UNIVERSITY OF LONDON THESIS

Degree phd Year 2007 Name of Author KONSTANTINOS KIAKOS

MOLECULAR AND CELLULAR PHARMACOLOGY OF NOVEL CHIRAL AND ACHIRAL CC-1065/DUOCARMYCIN ANALOGUES

KONSTANTINOS KIAKOS

A thesis submitted for the Degree of Doctor of Philosophy

Department of Oncology
Royal Free and University College Medical School
University College London

2006

ProQuest LLC
789 East Eisenhower Parkway
P.O. Box 1346
Ann Arbor, MI 48106-1346

In loving memory of Vagelitsa

ABSTRACT

CC-1065 and the duocarmycins are highly potent anticancer agents, exerting their biological activity through covalently reacting with adenine-N3 in the minor groove of AT-rich sequences. The alkylation properties and cytotoxicity of a series of novel chiral analogues are reported in this thesis. Structural modifications of established pharmacophores resulting in novel alkylating functionalities as well as variations of the DNA binding domain were introduced in the analogues considered, The sequence specificity of these compounds was assessed by a *Taq* Polymerase stop assay, identifying the sites of covalent modification on plasmid DNA and the purine-N3 adducts probed by a thermally-induced strand cleavage assay. The cytotoxic potency of the analogues was determined against human, chronic myeloid leukemia, K562, cells, using a MTT based growth inhibition assay.

The importance of the chiral centre present in the natural products was subsequently investigated with a series of achiral analogues. The studies established that the chiral centre is not absolutely required for DNA interaction and cytotoxicity. This finding offers the possibility of a new platform for the design of novel, active CC-1065/duocarmycin analogues.

A key chiral and an achiral analogue were selected for DNA repair studies. The sensitivity of yeast mutants deficient in specific DNA repair pathways was assessed in order to delineate the mechanisms involved in the repair of the relevant adenine-N3 adducts. Nucleotide excision repair (NER) and post replication repair mutants were the most sensitive to the two analogues. Single-strand ligation PCR was employed to follow the induction and repair of the lesions at nucleotide resolution. Adduct elimination of both agents was by transcription-coupled NER, and dependent upon functional Rad18. Finally, the involvement of NER as the predominant excision pathway was further confirmed in mammalian DNA repair mutant cells.

INDEX

Title..... 1

Abstract..... 3

Index..... 4

Lists of Figures and Tables..... 8

Abbreviations..... 16

Acknowledgements..... 20

CHAPTER 1: INTRODUCTION

1.1 Cancer: Facts and Figures..... 21

1.2 DNA as a target for chemotherapeutic agents..... 22

1.3 Sequence selective, DNA minor-groove interactive agents..... 28

1.3.1 Polyamides 29

1.3.2 SJG-136..... 37

1.3.3 Ecteinascidin-743..... 40

1.3.4 CC-1065 and the duocarmycins..... 45

1.3.4.1 Interaction with DNA..... 47

1.3.4.2 Modification of the pharmacophore..... 53

1.3.4.3 Origins of the sequence-selectivity..... 59

1.3.4.4 Biological properties..... 81

1.3.4.5 Cytotoxicity..... 92

1.3.4.6 Cell cycle effects – Cell death..... 97

1.3.4.7 Cellular uptake..... 97

1.3.4.8 Adverse toxicity..... 98

1.3.4.9 Novel analogues of CC-1065 and the duocarmycins. 100

1.3.4.10 Clinically investigated analogues..... 115

1.3.4.11 Yatakemycin..... 119

1.3.4.12 Consideration of the chiral centre..... 120

1.4 Experimental aims..... 125

CHAPTER 2: SEQUENCE SPECIFIC ALKYLATION AND CYTOTOXICITY OF A SERIES OF NOVEL CHIRAL CC-1065/DUOCARMYCIN ANALOGUES

2.1 Materials and Methods

2.1.1 Materials..... 126

2.1.2 Methods..... 130

2.1.2.1.Generation of a 5'-singly end labelled-fragment..... 130

2.1.2.2 Thermal Cleavage assay..... 132

2.1.2.3 *Taq* Polymerase stop assay..... 134

2.1.2.4 Detection of interstrand crosslinking in plasmid DNA..... 138

2.1.2.5 MTT cytotoxicity assay..... 140

2.2 C- and N- terminus conjugates of N-methylpyrrole polyamides with *seco*-cyclopropaneindole

2.2.1 Introduction..... 143

2.2.2 Compounds..... 148

2.2.3 Results and discussion..... 150

2.3 Furano analogues of Duocarmycin C1 and C2: *seco*-iso-CFI and *seco*-CFQ

2.3.1 Introduction..... 161

2.3.2 Compounds..... 163

2.3.3 Results and discussion..... 166

2.4 Hairpin conjugates of a racemic *seco*-Cyclopropaneindoline-2-benzofurancarboxamide and polyamides

2.4.1 Introduction..... 176

2.4.2 Compounds..... 178

2.4.3 Results and discussion..... 179

CHAPTER 3: SEQUENCE SPECIFIC ALKYLATION AND CYTOTOXICITY OF A SERIES OF NOVEL ACHIRAL CC-1065 / DUOCARMYCIN ANALOGUES

3.1 Introduction 186

3.2 Achiral *seco*-CI and achiral *seco*-amino-CI compounds

3.2.1 Compounds 192

3.2.2. Results and discussion 193

3.3 Achiral *seco*-CBI and *seco*-amino-CBI compounds

3.3.1 Introduction 200

3.3.2 Compounds 202

3.3.3 Results and discussion 202

3.4 Hairpin conjugates of achiral *seco*-cyclopropaneindoline-2-benzofurancarboxamide and pyrrole-imidazole polyamides

3.4.1. Introduction 210

3.4.2 Compounds 211

3.4.3 Results and discussion 212

CHAPTER 4: REPAIR STUDIES OF TH-III-151 AND AS-I-145 IN THE YEAST *Saccharomyces cerevisiae*

4.1 Introduction

4.1.1 Yeast as a model system 218

4.1.2 Yeast in drug discovery 220

4.1.3 Repair of minor groove adducts 224

4.1.4 Excision and post replication repair 225

4.1.5 Objectives of the study 234

4.2 Materials and Methods

4.2.1 Materials 236

4.2.2 Methods 236

4.2.2.1 Large scale sensitivity screen – Colony spotting assay..... 236
4.2.2.2 Yeast survival curves..... 238
4.2.2.3 Single strand ligation polymerase chain reaction (sslig-PCR). 238
4.2.2.4 DNA measurement by fluorimetry 244
4.2.2.5 DNA sequencing..... 244
4.2.2.6 PCR-based gene disruption..... 245
4.3 Results - TH-III-151 repair studies
4.3.1 NER-defective yeast cells are sensitive to TH-III-151. NER is the predominant excision repair event..... 250
4.3.2 *rad18* cells are sensitive to TH-III-151..... 256
4.3.3 Induction and repair of TH-III-151 adducts at nucleotide resolution in cells..... 258
4.3.4 Repair of TH-III-151 adducts is transcription-coupled..... 273
4.3.5 *RAD5* disruptants are extremely sensitive to TH-III-151..... 279
4.4 RESULTS - AS-I-145 repair studies..... 289
4.5 Discussion..... 297

CHAPTER 5: CYTOTOXICITY OF AS-I-145 IN NER DEFECTIVE CHINESE HAMSTER OVARY CELL LINES

5.1 Introduction – Aim..... 300
5.2 Materials and Methods
5.2.1 Materials..... 301
5.2.2 Methods; Sulphorhodamine B Growth Inhibition Assay..... 302
5.3 Results and discussion..... 303

CHAPTER 6: GENERAL DISCUSSION..... 309
APPENDIX..... 326
REFERENCES..... 329
PUBLICATIONS RESULTING FROM THIS THESIS..... 389

LIST OF FIGURES

CHAPTER 1

1.1	Nucleophilic centres in DNA as potential sites of alkylation.....	24
1.2	Modes of interaction of crosslinking drugs with DNA.....	25
1.3	Types of DNA-cisplatin adducts.....	26
1.4	Different types of interaction with DNA by DNA-interactive agents.....	28
1.5	Stuctures of netropsin and distamycin.....	29
1.6	Evolution of the rational design of GC recognising lexitropsins.....	32
1.7	Peptide fragments referred to in pairing rules.....	33
1.8	Inhibition of gene expression by Py/Im hairpin polyamides.....	36
1.9	Structures of DC-81, DSB-120 and SJG-136.....	38
1.10	Mechanism for the interstrand crosslinking of DNA by SJG-136.....	39
1.11	Structure and DNA interaction of ET-743.....	41
1.12	Structure of (+)-CC-1065.....	45
1.13	Structures of the duocarmycins.....	47
1.14	Reaction of (+)-CC-1065 with DNA.....	49
1.15	Reaction of (+)-DUMSA and (+)-DUMA with DNA.....	52
1.16	The CI pharmacophore.....	54
1.17	Structural modification of the natural pharmacophores CPI, DA and DSA..	57
1.18	Examples of other modifications of the alkylation subunits.....	59
1.19	Structures of partial analogues containing the CPI subunit.....	60
1.20	Proposed mechanism of catalysis of the adenine-N3-(+)-CC-1065 adduct....	64
1.21	Partial analogues for the evaluation of the (+)-CC-1065's subunit effects....	65
1.22	Analogues considered in the "first definitive test" by Boger.....	69
1.23	*seco*-CBI-indole analogues to test the role of electrostatic interactions.....	70
1.24	(+)-CBI-TMI and (+)-*iso*-CBI-TMI and their alkylation subunits.....	72
1.25	Structures of (+)-DSA-$CDPI_2$ and the reversed agent (+)-$CDPI_2$-DSA.....	73
1.26	Structure of (+) CDPI-DSA-CDPI, the "sandwiched" analogue.....	74

1.27 Torsion angles of (+)-DUMSA's intersubunit twist upon DNA binding..... 75
1.28 Structure of a modified (+)-CBI-TMI analogue lacking the linking amide..... 76
1.29 The minor groove imbedded substituents of (+)-DUMSA..... 77
1.30 (+)-DSI, an indole derivative of (+)-DUMSA..... 77
1.31 Structure of CBIn..... 79
1.32 Biological sites of action of (+)-CC-1065..... 91
1.33 Solvolysis and cytotoxicity of simple analogues of the alkylation subunits... 93
1.34 a. Effect of binding subunit on the cytotoxicity of CPI, CBI and DSA
b. C5 acyl derivatives of the CBI-indole agent..... 95
1.35 Analogues considered for the delayed toxicity phenomenon..... 99
1.36 Bizelesin..... 101
1.37 (+)(+)-DSA_2 102
1.38 Unsymmetrical bifunctional agents combining CPI, CBI and PBD..... 103
1.39 Hybrid molecules of CBI and bleomycin..... 104
1.40 Mitomycin A and duocarmyci hybrid..... 105
1.41 Structures of lexitropsin – CPI / CBI conjugates..... 106
1.42 Heterodimeric binding of DUMA and distamycin A..... 107
1.43 Examples of cooperative binding of DUMA with distamycin and triamides... 108
1.44 Hairpin polyamides incorporating the DUMA alkylation subunit..... 109
1.45 Hairpin conjugates incorporating Segment A of DU-86..... 110
1.46 a) Homodimeric and
b) heterodimeric binding of the ImPyLDu86 conjugate..... 112
1.47 Glycosides-prodrugs of *seco*-CI-TMI..... 114
1.48 Biotinylated CBI analogue..... 115
1.49 Structures of clinically evaluated CC-1065/duocarmycin analogues..... 116
1.50 Structure of (+)-Yatakemycin..... 119
1.51 Opposite direction of binding of (+)-DUMSA and (-)-DUMSA..... 121
1.52 Previously reported achiral agents..... 123

CHAPTER 2

2.1 Examples of hybrid molecules mentioned in the introduction..... 144

2.2 N-methyl pyrrole conjugates incorporating CPI..... 145

2.3 Natural and unnatural sets of the *seco*-CI hybrid agents..... 146

2.4 Pyrazole hybrids..... 147

2.5 Structures of JT-III-149A, JT-IV-31B and JT-IV-3..... 149

2.6 % Growth inhibition (absorbance plot) of K562 cells by JT-III-149A and JT-IV-31B for 1h exposure..... 151

2.7 *Taq* polymerase gel of JT-III-149A, JT-IV-31B and JT-IV-3..... 153

2.8 *Taq* polymerase gels of JT-III-149A, JT-IV-3 (left) and JT-IV-31B (right)... 155

2.9 Thermal cleavage gel of JT-III-149A, JT-IV-31B and JT-IV-3..... 157

2.10 Diagram showing the sequence of the resolvable portion of 2.9..... 158

2.11 % Growth inhibition (absorbance plot) of K562 cells by JT-III-149A, JT-IV-31B and JT-IV-3 for 4 days exposure..... 159

2.12 Structures of LY29632, LY29795 and LY307918..... 162

2.13 Structures of TH-III-149, BL-1-127, TH-III-151 and AS(BL)59..... 163

2.14 Stucture of the ultimate cyclopropane containing iso-CFI-TMI agent..... 164

2.15 Structures of the N3-N3, *seco*-iso-CFI dimers CP-75 and CP-67..... 165

2.16 Structure of the reference compound *seco*-CBI-TMI..... 166

2.17 *Taq* polymerase assay gel of TH-III-151 and AS(BL)59..... 168

2.18 *Taq* polymerase assay gel of TH-III-151, AS(BL)59, TH-III-149 and BL-1-127..... 169

2.19 Thermal cleavage gel of TH-III-149 and TH-III-151..... 171

2.20 DNA interstrand crosslinking gel of CP-75 and CP-67..... 172

2.21 Plot of the (%) DNA interstrand crosslinking induced by CP-75 in plasmid DNA against the agent's concentration..... 172

2.22 Structures of RBH-III-23, JT-IV-99, JT-IV-101 and JT-IV-83..... 178

2.23 Thermal cleavage gel for RBH-III-23, JT-IV-99, JT-IV-101 and JT-IV-83... 181

2.24 A. Diagram of the sequence and sites of alkylation from 2.23, for RBH-III-23 and JT-IV-99
B. Proposed mechanism of interaction of the two agents with 3'-GACT-5'..... 183

CHAPTER 3

3.1 Activation of the *seco* prodrugs by the loss of HCl in biological media..... 186
3.2 Formation of spiro[2,5]octa-1,4-dien-3-one as an intemediate in the reaction of bromide with a nucleophile..... 188
3.3 Analogues of 2-*p*-hydroxymethyl (HPE) compound..... 188
3.4 Proposed mechanism of activation and DNA alkylation of the achiral *seco*-CI moiety..... 189
3.5 Structures of SC-III-147 and JT-II-67..... 192
3.6 Proposed mechanism of activation and DNA alkylation of the achiral *seco*-amino-CI moiety of compound JT-II-67..... 193
3.7 A. *Taq* polymerase assay gel of SC-III-147
B. Thermal cleavage gel of SC-III-147..... 194
3.8 A. *Taq* polymerase assay gel of JT-II-67
B. Thermal cleavage gel of JT-II-67..... 196
3.9 Structure of TH-III-81..... 198
3.10 *Taq* polymerase assay gel on TH-III-81..... 199
3.11 Structures of AS-IV-104 and AS-I-145..... 202
3.12 Thermal cleavage gel of AS-IV-104 and AS-I-145..... 203
3.13 Proposed model of the activation and DNA alkylation of AS-I-145..... 204
3.14 Thermal cleavage gel comparing AS-I-145 to adozelesin..... 205
3.15 A.Thermal cleavage gel and
B.*Taq* polymerase stop assay gel comparing AS-I-145 with JT-II-67 and the racemic *seco*-CBI-TMI agent..... 207
3.16 Structures of CP-99A, CP-99B and BL-I-147..... 211
3.17 Thermal cleavage gel of CP-99A, CP-99B and BL-I-147..... 213

3.18 Sequence of the binding sites of CP-99A, CP-99B and BL-I-147..... 214
3.19 Model of molecular interaction of each compound with the sites of 3.18..... 215

CHAPTER 4

4.1 Example of a pathway-based, positive-selection screen in yeast..... 222
4.2 Oligopyrrole analogues of distamycin tethering BAM..... 226
4.3 Yeast NER damage recognition and incision steps..... 229
4.4 *RAD6* dependent post-replication repair subpathways..... 232
4.5 Experimental strategy followed for the yeast DNA repair studies..... 235
4.6 Schematic diagram of the sslig-PCR technique..... 240
4.7 Structure of TH-III-151..... 250
4.8 Sensitivity of the excision repair mutants *mag1* (BER) and *rad4* (NER) treated with TH-III-151. Colony spotting assay..... 251
4.9 TH-III-151 sensitivity of *rad4*, *mag1,* and *rad4 mag1* cells (survival curve).. 253
4.10 TH-III-151 sensitivity of *ogg1* with its isogenic parent W303a, *rad14* and the double mutant *ogg1 rad14*..... 254
4.11 Sensitivity of the BER repair mutants *ntg1*, *ntg2* and *ung1* treated with TH-III-151 (colony spotting assay)..... 255
4.12 TH-III-151 sensitivity of *rad4*, *rad18* and *rad4 rad18* cells..... 256
4.13 The region of the *MFA2* gene under study..... 259
4.14 Comparison of the levels of PCR signal detected in cells and isolated DNA with different TH-III-151 concentrations..... 260
4.15 Agarose gel showing the PCR fragments used for di-deoxy sequencing..... 261
4.16 Sequencing of the TS of *MFA2* to determine sites of TH-III-151 binding..... 262
4.17 Damage induced by 1 μM of TH-III-151 in isolated genomic DNA and that produced in cells by 10 μM of the agent..... 264
4.18 Repair of TH-III-151 adducts on the TS of *MFA2* in DBY747 cells..... 266
4.19 Sequence of the resolvable portion of the autoradiograph presented in Figure 4.18 and sites of binding of TH-III-151..... 267

4.20 Repair of TH-III-151 adducts on the TS of *MFA2* in *rad4* cells..... 269
4.21 Repair of TH-III-151 adducts on the TS of *MFA2* in *mag1*cells..... 270
4.22 Repair of TH-III-151 adducts on the TS of *MFA2* in *rad18 and rad6* cells... 271
4.23 Repair rates of TH-III-151 adducts on the TS of the *MFA2* gene in the DBY747 (parental), *rad4* and *rad18* strains..... 272
4.24 Sequencing of the NTS of *MFA2* gene..... 274
4.25 Repair of TH-III-151 adducts on the NTS of *MFA2* in DBY747 cells..... 275
4.26 TH-III-151 adducts on the NTS of *MFA2*, run alongside a molecular mass marker which generates bands at 10bp increments..... 276
4.27 Repair of the TH-III-151 adducts on the NTS of *MFA2* in *rad18* and *rad6* cells..... 277
4.28 TH-III-151 sensitivity of the *rev3* and *rad30* mutant cells..... 279
4.29 Sensitivity of *rev3* cells compared with the wild type DBY747..... 280
4.30 TH-III-151 sensitivity of *rad5*, *mms2*, and *rad5 mms2* cells..... 281
4.31 The PCR-mediated gene disruption procedure followed to create the *rad4 rad5* double mutant..... 283
4.32 Confirmation of *RAD4* disruption using PCR and *Pvu I* and *EcoR V* digestion..... 285
4.33 Gel analysis of undigested and *EcoR V* or *Pvu I* digested samples to confirm disruption of *RAD4*..... 286
4.34 TH-III-151 sensitivity of *rad5*, *rad4* and *rad4 rad5* cells..... 287
4.35 Comparison of the repair profiles of DBY747 and *rad5* cells on the TS of *MFA2*..... 288
4.36 Structure of AS-I-145..... 289
4.37 Sensitivity of the excision repair mutants *mag1* (BER), and *rad4* (NER) treated with AS-I-145 (colony spotting assay)..... 290
4.38 Sensitivity of the BER repair mutants *ntg1*, *ntg2* and *ung1* to AS-I-145..... 291
4.39 AS-I-145 sensitivity of *rad4*, *mag1,* and *rad4 mag1* cells..... 292
4.40 AS-I-145 sensitivity of *rad18*, *rad4,* and *rad4 rad18* cells..... 293
4.41 Repair of AS-I-145 adducts on the TS of *MFA2* in DBY474, *rad4* and *rad18* cells..... 294

4.42 Repair of AS-I-145 adducts on the NTS of *MFA2*..... 295

CHAPTER 5

5.1 Recognition and incision steps of human global genome NER..... 305
5.2 AS-I-145 sensitivity in parental AA8 cells and NER mutants..... 306

LIST OF TABLES

CHAPTER 1

1.1 Pairing code for minor groove recognition 33
1.2 Effect of the methoxy substituents on duocarmycin analogues..... 78
1.3 Summary of the main points of the Boger and Hurley models..... 80
1.4 Cytotoxic potencies and delayed lethality in animals of key CPI extended analogues 99
1.5 Cytotoxic potencies and delayed lethality in animals of various enantiomeric pairs..... 121
1.6 Cytotoxic potencies and alkylation efficiencies of enantiomeric pairs..... 122

CHAPTER 2

2.1 *In vitro* cytotoxicity data (IC_{50} values) of JT-III-149A, JT-IV-31B and JT-IV-3 for 1h exposure..... 151
2.2 *In vitro* cytotoxicity data (IC_{50} values) of JT-III-149A, JT-IV-31B and JT-IV-3 for a 4 days exposure..... 159
2.3 *In vitro* cytotoxicity (IC_{50} in μM) of the furano analogues in 2.3.2..... 174
2.4 *In vitro* cytotoxicity (IC_{50} in μM) of RBH-III-23, JT-IV-99, JT-IV-101 and JT-IV-83 (1 h and 4 days exposure)..... 184

CHAPTER 3

3.1 *In vitro* cytotoxicity data (IC_{50} values) of SC-III-147 and JT-II-67..... 197

3.2 *In vitro* cytotoxicity data (IC_{50} values) of AS-IV-104 and AS-I-145..... 208

CHAPTER 4

4.1 Conservation between yeast and human pathways altered in cancer..... 220

4.2 Properties of the three BAMs, tethering 1-3 pyrrole units..... 226

CHAPTER 5

5.1 The NER-deficient Chinese hamster cell lines used in this study..... 304

5.2 IC_{50} values of AS-I-145 in the CHO parental (AA8) and NER deficient mutant cell lines..... 306

ABBREVIATIONS

6-MP	6-Mercaptopurine
6-TG	6-Thioguanine
A	Adenine
ALL	Acute lymphoblastic leukaemia
APS	Ammonium persulphate
ATP	Adenine triphosphate
BAM	Benzoic acid mustard
BAP	Bacterial alkaline phosphatase
BER	Base excision repair
bp	Base pair
C	Cytosine
CBA	1,2,9,9a-tetrahydrocyclopropa[*c*]benz[*e*]-3-azaindol-4-one
CBI	1,2,9,9a-tetrahydrocycloporpa[c]benz[e]indol-4-one
CBIn	1,2,9,9a-tetrahydro-[H-cyclopropa[c]benz[e]inden-4-one
CBQ	2,3,10,10a-tetrahydrocyclopopa[d]-benzo[f]quinol-5-one
CD	Circular dichroism
CDPI	3-carbamoyl-1,2-dihydro-3H-pyrrolo[3,2-e]indole-7-carboxylic acid
CFI	1,2-dihydro-1-(chloromethyl)-5-hydroxy-8-methyl-3H-furano[3,2-*e*]indole
CHO	Chinese hamster ovary
CI	1,2,7,7a-tetrahydrocycloprop[1,2-c]indol-4-one
CLL	Chronic lymphocytic leukemia
CML	Chronic myeloid leukaemia
CNA	1,2,3,4,11,11a-Hexahydrocycloprop[c]naptho[2,1-b]azepin-6-one
CNS	Central nervous system
CPI	Cyclopropane[c]pyrrolo[3,2-*e*]indole-4(5H)-one
cps	Counts per second
CPyI	1,2,9,9a-tetrahydrocyclopropa[*c*]pyrido[3,2-*e*]indol-4-one-7-carboxylate

CPzI	1,2,8,8a-tetrahydro-5H-cyclopropa[c]pyrazolo[4,3-e]indol-4-one
CS in CSA, CSB	Cockayne's syndrome
CT	Calf thymus
DARP	Duocarmycin-DNA adduct recognising protein
DHFR	dihydrofolate reductase
DMA	N,N-dimethyl-acetamide
DMSO	Dimethyl sulfoxide
DNA	Deoxyribonucleic acid
dNTP	Deoxynucleoside triphosphate
Dp	3-(dimethylamino)propylamine
DTT	Dithiothreitol
DUMA	Duocarmycin A
DUMs	Duocarmycins
DUMSA	Duocarmycin SA
EDTA	Ethylemediamine tetraacetic acid
F_2CBI	9,9-difluoro-1,2,9,9a-tetrahydrocyclopropa[c]benz[e]indol-4-one
FCS	Foetal calf serum
FDA	Food and drug administration
Fn	Furan
FUra	5-Fluorouracil
GG-NER	Global genome nucleotide excision repair
G	Guanine
g	Gram
Hepes	N-[2-Hydroxyethyl]piperazine-N'-2[2-ethanesulfonic acid]
hnRNP L	Heterogenous nuclear ribonucleoprotein L
Hp	Hydroxypyrrole
HNSCC	Head and neck squamous cell carcinoma
Ht	3-hydroxythiophene
Hz	hydroxybenzimidazole
Im	Imidazole-2-carboxamide
IP	Intraperitoneally

Ip	imidazo[4,5-b]pyridine
ISC	Interstrand crosslink
IV	Intravenous
kb	kilobase
Kd	dissociation rate constant
kDa	Kilodalton
LTR	Long terminal repeats
M	Molar
MARs	Matrix associated regions
MAT	Mating-type genes
mg	Milligram
ml	Millilitre
mM	Millimolar
μM	Micromolar
MM	Multiple myeloma
MTD	Maximum tolerated dose
MTT	3-(4,5-dimethylthiazol-2-yl)-2,5-diphenyl tetrazolium bromide
MTX	Methotrexate
NCE	New chemical entities
NCI	National Cancer Institute
NCP	Nucleosome core particle
NER	Nucleotide excision repair
ng	Nanogram
NTS	Nontranscribed strand
OD	Optical density
ODN	Oligodeoxyribonucleotides
PBDs	Pyrrolo[2,1-c][1,4]benzodiazepines
PBS	Phosphate buffered saline
PCR	Polymerase chain reaction
PDE	1,2-dihydro-3H-pyrrolo[3,2-e]indole

pmol	Picomoles
Py	Pyrrole-2-carboxamide
Pz	N-methylpyrrazole
rpm	revolutions per minute
RPA	Replication protein A
SC	subcutaneous
SRB	Sulphorhodamine B
SSA	Single-strand annealing
SSB	Single-strand break
STS	Soft tissue sarcoma
SV40	Simian virus 40
T	Thymine
TAE	Tris-acetic acid EDTA buffer
TBE	Tris-boric acid EDTA buffer
TCA	Trichloroacetic acid
TC-NER	Transcription-coupled nucleotide excision repair
TFO	Triple helix forming oligonucleotide
TGCT	Testicular germ cell tumour
Th	4-methylthiazole
TLS	Translesion synthesis
TMI	Trimethoxyindole
Tn	3-methylthiopene
TS	Transcribed strand
U	Enzyme unit
UV	ultraviolet
XP in XPA, XPB etc	Xeroderma Pigmentosum
YEPD	Yeast extract-peptone dextrose

ACKNOWLEDGMENTS

I would like to thank Professor Hartley for giving me the opportunity to work in his lab. His guidance and support throughout the years, our work and his drive made me stay and stay and stay and eventually make England my home. For his ... Olympian patience regarding this thesis, he deserves the gold medal! I cannot thank him enough for all he has done for me, as a mentor, as a boss and as a friend. Special thanks for putting up with all those tears and all the drama every now and then-all too often !

I wholeheartedly thank Professor Moses Lee. For his compounds and for his friendship! He has inspired me and he has given me faith and vision. My visit to Furman is something I will never forget. As for his letters at the times of need, I will always be grateful!

Special thanks to Dr. McHugh for introducing me to the yeast world. It was great fun working with you. Thanks for all the support!

Lucia Christodoulides ... I will now stop hiding and stop not answering your calls. You were there, always. Thank you.

How can I possibly thank my parents? I must apologise for all this rollercoaster of emotions and for the unbearable burden I put on you. Yet you stood tall and helped me without never showing how hard it really was. Thank you. For always believing in me, for loving me unconditionally, for being you ... Hope one day to make up for all the years lost.

To all my friends in the lab, the people who came and left over the years, thanks you !

CHAPTER 1

INTRODUCTION

1.1 Cancer: Facts and Figures

Cancer is a group of diseases characterised by uncontrolled growth, accumulation and spread of abnormal cells. It involves a pathological breakdown in the processes that control cell proliferation, differentiation and death. The causal factors can be external (tobacco, chemicals, mutagens, radiation, sunlight, infectious organisms), internal (inherited faulty genes, mutations, hormones, immune conditions) and lifestyle factors such as obesity, physical inactivity, nutrition etc.
Worldwide, approximately 10 million people are diagnosed with cancer annually and more than 6 million die of the disease every year. Currently, over 22 million people are cancer patients rendering cancer a global major disease burden (Stewart & Kleihues, 2003).

Cancer is the second leading cause of death in the US (22.7% of all deaths) after heart disease (28% of all deaths-US mortality data 2003). However, compared to the rates in 1950, heart disease's death rate had decreased in 2003 by 60.6% while cancer death rate was marginally (0.2%) higher in 2001 and 2% lower in 2003. The American cancer society estimates that 564,830 cancer deaths were expected to occur in 2006, that is more than 1,500 people a day, with cancer accounting for 1 in every 4 deaths. Lung and bronchus (31% in men and 26% in women) are the leading sites of these fatal cancers, followed by colon and rectum (10%) in men and breast (15%) cancer in women. Lung cancer accounts therefore for most deaths of cancer. About 1.4 million new cancer cases were expected to be diagnosed in the US, in 2006, along with more than 1 million cases of basal and squamous cell skin cancers. Prostate (33%) in men and breast (31%) in women are the leading sites of the estimated new cases for 2006. In 2003 the first time since 1930, when relevant mortality data began to be compiled, a decrease in number of cancer deaths among

men was recorded. According to most recent data, the National cancer institute estimates that approximately 9.6 million Americans with a history of cancer were alive in January 2000, with some of these individuals being cancer-free, still having evidence of cancer and/or undergoing treatment (All US related data extracted from the American cancer society website; www.cancer.org).

In the UK, four types of cancer, breast, lung, large bowel (colorectal) and prostate, account for over half of the new diagnosed cases. Breast cancer is the most common, although rare in men, with over 40,000 new cases (15% of all cancers), followed by lung cancer with 38,000 diagnosed cases each year (incidence data refer to 2002). In the UK in 2004, there were 153,397 deaths from cancer, with lung cancer patients accounting for 22% of these deaths. Overall mortality from cancer has decreased in the period 1975-2004 by 14% despite increasing incidence. The state has a target of further reducing the cancer death rate in people under 75, by 20% by 2010. Approximately 1.2 million people, (2% of the population of the UK) are alive and have received a cancer diagnosis (All UK related data extracted from the Cancer research UK website; www.cancerresearchuk.org).

Cancer is treated by surgery, radiation, chemotherapy, hormones, and immunotherapy, either alone or in combination. Chemotherapy is now given in the setting of certain paediatric malignancies, germ cell tumours and some types of lymphomas with curative intent. The gains of cure rates however, in most other cases have been small (Stewart & Kleihues, 2003). Drugs are used at some time during the course of the illness of most cancer patients. The intracellular target of many such anticancer drugs used in the clinic is DNA.

1.2 DNA as a target for chemotherapeutic agents.

The emergence of DNA as a target for cancer therapy coincided with the dawning of modern cancer chemotherapy signalled by the clinical observation during the

World War II, that sulphur mustard gas, developed and used since 1917 as a war gas could lower the white-blood-cell count of exposed military personnel. The more stable nitrogen mustards followed and their therapeutic potential particularly against lymphomas was reviewed by Gilman and Philips in 1946, marking the introduction of this class of compounds as cancer therapeutics (Gillman & Philips, 1946). One of the first nitrogen mustards shown to be effective, mechlorethamine hydrochloride (or chlormethine) is still used as an anticancer drug. The nitrogen mustards were the archetypal DNA reactive drugs of the broader class of the alkylating agents.

Alkylating agents covalently interact with DNA. These are highly reactive compounds that form covalent bonds with a number of nucleophilic groups on DNA. Monofunctional agents having a single reactive group can induce single base modifications (monoadducts) at various nucleophilic centres in DNA (Figure 1.1). The positions N7 of guanine along with the N3 position of adenine are the most reactive DNA sites to alkylating agents. Two monofunctional alkylating agents, ET-743 and (+)-CC-1065 are discussed in sections 1.3.3 and 1.3.4. Base modifications by alkylation weaken the N-glycosidic bond, leading to depurination /depyrimidination and the appearance of alkali labile abasic sites (Friedberg *et al.*, 1995). Agents possessing two reactive groups can potentially react with two sites on DNA, are termed bifunctional and comprise the majority of the clinically used alkylating agents. They can form crosslinks by reacting with two nucleosides on the same (intrastrand) or opposites (interstrand) strands of DNA. Figure 1.2 shows the various modes of interaction of crosslinking drugs with DNA. Medicinal chemistry efforts during the 1950s resulted in the development of modified, crosslinking mustard derivatives such as chlorambucil and melphalan (phenylalanine mustard; Alkeran), both still being a mainstay of cancer treatment. Serendipity played a major role in the discovery of another clinically useful, bifunctional alkylating agent, cisplatin. In 1963, Rosenberg and co-workers observed that proliferation of *Escherichia coli* in an electrolysis chamber equipped with platinum electrodes and aerated with oxygen, was inhibited. The active agent was deduced to be a platinum salt (Rosenberg *et al.*, 1965). The compound cisplatin, (*cis*-

diamminedichloroplatinum (II)) is still one of the most widely used chemotherapeutic agents. Figure 1.3 shows the different, cisplatin-specific types of adducts, which can be formed following intracellular hydrolysis of the drug.

Alkylating agents have an extensive range of structures, differing though limited sequence specificities and often dramatically differing tumour specificities, potencies and toxicity profiles (Hartley, 2002).

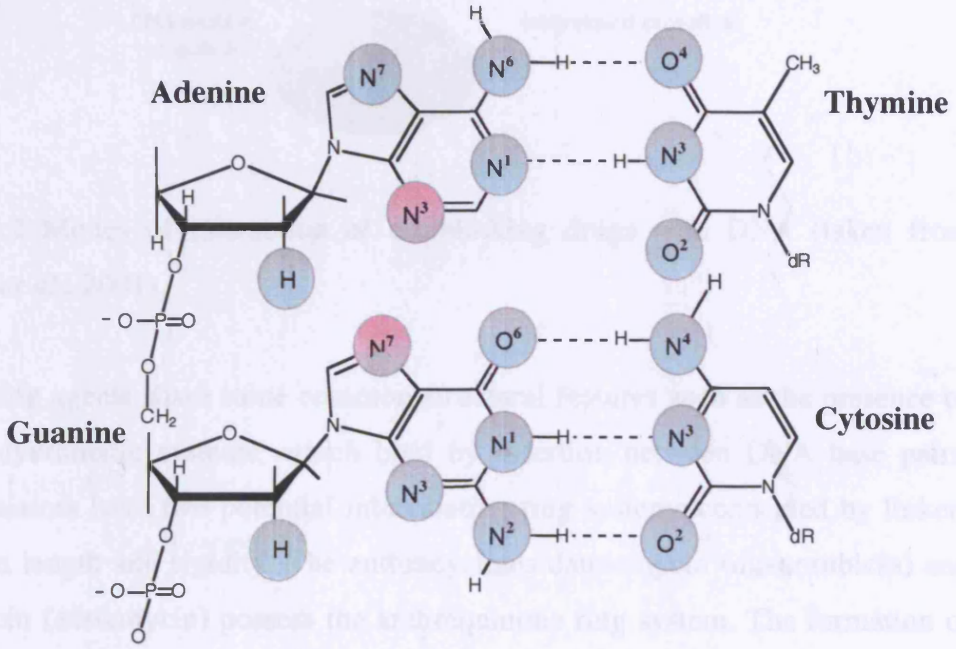

Figure 1.1 Nucleophilic centres in DNA, which are potential reaction sites for alkylation (adapted from Friedberg *et al.*, 1995). The N7 position of guanine and N3 of adenine are the most reactive (in pink). The alkylated N3 positions of adenine and guanine, the N2 of the guanine amino group and the O2 position of cytosine occupy the minor groove of the DNA helix. Other sites of alkylation in bases such as O6 in guanine, O4 in thymine and N7 in guanine occupy the major groove.

Antitumour antibiotics such as the anthracyclines have been part of the arsenal of chemotherapeutic drugs since the 1960s. In contrast to the agents mentioned

previously, these compounds bind to DNA primarily by intercalation, which is a non-covalent, reversible interaction.

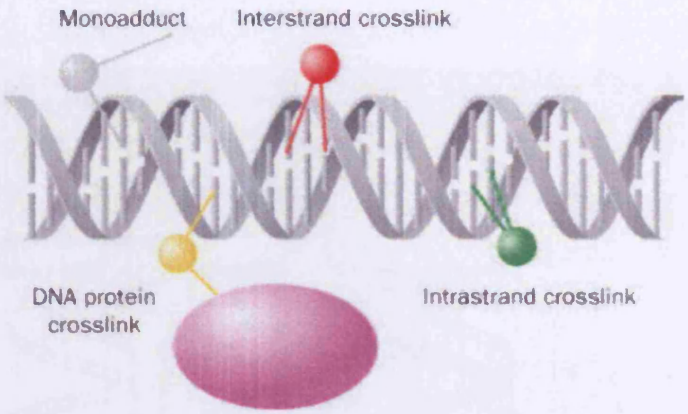

Figure 1.2 Modes of interaction of crosslinking drugs with DNA (taken from McHugh *et al.*, 2001).

Intercalating agents share some common structural features such as the presence of planar polyaromatic systems, which bind by insertion between DNA base pairs. Bisintercalators have two potential intercalating ring systems connected by linkers varying in length and rigidity. The anthracyclines daunomycin (duanorubicin) and doxorubicin (adriamycin) possess the anthraquinone ring system. The formation of a ternary complex with DNA and *topoisomerase-II*, trapping the "cleavable complex" and inhibiting the religation step, thus inducing *topoisomerase-II*-mediated, DNA double strand breaks is believed to be the critical event for their anticancer activity whereas free radical mediated DNA cleavage is possibly more closely related to their cardiotoxic side effects (reviewed by Braña *et al.*, 2001).

Apart from the DNA reactive agents, there are also drugs, which act by inhibiting nucleic acid synthesis. The antimetabolites such as antifolates, antipurines and antipyrimidines, interfere by inhibiting the production of precursors necessary for nucleic acid synthesis synthesis or they resemble in structure normal purines and

pyrimidines and they substitute them in the anabolic nucleotide pathways, eventually getting incorporated into RNA and DNA instead of their normal counterparts.

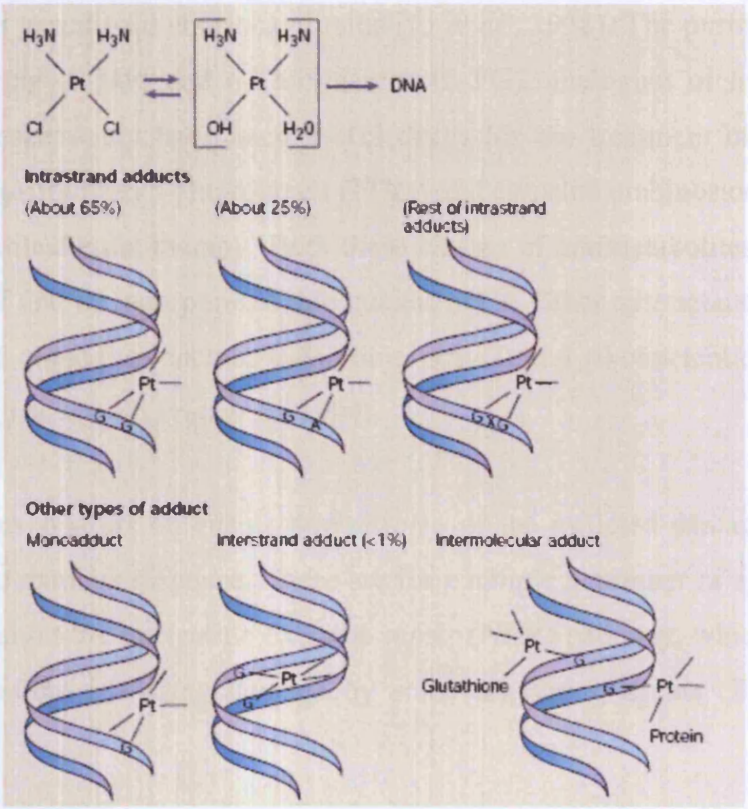

Figure 1.3 After undergoing hydrolysis in cells, cisplatin can attach to DNA. Intrastrand crosslinks between adjacent guanines are the adducts most frequently observed followed by the same type of adduct between adjacent adenine and guanines. It can also stretch across a base to link two guanines, on the same strand. Cisplatin can also form interstrand crosslinks (<1%), which although infrequent, they are believed to be the most toxic of the lesions, monoadducts and links between DNA and proteins (taken from Masters & Köberle, 2003).

Chronologically, this was the second class of anticancer drugs to be used in the clinic. Methotrexate, (MTX, amethopterin) inihibits the enzyme dihydrofolate reductase (DHFR) leading to inhibition of thimidylate synthesis and purine biosynthesis (Jolivet *et al.*, 1983). Eight years after the discovery of antifolates, methotrexate would provide the first example of drug-induced cure of a cancer, that of women with gestational choriocarcinoma (Li *et al.*, 1958). The purine analogues 6-Mercaptopurine (6-MP) and 6-Thioguanine (6-TG), analogues of hypoxanthine and guanine respectively have been useful drugs for the treatment of leukemias, while the antipyrimidines 5-fluorouracil (FUra) and cytosine arabinoside, are both a mainstay of antileukemic therapy. Both these classes of antimetabolites can inhibit the synthesis of and be incorporated into nucleic acids. Other antimetabolies include sugar modified analogues such as cytarabine (ara-C) and ribonucleotide reductase inhibitors (Hydroxyurea) (Pratt *et al*, 1994).

Compounds can also act on events downstream of the inflicted damage on DNA, like the evoked damage response. There are for example a number of agents, being developed to target the nucleotide excision repair (NER) pathway, which acts upon a variety of lesions including damage by some alkylating agents (Barret *et al.*, 2002).

DNA is an evolving target for cancer therapy offering various sites and modes of interaction for potential intervention with chemotherapeutic agents. Figure 1.4 summarises the molecular interactions with DNA, of various types of DNA-interactive agents. Secondary DNA structures, such as G-quadruplex formed at telomeres and also identified in promoter regions of a number of oncogenes, have emerged as such molecular targets for DNA-interactive compounds (Hurley, 2002) along with other domains of particular sequence content such as the AT-islands (Woynarowski, 2002) (the latter are discussed with respect to CC-1065 analogues in section 1.3.4.4).

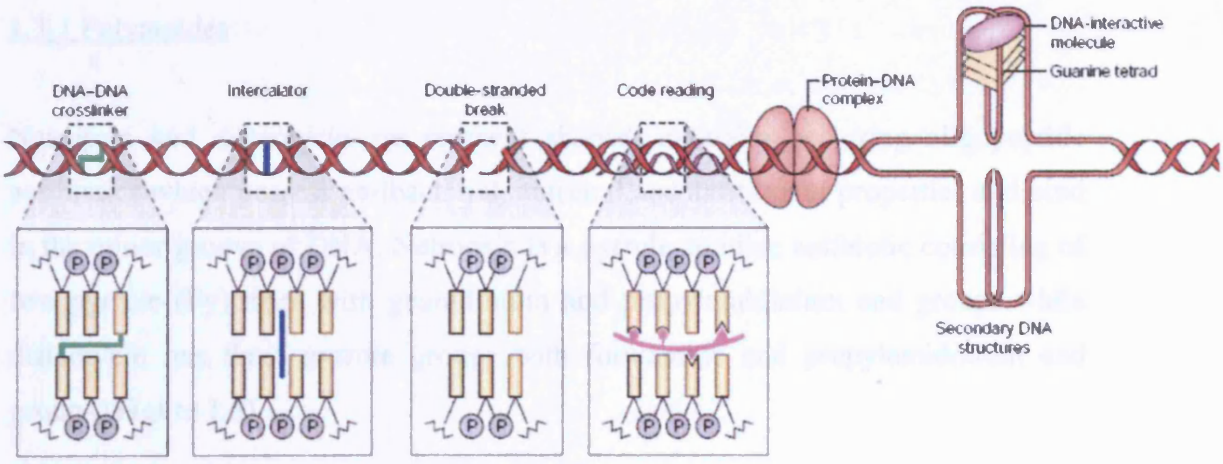

Figure 1.4 Different types of interaction with DNA by various classes of DNA-interactive agents.

The minor groove is one structural feature of DNA, which has been extensively pursued as the target for the design of a range of agents, often based on naturally occurring lead structures.

1.3 Sequence selective DNA minor groove-interactive agents

The minor groove of double helical B-DNA is the site of many non-covalent as well as covalent, highly sequence-specific interactions, for a large number of small molecules and as such, has been the target for the design of novel DNA ligands. DNA minor groove binders comprise a distinct class of DNA interactive agents, with some members possessing antiviral, antibacterial and antitumour properties (reviewed by Reddy *et al.*, 1999; Baraldi *et al.*, 2004). In the sections that follow, a class of agents that non-covalently interact with DNA, the polyamides, and agents, which can covalently modify DNA including SJG-136, capable of producing interstrand crosslinks and ET-743, CC-1065 and the duocarmycins, and yatakemycin, producing monoadducts and having different sequence specificitites, are discussed.

1.3.1 Polyamides

Netropsin and distamycin are crescent shaped, naturally occurring oligopeptide antibiotics which possess antibacterial, antiviral and antitumour properties and bind in the minor groove of DNA. Netropsin is a pyrrole amidine antibiotic consisting of two pyrrole (Py) rings with guanidinium and propylamidinium end groups while distamycin has three pyrrole groups with formamide and propylamidinium end groups (Figure 1.5).

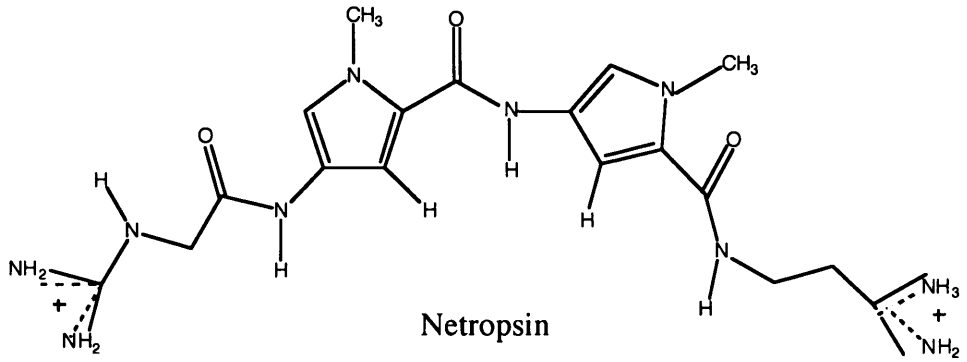

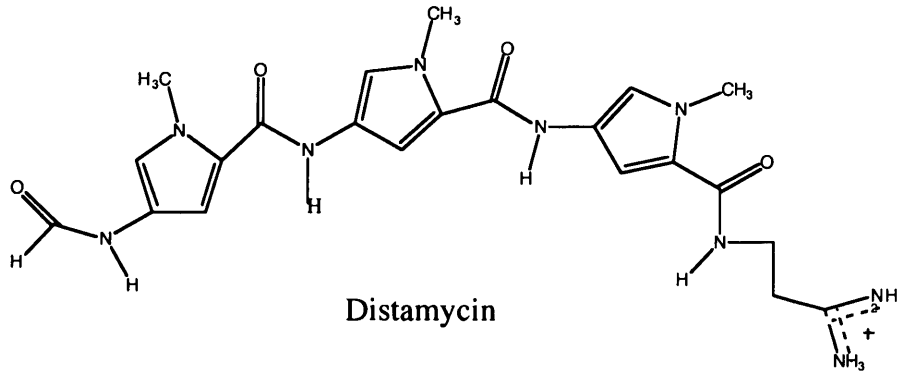

Figure 1.5 Structures of the minor groove antibiotics netropsin and distamycin.

The preference of the two agents for AT-rich regions has been established through biophysical methods (Wartell *et al.*, 1974) and footprinting experiments (Van dyke *et al.*, 1982; Fox & Waring, 1984; Portugal & Waring, 1987). Netropsin requires a

target site of four AT base pairs, while distamycin binds optimally to five contiguous AT base pairs, on account of its larger size. Both distamycin and netropsin bind to $d(A)_n \cdot d(T)_n$ better than $d(AT)_n$ (Zimmer *et al.*, 1979) and the presence of a TpA (but not ApT) step reduces the binding affinity (Ward *et al.*, 1988). However, distamycin is more tolerant of a GC base pair at the end of the binding site (Portugal & Waring, 1987; Churchill *et al.*, 1990). Since the main feature that distinguishes a GC base pair from an AT base pair in the minor groove, is the N-2 amino group of guanine, the lack of binding to GC rich regions was thought to be the result of steric clash between this protruding group and netropsin and distamycin. Replacement of one or more pyrrole units that consitute netropsin with a heterocycle capable of accepting a hydrogen bond from guanine-2-NH_2 should alter its strict preference for $(AT)_n$ binding and permit GC base pair recognition (Kopka *et al.*, 1985; Lown *et al.*, 1986). The resulting compounds were termed "lexitropsins" or information-reading oligopeptides and are currently referred to as polyamides due to their repeating peptide linkers. The imidazole group (Im), which bears an N atom in place of the C-H bond of the pyrrole (Figure 1.7), should correct the steric conflict and provide the opportunity for a hydrogen bond. The prototype lexitropsins incorporated one or more imidazole groups in place of the guanine-excluding pyrrole groups in the netropsin molecule (Lown *et al.*, 1986). These dicationic netropsin-based analogues exhibited a progressively decreasing preference for AT sites in binding studies and a corresponding acceptance of GC base pairs. *DNAse* I footprinting studies revealed that this series of compounds could recognize and bind GC rich sites yet still retained a strong memory for the original sequence selectivity of the parent netropsin (Lown *et al.*, 1986). In an attempt to further decrease the attraction for AT sites, which have a strong negative electrostatic potential, second generation lexitropsins were synthesized (Krowicki & Lown, 1987). These replaced the cationic N-terminal guanidinium head with a non-polar N-formyl end group, characteristic of distamycin, resulting to a singly positively charged molecule. Footprinting studies confirmed a dramatic change in the sequence specificity of these analogues, which

exhibited increased selecitivity for GC rich sites (Kissinger *et al.*, 1987). Studying the complex of a monocationic diimidazole polyamide and the oligonucleotide d[CATGGCCATG]$_2$, it was revealed that the analogue would bind over the 5'-CCAT-3' site, with its N-terminus oriented at the 5' end and the C-terminus located above the 3' thymine. It was deduced that the dominant factor determining the reading of the 3'-terminal AT base pair is the Van der Waals interaction between the methylenes at the carboxyl terminus of the lexitropsin and the DNA (Lee *et al.*, 1988a). These methylene groups enter into steric contact with the guanine-2-NH_2 group of a GC base pair, thereby preventing the binding of the C-terminus of netropsin analogues to a GC site and forcing the recognition of an AT pair instead. Removal of the offending methylene group resulted in a "truncated" lexitropsin, bearing only one methylene group at the C-terminus, allowing recognition of the 5'-ATTG site of a d[CGCAATTGCG]$_2$ oligonucleotide, in contrast to the unmodified lexitropsin which would bind to 5'-AATT (Lee *et al.*, 1988b). An overview of the strategy followed to obtain agents that would achieve GC recognition is presented in Figure 1.6.

A major advance was the discovery by NMR studies of a new type of complex, with distamycin being capable of binding in the minor groove of a 5'-AAATT-3' sequence as a side-by-side antiparallel homodimer, at higher concentrations and in a widened minor groove (Pelton & Wemmer, 1989). Study of the binding of the two peptides distamycin A and 1-methylimidazole-2-carboxamide-netropsin (2-ImN) revealed that they are also capable of a side-by-side antiparallel binding as a heterodimer allowing successful targeting of a single GC base pair (Mrksich & Dervan, 1993a). In light of the 2:1 binding mode of homodimeric or heterodimeric complexes, the recognition rules for the side-by-side pairing of pyrrole and imidazole groups in the minor groove with the geometry of hydrogen bonding, lending specificity, were elucidated. A pairing of an imidazole opposite a pyrrole targets a GC base pair, whereas a Py opposite an Im targets a CG base pair. The Py/Py could target both TA and AT pairs, in preference to GC/CG. The introduction of hydroxypyrrole (Hp) (Figure 1.7) as a thymine-selective recognition element,

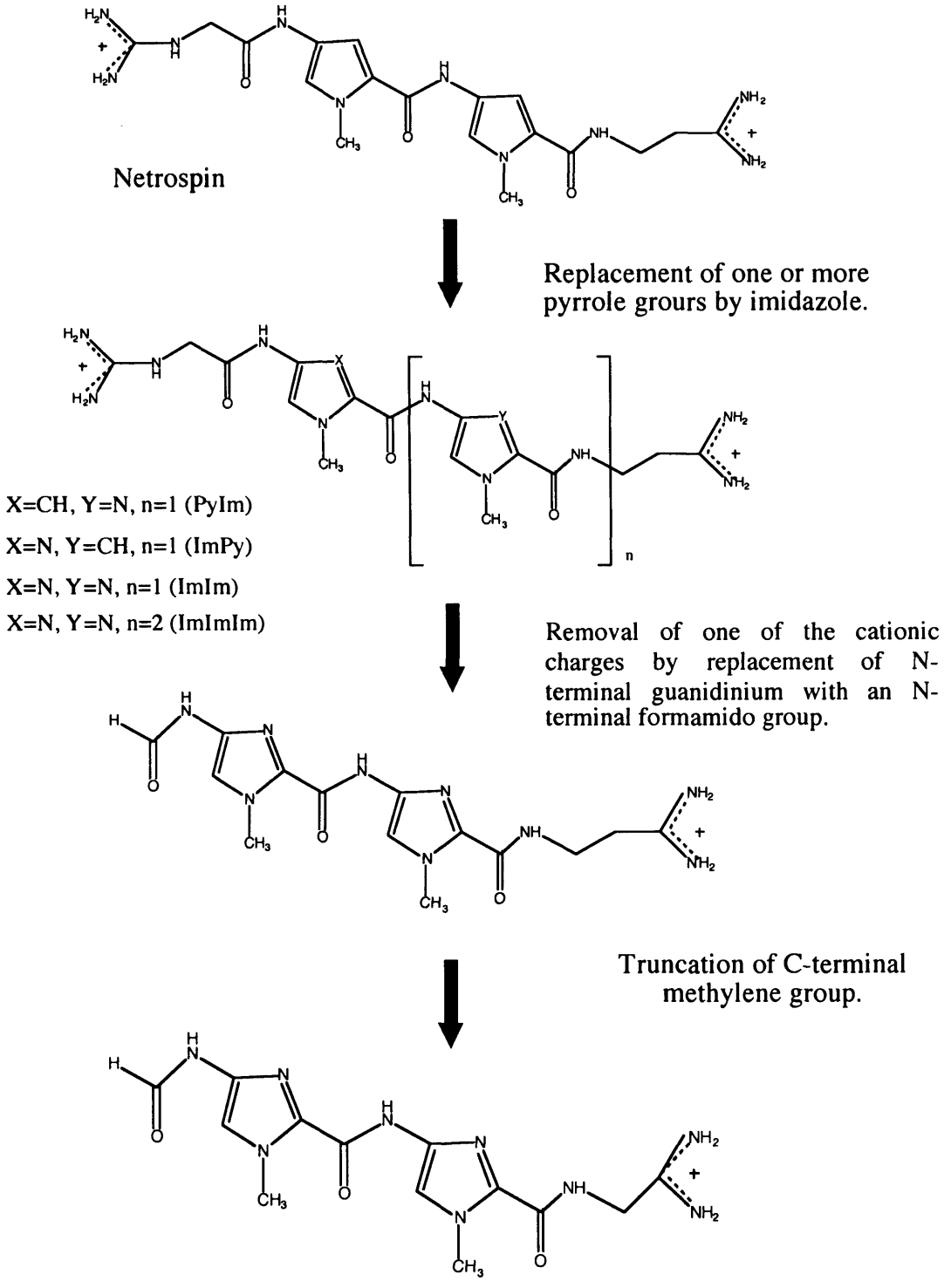

Figure 1.6 Evolution in the rational design of GC recognising polyamides.

designed to discriminate between AT and TA base pairs, thanks to specific hydrogen bonds between the 3-hydroxy and 4-carbomido groups of Hp with the O2 of T, completed the recognition code for all base pairs. The Hp/Py pair would specify TA from AT, while Py/Hp targets AT in preference to TA (White *et al.*, 1998; Kielkopf *et al.*, 2000). Table 1.1 shows the resulting recognition pairing rules and Figure 1.7 features the structures of the relevant peptide fragments.

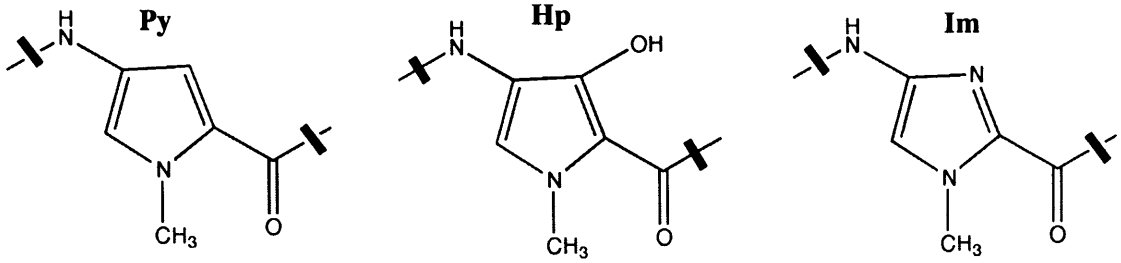

Figure 1.7 Peptide fragments referred to in the pairing rules of Table 1.1.

Pair	GC	CG	TA	AT
Im/Py	+	-	-	-
Py/Im	-	+	-	-
Hp/Py	-	-	+	-
Py/Hp	-	-	-	+

Table 1.1 Dimeric pairing rules for minor groove recognition by Py, Im and Hp. Plus and minus signs indicate favoured and disfavoured interactions, respectively.

In an attempt to further increase specificity for desired sequences, the covalent linking of the polyamide strands was considered, in order to achieve unambiguous register of the ring pairing, as opposed to homodimers, which could afford "slipped

motifs". A homodimer series of linked polyamide subunits (Mrksich & Devan, 1993b) with different length linkers and a heterodimer (Mrksich & Dervan, 1994) version were designed, both achieving enhanced sequence specific recognition of designated target sequences over the unlinked ligands. The second linking mechanism, entailing the attachment of the head of one molecule to the tail of the other with a group capable of a tight turn, fold back configuration, thus preserving the antiparallel binding, introduced the hairpin motif design strategy. Various linkers were subsequently investigated with the three carbon linker (gamma amino butaric acid – γ) providing the highest affinity (Swalley *et al.*, 1998). Different linking schemes have produced compounds ranging from polyamides of a cyclic configuration (Herman *et al.*, 1999a), to linking whole hairpin units and creating "tandem hairpin" ligands (Herman *et al.*, 1999b). Apart from the purely ring/ring paired analogues, incorporation of a flexible β-Alanine residue designed to relax the curvature of the polyamides allowed for improved selectivity and affinity of polyamides particularly towards GC base pairs with the β/Im pair being specific for CG base pairs and the β/Py and β/β pairs specific for A, T over G,C base pairs (Turner *et al.*, 1998). Other structural modifications to the classic Im/Py polyamide design include the incorporation of alternative five-membered aromatic heterocycles into DNA-binding polyamides. N-methylpyrazole (Pz) and 3-methylthiopene (Tn) retained AT selectivity when paired with Py while incorporation of 4-methylthiazole (Th), furan (Fr) or 3-hydroxythiophene (Ht) abolished binding, suggesting that there is a very narrow window of five-membered ring architectures that can be successfully accommodated in a polyamide conformation (Dervan & Edelson, 2003; References therein). While the above attempts did not yield any new specificities, the difficulty of targeting certain sequences that would evade the consensus of the pairing rules, probably due to sequence-dependent changes in the microenvironment of the DNA, maintained the interest to find novel recognition elements and new leads for sequence discrimination. The repertoire of aromatic heterocycles used for recognition was broadened with the introduction of the fused heterocycles imidazo[4,5-b]pyridine

(Ip) and hydroxybenzimidazole (Hz), paired with Py in eight-ring polyamides. It was shown that Ip/Py would mimic an Im/Py pair, exhibiting the same preference for GC, while most importantly the Hz/Py pair distinguishes a TA base pair from an AT base pair, rendering Hz a strong candidate to replace Hp which can degrade over time in the presence of acid or free radicals (Renneberg & Dervan, 2003). Pairing of Hz with benzimidazole (Bi) was also capable of discriminating TA from AT base pairs, successfully departing from the N-methylpyrrole-carboxamide framework (Marques *et al.*, 2004).

Polyamides can bind to a wide range of DNA sites and competitively displace proteins from their binding sites, as they possess comparable affinities and specificities (Trauger *et al.*, 1996, Dickinson *et al.*, 1998).

Transcription inhibition by blocking transcription factors from binding to their cognate sequences by polyamide binding has been demonstrated in various biological systems (Gottesfeld *et al.*, 1997; Dickinson *et al.*, 1998). Figure 1.8 presents various examples of DNA-binding proteins that have been inhibited by Py/Im hairpin polyamides.

Polyamides have also been used for the opposite effect of gene activation by recruiting or derepressing the transcriptional machinery. Inhibition of the binding of repressor IE86 to upregulate transcription of the human cytomegalovirus (Dickinson *et al.*, 1999) and inhibition of the binding of the human protein LSF involved in the derepression of the integrated HIV-1 long terminal repeats (LTR) (Coull *et al.*, 2002), have been reported. Additionally, polyamide-peptide conjugates can mediate transcriptional activation by functioning as artificial transcription factors (Mapp *et al.*, 2000).

Despite their documented *in vitro* biological effects, extention of these polyamide functions *in vivo* requires efficient cellular uptake and nuclear localisation. Initial studies revealed that polyamides would localise mainly in the cytoplasm with nuclear localisation observed only in CEM human cultured and human primary T-cells (Belitsky *et al.*, 2002).

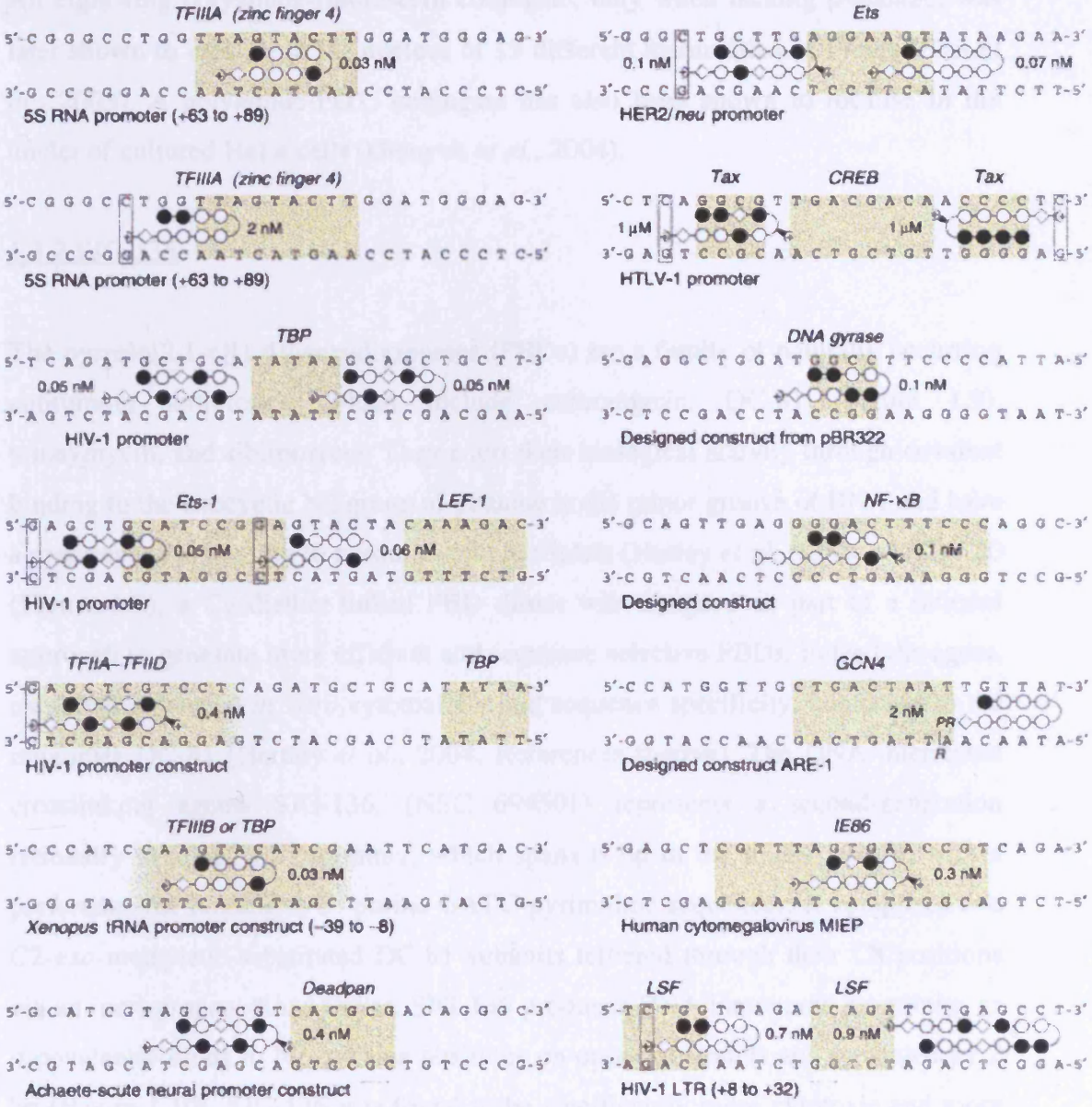

Figure 1.8 Examples of regulation of gene expression by competitive binding of Py-Im hairpin polyamides to binding sites of transcription factors. The coloured boxes indicate the binding site of the italicized protein. The promoter is identified below the DNA sequence. The black and open circles represent Im and Py rings respectively. Diamonds represent β-Ala residues. Plus signs next to diamonds represent 3-(dimethylamino)propylamine (Dp). The curved line connecting the sides of two circles represent the γ-turn. The half circle represents a propanolamine $-NH(CH_2)CH_3OH$ group. Approximate Kd values are given next to each polyamide. Open boxes indicate mismatches between the Dp tail and GC, base pairs (taken from Dervan & Edelson, 2003).

An eight-ring polyamide-fluorescein conjugate, only when lacking β-alanine, was later shown to localise in the nucleus of 13 different mammalian cell lines (Best *et al.*, 2003). A polyamide-FITC conjugate has also been shown to localise in the nuclei of cultured HeLa cells (Olenyuk *et al.*, 2004).

1.3.2 SJG-136

The pyrrolo[2,1-c][1,4]benzodiazepines (PBDs) are a family of naturally occurring antitumour antibiotics, which include anthramycin, DC-81 (Figure 1.9), tomaymycin, and sibiromycin. They exert their biological activity through covalent binding to the exocyclic N2 group of guanine in the minor groove of DNA and have a preference for binding to purine-G-purine triplets (Hurley *et al.*, 1988a). DSB-120 (Figure 1.9), a C8-diether-linked PBD dimer was designed as part of a rational approach to generate more efficient and sequence selective PBDs. Indeed the agent, exhibited enhanced *in vitro* cytotoxicity and sequence specificity, compared to the monomer DC-81 (Hartley *et al.*, 2004; References therein). The DNA interstrand crosslinking agents SJG-136, (NSC 694501) represents a second-generation rationally designed PBD dimmer, which spans 6 bp in the minor groove, with a preference for binding to 5'-purine-GATC-pyrimidine sequences. It comprises two C2-*exo*-methylene-substituted DC-81 subunits tethered through their C8 positions via an inert propanedioxy linker. SJG-136 produces DNA interstrand crosslinks, as it covalently binds to N2-guanine positions on opposite strands and separated by 2 bp (Figure 1.10). SJG-136 was found to be significantly more cytotoxic and more efficient DNA crosslinker than DSB-120 (Gregson *et al.*, 2001). More specifically, its high affinity for DNA and its ability to stabilise the helix is reflected in the increase in calf thymus, (CT) DNA melting temperature (ΔTm) of 33.6°C. Molecular modelling studies of an SJG-136 cross-link show a snug fit of the agent in the minor groove and very little helical distortion (Gregson *et al.*, 2001).

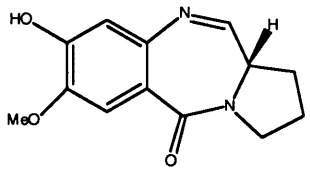

DC-81

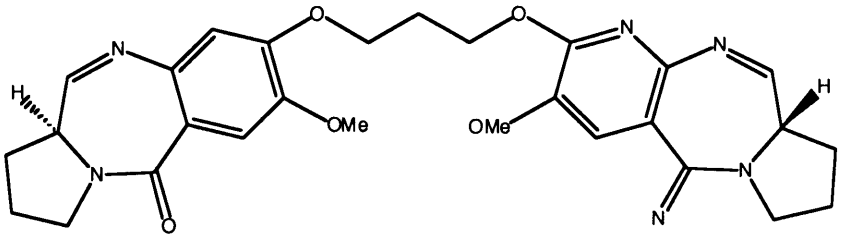

DSB-120

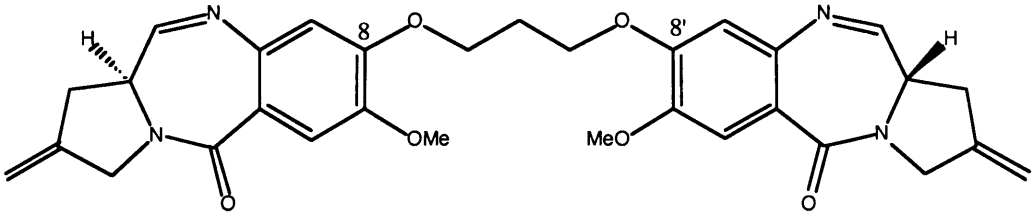

SJG-136

Figure 1.9 Structures of DC-81, DSB-120 and SJG-136.

SJG-136 is a highly efficient DNA interstrand crosslinking agent in naked DNA (XL_{50}=0.045 μM, 440-fold more potent than clinically used melphalan), as shown in a plasmid-based gel electrophoresis assay (Gregson *et al.*, 2001) and also in cultured cells and in human tumour xenografts, at a therapeutical relevant dose, as determined by the single cell gel electrophoresis (comet) assay (Hartley *et al.*, 2004). The agent's sequence selective crosslinking has beeen confirmed in footprinting studies, while single-strand ligation PCR (sslig-PCR) studies showed that the agent reaches the cellular genome and binds to DNA in a sequence selective manner (Martin *et al.*, 2005).

SJG-136 is also highly cytotoxic *in vitro*, exhibiting an IC_{50} value of 0.0425 μM in K562 cells following a 1 hour exposure and showing potent activity at the National cancer institute (NCI) 60 cell line anticancer drug screen with 50% net growth inhibition conferred within a range of 0.14 to 320 nmol/L (the mean concentration was 7.4 nmol/L). Sensitive cell lines exhibit total growth inhibition (TGI) and 50% lethality (LC_{50}) after treatment with as little as 0.83 and 7.1 nmol/L respectively. The mean-graph pattern of cell line sensitivity suggests that SJG-136 exerts a multilog, differential cytotoxicity. COMPARE analysis of the SJG-136 shows that the agent does not fit within clusters of other known agents, therefore might possess a distinct mechanism of action (Hartley *et al.*, 2004).

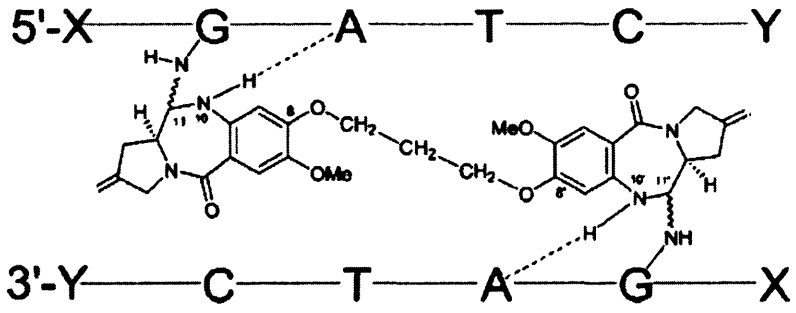

Figure 1.10 Schematic representation of the proposed mechanism for the interstrand crosslinking of DNA by SJG-136 (X=purine and Y=pyrimidine).

Because of its potent *in vitro* antitumour activity, the agent progressed in the standard NCI hollow fibre assay. Prominent *in vivo* antitumour activity was confirmed, with growth inhibition exhibited in 20 of 24 IP and 7 of 24 SC (total score of 54) and cell kill observed in 5 of the 12 cell lines tested, rendering this compound one of the most active compounds tested in this assay to date (top 5%). The agent proved highly efficacious and well tolerated in subsequent studies of ten human xenograft models including melanomas, ovarian, breast, colon, and lung carcinomas, gliomas and promyelotic leukemia. Significant growth delays occurred in nine models, cell kill in six models and there were 1 to 4/6 tumour-free responses

in six models (Alley *et al.*, 2004). This agent also appears to confer a preferential cytostatic and/or cytosidal effect *in vitro* upon leukemia cells *versus* normal bone marrow cells, as derived from a colony formation assay (Hartley *et al.*, 2004).
The SJG-136 induced crosslinks were shown to be more difficult to repair in human tumour cells (K562) than those formed by the clinically used agent melphalan. At a dose of 0.45 mg/kg of SJG-136, crosslinks formed rapidly and were also detected in tumour cells of mice bearing the LS174T human colon cancer xenograft, within 1 hour after administration. The level of this *in vivo* crosslinking persisted over 24 hours in this tumour, in contrast to crosslinks produced by conventional crosslinking agents over the same period. These observations suggest that the difficulty of the SJG-136 crosslinks to be repaired, possibly because of their poor recognition, must be an important determinant of sensitivity to the agent (Hartley *et al.*, 2004). The desirable pharmacological properties of SJG-136 derived from efficacy studies and its effective antitumour activity both *in vitro* and *in vivo*, render this agent the lead clinical candidate of the pyrrolobenzodiazepine class of compounds and is currently undergoing phase I clinical evaluation in the United Kingdom (through Cancer Research UK) and the United States (through the NCI).

1.3.3. Ecteinascidin-743

Ecteinascidin 743 (ET-743, NSC648766, Yondelis™, trabectedin) is a carbinolamine-containing antitumour antibiotic, composed of three fused tetrahydroisoquinolone subunits (designated A, B and C) forming a wedge-shaped molecule (Figure 1.11). It is a natural product isolated from the marine tunicate *Ecteinascidia turbinate* that grows preferentially on mangrove roots in the Caribbean sea. ET-743 binds in the minor groove of DNA and selectively alkylates the N2-position of a central guanine within sets of three consequtive nucleotides. The preferred sequences were determined to be 5'-PuGC-3' and 5'-PyGG-3' while the least favoured ones were 5'-NG(A/T)-3' (Pommier *et al.*, 1996; Seaman & Hurley, 1998). DNA covalent adduct formation is believed to be mediated through

an intramolecular acid-catalysed dehydration of the carbinolamine moiety (at the N-2 position), resulting in the formation of a cyclic electrophilic iminium, which is the DNA-reactive intermediate, as shown in Figure 1.11 (Pommier *et al.*, 1996).

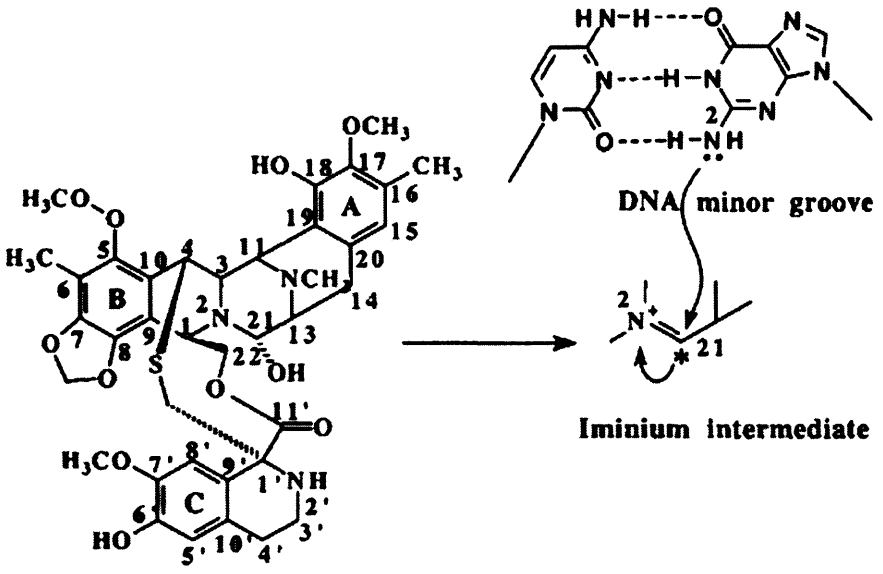

Figure 1.11 Chemical structure of ET-743 and proposed reaction of its reactive iminium intermediate with the guanine 2-amino group (Taken from Takebayashi *et al.*, 1999).

While the A- and B- subunits provide the scaffold for DNA recognition and bonding, based on the formation of a network of hydrogen bonds with the three base pairs of the binding site, the C-subunit protrudes out of the minor groove making limited contacts with DNA (Moore *et al.*, 1997). An important characteristic of this agent's interaction with DNA is the differential reversibility of its adducts, governed by the different patterns of hydrogen-bonding to DNA. It has been suggested that it is the differences in the rate of this reverse reaction at the non-preferred, 5'-NG(A/T) sequences that dictates the sequence selectivity of ET-743. The agent can migrate along DNA from its less favoured sequences and

eventually forms stable, irreversible covalent adducts at the preferred, target sequences (Zewail-Foote & Hurley, 2001). A unique feature of ET-743, among the DNA-interactive agents that occupy the minor groove, is that it bends DNA towards the major groove (Zewail-Foote & Hurley, 1999).

ET-743 targets DNA *topoisomerase I in vivo* but only at high concentrations while *topoisomerase-I* deficient cells showed no difference to sensitivity compared to normal cells indicating that the enzyme is not the primary target for the cytotoxic activity of the agent (Takebayashi *et al.*, 1999; 2001a). Nucleotide Excision Repair (NER)-defective mammalian cell lines were found to be more resistant rather than more sensitive to ET-743, compared to their isogenic parent cell lines (Takebayashi *et al.*, 2001b; Damia *et al.*, 1999). This NER-mediated cytotoxicity of ET-743, distinctly different from the other DNA-interactive agents investigated to date, was proposed by the Pommier group to be specifically dependent on the transcription-coupled (TC) pathway of NER. According to this model, ET-743 kills cells by inducing TC-NER-mediated, single strand breaks (SSBs) in transcribed genes. The TC-NER complex is stalled after DNA cleavage and produces irreversible SSBs, which become lethal to cells (Takebayashi *et al.*, 2001b). Based on this proposed mechanism, ET-743 was expected to be active against, for example, cisplatin-resistant cells, which have an enhanced NER system. Adducts at preferred binding sites were shown to be repaired less efficiently by the bacterial multisubunit nuclease system (UvrABC) than the non-preferred, less stable adducts. This differential incision efficiencies and the inefficient repair of the stable adducts which in the presence of intact NER become toxic lesions, were used to rationalise the repair-dependent toxicity of ET-743 (Zewail-Foote *et al.*, 2001).

Another characteristic of the mechanism of action of ET-743 is its ability to block transcription. Studies on the HSP70 promoter showed that the agent could rapidly block transcription at pharmacological concentrations (Minuzzo *et al.*, 2000). Transcriptional inhibition was also reported for several other promoters like the MDR1 promoter (Jin *et al.*, 2000) and p21 (Friedman *et al.*, 2002). Initially ET-743 was thought to target a single transcription factor (NF-Y) but it was later suggested

that it is a more general inhibitor of activated transcription by multiple stress inducers, with minimal effect on uninduced transcription (Friedman *et al.*, 2002).

ET-743 was shown to cause perturbation of the cell cycle, with a delay of cells progressing from the G_1 to the G_2 phase, an inhibition of DNA synthesis and causing an accumulation in the G_2/M phase. Cells in G_1 were the most sensitive to the agent (Erba *et al.*, 2001). At pharmacologically relevant concentrations (nM), the agent induces a potent apoptotic response, which can account for its cytotoxic activity, while at very low concentrations it produces transcription-dependent growth arrest (Gajate *et al.*, 2002).

ET-743 is active *in vitro* against a broad class of solid tumour cell lines in the nanomolar to subnanomolar range (Rinehart *et al.*, 1995). In phase I and II clinical trials in Europe and the USA, the agent has shown significant antitumour activity against several human malignancies, including soft-tissue sarcomas and ovarian carcinomas (Van Kesteren *et al.*, 2003). Combination with cisplatin was found to be synergistic against human tumour xenografts (D'Incalci *et al.*, 2003).

Sarcomas of soft tissue represent a heterogenous family of malignancies of mesenchymal origin that account for approximately 1% of adult neoplastic diseases diagnosed annually in the US. The median survival of patients with unresectable STSs is approximately 1 year. Therapy with conventional agents such as doxorubicin and ifosfamide demonstrated response rates ranging from 11% to 30%. However, after failure of first line therapy, there are no therapeutic options of proven benefit. Therefore effective new therapies are desperately needed. In phase II studies of patients with advanced pretreated STSs, ET-743 was able to induce long-lasting objective remissions and tumour control in a subset of patients (Van Glabbeke *et al.*, 2002; Garcia-Carbonero *et al.*, 2004). Therefore ET-743 represents the first active agent for this type of tumour in the last 25 years.

In October 2004, ET-743 was granted orphan drug status by the U.S. Food and Drug Administration (FDA) for the treatment of STSs and in April 2005, for the treatment of ovarian cancer. The European Comission had already granted orphan drug designation for the above mentioned cancer types, in 2001 and 2003

respectively. ET-743 is currently under study in a phase III pivotal trial in ovarian cancer, and is also being evaluated in phase II for prostate cancer. The agent is also being studied in phase I trials to evaluate its potential for use in combination with standard chemotherapies. It is being co-developed by PharmaMar (Madrid, Spain) and Johnson & Johnson Pharmaceutical Research & Development (www.pharmamar.com)

1.3.4 CC-1065 and the duocarmycins

(+)-CC-1065 (NSC-298223), the fermentation product of *Streptomyces Zelensis* is a naturally occurring cytotoxic antibiotic discovered by scientists at the Upjohn company in 1978 (Hanka *et al.*, 1978). Improved isolation and characterisation of this agent were reported by Martin, *et al.*, in 1981. Elucidation of the molecular and crystal structure of (+)-CC-1065 followed, along with initial circular dichroism (CD) studies, suggesting the compound's interaction with the minor groove of DNA (Chidester *et al.*, 1981). Structurally, the (+)-CC-1065 molecule consists of three repeating pyrroloindole subunits (subunits A, B, and C) linked by amide bonds. The A unit, which is the cyclopropane[c]pyrrolo[3,2-*e*]indole-4(5H)-one system, also referred to as CPI, constitutes the agent's pharmacophore containing the DNA reactive cyclopropyl ring (Figure 1.12). The B and C units, together comprising the PDE-I_2 dimer, are identical and display a strong influence on the binding and biological potency of the agent (Hurley *et al.*, 1988b; Boger *et al.*, 1990a).

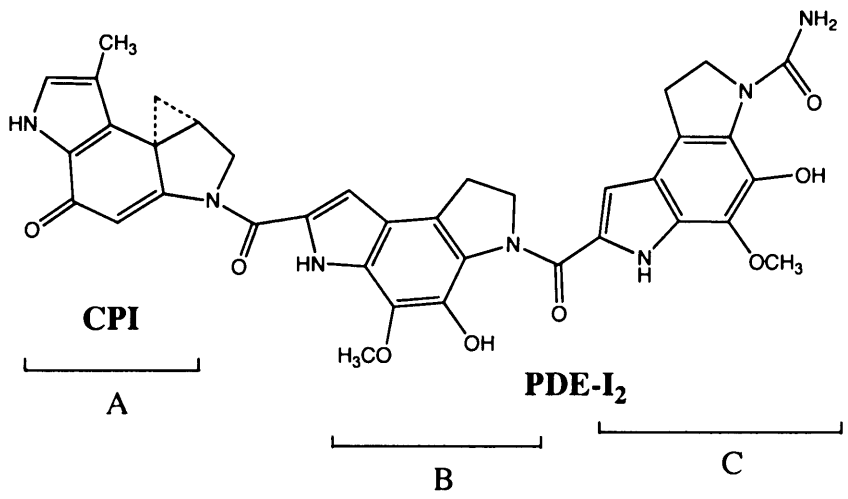

Figure 1.12 Chemical structure of the natural enantiomer of (+)-CC-1065. The component subunits are denoted as A, B and C.

(+)-CC-1065 has an overall curved shape with a lipophilic inner surface while the hydrogen-bond donors and acceptors are positioned on the molecule's outer periphery (Chidester *et al.*, 1981). It exhibits a right-handed twist that mimics the pitch of B-form DNA. The absolute configuration of the natural product was determined by X-ray crystallography to be that of Figure 1.12 (Martin *et al.*, 1988).
At the time of its identification, (+)-CC-1065 was the most potent, small molecular weight compound investigated, possessing exceptionally potent *in vitro* cytotoxic activity against a wide variety of human tumours (Bhuyan *et al.*, 1982). It was also found to be very active *in vivo* against a panel of experimental murine tumours (Neil *et al.*, 1981). Despite its high potency and broad spectrum of antitumour activity, CC-1065's further development into a clinical agent was precluded due to an irreversible, delayed hepatotoxicity in mice at subtherapeuric doses (McGovern *et al.*, 1984).

Later efforts disclosed another class of structurally related antitumour antibiotics, the duocarmycins (DUMs). The first of these agents, is (+)-duocarmycin A (DUMA), isolated from *Streptomyces* DO-88 and disclosed in 1988, concurrent with a series of related agents isolated from *Streptomyces* DO-89: duocarmycins B_1 and B_2, C_1 (pyrindamycin B) and C_2 (pyrindamycin A). The last addition to this family of natural products was (+)-duocarmycin SA (DUMSA), isolated from *Streptomyces* DO-113 and disclosed in 1990 (Figure 1.13) (Boger *et al.*, 1997b; References therein). Like (+)-CC-1065, the duocarmycins were also found to bind to the minor groove of DNA (Boger *et al.*, 1990b).
The duocarmycins A and SA are structurally different from (+)-CC-1065 in that they contain a unique left-hand alkylation subunit; a functionalised spirocyclopropylhexadione moiety. All of the duocarmycins incorporate the trimethoxyindole (TMI) group as their right hand, DNA binding subunit.
In a comparative evaluation, (+)-DUMA displayed the exceptionally potent *in vitro* activity characteristic of (+)-CC-1065 (Boger *et al.*, 1990b) and was the most potent agent among the duocarmycins. The enhanced potency of (+)-DUMSA was

attributed to its enhanced solvolytic stability relative to its predecessors, hence its name, DUMSA (SA stands for Stable A).

Like (+)-DUMA, (+)-DUMSA does not exhibit the delayed fatal hepatotoxicity characteristic of (+)-CC-1065 (Boger & Johnson 1996).

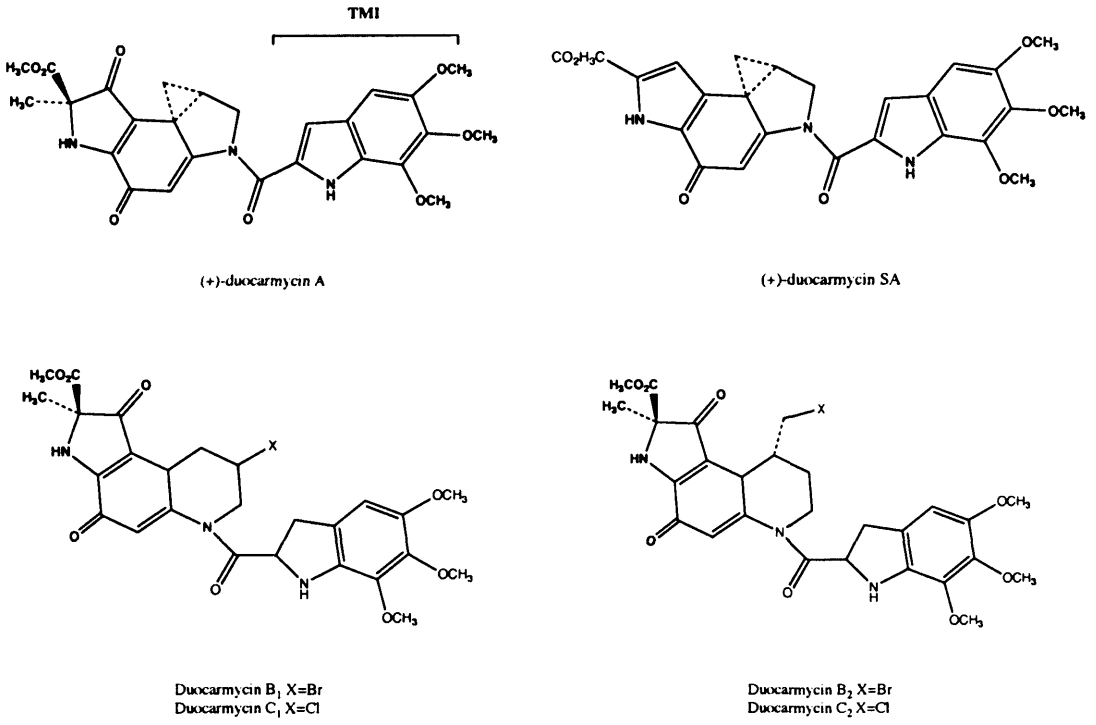

Figure 1.13 Structures of the main members of the duocarmycins.

Both classes of agents have been shown to exert their biological activity through a highly sequence selective alkylation of the minor groove of duplex DNA, at sequences rich in adenine-thymine (AT) base pairs.

1.3.4.1 Interaction with DNA

(+)-CC-1065 was shown to interact strongly with double stranded DNA by preferential interaction at AT-rich sites in a non-intercalative mode (Chiderster *et*

al., 1981; Li *et al.*, 1982) while showing weak and reversible or no interaction with other macromolecular targets (RNA, mouse chromatin, proteins like histones, human serum albumin (Moy *et al.*, 1989). The mechanism through which it exerts its cytotoxic activity was therefore suggested to be, at least partly, the preferential inhibition of DNA synthesis. Subsequent studies concentrated on determining the (+)-CC-1065's sites of covalent interaction with DNA. The evidence that (+)-CC-1065 binds primarily in the minor groove of DNA was provided by a series of observations. Firstly, (+)-CC-1065 was able to react with T4 DNA, which has a relatively inaccessible major groove due to glycosylation, at approximately the same extent as with calf thymus DNA, which contains no major groove modifications, suggesting that major groove binding is not involved (Swenson *et al.*, 1982). In competitive binding studies, the AT selective, minor groove agent netropsin, inhibited the binding of (+)-CC-1065. However (+)-CC-1065 could slowly displace netropsin from DNA. Netropsin on the other hand was unable to replace the bound (+)-CC-1065. Anthramycin, another reagent, that preferentially binds GC-rich sites and covalently reacts with the N2-guanine in the minor groove, could only partially block the binding of (+)-CC-1065, its inability of complete inhibition of binding reflecting the different base specificity of the two agents (Swenson *et al.*, 1982). Finally, preferential suppression of alkylation by methylnitrosourea and ethylnitrosourea of bases in the minor groove (and the N3 group of adenine in particular), when DNA was pretreated with (+)-CC-1065, pointed to this minor groove group as the major potential target of the drug (Swenson *et al.*, 1982).

The (+)-CC-1065 adduct was later obtained by thermal depurination of a defined oligonucleotide duplex (Needham-Van Devanter *et al.*, 1984), isolated, and NMR characterised (Hurley *et al.*, 1984), confirming the molecule's base (adenine) and heteroatom (N3) specificity. Other NMR studies of thermally released adenine adducts, derived by a 12bp, (+)-CC-1065-interacted oligonucleotide, determined the covalently modified adenine to be in the N6 doubly protonated (amino) form (Lin & Hurley, 1990), with the positive charge delocalised over the entire adenine molecule

and alkylation to be occurring between the extracyclic carbon of the cyclopropyl ring (C4) and the N3-adenine, with opening of the cyclopropyl ring system (Figure 1.14). This near exclusive alkylation event accounts for 80%-90% consumption of the agent in the presence of duplex DNA (Reynolds *et al.*, 1985).

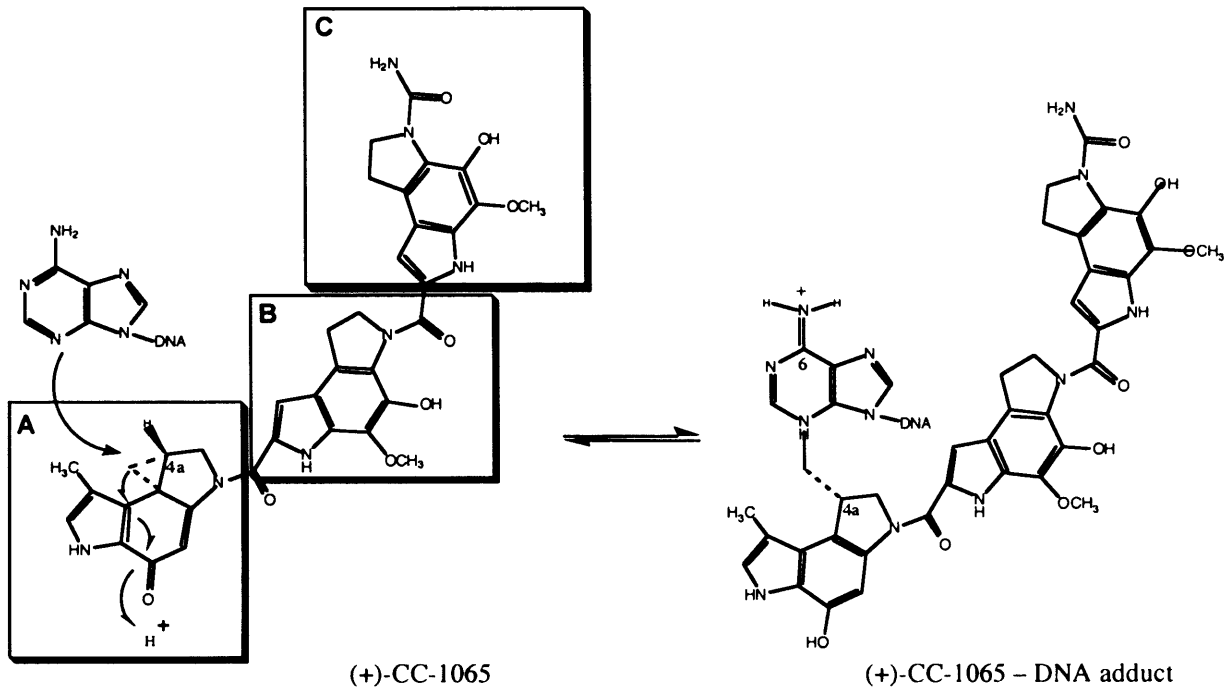

Figure 1.14 Reaction of (+)-CC-1065 with double stranded DNA at N3 of adenine to form the (+)-CC-1065-DNA adduct. The covalently modified adenine is in the doubly protonated 6-amino form.

(+)-CC-1065 binds covalently to N3 of adenine and lies within the minor groove, extending over a 5 bp AT-rich region for which sequence specificity exists. Each site of (+)-CC-1065 alkylation proved to be an adenine residue flanked by two 5'-A or 5'-T residues. The sequence preference for the three base AT-rich alkylation site follows the order: 5'-AA<u>A</u>-3' = 5'TT<u>A</u>-3' > 5'TA<u>A</u>-3' > 5'-AT<u>A</u>-3' (<u>A</u>; alkylated adenine). In addition, the agent exhibited a strong preference for the fourth 5' base to be A or T, and an extended, weaker preference for the fifth 5' base to be A or T and the same weak preference for the 3' base preceding the alkylation site to be a

purine base. This selectivity for AT-rich sites corresponds to the length of the agent and the size of the binding site required to accommodate it. The consensus sequences that (+)-CC-1065 is highly reactive with were therefore suggested to be: 5'-PuNTTA-3' and 5'-AAAAA-3' (Pu; purine, N; any nucleotide base, A; alkylated adenine) (Hurley *et al.*, 1984; Reynolds *et al.*, 1985). Another analysis, under different experimental conditions from the above mentioned (24h incubation at 4°C rather than 2h at 37°C), supported a consensus sequence of 5'-(A/T)(A/T)A-3' (Hurley *et al.*, 1990).

The orientation of the sequence specificity of (+)-CC-1065, in relation to the adducted adenine site, as established by the thermally induced cleavage assay, suggested the polarity of the molecule in the minor groove of DNA (Hurley *et al.* 1984) and was later confirmed by employing the footprinting assay (Needham-VanDevanter & Hurley 1986) and NMR (Scahill *et al.*, 1990). (+)-CC-1065 lies in the minor groove with a covalent bond between the opened cyclopropyl group and N3 of adenine and extends in the 3' -> 5' direction.

Oligonucleotide CD studies also revealed sequences that go through a transient phase of reversibly bound (+)-CC-1065 before converting to a covalent adduct, and others that create reversible only binding sites (e.g. 5'-GAATT-3'). Such reversibly bound species were found to compete with covalent adduct formation and inhibited the rates of DNA alkylation (Krueger *et al.*, 1991). The (+)-CC-1065 interactions with calf thymus DNA, however, unlike those of simpler analogues, could not be reversed by a variety of experimental manipulations. Additionally, the lack of observable cytotoxicity of the formed DNA-CC-1065 covalent adducts, indicates that (+)-CC-1065 interaction with DNA is effectively "irreversible" (Warpehoski *et al.*, 1992).

The structural similarities between the duocarmycins and (+)-CC-1065 suggest that these agents may be acting by a common mechanism derived from the reversible, stereoelectronically controlled adenine-N3 addition to the least substituted carbon of the activated cyclopropane within selected AT-rich minor groove regions of duplex DNA. Studies of the alkylation properties of (+)-DUMA and (+)-DUMSA

revealed that they participate in the characteristic DNA minor groove adenine-N3 alkylation, in a fashion and at concentrations similar to those of (+)-CC-1065. The adenine ring becomes protonated upon duocarmycin adduct formation, resulting in charge delocalisation over the purine ring system (Figure 1.15) (Boger *et al.*, 1990b).

Both (+)-DUMA and (+)-DUMSA exhibit strikingly similar DNA sequence selectivity to (+)-CC-1065. The site of the detected alkylations proved to be an adenine flanked by two 5'-A or T bases and the preference for the sequence of the three base pairs binding site, follows the order of 5'-AAA-3' > 5'-TTA-3' > 5'-TAA-3' > 5'-ATA-3'. There also proved to be a preference, though not absolute requirement, for the fourth 5' base to be A or T and a weak preference for the 3' base preceding the alkylation site to be a purine base. The high affinity consensus sequences for (+)-DUMA-DNA alkylation have therefore been suggested to be: 5'-(A/TAAA)-3' and 5'-(A/TTTAPu)-3'. Although each agent alkylates the same sites in DNA, two important distinctions lie in that the less reactive but more stable agent (+)-DUMSA is approximately 10-fold more efficient in alkylating duplex DNA compared to (+)-DUMA, and does so with a greater relative selectivity among the available alkylation sites (Boger *et al.*, 1994b). This selectivity extends in the 3' -> 5' binding directionality from the alkylation site, with the hydrophobic concave face of the duocarmycins deeply imbedded in the minor groove, the polar functionality lying on the outer face of the complex and the bound agent spanning 3.5 base pairs, complementing the topological curvature of the minor groove. Duocarmycins C_1 and C_2 also exhibited identical alkylation selectivity to (+)-DUMA (Boger *et al.*, 1990b).

The duocarmycin-adenine covalent adduct was isolated, characterised and quantified, establishing the N3-adenine alkylation as the near exclusive DNA alkylation event (accounting for 86%-92% consumption of (+)-DUMA and >92% of (+)-DUMSA, in the presence of duplex DNA (Figure 1.15) (Boger & Johnson, 1996; References therein). However, in conditions of DNA treatment with excess agent, and in the absence of high affinity adenine-N3 alkylation sites (Sugiyama *et*

al., 1993), or if such sites are protected from alkylation by pretreatment with another minor groove binding agent (e.g. distamycin A) (Yamamoto *et al.*, 1993), a minor guanine-N3 alkylation was detected, but only in the case of (+)-DUMA.

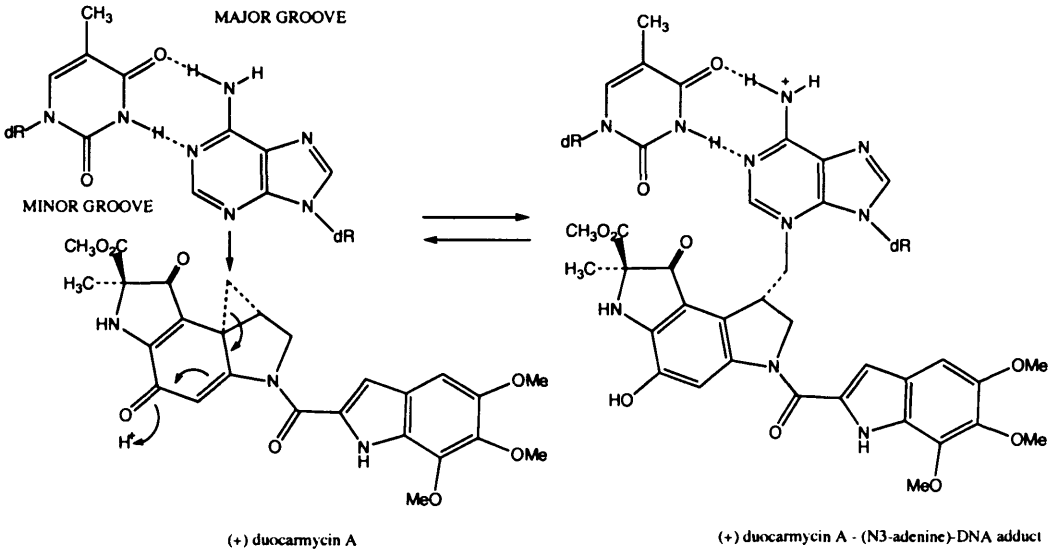

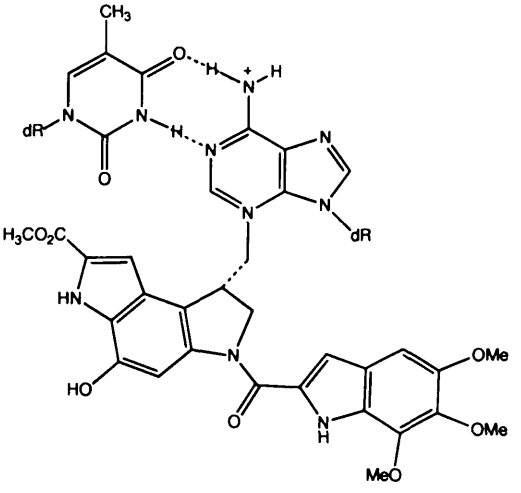

Figure 1.15 Schematic diagram of the alkylation of the N3 group of an adenine residue by (+)-duocarmycin A. The resulting adduct structure is also shown for (+)-DUMSA (bottom right).

Despite the similar nature of DNA alkylation by the two classes of agent, subtle differences in the alkylation profiles do occur, notably the lack of alkylation at 5'-

CAAAG-3' by (+)-CC-1065, attributed to its extended AT-rich binding site size (Boger *et al.*, 1994b). Another important distinction between those two classes of agents is the reversibility of the covalent reaction. Unlike (+)-CC-106, which essentially irreversibly alkylates double stranded DNA under the conditions of the relevant studies, (+)-DUMA and (+)-DUMSA have been shown to do so reversibly. The rate or ease of reversibility proved dependent upon the relative reactivity of the agent and the expected stability of adducts as well as the extent of the noncovalent interactions. Consistent with this interpretation, the (+)-DUMA retroalkylation reaction is much slower that that of (+)-DUMSA, as (+)-DUMA is more reactive. The reversibility of the DNA alkylation reaction was sensitive to the reaction conditions and parameters such as pH, temperature, time, and to a lesser extent salt concentration (Boger & Yun 1993).

1.3.4.2 Modification of the pharmacophore

As stated earlier, the duocarmycins and (+)-CC-1065 are not only structurally related but also share similarities in their properties of the DNA alkylation event. Between the two classes of agents a common pharmacophore has been identified. Synthesis of simplified functional analogues of (+)-CC-1065, incorporating the exceptionally reactive, parent left hand, (1,2,7,7a-tetrahydrocycloprop[1,2-c]indol-4-one) (CI) alkylation subunit, exhibit marked similarities in their DNA alkylation profiles with the authentic CPI bearing corresponding agents, hence CI constitutes the minimum potent pharmacophore of the agent (Figure 1.16) (Boger & Wysocki 1989). The CI subunit derives by the removal of the pyrrole segments from the CPI and the (+)-DUMA alkylation subunit (DA). The subsequent synthesis and comparative evaluation (*in vitro* cytotoxic activity, DNA alkylation properties) of the analogue CI-TMI, illustrated that this agent bears the minimum potent pharmacophore of the duocarmycin alkylation subunit and also the common pharmacophore of the duocarmycins / (+)-CC-1065 alkylation subunits (Boger *et al.*, 1990b; Boger *et al.*, 1990c) (Figure 1.16).

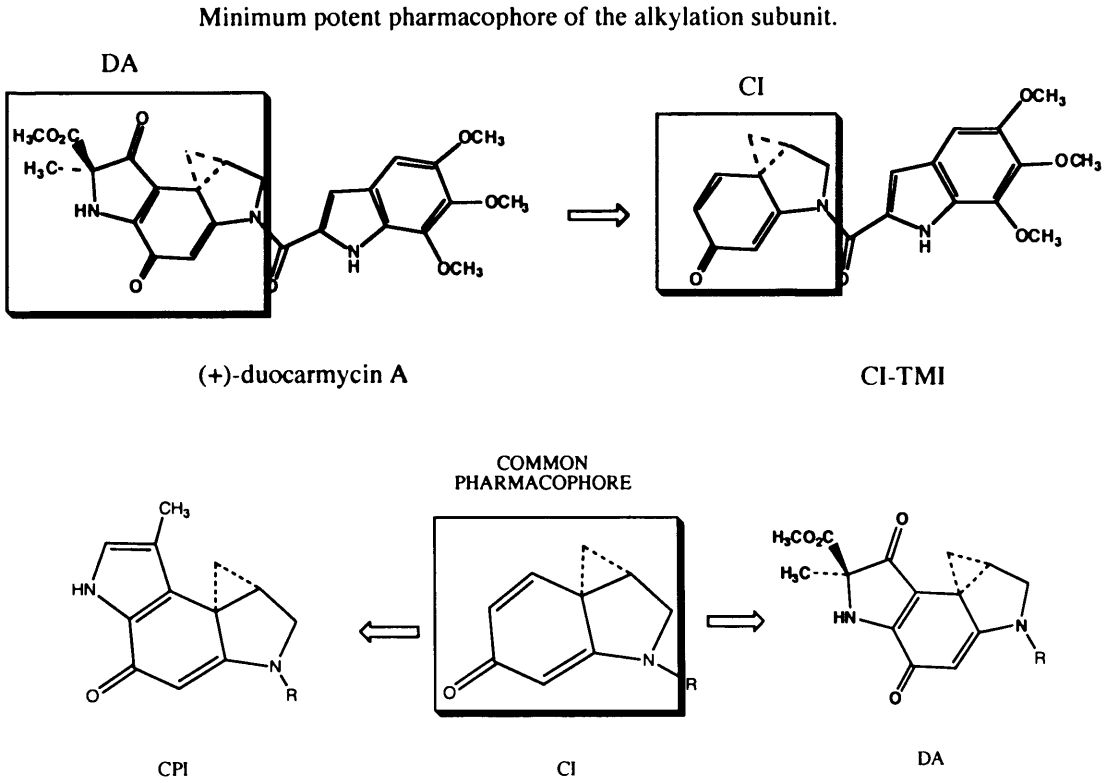

Figure 1.16 The minimum potent and common pharmacophore (CI), of the CPI and DA alkylation subunits.

However, CI alkylates DNA in a less efficient manner, resulting in decreased cytotoxic potency of its analogues, highlighting the need to further improve on the subunit's alkylation efficiency (Boger & Wysocki, 1989).

Replacement of the fused pyrrole ring with a fused benzene ring, results in the 1,2,9,9a-tetrahydrocycloporpa[c]benz[e]indol-4-one (CBI) subunit. Even though CBI is chemically less reactive, it was found that the more synthetically accessible CBI analogues were four times more stable and four times more potent than the corresponding CPI ones (Boger *et al.*, 1995a). CBI agents were found to alkylate DNA with an unaltered sequence selectivity, with greater intensity and at a faster relative rate than their CPI counterparts, resulting in enhanced cytotoxic potency, and indicating that the simplified CBI subunit possesses distinct advantages over

the authentic CPI pharmacophore (Boger *et al.*, 1989; Boger & Munk, 1992). These improved properties of the CBI analogues validate therefore the approach of introducing deep-seated modifications in the (+)-CC-1065 and duocarmycin alkylation subunits. Additionally such modifications seem to be well tolerated and can lead to potent cytotoxic agents that exhibit improved *in vivo* efficacy, as reported for the (+)-CBI-indole$_2$ agent, which also lacks the delayed hepatotoxicity of (+)-CC-1065. Extension of these studies includes the preparation of other CBI derivatives like MCBI (Boger *et al.*, 1996a), CCBI (Boger *et al.*, 1996b), C5-CO_2Me-CBI (Boger *et al.*, 2001), in an attempt to determine the substituent electonic effects on functional reactivity. The study of the CBI analogues also suggested that the CPI 7 centre (CH_3), may hinder the accessibility to the adenine-N3 alkylation site, decelerating the rate of the alkylation reaction and accounting for the lower efficiency of the CPI analogues. In addition, a direct relationship between stability and biological potency was confirmed by the observed trend of the solvolytically more stable derivatives to be the most potent (Boger *et al.*, 1995b).

An example of a substitution of the reactive centre of the natural products is the 9,9-difluoro-1,2,9,9a-tetrahydrocyclopropa[c]benz[e]indol-4-one (F_2CBI), a difluorocyclopropane analog of the (+)-CC-1065 and the duocarmycin alkylation subunits. The reactivity of the agents bearing this modified subunit was increased by 500-fold, and they were found to be (500-1000)-fold less cytotoxic than the corresponding unmodified CBI derivatives (Boger & Jenkins 1996). Fluorine substitution has played a key role in drug development with a number of fluorinated compounds and analogues currently investigated, among others, SJG-136 (Kamal *et al.*, 2004).

A ring expansion of the five-membered ring of the CBI to a fused six-membered ring, results in the formation of the 2,3,10,10a-tetrahydrocyclopopa[d]-benzo[f]quinol-5-one, (CBQ) subunit. CBQ agents were found to alkylate the same sites as their corresponding agents containing the DSA, CPI, CBI, or CI alkylation subunits. In agreement with their relative reactivity, they exhibited less selectivity

among the available alkylation sites, alkylating DNA with a lower efficiency (100- to 1000)-fold, while being equally less potent in cytotoxicity (Boger & Mesini 1995).

A seven-membered C-ring of the alkylation subunits of (+)-CC-1065 and the duocarmycins constitutes the 1,2,3,4,11,11a-Hexahydrocycloprop[c]naptho[2,1-b]azepin-6-one (CNA) pharmacophore. Incorproration of this seven-membered C-ring system to functionalised agents increased their reactivity by 4750-fold compared to the five-membered ring (CBI) bearing counterparts. The CNA based agents exhibited cytotoxic activity that was less potent than the corresponding duocarmycin based agents but more potent than the CI bearing ones (Boger & Turnbull, 1997).

Another reported variation is the 1,2,9,9a-tetrahydrocyclopropa[*c*]benz[*e*]-3-azaindol-4-one (CBA) alkylation subunit. CBA contains an aza variant of the natural products' subunit and proved structurally identical to its carbon analogue, CBI. However CBA-bearing derivatives were much less effective in DNA alkylation (1000-fold) and biologically much less potent (100- to 1000)-fold than the corresponding CBI analogues (Parrish *et al.*, 2003a).

A number of modified heteroaromatic core structures of the CC-1065 or duocarmycin alkylation subunits have also been reported, where the fused pyrrole is replaced with a different heterocycle.
Incorporation of the 1,2-dihydro-1-(chloromethyl)-5-hydroxy-8-methyl-3H-furano[3,2-*e*]indole (CFI) generated an agent which exhibited an identical alkylation profile with (+)-CC-1065 at the major site of alkylation, and was only subtly distinguishable, at the low-affinity sites. It was comparable or slightly less effective at alkylating DNA than (+)-CC-1065 (1-5 times), which was consistent with the relative *in vitro* cytotoxic potency (Mohamadi *et al.*, 1994).

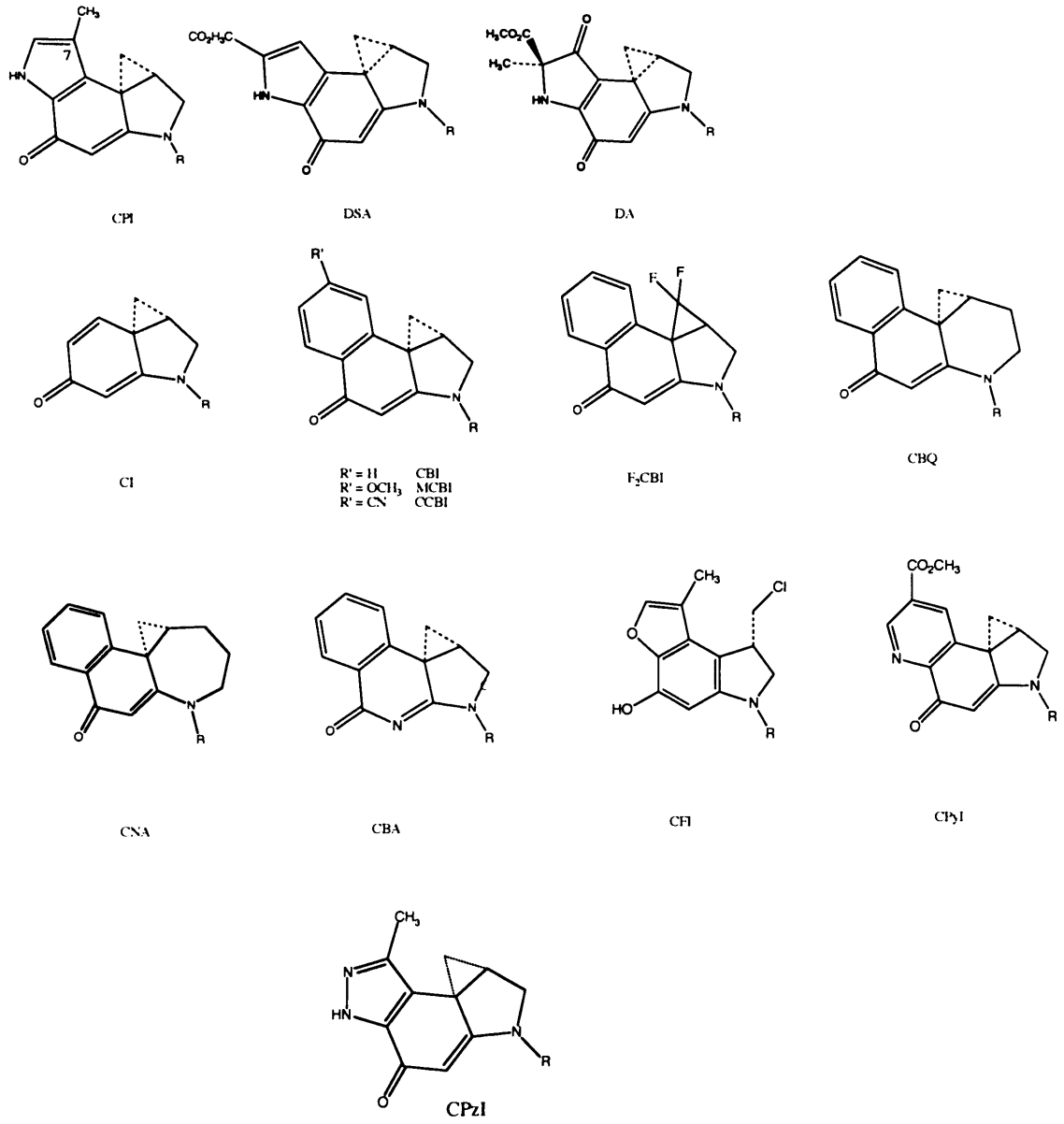

Figure 1.17 Structures of the authentic pharmacophores of (+)-CC-1065, (+)-DMA, (+)-DUMSA, and of those derivatives bearing the most profound structural modifications.

The methyl 1,2,9,9a-tetrahydrocyclopropa[*c*]pyrido[3,2-*e*]indol-4-one-7-carboxylate (CpyI), contains a one carbon expansion on the pyrrole ring found in DSA. Its unique 8-ketoquionoline core structure, was designed in an attempt to provide a means to effect activation via *in situ* selective metal cation complexation. CPyI was found to be (3-4)-fold less stable than CBI and DSA but possesses greater stability compared to (+)-CC-1065 and (+)-DUMA. CPyI analogues exhibited identical DNA alkylation sequence selectivity and near identical alkylation efficiencies compared to the natural products and displayed a trend of increasing cytotoxic potency with increasing the length of the DNA binding subunit (Boger & Boyce, 2000). In the presence of metal cations, the simplified (+)-N-BOC-CPyI agent exhibited dramatically enhanced levels and rates of alkylation, depending to the concentration of the cations and their established stabilities. Its resulting alkylation selectivity was identical to the (+)-DUMSA and (+)-CC-1065 lead compounds, and for one metal cation (Zn^{+2}) in particular, alkylation was achieved at unprecedently low concentrations for such a simple analogue, with an efficiency within only 10-fold of that of the natural products. In the absence of the metal cations, the CPyI bearing agents interact with DNA at an identical manner, albeit at a reduced rate and efficiency (Boger *et al.*, 2000a).

The pyrazole analogue of CPI, 1,2,8,8a-tetrahydro-5H-cyclopropa[c]pyrazolo[4,3-e]indol-4-one (CPzI) has also been reported (Baraldi *et al.*, 1997). This new derivative showed low cytotoxicity against L1210 murine leukemia (IC_{50}=3064 nM).
Figure 1.17 shows the structures of the modified alkylation subunits discussed above.

Other modifications include the study of the effect of even more pronounced structural changes as in the case of the isomeric analogues, iso-CPI, iso-CI, and iso–CBI, in efforts to address the importance of the location of the conjugated carbonyl and the impact on the reactivity of the activated cyclopropane. Additional

modifications in the DNA alkylation subunits in some other examples of heteroaryl derivatives are shown in Figure 1.18.

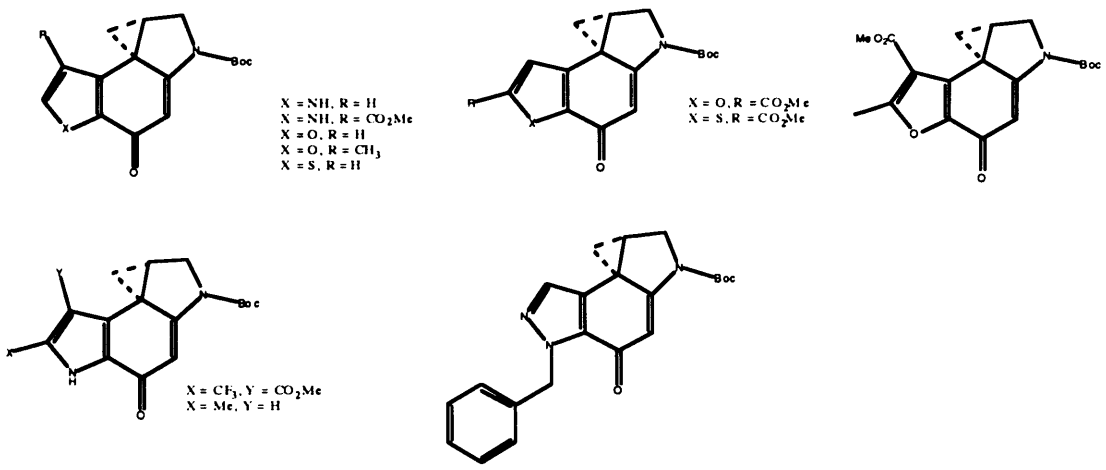

Figure 1.18 Some examples of other modifications of the alkylation subunits.

1.3.4.3 Origins of the sequence selectivity – Mechanisms of catalysis of the alkylation reaction.

There has been considerable debate over the primary driving force for the sequence selectivity and the source of catalysis of the DNA alkylation reaction by the CC1065/duocarmycin class of agents.

The relative importance of the covalent and noncovalent interactions provided by the component structural subunits of the (+)-CC-1065 molecule in mediating the agent's sequence specificity was initially probed by a series of selected synthetic analogues possessing structural modifications and variations to the natural product as well as a series of unnatural enantiomeric counterparts.

The alkylation model

The alkylating potency and sequence specificity of analogues containing the DNA reactive subunit (CPI) linked to zero, one or two indole subunits, as well as an analogue with the structure of (+)-CC-1065 but lacking the hydroxyl and methoxyl substituents in the B and C subunits (Figure 1.19), were determined using the thermally-induced strand breakage assay. Since all analogues exhibited nearly identical sequence selectivity, the Hurley/Upjohn group reported the key finding that the A subunit (CPI), plays the predominant role in sequence specific recognition, as it alone has sufficient structural information to mediate the sequence specificity of the entire molecule (Hurley *et al.*, 1988b).

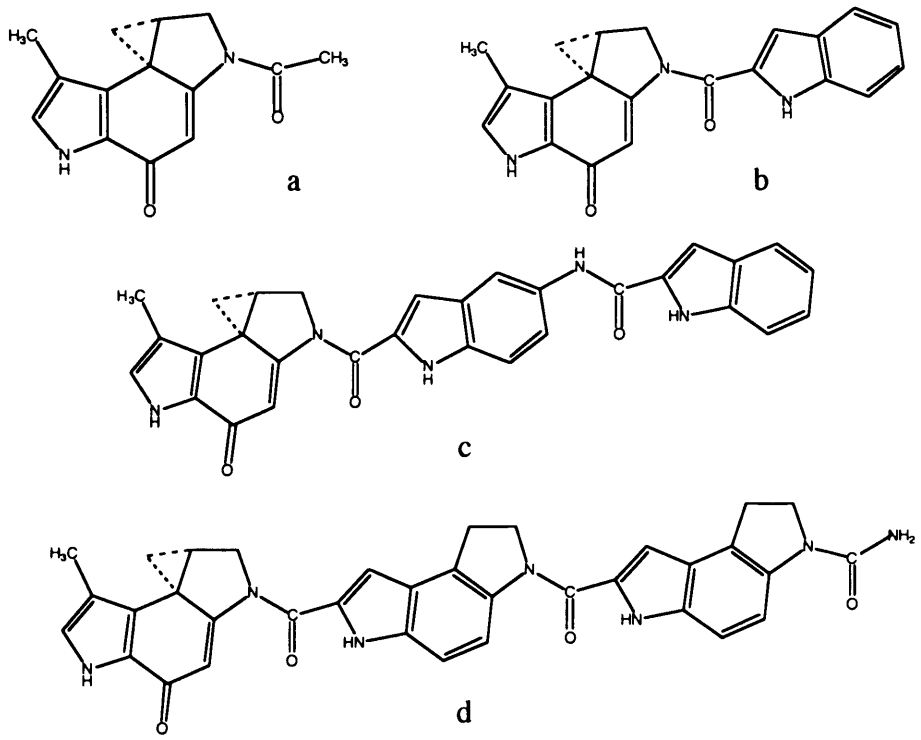

Figure 1.19 Structures of the partial analogues containing the DNA reactive cyclopropane ring, CPI, linked to (a) acetyl, (b) one, and (c) two indole groups, and (d) that of the (+)-CC-1065 structure lacking the hydroxyl and methoxyl substituents in the B and C subunits, all constructed to evaluate subunit effects on the sequence specificity of alkylation by (+)-CC-1065.

However, the a and b analogues, require 10^4 - and 10^3 - fold higher drug concentrations respectively, to show levels of covalent binding comparable to that of c. As the CPI group can contribute very little to the hydrophobic and van der Waals noncovalent interactions shown by the extended analogues and (+)-CC-1065, Hurley postulated that noncovalent interaction is not sufficient for determining the molecule's sequence selectivity. In agreement with that proposal was the finding in oligonucleotide studies that the 5'-GCGAATT-3' sequence would only bind (+)-CC-1065 reversibly (albeit strongly), and would fail to form a covalent bond, suggesting that high affinity binding is not the only prerequisite for bonding (Krueger *et al.*, 1991). Covalent bonding therefore appeared to be determined by a sequence-dependent reactivity of certain adenines with the DNA alkylating subunit CPI. The two pyrroloindole units (subunits B and C), however, are not entirely passive as they dramatically increase the rate of adduct formation and "modulate or fine-tune" the sequence specificity through binding interactions between the inside edge substituents of B and C and the floor of the minor groove (Hurley *et al.*, 1988b). This is particularly evident in certain incubation conditions (e.g. 37°C) where alkylation patterns are indistinguishable only between the fully carbon framework trimeric analogue d and (+)-CC-1065. While noncovalent binding is required to take place in the minor groove of DNA before bonding can be achieved, this binding can be very weak and need not be sequence selective, as in the case of a. Therefore, according to the Hurley group, the reported selectivity must originate in the bonding reaction.

The Hurley/Upjohn group were also the first to report a "telestability" effect of (+)-CC-1065 observed in their thermally-induced strand breakage studies, in the form of either an enhanced background strand breakage, and / or evidence of breakage at one presumably non-(+)-CC-1065-binding position (Reynolds *et al.*, 1985). They also demonstrated the asymmetric effect of (+)-CC-1065 on local DNA structure, as revealed by the strand selective inhibition of both *DNase* I and *Alu* I cleavage, using a site-directed adduct (Hurley *et al.*, 1987). (+)-CC-1065 was shown to produce a selective conformational change in the structure of the covalently modified strand,

which extends as far as 11 bases to the 5' side of the covalent modification site. Since only adenines in certain sequence contexts react with (+)-CC-1065, and since covalent binding of (+)-CC-1065 to DNA appears to require a deformation of DNA structure, they proposed that the relative propensity of the reactive sequences to undergo such conformational changes may play a role in the sequence selectivity of the alkylation event. Based on footprinting studies of their simplest synthetic analogue a (Figure 1.19), they proposed that the CPI group could alone mediate this asymmetric effect, offering further evidence against a productive role of the noncovalent interactions in those important DNA topological changes (Hurley *et al.*, 1988). Relevant to this, the DNA helix distortions also proved to be highly sequence dependent, since the relative distortion energies of different sequences seemed to be predictive of the experimentally determined DNA sequence specificity of (+)-CC-1065 (Zakrzewska *et al.*, 1987).

This *sequence dependent conformational flexibility* theory put forward would refer to adenines in certain environments that would be able to approach the methylene carbon of the cyclopropane, sufficiently closely for bond formation. It was later observed that DNA structure would bend upon covalent modification by (+)-CC-1065 (Lee *et al.*, 1991; Lin *et al.*, 1992), resembling the intrinsic bending associated with poly-adenine tracts. Again the CPI subunit of (+)-CC-1065 was claimed to have sufficient structural information to mediate this effect. The reactivity of the established consensus sequence 5'-AAAAA-3' towards (+)-CC-1065 and the observation of the above mentioned bending of DNA upon covalent bonding, both suggest a critical involvement of a bent DNA conformation in the (+)-CC-1065 sequence selectivity, accounting for at least one set of the reported optimum bonding/consensus sequences. Sequences such as 5'-TTA-3' which are equally, if more, reactive do not exhibit an intrinsically bent DNA structure, but possess several local structural perturbations (propeller twisting, narrowing of the minor groove) which upon reaction with (+)-CC-1065 induce bending (Lin *et al.*, 1992; Sun *et al.*, 1993). The reaction of (+)-CC-1065 with DNA was envisaged to entrap this transient bending of the DNA duplex to eventually form covalent bonding.

In conjunction with the *sequence dependent conformational flexibility* proposal as the basis for sequence selectivity, Hurley also developed a *sequence dependent catalytic activation* model, an adduct formation mechanism involving positioning of the N3 group of adenine of an "active site" within bonding distance of the cyclopropyl methylene carbon and at the same time, positioning a proton, from a phosphate group close to the C4 carbonyl oxygen atom which eventually becomes a phenolic group in the final adduct. The hydrogen bonding interaction between the new phenolic group and an anionic oxygen of the phosphate on the noncovalently modified strand, distant by two base pairs from the covalently modified adenine in the 5'direction, was suggested to be involved in general acid catalysis of the alkylation reaction (Warpehoski & Hurley, 1988). This proposed model was later further refined with the addition of two critically positioned water molecules at opposite ends of the covalent reaction site. One bridging water molecule is placed between a phenolic proton on the alkylating subunit of (+)-CC-1065 and an anionic oxygen in the phosphate on the noncovalently modified strand, and a second ordered water molecule is associated with one of the protons on N6 of the covalently modified adenine (Figure 1.20) (Lin *et al.*, 1991).

In contrast to the natural enantiomeric analogues, Hurley concluded that the mode of sequence recognition for the unnatural enantiomer (-)-CC-1065-DNA adduct formation, was different from the natural product and was primarily governed by the AT-rich sequence selective noncovalent minor groove interactions (Hurley *et al.*, 1990). They reported that (-)-CC-1065 lies in the opposite direction in the minor groove, alkylates a distinct set of adenines and exhibits a different selectivity for covalent adduct formation, while the smaller simplified analogues do not alkylate DNA, (with the exception of the smallest (-)-N-acetyl-CPI). The dramatic increase in the alkylation rate achieved by attachment of the full carbon skeleton of the natural product to (-)-CPI, implied that it is the specific AT-recognising interactions associated with the pyrroloindole groups which play the dominant role in (-)-CC-1065's reactivity (Hurley *et al.*, 1990).

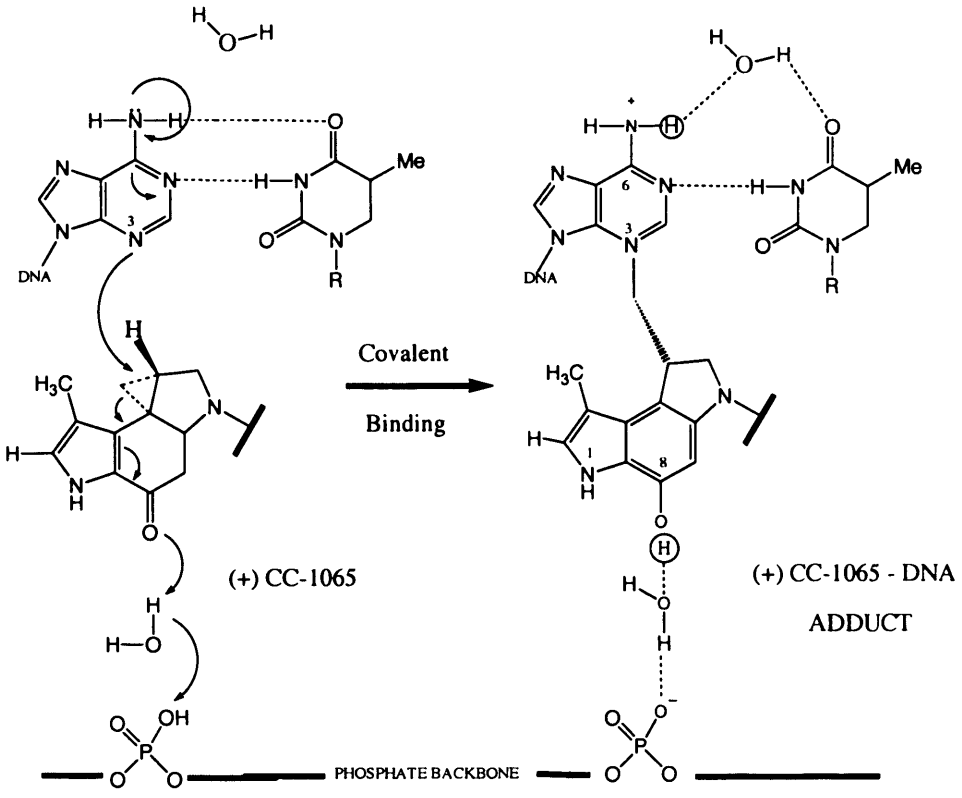

Figure 1.20 Proposed mechanism for the catalysis of the covalent bond formation of the cyclopropane ring of (+)-CC-1065 with an adenine-N3 group, involving two strategically placed water molecules (taken from Lin *et al.*, 1991).

The noncovalent model

An alternative theory about the relative role of the central and right hand segments of the (+)-CC-1065 molecule in its reported alkylation selectivity was put forward by the Boger group. Boger initially focused on the synthesis and evaluation of aborted and extended synthetic analogues of the CDPI and PDE-I frameworks (Kelly *et al*, 1987; Boger *et al.*, 1987). These analogues were structurally related to CC-1065 but incapable of covalent bond formation, constituting potentially selective, high affinity, noncovalent, minor groove binding agents (Figure 1.21). The group initially provided experimental evidence of a substantial preference for

AT-rich noncovalent binding of the simplified agent $CDPI_3$ methyl ester. The studies were later extended to include a whole series of $CDPI_n$ methyl esters (n=1-5) and PDE-I_n methyl esters (n=1-3), all exhibiting high affinity, AT rich, minor groove binding (Boger *et al.*, 1990d). This binding, principally derived from hydrophobic interactions and noncovalent van der Waals contacts was shown to be sufficient to produce a potent cytotoxic effect. The initial noncovalent, AT-specific, minor groove interaction, is optimal for the trimeric $CDPI_3$/PDE-I_3 agents, while $PDEI_3$/DNA complexes were shown to be more stable. Those findings led the Boger group to suggest that (+)-CC-1065 is best represented as a selective alkylating group superimposed on the rigid $CDPI_3$ skeleton. The removal of the hydroxy and methoxy substituents ($PDEI_n \rightarrow CDPI_n$) had only a small impact on the binding affinity and no effect on the AT-rich binding selectivity.

In later similar studies, the Boger group synthesised and studied the DNA binding properties of two other series of agents, $ACDPI_n$ (n=1-4) and $TACDPI_n$ (n=1-3) (Figure 1.21) (Boger & Sakya, 1992).

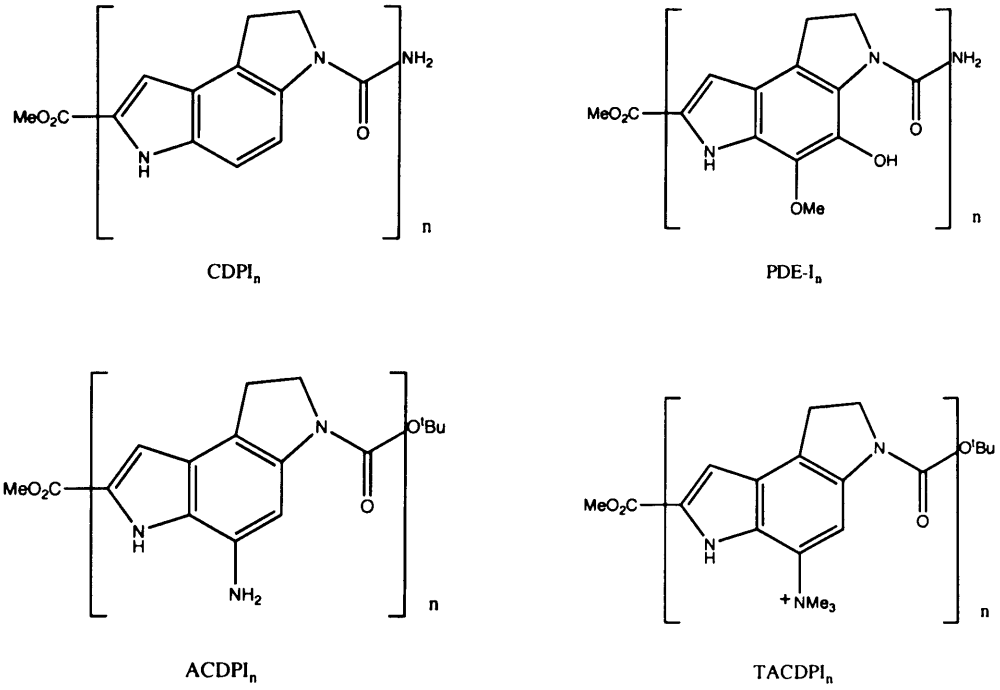

$CDPI_n$ PDE-I_n

$ACDPI_n$ $TACDPI_n$

Figure 1.21 Structures of the partial analogues constructed to evaluate subunit effects on the sequence specificity and affinity of binding.

Comparable to observations made with the $CDPI_n$ series, both the $ACDPI_n$ and $TACDPI_n$ agents exhibited a marked selectivity for AT-rich versus GC-rich DNA (most pronounced for $ACDPI_n$). Again, the trimeric agents $ACDPI_3$ and $TACDPI_3$ proved to be the optimal agents for groove binding. However, the $ACDPI_n$ series exhibited a substantially reduced DNA binding affinity, compared to the parent $CDPI_n$ agents, while in contrast, the $TADCPI_n$ series significantly surpassed it. In the case of $ACDPI_n$ agents, the reduced binding affinity was attributed to the destabilising electrostatic interaction of the amine group on the peripheral face of the agent, with the negatively charged phosphate backbone of DNA. When this amine group was converted to an electropositive substituent, such as a quarternary amine (as is the case of the $TACDPI_n$ series), DNA binding affinity was increased. The introduction of stabilising electrostatic interactions, therefore, greatly enhanced the noncovalent affinity for DNA minor groove binding, whilst having little impact on the intrinsic, preferential AT-rich binding selectivity.

When coupling such simplified analogues to the CPI pharmacophore, the resulting (+)-CPI-$CDPI_2$ agent proved indistinguishable from (+)-CC-1065 in both *in vitro* cytotoxic potency (Boger & Coleman, 1988) and alkylation selectivity profile (Boger *et al.*, 1990a). The profile of covalent alkylation by (+)-CPI-$CDPI_3$ proved nearly identical to that of (+)-CC-1065/(+)-CPI-$CDPI_2$, however, (+)-CPI-$CDPI_1$ exhibited a perceptibly different profile. It was this indistinguishable alkylation pattern of (+)-CC-1065/(+)-CPI-$CDPI_2$ versus that of (+)-CPI-$CDPI_1$ (for the enantiomeric counterparts it was (-)-CC-1065 = (-)-CPI-$CDPI_2$ $\neq$ (-)-CPI-$CDPI_1$) that lead Boger suggest that it is the structural differences of (+)-CPI-$CDPI_2$ versus (+)-CPI-$CDPI_1$ which embody the principal determinant of (+)-CC-1065's sequence selectivity. Hence, Boger assigned a critical role to the potential of the CPI-$CDPI_2$ agent for additional noncovalent binding interaction (Boger *et al.*, 1990a).

Central to the interpretations of the two distinct proposals for the origin of the DNA alkylation selectivity that emerged have been the perceived similarities or

distinctions in the alkylation profiles of the simple derivates of the alkylation subunit versus the natural products. A key finding of the Boger group, was therefore the demonstration that the simplified analogues, (+)-N-acetyl-CPI and (+)-N-BOC-CPI, apart from being far less potent in cytotoxicity and alkylation potency (requiring 10^4- to 10^7- fold the concentration of (+)-CC-1065 to achieve comparable potency), they also exhibited substantially different and less selective alkylation profiles (Boger *et al.*, 1990a), albeit in a different DNA fragment and with different experimental conditions to those employed by Hurley. That finding alone directly conflicted one of the main arguments of Hurley's proposed model.

The above pattern also applies to (+)-DUMSA and its simple derivative, (+)-N-BOC-DSA, which was also shown to possess a substantially reduced cytotoxic and alkylation potency (10^4- fold less efficient compared to the parent agent), while exhibiting a clearly distinct and less selective DNA alkylation profile (Boger *et al.*, 1994b; Boger *et al.*, 1997d). Unlike (+)-CC-1065, the structurally and chemically related agents (+)-DUMSA, (+)-DUMA and the simplified (+)-N-BOC-DSA, were found to reversibly alkylate DNA under the relevant study's experimental conditions (Boger *et al.*, 1994b). The faster rate of retroalkylation exhibited by (+)-N-BOC-DSA, as well as the lack of such alkylation reversibility by (+)-CC-1065, suggests that the extent and the rate of this reverse reaction is inversely dependent upon the extent of the noncovalent binding stabilisation of the agents, provided by the PDE-I_2 and the trimethoxyindole (TMI) subunits of the CC-1065 and the duocarmycins, respectively.

The near thermally neutral and inherently reversible alkylation reaction is, therefore rendered less reversible or irreversible by the stabilising effect of the noncovalent interactions. Consistent with this interpretation, simplified analogues of (+)-CC-1065 with aborted binding subunits, also reversibly alkylate DNA. Another functional role of the (+)-CC-1065 central and right-hand subunits, therefore, is that of promoting and stabilising a thermodynamically poor and potentially reversible covalent alkylation, a theory also known as *binding – driven bonding* (Boger *et al.*, 1989: footnote (14); Boger *et al.* 1990a).

Retaining the $CDPI_1$ and $CDPI_2$ framework, Boger synthesised a number of analogues incorporating different alkylating pharmacophores, such as the exceptionally reactive CI (Boger & Wysocki 1989; Boger *et al.*, 1991a) and the CBI (Boger *et al.*, 1989) electrophiles. As in the case of the CPI containing analogues, the incorporation of the CI subunit into the (+)-CI-$CDPI_2$ agent, conveyed enhanced alkylation specificity compared to the simple (+)-N-BOC-CI analogue, and remarkably similar to that of (+)-CC-1065. This was attributed to the restriction in the number of available alkylation sites dictated by the enhanced noncovalent selectivity of the agent. The identical DNA binding properties of (+)-CBI-$CDPI_2$ and (+)-CC-1065 and their equipotent cytotoxic activity, proved that alternative electrophiles incorporated into structurally related agents act similarly and can participate in the characteristic sequence selective alkylation reaction.

In what was later described as "the first definitive test" of Boger's proposed model, the agents of Figure 1.22 were considered (Boger *et al.*, 1991b). It was demonstrated that agents 1-3 had identical DNA alkylation profiles, irrespective of their absolute configuration, and were in turn identical to the selectivities of both enantiomers of N-BOC-CI and N-BOC-CPI. Similarly the DNA alkylation profiles of the natural enantiomers of 4-6 were identical, indistinguishable from that of (+)-CI-$CDPI_2$. The selectivities of the $CDPI_2$ agents were strikingly similar to that of (+)-CC-1065 and substantially more selective that that of N-BOC-CI and of agents 1-3. One conclusion drawn from the above studies is that absence of noncovalent binding (afforded by the $CDPI_2$ framework) allows a "nonselectivity" of the simple alkylation event, which would proceed with identical selectivities, independently of the nature of the incorporated electrophile. This "nondiscriminant" nature of the alkylation event indicated yet again a more prominent role for (+)-CC-1065's noncovalent binding. Another important point is that the methyl ether 2 and agent 3 and similarly the methyl ether 5 and agent 6, cannot close to the putative corresponding CI agents, yet alkylate the same sites. This finding illustrates that the

cyclopropane is not obligatory for observation of the CI characteristic DNA alkylation and therefore a sequence dependent phosphate protonation and activation cannot be the critical event that determines the alkylation selectivity (Boger *et al.*, 1991b).

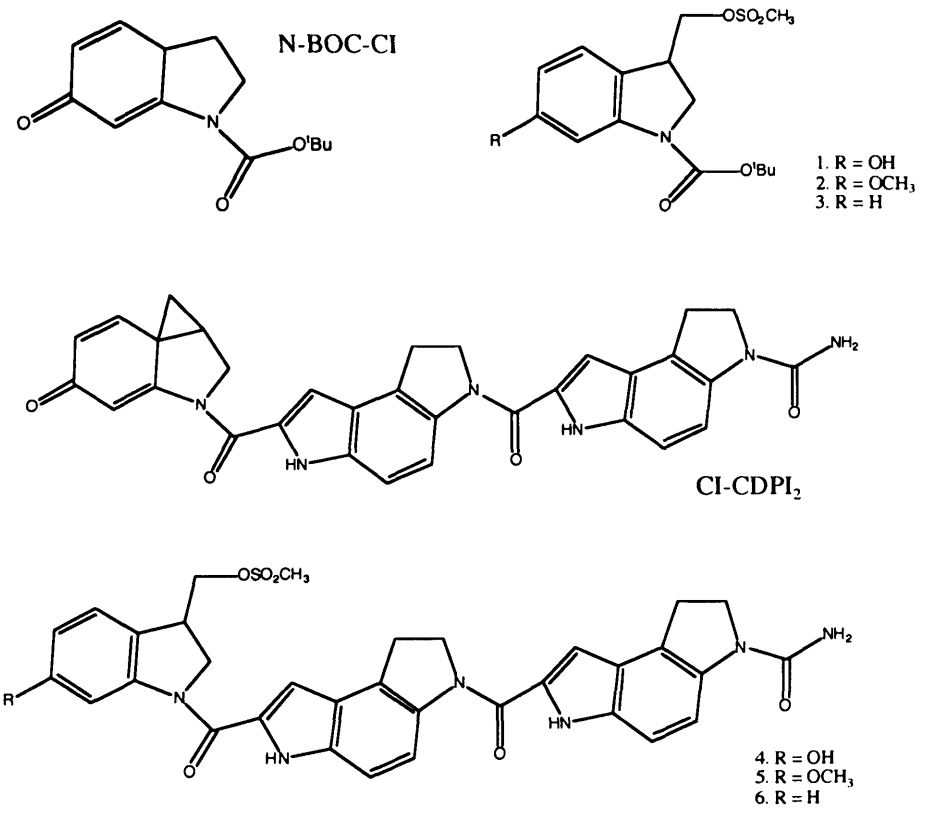

Figure 1.22 Structures of the agents considered in the "first definitive test" of Boger's proposed model of the role of the noncovalent binding in the reported sequence selectivity of CC-1065 and the duocarmycins.

Two structural characteristics of a run of AT base pairs as opposed to GC base pairs are of particular importance for this noncovalent binding selectivity and stabilisation. The lack of the amino substituent that extends in the minor groove, present in a GC base pair, and the constricted width associated with AT

attenuations, renders an AT-rich minor groove more sterically accessible, permiting deeper penetration and most fully achieving the stabilising hydrophobic contacts (Boger *et al.*, 1991a; References therein).

In an extention of the earlier mentioned studies with $ACDPI_n$ and $TACDPI_n$ agents, the role of such stabilising electrostatic interactions, was again highlighted through the introduction of the positively charged trimethylammonium group on the peripheral face of a series of *seco*-CBI-indole agents (Figure 1.23). That structural alteration, as in the previous case, resulted in enhanced DNA alkylation efficiencies. The agents b-d were found to be 100-fold more effective than a, which lacks the positively charged group. This was attributed to the increased noncovalent DNA binding affinity (Boger *et al.*, 1995a). Additionally, the alkylation selectivity of these analogues was influenced by the exact positioning of the positively charged substituent. When lying on the peripheral face of the agents (b and c), the positively charged substituent did not alter the DNA alkylation selectivity. In contrast, groove placement of the large trimethylammonium salt (d) resulted in an altered and more discriminating AT-rich adenine N3 alkylation.

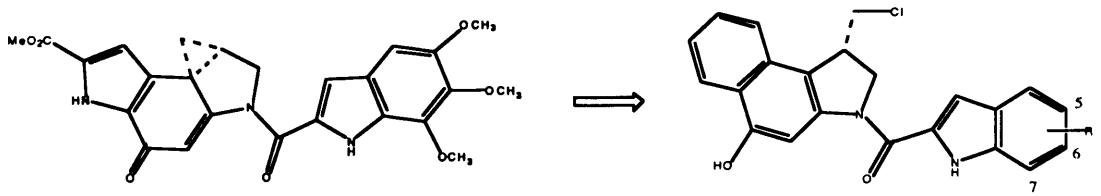

(+)-duocarmycin SA

a. R = H
b. R = 7-NMe^+
c. R = 6-NMe^+
d. R = 5-NMe^+

Figure 1.23 Structure of the *seco*-CBI-indole parent agent (a) and those analogues resulting from strategic placement of the positively charged trimethylammonium substituent on the peripheral face (b, c) of the agents, or within the minor groove (d).

Boger's model in which the alkylaton selecitivity derives from the noncovalent binding selectivity, preferentially in the narrower, sterically more accessible AT - rich minor groove, was also used to accommodate the observed reverse and offset AT-rich adenine-N3 alkylation selectivity of the enantiomeric pairs of agents related to CC-1065 (Boger *et al.*, 1994a) and the duocarmycins (Boger *et al.*, 1994b; Boger *et al.*, 1997d).

The unnatural enantiomers bind in the reverse 5'→3 direction in the minor groove, so as to permit access to the electrophilic cyclopropane and resulting in an offset AT-rich selectivity, since the binding site necessarily starts at the 5' base adjacent to the alkylation site. This alkylation selectivity within an offset AT-rich site is the natural consequence of the diastereomeric relationship of the adducts. This model requires that (+)-CC-1065 / (+)-DUMSA / (+)-DUMA and (+)-N-BOC-CPI / (+)-N-BOC-DSA exhibit distinct alkylation selectivities. For the simple derivatives of the alkylation subunit, sufficient minor groove access to the reacting centre is possible with a single 5' A or T base adjacent to the alkylation site. However for the extended agents sufficient minor groove penetration requires a larger 3.5 or 5 bp, AT-rich region, with two or more adjacent A or T bases. This AT-rich selectivity nicely corresponds to the size of the agent and conflicts Hurley's proposal of an identical sequence selectivity of (+)-CC-1065 and (+)-N-BOC-CPI.

Another observation that supports Boger's proposal of a dominant role of the AT-rich noncovalent binding selectivity and steric accessibility of the N3 alkylation site, derived from the study of the impact of relocation of the C4 carbonyl of the (+)-CC-1065 and the duocarmycin alkylation subunits. It was revealed that despite this most substantial structural modification, the resulting agents (Figure 1.24) react at comparable rates and possess identical sequence selectivity to the parent agents (Boger *et al.*, 1997c). The natural enatiomer *iso*-CBI-TMI, although having the carbonyl buried in the minor groove and therefore no more accessible to the DNA phosphate backbone, as is the case of the parent compounds, alkylates in an identical manner, albeit 50- to 100-fold less efficiently, and at comparable rates.

This observation is inconsistent with Hurley's proposal of alkylation selectivity being controlled by a sequence dependent C4 carbonyl protonation by strategically located DNA backbone phosphates (Boger *et al.*, 1997c).

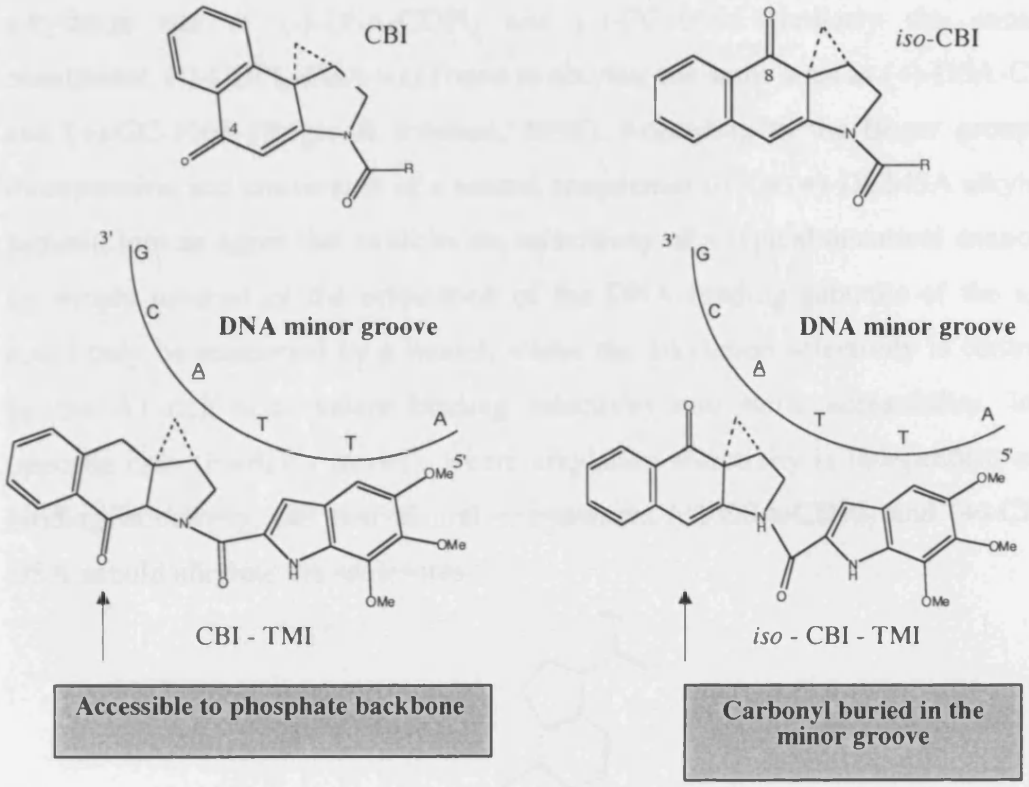

Figure 1.24 Structures of the natural enantiomers of (+)-CBI-TMI and (+)-*iso*-CBI-TMI and their corresponding alkylation subunits, the latter containing an isomeric structural modification of the C4 carbonyl relocated to the C8 position.

Further support for the *noncovalent binding* model was the disclosure, in what is referred to as the second definitive test of Boger's proposed model, that a simple reversal of the orientation of the DNA binding subunits of the agent (+)-DSA-$CDPI_2$, results in reversal of the enantiomeric alkylation selectivity (Boger & Johnson 1995). One unique feature of (+)-DUMSA is the C6 methyl ester on the left hand side of DSA which complements the right-hand side linking amide,

providing the ability to introduce DNA binding subunits on either side of DSA. Both (+)-DSA-$CDPI_2$ and (-)-DSA-$CDPI_2$ agents alkylate the single high affinity sites of (+)- and (-)- CC-1065, respectively. The natural enantiomer of the reversed agent, (+)-$CDPI_2$-DSA (Figure 1.25), was shown to alkylate the same high affinity alkylation site of (-)-DSA-$CDPI_2$ and (-)-CC1065. Similarly the unnatural enantiomer, (-)-$CDPI_2$-DSA was found to alkylate the same sites as (+)-DSA-$CDPI_2$ and (+)-CC-1065 (Boger & Johnson, 1995). According to the Boger group this incorporation and conversion of a natural enantiomer of the (+)-DUMSA alkylation subunit, into an agent that exhibits the selecitivity of a typical unnatural enatiomer, by simple reversal of the orientation of the DNA binding subunits of the agent, could only be supported by a model, where the alkylation selectivity is controlled by the AT-rich noncovalent binding selectivity and steric accessibility. In the opposite case (Hurley's model), where alkylation selectivity is independent of the binding selectivity, the two natural enantiomers (+)-DSA-$CDPI_2$ and (+)-$CDPI_2$-DSA should alkylate the same sites.

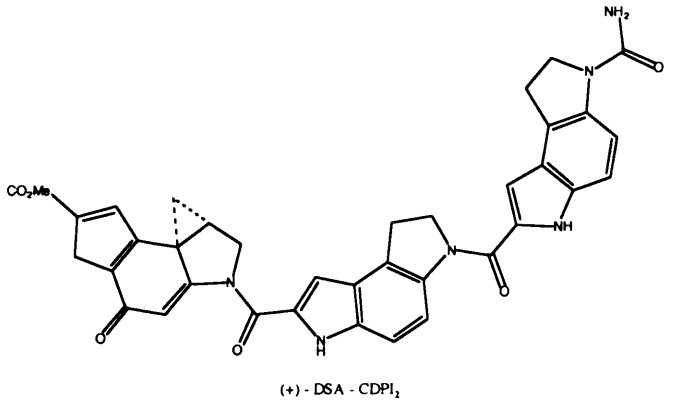

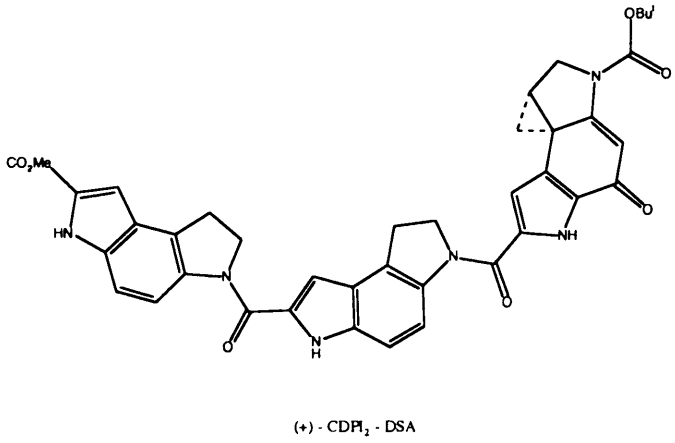

Figure 1.25 The natural enantiomers of the extended: (+)-DSA-$CDPI_2$, and reversed: (+)-$CDPI_2$-DSA, analogues of (+)-duocarmycin SA.

Complementary to the above study, was that of another structurally novel analogue of (+)-DUMSA, CDPI-DSA-CDPI, referred to as the "sandwiched" analogue (Figure 1.26). Both enantiomers of this agent, containing a single DNA binding subunit attached to each side of the alkylation subunit, alkylated the same sites and their selectivity proved distinct from either enantiomer of the previously mentioned extended or reversed agents, consistent with the noncovalent binding model (Boger *et al.*, 1997a).

These studies established that the preferential AT-rich noncovalent binding selectivity of the agents controls the DNA alkylation selectivity and that both natural and unnatural enantiomers of this class of agents are subject to the same polynucleotide recognition features.

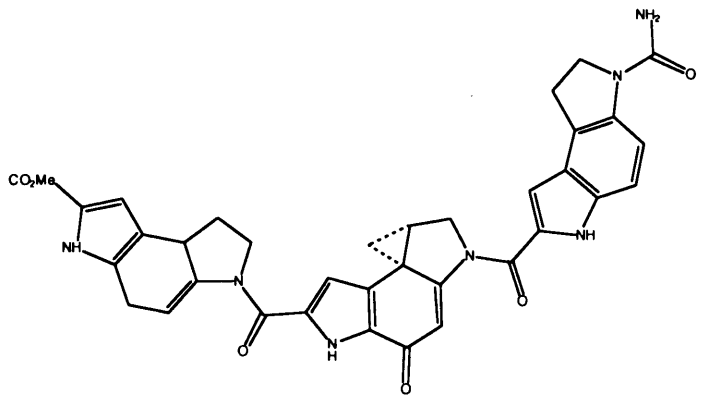

(+) CDPI-DSA-CDPI

Figure 1.26 The natural enantiomer of the "sandwiched" analogue of duocarmycin SA, (+) CDPI-DSA-CDPI.

While alkylation by the reversed agents proceeds at exceptionally low rates (comparable to the small simple derivatives), a rapid rate of DNA alkylation was observed for the sandwiched analogue at a new set of alkylation sites, and independently of the absolute configuration of the agent. This observation suggests that the source of catalysis is not uniquely embedded in the original DNA alkylation

sites but could be a function of the presence of the right-hand heteroaryl N^2 amide substituent. This substituent is the distinguishing feature between the reversed and the extended or sandwiched analogues and could be the factor conveying this enhanced DNA reactivity. It was suggested that the inherent twist of the N^2 amide of the reversed agents is not altered upon binding, thus the agents are not activated for nucleophilic addition. This explains why they undergo DNA alkylation at rates comparable to those of the simple derivatives. Therefore, in addition to the the alkylation selectivity being governed by the noncovalent binding selectivity, Boger also proposed as a source for catalysis, a binding-induced conformational change in the agent that disrupts the ability of the N^2 nitrogen to convey stability to the alkylation subunit through vinylogous amide conjugation (Boger *et al.*, 1997d).

The rigid, bridged aromatic A and B subunits of the duocarmycins and CC-1065 molecules are coplanar in the X-ray structure of the free agents. Upon binding in the minor groove, an intersubunit twist is observed, as the two subunits are driven to maximize hydrophobic contacts with the DNA, as shown in Figure 1.27. This twist is distributed across the torsion angles χ_1 , χ_2 and χ_3 in the linkage between them. The perturbation of χ_1 dihedral angle (the vinylogous amide) is found to correlate very well with the rate of the reaction and most directly relates to DNA alkylation activity (Boger & Garbaccio 1999a; Smith *et al*, 2000).

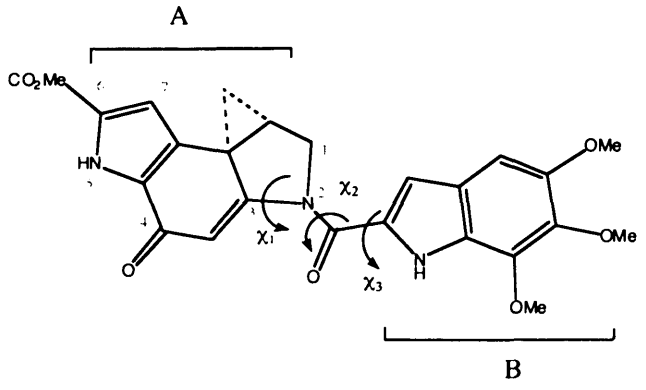

Figure 1.27 Structure of the natural enantiomer of (+)-DUMSA. The subunit naming and atom numbering scheme is shown, and the torsion angles χ_1 , χ_2 and χ_3 indicated.

This activation is not uniquely alkylation site dependent, but rather a consequence of forced adoption of a helical conformation upon AT-rich minor groove binding. This source of catalysis requires an extended and rigid N^2 amide substituent.
The amide's fundamental role in catalysis was established in experiments where replacement of the amide by a methylene group in the (+)-CBI-TMI agent, therefore essentially eliminating the source of catalysis, resulted in complete abolishment of any DNA alkylation capabilities for the modified analogue accompanied by a 10^5-fold loss in cytotoxic potency (Boger *et al.*, 1998) (Figure 1.28).

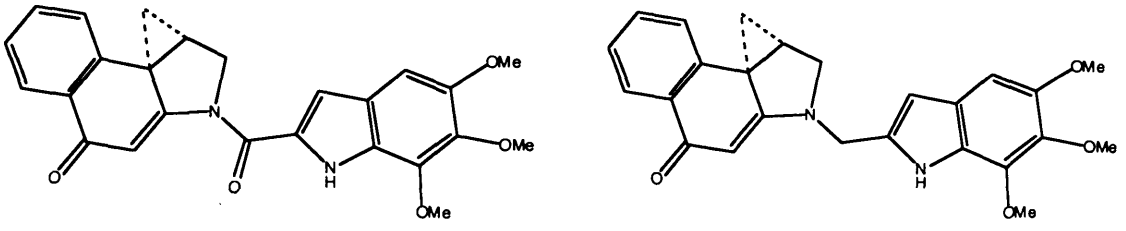

(+)-CBI-TMI

Figure 1.28 Structures of the (+)-CBI-TMI agent (left) and a modified analogue (right), which replaces the linking N^2 amide with a methylene group.

Since the extent of this binding induced conformational change is dependent on the shape of the minor groove, the agent's destabilisation would be greater within the narrower, deeper AT-rich minor groove sites, where the inherent twist in the linking amide and helical rise of the bound conformation is greatest. Therefore, the shape-selective recognition (preferential AT-rich noncovalent binding) and shape-dependent catalysis (binding induced twist of the amide), work in concert to restrict alkylation to accessible adenine N3 sites. This synergism is epitomised by the left-hand subunit C6 methyl ester and the C5 methoxy substituent of the TMI subunit of the duocarmycins, which both substantially enhance alkylation potency and increase biological potency. Not only do these two substituents contribute to the

noncovalent binding stabilisation by being imbedded in the minor groove, but they also increase the rigid length of each subunit and the inherent twist in a DNA-bound helical conformation (Figure 1.29).

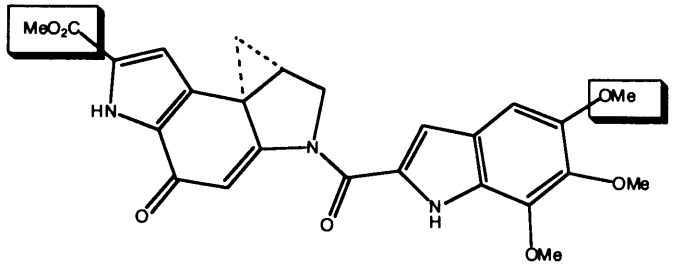

Figure 1.29 Structure of the natural enantiomer of (+)-duocarmycin SA. The minor groove imbedded substituents that extend rigid subunit lengths are indicated.

The effect of methoxy substituents on the activity of (+)-DUMSA analogues is summarised in Table 1.2.

Replacement of the TMI binding subunit of (+)-DUMSA with a simple indole results to the DSI agent (Figure 1.30). This modification not only alters the noncovalent binding potential of the agent but also allows for deeper penetration into the DNA minor groove due to the absence of the bulky methoxy groups of TMI and more extensive favourable van de Waals interactions. Despite the fact that the deeper groove penetration accentuates the twisting requirement, the intersubunit twist angle is decreased by 8° and results in less disruption of the ligand vinylogous amide, manifested as a 20-fold slower rate in DNA alkylation (Schnell *et al*, 1999).

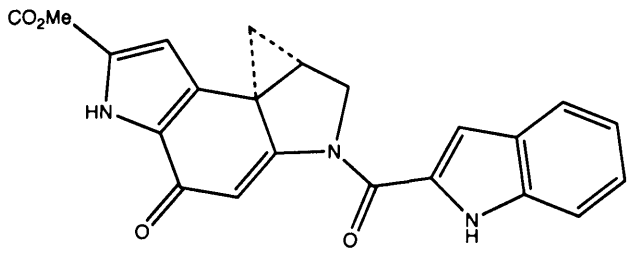

Figure 1.30 Structure of the indole derivative of (+)-duocarmycin SA, DSI.

R =	Relative DNA Alkylation efficiency	IC_{50}, L1210, pM
TMI 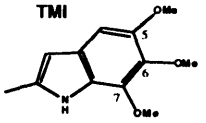	1.0	10
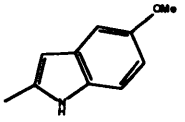	1.0	12
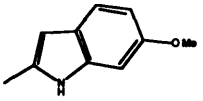	0.2	25
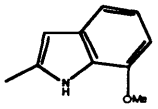	0.1	60
Indole$_1$ 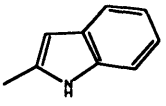	0.05	65

Table 1.2 The effect of methoxy substituents on the activity of the corresponding duocarmycin SA analogues (taken from Boger & Garbaccio 1999a).

In conclusion, in the absence of an extended right-hand subunit, DNA minor groove binding no longer requires an induced twist in the N^2 amide linkage, depriving the agent of the additional activation toward DNA alkylation. This in turn results in the slow alkylation rates observed with simple derivatives of the alkylation subunits.

This theory further contributes to the distinction in the behaviour of the enantiomeric pairs. From NMR studies of oligonucleotides, it has been reported (Boger & Garbaccio 1997) that the natural enantiomer of (+)-DUMSA, in its bound adopted conformation, contains an average twist of 41°, while in contrast, the unnatural enantiomer, within the same binding site, when bound, exhibits a much smaller, 28° twist between the right and left-hand subunits. This greater twist angle

is thought to result in greater disruption of the vinylogous amide stabilisation and preferentially accelerates the alkylation event for the natural enantiomer.

The role of the vinylogous amide was further clarified with the synthesis and evaluation of a carbocyclic analogue of the (+)-CC-1065 and the duocarmycins, CBIn, which lacks N^2 and the vinylogous amide (Figure 1.31) (Boger & Turnbull, 1998).

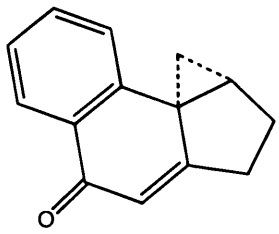

CBIn

Figure 1.31 Structure of the 1,2,9,9a-tetrahydro-[H-cyclopropa[c]benz[e]inden-4-one (CBIn), a carbocyclic C-ring analogue of the alkylation subunits of (+)-CC-1065 and the duocarmycins.

The comparison of CBIn with CBI directly established that the presence of N^2 and the vinylogous amide increases stability by 3200-fold at pH3, and by ($>10^3$ to 10^4)-fold at pH 7, relative to its structural CBI homologue. The expanded analogues CNA and CBQ (Figure 1.17) exhibited increased reactivity in the order CAN > CBQ > CBI, mirroring the relative extent of vinylogous amide conjugation. Thus, the vinylogous amide found in the naturally occurring alkylation subunits is responsible for their unusual stability, while disruption of the vinylogous amide stabilisation caused by a DNA binding-induced conformational change, seems to be providing the necessary activation (reactivity) for the alkylation reaction (Boger & Turnbull, 1998). A study of the solvolysis pH-rate profiles of the N-BOC analogues of CBQ and CAN, which are reactive throughout the pH range 2-12, showed no evidence of solvolysis rate - pH dependence, indicating that the DNA alkylatiojn reaction need not be acid-catalysed (Boger & Garbaccio 1999b).

Finally, in another demonstration of the duocarmycin and (+)-CC-1065 DNA alkylation reaction not relying on the DNA phosphate backbone for catalysis, the Boger group replaced the backbone phosphates proximal to the C4 carbonyl of a (+)-DUMSA molecule bound to an oligonucleotide containing a single high affinity alkylation site, by methylphosphonates. Despite this modification, alkylation proceeded at comparable rates (Ambroise & Boger 2002). This observation is again incompatible with an active backbone participation in the DNA alkylation reaction as proposed by Hurley. The main findings concerning the two models are summarised in Table 1.3.

Alkylation site model	Non covalent Binding model
• (+)-CC-1065 and the (+)-CPI have identical alkylation selecitivities. • Selectivity inherent and embodied in the CPI subunit. • The alkylation reaction controls the selectivity irrespective of noncovalent binding. • Sequence dependent phosphate activation through carbonyl complexation / protonation. C4 carbonyl required. • Alkylation at junctions of bent DNA. • Different features control (-)-CC-1065 enantiomeric selectivity.	• (+)-CC-1065 and the (+)-CPI selectivtities are distinct. • (+)-CC-1065 is best represented as a selective alkylating agent superimposed on the CDPI trimer skeleton • Alkylation selectivity is controlled by binding selectivity • Alkylation within sterically accessible, AT rich sites. • Alkylation not controlled by phosphate protonation, not relying on phosphate backbone for catalysis. C4 carbonyl not required. • Same features control (-)-CC1065 enantiomeric selectivity. • pH independent catalysis derived from a DNA binding induced conformational change.

Table 1.3 Summary of the most important features of the two proposed models regarding the origin of sequence specificity and alkylation catalysis of CC-1065 and the duocarmycins.

1. 3.4.4 Biological Properties

The potent cytotoxic and antitumour effects of (+)-CC-1065 have been attributed to the DNA alkylation event addressed earlier and are thought to be produced as a direct consequence of the formation of the (+)-CC-1065 – DNA covalent adduct. This results in characteristic structural modifications on the DNA, which can be linked to the observed biological properties of the agent.

Effects on local DNA structure

DNA helix

Early studies suggested that (+)-CC-1065 stabilises the DNA helix. Evidence came from a dose dependent increase in the melting temperature of calf thymus DNA, inhibition of S_1 nuclease activity and resistance to ethidium-induced intercalative unwinding attributed to stiffening of the helix (Swenson *et al.*, 1982).
(+)-CC-1065 induces DNA bending of about 14-19°, with a directionality towards the minor groove (Lee *et al.*, 1991). The direction and the magnitude of the drug-induced bending, and the associated narrowing of the groove, correspond well with the general features of the intrinsic bending in a 5-6 bp, AT tract. Drug modification however results in loss of temperature dependency of the intrinsic bending (Sun *et al.*, 1993). The special reactivity of the 3' adenine of the consensus sequences to (+)-CC-1065, the shift in the locus of bending of an A_5 tract about 0.5 base pairs toward the 3' of its centre, and the additive effect on the magnitude of bending upon drug modification, provide support for the proposed "junction bend" model. The interaction of the inside edge substituents of the B and C subunits of (+)-CC-1065 with the floor of the minor groove cause winding of the DNA helix and are also associated with DNA stiffening (Lee *et al.*, 1991; Hurley & Sun, 1994a). The helix stabilising property of (+)-CC-1065 also extends to RNA-DNA duplexes as well as DNA with modified internucleotide linkages (Kim *et al.*, 1995).

Chromatin

The interaction of (+)-CC-1065 with DNA was also characterised when DNA is in the form of chromatin. (+)-CC-1065 does bind to chromatin isolated from P388 mouse leukemia cells but significantly less strongly compared to naked DNA and through what is a primarily reversible reaction. (+)-CC-1065 was also found to bind very weakly and nonspecifically to histones (Moy *et al.*, 1989).
In a study of drug-induced damage to cellular DNA, more damage (at the same drug to DNA ratio) was observed in cell lysates than to whole cell DNA. This was attributed partly to a greater accessibily of the drug to the protein-dissociated DNA (Zsido *et al.*, 1991). However, extensive formation of irreversibly bound (+)-CC-1065 covalent adducts, both in the absence and in the presence of chromatin proteins, in purified and intracellular SV40 DNA, respectively, has also been reported (McHugh *et al.*, 1994). Increased concentration of drug was nonetheless required to react with SV40 DNA in infected cells in order to achieve the same level of damage as with purified DNA. Matrix associated regions (MARs), are domains that anchor cellular DNA to the nuclear matrix, a proteinaceous scaffolding that organizes chromatin fibres into looped domains. Given their critical role in the organisation of nuclear chromatin, they too have been investigated as targets of the (+)-CC-1065 and analogues and are discussed later.

The structural changes in DNA induced by its interaction with (+)-CC-1065 have biochemical consequences as they affect the activity of, and reactions mediated by, enzymes which are highly sensitive to such structural changes and which play key roles in various aspects of the DNA metabolism. Such examples include:

DNA polymerases

Inhibition of DNA synthesis represents a major mode of action of (+)-CC-1065, which exhibited a pronounced inhibitory effect on purified DNA polymerase α (Li

et al., 1982). A single stranded template containing a site-directed adenine adduct induced by (+)-CC-1065 and analogues, was also shown to block (though not absolutely) the *in vitro* DNA synthesis mediated by Klenow fragment, *E.Coli* DNA polymerase I, and T4 DNA polymerase. A strong selective hinderance of polymerisation from a primer site containing a drug lesion in a duplex region, was associated with the ethano bridges of the pyrroloindole subunits of the parent agent and the relevant analogues (Sun & Hurley, 1992a). The (+)-CC-1065–DNA adduct was particularly prone to misincorporation of the nucleotide prior to the modified adenine in the highly reactive sequence 5'-GATTA-3' (A; adducted adenine).

The sequence specificity of adozelesin bound on purified plasmid DNA was previously determined based on the identification of termination sites of a modified form of bacteriophage T7 polymerase, *Sequenase* (Weiland & Dooley, 1991). This property of (+)-CC-1065 and analogues to impede the progression of DNA polymerase was further utilised by polymerase chain reaction (PCR) based assays, to map DNA alkylation sites of selected analogues at the single-nucleotide level in human genomic DNA (Passadore *et al.*, 1997; Lee *et al.*, 1994; Bianchi *et al.*, 1999). In all these studies the inhibition of DNA replication due to the strong irreversible binding of (+)-CC-1065 to double stranded DNA was considered to be responsible for its cytotoxicity.

Helicases

The DNA helicases are enzymes that separate the strands of DNA, coupling the hydrolysis of ATP, which provides the necessary energy, with the unwinding of duplex DNA at the replication fork and providing the DNA polymerase with a single standed template. The helicases therefore play an important role in nearly all aspects of nucleic acid metabolism, including replication, repair, recombination, and transcription.

(+)-CC-1065 was found to inhibit unwinding of duplex DNA catalysed by the dda protein of phage T4 and DNA helicase II (UvrD) of *Escherichia coli*, relative to

unmodified substrates. Strand-specific inhibition was strictly exhibited for the dda protein-mediated reactions. Yet, both helicases were shown to get trapped by the drug-DNA complex, generating an unusual secondary structure in the DNA during the protein mediated unwinding (Maine *et al.*, 1992).

The *E.Coli* rep protein was also found to be inhibited, in the same pattern as helicase II with which it shares the same polarity of translocation (Sun & Hurley, 1992b). The extent of DNA unwinding inhibition by helicase II is much more significant for extended analogues that bear the full carbon skeleton of the (+)-CC-1065, responsible for the unique winding effect of the parent molecule (Sun & Hurley, 1992b; Aristoff *et al.*, 1993). The increase in the extent of inhibition is also dependent upon the orientation of this winding effect which has to be opposite with respect to the direction of the helicase II translocation.

The activity of another DNA helicase, Rad3, was also reported to be inhibited by (+)-CC-1065 adducts (Naegeli *et al.*, 1993). Rad3 activity inhibition is strand specific and was observed only when damage was confined to the DNA strand on which Rad3 binds and translocates.

Chinese hamster ovary (CHO) cell lines, deficient in the XPB/ERCC3 and XPD/ERCC2 helicases, both exhibited the same, increased sensitivity to (+)-CC-1065 compared to the parental repair proficient cell line (Damia *et al.*, 1996). These observations indicate the involvement of functional helicases in the repair of the (+)-CC-1065 adducts.

Ligase

T4 DNA ligase catalyses the formation of a phosphodiester bond between juxtaposed 5' phosphate and 3' hydroxyl termini in duplex DNA. Covalent modification by (+)-CC-1065 and analogues was found to preferentially inhibit the T4 DNA ligase catalysed reaction and to prevent nick sealing on the non-drug modified stand of DNA to the 5' side of the covalent adduct, but enhanced ligation of the covalently modified strand. Two types of inhibition have been described, a

proximal one attributed to the DNA winding and helix stabilising effects of (+)-CC-1065 which causes the differential effect on each strand, and a distal one, associated with an unusual helix stiffening effect of the parent molecule and extended analogues (Sun & Hurley, 1992c).

Protein – DNA complexes

DNA complexed with proteins, rather than naked DNA, presents a more accurate consideration of the ultimate cellular target of (+)-CC-1065.

Transcription is regulated by promoter and enhancer elements recognized by gene-specific DNA-binding proteins, by general transcription factors, and, at a higher level, by chromatin structures. Impairment of the complex interactions between activators and their DNA targets could lead to a change in the pattern of gene expression. Interference at this level by alkylating drugs through DNA conformational changes, direct occupation of recognition sites or interference with crucial protein-protein interactions essential for promoter activation, might be responsible for critical biological functions.

(+)-CC-1065 has been shown to prevent the general transcription factor TATA box binding protein (TBP) from binding to the adenovirus major late promoter, with a much greater efficiency (at nM doses) than reversible minor groove binding agents (200-fold more effective than distamycin A) or intercalating agents (8000-fold more effective than ethidium bromide and 300-fold more effective than hedamycin) (Chiang *et al.*, 1994). Preincubation of DNA with TBP alone or with TBP and TFIIA, a factor that enhances TBP association with DNA, followed by drug addition, requires 10-fold greater (+)-CC-1065 concentration to prevent complex formation, suggesting that access to DNA is important for the drug binding. In this case, drug binding was thought to directly hinder minor groove binding of TBP to the TATA box.

Binding of Specificity Protein 1 (Sp1) to 6 GC boxes present in the simian virus 40, (SV40) promoter region has also been shown to be inhibited by (+)-CC-1065

binding to the two 5'-AGTTA drug modification sites in the GC box region. In this case, the inhibition in Sp1 binding, particularly at the 3'-GC box is attributed to structural distortions in DNA associated with helix stiffening caused by the covalent adduct formation (Hurley & Sun, 1994b).

(+)-CC-1065 has also proved to be a useful probe for monitoring protein-induced DNA structural alteraltions such as bending, due to its own unique entrapped/induced bend in DNA and its similarities to an A-tract's structural properties. In such studies the directionality and locus of the phage Mu transposase (A-protein) induced bending have been elucidated (Ding *et al.*, 1993) while the Sp1 binding sites (GC boxes) within the three 21 base pairs repeat region of the SV40 promoter were shown to assume a looping structure, based of their interaction with (+)-CC-1065 (Sun & Hurley, 1994). CC-1065 has also offered insights into binding of the SV40 large tumour antigen, T-antigen (T-ag) with the SV40 replication origin. Based on observations of the differential effect this interaction had on the ability of (+)-CC-1065 and bizelesin to alkylate the AT tract located in that region, it was deduced that the SV40 origin is in a straight conformation upon T-ag binding (Han & Hurley, 1996).

Judging from the extent and nature of the structural effects of (+)-CC-1065 on transcription binding sites, it can be envisaged that (+)-CC-1065 could additionally modulate transcription by trapping the DNA in a transcriptionally active state, mimicking the activation by transcription factors. Alternatively the induced structural modifications could potentially create artificial binding sites.

The (+)-CC-1065 class of compounds has also been shown to affect cellular processes such as DNA replication, in an "indirect" way. Adozelesin selectively blocks SV40 DNA replication at the level of initiation of nascent DNA chains (Cobuzzi *et al.*, 1996). Bizelesin on the other hand inhibits both initiation and, at greater doses, elongation of SV40 replication. While the inhibition of elongation was suggested to occur in a direct / "cis" manner through the covalent adduct

formation, the inhibition of initiation was thought to be mediated through a secondary factor which acts indirectly i.e. in a "trans" manner. That would probably involve the induction of production of a SV40 DNA replication inhibitor (McHugh *et al.*, 1999a).

Altering the DNA helix and the chromatin structure and hence affecting processes such as transcription and ultimately gene expression can also occur at critical sites at some distance from the actual drug binding site due to the asymmetric "telestability" effect, addressed earlier. Bizelesin adducts have been suggested to exert inhibitory effects on cellular DNA replication at a substantial distance from the actual location as only one to two bizelesin adducts per $\sim 10^6$ are needed for a genome-wide inhibition of replicon initiation (Woynarowski 2002). The targeting of crucial genes or nearby regulatory sequences offers therefore a plausible rationale for the exceptional cytotoxic efficiency exerted by the adduct formation of this class of compounds.

Targeting the genome

Since the early studies of the (+) CC-1065-induced damage to cellular DNA, it was speculated that part of the drug's exceptional potency could be due to its selective reactivity with critical targets within the genome (Zsido *et al.*, 1991).
The availability of tritiated adozelesin enabled the investigation of the intracellular localization of CPI adducts on nuclear DNA of cultured human HT-1080 cells through restriction enzyme analysis. The telomeres of each human chromosome possess clusters of the repetitive DNA sequence $(TTAGGG)_n$ that are potential binding sites for the agent and comprise a critical and highly abundant target. It was observed in that study that adozelesin binds predominantly to nuclear DNA at sites other than those telomeric repeat sequences. However, there were other distinct repeat elements that clearly exhibited increased drug bonding, relative to other regions of the genome (Weiland & Dooley, 1991).

The formation and location of (+)-CC-1065 adducts within the SV40 DNA genome have also been reported (McHugh *et al.*, 1994). Structural damage to DNA has been monitored by assaying the conversion of SV40 topological forms with increasing concentrations of (+)-CC-1065. The extensive conversion to the linear form, indicative of double-strand damage, at even low drug concentrations suggested a clustering of highly reactive bonding sites.

AT-rich region specific damage on eukaryotic genomic DNA has been demonstrated for (+)-CC-1065 (McHugh *et al.*, 1994), adozelesin and bizelesin (Woynarowski & Beerman, 1997). The AT-rich, matrix-associated region (MAR) of intracellular SV40 DNA was among the preferred targets of those CPI drugs, consistent with their binding specificity on naked DNA.

Study of the genome targeting by those agents has also been further refined with the use of PCR-based technology. The distribution and the binding motifs of the targeted adducts have been assessed by quantitative polymerase chain reaction (QPCR) on specific human gene sequences. One such study involved the "AT islands". These constitute another paradigm of a repetitive and critical domain of clusters of potential binding sites for the (+)-CC-1065 class of compounds, other than the telomeric $(TTAGGG)_n$ sequence mentioned earlier. AT islands are distinct minisatellite regions which consist typically of 200-1000 bp long tracts, of up to ~85-100% A/T DNA. Such domains are believed to function as strong MARs, responsible for organising DNA loops on the nuclear matrix. Long AT islands were shown to represent a critical, selective target for bizelesin. While adozelesin induces more frequent, less strictly localised lesions, bizelesin preferentially targeted the MAR domains of the *c-myc* and apolipoprotein B (*apoB*) genes (Woynarowski *et al.*, 2000). This targeted damage by bizelesin markedly exceeds genome average and preferentially occurs within MAR regions over non-MAR domains as clearly exhibited by the lack of binding to a non-MAR, AT-poor domain in the *β-globin* gene.

This directed, nonrandom, clustering of bizelesin lesions in the AT islands is observed along with the need of formation of very few lesions for bizelesin to block cell growth. More specifically two bizelesin adducts per cell are estimated to be required for a GI_{50} lethality compared to other, non-region specific alkylating agents, such as tallimustine and cisplatin (220 and 14,000 estimated adducts per cell at GI_{50}, respectively) (Woynarowski 2002). Overall, bizelesin induces two orders of magnitude fewer lesions in cellular DNA than (+)-CC-1065 and adozelesin.

The interaction of another (+)-CC-1065 analogue, U-71184 (analogue c in Figure 1.19) with human genomic DNA has been documented as selective inhibition of PCR-mediated amplification of a 5' upstream region of the human estrogen receptor gene, from DNA derived from drug-treated MCF7 human breast cancer cells, known to possess many AT-rich, binding motif sites. The lack of such inhibition on *Ha-ras* oncogene and the chromosome X-linked, (CGG)-rich fragile X mental retardation-1 gene (*FMR-1*) sequences, which are both GC-rich, further demonstrates the agent's expected region specific and sequence selective effect (Passadore *et al.*, 1997). In a similar study for analogues possessing a pyrazole substituted CPI grpup (CPzI), the same sequence–dependent inhibition of PCR-amplification of genomic regions was observed (Bianchi *et al.*, 1999).

AT islands, such as those targeted by bizelesin, are in general inherently unstable (expandable) domains found in various loci of genomic instability, such as AT-rich fragile sites. The cellular MAR function of AT islands may differ in cancer and normal cells. The abnormally expanded AT islands in the FRA16B fragile site in leukemic CEM cells act as strong, permanent MARs, while their unexpanded counterparts in normal cells are loop localized. Given their instability and involvement in the remodelling of the nuclear architecture, AT islands may actually contribute to cancerous phenotypes. They have been in particular implicated in leukemias and lymphomas, including acute lymphoblastic leukemia (ALL), one of the most frequent pediatric malignancies (Wyonarowski, 2002; References therein). The abnormal structure/function of AT islands, such as their expansion and

acquired strong MAR properties and their increased abundance in hypersensitive cell lines, like the CEM cells, may sensitize certain tumours to the bizelesin-type drugs. Highly localised lesions such as the ones described above are several orders of magnitute more lethal than non-region-specific damage, consistent with the critical role of MAR domains in DNA replication (Wyonarowski, 2002).

An agent's preference for region specific damage does not always coincide with its inherent binding specificity. This is clearly demonstrated by the bizelesin analogue U-78779. U-78779 was designed to recognise mixed A/T – G/C motifs, that distribute uniformly at the genome level. However, the clustering of the minor, pure AT, binding motifs take precedence over drug binding preference and outcompetes isolated, mixed sites in drug binding (Herzig *et al.*, 2002). Sequence specificity alone, on the other hand, is not sufficicent for region specificity. Tallimustine for example, which also prefers mixed motifs and is highly sequence specific (consensus sequence: 5'-TTTTGPu-3') fails to induce region-specific lesions and is less lethal that both bizelesin and U-78779 (Herzig *et al.*, 2002). These observations highlight the importance of region specific targeting and its potential implication in the biological outcome of the drug action.

DNA repair

(+)-CC-1065 adducts are probably the best characterised minor groove sequence specific lesion in terms of DNA repair. These adducts are known to be substrates for bacterial and human nucleotide excision repair *in vitro* (Gunz et al., 1996; Selby & Sancar 1988). A protein, named duocarmycin-DNA adduct recognising protein (DARP), which binds with increased affinity to duocarmycin damaged DNA has also been identified (Asai *et al.*, 1999).

This topic is covered in more detail in chapter 4 and in the general discussion (Chapter 6).

Figure 1.32 summarises the biological sites of action of (+)-CC-1065 and the affected cellular processes covered in the text.

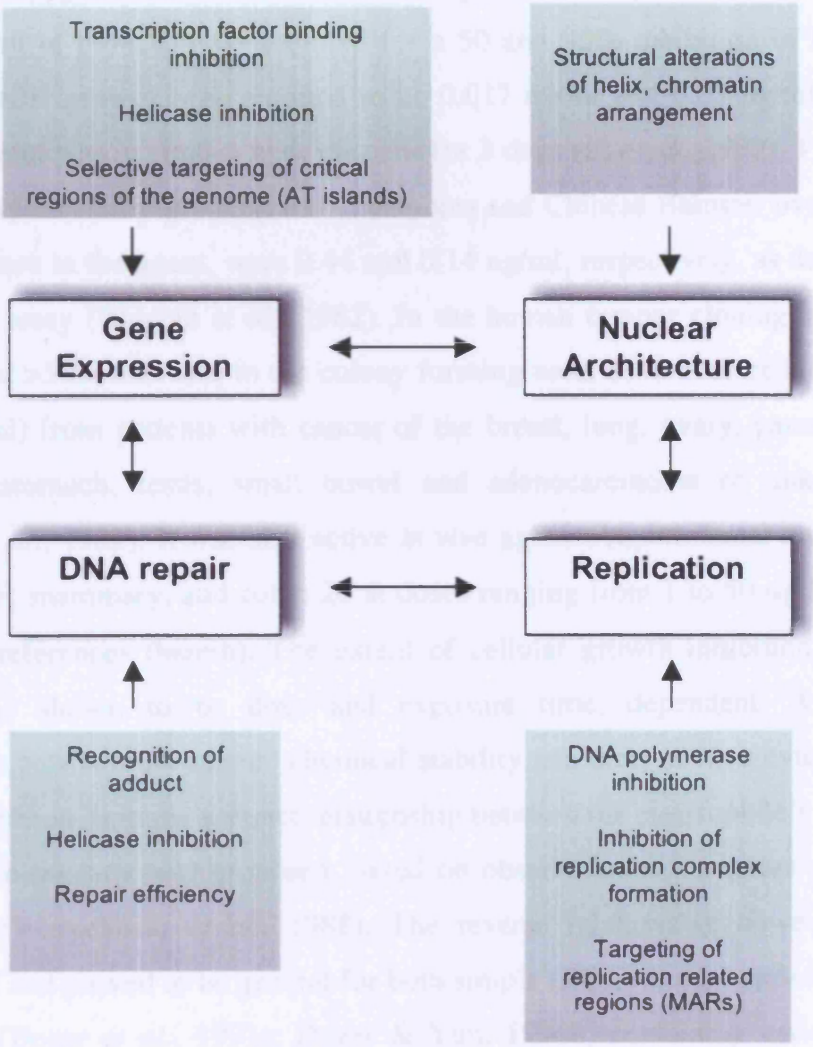

Figure 1.32 Summary of the inter-related biological sites of action/cellular processes, of (+)-CC-1065 and analogues, addressed in the text. (adapted from Turner & Denny, 2000).

1.3.4.5 Cytotoxicity

(+)-CC-1065 and the duocarmycins are extremely potent cytotoxic agents, as demonstrated by *in vitro* studies, achieving cytotoxicity in the pM range. The concentration of (+)-CC-1065 required for a 50 and 90% inhibition of L1210 mouse leukemia cells' growth, was reported to be 0.017 ng/ml and 0.05 ng/ml respectively, when the agent was in contact with the cells for 3 days (Li *et al.*, 1982). The 50% lethal doses for exponentially growing B16 melanoma and Chinese Hamster ovary cells, after a 2 h exposure to the agent, were 0.44 and 0.14 ng/ml, respectively, as determined in a clonogenic assay (Bhuyan *et al.*, 1982). In the human tumour cloning assay, (+)-CC-1065 caused >50% decrease in the colony forming units of tumour cells (1 h exposure to 0.1 ng/ml) from patients with cancer of the breast, lung, ovary, pancreas, multiple myeloma, stomach, testis, small bowel and adenocarcinoma of unknown origins (Bhuyan *et al.*, 1982). It was also active *in vivo* against experimental tumours such as P388, CD_8F_1 mammary, and colon 26 at doses ranging from 1 to 50 μg/kg (Bhuyan *et al.*, 1983, references therein). The extent of cellular growth inhibition in the above studies was shown to be dose and exposure time, dependent. A fundamental relationship between the agents' chemical stability and their *in vitro* cytotoxic potency has been defined. Initially a direct relationship between the electrophile's reactivity and its cytotoxic potency was proposed, based on observations of a series of simple CPI analogues (Warpehoski *et al.*, 1988). The reverse relationship however, was later established and proved to be general for both simple (BOC) and extended (CDPI, TMI) analogues (Boger *et al.*, 1991c; Boger & Yun, 1994b) containing various alkylation subunits. As shown in Figure 1.33, in the series of the simple BOC analogues, the compound with the greatest solvolytic stability ($t^1/_2$) exhibits the most potent cytotoxic activity against L1210 cells.

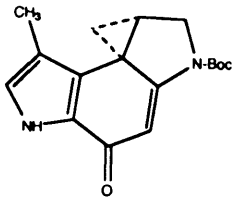

(+)-N-Boc-C7-MeCPI

IC_{50} = 330 nM

$t^1/_2$ = 37 h

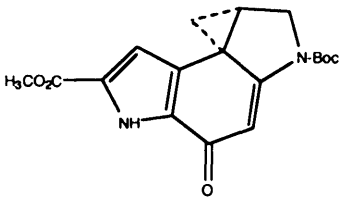

(+)-N-Boc-DSA

IC_{50} = 6 nM

$t^1/_2$ = 177 h

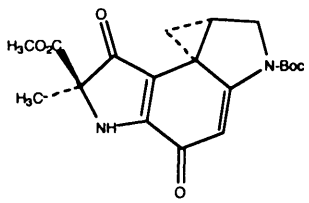

(+)-N-Boc-DA

IC_{50} = 1000 nM

$t^1/_2$ = 11 h

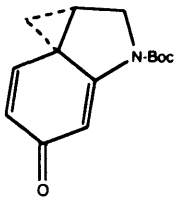

(+)-N-Boc-CI

IC_{50} = 18000 nM

$t^1/_2$ = 0.01 h

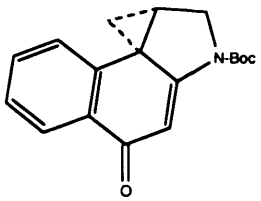

(+)-N-Boc-CBQ

IC_{50} = 4000 nM

$t^1/_2$ = 21 h

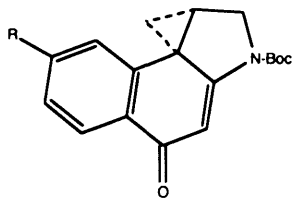

R=H, (+)-N-Boc-CBI

IC_{50} = 80 nM

$t^1/_2$ = 133 h

R=OCH_3, (+)-N-Boc-MCBI

IC_{50} = 90 nM

$t^1/_2$ = 110 h

R = CN, (+)-N-Boc-CCBI

IC_{50} = 20 nM

$t^1/_2$ = 213 h

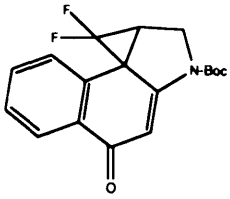

(+)-N-BocF_2-CBI

IC_{50} = 55000 nM

$t^1/_2$ = 0.26 h

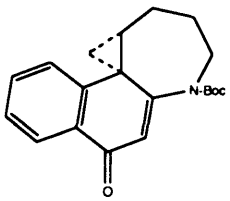

(+)-N-Boc-CNA

IC_{50} = 5000 nM

$t^1/_2$ = 0.03 h

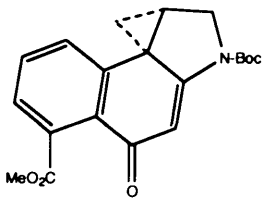

(+)-C_5-CO_2Me-CBI

IC_{50} = 70 nM

$t^1/_2$ = 236 h

Figure 1.33 The stability towards solvolysis ($t^1/_2$ in h, at pH 3) and *in vitro* cytotoxicity (IC_{50} in nM, against the L1210 cells) for the simple analogues of a range of alkylation subunits.

This is interpreted to reflect the ability of the chemically more stable derivatives to more effectively reach their intracellular biological target, the DNA. This same relationship between an agents's solvolysis stability and its *in vitro* cytotoxic potency is also mirrored in extended analogues such as (+)-DUMSA. The most chemically stable of the duocarmycins. (+)-DUMSA also exhibits the greatest cytotoxic activity with an IC_{50} value of 6 pM in L1210 cells. At the same time the IC_{50} value for the less stable (+)-duocarmycin A is only 100pM (Boger, 1994).

Exceptions to this general correlation have been reported for a series of cyclopropaneindolones, which exhibited the originally described direct relationship between solvolytic reactivity and cytotoxic potency (Castedo *et al.*, 2001).

A more recent study of N2-aryl derivatives of CBI however, served to further establish a parabolic relationship between solvolysis stability (-log k, pH3) versus cytotoxic potency (-log IC_{50}, L1210), also applicable to all the N-BOC derivatives of Figure 1.33 (Parrish *et al.*, 2003b). The correlation between solvolytic stability and potency displays the following order of cytotoxicities for the main alkylation subunits: N-BOC-DSA>N-BOC-CBI>N-BOC-CPI>N-BOC-DA>N-BOC-CBQ>N-BOC-CI (Boger & Johnson, 1996).

The general consensus suggests that an analogue should possess sufficient stability to reach their target (DNA), yet maintain sufficient reactivity upon binding, in order to alkylate DNA, describing in this way a balance between stability and reactivity (Parrish *et al.*, 2003b).

The cytotoxic activity has also been shown to be influenced by the structural variations of the DNA binding domain linked to the various alkylation subunits. The DNA binding subunits of (+)-CC-1065 and the duocarmycins contribute in several ways to the properties of the natural products. As discussed earlier, extensive structure- activity

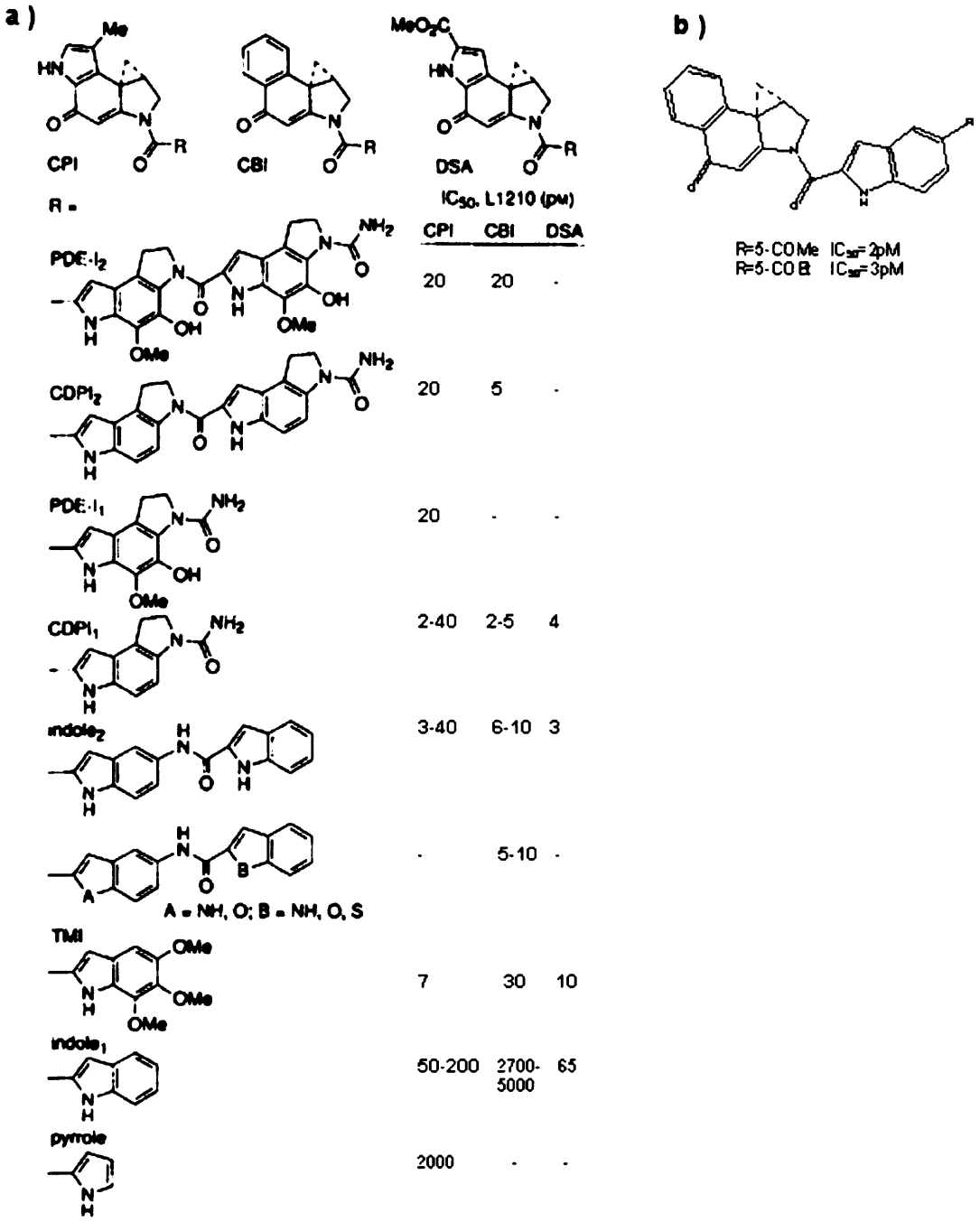

Figure 1.34 a. The cytotoxic potency resulting from attachment of different DNA binding subunits to the CPI, CBI and DSA natural pharmacophores (adjusted from Boger & Johnson, 1996. so as to include all (differing) reported IC_{50} values. b. structure of the C5-substituted CBI-indole derivatives.

relationship studies of a series of modifications confirmed that it is this portion of the molecule that conveys binding affinity to the DNA minor groove, selectivity for binding at AT-rich sites, stabilises the covalent adduct formation, accelerates the rate of DNA alkylation and overall plays an important role (the degree varying according to the distinct models of the catalysis of alkylation proposed) in the alkylation event.

The potentiation of the cytotoxic activity of agents bearing the CPI, CBI and DSA pharmacophores tethered to varying binding subunits is shown in Figure 1.34a.

Further to this, variations in the size, rigid length, and shape of the binding subunits afforded by appropriate substitutions can have a profound effect in the resulting cytotoxicity. This is exemplified by the C5 acyl derivatives of the CBI-indole agent featured in Figure 1.34b. The derivatives possessing the methyl and ethyl group at the indole C5 position were 1000-fold more potent (IC_{50}=2-3pM) than the parent CBI-indole$_1$ agent (IC_{50} =2700pM), also surpassing the activity of both the CBI-TMI (IC_{50}=30pM) and even the natural parent compounds CC-1065 (IC_{50}=20 pM) and DUMSA (IC_{50}=6-10pM) (Boger *et al.*, 2001b),

Apart from variations in the size (extensions and simplifications) of the attached binding subunits or crucial substitutions, other approaches include the design of analogues bearing deep seated structural modifications. Such modifications may involve the incorporation of heteroatoms, as is the case of a nitrogen capable to function as a hydrogen bond acceptor or donor (Boger *et al.*, 1995c) or introduction of different linkers and terminal amides (Wang *et al.*, 1996; Wang *et al.*, 2000)

The role of the nature of the DNA binding domain is now believed to extend beyond simply providing DNA binding selectivity and affinity, but also actively contributing to the catalysis of the DNA alkylation reaction, through the shape-dependent catalysis model of the binding induced activation (Boger & Garbaccio, 1999a).

1.3.4.6 Cell Cycle Effects-Cell death

The effects of (+)-CC-1065 and analogues have also been studied on CHO and B16 cell progression and their phase-specific toxicity. (+)-CC1065 was most cytotoxic to mitotic cells, and toxicity decreased as cells entered the S-phase however, other analogues exhibited a different phase specific toxicity profile. In general, this class of compounds, does not inhibit progression from G1 to S, but slows progression through S and blocks cells in G2-M (Bhuyan *et al.*, 1983; Adams *et al.*, 1988). As shown for CBI bearing analogues (Wang *et al.*, 2000), as well as the duocarmycins (Wrasidlo *et al.*, 1994), the mechanism of tumour cell death is through induction of apoptosis, and is accompanied by morphological changes and internucleosomal DNA fragmentation.

1.3.4.7 Cellular uptake

The cytotoxic activity exerted by the alkylation of DNA which is the ultimate intracellular target of the CC-1065 class of compounds, is also a function of effective cellular uptake. This is manifested particularly in cases where, in contrast to expectations based on the relative efficiencies of alkylation of naked DNA, analogues exhibited diminished cytotoxic potencies. Such an example are the CBI-indole analogues containing a peripheral quaternary ammonium salt which, although shown to alkylate DNA at the same relative efficiency as (+)-CC-1065 and (+)DUMSA, were approximately 1000 times less potent (Boger *et al.*, 1995b). This diminished cytotoxic potency was attributed to ineffective cellular penetration.

The alkylation of intracellular DNA by CC-1065 and analogues has been demonstrated as discussed earlier. The only study, however, of intracellular distribution and cellular uptake involved a fluorescently labelled *seco*-CBI-pyrrole polyamide conjugate (Kumar *et al.*, 2004). Cellular localisation was evaluated using confocal laser scanning microscopy and the molecule was shown to be located primarily in the cytoplasm and

organelles. However, this is a hybrid molecule with relatively large molecular weight, which may hinder its cellular uptake, as observed for other functionalised polyamides examined to date.

1. 3.4.8 Adverse Toxicity

Despite CC-1065's potent cytotoxic properties described earlier, clinical development of the agent as an anticancer therapeutic was precluded due to its limiting toxicity of delayed lethality in mice, at subtherapeutic doses. More specifically, initial toxicity studies showed that mice receiving high doses of the drug (400-800 μg/kg single dose, 50-200 μg/kg/day, five daily doses) died by day 9. Mice receiving lower doses, appeared normal between days 6-30, but on day 30 expressed loss weight, hunched posture and ruffled fur. Between days 32 and 38, all of the mice at every dose level died. Observations of the high-dose dead animals revealed pale livers and kidneys. The low-dose animals displayed ascites and a lack of body fat. Noted cellular changes included marked morphological alterations of the mitochondria. Studies of tissues other than the liver appeared normal (McGovern *et al.*, 1984).

Several analogues of (+)-CC-1065 were studied in an attempt to separate the cytotoxic from hepatotoxic properties of the molecule by tracing the structural element of the parent agent responsible for the delayed lethality (Figure 1.35). This undesired property was finally attributed to the ethano bridges of the central and right-hand pyrroloindole units. Their removal, apart from elimination of the characteristic delayed death also results in increase of the activity against P388 and L1210 cells (Table 1.4). It has been suggested that the delayed lethality of (+)-CC-1065 or (+)-CPI-$CDPI_2$ may be directly related to the irreversibility of the alkylation reaction due to the extended noncovalent binding stabilisation provided by the full carbon skeleton of the pyrroloindoles. The ethano groups contribute to the stong noncovalent binding through van der Waals and hydrophobic interactions with the floor of the minor groove. This noncovalent binding

stabilisation may either prevent the reverse reaction after alkylation has occurred (Boger *et al.*, 1994b) or keep the drug bound so that it realkylates the same site (Warpehoski *et al.*, 1992).

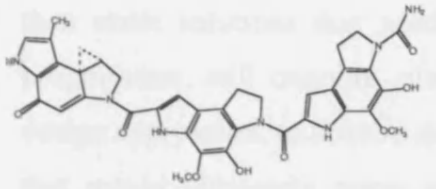

(+)-CC-1065

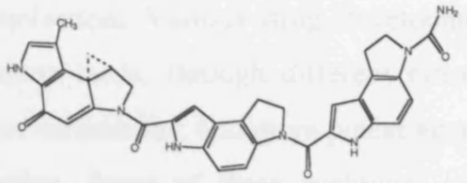

(+)-CPI-$CDPI_2$

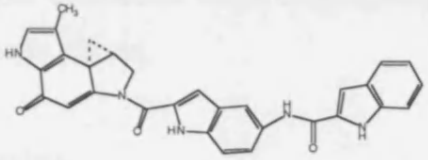

(+)-CPI-$indole_2$

Figure 1.35 Analogues considered in order to determine the structural feature responsible for the delayed toxicity phenomenon

Agent	IC_{50} (L1210)	% ILS (P388 *in vivo*)	Delayed Death
(+)-CC-1065	0.05	62	Yes
(+)-CPI-$CDPI_2$	0.05	77	Yes
(+)-CPI-$indole_2$	0.004	4/6 [a]	No

Table 1.4 *In vitro* (IC_{50} = Drug concentration causing 50% inhibition of cell growth with 3-days incubation) and *in vivo* (%ILS = percent increase in life span of treated compared to control mice) activities of the analogues of Figure 1.35. [a] Number of day 30 survivors/total number mice in test group. (Data as reported in Hurley *et al.*, 1988b).

Other analogues such as adozelesin or DUMSA, which lack those ethano bridges or the full carbon framework are devoid of the delayed lethality.

1.3.4.9 Novel analogues of CC-1065 and the duocarmycins

CC-1065 and the duocarmycins are naturally occurring agents with potent anticancer activity and they should be considered as "dynamic" leads provided by nature, rather than static solutions that need no further optimisation. Various drug development programmes, still ongoing, aim in exploiting those leads, through different rational design approaches, to acquire more selective, more efficacious, and more potent agents, that would ultimately prove useful as therapeutics. Some of these analogues have reached the clinical trial evaluation stage, highlighting the potential and the positive outcome of such synthetic efforts.

Rational design approaches

Bisalykylators

The pharmacophores of both CC-1065 and the duocarmycins have been used as monomeric units for dimerisation, leading to novel crosslinking agents. Such agents are anticipitated to have increased sequence selectivity as they should be more sequence discriminating, possess enhanced cytotoxicity, increased size of recognition site, and ideally an increased selectivity for predefined DNA sites in tumour cells, compared to the parent monoalkylating compounds. Unsymmetrical cross-linking agents derived from the combination with a PBD pharmacophore have also been reported.

Bifunctional Alkylating agents derived from (+)-CC-1065

Early studies showed that some synthetic compounds which contain two CPI moieties linked by variable length flexible methylene chains, are significantly more potent than

CC-1065 both *in vitro* and *in vivo* (Mitchell *et al.*, 1989). Such dimers are exemplified by bizelesin (Figure 1.36).

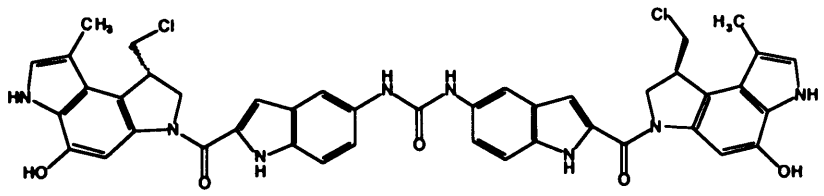

Figure 1.36 Structure of bizelesin, (U-77,779).

Bizelesin (U-77,779) is a symmetrical dimer of the spiro cyclopropyl alkylating subunit of (+)-CC-1065. The two *seco*-CPI units are linked by a rigid bis (indolecarboxylic acid) linker. Bizelesin very efficiently induces 6- or 7- nucleotide interstrand crosslinks (ISC) and has also been shown to induce monofunctional alkylation of DNA within sites of potential ISC. The most preferred site for ISC formation is the 6-nucletodie sequence 5'-TAATTA, where A is the alkylated adenine, which represents a palindromic sequence joining two adjacent 5'-TTA triplets. Thus, the two adenine alkylation sites are located on opposite strands of DNA and are separated by 4 nucleotides. There is also a preference for the 6-nucleotide sequence 5'-TAAAAA* where the asterisk represents the alkylation site on the top strand and the underlined T indicates the location of alkylation on the complementary strand (Lee & Gibson 1993). Bizelesin also induces a 7-nucleotide DNA ISC at the sequence 5'-TAAAAAA-3'. An ISC at this sequence occurs to a 2-fold greater degree than the corresponding 6-nucleotide DNA ISC 5'-TAAAAA*A-3' when both sites are located within the same duplex. The monoalkylation sequences are generally of the sequence 5'-(A/T)(A/T)A, Bizelesin is both more sequence selective and cytotoxic than the monomeric agents from which it derived (Lee *et al.*, 1994).

Another variation of this rational design approach includes the synthesis of *seco*-CBI dimers. Some of those analogues showed promising activity in the NCI *in vitro* preclinical screening assay (Jia & Lown, 2000).

Bifunctional agents derived from the duocarmycins.

A series of four dimers derived from head to tail coupling of the two enantiomers of the duocarmycin SA alkylation subunit have been reported (Boger *et al.*, 2000b).

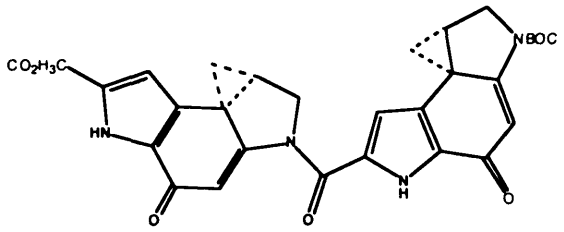

Figure 1.37 Structure of the (+)(+)-DSA_2 analogue.

The (+)(+)-DSA_2 and (+)(-)-DSA_2 agents proved to be 2-3-fold more potent than (+)-DUMSA and approximately 2000-fold more potent than the simplified N-BOC-DSA. The left-hand subunit was found to dominate the charactreristics of the agents, responsible for the first and primary site of DNA alkylation, while the right hand DSA alkylation subunit serves the same function as TMI subunit of the duocarmycins. The agent in Figure 1.37 as well as the (-)(-)-DSA_2 are capable of intrastrand crosslinks only, as both cyclopropanes are oriented toward the same strand of DNA, while the agents (+)(-)-DSA_2 and (-)(+)-DSA_2 were expected to display ISCs.

Unsymmetrical bifunctional agents

Given the initial success of dimerisation in providing biologically active molecules, the CPI, CBI and PBD units have since been combined to generate a new class of unsymmetrical crosslinking agents. The advantage of this approach is the creation of interstrand crosslinking agents that could alkylate guanines on one strand and adenines on the opposite strand, enabling recognition and binding to mixed DNA sequences.

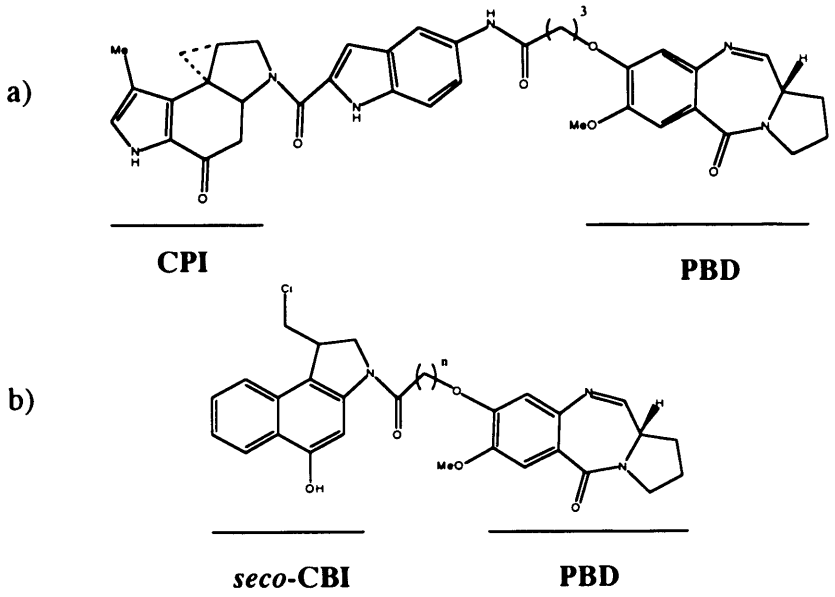

Figure 1.38 Structure of reported agents combining the CPI, CBI and PBD pharmacophores.

The single CPI-PBD dimer (a) was demonstrated to crosslink the 6 bp sequence 5'-CAATTA-3' (Zhou *et al.*, 2001). The set of compounds depicted in structure (b), designed to crosslink between N3 of adenine and N2 of guanine, in the minor groove of DNA, showed great variation in cellular toxicity with the most potent ones exhibiting IC_{50}s in the pM range. One CBI-PBD dimer from this set was observed to crosslink

cellular DNA at 1000-fold lower concentrations than the related symmetrical PBD dimer. The CBI portion of the agents controlled the alkylation selectivity while the PBD substituent increased the overall efficiency of the reaction (Tercel *et al.*, 2003).

Hybrid molecules

CC-1065 pharmacophores have also been used as scaffolds to attach other chemical moieties in an attempt to acquire hybrid agents with an altered sequence selectivity. Some examples of these efforts are presented below.

Bleomycin A_2

Hybrid agents incorporating the C-terminus DNA domain of bleomycin A_2, linked to the CBI have been reported (Figure 1.39).

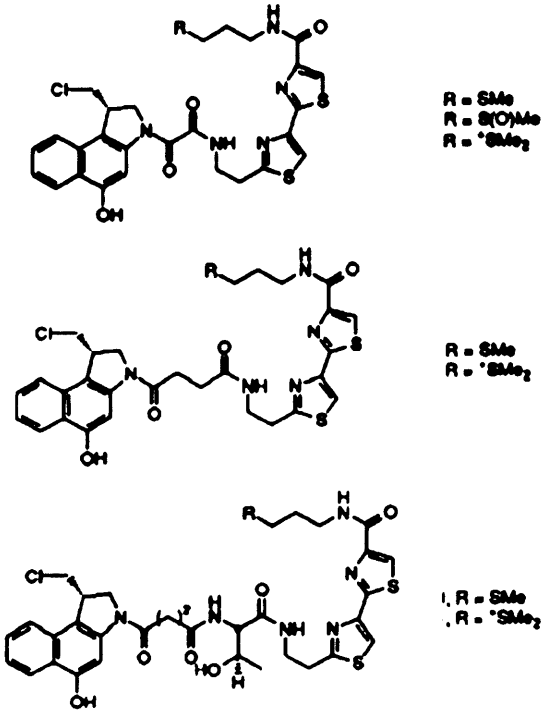

Figure 1.39 Structures of the CBI and bleomycin A_2 hybrid agents incorprorating a shorter rigid or longer flexible linkers

The resulting agents exhibited little or no enhancement of DNA alkylation efficiency and demonstrated identical selectivity to that of simple CBI derivatives such as N-BOC-CBI. They also possessed diminished cytotoxic activities (Boger & Han, 1997).

Mitomycin

Synthetic hybrids have been prepared combining the DNA alkylation features of the duocarmycins and the reductive activation of the mitomycins, by incorporation of the quinone of the mitomycins, which is thought to confer tumour selectivity as a result of preferential reduction in hypoxic environments, into the AT-selective binding framework of the duocarmycins. An activation cascade for such agents was envisioned to involve bioreduction, followed by spirocyclization and eventual alkylation.
The resulting agents confirmed the proposed reaction cascade, as the quinone-based analogue would not alkylate DNA under nonreductive conditions. In its reduced form, as a hydroquinone, it would alkylate DNA in a sequence specific manner identical to (+)-DUMSA, albeit 100-fold less efficiently.

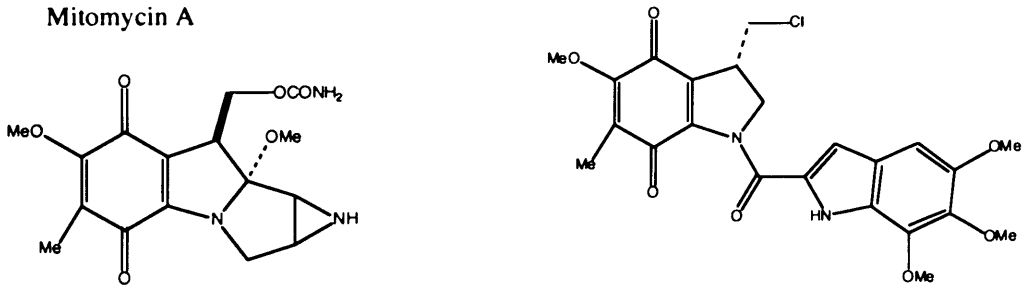

Figure 1.40 Chemical structures of mitomycin A and the hybrid agent bearing the quinone group of the mitomycins incorporated in the AT-selective binding framework of the duocarmycins and designed to be capable of mitomycin-like reductive activation and duocarmycin-like DNA alkylation.

A study of the cytotoxic potency of these analogues established that they were more potent in a DT-Diaphorase-enriched cell line versus a deficient one, consistent with a preferential activation by DT-Diaphorase (Boger & Garbaccio 1999c).

Lexitropsins

Another approach for the design of hybrid molecules is coupling the reactivity and alkylation function of a CC-1065/duocarmycin moiety with the DNA-reading ability of the imidazole (Im) and/or pyrrole (Py) moieties, aiming to further exploit binding-driven bonding, tailor the binding preference and manipulate sequence specificity.
Initital studies involved simple CPI-oligopyrrole conjugates incorporating amide groups of different sizes and flexible or rigid linkers (Wang *et al.*, 1996). Certain such conjugates exhibited up to 10,000 higher potency than CC-1065 against KB cancer cells. Another variation was the design of unsymmetrical bis-lexitropsin conjugates incorporating the CBI pharmacophore (Jia *et al.*, 1999) (Figure 1.41 a and b)

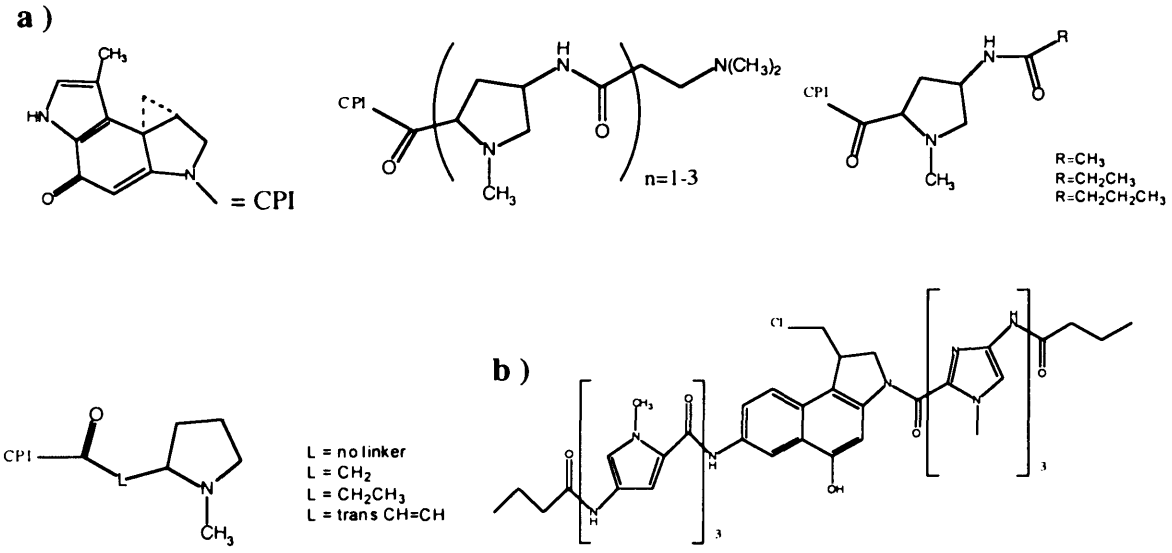

Figure 1.41 Chemical structures of a) the CPI-N-methylpyrrole synthetic conjugates and b) and usymmetrical bis-lexitropsin-CBI.

The discovery that distamycin A dramatically modulates the sequence specificity of DNA alkylation by DUMA, so to preferentially alkylate G-N3 groups through cooperative binding of a heterodimer between DUMA and distamycin in the minor groove (Yamamoto *et al.*, 1993) (Figures 1.42 and 1.43a) presented the possibility of controlling the sequence specificity of DUMA in a predictable manner in the presence of Py / Im triamides and following Dervan's binary code of the side-by-side pairing between Py and Im carboxyamides (Figure 1.43) (Fujiwara *et al.*, 1999).

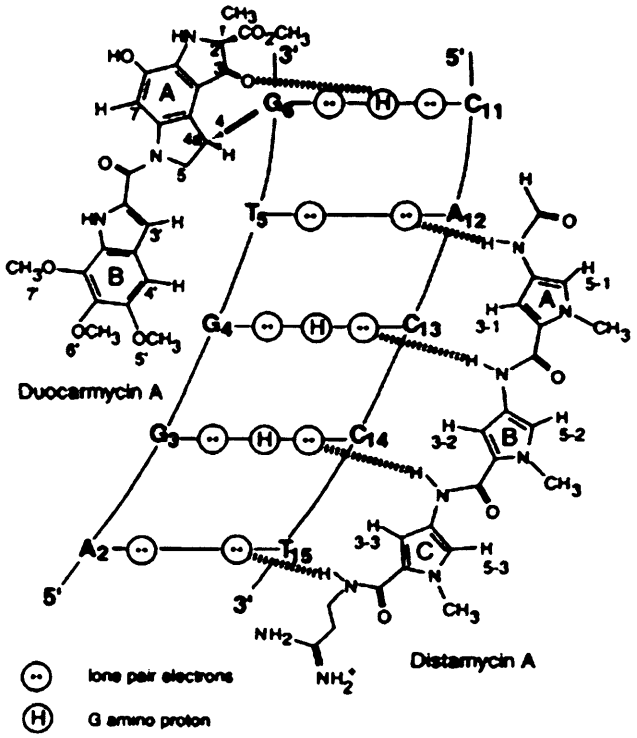

Figure 1.42 Schematic representation of the heterodimeric binding model of duocarmycin A and distamycin to the minor groove of d(CAGGTGGT)-d(ACCACCTG). Hydrogen bonds between the drugs and DNA are in dashed lines. The hydrogen bond between the O3 of duocarmycin A and the N2 amino group of G6 helps anchor the drug in its position (Taken from Sugiyama *et al.*, 1996).

After modulation of specificity was achieved in the presence of appropriate triamides, novel hybrids were created coupling the alkylation subunit of duoacarmycin A (DA) to

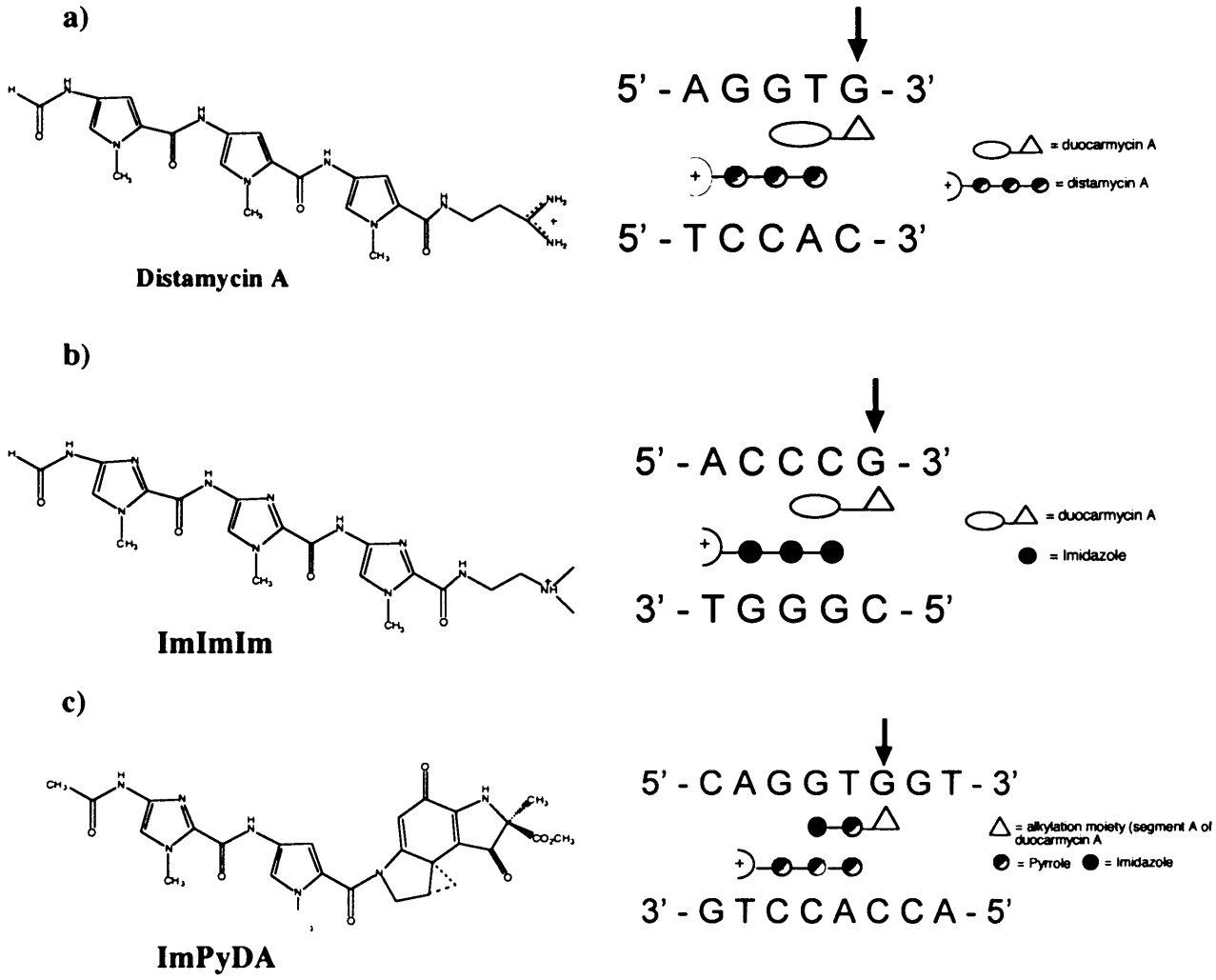

Figure 1.43 The chemical structures of the agents / conjugates and a schematic representation of examples of recognition and alkylation through cooperative binding with distamycin and relevant triamides. The arrows denote the location of alkylation (adapted from Fujiwara *et al.*, 1999).

Py/Im diamides, and targeting the heterodimeric binding with distamycin, efficiently and with high specificity at predetermined DNA sequences (Tao *et al.*, 1999a).

This approach evolved to the rational design of conjugates incorporating the DUMA alkylation moiety into Im /Py hairpin polyamides. Such molecules demonstrated the altered reactivity at guanine and targeted purines proximal to the polyamide binding site (Tao *et al.*, 1999b). Conjugate a of Figure 1.44 exclusively alkylated an adenine of a seven base pairs target site, within a ~ 400 bp DNA fragment.

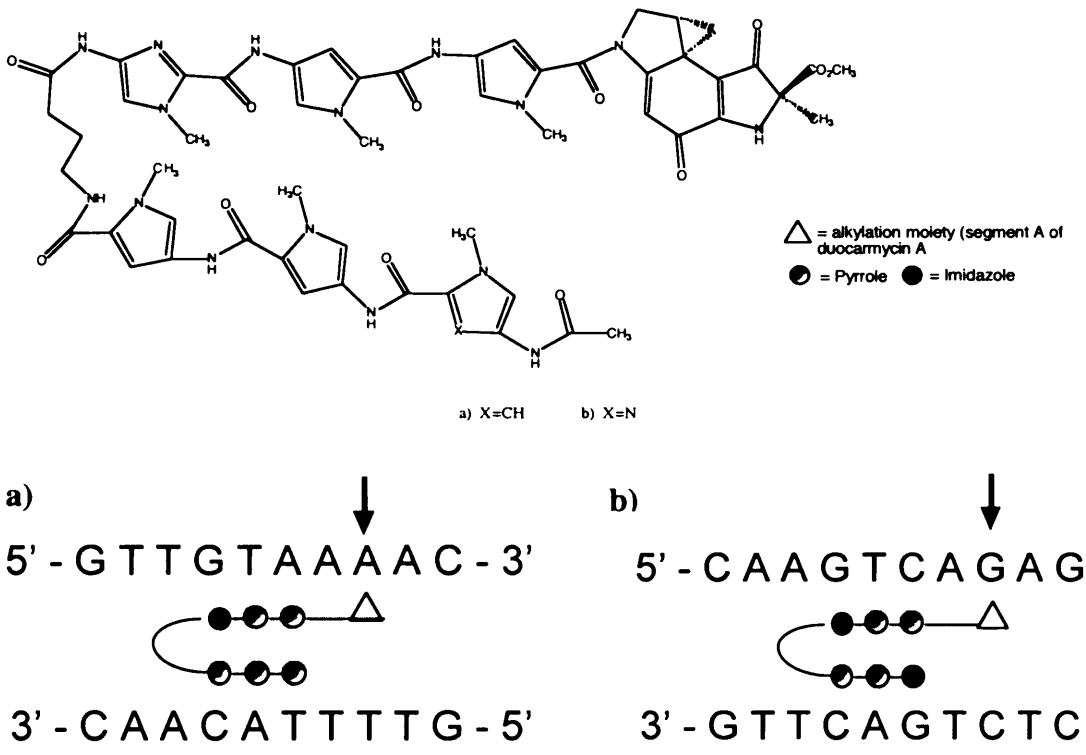

Figure 1.44 Chemical structure and schematic representation of recognition and alkylation of target sequences in oligonucleotides, by conjugates of duocarmycin A alkylation subunit and Im/Py hairpin polyamides. The arrows represent the location of alkylation (adapted from Tao *et al.*, 1999b).

Similarly alkylation by conjugate b occurred exclusively at a G of a target site. Alkylation of target sequences by both conjugates was however of very low efficiency, even after 7 days (Tao *et al.*, 1999b).

The alkylating moiety incorporated in subsequent conjugates was therefore changed to segment A of DU-86 (segA-Du86). That in combination with the introduction of a vinyl linker, dramatically enhanced alkylating efficiency, while a new mode of recognition in which the Im/vinyl linker (L) pair targets GC base pairs, emerged (Bando *et al.*, 2002) (Figure 1.45).

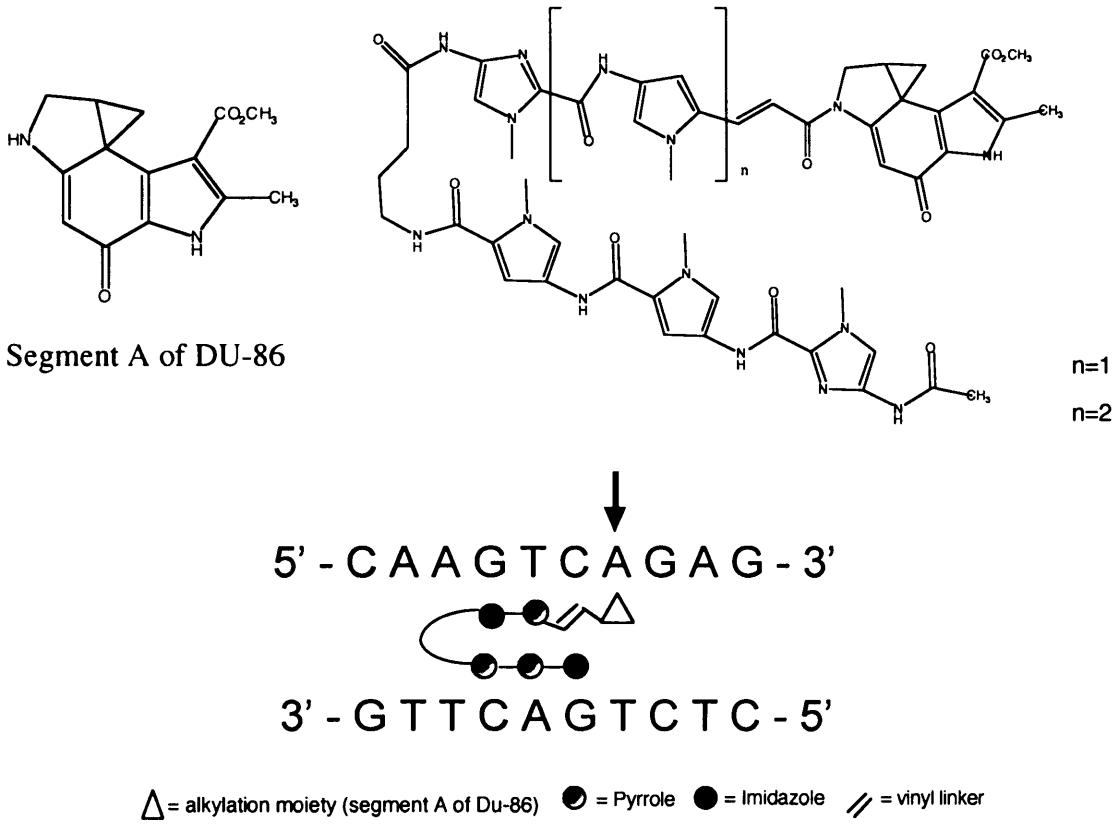

Figure 1.45 Chemical structures and schematic representation of the recognition and alkylation of target sequences in oligonucleotides by conjugates of segment A of DU-86 and Im / Py hairpin polyamides. The arrows indicate the location of alkylation. Adapted from Bando *et al.*, 2002)

More extended hairpin conjugates, such as ImPyPy-γ-ImPyLDu86 (Oyoshi *et al.*, 2003) or PyImImImIm-γ-PyPyPyLDu86 (Takahashi *et al.*, 2003) have also been reported and their biological effect investigated in studies examining inhibition of transcription and targeting of the human telomere repeats, respectively. Such studies further highlight the potential use of Py/Im polymides as versatile recognition components of novel CC-1065 / duocarmycin conjugates.

Another application of the use of the Py/Im polyamides was the design of novel CC-1065/duocarmycin conjugates that could produce highly sequence selective ISCs, and unlike bizelesin which possesses intrinsic sequence selectivity, could target predetermined base pairs. One mode of crosslinking involved DNA dialkylation by the formation of a homodimer by Im/Py diamide-(segA-DU86) conjugates incorporating a vinyl linker. Highly efficient alkylation occured at predetermined sequences, simultaneously on both strands at nanomolar concentrations. Again, the homodimer would dialkylate both strands according to the base-pair recognition rule of the Py/Im polyamides (Tao *et al.*, 2000) (Figure 1.46a). This concept was further extended by synthesising alkylating triamides (Fujimoto *et al.*, 2002).

Crosslinking would also be achieved by covalent dimers of Im/Py and segADu86, connected using different linkers, by the formation of a heterodimer in the presence of a partner triamide (Bando *et al.*, 2003). Interstrand crosslinking proceeds sequence-specifically according to Dervan's pair recognition rule (Figure 1.46b). Alternatively, conjugates were designed bearing two alkylating moieties linked with pyrrole and imidazole bearing polyamides by a flexible methylene chain of variable length, as in the case of a series of bis-(*seco*-CBI)-Py/ Im polyamides (Kumar & Lown, 2003).

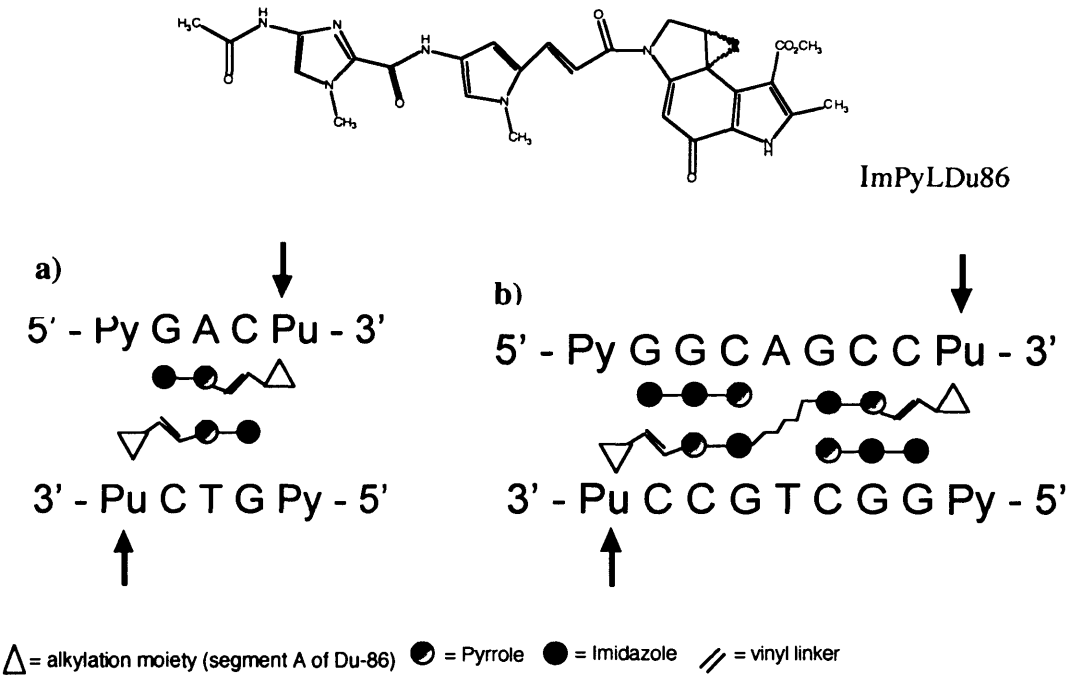

Figure 1.46 The chemical structure of the ImPyLDu86 conjugate and a schematic representation of the recognition mode of the depicted selected oligonucleotides and their crosslinking through the formation of a a) homodimer of two conjugate molecules and b) heterodimer of the covalent dimer of the conjugate, with the ImImPy triamide. The arrows indicate the location of alkylation. Adapted from Tao *et al.*, 2000 and Bando *et al.*, 2003.

CPI – ODN complexes

Racemic CPI has been conjugated to the 3' and 5'-end of 18-mer oligodeoxyribonucleotides (ODN), thereby replacing the B and C subunits of CC-1065

with a much more sequence specific moiety (the ODN). The 3'-CPI-ODN conjugate, once hybridised to a complementary 30-mer target DNA strand, showed highly efficient and rapid alkylation of the complementary strand in the duplex, with the same polarity and preference for AT-rich regions as observed for CC-1065, while remaining totally inactive when incubated with a non-complementary control. This result suggests that CPI-ODNs could be potential candidates as sequence-specific hybridisation-triggered crosslinking agents for targeted gene modification (Lukhtanov *et al.*, 1996).
Conjugation of the non-reactive $CDPI_3$ binding framework of CC-1065 to various ODNs has also been reported. Such conjugates form unusually stable and specific hybrids with complementary DNA in which the tethered $CDPI_3$ group resides in the minor groove (Kumar *et al.*, 1998). ODN conjugates with $CDPI_3$ can make effective primers (as short as 8-10 mers) for PCR amplification (Afonina *et al.*, 1997),
Finally, CPI has been attached to triplex-forming oligonucleotides (TFOs), for triplex-directed covalent modification, in such a way to either reach from the major to a minor groove by wrapping around one DNA strand via long linkers (Lukhtanov *et al.*, 1997) or to "thread" DNA from the major-groove bound TFO to the minor groove binding site of CPI via linkers containing aromatic rings (Dempcy *et al.*, 1999). In the latter case, efficient alkylation of the duplex target was achieved.

Other analogues

Three different glycosides of the *seco*-CI-TMI (Figure 1.47) have been reported, as prodrugs. Glycosides can be cleaved by glycohydrolases in order to release the cytotoxic *seco*-CI-TMI agent. In the presence of the corresponding glycohydrolases, which removed the sugar moiety from the phenolic hydroxy group, all three prodrugs displayed nearly the same cytotoxicity as that of *seco*-CI-TMI. With the exception of the *seco*-CI-TMI-glycoside, which possessed an inherent high cytotoxicity, the two

other prodrugs displayed a highly differential cytotoxicity in the presence and absence of β-galactosidase and α-D-mannosidase (Tietze *et al.*, 2001a).

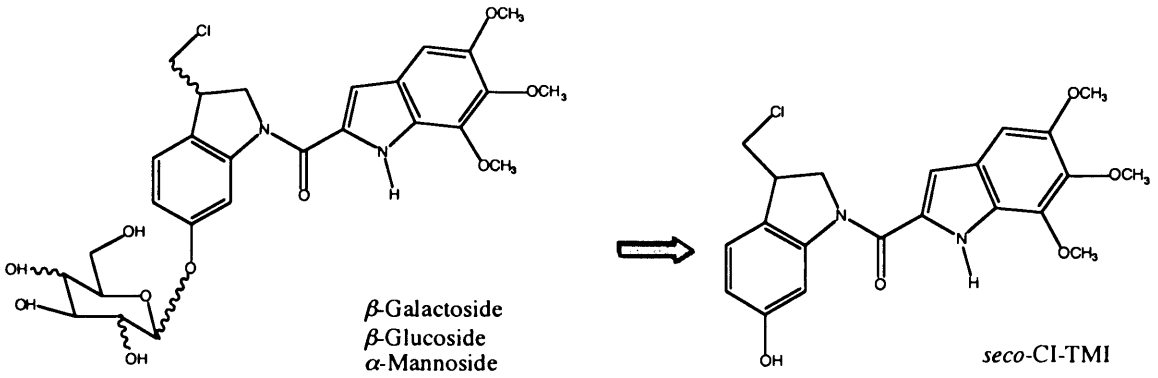

Figure 1.47 Structures of the glycosides – prodrugs and the "released" *seco*-CI-TMI active agent.

Glycosylated prodrugs of a *seco*-CBI and a methyl-*seco*-CBI analogue have also been reported (Tietze *et al.*, 2001b).

In another such effort a conjugate comprised of a cephalosporin and a CC-1065 analogue has been synthesized. Activation of the prodrug to the toxic CC-1065 derivative would in this case be effected by β-lactamase. The preliminary *in vitro* studies show that the prodrug was 10-fold less toxic that the free drug, validating the approach (Wang *et al.*, 2001). Finally, a biotinylated, CBI-bearing CC-1065 analogue was synthesised and its cytotoxicity against U937 leukemia cells assessed (Figure 1.48) (Wang *et al.*, 2002). Although the biotinylated compound was 7-fold less toxic than its unconjugated precursor (IC_{50} values of 0.7 and 0.09 nM respectively), it was still much more potent than doxorubicin (IC_{50} = 100 nM).

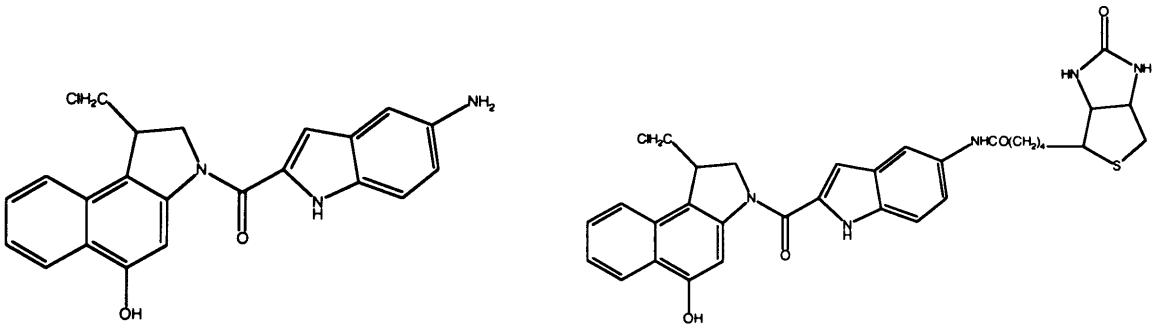

Figure 1.48 Structures of the biotinylated, CBI-bearing analogue (right) and its unconjugated precursor (left).

1.3.4.10 Clinically investigated analogues

Adozelesin (U-73,975) (Figure 1.49) is a synthetic, highly potent, monofunctional, CPI analogue of the antitumour antibiotic CC-1065, Like CC-1065, adozelesin's primary intracellular target is DNA and does not react appreciably with protein, RNA or single-stranded DNA (Weiland & Dooley 1991). A consensus sequence for adozelesin bonding is: 5'-(T/A)-T/A-A, where A is the site of alkylation, while the parentheses indicate a bias but not absolutely required occurrence of those deoxynucleotides (Weiland & Dooley, 1991). Two bonding consensus sequences on genomic DNA have been identified: 5'- (A/T)(A/T)A and 5'-(A/T)(G/C)(A/T)A, where A is the alkylated 3' adenine (Lee *et al.*, 1994). Adozelesin has a broad spectrum of antitumour activity against a variety of murine and human tumour xenograft models and does not produce the CC-1065 characteristic delayed lethality. Because of its solubility, stability and extreme potency, adozelesin was the first of the CC-1065 analogues to enter into clinical trials. A number of phase I trials were conducted, and myelosuppresion was the dose limiting toxicity in all cases (Shamdas *et al.*, 1994, Foster *et al.*, 1996, Fleming *et al.*, 1994). In a study involving 33 patients who had refractory solid tumours,

adozelesin was given at a range of 6-30 μg/m^2/day through a 10min IV infusion, for 5 consecutive days every three weeks. The maximun tolerated dose (MTD) was determined to be at 30 μg/m^2/day. A partial response was observed in a patient with refractory soft tissue carcinoma (Foster *et al.*, 1996). In another study, involving 47 adult patients with solid malignancies, the MTD was defined at 180 μg/m^2. A minor response with a 4 month duration was reported in one previously treated patient with melanoma (Shamdas *et al.*, 1994). In either studies, there was no objective clinical responses.

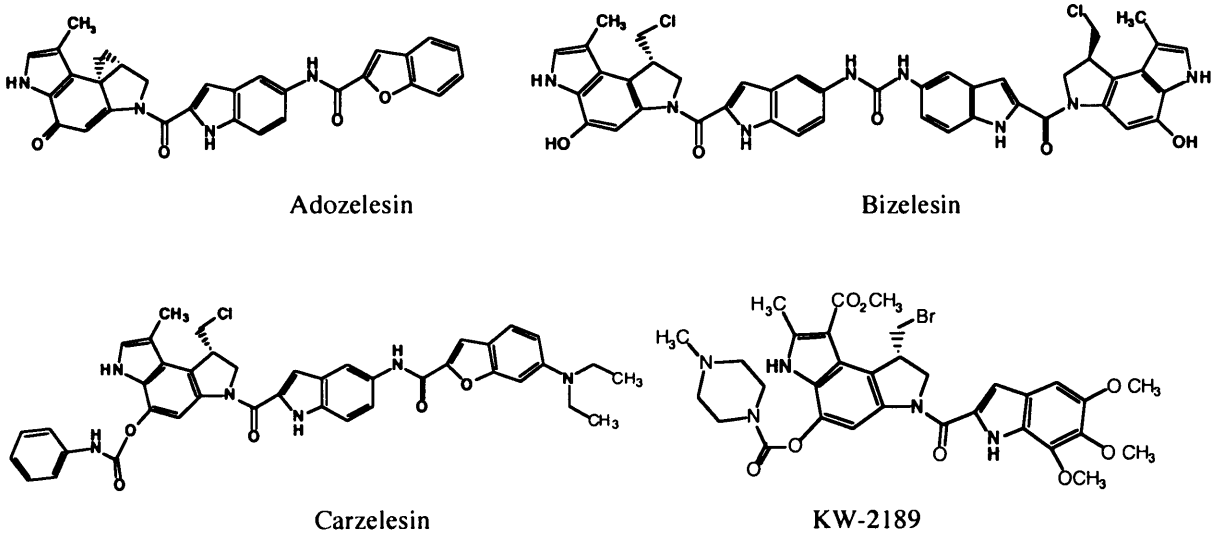

Figure 1.49 Structures of the CC-1065/duocarmycin analogues that have been clinically evaluated; adozelesin, bizelesin, carzelesin, and KW-2189.

Bizelesin (U-77,779, NSC 615291) (Figure 1.49) serves effectively as a prodrug which can form two DNA-reactive cyclopropylpyrroloindole subunits connected by a rigid indole–ureido-indole segment. As a symmetrical dimer, bizelesin is capable of forming ISCs. Bizelesin was active against a broad spectrum of murine tumours and human

tumour xenografts in mice and did not produce delayed deaths at therapeutic doses (Carter *et al.*, 1996). Again myelosuppression was the dose-limiting toxicity. Preliminary testing of *in vitro* myelotoxicity with bizelesin demonstrated significant (>10,000-fold) difference between species (Volpe *et al.*, 1996). A starting dose of 0.1 $\mu g/m^2$/day was chosen for a phase I clinical trial, involving 19 patients. Bizelesin administered every 4 weeks as an IV push was well tolerated with a dose-limiting toxicity of neutropenia. The MTD was defined as 0.8 $\mu g/m^2$, administered once every 4 weeks. However no objective responses were seen in these 19 patients (Pilot *et al.*, 2002). In another phase I study, 62 patients were treated with 185 courses of bizelesin at eight dose levels ranging from 0.1 to 1.5 $\mu g/m^2$. Myelosuppression was the most common toxicity observed. A 40% reduction in measurable disease lasting 24 months was noted in one patient with advanced ovarian carcinoma (Schwartz *et al.*, 2003).

Carzelesin (U-80244) (Figure 1.49) is a synthetic cyclopropylpyrroloindole prodrug containing a relatively nonreactive chloromethyl precursor to the cyclopropyl function. Activation of carzelesin requires two-steps. Hydrolysis of the phenylurethane substituent followed by a ring closure produces the CPI-containing product. In its prodrug form, carzelesin is relatively non-reactive and thus may be capable of penetrating deeper into tissues before being converted to the active species. Although less potent in terms of *in vitro* cytotoxicity, carzelesin proved to be more efficacious than adozelesin, against mouse L1210 leukemia and mouse pancreatic ductal 02 adenocarcinoma (Li *et al.*, 1992).

In a phase I study, carzelesin was given as a 4-weekly 10 min IV infusion to 51 patients with advanced solid tumours. Again the dose limiting toxicity was haematological and consisted mainly of neutropenia and to a lesser extent thrombocytopenia. The MTD for a single course was 300 $\mu g/m^2$ while the dose level with the best dose intensity for multiple courses was 150 $\mu g/m^2$ (Awada *et al.*, 1999).

A total of 140 patients were entered in a phase II trial. The drug was given as a bolus infusion at a 4-weekly dose of 150 $\mu g/m^2$. In general the compound was well tolerated. Myelotoxicity was the most common toxicity. Only one partial response in a patient with melanoma was seen, hence at this dose and schedule, carzelesin did not yield activity in the types of tumours studied (Pavlidis *et al.*, 2000).

KW-2189 (Figure 1.49) is a water soluble, semi-synthetic derivative of duocarmycin B_2. It was designed to be a prodrug requiring enzymatic hydrolysis of the carbomoyl moiety, however research demonstrated that the prodrug itself covalently alkylated DNA without activation of the prodrug to the drug. It was proposed that this mechanism occurs by a rate-determining formation of the reactive cyclopropane in aqueous solution. In a phase I trial involving 22 patients with solid tumours, KW-2189 was administered as a rapid IV bolus daily for 5 days every 6 weeks. Leukopenia, neutropenia, and thrombocytopenia were the dose limiting toxicities. Four patients had stable disease over two to four cycles of treatment and showed no cumulative toxicity (Alberts *et al.*, 1998).
In a phase II trial, 40 patients with metastatic renal cell carcinoma, received 0.4 mg/m^2 as an IV infusion for cycle 1. Cycles were repeated every 5 to 6 weeks with escalations to 0.5 mg/m^2. The most common drug-related toxicity was haematological-delayed neutropenia and thrombocytopenia. No patient had an objective response (Small *et al.*, 2000). Two other concurrent Phase II trials accrued patients with advanced malignant melanoma, with and without prior treatment. KW-2189 was administered IV on day 1 of a 6-week cycle. None of the 15 previously treated patients responded to therapy. Five of the previously untreated patients achieved a partial remission / regression. Response duration ranged from 2.8 to 16.6 months (Svetomir *et al.*, 2002).

Presently, only bizelesin remains under clinical evaluation. Clinical studies on the other three compounds were discontinued. The most significant factor that undermined the

clinical effectiveness of those analogues, still remains a severe nonselective bone marrow toxicity. Therefore the need to design novel analogues is still a very pragmatic one.

1.3.4.11 Yatakemycin

Yatakemycin represents the newest and now most potent (IC_{50} = 3 pM, L1210) member of the CC-1065/duocarmycin class of naturally occurring antitumour compounds. It was isolated from the culture broth of *Streptomyces sp.* TP-A0356, in the course of screening for novel antifungal agents (Igarashi *et al.*, 2003).

Yatakemycin represents a remarkable hybrid of the preceding natural products containing a central alkylation subunit identical to that of duocarmycin SA, a right-hand indole based DNA binding subunit similar to that found in duocarmycin SA and a unique, left-hand binding subunit similar in structure to the central and right-hand subunits of CC-1065, a structure reminiscent of the previously reported synthetic "sandwiched" duocarmycin analogues. Distinct from the preceding natural products, it represents the first naturally occurring member of this class that incorporates DNA binding subunits flanking each side of the alkylation pharmacophore.

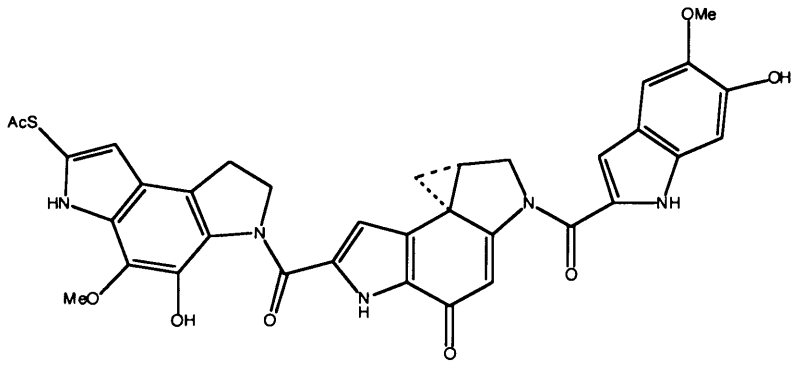

Figure 1.50 Structure of (+)-Yatakemycin.

(+)-Yatakemycin alkylated DNA with a selectivity distinct from either (+)-CC-1065 or (+)-duocarmycin SA/A (Parrish *et al.*, 2003c). All alkylation sites were adenines, flanked essentially exclusively by a 5' and 3' A or T base with a preference that follows the order : 5'-A<u>A</u>A > 5'-A<u>A</u>T ≥ 5'-T<u>A</u>A > T<u>A</u>T, where <u>A</u> is the alkylated adenine. In addition, there was a strong preference, but not absolute requirement for both the second 5' and 3' bases to be A or T. Thus, yatakemycin preferentially alkylates the central adenine of a five base pair AT site (e.g., 5'-AA<u>A</u>AA), differing significantly from (+)-CC-1065 or (+)-duocarmycin SA/A, which alkylate the 3' terminal adenine of a 5 base pair (CC-1065) or 3-4 base pair (duocarmycins) A/T sites (Parrish *et al.*, 2003c). Relative efficiencies of DNA alkylation by yatakemycin, CC-1065 and duocarmycin SA were indistinguishable. Yatakemycin, however, alkylated DNA faster than the other natural products, 1.2-fold faster than the previsouly reported sandwiched analogue CDPI-DSA-CDPI, and 200,000-fold faster than the simple derivative N-BOC-DSA. In addition, like CC-1065, the yatakemycin DNA alkylation is essentially irreversible under the conditions employed, distinguishing it in that respect from the duocarmycins (Parrish *et al.*, 2003c).

1.3.4.12 Consideration of the chiral center in the duocarmycins and CC-1065

One issue of potential concern in the development of novel analogues of CC-1065 and the duocarmycins is chirality. The analogues discussed thus far, all contain a chiral centre. Their enantiomeric pairs can display distinctly different properties ranging from opposite binding orientation in the minor groove (Figure 1.51) to different rates and efficiency of alkylation (Table 1.6), and differing cytotoxic potencies and/or biological outcome in experimental animals (Table 1.5).

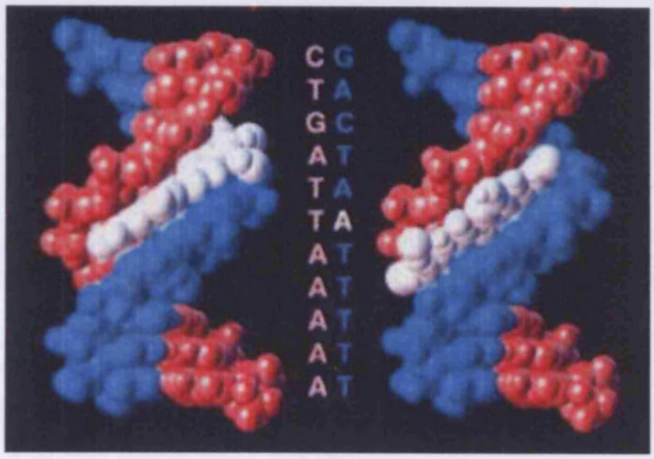

Figure 1.51 Space-filling model illustrating the alkylation at the same site within w794 DNA (duplex 5'-d(GACTAATTTTT)) by (+)-DUMSA (left) and (-)-DUMSA (right). The binding of the natural enantiomer extends in the 3'→ 5' direction from the alkylated adenine, across the sequence 5'-CTA, while the unnatural enantiomer binds in the reversed 5'→ 3' direction, across the 5'-AATT site (taken from Boger & Johnson, 1996).

Agent	IC_{50} (L1210 pM)	Delayed death
(+)-DUMSA	10	no
(-) -DUMSA	100	no
(+)-CC-1065	20	yes
(-) -CC-1065	20	no
(+)-CPI-$CDPI_2$	20	yes
(-) -CPI-$CDPI_2$	20	no
(+)-CPI-In-In	40	no
(-)- CPI-In-In	1000	no

Table 1.5 Cytotoxic potencies and occurrence of the delayed lethality in experimental animals for a number of enantiomeric pairs (Data from Hurley *et al.*, 1990; Boger *et al.*, 1995b).

Agent	rel IC_{50} [a]	rel DNA alkylation [b]
Duocarmycin SA	10	10
Duocarmycin A	≥ 110	≥ 100
CBI-TMI	100	100
CI-TMI	1.0	0.5-2.0

Table 1.6 [a] IC_{50} (L1210) of unnatural (-)/natural (+) enantiomer. [b] Relative concentrations of unnatural (-)/natural (+) enantiomer, required to detect w794 DNA alkylation (taken from Boger & Yun, 1994b).

The differences between enantiomeric pairs have proven clearly distinguishable with simple derivatives of the alkylation subunits themselves (e.g. N-BOC analogues), are most prominent with the dimer based agents (e.g. TMI bearing analogues) and are less prominent or not readily distinguishable with the larger trimer- or tetramer- based agents (e.g. $CDPI_2$ bearing agents). While the unnatural enantiomers in general form intrinsically less stable adducts which are more readily reversed, full biological potency and efficient DNA alkylation have been achieved only with elaborate unnatural enantiomeric analogues that contain two large binding subunits. That is because of the additional noncovalent binding interactions of the extended analogues, which can overcome the destabilising steric interactions of the unnatural enantiomer alkylation (Boger *et al.*, 1995b; Boger & Johnson 1996). The extended unnatural enantiomeric analogues are strikingly differentiated in their biological action, from their naturally occurring counterparts, in that they are devoid of the characteristic delayed lethality phenomenon (Hurley *et al.*, 1990). In agreement with these observations, (-)-CC-1065 alkylates DNA with the same efficiency to that of the natural enantiomer (albeit at a nonidentical set of adenines), exhibits indistinguishable cytotoxic potency and *in vivo*

antitumour activity, and importantly does not cause delayed lethality. The distinguishing behaviour of the unnatural enantiomers is suggested to derive from a pronounced steric interaction of the CPI/DSA C7 (CH_3) or CBI C8 centre with the 5' base adjacent to the adenine N3 alkylation site present in the unnatural enantiomeric 5'→3' binding model. As the steric bulk surrounding this centre is reduced or removed, the distinguishing differences in DNA alkylation efficiencies and biological potencies of the pairs of enantiomers are diminished (Boger & Yun, 1994b). Fully consistent with this proposal is the fact that less distinctions were observed with the CI and DSA enantiomeric pairs, both of which lack substituents or steric bulk at this position (Table 1.6).

In a racemic drug formulation, one enantiomer may affect the activity and the properties of the other enantiomer, and they can exhibit different activities *in vivo* due to varying interactions with their target. The differences displayed by the enantiomeric pairs discussed above, warrants the preparation of enantiomerically pure compounds and full characterisation of their properties. This can be both time-consuming and costly. Importantly, the synthesis of pure enantiomers requires an assymetric synthesis or resolution of racemates, decreasing the net yield.

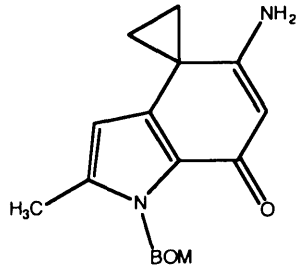

Cyclopropylindolone

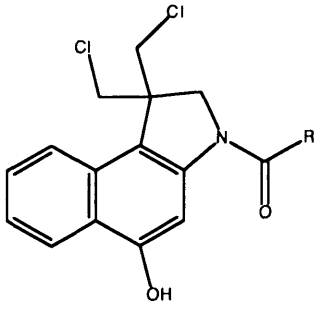

Bischloromethyl-*seco*-C_2BI

Figure 1.52 Structures of the previously reported achiral analogues.

Thus far, only two synthetic efforts of achiral analogues of CC-1065 and the duocarmycins have been reported. One report described the synthesis of a spiro[2,5]cyclopropanecyclohexadienone derivative, but no biological evaluation was conducted (Figure 1.52-left) (Bryson& Roth, 1988). Another effort involved the synthesis of the bischloromethyl-*seco*-C_2BI) subunit (Figure 1.52-right), and its incorporation to various functional analogues bearing the $CDPI_1$, $CDPI_2$, TMI and $indole_2$, DNA binding subunits. The achiral, precursor, *seco*-C_2BI were designed as adenine-adenine interstrand crosslinking agents (Figure 1.25) (Boger & Palanki, 1992; Boger *et al.*, 1993). The C_2BI agents were shown to constitute efficient crosslinking agents. However, in comparison to the parent CBI-agents, the C_2BI analogues proved (100-10,000)-fold less effective at DNA alkylation and less potent in *in vitro* cytotoxic activity (Boger *et al.*, 1993).

1.4 Experimental aims

The aim of chapters 2 and 3 is to evaluate the alkylation properties and cytotoxic activities of a number of novel chiral and achiral CC-1065/duocarmycin analogues. The effect of modification on the non-covalent DNA binding component of chiral agents bearing the established CI functionality as well as the introduction of a novel alkylation subunit as a possible alternative to the established pharmacophore CBI, are being investigated in Chapter 2. The *Taq* polymerase stop assay is employed to reveal the sites of covalent modification by the agents, on plasmid DNA. Comparison of the efficiency and the sequence selectivity of the DNA alkylation by the novel analogues will define the effect these structural modifications have on the sequence specific interactions of this class of compounds with DNA. The thermally-induced cleavage assay is also employed to specifically probe the A-N3 alkylations of the agents in the minor groove of DNA. The MTT cytotoxicity assay is used to investigate the effect of the modifications on the potency of the agents to inhibit the growth of tumour cells.

The effect of the chiral centre present in the natural lead compounds and all the synthetic analogues reported to date, on the biological activity of this class of compounds and their interaction with DNA is investigated in Chapter 3. A series of achiral analogues was synthesised to this effect and are evaluated as the chiral ones, in order to establish whether the chiral centre is absolutely required for the characteristic DNA alkylation and cytotoxicity. The result of this study would confirm whether this synthetic strategy can generate active compounds which could potentially comprise a new class of agents and a new focus for the design of novel CC-1065/duocarmycin analogues.

CHAPTER 2

SEQUENCE SPECIFIC ALKYLATION AND CYTOTOXICITY OF A SERIES OF NOVEL CHIRAL CC-1065/DUOCARMYCIN ANALOGUES

2.1 Materials and Methods

2.1.1 Materials

Investigational compounds

All compounds were kindly provided by Professor Moses Lee, Department of Chemistry, Furman University, Greenville, South Carolina, USA. A minimum of 1 mg of each compound was dissolved in DMA at a 10 mM stock concentration and stored at -20°C until immediately prior to use. Dilutions were freshly prepared for each experiment in 1xTEOA buffer. Adozelesin was a kind gift from Dr. Robert Kelly of Pharmacia & Upjohn.

Plasmid DNA

Plasmid pUC18 was purchased from Sigma, at a concentration of 237 μg/ml and stored at a 10 mM Tris-HCl, pH 8.0, 1mM EDTA storage buffer, at -20°C until use.

Radioisotope

[γ-^{32}P] ATP (5000 Ci/mmol, 10mCi/ml) was purchased from Amersham International.

Chemicals

Tris-hydroxymethyl-methylamine (Trizma® base), ethylemediamine tetraacetic acid disodium salt (dihydrate) (disodium EDTA), boric acid (H_3BO_3), sucrose,

bromophenol blue, xylene cyanol, formic acid, phenol:chloroform:isoamylalcohol (25:24:1), ethidium bromide, magnesium chloride, ammonium persulphate (APS), piperidine, phenol, tetranolamine (hydrochloride), phosphate buffered saline (PBS), sodium acetate, sodium chloride, N,N-dimethyl-acetamide (DMA), dimethyl sulfoxide (DMSO), ammonium acetate, and MTT were purchased from Sigma.
Isopropanol, ethanol, triethylamine ($(C_2H5)_3N$), trisodium citrate, formamide, and concentrated hydrochloric acid were purchased from BDH.
Biogel-P6 gel (fine grade 45-90 μm) was purchased from Biorad.
Electrophoresis grade agarose was purchased from Invitrogen.
Glycogen (20 mg/ml) was purchased from Boehringer Mannheim.
Ultrapure deoxynucleoside triphosphates (dNTPs) solutions (100 mM) were purchased from Pharmacia.
X-Omat (35x43 cm) Kodak film was purchased from Anachem.

Enzymes

T4 polynucleotide kinase (10 units/μl) supplied in 50 mM Tris-HCl (pH 7.6), 25 mM KCl, 5 mM DTT, 0.1 μM ATP, 0.2 mg/ml BSA and 50% (v/v) glycerol was purchased from Invitrogen.
Taq DNA polymerase (5 units/μl) supplied in 50mM Tris-HCl (pH 8.0 at 25°C), 100mM NaCl, 0.1mM EDTA, 1mM DTT, 50% glycerol and 1% Triton® X-100, was purchased from Promega.
Hind III (10 units/μl) supplied in 10mM Tris-HCl (pH 7.4), 250mM NaCl, 0.1mM EDTA, 1mM DTT, 0.5 mg/ml BSA, 50% glycerol was purchased by Promega.
Bacterial Alkaline Phosphatase (BAP), (10 units/μl) supplied in 10mM Tris-HCl (pH 8.0), 120 mM NaCl and 50% (v/v) glycerol was purchased by Invitrogen.

Buffers

Forward reaction buffer (5X) consisting of 350 mM Tris-HCl (pH 7.6), 50 mM $MgCl_2$, 500 mM KCl and 5 mM 2-mercaptoethanol was supplied with the purchased T4 polynuleotide kinase from Invitrogen.

Thermophylic DNA polymerase 10X, magnesium free buffer (when diluted 1:10 it has a composition of 10 mM Tris-HCl (pH 9.0 at 25°C), 50 mM KCl and 0.1% Triton® X-100) was supplied with the purchased *Taq* DNA polymerase from Promega.

10X Restriction Enzyme buffer consisting of 60 mM Tris-HCl (pH 7.5), 1 M NaCl, 60 mM MgCl2 and 10 mM DTT was supplied with the purchased *Hind* III from Promega.

10X Dephosphorylation Buffer consisting of 100 mM Tris-HCl (pH 8.0) was supplied with the purchased BAP from Invitrogen.

Biogel-P6 spin column solution: 8% P-6-biogel (w/v), 0.02% sodium azide (w/v) in distilled and deionised water.

Sucrose loading buffer: 6% sucrose (w/v), 0.04% bromophenol blue (w/v) and 0.04% xylene cyanole (w/v) in distilled and deionised water.

Formamide loading dye: 0.04% bromophenol blue, 0.04% xylene cyanol, 98% deionised formamide.

10X TEOA buffer: 1 mM disodium EDTA, 25 mM triethanolamine, pH 7.2

50X TAE agarose gel running buffer: 40mM Tris, 20mM acetic acid, 2mM disodium EDTA, pH 8.1.

10X Tris-boric acid buffer (TBE): 89mM Tris, 89mM boric acid, 2mM EDTA, pH 8.3.

Stop solution: 0.6M sodium acetate, 20 mM Na_2EDTA, 100 μg/ml Yeast tRNA

Strand Separation Buffer: 30% DMSO, 1mM Na_2EDTA, 0.04% bromophenol blue, and 0.04% xylene cyanol in distilled and deionised water.

DNA size markers

1 kb DNA ladder (1mg/ml) in 10 mM Tris-HCl, pH 7.5, 50mM NaCl and 1 mM EDTA was purchased from Invitrogen.
10 bp DNA ladder (1μg/μl) in 10 mM Tris-HCl (pH 7.5), 1 mM EDTA was purchased from Invitrogen.

Kits

A ready-to-use SequaGel®-6 sequencing system, consisting of SequaGel-6 monomer solution (19:1 acrylamide: bisacrylamide, 8M urea) and SequaGel complete buffer solution (0.89 M Tris borate, 0.89 M boric acid, 20 mM EDTA) was purchased from National Diagnostics.
A Bio101 GENECLEAN® II kit comprising of a 6 M solution of NaI, Glassmilk®, a specially prepared aqueous suspension of proprietary silica matrix, TBE modifier, a proprietary mixture of concentrated salts from removing DNA from TBE-buffered gels, and "NEW wash concentrate", a concentrated solution of NaCl, Tris, and EDTA to which water and ethanol are added, was purchased from Q-biogene.
BESS Mutascan™ Mutation characterisation Kit comprising of d-UTP containing dNTP mix, BESS T-Scan excision/cleavage enzyme mix, BESS G-Tracker modification reagent, a 10X Excision Reaction buffer and a stop/loading buffer, was purchased by Epicentre.

Synthetic oligodeoxynucleotide primers

The synthetic primer 5'-CTC ACT CAA AGG CGG TAA TAC-3', identified as pUC1, binds to the sequence region 749 to 769 of the bottom strand of the pUC18 plasmid and was used to extend the top strand.
The synthetic primer 5'-TGG TAT CTT TAT AGT CCT GTC G -3', identified as pUC5, binds to its complementary (top) strand at position 956-935 and was used to extend the bottom strand.
Both primers were purchased from MWG Biotech, and were used to examine drug-induced damage on the bottom strand of pUC18.

2.1.2 Methods

2.1.2.1.Generation of a 5'-singly end-labelled fragment.

5'end labelling of primer pUC5 with [γ-^{32}P] ATP.

4 pmol of primer pUC5 (stored in a stock of 2 pmol/µl) were 5' end-labelled with 2 µl (20 units) of the purchased stock T4 polynucleotide kinase and [γ-^{32}P] ATP (30 µCi) in 1x forward reaction buffer in a final volume of 10 µl made up with distilled and deionised H_2O (dd H_2O). The reaction mixture was incubated at 37°C for 45 minutes. Following incubation, the labelled primer was placed at a 65°C heat block for 20 minutes to heat inactivate the kinase reaction and was then stored until use at 4°C.

Exponential Primer Extension:

The exponential amplification of the 749-956 region of pUC18 was carried out with the 10 µl of the above reaction mix containing 4 pmoles of the labelled pUC5 and an equal amount of the unlabelled primer pUC1 (from a stock of 2 pmol/µl) specific for the complementary strand. Extension proceeded in a total volume of 50 µl also containing 10 ng of template DNA (linearised pUC18 plasmid, from a stock of 10

ng/μl). 2 μl of dNTPs prepared as a 10 mM mix, 2 μl of the supplied 25 mM stock of $MgCl_2$, 4.5 ml of the 10X stock reaction buffer provided with *Taq* polymerase and 1 unit of the enzyme. PCR was carried out using a PTC-100 Programmable Thermal Cycler (MJ Research) and the cycling conditions consisted of an initial 4 minute denaturation step at 94°C, followed by a cycle of 1 minute at 94°C, 1 minute annealing at 56°C and 1 minute extension at 72°C, for a total of 35 cycles. An unlabelled extension reaction was carried out in parallel.

Purification of the double stranded single-end labelled fragment:

Following amplification of the target pUC18 sequence defined by the two primers, pUC1 and pUC5, 30 μl of ddH_20 were added to the 50 μl of the PCR product and a total volume of 80 μl was loaded onto a Biospin-6 column. The column was prepared immediately prior to use by loading 1 ml of Biospin-6 solution into an empty column, which was then spun at 1200 g to pack and remove residual storage buffer. The packed column was then washed through twice with 200 μl of distilled H_20. The 80 μl of the PCR product were loaded onto the dry column and spun for 5 minutes at 1200 g to elute the end-labelled fragment. The eluant was taken up in 10 μl of 10x sucrose loading buffer and loaded in aliquots onto a 2% agarose gel (dimensions 8 x 10.5 x 1cm) containing 0.4 μl/ml of ethidium bromide, alongside 1 μg of a 1 kb DNA size marker. Electrophoresis was carried out for 2 hours at 50 volts in 1X TAE buffer. At the end of the electrophoresis, the 208 base pair fragment was visualised using UV fluorescence, generation of a single product was confirmed and the band corresponding to the amplified target DNA excised. The DNA fragment was then recovered from the agarose gel slices using the constituent reagents of the GENECLEAN® II Kit, following the manufacture's standard protocol.

2.1.2.2 Thermal Cleavage assay

The thermal cleavage assay described by Reynolds *et al.* (1985), detects adducts susceptible to thermal glycosidic bond cleavage, and in the form employed in our studies, exclusively A-N3 and G-N3 alkylations, which constitute the suspected type of lesions induced by our investigational compounds.

Buffers:

Sodium Citrate buffer: 1.5 mM sodium citrate, 15 mM NaCl, pH 7.2.

Drug:DNA reactions:

The compounds under investgation in each instance, were incubated at various concentrations, with 500 cps of the 5' singly end-labelled fragment of the pUC18, prepared as described above in a TEOA buffer solution (final volume of 50 μl) at 37°C for five hours. Upon completion of the incubation, the reaction mixtures were precipitated with 0.3 M sodium acetate and 3 vol of 95% ethanol, in a dry ice/ethanol bath for 15 min. Samples were spun at 13000 rpm, for 5 min at 4°C. The resulting pellet was washed twice with 200 μl of 70% ethanol and spun for a further 10 mins, at 13000 rpm. After the final wash, the supernatant was removed and the samples were lyophilised to dryness.

Thermally induced cleavage:

It has been established in prior studies by the Boger group, that rapid thermolysis at high temperature (95-100°C), neutral to low pH (6-7) and at low salt concentration, minimizes a potentially competitive reversible DNA alkylation reaction and optimises thermal depurination leading to stoichiometric thermal strand cleavage at the sites of DNA alkylation Conversely, thermal depurination conducted at lower temperature or higher pH (8.0) favoured the retroalkylation reaction. It was also demonstrated that thermal treatment of the alkylated DNA for longer than 30 mins at 100°C does not lead to additional cleavage (Boger *et al.*, 1994b).

The dried samples were taken up in 100 µl of sodium citrate buffer (pH 7.2) and heated at 95°C for 30 minutes. Following heat treatment, samples were chilled in an ice bath, precipitated with 0.3 M sodium acetate and 3 vol of 95% ethanol, spun and lyophilised dry. Samples were finally resuspended in 4 µl of formamide loading dye, heat denatured for 5 minutes at 90°C and cooled on ice prior to loading on a 6% denaturing polyacrylamide gel.

Maxam Gilbert Sequencing Lanes:

A purine specific marker lane was generated using ~1000cps each time, of the same 5' single-end labelled DNA. 20 µl total volume of labelled DNA in ddH_20, was incubated at room temperature for 5 minutes with 50 µl of 95% stock of formic acid. Following incubation, samples were snap frozen with a dry ice/ethanol bath and dried by lyophilisation. The DNA pellet was resuspended in 65 µl of a freshly diluted and kept chilled on ice, 10% piperidine solution and incubated at 90°C for 30 minutes. DNA was then precipitated with 0.3 M sodium acetate and 2 volumes of absolute isopropanol and left on a dry ice bath for 15min. The pellet was spun and washed twice with 80% ethanol and lyophilised dry. Samples were taken up in 4 µl of formamide loading dye and prior to loading onto the polyacrylamide gel, heat denatured at 90°C for 5 minutes and placed on ice until loading.

Polyacrylamide Gel Electrophoresis:

Electrophoresis was carried out on a BioRad Sequi-Gen sequencing gel apparatus using a gel size of 21cm x 50cm x 0.4mm. Gel plates were tightly clamped in a 21 cm casting tray containing a silicone gasket. The 6% polyacrylamide denaturing sequencing gels were prepared from a National Diagnostics SequaGel-6 kit comprised of a ready-to-use SequaGel-6 monomer solution and a SequaGel complete buffer solution. For each gel, 94 ml of SequaGel-6 monomer and 24 ml of complete buffer were mixed with 300 µl of 25% freshly prepared APS solution. Following polymerisation, each gel was prerun with TBE buffer for approximately 30 minutes in order to bring the temperature of the gel up to approximately 50°C.

Once loaded, samples were electrophoresed at 1500-1800V, maintaining the gel temperature at 50-55°C at all times. Each electrophoresis run was terminated when the bromophenol blue marker had migrated approximately 40cm. Gel plates were then separated and the gel peeled away from the back plate using a sheet of Whatman 3MM chromatography paper. An extra sheet of DE81 filter paper was placed underneath and onto the porous gel drying support. Gels were dried under vacuum for 2 hours at 80°C using a Biorad 5850 gel dryer and exposed to X-ray film (X-OMAT, Kodak) overnight. Exposure times for the gels varied, but were on average overnight for both thermal cleavage and *Taq* polymerase stop assay gels, without an intensifying screen.

2.1.2.3 *Taq* Polymerase stop assay

This assay previously described by Ponti *et al.* (1991), is used for the identification of the sites of covalent DNA modification and it is not limited to a single type of DNA lesion, as is the thermal cleavage assay, which is purine-N3 damage specific only.

Plasmid linearization:

The plasmid pUC18 was linearised with the restriction enzyme *Hind* III, which has a unique recognition site at position 399 of pUC18 and will provide a downstream block for the *Taq* polymerase. The 20 μg of the purchased plasmid DNA were linearised with 30 units of enzyme in the provided reaction buffer, for one hour at 37°C. The restriction reaction was terminated with ethanol precipitation and the pelleted DNA was resuspended into an appropriate volume to provide a stock solution of 0.5 μg/10 μl.

In all the *Taq* polymerase stop assay experiments, linearised DNA was used as the template DNA for primer extension. However, it has been previously reported that plasmid DNA in a negative supercoiled state, when linearised with a restriction endonucleose and subsequently treated with adozelesin, yielded a result identical

with that of unrelaxed DNA. Identical sites were occupied by adozelesin at equal intensities in both types of DNA, suggesting that negative supercoils have little, if any, effect on the agent's sequence selectivity (Weiland & Dooley, 1991).

Drug:DNA reactions:

0.5 μg of DNA were used per experimental point and drug reactions were performed in a total volume of 50 μl TEOA buffer. Incubations were for 5 hours at 37°C, followed by precipitation with sodium acetate and 95% ethanol. Samples were washed with 70% ethanol twice and dried by lyophilisation. Drug-reacted DNA was resuspended in 50 μl of ddH_20.

5-end labelling of primer with [γ-^{32}P] ATP:

For examination of the damage on the bottom strand of pUC18, the synthetic primer pUC1 primer was labelled. A standard reaction mix was prepared for 10 samples. For more experimental points, the mix volumes were adjusted accordingly. 5μl of pUC1 (from a stock of 10 pmoles/μl) were incubated with [γ-^{32}P] ATP (30 μCi) and 10 units of polycleotide T4 kinase in 1x forward reaction buffer, in a total volume of 25 μl. Incubation and heat inactivation conditions were as described in the relevant section of 2.1.2.1. Following incubation, the primer reaction mixture was loaded onto a Biospin column, freshly prepared as before. As 5 μl of labelled primer are required per experimental point (i.e. 50 μl for the planned mix for 10 samples), at least 25 μl of ddH_20 are added on top of the 25 μl of the labelling reaction mix so as the collected eluant can provide the required volume of labelled primer which is then aliquoted directly into the primer reaction mixtures.

Primer extension:

In a total volume of 100 μl per sample containing the 50 μl of template DNA (0.5 μg per experimental point), 5 μl of the labelled primer from the eluted stock (5 pmoles) were added, along with 125 mM of each dNTP, 1 unit of *Taq* polymerase, the provided 10x reaction buffer, 2.5 mM $MgCl_2$, and 0.05% gelatin. PCR was

carried out using cycling conditions consisting of an initial 4 minute denaturation step at 94°C, one minute at 60°C and one minute at 72°C, for a total of 30 cycles. After primer extension the samples were precipitated, washed and dried by lyophilisation. They were finally taken up in 4 μl of formamide loading dye prior to polyacrylamide electrophoresis.

Electrophoresis was carried out as described before.

Sequencing lanes

During electrophoresis, the drug reacted DNA samples were run with internal controls with known sequence specificity (such as adozelesin) or sequencing lanes to help identify and appoint the exact sequence on the band corresponding to each polymerase block.

One way for obtaining a sequence reference was the amplification of the pUC1-pUC5 template DNA, with pUC1 being the labelled primer, extending the top strand. The resulting fragment was then subjected to a Maxam and Gibert formic acid treatment, to provide cleavage at purines. When run alongside the *Taq* Polymerase assay samples, this sequencing lane would provide the sequence of the top strand and would therefore be complementary to the sequence of the observed polymerase termination sites at damaged bases situated on the bottom strand.

An alternative method employed in these studies involved utilisation of the BESS Mutascan™ mutation characterisation kit, which allows detection of sites involving thymine (BESS T-Scan system) or guanine (BESS G-tracker system). The BESS T-Scan system detects mutations by incorporating limiting amounts of dUTP into a PCR product. Subsequent treatment of the product results in removal of uracil and cleavage of the phosphodiester bonds at these sites to produce a DNA ladder virtually identical to a "T" sequencing ladder. The BESS G-tracker system involves treatment of a PCR product to modify guanine residues followed by enzymatic cleavage at the modified bases, generating a "G" sequencing ladder.

For the *Taq* stop gel of Figure 2.7 for example, the following procedure was followed:

The primer pUC1 was 5'labelled with [γ-^{32}P] ATP and T4 polynucleotide kinase in a final volume of 10 µl, as described in 2.1.2.1.

Subsequently a PCR amplification reaction was set in a final volume of 25 µl containing 10 ng of the template DNA, 2 µl of the modified dNTPs mix supplied in the kit (dUTP-containing dNTP mix) (200 µM dATP, dTTP, dGTP, dCTP, and 16 µM dUTP final concentrations), 5 pmoles of the reverse primer pUC5 and half the kinase reaction volume (therefore half the amount of the labelled forward primer pUC1, i.e. 2 pmoles). The reaction mixture is then subjected to PCR amplification. Following PCR, 25 µl of dH_20 is added to the PCR products containing dUTP and loaded onto a Biogel column to remove unicorporated radiocactivity. The eluant is then collected and constitutes the probe for the subsequent excision/cleavage reactions.

A. BESS T-Scan Excision/Cleavage Reaction: For a single cleavage reaction containing a total reaction volume of 10 µl, 3 µl of PCR product containing dUTP is incubated with 0.5 µl of BESS T-Scan excision enzyme mix, 1 µl of 10X Excision Enzyme buffer (1X final concentration) and the remaining volume, ddH_20. All the reagents are kept on ice prior to use. Reactions are incubated at 37°C for 30 minutes and terminated with addition of 5 µl of the kit supplied stop/loading buffer (containing xylene cyanol and bromophenol blue like the loading buffer prepared in the lab). The cleavage products can then be run on the polyacrylamide sequencing gel (following heat denaturation prior to loading), alongside the drug-treated, PCR amplified, *Taq* stop assay samples.

B. BESS G-Tracker Excision/Cleavage reaction: 5 µl of the PCR product containing dUTP is incubated with 1 µl of BESS G-Tracker modification reagent and 1 µl of BESS 10x excision enzyme buffer (1X final concentration) in a total volume of 10 µl (the remaining made up with

dH_20). A light box is turned on 5 minutes before using. The reactions are placed on the pre-warmed light box and the following steps are performed:

- Illuminate 5 minutes
- Vortex mix samples for 30 seconds
- Illuminate 5 minutes
- Vortex mix samples for 30 seconds
- Illuminate 5 minutes

An extra 1 µl of BESS G-tracker Excision Enzyme mix is added to the tube and mixed thoroughly. The reactions are incubated at 37°C for 30 minutes and terminated with the addition of 5 µl of the stop/loading buffer.

The cleavage products can then be subjected to electrophoresis after being heat denatured prior to loading

As mentioned before, the results produced by the BESS mutascan kit are virtually identical to the "T" (NESS T-scan) and "G" (BESS G-tracker) lane sequence of the DNA product being analysed. The products generated by the kit's reactions, will migrate approximately 1 base faster than those products generated by dideoxynucleotide sequencing. Approximately 40-50% of the PCR product will remain full length after treatment with the Excision Enzyme mix.

In the case of the gel in Figure 2.7, the labelled top strand was subjected to T and G cleavage using the kit's reactions. The bands visualised on the gel, correspond therefore to "A" and "C" sequencing lanes of the bottom strand. This allows for a direct identification of the covalently modified bases located on the bottom strand.

2.1.2.4 Detection of interstrand crosslinking in plasmid DNA

This agarose gel-based method was previously described by Hartley *et al.* (1991).

Dephosphorylation of linear DNA:

20 μg of pUC18 DNA were linearised by digestion with *Hind* III and taken up in 304 μl of ddH_20. DNA was incubated with 3 μl of Bacterial Alkaline Phosphatase (BAP) (stock of 10 units/μl) and 80 μl of 5X BAP buffer (1X final concentration) in a total volume of 400 μl made up with ddH_20. Incubation lasted for an hour at 65°C. The mixture was then left to cool at room temperature and DNA phenol:chloroform extracted by vortexing with an equal amount of phenol: chloroform: isoamylalcohol (25:24:1), spinning for 5 minutes at 13000 rpm and removing the upper aqueous layer containing the dephosphorylated DNA into a fresh Eppendorf. This was then ethanol precipitated with sodium acetate and 95% ethanol, left for 15 mins in a dry ice/ethanol bath and lyophilised dry. The 20 μg of linearised dephosphorylated DNA were resuspended in a final volume of 40 μl of ddH_20 (5 μg/10 μl) and stored at -20°C.

5'-end labelling of the linearised and dephosphorylated DNA:

10 μl of the above "stock DNA" was radiolabelled with [γ-^{32}P] ATP and T4 polynucleotide kinase in a final volume of 20 μl, as detailed before. The reaction was terminated with the addition of an equal volume of 7.5 M ammonium acetate (NH_4OAc) and 3x vol 95% ethanol. The resulting DNA pellet was further resuspended in 50 μl of 0.3 M sodium acetate and 10 mM EDTA and precipated again with 3x vol of 95% ethanol. Once dry, DNA was redissolved in 40 μl of ddH_20, resulting in a concentration of 125 ng/μl. From this, 8 μl (1μg) of radiolabelled DNA was further diluted in a total volume of 100 μl of 1X TEOA buffer allowing 100 ng of DNA per experimental point, for a 10 samples experiment. For more samples, volumes were adjusted accordingly.

Drug:DNA reactions:

10 μl (containing 100 ng) of the above diluted, radiolabelled plasmid DNA, were treated with a range of drug concentrations in TEOA, in a total volume of 50 μl. Reactions were terminated by the addition of an equal volume of stop solution and

DNA was precipitated by the addition of 3 vol of 95% ethanol. The DNA pellet was dried by lyophilisation and the samples redissolved in alkali loading buffer (6% sucrose, 0.4% sodium hydroxide, 0.04% bromophenol blue). The alkali denatured samples were vortexed well, pulse centrifuged and loaded onto the gel. Control undenatured samples were dissolved in 10 µl sucrose loading buffer and loaded directly on the gel.

Agarose Gel Electrophoresis:

Electrophoresis was performed on 20 cm long 0.8% submerged horizontal agarose gels (20cm x 25cm x 0.5cm; made up by 2.4g agarose in 300 ml 1X TAE buffer) at 20V for 16 hours, in TAE buffer. After electrophoresis the gels were placed onto a sheet of 3MM Whatman filter paper and one layer of DE81 filter paper and dried on a BioRad Model 5850 gel dryer for 2 hours at 80°C. The dried gels were exposed on X-ray film overnight (X-OMAT, Kodak) or until an image of satisfactory intensity was obtained. Densitometry was carried out on a BioRad GS-670 imaging densitometer.

2.1.2.5 MTT cytotoxicity assay

The ability of agents to inhibit the growth of human myeloid leukemia K562 cells in culture was measured using the MTT assay (Mosmann *et al.*, 1983). The original assay was later modified by Carmichael *et al.* (1987) to give better solubilisation of the MTT formazan crystals by using the DMSO solvent.

Cell line and Cell Culture conditions:

The human chronic myelogenous leukameic cell line K562 was grown as a suspension culture at 37°C in an atmosphere of 5% (v/v) CO_2 in RPMI 1640 medium purchased by VWR and supplemented with 5% fetal calf serum and 2 mM glutamine. Cells were maintained at a concentration of between $5x10^4$ and $1x10^6$, within log phase growth.

Drug treatment:

Cells from the culture were spun, their supenatant discarded and diluted in a total volume of 25 ml of fresh serum free medium, at a density of $5x10^4$ cells/ml. This is sufficient for 10 experimental points, each consisting of 2 ml of cell suspension and allowing for pipetting errors. The final number of cells to be plated out per well is $1x10^4$ cells/ml.

The 25 ml of cell suspensions were aliquoted out into 2 ml volumes, in 10 ml tubes. Drug was then added at an appropriate concentration and the tubes were inverted to mix the cells with the agent and then left to incubate for one hour in the dark at 37°C. Drug dilutions were all performed in sterile filtered PBS or ddH_20, with the drug concentrations calculated for a final volume of 2 ml. In a continuous drug exposure experiment cells at this point were transferred to plates. For an 1-hour exposure and following incubation, the tubes were spun down (1200 rpm for five minutes, at 37°C), the supernatant poured off and cells were resuspended in 2 ml of fresh serum-free medium. Tubes were respun, supernatant discarded and cell pellets resuspended in 2 ml of fresh medium with 10% serum. The cells were plated at 200 µl/well, in a 96-well round bottom microtitre plate, allowing 8 wells per sample. The plates were left to incubate for three nights in the dark, at 37°C in a humidified atmosphere containing 5% $C0_2$. The assay is based on the ability of viable cells with active mitochondria to reduce a yellow soluble tetrazolium salt, 3-(4,5-dimethylthiazolyl-2,5-diphenyltetrazolium bromide) (MTT) to a blue formazan precipitate. At the end of incubation, 20 µl of a 5mg/ml solution of MTT in phosphate-buffered saline (PBS) were added to each well and the plates were left to incubate at 37°C for a further 5 hours. The plates were subsequently centrifuged for 5 min at 1200 rpm and the bulk of the medium is carefully aspirated from the cell pellet, leaving 10 to 20 µl in each well. DMSO (200 µl) is finally added to each well and the pellets are completely dissolved in the solvent by mixing, ensuring that no air bubbles form in the wells during resuspension.

The optical density is then read at a wavelength of 550 nM on a Titertek Multican ELISA plate reader. The absorbance reading, an average of the eight wells per sample is calculated as a percentage of the absorbance of the control untreated lane. The IC_{50} values are extrapolated from the percent absorbance versus drug concentration plots, and correspond to the concentration of drug at which the absorbance percentage has been reduced by half.

2.2 C- and N- terminus conjugates of N-methylpyrrole polyamides with *seco*-cyclopropaneindole

2.2.1 Introduction

Distamycin and Netropsin are well studied, naturally occurring oligopeptides that exhibit antiviral activities and reversibly bind at AT rich sites of the DNA minor groove. The reactive moieties of several antitumour compounds have been tethered to the distamycin or netropsin pyrrole-amide framework, to form novel hybrid compounds. DNA binding agents of this type are known as lexitropsins or information reading oligopeptides (Lown, 1988). The rationale has been to use such polyamides as "vectors" for the delivery and targeting of a DNA reactive appendage (e.g. the pharmacophore of an alkylating agent), in an attempt to alter the individual component's mode of interaction with the DNA, or to develop novel properties for the conjugates. This hybrid approach has had varied results. Tethering DNA minor groove binders structurally related to distamycin, to the antitumour antibiotic enediyne, for example, did not yield any increase in potency compared to the enediyne effector alone (Xie *et al.*, 1997). There have been cases where the conjugates lost the activity of the antitumour moiety incorporated, as when combining the anticancer bioreductive mitomycin C with a distamycin-like frame (Paz *et al.*, 1999). In sharp contrast, attachment of the polypyrrolic frame of distamycin A to benzoic acid mustard (BAM) produces the conjugate tallimustine (FCE 24517), which alkylates DNA more efficiently and is more cytotoxic than BAM alone. In this case the hybrid molecule would exhibit new properties, as the tethered benzoyl mustard moiety changed from being exclusively a major groove alkylator (N7 of guanine) to a highly sequence specific minor groove one, when part of the conjugate (Broggini *et al.*, 1995). Enhanced potency was also reported for a distamycin A – Uramustine (uracil mustard) hybrid, compared to each of its individual components, with maximal activity shown by the analogue containing six pyrrole units (Baraldi *et al.*, 2002). Linking a distamycin-like frame with a

podophyllotoxin derivative generated novel agents that were (10-100)-fold more potent than etoposide (Ji *et al.*, 1997). Hybrid molecules containing a PBD moiety and minor groove oligopyrrole carriers (1-4 pyrrole units) have also been designed and evaluated (Baraldi *et al.*, 1999). The hybrids exhibited different DNA binding activity to both distamycin A and PBD, and a direct relationship between the number of pyrroles present in the hybrid molecule and the stability of the DNA/drug complexes was established. Increase in the length of the polypyrrole backbone leads to an increase of *in vitro* antiproliferative activity, with the congugate containing four pyrroles being the most active.

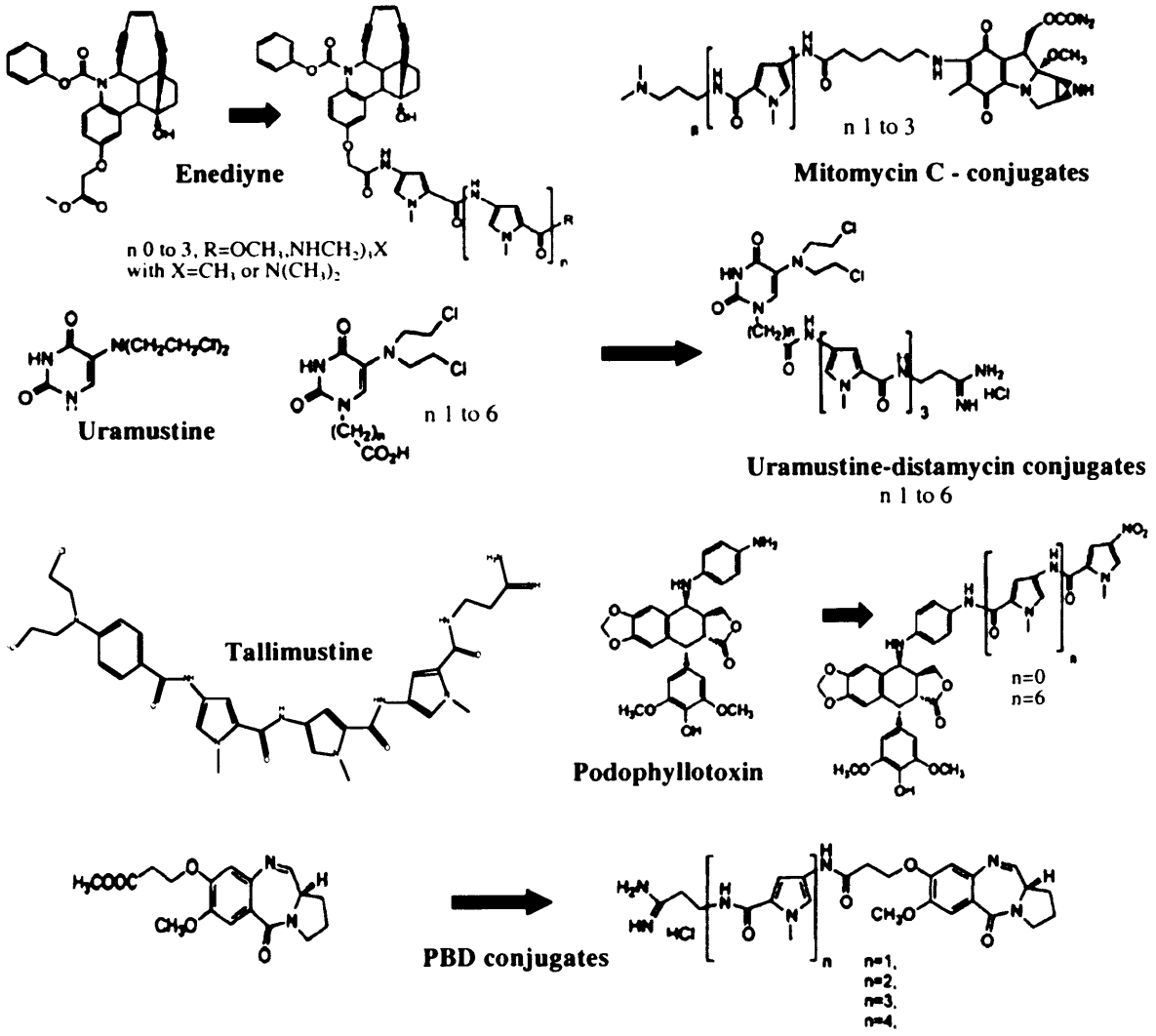

Figure 2.1 Structures of the examples of hybrid molecules mentioned in the text.

The hybrid approach has also been applied for the design of novel CC-1065 analogues. The objective has been to modify the selectivity of alkylation and/or enhance the DNA binding characteristics of the lead compound, aiming to obtain compounds that would retain CC-1065's potency in tumours but would avoid its unwanted side effects. The CPI pharmacophore was the first to be studied due to its natural occurrence in CC-1065. For that reason, the racemic compounds shown in Figure 2.2, were synthesised, retaining the CPI pharmacophore and replacing the B and C subunits of CC-1065, which have been shown to influence DNA binding, with N-methyl pyrrole moieties as the DNA binding domain of the hybrid molecules. Among the synthesised compounds, the two most potent hybrids were the compounds having the CPI unit linked to one or two N-methyl pyrroles via a *trans* double bond (Figure 2.2-d). The propyl end group has also been found to increase the bioactivity of these compounds, which were shown to be extremely cytotoxic (IC_{50} for KB cells of 0.76 and 0.95 fg/L, respectively) (Fregeau *et al.*, 1995; Wang *et al.*, 1996).

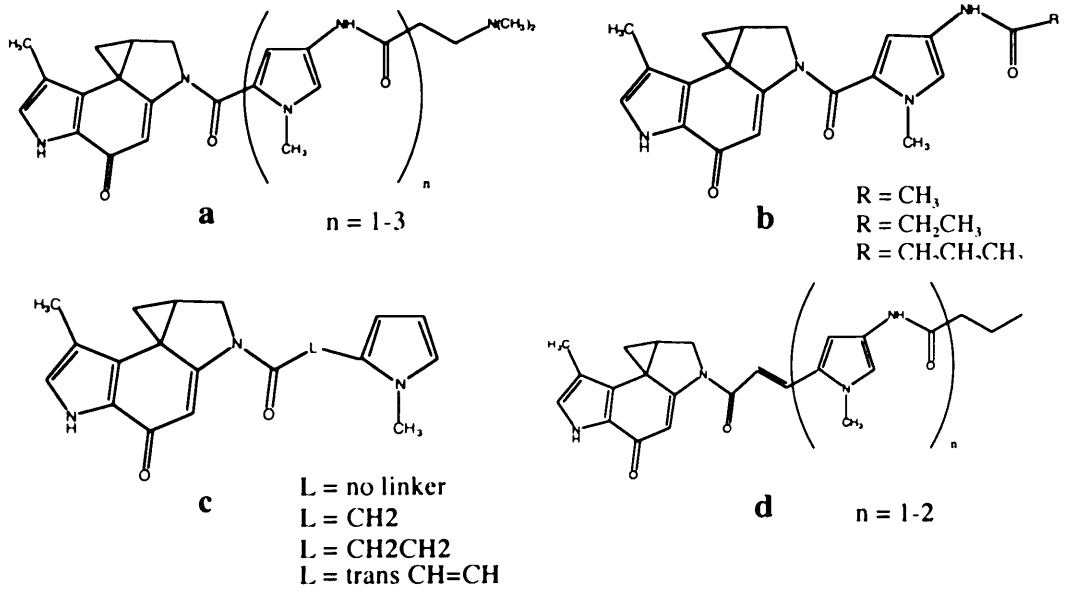

Figure 2.2 Structures of reported N-methylpyrrole conjugates incorporating the CPI alkylation functionality.

DNA cleavage studies revealed that the DNA alkylation selectivity pattern for the synthetic agents of the a category in Figure 2.2, was distinct from that of CC-1065 (Wang *et al.*, 1996). Agents of the d category also had different sequence preference from CC-1065 (Fregeau *et al.*, 1995). The covalent adduct of the racemic conjugate d for n=1, appeared to be quite stable, showing no sign of reversibility as has been earlier reported with other CPI-derived agents.

Individually, CPI and the pyrrole groups, both prefer to non-selectively bind to AT-rich minor groove sequences. When joined together, the CPI-N-methylpyrrole hybrids of Figure 2.2 avoid the major alkylation sites of CC-1065, yet all alkylated minor sites such as 5'-AATA-3'. The alkylation patterns were exclusive at adenines, within the binding site consensus sequence of 5'-N(A/T)(A/T)A-3' (Wang *et al*, 1996).

Other hybrid molecules studied include the enantiomeric pairs in Figure 2.3. In this case, the alkylating moiety chosen was a chemically stable 3-chloromethyl-6-hydroxy-2,3-dihydroindole, which is a precursor of the pharmacophore commonly present in CC-1065 and the duocarmycins. Different sized pyrrole amides were chosen as the DNA minor groove-binding portion of the conjugates. While the hybrid molecules with natural configuration showed moderate DNA-cleaving activity, their unnatural counterparts exhibited potent activities depending upon the length of the binding moiety, drug concentrations and reaction times.

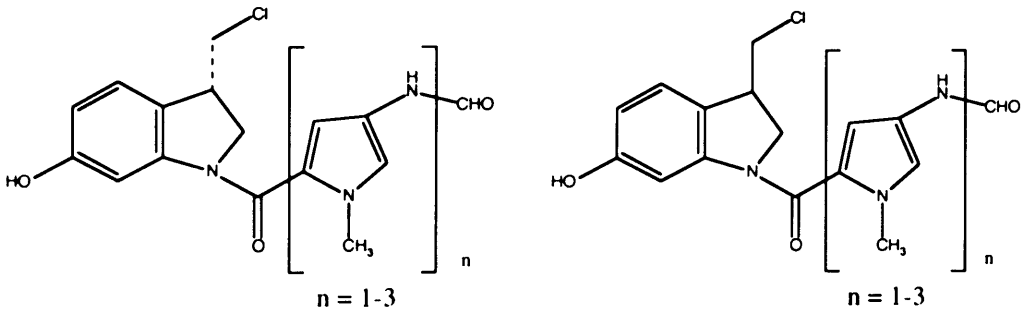

Figure 2.3 Structures of the natural and unnatural sets of the *seco*-CI hybrid agents.

The site of alkylation was shown to be an adenine by DNA cleavage studies. As for the difference in potency of both enantiomers, this was attributed to the closer proximity in the case of the unnatural enantiomer between the least substituted carbon of the cyclopropane and adenine-N3, as derived from molecular models (Shishido *et al.*, 1997).

Another set of reported conjugates involves the combination of an oligopolypyrrolic frame and two pyrazole analogues of the CPI (Figure 2.4, structures 1 and 2).

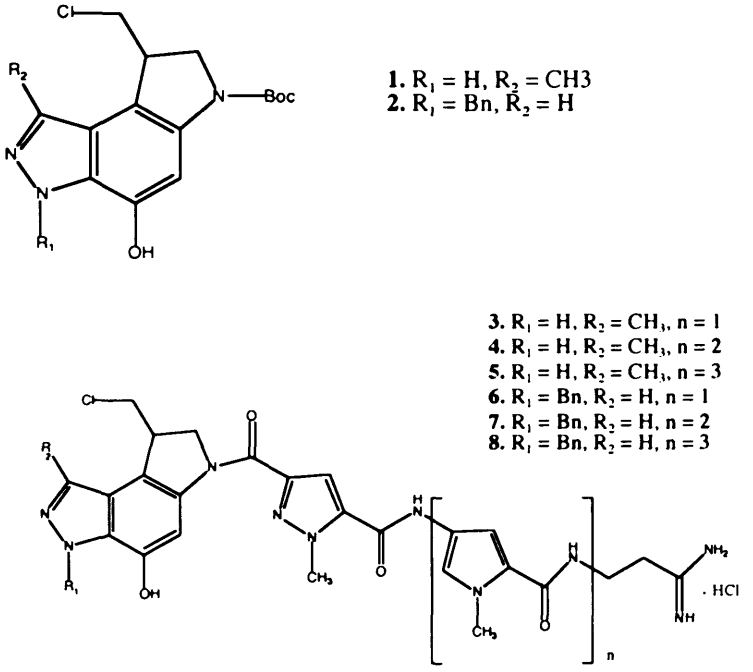

Figure 2.4 Structures of the two pyrazole alkylating moieties (up) and the series of hybrids (bottom) reported by Baraldi *et al.* 2001.

Simplified pyrazole agents (N-BOC-CPzI) showed limited sequence specificity, low affinitiy for DNA and poor water solubility. The objective again was to increase the potency of the pyrazole CPI analogues by increasing their affinity to DNA through tethering these alkylating compounds to DNA minor groove "vectors" such as polypyrrole amides. The hybrid agents 3-8, shown in Figure 2.4 were approximately 8- to 70- fold more potent than the original alkylating unit against five different

cancer cell lines *in vitro*. The group of analogues bearing the benzyl group at the azaindole moiety (6-8) failed to exhibit significant DNA alkylation. However the other hybrids (3-5), lacking the benzoyl group, showed unique DNA sequence specific alkylation in AT rich sequences. The three pyrrolic ring bearing analogue (agent 3) alkylates the denoted underlined adenine, in the sequence 5'-ACAAAAATCG-5', within a 400 bp fragment, eliciting the strongest and most highly sequence specific alkylation activity. This compound was also the most cytotoxic with an IC_{50} of 7.4 nM against L1210 cells (Baraldi *et al.*, 2001).
Synthesis of unsymmetrical bis-lexitropsin-CBI precursor conjugates has also been reported (Jia *et al.*, 1999).

From the above studies, it is highlighted that the hybrid approach can generate conjugates capable of enhanced DNA binding and thus increased cytotoxic activity. In the case of the CPI analogues proposed by Lown, reversibility of alkylation was overcome, while in the case of the pyrazole analogues, a weak effector (N-Boc-CPzI exhibiting 10-fold lower cytotoxicity in L1210 than the reference compound N-Boc-CPI), when tethered with the appropriate binding domain, afforded a hybrid agent both highly sequence selective and more cytotoxic.

2.2.2 Compounds

Three novel racemic conjugates of polyamides and the *seco*-propaneindoline (*seco*–CI) alkylation subunit are studied in this section. Extensive structure-activity relationship studies, as discussed in the introduction, have previously identified CI as the minimum potent and common pharmacophore of CC-1065 and the duocarmycins (Boger *et al.*, 1990b; Boger *et al.*, 1990c).

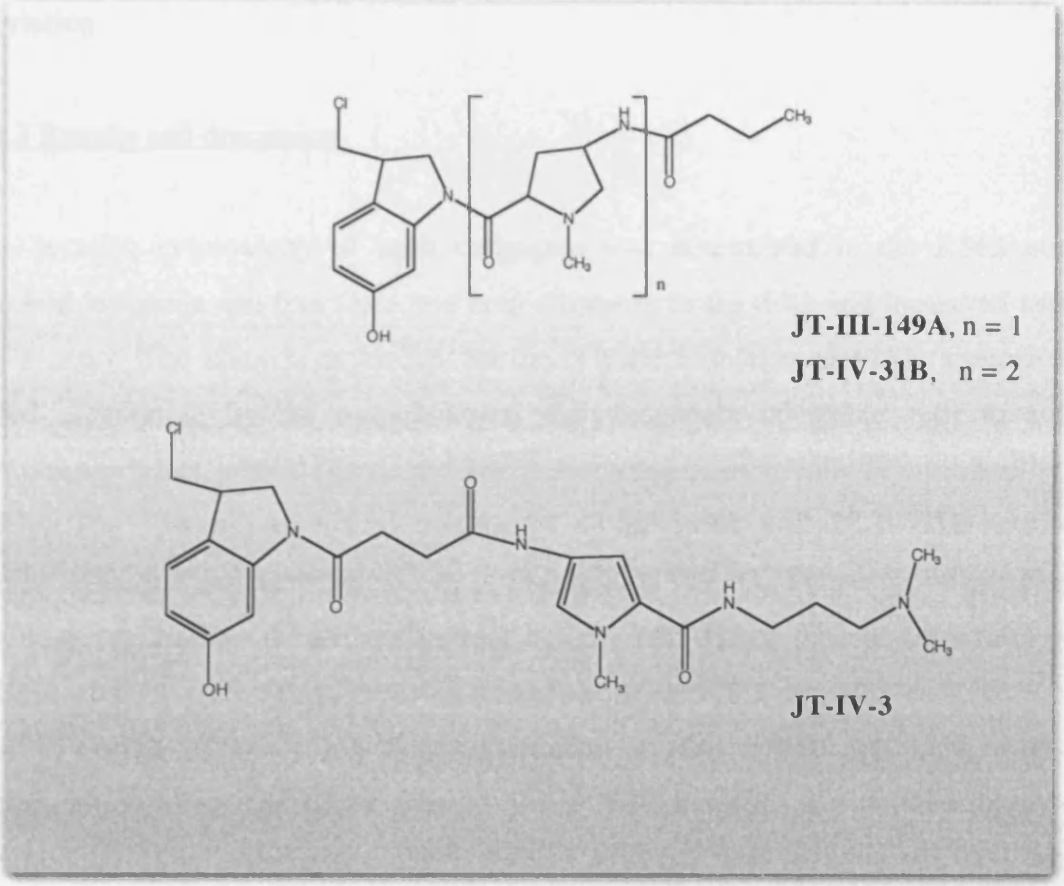

Figure 2.5 Structures of the compounds investigated in this study.

Compounds JT-III-149 and JT-IV-31B consist of a *seco*-CI group attached to the C-terminus of either one or two N-methylpyrrole units, respectively. These compounds are linked to the CI pharmacophore via the carboxylic acid moiety on the pyrrole unit and the amine on the CI. JT-IV-3 in contrast is unique in that the *seco*-CI effector is attached to the N-terminus of a one pyrrole-containing analogue of distamycin. The N-terminus of this compound contains a butanamide moiety. The longer alkyl moiety is incorporated to enhance activity, as previously shown for CPI hybrids (Wang *et al.*, 1996).

The aim of this study was to determine the effect of two structural variations, the size of the oligopyrrole frame and the orientation of the attachment of the alkylating

moiety, on the cytotoxic activity of the conjugates and the sequence selectivity of alkylation.

2.2.3 Results and discussion

The *in vitro* cytotoxicity of each conjugate was determined in the K562 human myeloid leukemia cell line for a one hour exposure to the drug and measured using a MTT assay. The assay is dependent on the cellular reduction of MTT, a tetrazolium based compound, by the mitochondrial dehydrogenase of viable cells to a blue formazan product, which can be measured spectrophotometrically (Carmichael *et al.*, 1987). The C-terminus linked conjugates JT-III-149A and JT-IV-31B exhibited similar cytotoxic potencies as shown in Figure 2.6. The IC_{50} values (corresponding to the dose required to reduce the optical density to 50% of the control value) were extrapolated from the relevant curves and are presented in Table 2.2.

The extension of the DNA binding domain of the hybrid molecule, with the incorporation of an additional pyrrole group did not result in a marked increase in cytotoxicity. The N-terminus linked hybrid JT-IV-3 was substantially less active, despite bearing one pyrrole unit, just like JT-III-149A. JT-IV-3 constitutes the first reported example of a CI-polyamide conjugate with the alkylating moiety attached to the N-terminus of the polyamide. At physiological conditions, this agent would bear a positively charged dimethylpropylamino group. The protonated functionality should increase the conjugate's affinity for DNA, but it has also been suggested that it might actually contribute to reduced cytotoxicic potency by reducing intracellular accessibility. More specifically, conjugates of the "b" class (Figure 2.2) which incorporated uncharged alkyl groups were found to be much more potent towards KB cells than conjugates of the "a" type which bear a protonated dimethylamino group, supporting the view of a reduced cellular uptake of the latter (Wang *et al*, 1996). The lack of activity of JT-IV-3 could also infer that this particular orientation of the alkylating species has a detrimental effect on its ability to interact and alkylate DNA, reflected in its lack of cytotoxic potency.

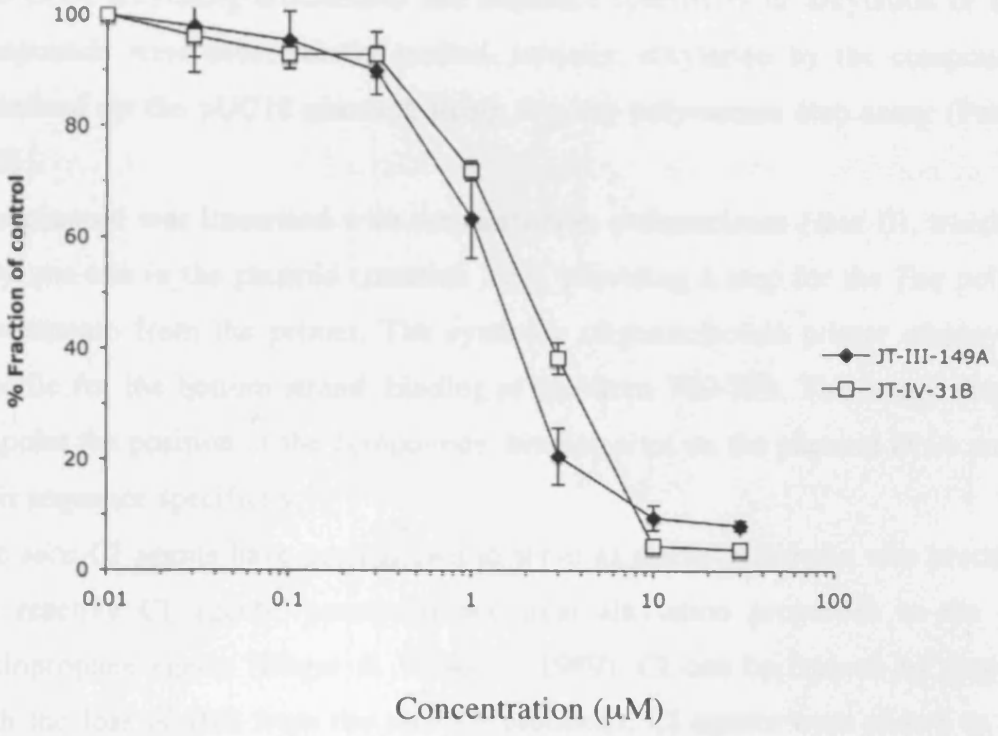

Figure 2.6 Plot of the absorbance as a fraction of the control (untreated cells) versus the concentration of JT-III-149A and JT-IV-31B (in μM). JT-IV-3 is not included as no increase in sensitivity was observed even at a concentration of 30 μM. The error bars represent the standard error of the mean of three independent experiments.

Compounds	IC_{50} values (μM)
JT-III-149A	1.6 ± 0.36
JT-IV-31B	2.1 ± 0.26
JT-IV-3	>30

Table 2.1 *In vitro* cytotoxicity of the three conjugates against human chronic myeloid leukemia K562 cells, following a one hour drug exposure. The IC_{50} values represent the average of three independent experiments and the S.D values are also included.

The DNA alkylating efficiencies and sequence specificity of alkylation of the three compounds were subsequently studied. Initially, alkylation by the compounds was examined on the pUC18 plasmid, using the *Taq* polymerase stop assay (Ponti *et al*, 1991).

The plasmid was linearised with the restriction endonuclease *Hind* III, which cuts at only one site in the plasmid (position 399), providing a stop for the *Taq* polymerase downstream from the primer. The synthetic oligonucleotide primer employed, was specific for the bottom strand, binding at positions 749-769. This assay should help pinpoint the position of the compounds' binding sites on the plasmid DNA and reveal their sequence specificity.

The *seco*-CI agents have been shown to serve as stable *in vitro/in vivo* precursors of the reactive CI agents, possessing identical alkylation properties to the putative cyclopropane agents (Boger & Wysocki, 1989). CI can be formed by ring closure with the loss of HCl from the *seco*-CI precursor. CI agents were shown to alkylate DNA at the same sites as the corresponding CPI based agents but with lower efficiency and less selectivity among the available sites (Boger *et al.*, 1991a).

Figure 2.7 shows the autoradiographs of *Taq* polymerase gels examining the damage patterns of the three agents on pUC18. A predominant site of polymerase stop for all three compounds was the cluster of the five adenines ^{869}5'-AAAAA-3'^{865}, which constitutes one of the reported consensus sequences of CC-1065 (Hurley *et al.*, 1984). Unlike previously reported CPI-N-methylpyrrole hybrids, which avoided the CC-1065 major sites of alkylation, these *seco*-CI hybrid compounds therefore retain the pharmacophore's intrinsic selectivity for its consensus sequence. The sequencing lanes specific for the upper strand were produced by the BESS (Base Excision Sequence Scanning) Mutascan^{TM} Mutation detection and localisation kit, utilising the BESS T-Scan and BESS G-Tracker systems and offering an alternative way for producing sequencing lanes. Due to complementarity, these sequencing ladders can be considered as A and C specific respectively, for the bottom strand which is the relevant strand for the drug induced damage assessment.

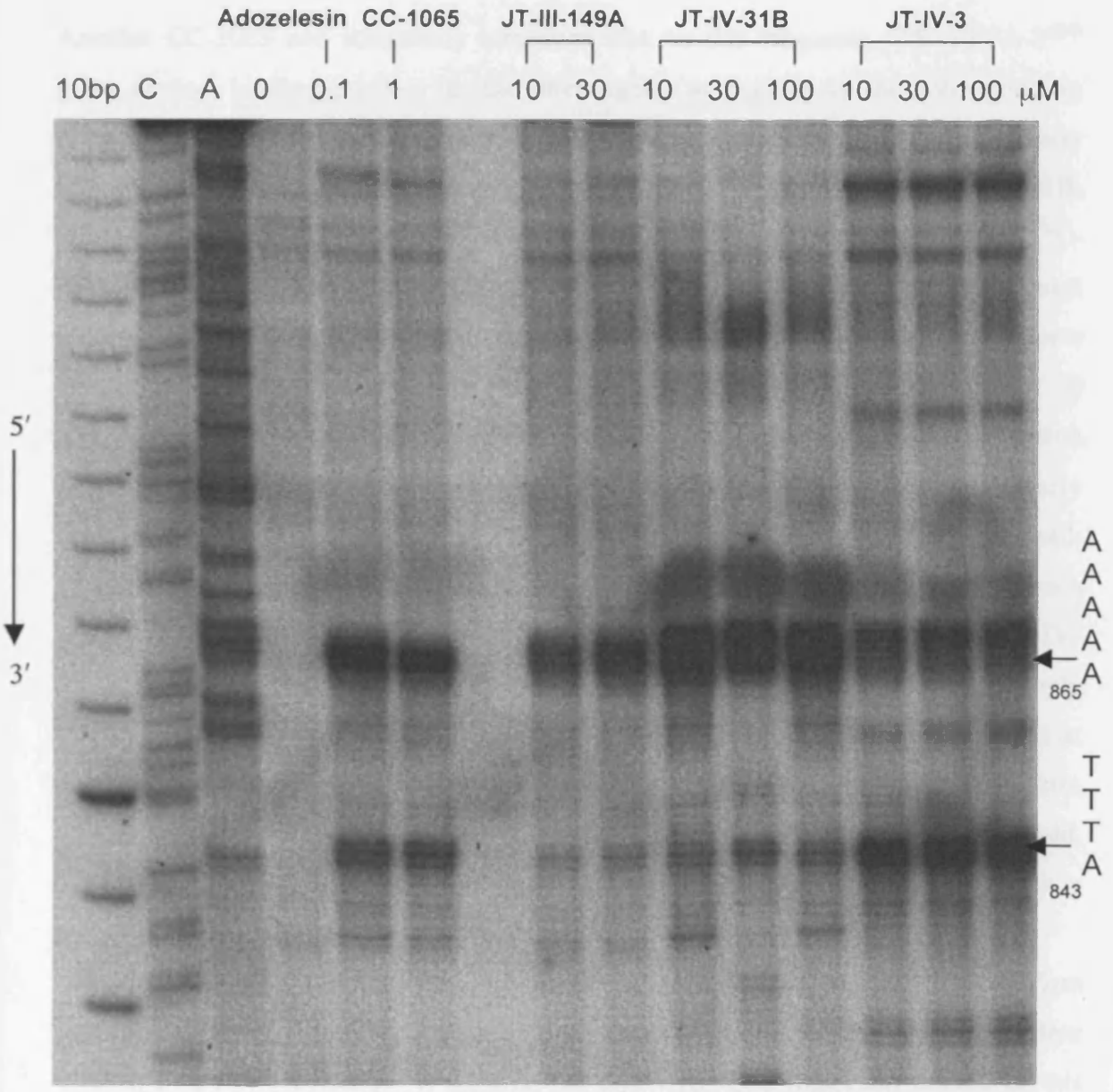

Figure 2.7 Portion of an autoradiograph from a *Taq* polymerase gel examining damage on the bottom strand of pUC18. For comparison, damage induced by 100 nM adozelesin and 1 μM CC-1065 is also assessed. 10 bp is a DNA molecular weight marker, while 0 is the untreated control. C and A sequence lanes refer to the bottom strand. Arrows indicate the positions and sequence of the binding sites. Drug: DNA incubations were for 5 hours at 37°C.

Another CC-1065 and adozelesin alkylation site on this fragment, ^{846}5'-TTTA-3'^{843} gives distinct binding profiles for the three agents as evident by the corresponding cluster of stopping sites. JT-IV-3 alkylates this site at least as efficiently as the cluster of the five adenines and more efficiently than CC-1065 and adozelesin. JT-IV-31B, while there are traces of covalent binding at this site, overwhelmingly favours ^{869}5'-AAAAA-3'^{865} for interaction. Finally, JT-III-149 interacts with the AT site to the least extent of all the agents featured in the gel. At the concentration range of the agents studied in Figure 2.7, considerable damage is induced even at the lowest value of 10 μM. In Figure 2.8 smaller concentrations were used allowing for the early detection and a gradual increase of the damage load on the plasmid. This is particularly important for the ^{846}5'-TTTA-3'^{843} site, which the agents discriminately recognised. The relative reactivity of this site, as judged by the minimum concentration of each agent required for the appearance of polymerase blocks, follows the order JT-IV-3>>JT-IV-31B>JT-III-149A with JT-III-149A barely showing any binding. Strikingly JT-IV-3 binds to this sequence with the same efficiency as the cluster of adenines at 865. Regarding this latter site and the C-terminus compounds, the addition of an extra pyrrole group increased JT-IV-31B's affinity for the site by approximately 10-fold, compared to JT-III-149A. JT-IV-3 binds to this site with an intermediate efficiency compared to the other two.

A thermally-induced strand cleavage study was subsequently performed to confirm the binding of the three conjugates in the minor groove and probe the covalent modifications as alkylations at adenine-N3 positions. One important feature of this strand breakage assay, previously extensively applied for the study of other (+)-CC-1065 analogues, is that the reactivity of the agents for a specific site can be gauged by the concentration of drug required to produce detectable cleavage. Also the extent of covalent adduct formation, as established by this assay, correlated closely with the biological potency of the analogues studied (Hurley *et al.*, 1988b; Hurley *et al.*, 1990).

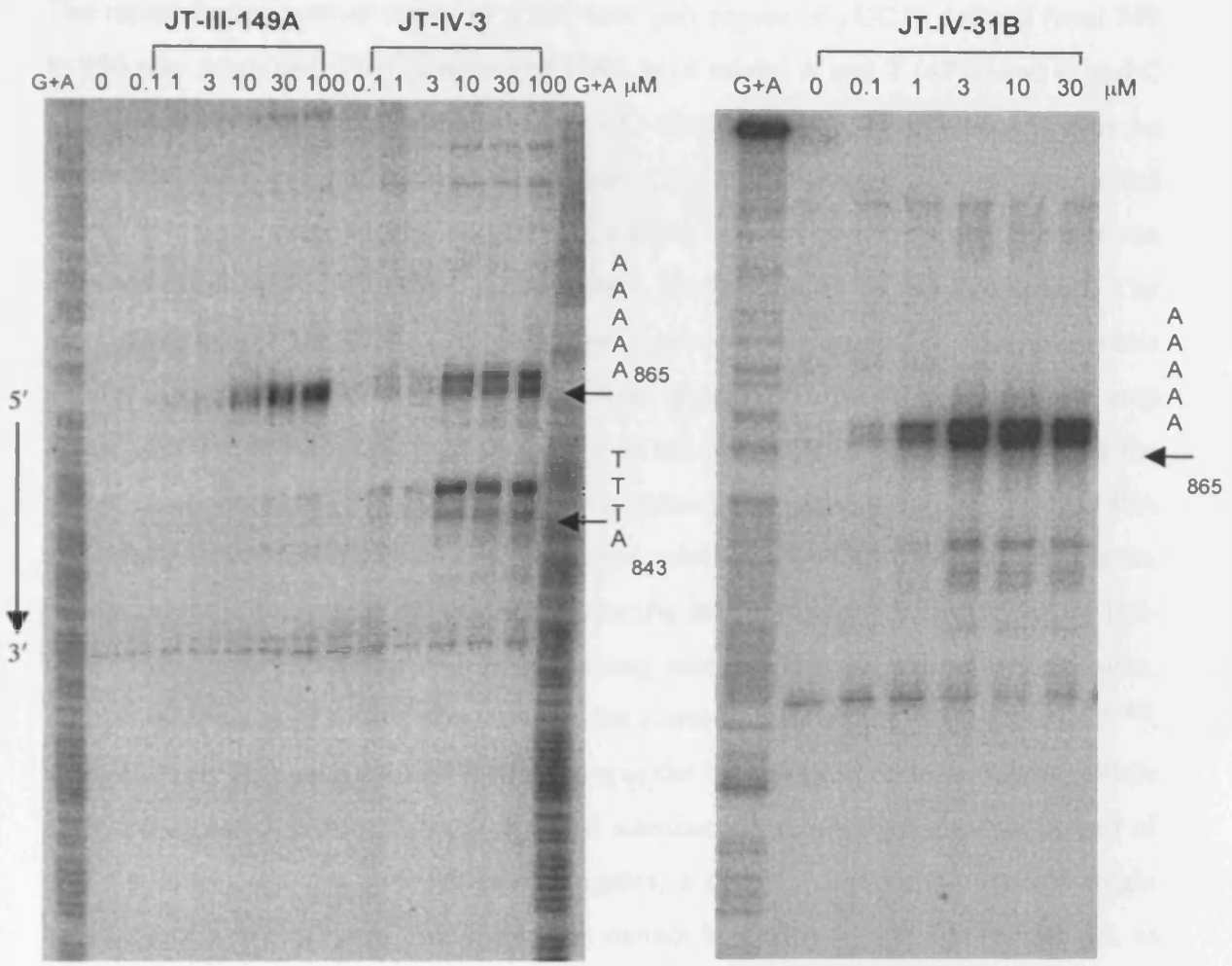

Figure 2.8 Portions of the autoradiographs from *Taq* polymerase gels examining damage to the bottom strand of pUC18, induced by the conjugates JT-III-149A, JT-IV-3 (left) and JT-IV-31B (right), at the denoted concentrations. G+A is the purine marker (formic acid) specific for the 5'-^{32}P radiolabelled, 208 bp fragment of the upper strand of the plasmid. The sequence of the detected bands has been assigned based on their complementarity to the G+A sequencing lane. 0 is the untreated control. Arrows indicate the position and sequence of the binding sites.

The radiolabelled bottom strand of a 208 base pair region of pUC18 defined from 749 to 956 was examined. This sampling of DNA is of mixed A and T (47%) and G and C (53%) base content, contains high affinity CC-1065 sequences (runs of contiguous As and mixed AT sites), and includes the region of the strand employed as a template and visualised in the original *Taq* polymerase studies. This allows for direct comparison between the alkylation profiles of the agents, as determined by the two assays. The autoradiograph of the thermal-cleavage gel is shown in Figure 2.9. The gel reveals similar sites of covalent reaction on DNA as observed in the *Taq* polymerase stop assay. Relative band intensity is indicative of the reactivity of the agents for, and the extent of alkylation of the adenine at which subsequent cleavage occurs. JT-III-149A and JT-IV-31B exhibit an identical sequence selectivity to CC-1065 and adozelesin, on this specific fragment and under the specific incubation conditions, albeit at 100-fold greater concentrations and with varying intensities among the alkylated sites. Again a predominant site of alkylation is the consensus sequence ^{869}5'-AAAAA-3'^{865}, most strongly alkylated by JT-IV-31B, as was the case in the *Taq* stop studies. While for CC-1065 and adozelesin the alkylated adenine is the one lying on the 3' end of this alkylation site, for these three conjugates, a directly adjacent 5' adenine might also be prone to alkylation. However, this cannot be verified on this particular gel, as the fragment examined for damage in this assay and subjected to sequencing is 5'-labelled, and the heat cleavage products containing a modified sugar (Sugiyama *et al.*, 1994) do not comigrate with the fragments produced by the Maxam And Gilbert sequencing reactions, which possess a 3'-phosphate terminus. For the other CC-1065 site, ^{846}5'-TTTA-3'^{843}, JT-IV-3 exhibits the greatest affinity among the conjugates and seems to alkylate the A (843) with the same efficiency as it alkylates the 3' adenine within the A_5 cluster (869-865). Again, the other two agents alkylate this site to a much lesser degree. In all instances, the alkylation sites detected by the thermally-induced cleavage assay, proved to be an alkylated adenine flanked by at least two 5'-A or T bases.

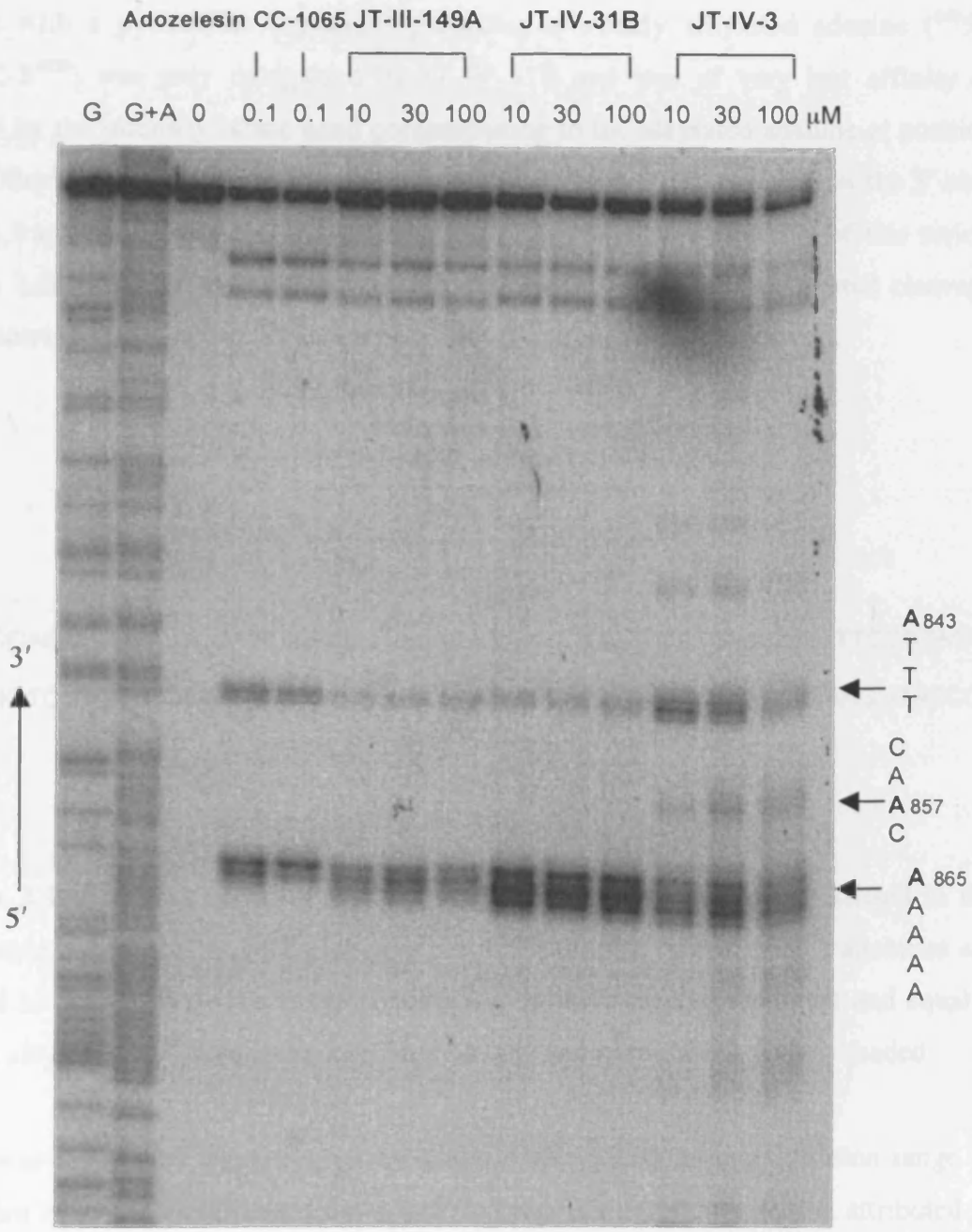

Figure 2.9 Thermal cleavage gel showing purine-N3 lesions to the bottom strand of a 5'-^{32}P labelled 208 bp fragment of pUC18, defined from 749 to 956. G and G+A are the sequencing lanes, specific to the (same) bottom strand. 0 is the untreated control. Thermal cleavage conditions as described in the Methods section. Arrows indicate the position and sequence context of the alkylated adenines (underlined and in bold). Drug: DNA incubations were for 5 hours at 37° C.

A site with a pyrimidine (cytosine) preceding a weakly alkylated adenine (^{858}5'-CAAC-3'^{855}) was only recognised by JT-IV-31B and was of very low affinity as judged by the intensity of the band corresponding to the alkylated adenine at position 857. Other minor alkylation sites specific for JT-IV-3 are also revealed in the 3' side of this fragment, rendering this compound the least sequence selective of this series. Figure 2.10 provides the sequence of the resolvable portion of the thermal cleavage gels showing the adenines alkylated by JT-IV-3 in their sequence context.

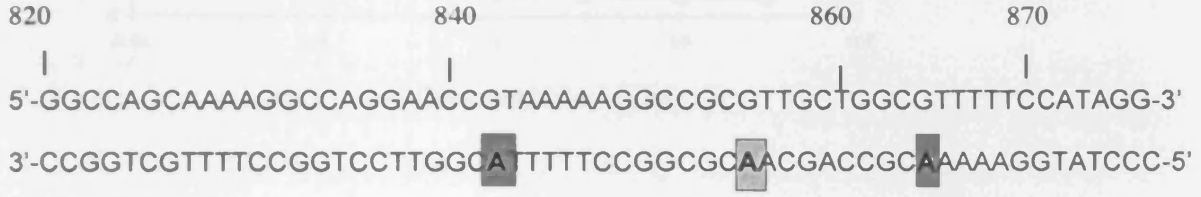

Figure 2.10 Diagram showing the portion of the pUC18 sequence visualised in the resolvable part of the thermal cleavage gel in Figure 2.9. The alkylated adenines are printed in bold. The darker shade denotes a greater affinity by the agent and equally strong alkylation of the specific adenines, as opposed to the weak, lighter shaded.

As it was capable of alkylating naked DNA within the same concentration range as the other two compounds, JT-IV-3's lack of cytotoxic potency could be attributed to poor or slow cellular uptake. A continuous drug exposure, 4 day MTT assay, would help distinguish between the two possibilities. The curves for the three agents are shown in Figure 2.11 and the corresponding IC_{50} values are presented in Table 2.2.

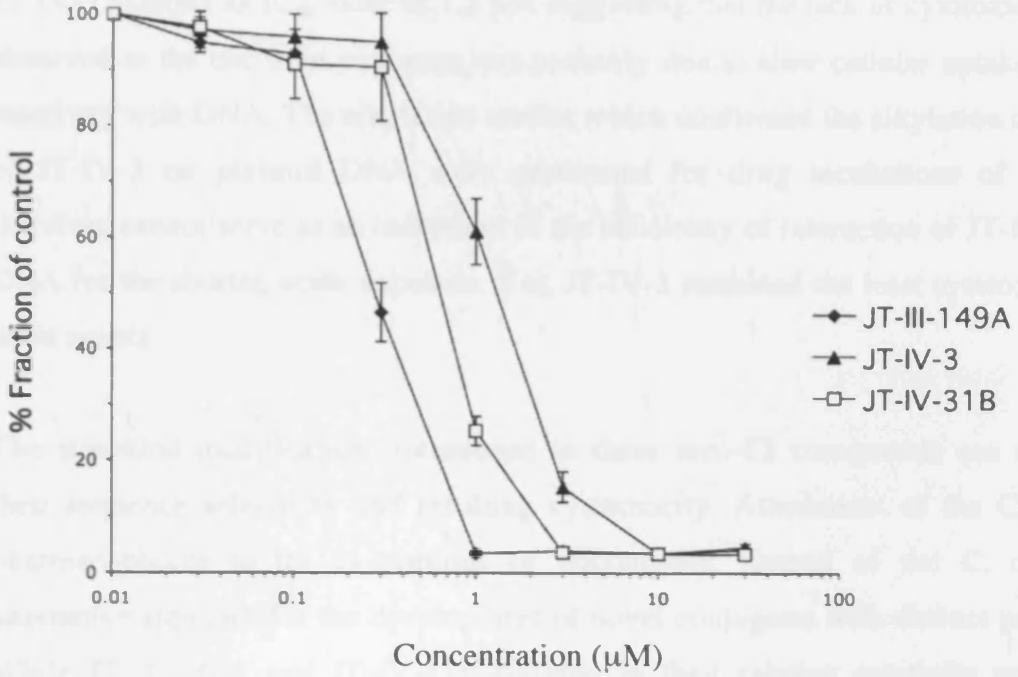

Figure 2.11 Plot of the absorbance as a fraction of the control (untreated cells) versus the concentration of JT-III-149, JT-IV-31B and JT-IV-3 (in μM). The error bars represent the standard error of the mean of three independent experiments.

Compounds	IC_{50} values (μM)
JT-III-149A	0.28 ± 0.05
JT-IV-31B	0.6 ± 0.08
JT-IV-3	1.3 ± 0.26

Table 2.2 *In vitro* cytotoxicity of the three conjugates against human chronic myeloid leukaemia K562 cells, following continuous, 4 days drug exposure. The IC_{50} values represent the average of three independent experiments. The S.D values are also included.

JT-IV-3 exhibits an IC_{50} value of 1.3 μM suggesting that the lack of cytotoxic potency observed in the one hour exposure was probably due to slow cellular uptake or slow reactivity with DNA. The alkylation studies which confirmed the alkylation capability of JT-IV-3 on plasmid DNA were performed for drug incubations of 5 hours, therefore cannot serve as an indication of the efficiency of interaction of JT-IV-3 with DNA for the shorter, acute exposure. Yet, JT-IV-3 remained the least cytotoxic of the three agents.

The structural modifications introduced to these *seco*-CI compounds can influence their sequence selectivity and resulting cytotoxicity. Attachment of the CPI or CI pharmacophores to the N-terminus of polyamides, instead of the C, offers an alternative approach for the development of novel conjugates with distinct properties. While JT-III-149A and JT-IV-31B differed in their relative reactivity among the alkylation sites, the different orientation of the CI appendage to the polyamide of JT-IV-3 produced a compound with alterations in the intrinsic sequence selectivity of the pharmacophore. Even subtle differences in sequence specificity, among structurally related agents, if occuring *in vivo* can have possibly important biological consequences, as proved in early studies between (+)-CC-1065 and the (+)-CPI-indole$_2$ ((+)-U_{71184}, (+)-ABC) and (+)-CPI-$CDPI_2$ ((+)-AB'C') analogues (Hurley *et al*, 1990).

2.3 Furano analogues of Duocarmycin C1 and C2: *seco*-iso-CFI and *seco*-CFQ

2.3.1 Introduction

Since the disclosure of CC-1065 and later the duocarmycins, extensive efforts have been made to define the role of their structural features and subunits in the alkylation event considered to be the source of the agents' biological effect. Part of this effort to determine the fundamental principles underlying the relationships between stucture, chemical reactivity and biological activity was the synthesis and evaluation of key partial structures and modified analogues as well as structurally modified alkylation subunits. A relationship between functional reactivity, solvolytic stability and cytotoxic potency has been established (as discussed in section 1.3.4.5).

As a successful example of modification of the parent CPI pharmacophore, Boger first reported the synthesis of CBI (Boger & Ishizaki, 1990), where the fused pyrrole ring of the CPI is replaced with a fused benzene ring. Incorporation of CBI into functional analogues results in chemically more stable and biologically more active agents than their CPI counterparts. Since increasing the stability of the alkylation subunit has proved a key determinant of the exerted biological potency, another modification to this effect was the replacement of CPI with a fused furan ring, which is metabolically more inert than the pyrrole ring, resulting in the CFI subunit (Mohamadi *et al.*, 1994). One analogue bearing the CFI subunit in place of the CPI was LY296329 shown in Figure 2.12. This agent had identical alkylation selectivity and alkylated DNA at comparable or slightly less effective rate (1-5 times) to (+)-CC-1065. Its unnatural enantiomeric counterpart, LY2979 (figure 2.12) exhibited an alkylation profile essentially identical to that of (-)-CC-1065, alkylating DNA, 33-100 times less efficiently than LY296329. LY296329 was toxic with an IC_{50} of 0.17 ng/mL against human lung epidermoid carcinoma (T222) *in vitro*, but also inhibited the growth of T222 solid tumours in mice by up to 85% at a dose of 0.2 mg/kg, administered IV (Mohamadi *et al.*, 1994). In another study, the

alkylation subunit of (+)-DUMSA was also modified by again incorporating the fused furan ring, generating the *seco*-prodrug LY307918 with the construction of the (chloromethyl)indoline alkylation subunit (Figure 2.12). The natural enantiomer was active at pM concentrations and was 5-70 fold more potent than its unnatural enantiomeric counterpart in *in vitro* cytotoxicity assays (Patel *et al.*, 1997). These studies highlighted the potential of the use of the CFI subunit in the design of novel active analogues of CC-1065 and the duocarmycins.

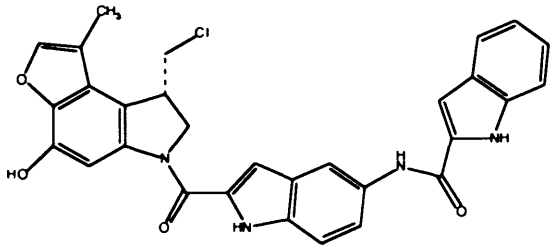

LY29632

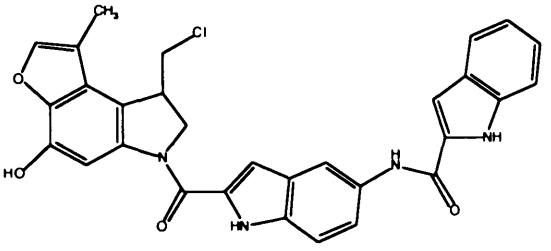

LY29795

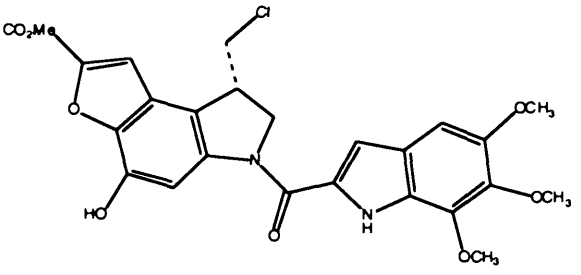

LY307918

Figure 2.12 Structures of the reported analogues incorporating a fused furan ring in the alkylation subunit.

In studies of CPI derivatives, it has been shown that the introduction of electron-withdrawing groups causes a linear decrease in speed of the acidic solvolysis. This in turn, enhances the stability of cyclopropaindolines in plasma and causes an increase in *in vivo* cytotoxic potency. The effects of the introduction of electron-withdrawing groups in the stability of an analogue can vary from significant, as in

the case of N2 substituents (Boger & Yun, 1994), to more moderate or minimal as in the case of a C7 substituent which is *para* to C4 carbonyl (Boger *et al.*, 1996a Boger *et al.*, 1996b). Attachment of an electron withdrawing group to the extended aromatic moiety also improves the chemical stability of the pharmacophore. These findings suggested that the best candidates for drug development would be those analogues with greater electron – deficiency.

2.3.2 Compounds

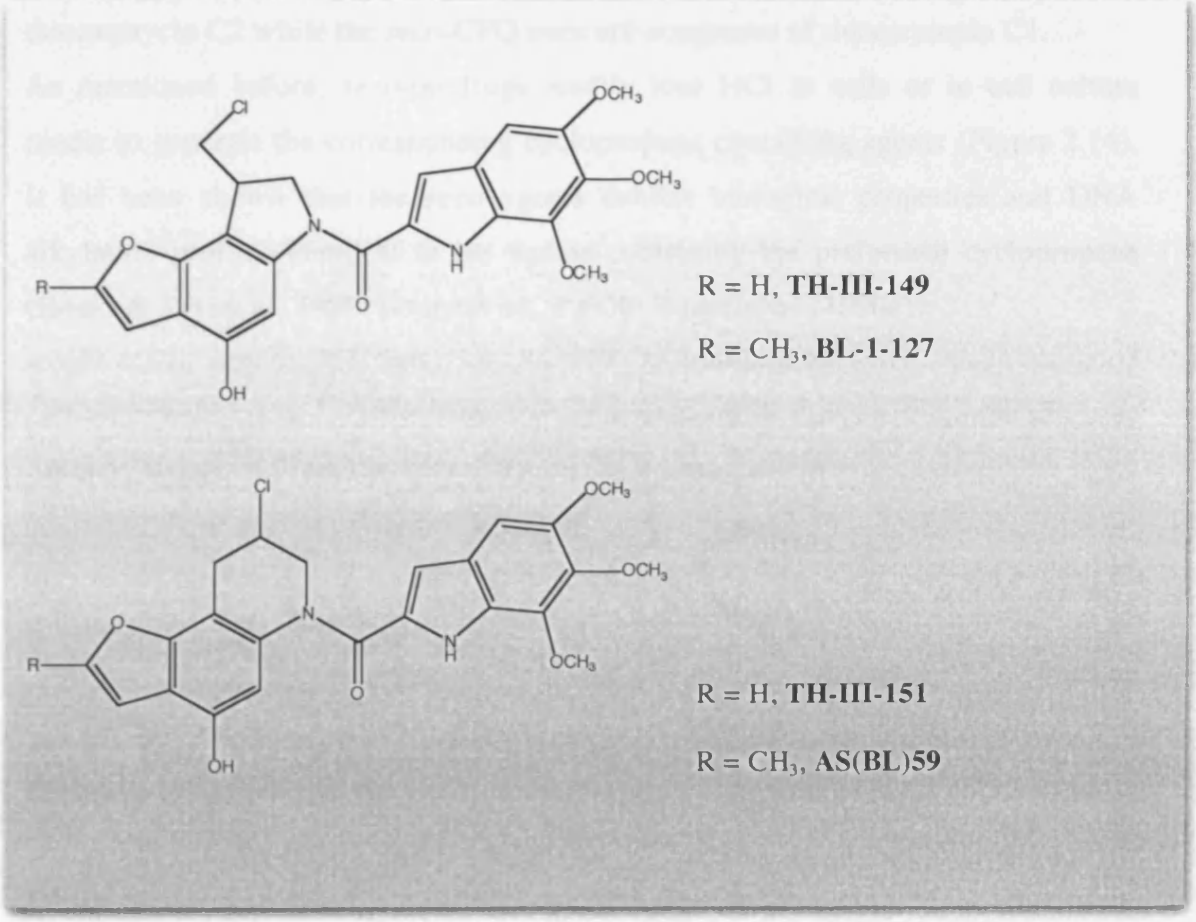

Figure 2.13 Structures of the *seco*-iso-CFI indoline (top) and the *seco*-CFQ quinoline (bottom) compounds along with their respective methylated counterparts.

In the present study, novel racemic *seco*-prodrugs of iso-CFI analogues of duocarmycins are being investigated. This subunit has a fused furan ring in place of the benzene ring of CBI. The difference between these analogues and the previously reported ones (Figure 2.12) lies in the orientation of the fused ring. During preparation, radical cyclisation of the iso-CFI intermediate gave equal amounts of the iso-CFI indoline and quinoline CFQ precursors (Pati *et al.*, 2004). Subsequent conjugation to the TMI moiety provided the indoline (TH-III-149 and BL-1-127) and quinoline (TH-III-151 and AS(BL)59) analogues of the duocarmycins as shown in Figure 2.13. More specifically, the *seco*-iso-CFI compounds are analogous to duocarmycin C2 while the *seco*-CFQ ones are congeners of duocarmcyin C1.
As mentioned before, *seco*-prodrugs readily lose HCl in cells or in cell culture media to generate the corresponding cyclopropane containing agents (Figure 2.14). It has been shown that the *seco* agents exhibit biological properties and DNA alkylation profiles identical to the agents containing the preformed cyclopropane (Boger & Wysocki, 1989; Boger *et al.*, 1990b; Boger *et al.*, 1990c).

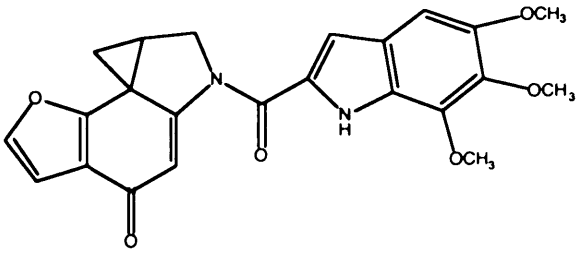

Figure 2.14 Stucture of the ultimate cyclopropane containing iso-CFI-TMI agent.

The ultimate alkylating agent iso-CFI was designed on the basis that the attachment of the furan ring containing the electron withdrawing oxygen atom would stabilise the cyclopropylindoline functionality toward nucleophiles. The extension of the CI unit with inclusion of the furan ring, should, as in the case of the extension of CI to CBI, enhance chemical stability and cytotoxicity.

Many antitumour agents act by crosslinking DNA. Synthetic compounds containing two CPI moieties and able to interstrand crosslink DNA, have been shown to be significantly more potent than CC-1065 both *in vitro* and *in vivo* (Mitchell *et al.*, 1989; Mitchell *et al.*, 1991). Cyclopropaindolone dimers are exemplified by bizelesin which proved both more sequence selective and cytotoxic than the monomeric agents it derived from and is the only CC-1065 analogue to be still undergoing clinical trials. Synthesis and biological evaluation of *seco*-CBI dimers bearing flexible methylene linkers (Jia & Lown, 2000) and *seco*-CBI with pyrrole and imidazole bearing polyamide conjugates (Kumar & Lown, 2003) have been previously reported. In an attempt to improve the potencies of the novel furano analogues, two N3-N3 dimers, shown in Figure 2.15 were synthesised and evaluated.

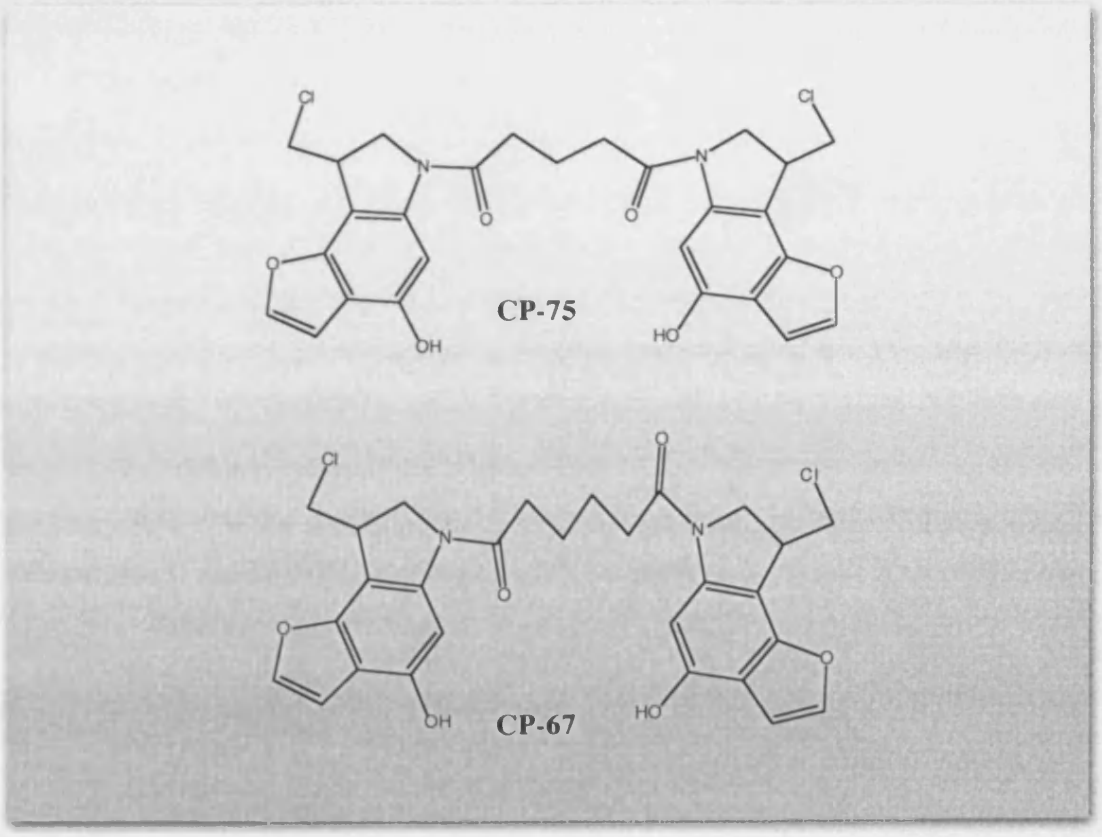

Figure 2.15 Structures of the N3-N3, *seco*-iso-CFI dimers incorporating a linker of 3 (top) and 4 (bottom) carbons.

Finally, the *seco*-CBI-TMI agent in Figure 2.16 has also been included as a control in some cases, for comparison.

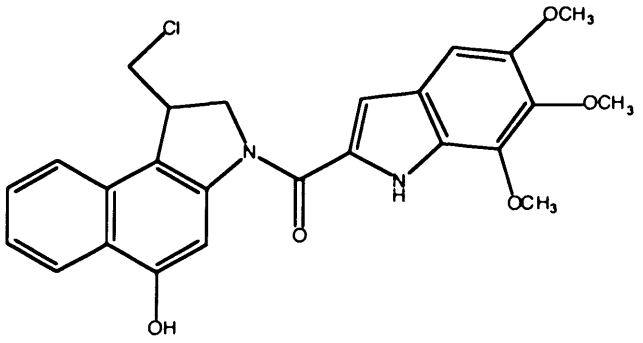

Figure 2.16 Structure of the reference compound *seco*-CBI-TMI (Boger & Yun, 1994; Atwell *et al.*, 1997).

2.3.3 Results and discussion

The sites of covalent modification induced by the compounds under investigation, were examined using the *Taq* polymerase stop assay. The same set of sequences that react with adozelesin, also reacted with the four furano analogues. Figure 2.17 shows the polymerase stop sites induced by the binding to DNA of adozelesin, the *seco*-CFQ agent, TH-II-151 and its methylated counterpart, AS(BL)59. The predominant site of drug binding for all three compounds is the cluster of five adenines at positions 865-869 which constitutes a (+)-CC-1065 consensus sequence. While the sequence selectivity of covalent alkylation for the two investigational agents is indistinguishable, the intensity of the DNA modification is much greater for TH-II-151. The A_5(865) cluster is far more reactive to this agent, judging by the at least 10-fold greater concentration required for AS(BL)59 to induce detectable damage at that site, and still not at a level comparable to TH-III-151. The presence of the methyl substituents should provide compounds AS(BL)59 and BL-1-127 with added stability. Incorporation of the methyl group in the iso-CFI pharmacophore should provide rigidity between the two portions of the molecule

(iso-CFI and TMI) and enhance the DNA-binding activation of the agent towards alkylation at the N3 of adenine. As in the case of the left-hand subunit C6 methyl ester of (+)-DUMSA and the C7 substituent of CBI-TMI analogues, simply the presence of the methyl which extends the length of the rigid furanoindole group, would cause upon binding, a larger angular twist between the alkylation pharmacophore and TMI, and should serve to enhance DNA alkylation efficiencies and biological properties (Boger & Garbaccio 1999a). Yet, as shown in Figure 2.17, the methylated CFQ agent, AS(BL)59 has poor alkylation capabilities.

Figure 2.18 shows the gel of another *Taq* polymerase stop assay which also features the *seco*-iso-CFI indoline analogues. In this case, the methylated iso-CFI agent, BL-1-127 has an indistinguishable alkylation profile (regarding both selectivity and intensity) to TH-III-149. It produces equally strong, dose-dependent bands at the ^{869}5'-AAAAA-3'^{865} binding site. In the same gel, AS(BL)59 again demonstrates limited alkylation efficiency.

The thermally-induced strand cleavage assay was subsequently performed to confirm the covalent interaction of the furano analogues with the N3 position of adenine bases in the minor groove.

The probe DNA sequence was obtained from PCR amplification of base pairs 749-956 of the linearised with *Hind* III, pUC18 plasmid, so that it contains the DNA fragment previously visualised and examined with the *Taq* polymerase gels.

Figure 2.19 shows the autoradiograph of a thermal cleavage gel confirming the ability of TH-III-149 and TH-III-151 to recognise and alkylate the 3' adenine of the ^{869}5'-AAAAA-3'^{865} site with similar efficiencies. The pattern of alkylation was similar to that produced by the reference compound *seco*-CBI-TMI. However, the *seco*-CBI-TMI agent slightly differentiates in its ability to alkylate adenines even at the lower concentration employed, at the AT site ^{794}5'-TTAT-3'^{791} and the ^{861}5'-CAAC-3'^{858} site.

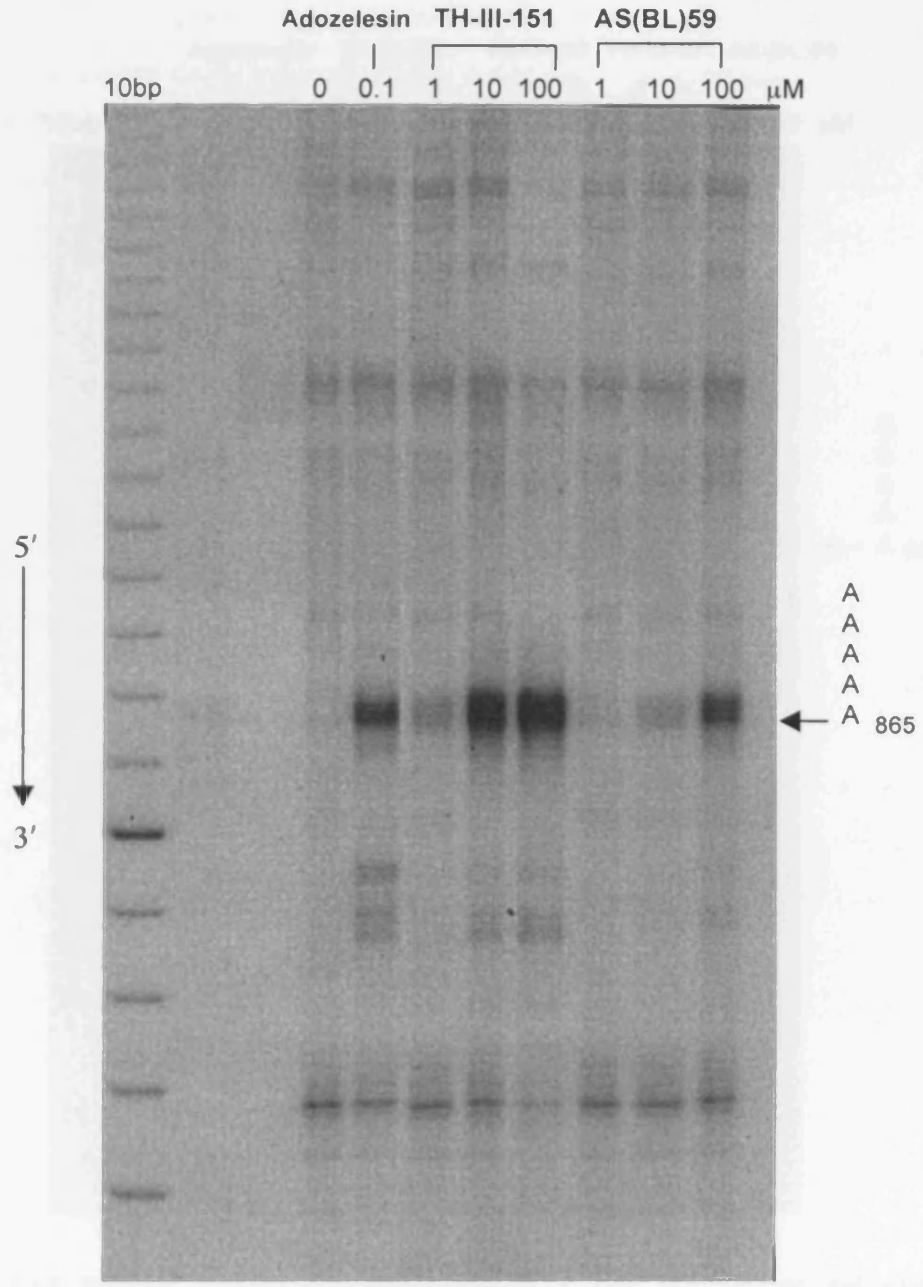

Figure 2.17 Portions of the autoradiograph of a *Taq* polymerase assay gel examining damage to the bottom strand of pUC18, induced by the *seco*-CFQ agent, TH-III-151 and its methylated counterpart AS(BL)59, at the denoted concentrations. Adozelesin was included as an internal standard. 10bp is a DNA molecular weight marker. 0 is the untreated control. The arrow indicates the position and sequence of the common major binding site. Drug: DNA incubations were for 5 hours at 37° C.

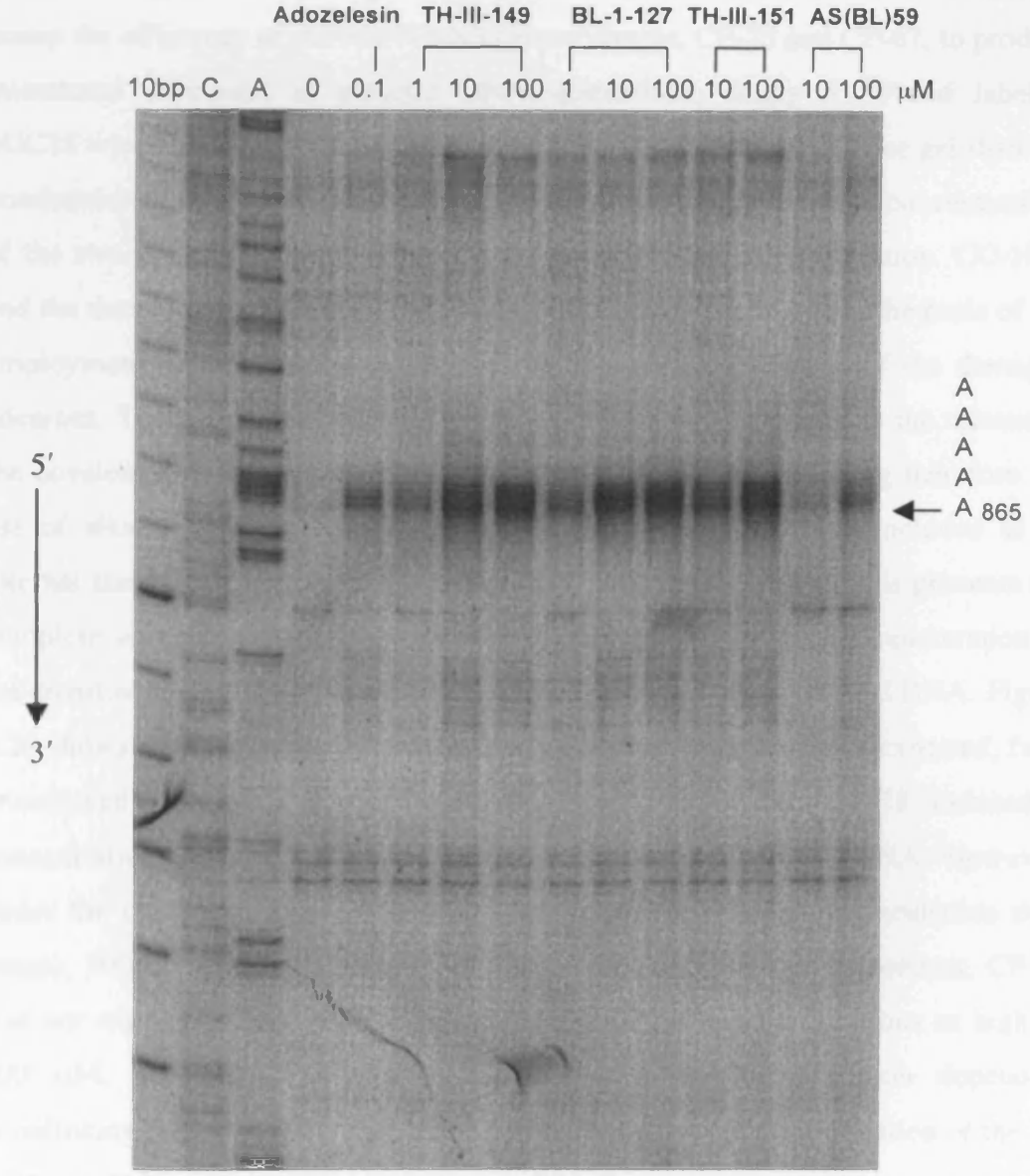

Figure 2.18 Portion of the autoradiograph of a *Taq* polymerase gel examining damage to the bottom strand of pUC18, induced by both the iso-CFI and *seco*-CFQ agents and their methylated counterparts, at the denoted concentrations. Adozelesin was included as an internal standard. 10bp is a DNA molecular weight marker, while C and A are sequencing lanes specific for the Gs and Ts respectively, of the upper strand, produced by the BESS (Base Excision Sequence Scanning) Mutascan™ Mutation detection and localisation kit. Due to complementarity, these sequencing ladders can be read as A and C specific for the bottom strand which is the relevant strand for the drug induced damage assessment. 0 is the untreated control. The arrow indicates the position and sequence of the common, major binding site. Drug: DNA incubations were for 5 hours at 37° C.

An agarose gel electrophoresis method (Hartley *et al.*, 1991) was employed to assess the efficiency of the two N3-N3 furano dimers, CP-75 and CP-67, to produce interstrand crosslinks in plasmid DNA. Linearised, singly 5'-^{32}P-end labelled pUC18 was completely denatured, thus migrating faster in the agarose gel than the nondenatured, double stranded control. DNA treated with a range of concentrations of the two investigational analogues was also subjected to denaturation. CC-1065 and the duocarmycins produce heat-labile adducts and this has been the basis of the employment of the thermal-cleavage assay for the identification of the damaged adenines. Thermal denaturation of the DNA would therefore lead to the release of the covalently modified bases introducing single nicks, necessitating therefore the use of alkaline denaturation instead. Cisplatin treated DNA was included as an internal standard. The presence of a crosslink between the two strands prevents the complete separation of the strands upon denaturation, resulting in renaturation of the crosslinked DNA in the neutral gel, which runs as double stranded DNA. Figure 2.20 shows the autoradiograph of such an agarose gel. Cisplatin, as expected, fully crosslinked plasmid DNA at a concentration of 10 μM. CP-75 induced a concentration-dependent increase in the amount of cross-linked DNA. However, under the conditions employed for this assay (concentration and incubation time range), 100% crosslinking of pUC18 DNA was not achieved. In contrast, CP-67 was not capable of any interstrand crosslinking even at concentrations as high as 100 μM. The graph in Figure 2.21 presents the concentration dependent crosslinking ability of CP-75 as derived from densitometric quantification of the gel in Figure 2.20. Previously reported *seco*-CBI dimmers have not been assessed for their crosslinking efficiencies. However the position and length of the linker greatly affected the biological potency of those compounds with the N3-N3 linked dimers being the most potent set investigated (Jia & Lown, 2000). In flexibly linked *seco*-CPI dimers, crosslinking ability and cytotoxicity were found to be related to the number of carbons in the linking polymethylene chain (Mitchell *et al.*, 1989).

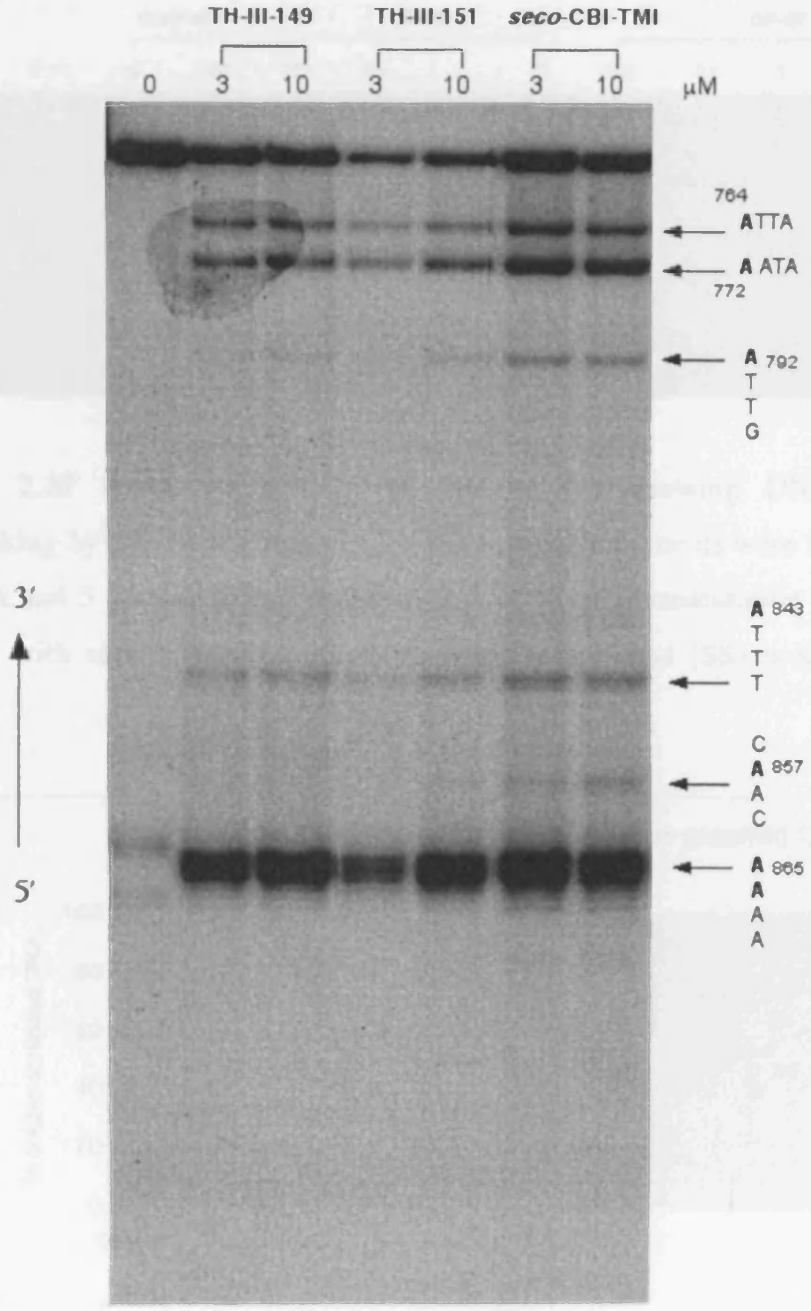

Figure 2.19 Thermal cleavage gel showing purine N-3 lesions to the bottom strand of a 5'-^{32}P labelled 208 bp fragment of pUC18, defined from 749 to 956. 0 is the untreated control. Thermal cleavage conditions as described in the Methods section. Arrows indicate the position and sequence context of the alkylated adenines (underlined and in bold). Adenines on the upper portion of the gel have been appointed from previous experiments Drug: DNA incubations were for 5 hours at 37° C.

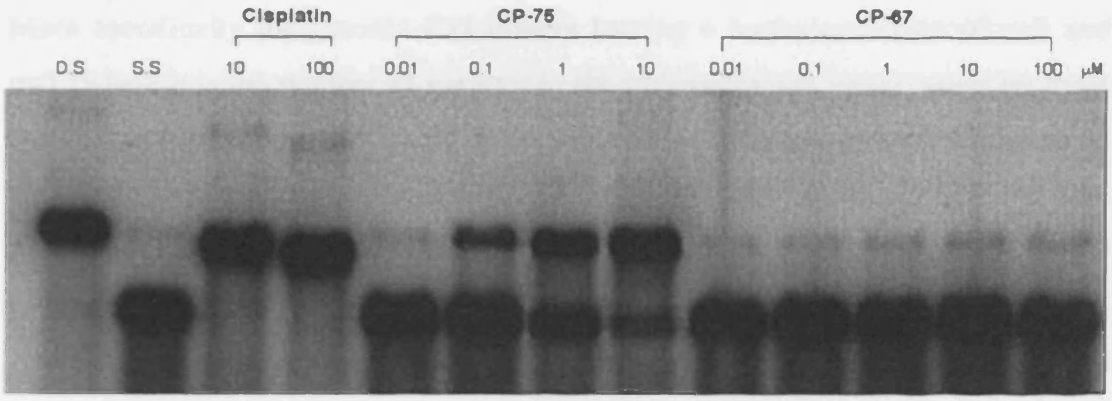

Figure 2.20 Autoradiograph of an agarose gel showing DNA interstrand crosslinking by CP-75 in linear pUC18 DNA. Drug treatments were for 2 hours for cisplatin and 5 hours for the furano dimers, at 37° C. Denaturation for 2 mins by treating with alkali. (DS) is double stranded control and (SS) is single stranded control.

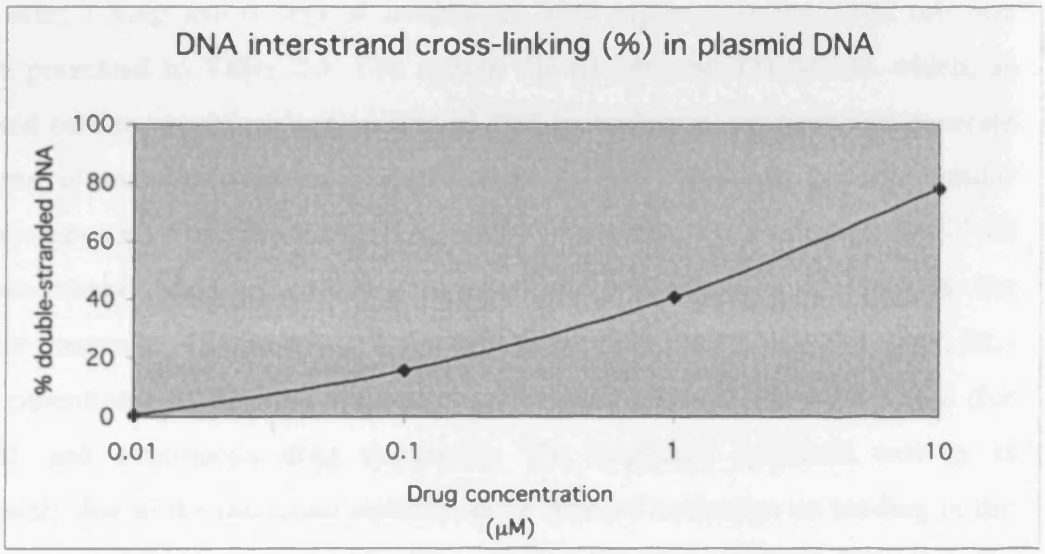

Figure 2.21 Double stranded and single stranded DNA bands from the above gel were quantified using laser densitometry to produce the dose response curve for CP-75 induced crosslinking.

More specifically the flexible CPI dimers bearing a methylene chain of n=3 and n=5 (where n is the number of carbons in the polymethylene linker) were far more toxic and efficient in crosslinking DNA, than the ones of n=2 and n=4. This same clear pattern has also been seen for PBD dimmers (Bose *et al.*, 1992b) and also unsymmetrical crosslinking agents combining the *seco*-CBI and PBD pharmacophores where again crosslinking ability and toxicity was dependent on chain length and was of the order n=2< 1< 4< 5≤ 3 (Tercel *et al.*, 2003). That pattern was also seen for the furano dimers examined in this study, with CP-75 which incorporates a methylene chain of n=3, being able to crosslink DNA, unlike CP-67 where n=4. Presumably this is due to a better match between the separation of the alkylating subunits of the dimer with n=3 and the base pair register.

The novel agents were also tested for their *in vitro* cytotoxicity potency using an MTT based growth inhibition assay. Cellular toxicities were determined as IC_{50} values after 1 hour and 4 days of continuous drug exposure in the K562 cell line and are presented in Table 2.3. The agents TH-III-149 and TH-III-151 which, as discussed earlier, would undergo a loss of HCl in biological medium and generate the same ultimate cyclopropane agent were indeed shown to possess similar cytotoxicities and were approximately 6-fold less potent than the *seco*-CBI-TMI reference compound in a continuous exposure and approximately 15 times for the one hour treatment. The presence of the methyl group in the iso-Me-CFI agent, BL-1-127, potentiated its cytotoxicity compared to that of TH-III-149 by 4-6 fold (for both 1h and continuous drug exposure). The improved cytotoxic activity is presumably due to the increased stability and enhanced activation on binding in the minor groove of DNA, conferred by the extended alkylation subunit. However, the *seco*-Me-CFQ agent, AS(BL)59 failed to demonstrate the same effect. On the contrary its cytotoxicity was lower than its non-methylated counterpart, in accordance with its decreased DNA alkylation capability as demonstrated in the alkylation studies. The IC_{50} values of all the agents were comparable between the 1 hour and the 4 days exposure. The lack of potentiation of the cytotoxicity during the

extended exposure suggests that the cells are affected, presumably through the reaction of the agents with DNA and the induced alkylation event, within the first hour of exposure.

Compounds	IC_{50} values (μM)	
	4 days	1 hour
TH-III-149	0.019 ± 0.002	0.017 ± 0.002
BL-1-127	0.003 ± 0.002	0.004 ± 0.0014
TH-III-151	0.018 ± 0.003	0.015 ± 0.02
AS(BL)59	0.037 ± 0.017	0.075 ± 0.025
CP-75	0.0018 ± 0.0008	0.002 ± 0.0005
CP-67	0.03 ± 0.015	0.04 ± 0.007
seco-CBI-TMI	0.0028 ± 0.001	0.0011 ± 0.0004

Table 2.3 *In vitro* cytotoxicity (IC_{50} in μM) of the investigational agents and the reference compound, *seco*-CBI-TMI, against human chronic myeloid leukaemia K562 cells, following a one hour and 4 days continuous drug exposure. The IC_{50} values represent the mean of at least two independent experiments. S.D values are also presented.

CP-75, the dimer with the linker chain size previously identified as optimal for both toxicity and crosslinking ability, was the most toxic agent, suggesting that its crosslinking ability could be a contributor to its enhanced cytotoxic potency. It exhibited a 10-fold increase in cytotoxicity compared to its parent monoalkylator, TH-II-149 and was comparable to the *seco*-CBI-TMI agent. In contrast, CP-67 that failed to crosslink DNA was more than 20-fold less toxic. The enhanced cytotoxic

activity exhibited by CP-75 is in agreement with previous studies comparing bifunctional and monofunctional agents. The IC_{50} of the monofunctional counterparts of melphalan and SJG-136 were shown to be 4- and 60-fold higher then the parent bifunctional agents in wild type CHO cells. Thus it was suggested that bifunctional adducts are a more cytotoxic form of DNA damage than the respective monoadducts (Clingen *et al.*, 2005). Similarly, in earlier studies, DSB-120, a PBD dimer forming interstrand crosslinks by covalently interacting with guanines on opposite strands was found to be > 650-fold more cytotoxic than the parent DC-81 molecule, presumably as a result of the formation of the crosslinks (Bose *et al.*, 1992a).

2.4 Hairpin conjugates of a racemic *seco*-Cyclopropaneindoline-2-benzofurancarboxamide and polyamides

2.4.1 Introduction

Hairpin polyamides are the only cell permeable small molecules capable of recognising extended, specific, predetermined sequences of DNA with an affinity comparable to DNA binding proteins, as discussed in Chapter 1. Hence their potential role in molecular biology and medicine as diagnostic tools and as reagents capable of modulating gene expression has attracted much attention and various synthetic efforts in designing such agents have been reported. Hairpin polyamides have been linked to various DNA modifying agents, one of which has been duocarmycin. What initiated this approach of combining the hairpin motif and the DUMA alkylating subunit was the initial observation of the ability of distamycin A to dramatically modulate the sequence specificity of DUMA, causing the alkylation to shift primarily to the G residues in GC-rich sequences (Yamamoto *et al.*, 1993). NMR strectroscopy later revealed that this modulation of sequence specificity involves the cooperative heterodimeric binding of DUMA and distamycin to the minor groove in a side-by-side arrangement (Sugiyama *et al.*, 1996). Apart from DUMA's ability to form heterodimers with distamycin, cooperative alkylation was later also observed in the presence of Py / Im triamides (Fujiwara *et al.*, 1999). This approach consequently evolved in the design of hybrid molecules between segment A of DUMA and Py/Im diamides. Such hybrids would retain the parent DUMA's alkylation selectivity, primarily alkylating the 3' A of AT-rich sequences. However they would be able to specifically and efficiently alkylate G residues of predetermined DNA sequences through formation of a heterodimer in the presence of distamycin, following Dervan's binary code for base pair recognition by Py/Im polyamides (Tao *et al.*, 1999a). In concurrent and later attempts to further modify the sequence selectivity of duocarmycin's alkylation in a predictable manner, hairpin polyamides were synthesised.

The hairpin polyamide motif which was first envisaged to mimic the 2:1 side-by-side antiparallel binding of unlinked polyamides, proved to have some distinct advantages over the traditional dimer systems. Previous studies have shown that covalently linking two antiparallel polyamide strands with γ-aminobutyric acid (GABA), forms a hairpin structure which exhibits specific binding to designated target sites with >100-fold enhanced affinity relative to the unlinked dimers (Mrksich *et al.*, 1994). Unlike the homodimeric binding of unlinked polyamides, which can afford "slipped motifs", hairpins are positioned unambiguously between the two DNA strands, as the γ-turn "locks" the register of the ring pairings. Also the individual compounds no longer have to interact in the minor groove to form the dimer, which is a significant advantage, particulary in the case of a heterodimer, as a secondary homodimer forming is possible since a complex equilibrium dictates the formation of a homodimer or heterodimer. With the hairpin approach, the alkylating moiety incorporated in the conjugates, such as that of DUMA can display a different DNA sequence specificity afforded by the polyamide's heterocycles' sequence and selectively alkylate matched sequences. Also the hairpin motif offers a means to target an alkylating pharmacophore to either more biologically relevant sites or to increase the actual size of the targeted binding site and hence the chances of recognising a unique site in the genome. On the other hand, polyamides linked to an alkylating effector can benefit from a covalent binding to DNA, which would enhance the stability of the polyamide-DNA complex and influence the ensuing biological activity, which could be also affected by the alkylation-induced DNA damage.

Pyrrole-imidazole polyamide conjugates incorporating the natural enantiomer of segment A of DUMA (Tao *et al.*, 1999b) and segment A of DU-86 along with a trans-vinyl (L) linker (Bando et *al.*, 2002) have been discussed in Chapter 1 (section 1.3.4.9). Finally, in another study, an eight-ring hairpin polyamide was shown to be able to target opposite strands of the DNA depending on the enantiomer of *seco*-CBI conjugated at its turn (Chang & Dervan, 2000).

2.4.2 Compounds

Conjugates of racemic *seco*-cyclopropaneindoline-2-benzofurancarboxamide (CI-Bf) and four diamides (ImIm (RBH-III-23), ImPy (JT-IV-99), PyIm (JT-IV-101) and PyPy (JT-IV-83), where Py is pyrrole and Im is imidazole), linked by a γ-aminobutyrate group, were synthesised and their structures are presented in Figure 2.22.

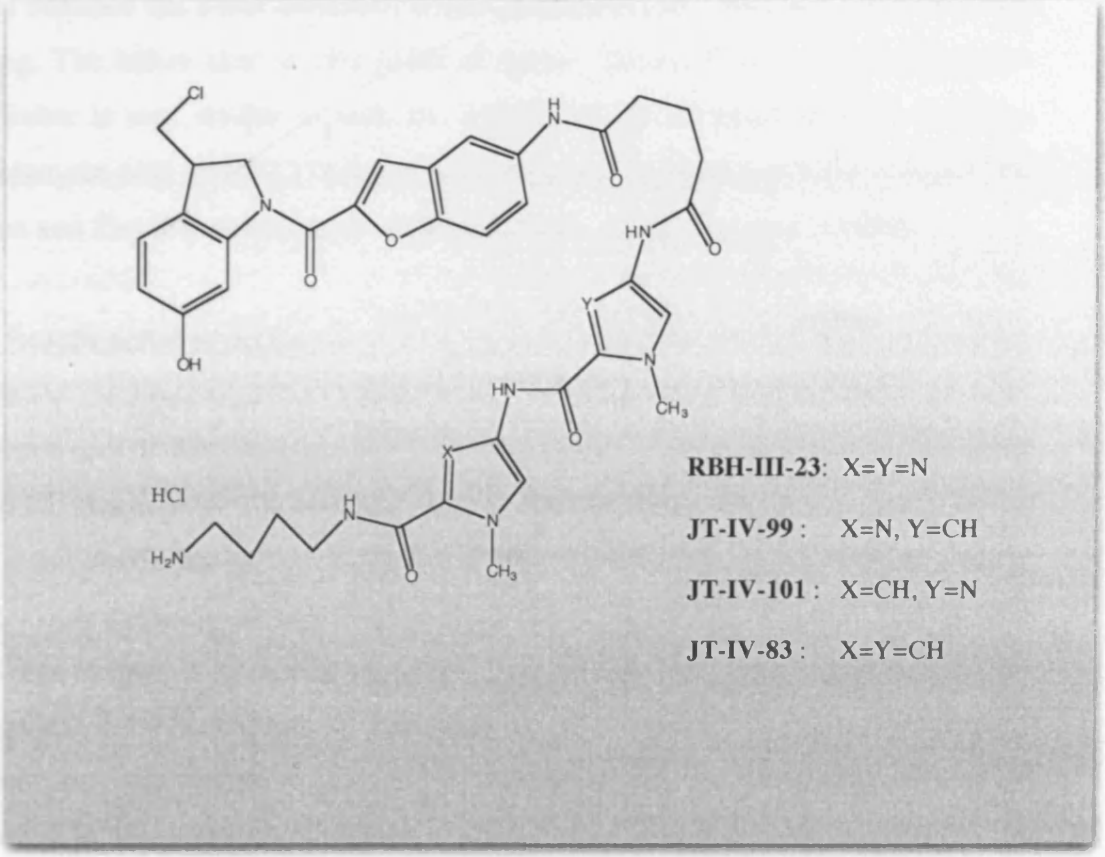

Figure 2.22 Structures of the agents under investigation in this study.

In these agents, as in the analogues discussed in section 2.2, the *seco*-CI pharmacophore was utilised as the alkylating "warhead", unlike the previously reported studies employing the DUMA and DU-86 alkylation subunits and the CBI.

Although DUMA prefers to alkylate the N3 of A at the 3' ends of consecutive AT sequences, it has been observed that DUMA could also undergo a N3 alkylation of guanine as in the case of (G_7) of d(GCAATTGC)$_2$ (Sugiyama *et al.*, 1993). DUMA's potential for guanine alkylation, not observed for DUMSA or CC-1065, is attributed to its greatest reactivity among all members of the duocarmycin class of agents. CI on the other hand, is also an exceptionally reactive electrophile (Boger *et al.*, 1991a). The terminal free amine of the conjugates, at physiological pH of 7.4, will remain protonated, resembling the distamycin A termini. This charged species should enhance the water solubility of the conjugates and could also enhance DNA binding. The linker used in this series of agents, derives from glutaric anhydride. This linker is very similar in both the length and the chemical structure to the γ-aminobutyric acid (GABA) linker employed in the hairpin molecules designed by Dervan and Tao in previous studies (Mrkish *et al.*, 1994; Tao *et al.*, 1999b).

2.4.3 Results and discussion

The main goal of designing the above agents was to combine the inherent reactivity of the CI pharmacophore with the binding specificity of the hairpin polyamides. Such compounds can potentially be endowed with the ability to more efficiently recognise distinct and unique sequences of DNA. The thermally-induced cleavage assay was utilised to probe the sites of covalent interaction of this series of hairpin conjugates with purine-N3 in the minor groove.

Damage was examined on the bottom strand of the same fragment of pUC18 employed as the reference DNA in the previous studies. As can be seen on the autoradiograph in Figure 2.23, all four compounds retain a memory for alkylating adenine N3 within the A_5(865) cluster, ^{869}5'-AAAAA-3'^{865}, a site that constitutes a consensus sequence for CC-1065 and which was readily recognised by the compounds in section 2.2 which also incorporate the same *seco*-CI pharmacophore.

Covalent A-N3 alkylation is also evident by all four hairpin conjugates, at the AT sites situated 3' of the common major A_5 cluster, 5'-^{767}ATTA-3'^{764}, ^{775}5'-ATAA-3'^{772} and ^{846}5'-TTTA-3'^{843} (the 3'-alkylated adenine is underlined). What differentiates the alkylation profiles of these agents is the ability of the imidazole bearing compounds RBH-III-23 (ImIm) and JT-IV-99 (PyIm) to alkylate the minor but unique for these two conjugates, site ^{890}5'-TCAG-3'^{887}. This sequence is less reactive than the run of the five adenines, as alkylation is only evident at the higher (10 μM) concentration studied. Since the DNA fragment in Figure 2.23 has been 5'-^{32}P-radiolabelled, a 3'- end heterogeneity is evident, manifested by the presence of a pair of closely migrating bands (more pronounced for the ^{890}5'-TCAG-3'^{887} site at the bottom part of the gel, due to increased band separation). The band that migrated slower, is thought to represent a species containing the modified deoxyribose moiety, while the lower molecular weight band (higher gel mobility), constitutes a thermal cleavage product that has resulted from the loss of the modified sugar, and as such constitutes a 3'phosphate terminated molecule, therefore comigrating with the Maxam and Gilber sequencing products. Thus the bands observed at the bottom of the gel in Figure 2.23, unique for RBH-III-23 and JT-IV-99, represent the thermal cleavage product of the adenine at position 888, which is thought to be the reacting base within this specific sequence context. These two compounds therefore exhibit the ability to recognise a GC-containing sequence. Alkylation at the ^{890}5'-TCAG-3'^{887} can be explained by the mode of recognition shown in Figure 2.24-B.

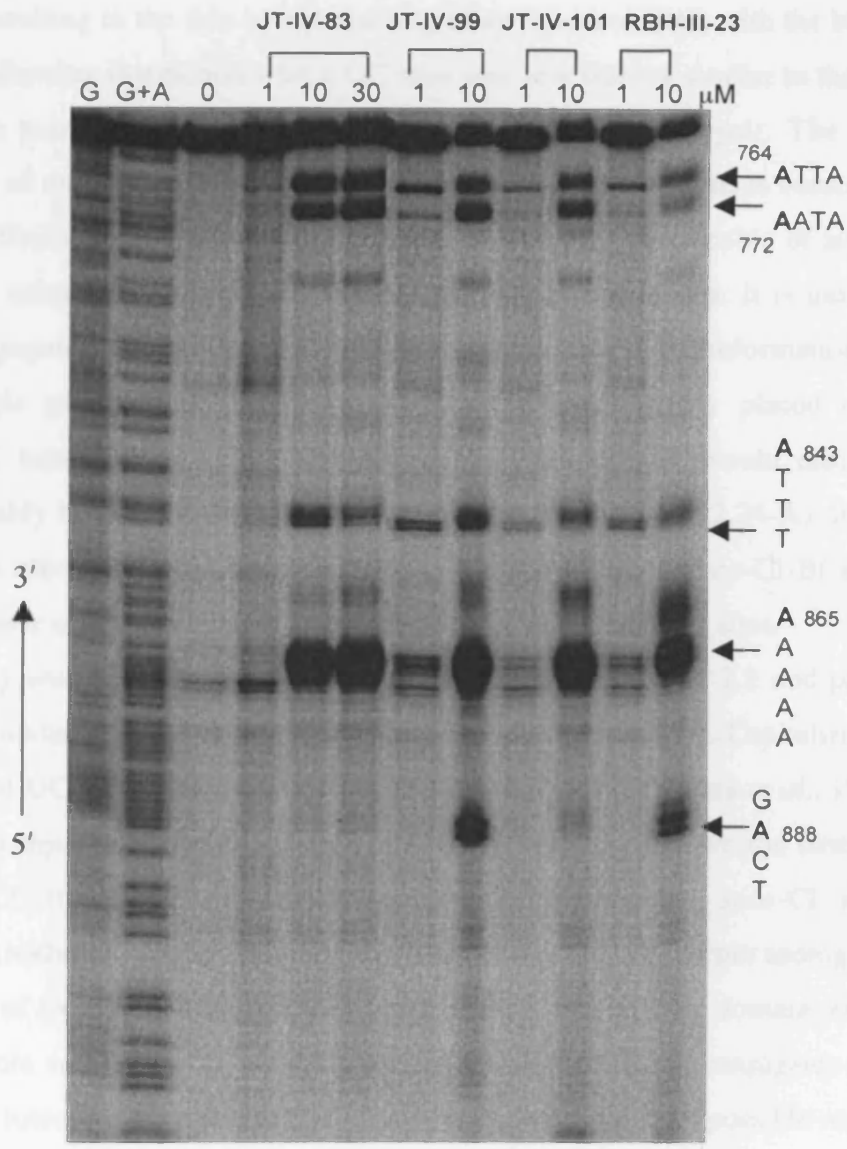

Figure 2.23 Thermal cleavage gel showing purine-N3 lesions to the bottom strand of a 5'-^{32}P labelled 208 bp fragment of pUC18, defined from 749 to 956 induced by the denoted hairpin polyamide agents. 0 is the untreated control. G / G+A are the sequencing markers. Thermal cleavage conditions as described in the Methods section. Arrows indicate the position and sequence context of the alkylated adenines (underlined and in bold). Adenines on the upper, non resolvable portion of the gel have been appointed from previous experiments. Drug: DNA incubations were for 5 hours at 37° C.

In this proposed model the *seco*-CI-Bf and polyamide subunits fold to form a hairpin resulting in the side by side pairing of an imidazole unit with the benzofuran moiety, allowing interaction with a GC base pair in a fashion similar to the pyrrole / imidazole pairing that is capable of recognising a C/G base pair. The enhanced tolerance of mixed AT/GC sequences exhibited by the two agents is consistent with previous findings that imidazole containing polyamides are capable of altering the sequence selectivity of DUMA from AT to GC-rich sequences. It is unlikely that these conjugates would bind to this sequence in an extended conformation because the pyrrole group of JT-IV-99 would then be unfavourably placed next to a G(891)/C base pair. Additionally, the benzofuran moiety, would also have to unfavourably bind to a C(889)/G base pair (sequence in Figure 2.24-A). It has been shown, in other studies in our group, that like *seco*-CI-TMI, *seco*-CI-Bf also binds to the cluster of the A adenines at 865 and not to GC-containing sites.

This study was an extension of the study described in section 2.2 and part of the effort to modulate the sequence specificity of the duocarmycins. Capitalising on the findings of GC recognition in the presence of triamides (Fujiwara *et al.*, 1999), this series of conjugates adopted the hairpin motif. These agents are the first reported hairpin CC-1065/duocarmycin analogues incorporating the *seco*-CI alkylating moiety. Another distinctive feature from other duocarmycin hairpin analogues is the inclusion of the benzofuran moiety as part of the DNA binding domain, rather than only pyrrole and imidazole groups. Two imidazole containing conjugates exhibited enhanced tolerance to mixed GC/AT sequences, highlighting a possible recognition mode for the benzofuran / Imidazole pairing.

The cytotoxic potency of these agents was also determined against the K562 cells for both a one hour and 4 days continuous drug exposure, using the MTT assay. The IC_{50} values are presented in Table 2.4.

A.

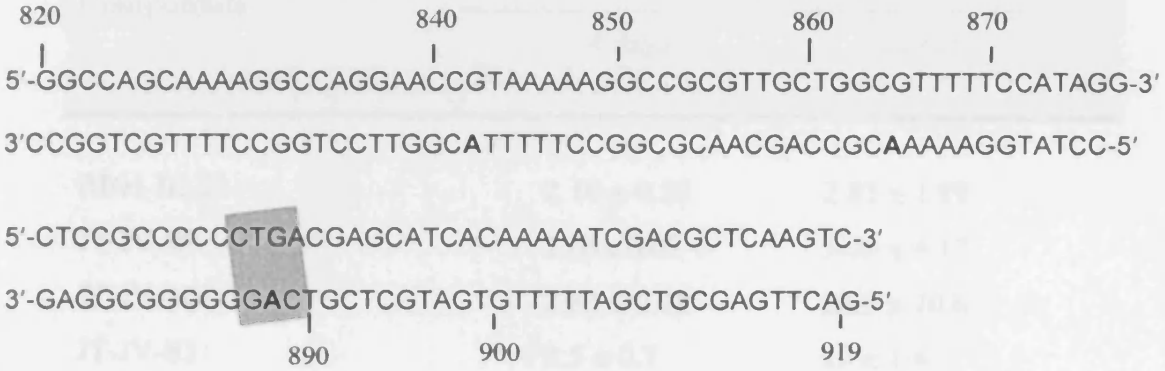

B.

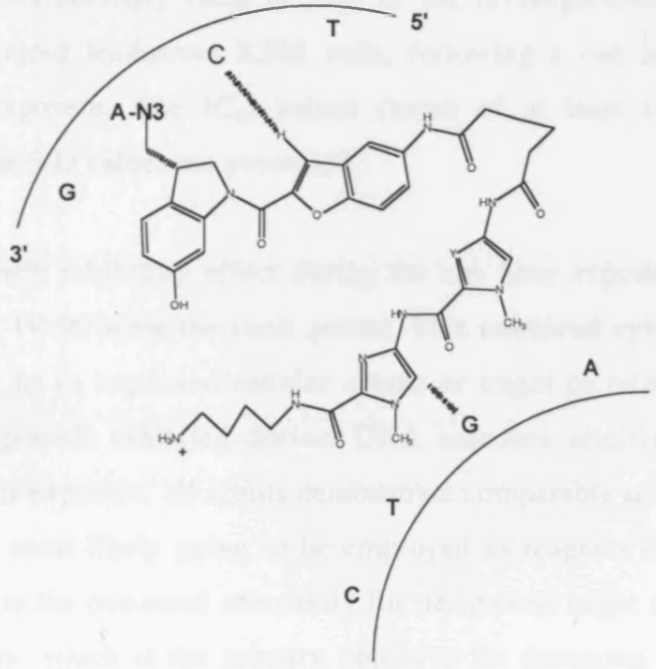

Figure 2.24 A. Diagram showing the sequence of the resolvable portion of the thermal cleavage gel of Figure 2.23, examining the damage on the bottom strand of pUC18 induced by compounds RBH-III-23 and JT-IV-99. The alkylated bases are in bold. The GC/AT mixed binding site, unique for these two compounds in that series of conjugates, is shaded. **B.** Proposed model of the molecular interactions between the natural (S)-enantiomers of compounds RBH-III-23 (Y=N) and JT-IV-99 (Y=CH) with the site 3'-GACT-5' (shaded in A.).

Compounds	IC_{50} values (μM)	
	4 days	1 hour
RBH-III-23	2.16 ± 0.28	2.83 ± 1.89
JT-IV-99	2.05± 0.07	5.05 ± 4.17
JT-IV-101	2.83 ± 0.28	22.5 ± 10.6
JT-IV-83	2.5 ± 0.7	19 ± 1.4

Table 2.4 *In vitro* cytotoxicity (IC_{50} in μM) of the investigational agents against human chronic myeloid leukaemia K562 cells, following a one hour and 4 days continuous drug exposure. The IC_{50} values (mean of at least two independent experiments) and the S.D values are presented.

Judging by the growth inhibitory effect during the one hour exposure, the agents RBH-III-23 and JT-IV-99 were the most potent. This enhanced cytotoxic activity could either be due to an improved cellular uptake or might be related to the fact that these two compounds exhibited distinct DNA sequence selectivity. After the extended, continuous exposure, all agents demonstrate comparable activity.

As such agents are most likely going to be employed as reagents for modulating gene expression, it is the enhanced selectivity for designated target sequences and not the high toxicity, which is the primary objective for designing them. To this effect, hairpin pyrrole-imidazole polyamides incorporating the DU-86 alkylating moiety have been shown to target and bind adenine in the telomere repeats 5'-CCCTAA-3' extending sequence recognition to a six-base pair sequence (Takahasi *et al.*, 2003). Another DU-86 incorporating hairpin has been shown to inhibit transcription in the coding region of the *GFP* gene (Oyoshi *et al.*, 2003) while longer polyamide-DU-86 hybrid hairpins could selectively suppress the expression of luciferase activity in living cells by targeting coding regions of renilla and firefly

luciferase (Shinohara *et al.*, 2004). These findings highlight the potential of "effective" DNA alkylation as a promising strategy for designing new types of gene-regulating agents. The hairpin motif provides therefore the framework for "tailor-made" antitumour agents by introducing further sequence selectivity or a modified sequence specificity for predetermined, site-specific targeting to established alkylating agents.

CHAPTER 3

SEQUENCE SPECIFIC ALKYLATION AND CYTOTOXICITY OF A SERIES OF NOVEL ACHIRAL CC-1065 / DUOCARMYCIN ANALOGUES

3.1 Introduction

Three of the four CC-1065/duocarmycin analogues that have advanced into clinical trials, bizelesin, carzelesin and KW-2189 are *seco* prodrugs, as they do not incorporate the preformed cyclopropane ring of the parent compounds. As has been mentioned before, *seco* agents readily close to the corresponding cyclopropane containing agents in biological media, through elimination of HCl prior to induction of alkylation (Figure 3.1).

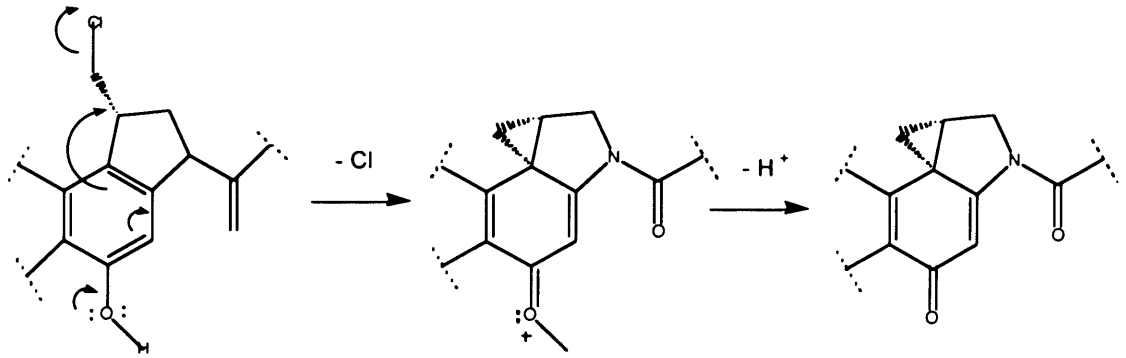

Figure 3.1 Activation of the *seco* prodrugs by the loss of HCl in biological media.

Past studies have shown that *seco* agents incorporating the CI (Boger & Wysocki, 1989; Boger *et al.*, 1990c; Boger et al., 1990b) or the CBI (Boger & McKie, 1995; Boger *et al.*, 1995b, Boger *et al.*, 1995c) pharmacophores, exhibit biological properties and DNA alkylation efficiencies and selectivities, identical to those of

their cyclised counterparts. In one instance, the *seco*-CI-TMI precursor proved to be (10-100)-fold more efficient alkylator than CI-TMI and five times more toxic in L1210 cells, attributed to the relative instability of the latter agent to the conditions of the assay (Boger *et al.*, 1990c). The stability of the analogues in the *seco* configuration and their ability to serve as stable *in vivo* precursors of the reactive agents provides an attractive strategy for drug design. Hence, all the analogues in the studies presented thus far have been uncyclised precursors. However, just like the three clinically investigated compounds, they all possess a chiral centre. The advantages of the omission of this feature and alternatively the development of active achiral analogues have been outlined in the Introduction (section 1.3.4.12).

In the quest for improved antitumour agents of this type and based on previous studies on *seco* versions of CC-1065 analogues, we sought to develop an achiral pharmacophore that would be capable of the CC-1065 characteristic, sequence specific, minor groove alkylation and subsequently incorporate it into functional analogues. In order to determine the minimum structural requirements of a potential achiral pharmacophore, for a "CC-1065 mode" of interaction with DNA, the 2-*p*-hydroxyphenethyl (HPE) halides were considered, previously studied for their cytotoxicity and DNA alkylating ability (White *et al.*, 1995). These analogues which are the simplest *seco* CPI functional agents were chosen in place of the spiro[2.5]octa-1,4-dien-3-one group (Figure 3.2). This group lacks the fused aromatic and pyrrolidine functionality of the CPI and other known alkylating subunits and is formed as an intermediate in a reaction involving Ar-3' participation in the phenoxide anion of 2-aryl-1-ethyl halides. However, it is too hydrolytically unstable to be studied in biological systems (Baird & Winstein, 1963).

Assessment of the *in vitro* cytotoxicity of the 2-*p*-hydroxyphenethyl (HPE) halides featured in Figure 3.3 showed that the alcohols were much less cytotoxic than the corresponding halides against the cell lines HeLa and MM96L. The IC_{50} value of *p*-hydroxyphenethyl bromide (HPEB) was determined to be 32 μM towards the murine melanoma B16 cell line, which is comparable to the reported values for N-BOC-CPI (>3.3 μM) and is approximately 34 times that for N-BOC-CBI.

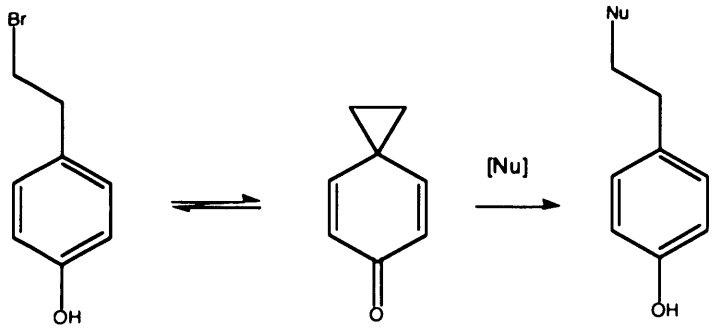

Figure 3.2 The formation of spiro[2,5]octa-1,4-dien-3-one as an intemediate in the reaction of bromide with a nucleophile.

The decreased activity of the halide compared to these other alkylating subunits, is consistent with the inverse relationship between chemical stability and cytotoxic potency as previously suggested (Boger & Yun, 1994). Overall, the *p*-hydroxyphenethyl chloride and bromide (HPEC and HPEB) exhibited the greatest potency and were more cytotoxic than the *m*-methoxy and *p*-methoxy derivatives. The relative cytotoxicities of the methoxy derivatives correlated with the leaving group ability, i.e. I > Br > Cl. A derivatised hydroxy group for HPEC and HPEB is therefore detrimental for the cytotoxicity of these agents.

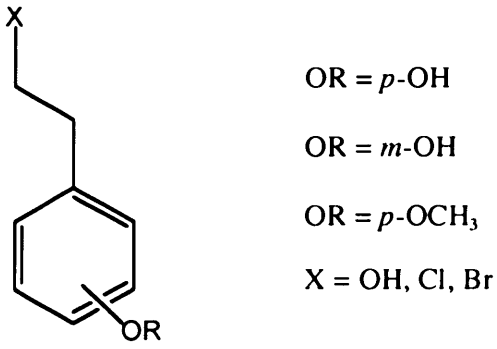

OR = *p*-OH

OR = *m*-OH

OR = *p*-OCH_3

X = OH, Cl, Br

Figure 3.3 Analogues of 2-*p*-hydroxymethyl (HPE) compound.

The above results indicated the importance of the presence of an intact *p*-hydroxy group for the elimination of HX in order to produce the reactive cyclopropylhexadienone intermediate.

The hydroxyphenethyl halides readily eliminate hydrogen halide and cyclise to form the reactive spiro[2.5]cyclopropylcyclohexadienone intermediate which covalently reacts with DNA. The alkylation ability of *p*-HPEB was comparable to that of the CPI and CI derivatives, and demonstrated a strong preference for adenines especially when flanked by a 5' T, mirroring the sequence specificity of CC-1065. However, it was less sequence discriminating compared to the CI and CPI pharmacophores and their *seco* precursors (White *et al.*, 1995).

The above studies suggest that the *p*-hydroxyphenyl halides feature the minimum structural requirements for DNA alkylation and biological activity, and therefore offer the potential of being developed as an achiral pharmacophore. The basic *seco*-achiral CI structure constitutes the first step in this general drug design strategy for the development of achiral analogues. An amino group is introduced to position-3 of the spiro[2.5]cyclopropylcyclopropylcyclohexadienone (Figure 3.4, structure 2).

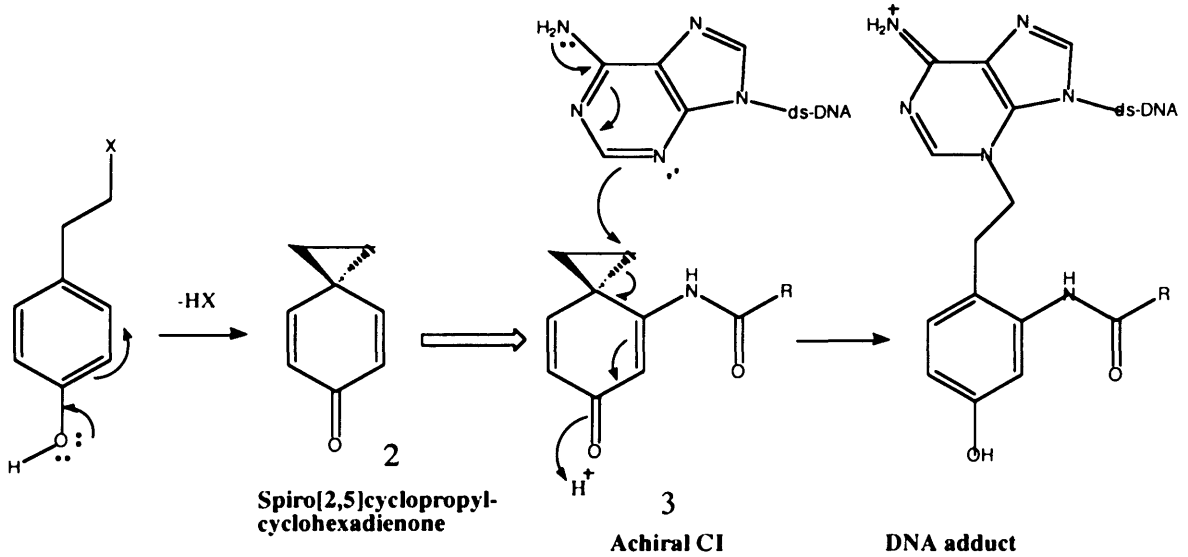

Figure 3.4 Rationale of design and proposed mechanism of activation and DNA alkylation of the achiral *seco*-CI moiety.

This structural addition should provide stability to the intermediate towards solvolysis and would allow coupling with various DNA binding domains (Figure 3.4, stucture 3).

According to this hypothesis, compounds of the general formula 3, could induce highly sequence specific, minor groove DNA alkylation, consistent with the mechanism of action of CC-1065 and the duocarmycins and exert potent biological activity. Attachment of appropriate noncovalent subunits could endow the novel conjugates with cytotoxicities comparable to those of the previously reported, chiral, CI or CPI analogues.

Utilising the basic *seco* achiral CI structure and coupling it to the trimethoxyindole (TMI) subunit of the duocarmycins, the "first generation" of achiral analogues were synthesised and evaluated for their sequence specificity and cytotoxic potency. Such studies would reveal whether the chiral centre present in all analogues of the CC-1065 class of compounds, is absolutely necessary for DNA interaction and cytotoxicity. The achiral CI pharmacophore was subsequently replaced with the achiral CBI alkylation subunit. In all instances, the TMI group was maintained as the DNA binding domain.

The full complexity of the natural products is not required for high potency, as exemplified by the analogue (+)-CBI-TMI which is essentially as cytotoxic as (+)-DUMSA in cell culture (IC_{50}s of 30 and 10 pM, respectively, in L1210 leukemia) (Boger & Yun 1994b). The DNA binding subunit is also thought to be implicated in the occurrence of the delayed fatal toxicity, characteristic of (+)-CC-1065, whose adducts are essentially irreversible. The rate of adduct reversibility is dependent upon the extent of the noncovalent binding stabilisation. The simplified and smaller structure of TMI, found in the parent compounds of the duocarmycins seems to be providing sufficient binding stabilisation for the induction of a "more reversible" adduct and of such an extent as to not induce delayed lethality. TMI is also proposed to be actively contributing to the catalysis of the DNA alkylation reaction, being of sufficient rigid length (provided by the presence of the C5' methoxy

group) to increase the inherent twist of the linking N2 amide upon DNA minor groove binding (Boger & Garbaccio, 1997; Boger & Garbaccio, 1999a).

Finally the novel achiral pharmacophores were incorporated into hairpin polyamide conjugates, in a further attempt to obtain analogues with modified sequence selectivity.

Two of the clinically investigated CC-1065 analogues, the carbamate-type prodrugs carzelesin and KW-2189, are prodrugs of the corresponding highly potent phenolic *seco* compounds and undergo rapid and non-specific hydrolysis to the phenols by plasma esterases. This type of prodrugs could potentially be used in tumour-specific targeting applications. However, as in the case of the two CC-1065 analogues, ester types of prodrugs of phenols are prone to non-specifically releasing the corresponding phenol in plasma, undermining their potential as effectors in prodrug strategies. To address this problem, in an alternative synthetic approach, amino analogues of the phenolic *seco* forms of cyclopropanoindolinones have been developed (e.g. 6-amino-*seco*-CI-TMI, 5-amino-*seco*-CBI-TMI), aiming to prepare relatively more stable prodrugs (Milbank *et al.*, 1999; Atwell *et al.*, 1998). Similarly in the following studies, amino analogues of both achiral pharmacophores were also synthesised and incorporated to the corresponding conjugates.

3.2 Achiral *seco*-CI and achiral *seco*-amino-CI compounds

3.2.1 Compounds

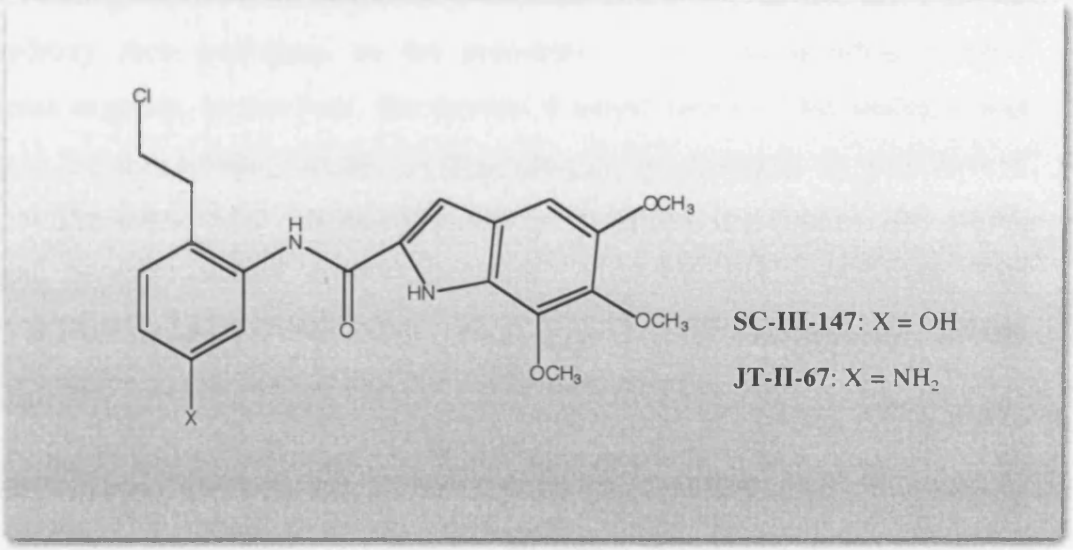

Figure 3.5 Structures of the novel achiral *seco*-CI (SC-III-147) and achiral *seco*-amino-CI (JT-II-67) compounds.

The achiral *seco*-CI analogues shown in Figure 3.5 were the first of this series of compounds to be designed due to their structural simplicity. Compound SC-III-147 contains the hydroxyphenylethyl halide functionality, coupled to the TMI DNA binding side chain. As discussed earlier, and according to the general scheme of Figure 3.4, the SC-III-147 analogue should lose HCl to produce the putative cyclopropane containing DNA alkylating agent which was hypothesised to be able to react with an adenine-N3 group in AT-rich sequences. Compound JT-II-67 incorporates a 4-aminophenylethyl functionality, possessing an amino group *para* to the *seco*-chloroethyl group and the same, TMI subunit attached to the pharmacophore. Similar to the loss of HCl in *seco*-CC-1065 and *seco*-duocarmycin analogues, and in an analogous fashion to SC-III-47, JT-II-67 should revert to the

ring-closed form in biological media, according to the scheme in Figure 3.6. In the case of the *p*-hydroxyphenyl halides, the presence of an underivatised *p*-hydroxy group was shown to be essential for the generation of potent DNA reactive analogues (White *et al.*, 1995). We wanted to assess whether, in the case of the *seco*-CI analogues, the 4-aminophenethyl chloride moiety is a feasible substitute for the hydroxy *seco* analogues, as the precedent of the corresponding racemic analogues suggests. In that case, the racemic 6-amino-*seco*-CI TMI analogue was shown to function similarly to the corresponding phenol analogue, by alkylation of DNA at the adenine-N3 group, with similar sequence specificity. The amino analogue however was a moderately potent cytotoxin and considerably less cytotoxic than its hydroxy counterpart (IC_{50}s in AA8 cells, 4 h exposure; 320 and 6nM, respectively) (Milbank *et al.*, 1999, references therein).

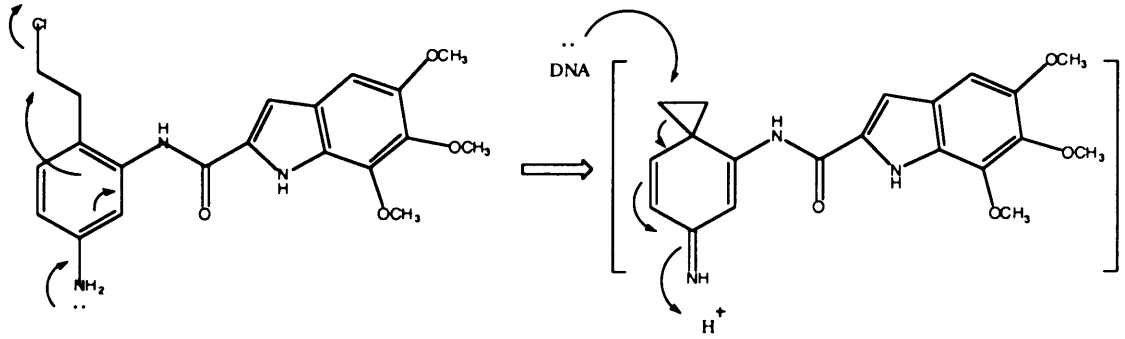

Figure 3.6 Proposed mechanism of activation and DNA alkylation of the achiral *seco*-amino-CI moiety of compound JT-II-67.

3.2.2 Results and discussion

The DNA alkylation ability by the novel achiral agents was initially tested using the PCR-based, *Taq* polymerase stop assay, to pinpoint the exact sites of covalent binding on the reference pUC18 DNA fragment. As shown in Figure 3.7-A, SC-III-

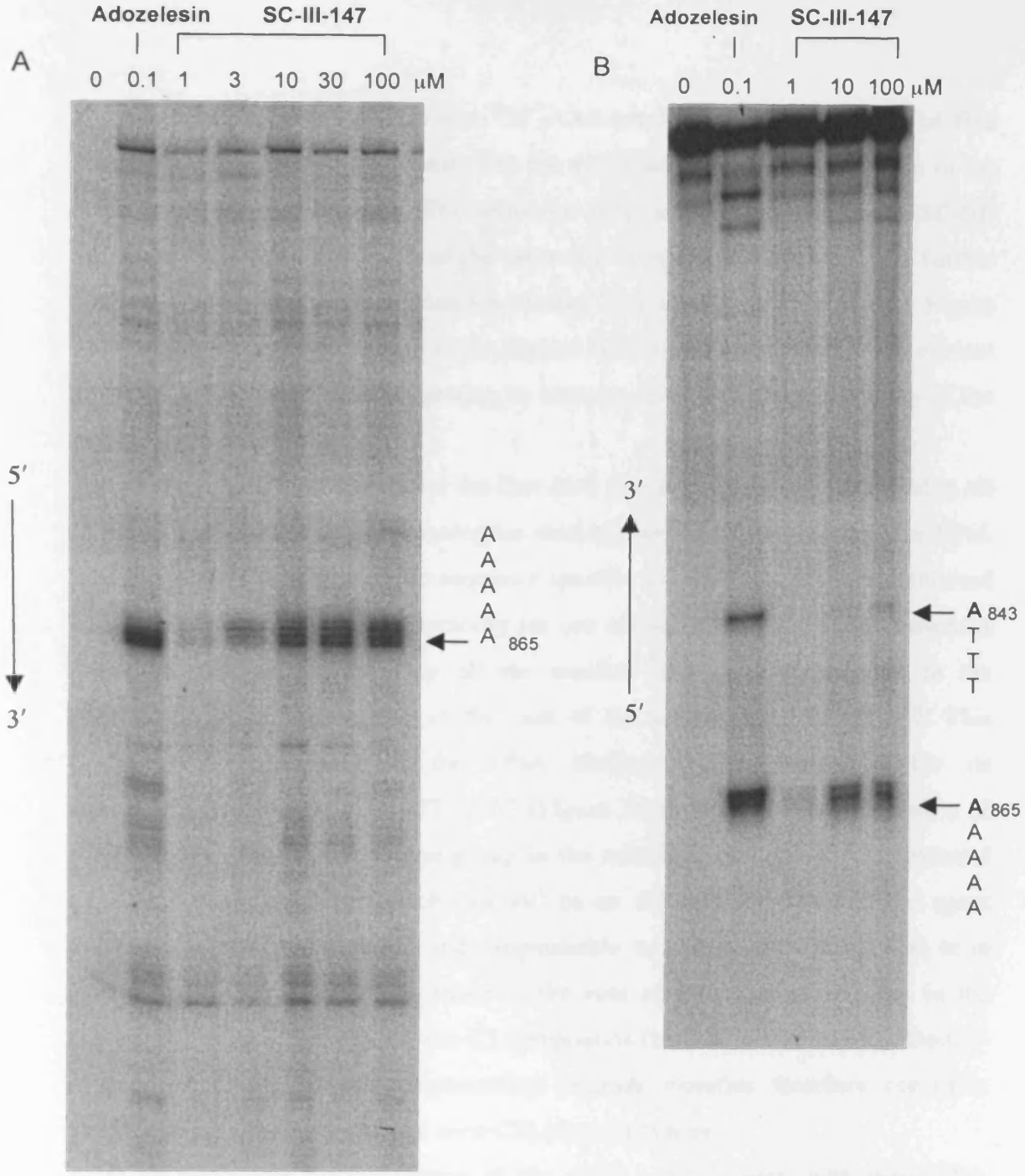

Figure 3.7 A. Portion of the autoradiograph of a *Taq* polymerase assay gel examining damage to the bottom strand of pUC18, induced by the achiral *seco*-CI agent, SC-III-147 at the denoted concentrations. Adozelesin was included as an internal standard. 0 is the untreated control. The arrow indicates the position and sequence of the common major binding site. Drug: DNA incubations were for 5 hours at 37° C. **B.** Thermal cleavage gel showing purine-N3 alkylations to the 5'-^{32}P labelled bottom strand of pUC18. 0 is the untreated control. Arrows indicate the position and sequence context of the alkylated adenine (underlined and in bold). Drug: DNA incubations were for 5 hours at 37° C.

147 strongly interacts with the site ^{869}5'-AAAAA-3'^{865}, containing a run of five adenine residues, which also constitutes the major binding site of adozelesin in the fragment under consideration. The sequence specific covalent reaction of SC-III-147 with the adenine-N3 group at the same site of contigious adenines was further confirmed using the thermally-induced strand cleavage assay as shown in Figure 3.7-B. Only traces of alkylation at the highest SC-III-147 concentration are evident at the ^{843}5'-ATTT-3'^{846} site, suggesting an increase in the sequence selectivity of the achiral agent over adozelesin.

The above results demonstrate for the first time that the chiral centre featured in all of the CC-1065/duocarmycins analogues studied thus far is not necessary for DNA interaction and the characteristic sequence specific adenine-N3 alkylation exhibited for this class of compounds. Selectivity for one of the reported CC-1065 consensus sequence readily recognised by all the racemic analogues investigated in the previous chapters is preserved in the case of the achiral agent SC-III-147. This finding was reproduced in the DNA binding studies performed for its aminophenelethyl counterpart, JT-III-67 (Figure 3.8-A and B). The substitution of the hydroxyl group by the amino group in the achiral alkylating subunit produced an achiral pharmacophore which can still be an effective alkylator, as the agent exhibited an alkylation profile, indistinguishable to that of adozelesin. This is in accordance to the observations made in the case of the same substitution in the corresponding pair of racemic *seco*-CI compounds (Millbank *et al.*, 1999). Both 4-hydroxyphenethyl and 4-aminophenethyl chloride moieties therefore constitute possible substitutes for the chiral *seco*-CPI pharmacophore.

After characterising the interaction of the novel achiral agents with their DNA target, their biological activity was assessed by determining their cytotoxicity against the K562 cells, using a MTT based growth inhibition assay. The IC_{50} values of SC-III-147 and JT-II-67 for a continuous, 4-day exposure of the cells to the agents, are presented in Table 3.1

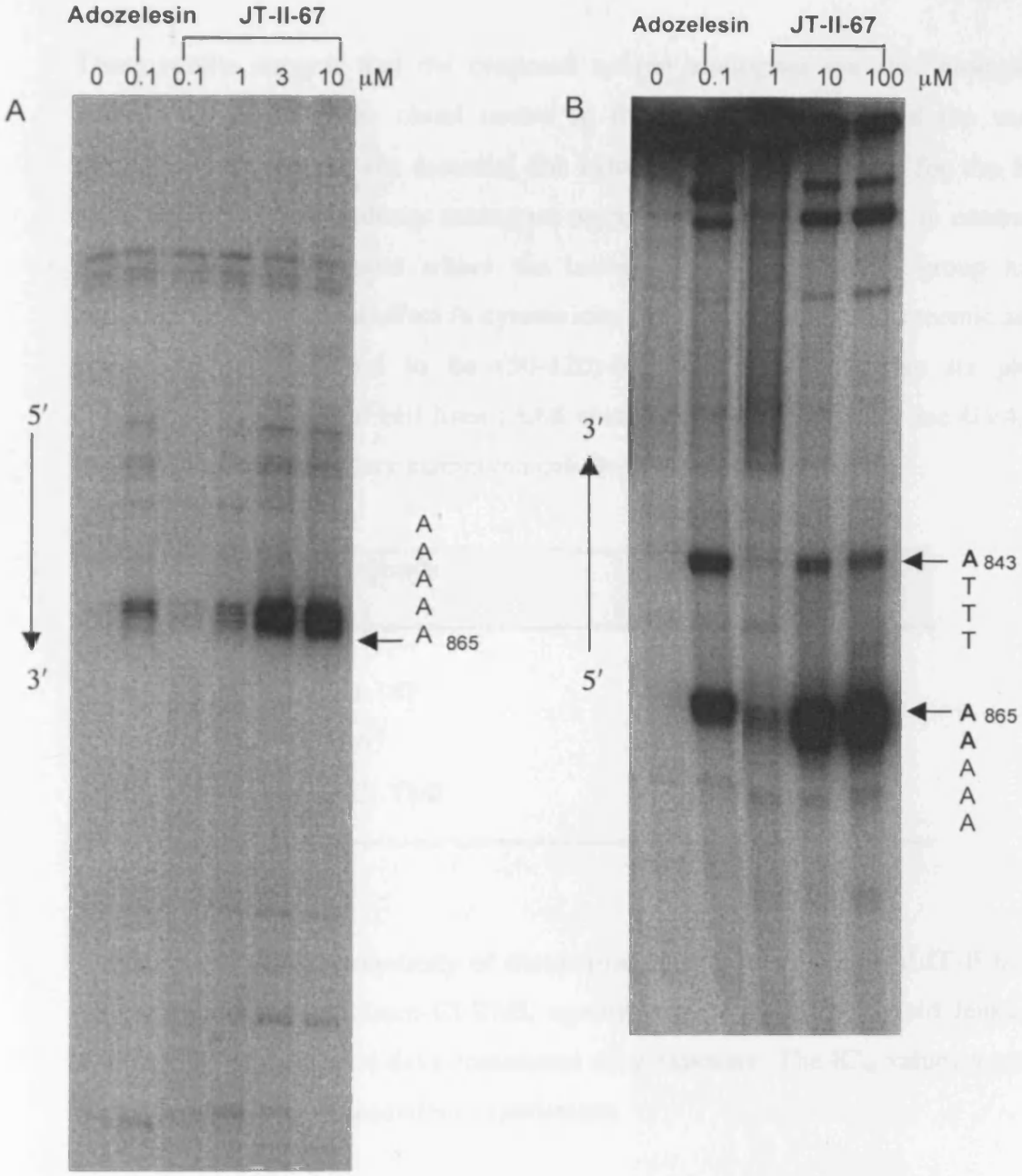

Figure 3.8 A. Portion of the autoradiograph of a *Taq* polymerase assay gel examining damage to the bottom strand of pUC18, induced by the achiral *seco*-amino-CI agent, JT-II-67, at the denoted concentrations. Adozelesin was included as an internal standard. 0 is the untreated control. The arrow indicates the position and sequence of the common major binding site. Drug: DNA incubations were for 5 hours at 37° C. **B.** Thermal cleavage gel showing purine-N3 lesions to the 5'-^{32}P labelled bottom strand of pUC18. 0 is the untreated control. Arrows indicate the position and sequence context of the alkylated adenine (underlined and in bold) at the readable portion of the gel. Drug: DNA incubations were for 5 hours at 37° C.

These results suggest that the proposed achiral analogues are also biologically active and therefore the chiral centre in the natural products and the various synthetic analogues is not essential for cytotoxicity. Interestingly, for the K562 cells, the amino and hydroxy analogues were comparably cytotoxic, in contrast to their racemic counterparts where the introduction of the amino group had a considerable detrimental effect in cytotoxicity. More specifically the racemic amino compound was reported to be (50-120)-fold less cytotoxic than its phenol counterpart in a panel of cell lines (AA8 chinese hamster ovary cell line UV4, and EMT6, a murine mammary carcinoma cell line (Tercel *et al.*, 1996).

Compounds	**IC_{50} values (μM)**
SC-III-147	1.43 ± 0.273
JT-II-67	1.7 ± 0.173
seco-CI-TMI	0.15

Table 3.1 *In vitro* cytotoxicity of the achiral agents SC-III-147 and JT-II-67 and the racemic compound *seco*-CI-TMI, against human chronic myeloid leukaemia K562 cells, following a 4-days continuous drug exposure. The IC_{50} values represent the average of three independent experiments.

Protection of the hydroxyl group in SC-III-147, led to a dramatic decrease in cytotoxicity. The carbamate agent TH-III-81 shown in Figure 3.9 gave IC_{50} values of 75 μM and >100 μM against L1210 and P815 cells, while the IC_{50} values of SC-III-147 for the same cell lines were 1.5 and 5.6 μM, respectively (Prof. Lee – personal communication).

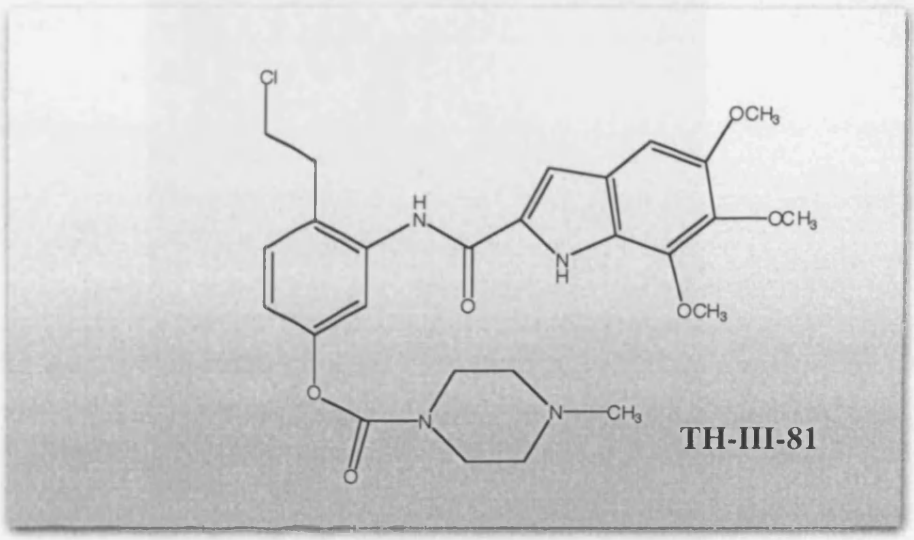

Figure 3.9 Structure of the protected SC-III-147 analogue, TH-III-81

The diminished cytoxic potency by TH-III-81 coincides with the expected lack of covalent binding on naked DNA, as shown in Figure 3.10, which confirms the agent's inability to interact with DNA when having an inaccessible hydroxy group. This further confirms the importance of the unprotected hydroxy group (or equally effective amino) and indicate that the *seco*-achiral halide compounds must eliminate HCl to form spiro[2,5]cyclopropanecyclohexadienone intermediates that react with DNA (Figure 3.6) to elicit cytotoxic activity.

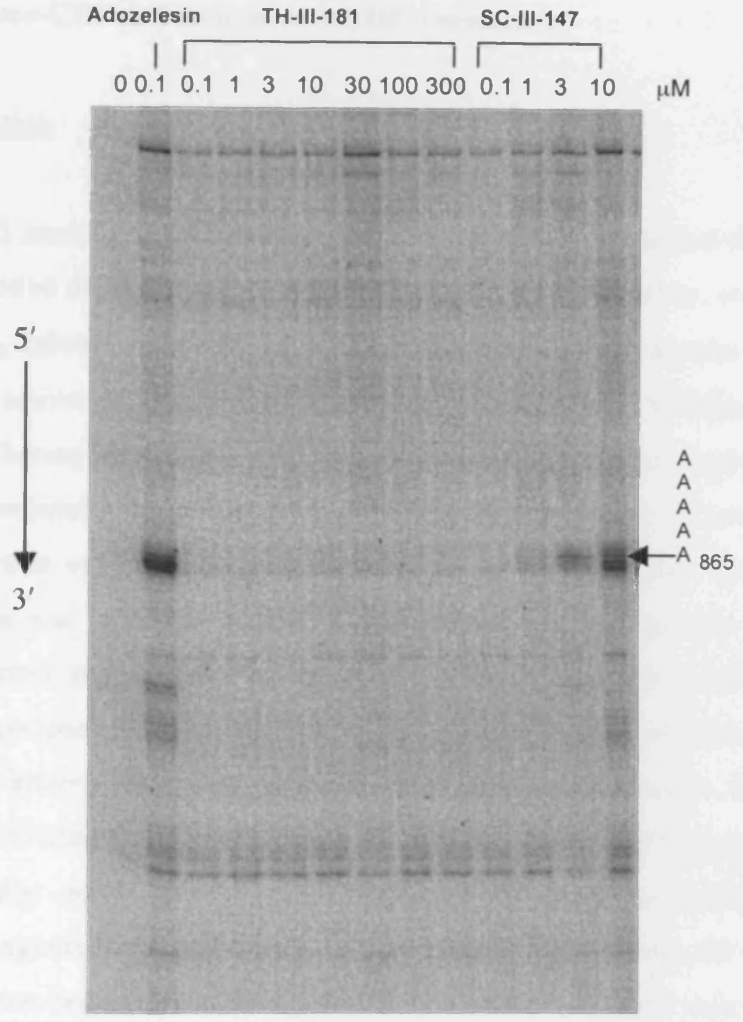

Figure 3.10 *Taq* polymerase assay gel examining damage to the bottom strand of pUC18, induced by the agent, TH-III-81, at the denoted concentrations. Adozelesin and SC-III-147 were included as controls. 0 is the untreated control. The arrow indicates the position and sequence of the common major binding site. Drug: DNA incubations were for 5 hours at 37° C.

3.3 Achiral *seco*-CBI and *seco*-amino-CBI compounds

3.3.1 Introduction

The achiral CI analogues reported in the previous section, retained the ability for sequence selective alkylation at the 5'-AAAAA and 5'-ATTT sites, were cytotoxic exhibiting IC_{50} values in the μM range and comparable to the racemic compounds, and proven active in preliminary *in vivo* studies (see Chapter 6-General Discussion). Having established that the chiral centre of duocarmycins and CC-1065 is not absolutely needed for DNA interactions and anticancer activities, in an attempt to further enhance the properties of the novel analogues, the achiral CI pharmacophore was replaced by the achiral CBI alkylation subunit. There are a number of distinct advantages into incorporating the CBI pharmacophore over CI and CPI, as have been established from early structure activity relationship studies of structurally altered alkylation subunits. The natural enantiomers of CBI-based analogues of CC-1065 have been shown to be four times more biologically stable and biologically more potent, and more synthetically accessible that the corresponding agents featuring the natural CPI subunit. In addition, the less reactive CBI agents have been shown to alkylate DNA at an enhanced rate (due to the absence of the C7 methyl group of CPI which sterically decelerates the rate of DNA alkylation) with greater efficiency and with a slightly greater selectivity among the available sites (Boger *et al.*, 1989; Boger & Ishizaki, 1990; Boger *et al.*, 1992; Boger *et al.*, 1995b). These observations are in agreement with the model of reverse relationship between the electrophile's reactivity and *in vitro* cytotoxic potency, proposed by Boger. Incorporation of the CBI pharmacophore should therefore endow the novel achiral analogues with increased solvolytic stability, which should in turn confer enhanced potency.

Apart from being potent cytotoxic agents, CBI-based agents have also proved to be efficacious antitumour compounds. The (+)-CBI-indole$_2$ agent has been evaluated *in vivo* against the murine P388 leukemia, murine M109 lung carcinoma and B16

melanoma, and human A2780 ovarian carcinoma, achieving some inhibition of growth and increase in lifespan (Boger *et al.*, 1995b). Significant activity by other CBI analogues has been shown in mice bearing L1210 leukemia cells (Wang *et al.*, 2000). Finally certain *seco*-CBI dimers have been evaluated *in vitro* by the NCI and showed significant activity against leukaemia, CNS cancer, melanoma and prostate cancer cell lines with GI_{50} values < 0.01 μM (Jia & Lown, 2000).

Another advantage of the use of the CBI pharmacophore, is the earlier observation that the natural enantiomers of CBI analogues are substantially more potent than their CPI counterparts against resistant cell lines. The cell lines considered were a human colon carcinoma cell line (HCT116) and two resistant variants HCT116/VM46 (MDR cell line) and HCT116/VP35 (resistant to *topoisomerase II* inhibitors). This hypersensitivity of the resistant cell lines was more pronounced for the (+)-CBI-TMI agent in particular, which was even more cytotoxic than the parent compound, (+)-DUMSA (Boger *et al.*, 1995b). This particular property makes the CBI-TMI an interesting lead for further drug development as resistance is one of the most acute problems of conventional chemotherapy and particularly so, for alkylating agents.

The delayed hepatotoxicity associated with (+)-CC-1065, precluded its clinical development. The only CBI agent that has exhibited this phenomenon is (+)-CBI-$PDEI_2$ (Aristoff *et al.*, 1993). However another form of systemic toxicity, suppression of human bone marrow has proved to be the major limiting factor in the development of otherwise potent CC-1065 analogues into therapeutics. Bone marrow toxicity has been shown to undermine the clinical effectiveness of carzelesin and KW2189 in early clinical trials. In previous studies of novel CBI congeners, two CBI-based agents, one bearing two indoles as the DNA binding subunit and a cyclised analogue bearing one indole and one benzofuran group (both analogues possessing a terminal acetamino group), were shown to be highly active against L1210 leukemia in mice and most importantly, not to be myelosuppresive at therapeutically effective doses. While CC-1065, at a dose of 25 μg/kg, severely suppressed white blood cells (WBC), both these novel analogues had no effect on

WBC and platelet counts at double the dose (50 μg/kg), 27 days after administered to mice (Wang *et al.*, 2000). This critically desirable biological property further supports the pursuit of designing CBI based analogues.

3.3.2 Compounds

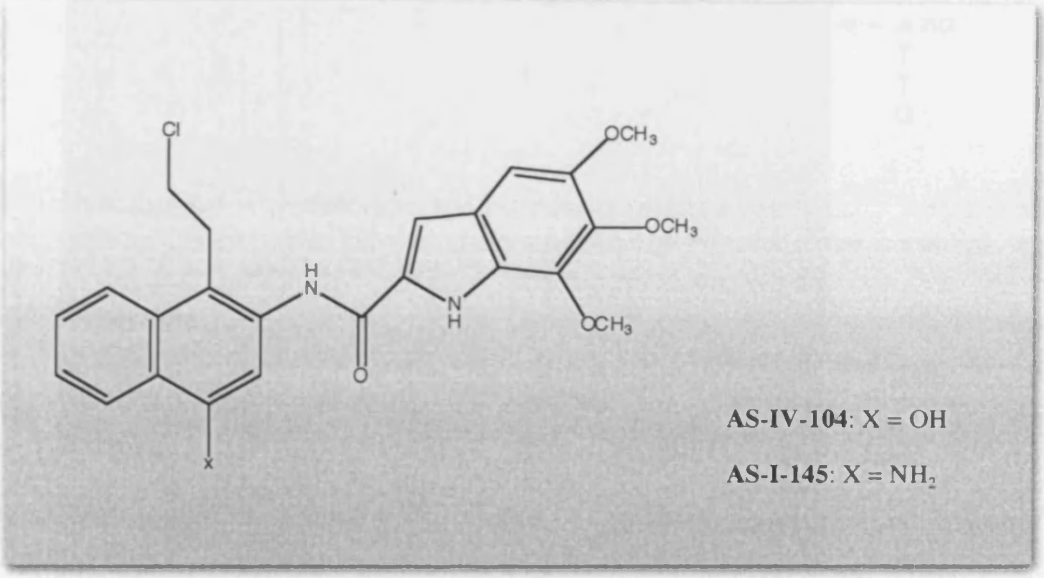

Figure 3.11 Stuctures of the novel achiral *seco*-CBI (AS-IV-104) and achiral *seco*-amino-CBI (AS-I-145) compounds.

3.3.3 Results and discussion

The alkylation ability of the novel achiral CBI compounds and sequence specificity for purine-N3 groups in the minor groove was assessed using the thermally-induced DNA strand cleavage assay. The bottom strand of the pUC18 fragment was used to probe the damage induced by these achiral compounds. Initially, the alkylation ability of both the phenolic and amino achiral CBI agents was compared to the racemic *seco*-CBI-TMI compound, also used as the reference compound in section 2.3. The autoradiograph of this thermal cleavage experiment is shown in Figure 3.12.

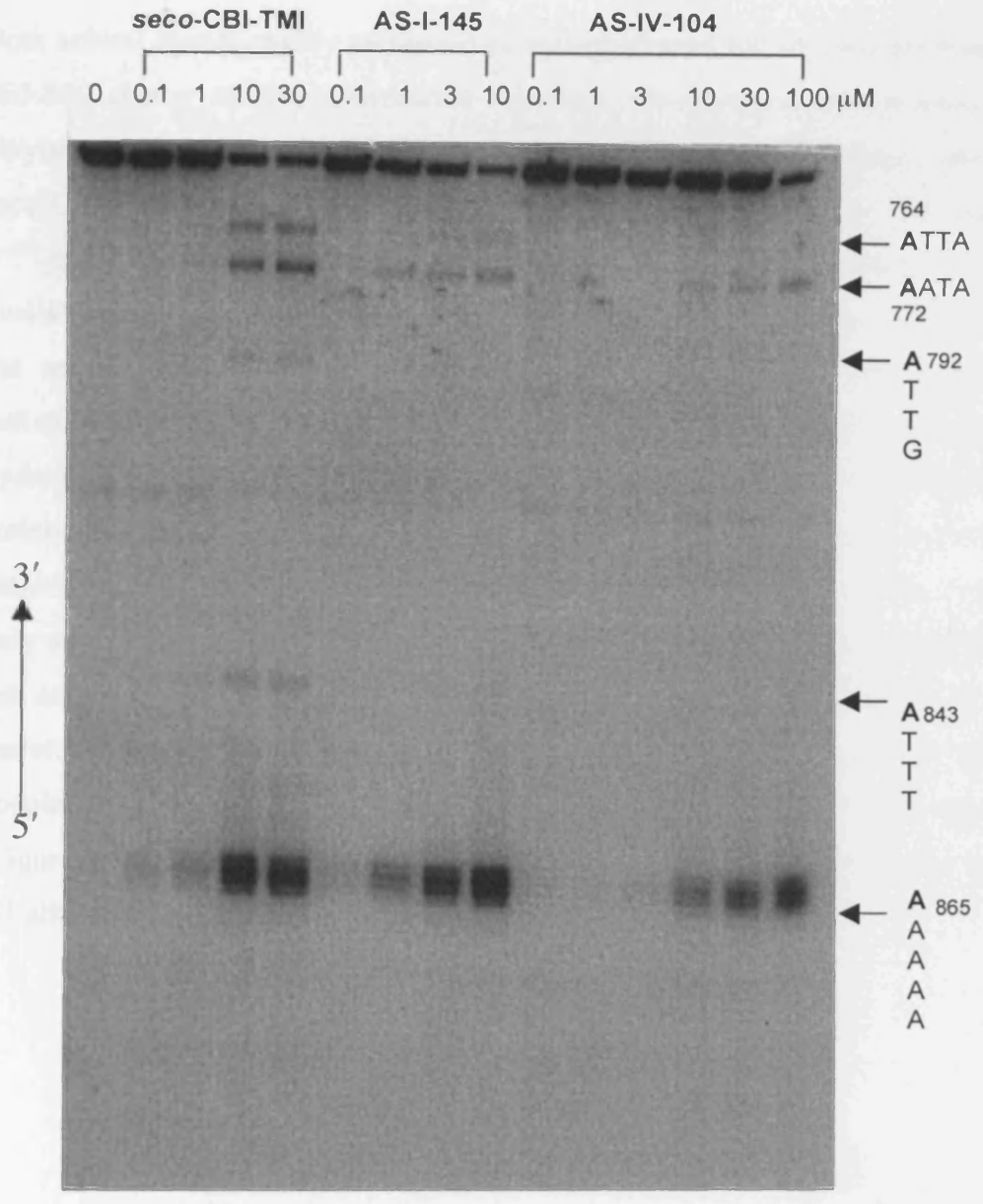

Figure 3.12 Thermal cleavage gel showing purine-N3 lesions to the bottom strand of a 5'-^{32}P labelled, 208 bp fragment of pUC18, defined from 749 to 956 induced by the achiral *seco*-CBI-TMI (AS-IV-104) and its amino counterpart (AS-I-145). 0 is the untreated control. The racemic *seco*-CBI-TMI is included as internal control. Arrows indicate the position and sequence context of the alkylated adenines (underlined and in bold). Adenines on the upper, non-resolvable portion of the gel have been appointed from previous experiments. Drug: DNA incubations were for 5 hours at 37° C.

Both achiral agents readily recognise as their preferred site of covalent binding the 865-869 cluster of five consecutive adenines, displaying a dose-response DNA alkylation effect. This site is also the common, high affinity alkylation site for the *seco*-CBI-TMI control. For all three instances, the 3' adenine of the ^{869}5'-AAAAA-3'^{865} is the most reactive and this site the most prominently alkylated among the available sites judging by the intensity of the band of the cleavage product. While the sequence selectivity of covalent alkylation for the two achiral agents is indistinguishable, the intensity of DNA modification is slightly different. The *seco*-hydroxy compound, AS-IV-104, required a 10-fold higher concentration than its amino counterpart (AS-I-145), to induce a comparable covalent alkylation at the major $(A)_5$ site. Of the AT mixed sequences alkylated by the racemic analogue, only one, ^{772}3'-AATA-5'^{775}, is poorly alkylated by the achiral agents, while there are just traces of alkylation at the ^{764}3'-ATTA-5'^{767}. Both AS-IV-104 and AS-I-145 therefore were more sequence discriminating than their racemic phenolic counterpart. The same is also true when comparing AS-IV-145 with adozelesin (Figure 3.14). Figure 3.13 shows the proposed model for the activation and adenine-N3 alkylation by AS-I-145.

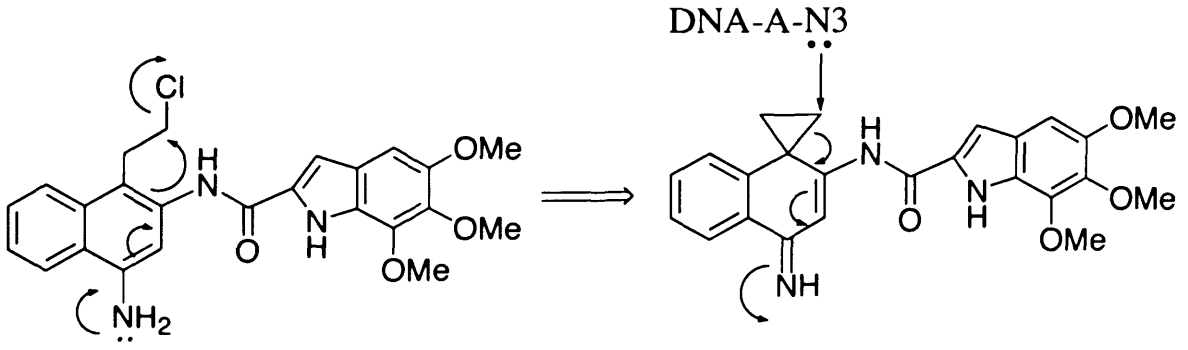

AS-1-145
NSC D716970

Figure 3.13 Proposed model of the activation and DNA alkylation of the achiral AS-I-145 agent.

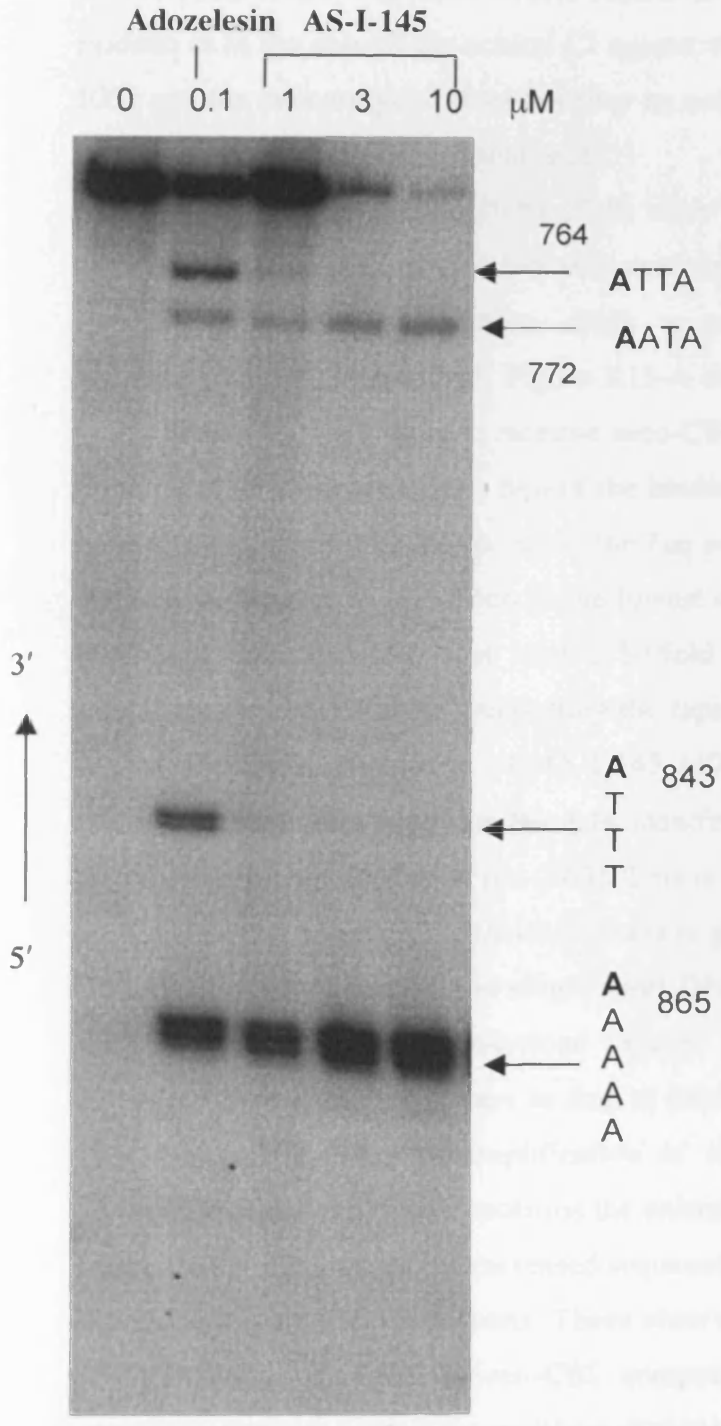

Figure 3.14 Thermal cleavage gel showing the enhancement of the sequence selectivity of AS-I-145 over adozelesin.

On the basis of the alkylation studies results of the achiral CBI agents, it became evident, as in the case of the achiral CI agents, that the stereocentre present in CC-1065 and the duocarmycins does not play an essential role in controlling the DNA interaction properties of these analogues.

The alkylation efficiency/specificity of the more potent CBI based achiral agent, the amino bearing congener, AS-I-145 was compared to its CI counterpart, JT-II-67, studied in the previous section. Such a comparison can be seen on the autoradiographs of Figure 3.15. Figure 3.15-A shows the thermal cleavage analysis of AS-I-145, JT-II-67, and the racemic *seco*-CBI-TMI reference compound, while Figure 3.15-B confirms the position of the binding sites on the bottom strand of the same DNA fragment and region, using the *Taq* polymerase stop assay. Based on the intensity and extent of alkylation at the lowest drug concentration, as observed on Figure 3.15-A, AS-I-145 is at least a 10-fold more efficient alkylator than the achiral *seco*-amino-CI agent, supporting the replacement of the CI pharmacophore. At the highest concentration of AS-I-145 (100 μM) there is a near complete consumption of radioactivity on the gels, manifested as fading of the bands even at the most prominent alkylation site (865). This is due to complete cleavage of all 5'-end labelled fragments (in the thermal cleavage gel) and an overload of non-specific multiple alkylations resulting in single short DNA fragments, not examined on the gel. Accordingly, a damage overload induced by binding at even non-preferred sequences, forces the polymerase to stop at sites prior to the ones examined on the *Taq* stop gel, resulting in amplification of shorter DNA fragments. The *Taq* polymerase assay once again confirms the enhanced alkylating ability of the achiral amino-CBI compound and its increased sequence selectivity over both its achiral CI and racemic phenolic counterparts. These observations coupled to the relative ease of synthesising the achiral-*seco*-CBI compounds, render AS-I-145 the most attractive candidate among the members of this new class of achiral compounds for future development.

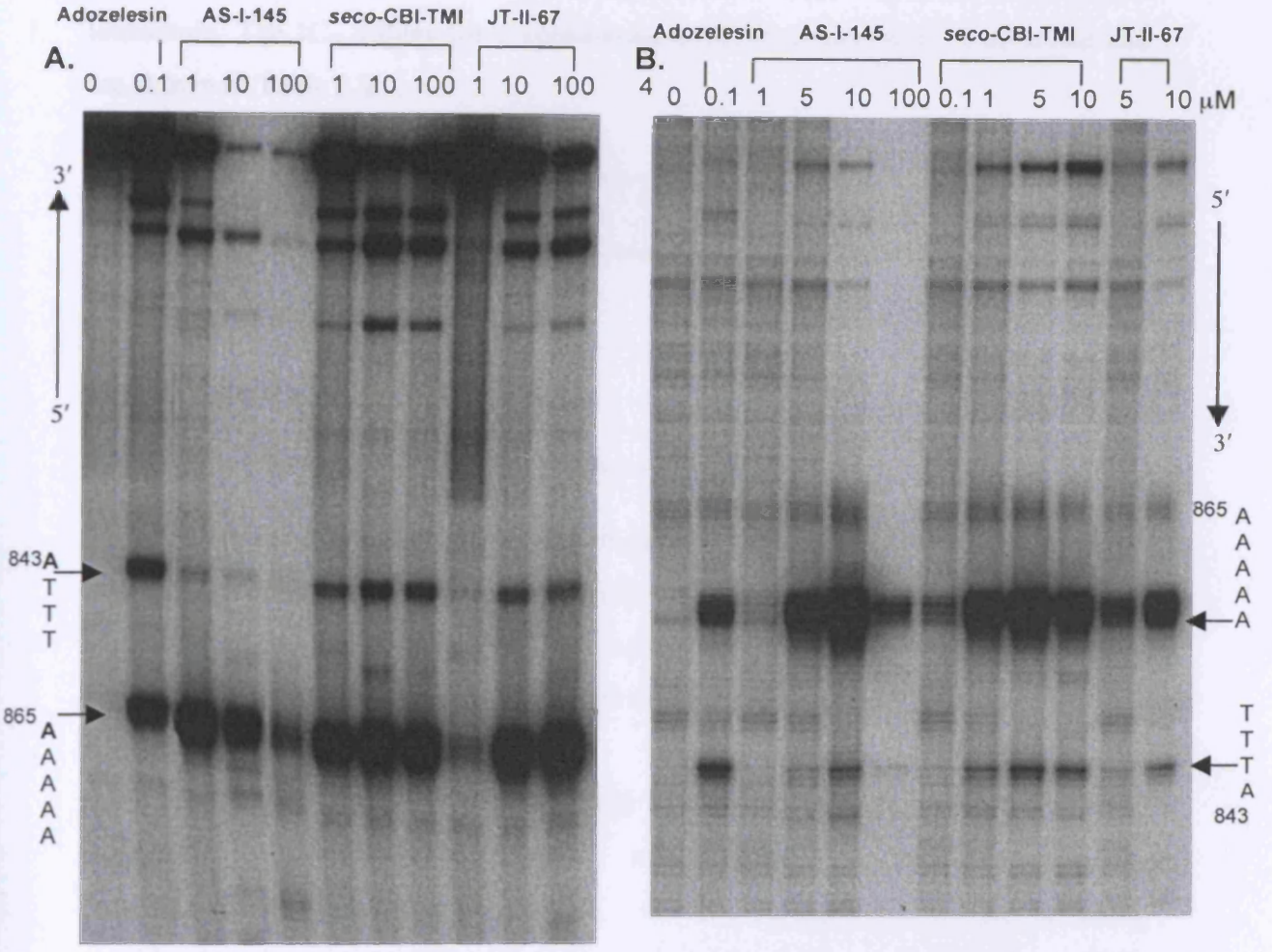

Figure 3.15 A. Thermal cleavage gel, comparing the purine-N3 alkylation ability of the achiral *seco*-amino-CBI analogue (AS-I-145) and its CI counterpart (JT-II-67) along with the racemic *seco*-CBI-TMI agent. **B.** *Taq* Polymerase stop gel, examining the sites of covalent modification, on the same DNA region by the same set of agents. 0 is the untreated control. Arrows indicate the position and sequence context/binding sites of the alkylated adenines. Drug: DNA incubations were for 5 hours at 37° C.

However, it remains critical for these analogues to possess cytotoxic potency and anti tumour efficacy. A MTT-based growth inhibition assay was used to assess the

cytotoxicity of the new achiral agents against the human K562 chronic myeloid leukaemia. The IC_{50} values for a continuous 4-day exposure were determined and are shown in Table 3.2.

Compounds	IC_{50} values (μM)
AS-IV-104	0.15 ± 0.05
AS-I-145	0.045 ± 0.015
(±)-*seco*-CBI-TMI	0.0028 ± 0.001

Table 3.2 *In vitro* cytotoxicity of the achiral CBI agents AS-IV-104 and AS-I-145 and the racemic compound *seco*-CBI-TMI, against human chronic myeloid leukaemia K562 cells, following a 4-day continuous drug exposure. The IC_{50} values represent the average of three independent experiments.

Both achiral CBI-based agents inhibited the growth of tumour cells at sub-micromolar concentrations and proved more active than their corresponding indoline (CI) analogues. Additionally, the amino substitution had a more considerable effect in the CBI series of compounds, with the amino CBI agent, AS-I-145 being approximately 3-fold more potent than the hydroxy derivative, AS-IV-104. In a previous assessment of cytotoxicity of the corresponding chiral agents, no such potentiation was evident. In that case the natural enantiomer of the *seco*-amino-CBI agent exhibited an identical cytotoxicity across a panel of cell lines (the Chinese hamster ovary AA8, UV4 and the human EMT6) to the natural enantiomer of the *seco*-phenolic counterpart (Atwell *et al.*, 1998). That finding was in marked contrast to the CI series, where the nature of the substituent group at the 6-position (*seco*-CI numbering) had a very large influence on cytotoxicity with the racemic *seco*-amino-CI compound being (55-122)-fold less cytotoxic than the corresponding phenol, in the same panel of cell lines (Tercel *et al.*, 1996; Milbank *et al.*, 1999). In all cases the CBI analogues were consistently much more potent than the CI

derivatives. In conclusion, the cytotoxicity results show the present design of the achiral CBI analogues to be successful, with the amino substitution resulting in a more potent product. However past studies of racemic *seco*-amino-CBI agents have indicated the possibility of dissociating cytotoxicity against tumour cells from chronic host toxicity. More specifically while the racemate and unnatural enantiomer of the *seco*-amino-CBI-TMI agent both produced a delayed toxicity effect in treated mice, the more cytotoxic natural enantiomer-treated animals, at the same dose regime, had no histological manifestations of such toxicity at necropsy (Atwell *et al.*, 1999). This result further supports the concept of designing achiral agents, particuarly of this class of compounds, as *in vivo* studies would lack the ambiguity of the enantiomeric pairs often having conflicting biological effects.

The above studies have established the achiral *seco*-amino-CBI agent, AS-I-145, as the best candidate for further development and the leading compound in this new class of agents, endowed with an increased ability to alkylate DNA, possessing enhanced sequence selectivity and resulting cytotoxic potency, among all members of this series of newly synthesised CBI and CI agents lacking the characteristic stereocentre of CC-1065/duocarmycins.

3.4 Hairpin conjugates of achiral seco-cyclopropaneindoline-2-benzofurancarboxamide and pyrrole-imidazole polyamides

3.4.1 Introduction

In section 3.2 it was established that the achiral *seco*-CI pharmacophore can be incorporated into functional analogues and afford potent alkylating agents, despite lacking the parent compounds' stereocentre. Yet, all the achiral compounds synthesised and evaluated for their sequence specificity retain the original chiral CI alkylation subunit's memory for a 3' adenine alkylation within the consensus 5'-AAAAA-3' and AT mixed sequences.

The racenic *seco*-cyclopropaneindoline-2-benzofurancarboxamide (CI-Bf) hairpin polyamides discussed in chapter 2 offered further proof that the concept of conjugating the alkylating pharmacophore of CC-1065 and the duocarmycins with pyrrole/imidazole polyamides in a hairpin configuration may provide an attractive strategy for the discovery of a new class of minor groove sequence specific alkylating agents. The Im-containing conjugates of that series were found to accept G residues within their binding and alkylating site, reminiscent of the DUMA's sequence modulation demonstrated in the presence of imidazole-containing triamides, where the formed - in that case - heterodimer was forced to alkylate guanine-N3 groups within exclusively GC sequences (Fujiwara *et al.*, 1999). Hybrid compounds of a hairpin configuration have been synthesised with the strategy of using the Py/Im polyamides as recognition components to deliver alkylating agents to a target sequence. Hairpin polyamide hybrids incorporating segment A of DUMA (DA) have been shown to alkylate with high specificity and with a fashion that is thought to be a combination of the inherent reactivity of the alkylation effector (such as DA) and the binding specificity of the hairpin polyamides (Tao *et al.*, 1999b). DUMA being the most reactive of the duocarmycins has been shown to be capable of G-N3 alkylation (Sugiyama *et al.*, 1993). The racemic *seco*-CI, Im-containing conjugates in Chapter 2 were also found

to tolerate the presence of a G residue adjacent to an alkylated adenine. However, those chiral analogues retained - as all chiral and achiral analogues considered in this thesis – a significant "memory" for the 5'-AAAAA-3'site, the common, shared most reactive alkylation site. The challenge therefore for analogues possessing an altered reactivity to that of he parent compounds remains.

3.4.2 Compounds

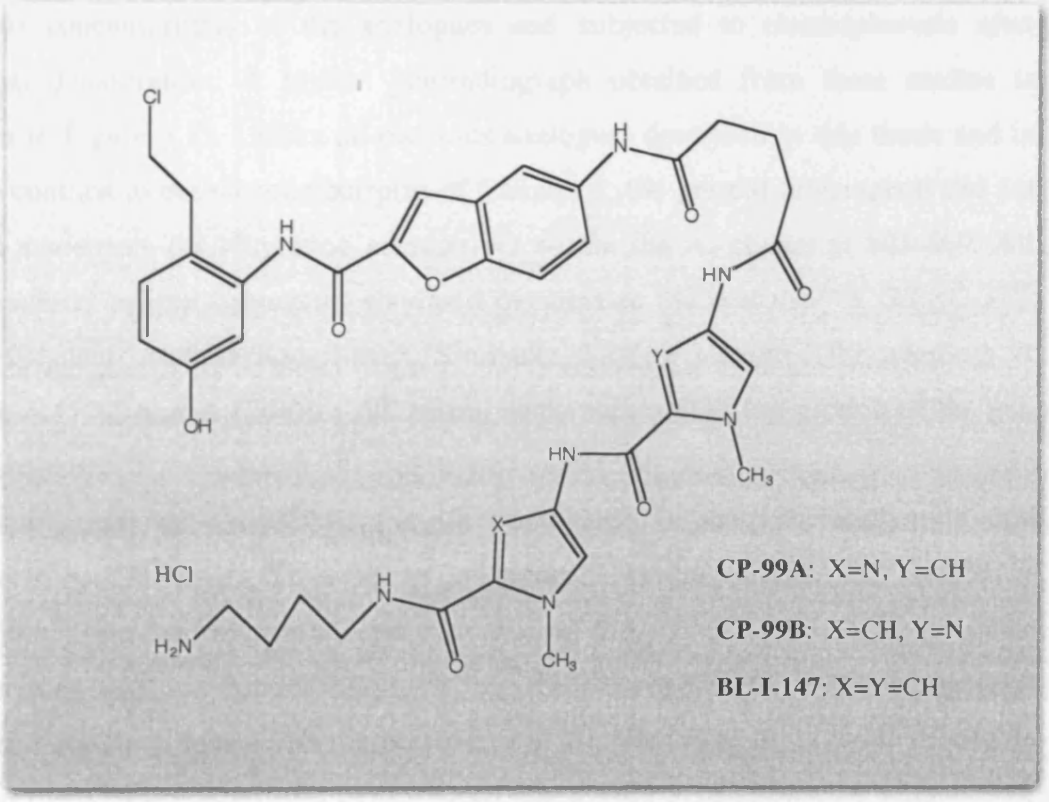

Figure 3.16 Structures of the achiral *seco*-CI hairpin polyamide compounds investigated in this study.

Three novel hairpin compounds have been synthesised incorporating the achiral *seco*-CI as the alkylating "warhead". These are CP-99A (achiral-CI-Bf-Glutaryl-Py-Im-NH_3Cl), CP-99B (achiral-CI-Bf-Glutaryl-Im-Py-NH_3Cl) and BL-I-147 (achiral CI-Bf-Glutaryl-Py-Py-NH_3Cl) (where Py is pyrrole and Im is imidazole). The linker

is the same as the one employed in the racemic *seco*-CI hairpin analogues in Chapter 2. Just like those, the terminal free amine of the conjugates, at physiological pH will remain protonated.

3.4.3 Results and discussion

The covalent sequence specificity of the analogues was assessed by the thermally-induced strand cleavage assay. The same radiolabelled probe was treated with various concentrations of the analogues and subjected to electrophoresis after thermal denaturation. A typical autoradiograph obtained from these studies is shown in Figure 3.17. Unlike all previous analogues described in this thesis and in sharp contrast to the racemic hairpins of Chapter 2, the present three agents did not retain a memory for alkylating adenine-N3 within the A_5 cluster at 865-869. All three achiral hairpin conjugates alkylated the adenine (843) at the ^{845}5'-TT<u>A</u>C-3'^{842} site (alkylated adenine underlined). Similarly they all alkylated the adenines A (792), A (772) and A (764) in AT mixed sequences on the top portion of the gel. The sequence ^{890}5'-TC<u>A</u>G-3'^{887}, which was selectively alkylated by the imidazole containing racemic *seco*-CI-Bf hairpin conjugates, is uniquely recognised and alkylated by CP-99A in this series of analogues. Conversely, conjugate CP-99B is the only agent to react with the A (856) of the ^{858}5'-CA<u>A</u>C-3'^{855} site. The distinctions in the sequence selectivity of the two agents suggest a recognition pattern intimately linked with the presence and the relative position of the imidazole within the polyamide portion of the molecule. Figure 3.18 shows the sequence of the resolvable portion of the gel in Figure 3.17 and highlights the binding sites of all three agents. Based on the model proposed for the binding of the imidazole containing racemic hairpins (JT-IV-99 and RBH-III-23), where an imidazole unit would pair side-by-side with the benzofuran moiety and interact with a GC base pair (Chapter 2), a model of molecular interaction between CP-99A and its unique site of alkylation is shown in Figure 3.19-1. Again, the imidazole group of CP-99A is envisioned to stack with the benzofuran to form a complex similar to the pyrrole / imidazole pairing, capable of recognising a C / G base pair.

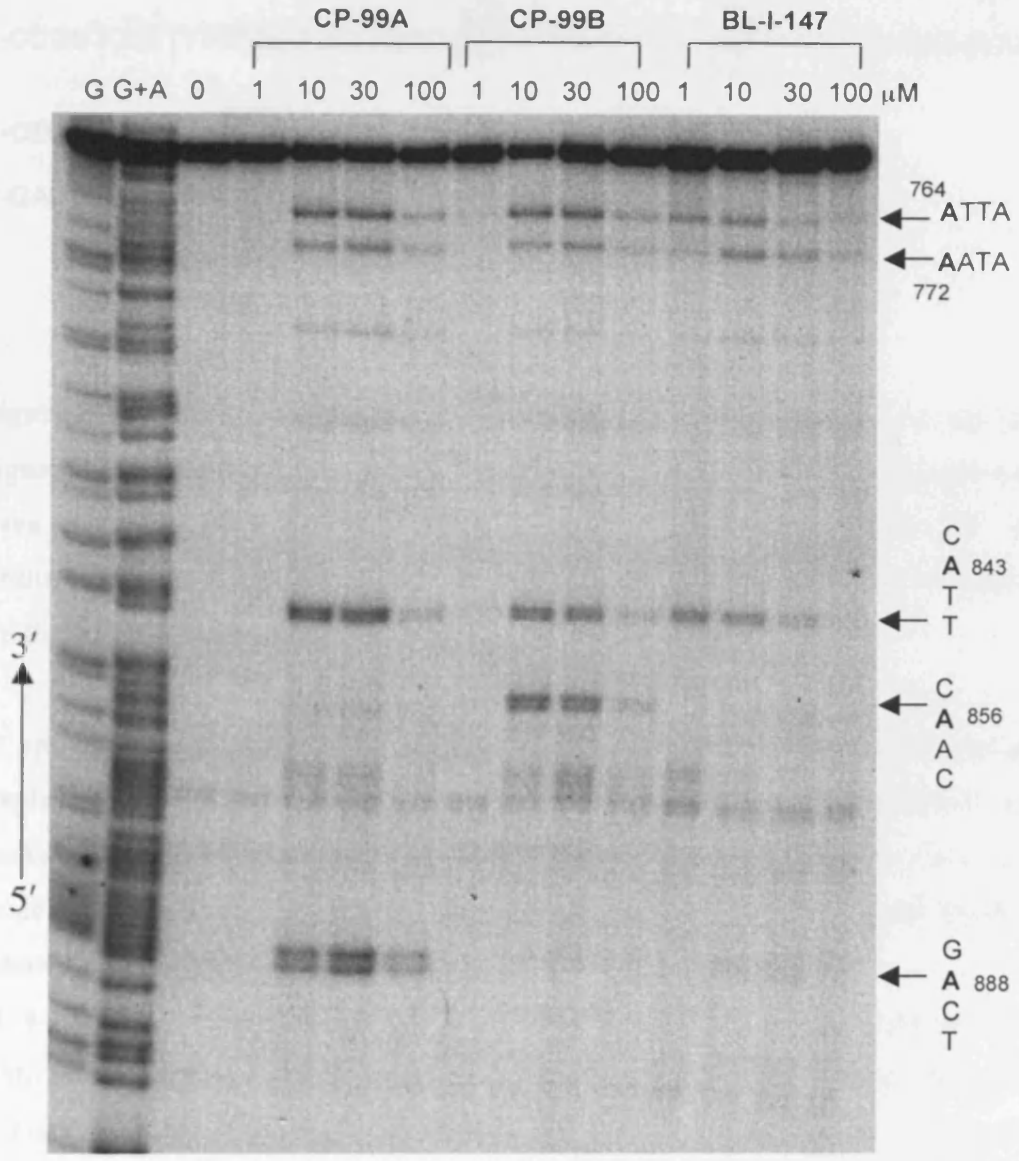

Figure 3.17 Thermal cleavage gel showing purine-N3 lesions to the bottom strand of a 5'-^{32}P labelled, 208 bp fragment of pUC18 (defined from 749 to 956), induced by the denoted achiral *seco*-CI-Bf hairpin polyamide agents. 0 is the untreated control. G / G+A is the purine marker (formic acid). Thermal cleavage conditions as described in the Methods section. Arrows indicate the position and sequence context of the alkylated adenines (underlined and in bold). Drug: DNA incubations were for 5 hours at 37° C.

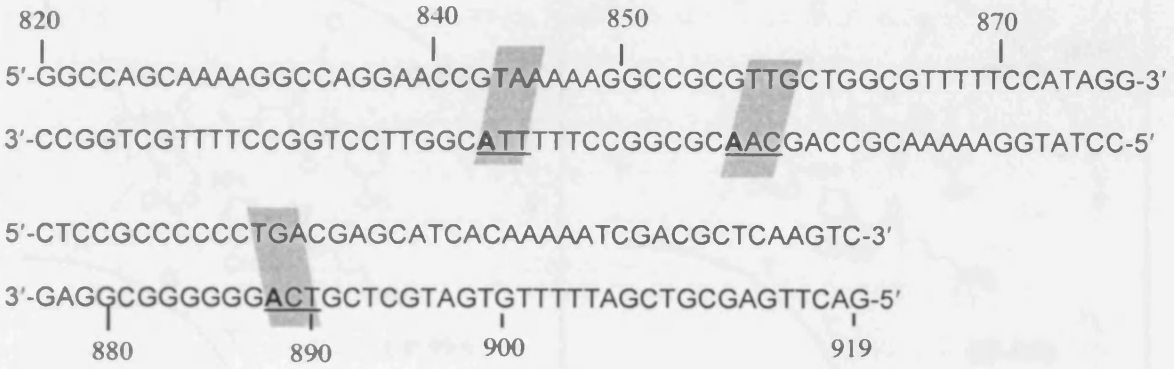

Figure 3.18 Diagram showing the resolvable portion of the thermal cleavage gel of Figure 3.17 examining the damage on the bottom strand of pUC18 induced by the three achiral *seco*-CI hairpin conjugates CP-99A, CP-99B and BL-I-147. Their binding sites are shaded and underlined while the alkylated adenine as identified by the thermal cleavage assay is bolded.

In an analogous manner, the sequence preference of CP-99B which uniquely alkylated the 5'-CAAC-3' site can be attained, by having its imidazole group stacked with the linker and the pyrrole with the benzofuran. In this case, a new mode of recognition involving the benzofuran is proposed, in which the Py/Bf pair behaves like the Py/Py pair of the polyamides (Figure 3.19-2).

BL-I-147 which lacks an imidazole group, failed to produce any alkylation at the A (856) and A (888) sites. This could be attributed to the steric hindrance between the G-2-amino group and the pyrrole-H3 atom, which is responsible for the pyrrole's lack of tolerance for G/C or C/G sites. Consequently BL-I-147 would only bind to the 5'-TTA(843)-3' site with the Bf/Py behaving like a Py/Py pair of the polyamide (Figure 3.19-4). This sequence however must be a conformationally preferred site for this class of compounds as it is also receptive for binding by CP-99A and CP-99B, agents which do not possess structurally discriminating pyrrole-H3 atoms.

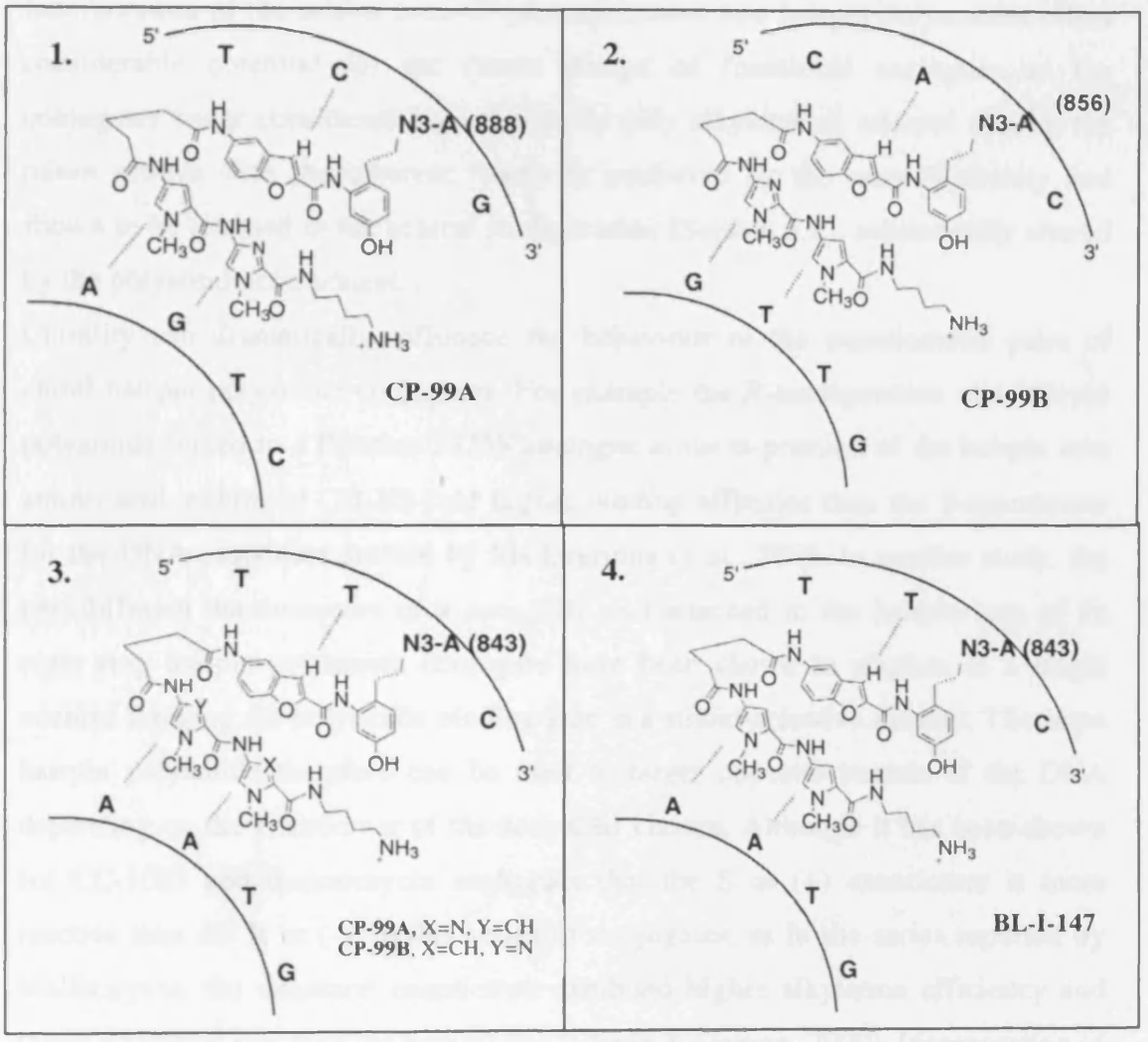

Figure 3.19 Model of molecular interaction between 1. CP-99A (achiral-Cl-Bf-Glutaryl-Py-Im-NH_3Cl) with its unique site 5'-TCA(888)G-3', 2. CP-99B (achiral-Cl-Bf-Glutaryl-Im-Py-NH_3Cl) with its unique site 5'-CAA(856)C-3', 3. CP-99A (for X=N, Y=CH) and CP-99B (for X=CH, Y=N) with their common 5'-TTA(843)C-3', and 4. BL-I-147 with the same site. The adenine-N3 is covalently bonded to the bolded A residue in each of the sequence in the pUC18 plasmid given in Figure 3.18.

Incorporation of the achiral *seco*-CI pharmacophore into hairpin polyamides offers considerable potential for the future design of functional analogues as the conjugates under consideration in this study only alkylated at selected sites in the minor groove with the inherent reactivity conferred by the *seco*-CI moiety and shown to be retained in the achiral configuration (Section 3.2), substantially altered by the polyamide component.

Chirality can dramatically influence the behaviour of the enantiomeric pairs of chiral hairpin polyamide conjugates. For example the *R*-configuration of a hairpin polyamide linked to a Hoechst 33258 analogue at the α-position of the hairpin turn amino acid, exhibited (10-30)-fold higher binding affinities than the *S*-enantiomer for the DNA sequences studied by Mallikarjuna *et al.*, 2005. In another study, the two different diastereomers of a *seco*-CBI unit attached to the hairpin turn of an eight ring hairpin polyamide conjugate have been shown to alkylate at a single adenine flanking the polyamide binding side in a strand-selective manner. The same hairpin polyamide therefore can be used to target opposite strands of the DNA depending on the enantiomer of the *seco*-CBI chosen. Although it has been shown for CC-1065 and duocarmycin analogues that the S or (+) enantiomer is more reactive than the R or (-), in this series of conjugates, as in the series reported by Mallikarjuna, the unnatural enantiomer exhibited higher alkylation efficiency and faster alkylation rate than the natural one (Chang & Dervan, 2000). Incorporation of an achiral pharmacophore can therefore provide a more simplified interaction of the hybrid molecules with DNA.

In a recent study of Py-Im hairpin polyamides which incorporate the CBI and CPI groups as their DNA alkylating moieties, it was revealed that alkylation by the CBI conjugates occurred specifically at adenines in matched sequences, whereas the CPI conjugates alkylated both adenines and guanines in matched sequences, despite having similar orientations. The enhanced, adenine-exclusive, sequence selectivity of the CBI bearing conjugates was attributed to the alkylation group's lower electrophilicity and higher stability compared to the CPI (Bando *et al.*, 2005). The conjugates of the present study also exhibited enhanced sequence selectivity. It is

therefore conceivable that incorporation of the achiral *seco*-CBI pharmacophore (section 3.3), could endow a next generation of hairpin polyamide conjugates as the ones in this study with additional sequence selectivity for target sequences.

CHAPTER 4

REPAIR STUDIES OF TH-III-151 AND AS-I-145 IN THE YEAST *Saccharomyces cerevisiae*

4.1 Introduction

The definition of the molecular context that confers chemosensitivity is essential for the improvement of the efficacy of antitumour drugs. The recognition and the extent of the repair of specific drug-induced DNA lesions are critical determinants of the cellular response to DNA damaging agents, the resulting sensitivity or resistance and can greatly influence their clinical outcome. The reduced levels of the XPA protein in testicular germ cell tumours, for example, and the ensuing defective repair of cisplatin-induced damage, was considered to be a major factor determining the enhanced sensitivity to the drug (Koberle *et al.*, 1999). In contrast, the increased level of repair of the interstrand crosslinks induced by melphalan in patients treated with the agent is thought to constitute a mechanism of clinical resistance to the drug in multiple myeloma (Spanswick *et al.*, 2002).

The yeast *Saccharomyces cerevisiae* has been exploited in the field of drug discovery and in particular the study of the repair mechanisms of many established and experimental anticancer agents.

4.1.1 Yeast as a model system

The budding yeast *Saccharomyces cerevisiae* presents a valuable model system for the study of processes and pathways of eukaryotic cells including their DNA repair mechanisms. As an experimental organism, yeast has a small genome (1.4×10^7 bp/cell), requires simple and inexpensive conditions and media for growth, and has a rapid cell division (90-minute population doubling time), allowing for relatively short experiments, examining effects of e.g. drug exposure over many population

doublings. Importantly, *S.cerevisiae* was the first eukaryote to have its genome fully sequenced (Goffeau *et al.*, 1996) and extensive annotation of most yeast genes has been compiled, yet still remains an ongoing process and is constantly being updated. To this effect, a new resource at the *Saccharomyces* Genome Database, called "Genome Snapshot", has been created and can be found at http://db.yeastgenome.org/cgi-bin/genomeSnapShot.pl). Additionally, a number of methodologies allow for accurate and versatile genetic manipulation, easy gene deletions, characterisation, and assignment of distinct genes to different pathways etc.

A high degree of evolutionary conservation between yeast and mammalian cells in terms of protein functions and cellular processes exists, reflected as gene functional analogy or even interchangeability (Liu *et al.*, 1997; Teichmann *et al.*, 1997). The knowledge gained in yeast can often lead to an understanding of how similar genes might function in mammals and predict their function even before being cloned. This is particularly important since several yeast proteins possess sequence similarity to proteins implicated in human diseases including cancer (Hughes, 2002; Foury, 1997). Xeroderma Pigmentosum for example is a recessive skin disease associated with high predisposition to skin cancers. The xeroderma associated gene *XPD* was cloned and found to be the homologue of the yeast *RAD3* which was the first NER gene to be sequenced and the DNA helicase activity of the gene product to be associated with the repair defect (Weber *et al.*, 1990; Sung *et al.*, 1987). Later, XPA and XPB proteins were shown to be essential components of the TFHII complex of the transcription machinery, the same also holding true for the yeast counterparts Rad3 and Rad25. It was progressively established that all human NER genes have a yeast homologue. The high degree of conservation with mammalian cells therefore, does not only apply to gene sequences and proteins but extends to the function of whole pathways. Table 4.1 highlights this functional conservation of key pathways between humans and yeast, which when altered are related to malignant phenotypes.

Cancer-related pathway	Human genes	Yeast genes
DNA-damage checkpoint	*ATM, ATR*	*RAD53*
Replication checkpoint	*BLM, WRN1*	*SGS1*
Mitotic-spindle-assembly checkpoint	*BUB1, BUBR1*	*BUB1*
Mismatch repair	*hMLH1*	*MLH1*
Repair of DNA double-strand breaks	*BRCA1*	*RAD50, RAD52*
G1- to S-phase transition	*Cyclin D1, cyclin E*	*CLN2*

Table 4.1 Conservation between yeast and human pathways altered in cancer. The human and yeast genes shown are functional homologues and do not necessarily share sequence homology (taken from Simon & Bedalov, 2004).

Since genetic alterations of human tumour cells frequently involve functional homologues in yeast, many of the insights gained using yeast can be extrapolated to mammalian systems. These characteristics have expanded the application of yeast as a screening tool to the field of drug discovery, as it represents an inexpensive and alternative system to mammalian culture cells and enables screening of compounds in a cellular, eukaryotic environment.

4.1.2 Yeast in drug discovery

Target-based anticancer screens

Yeast-based screens can be used as a tool for the identification of targets, which can be pharmacologically modulated by appropriate inhibitors, thus providing novel leads for drug development. Proteins that are linked with accelerated growth in human cancers, when expressed in yeast, can lead to an arrest in cell growth and division by interfering with growth-regulatory pathways. Inhibition of the enzymatic activity of the foreign protein restores normal yeast growth. This principle allows for the screening of potential inhibitors of the human enzymes in

yeast. In such yeast anticancer screens, candidate cDNAs that encode cancer-related proteins are transformed in yeast. Those that block growth are identified as potential anticancer targets and can be used in small-molecule screens for agents that could restore growth and therefore function as inhibitors of the human proteins.

One such screen identified several novel submicromolar inhibitors of poly(ADP-ribose) polymerase, PARP1, which is responsible for addition of ADP-ribose units to nuclear proteins. PARP activity in human cells is induced by DNA strand breaks. The inhibition therefore of PARP could improve the efficacy of DNA-damaging agents. PARP is not found in yeast but when expressed causes a growth reduction phenotype. Based on their ability to reverse growth inhibition in PARP1-expressing yeast, several small molecule inhibitors have been identified. These were also shown to be active in a mammalian PARP biochemical assay, further validating the usefulness of the yeast screen (Perkins *et al.*, 2001). Similarly, the p16 (INK4A) protein and flavopiridol were identified as cyclin-dependent kinase (CDK) inhibitors, as they were shown to restore yeast cell growth inhibited by overexpression of human CDK4 (Moorthamer *et al.*, 1998).

Pathway-based screens

As well as the basis for screening inhibitors of identified targets, yeast can also be used for pathway-based anticancer screens. In this case, the focus shifts on the inactivation of any one of several enzymes that participate in a single functional pathway. A high degree of conservation of epigenetic regulation of gene expression exists between yeast and mammals. Therefore agents identified in yeast-based screens to inhibit the activity of e.g. yeast histone-modifying enzymes, could also serve as potential anticancer drugs.

Yeast Sir2 is a NAD^+-dependent histone deacetylase required for chromatin-dependent silencing in yeast, and functions in a complex with Sir3 and Sir4 to maintain silencing. Yeast cells cultured in uracil-deficient media require expression of the *URA3* gene for growth. In cells lacking the endogenous *URA3* gene (which

encodes a protein required for the biosynthesis of uracil), a *URA3* reporter gene is inserted within an area of silenced chromatin, near a telomere. As expression of this telomeric *URA3* is blocked by the activity of the pathways comprising of Sir2, Sir3 and Sir4, a screen for growth in these conditions can identify those compounds that are capable of interfering with the function of any of the pathway components. The principle of such a positive-selection screen, where inhibition of the target leads to growth, is shown in figure 4.1.

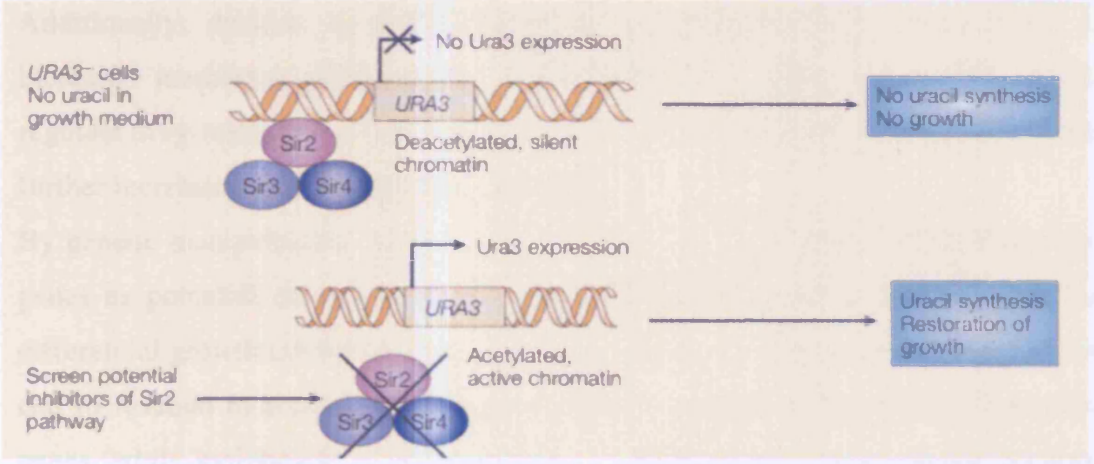

Figure 4.1 Example of a pathway-based, positive-selection screen in yeast (taken from Simon & Bedalov, 2004).

This screen helped identify a compound, splitomycin, which disrupts telomeric silencing from a collection of 6,000 compounds from the NCI repository. Whole genome microarray experiments further confirmed that splitomycin selectively inhibits the Sir2 protein (Bedalov *et al.*, 2001).

Positive growth selection assays with appropriately engineered yeast strains have also been successfully performed for the identification of inhibitors of tyrosine kinases receptors (RTKs) (Barberis *et al.*, 2005), ion channel-forming protein of the influenza virus (Kurtz *et al.*, 1995) and enzymes like β-secretase (BACE) implicated in Alzheimer's disease (Middenodorp *et al.*, 2004). Thus the

applicability of yeast as a screening tool extends to a variety of drug targets associated not only with cancer but also other diseases.

Context-based anticancer screens - Yeast mutants for identification of determinants of chemosensitivity

One important application of yeast is its use for anticancer drug screens, as a large number of biologically active compounds can penetrate the yeast cell membrane. Additionally, deletion in *ERG6* (involved in ergosterol biosynthesis) leads to increased membrane permeability, while deletions in *PDR1* and *PDR3* (which regulate drug-resistance efflux pumps) reduces efflux-mediated detoxification, thus further increasing yeast's sensitivity to drugs.

By genetic manipulations, such as gene deletions, it is possible to evaluate certain genes as potential determinants for sensitivity to anticancer drugs based on the differential growth inhibition. Single gene alterations can highlight the ability of the cell to respond to a particular cytotoxic injury focusing on the effects of specific genes, while assignment of distinct genes to different pathways can be obtained through epistasis analysis, in which the phenotype of a double mutant strain is compared to the corresponding single mutant strain.

The developmental therapeutic program of the NCI has developed a yeast anticancer drug screening employing key selected *Saccharomyces cerevisiae* single and double mutant strains, each defective in a particular DNA damage repair or cell cycle control function. Tens of thousands of compounds have been tested for their ability to inhibit the growth of these yeast strains. All screening was performed as part of the "Seattle Project" at the Fred Hutchinson Cancer Research Center in Seattle, Washington. The project involved a panel of isogenic strains bearing several DNA repair mutations (including nucleotide excision, base excision, mismatch, post-replication, recombinational repair and reversal of O^6-alkylguanine) and cell cycle checkpoint mutations (including DNA damage G2/M, and S phase checkpoint, mitotic spindle assembly checkpoint). The strains were also mutant for

the three genes *ERG6*, *PDR1* and *PDR3* to increase cell permeability and decrease efflux. The experimental design comprise three stages, stage 0 (crude sensitivity screen), stage 1 (crude selectivity screen) and stage 2 (dose response) (DTP Yeast Anticancer drug screen website http://dtp.nci.nih.gov/yacds/).

The cytotoxicity profiles obtained for selected yeast mutants, help to highlight the importance of defects in specific DNA repair pathways as a determinant of chemosensitivity, clarify the contribution of specific eukaryotic genes in regulating sensitivity or resistance to antitumour drugs, and identify agents selective for specific genetic defects.

4.1.3 Repair of minor groove adducts

Key yeast mutants have been studied previously in the laboratory, in order to elucidate the mechanisms involved in the excision repair of the untargeted *N*-alkyl purine adducts induced by clinically important anticancer drugs like the nitrogen mustards. The involvement of both base excision repair (BER) and nucleotide excision repair (NER) was confirmed with NER clearly dominating (McHugh *et al.*, 1999b; McHugh *et al.*, 2000).

Little is known however, about the repair of damage produced by complex agents that bind in the DNA minor groove. CC-1065, an archetypal representative of this class of compounds reacts with the N3 position of adenine to produce minor-groove targeted adducts. These sequence-specific adducts have been shown to be substrates for bacterial and human NER *in vitro* (Gunz *et al.*, 1996; Selby & Sancar, 1988).

In previous work in this laboratory, benzoic acid mustards (BAMs) tethering 1-3 pyrrole units (Figure 4.2) showed increasing DNA sequence selectivity ranging from primarily guanine-N7 alkylation in the major groove (BAM and BAM-Py) to highly sequence specific alkylation in the minor groove (BAM-PyPyPy) in the sequence 5'-TTTTGPu (Pu=guanine or adenine) (Wyatt *et al.*, 1995). Cytotoxicity of these analogues in human cells increased with increasing the number of the incorporated pyrrole units, reflecting the increasing sequence selectivity. A panel of

yeast mutants disrupted in BER, NER, recombination, and post-replication repair functions, was screened for sensitivity against the three analogues. Table 4.2 shows the involvement of the repair pathways in the elimination of the DNA adducts produced by the three oligopyrrole compounds, as suggested by the survival studies. The primarily purine-N7 adducts produced by BAM-Py, in the major groove, are repaired by both BER and NER with a clear dominance of the BER pathway (unlike the nitrogen mustard major groove adducts) (Brooks *et al.*, 2000). The purine-N3 minor groove adducts induced by BAM-PyPy, which possesses limited sequence selectivity, are good substrates for both BER and NER. In contrast, the highly sequence specific, minor groove-targeted adducts by BAM-PyPyPy were not processed by any known BER or NER activities as no increased sensitivity over their isogenic parent, was evident in any BER or NER deficient yeast strains studied, even at the highest concentration of the agent employed. However, these adducts do get excised in the parental, repair proficient strain as revealed by a PCR-based technique, yet the *rad18* strain failed to eliminate them. Therefore a process requiring Rad18 is employed for the excision of this type of minor groove damage (Brooks *et al.*, 2000).

4.1.4 Excision and Post-Replication repair

Excision repair is an important cellular response to DNA damage by a broad spectrum of physical and chemical agents. The two principal excision repair pathways, from *E.coli* to human cells are base excision repair (BER) and nucleotide excision repair (NER).

Excision repair initiated by the action of DNA glycosylases, a specific class of DNA repair enzymes, is called base excision repair. DNA glycosylases incise the chemically modified bases by hydrolysis of the N-glycosyl bond linking the base to the sugar-phosphate backbone (Sancar & Sancar, 1988; Cunningham, 1997).

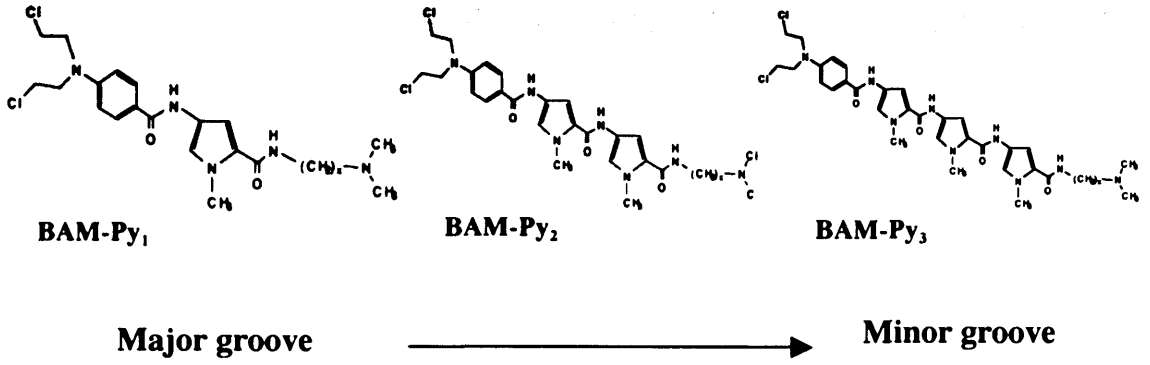

Figure 4.2 Structures of the three oligopyrrole analogues of distamycin tethering BAM. The shift of the targeting from major to minor groove is denoted.

Compound	Target	Cytotoxicity	Sequence specificity	Repair mechanism
BAM-Py_1	Major groove	+	G-N7 A-N3	**BER**, NER
BAM-Py_2	Minor groove	++	AT tracts	BER, NER Rad18, Rad52
BAM-Py_3	Minor groove	+++	5'-TTTTGPu	**Rad18**

Table 4.2 Summary of the properties of the three BAMs, tethering 1-3 pyrrole units, as extracted from Wyatt *et al.*, 1994; 1995. The repair mechanism in bold, denotes the primary repair process acting upon the corresponding adducts, as determined by the sensitivity screen of the relevant yeast mutants (Brooks *et al.*, 2000).

The resulting sites of base loss, called apurinic or apyrimidinic (AP) sites are removed by a second class of base excision repair enzymes, the apurinic/apyrimidinic (AP) endonucleases, which cut the DNA phosphodiester backbone at the 5' side of the abasic site. Some glycosylases (bifunctional) also possess an associated AP lyase activity (Doetsch & Cunningham, 1990). The sequential action of the two types of enzymes results in a single nucleotide gap in the DNA duplex during base excision repair. Following the processing of the 5' terminus by deoxyribose phosphodiesterase, which excises the 5'-terminal sugar phosphate, the gap is filled by repair synthesis by DNA polymerase and DNA repair is completed by DNA ligase (Reviewed by Friedberg *et al.*, 1995). BER processes DNA base damage that causes relatively minor disturbances to the helical DNA structure and includes primarily oxidative damage, alkylation damage such as methylation, damage induced by radiation, or replication errors, all induced from environmental agents and endogenous sources (Memisoglu & Samson, 2000).

Another mode of excision repair involves the incision of the affected DNA strand on both sides of the base damage, generating a lesion-containing oligonucleotide fragment. This excision phenomenon is mainly targeted to helix-distorting bulky base adducts produced by physical agents, such as UV radiation, or a variety of chemical agents (e.g. cisplatin-induced intrastrand crosslinks). In eukaryotes NER is a multi-step process involving damage recognition, DNA unwinding and dual incision. This entails the coordinated action of around 30 polypeptides and eventually leads to the release of a damage-containing 25-30-mer oligonucleotide (reviewed by Friedberg *et al.*, 1995; Prakash & Prakash, 2000). The gap created is filled in by a DNA polymerase and ligation completes the repair. In *Saccharomyces cerevisiae*, NER is dependent upon genes of the *RAD3* epistasis group. Of these genes, *RAD1, RAD2, RAD3, RAD4, RAD10, RAD14* and *RAD25* are absolutely required for the recognition and incision steps of NER in *S. cerevisiae*. More specifically, the initial recognition of a DNA lesion is probably mediated by the Rad4/Rad23 (nucleotide excision repair factor; NEF2) and the Rad7/Rad16 (NEF4) complexes, the latter showing ATP dependence for damage binding and is crucial

for the global genome repair (Guzder *et al.* 1997) (Figure 4.3). Other damage binding protein factors are Rad14 which has an affinity for UV-damaged DNA and replication protein A (RPA), which binds single stranded DNA and is also required for the incision step of NER (Guzder *et al.* 1993; 1995). Rad3 and Rad25 (part of the NEF3 complex) are DNA helicases, which translocate on single stranded DNA in the 5'→3' and 3'→5' direction, respectively, topically unwinding the DNA (Sung *et al.*, 1996). These two proteins constitute two of the subunits of the transcription factor TFIIH and are both essential for the incision step of NER (Sung *et al.*, 1996). Rad4 and Rad23, which together form NEF2, have been implicated in an early step of NER, as damage recognition factors, and no incisions are observed in a *rad4* mutant (Guzder *et al.*, 1998). Rad1-Rad10 which form a tight heterodimeric complex (NEF1) and Rad2 (NEF3), introduce incisions on the 5' and the 3' side of the damage, respectively (Bardwell *et al.*, 1994; Habraken, *et al.*, 1993). After the release of the lesion-containing oligonucleotide, resythesis is performed by DNA polymerase δ and ε and ligation by Cdc9 (DNA ligase I) (Prakash & Prakash, 2000).

NER proceeds at a faster rate on the transcribed strand of active genes than the non-transcribed strand, and this phenomenon is known as transcription-coupled repair (TCR). Yeast *RAD26* disruption, severely impaired the preferential repair of UV-induced cyclobutane pyrimidine dimers in the transcribed strand of the active *RBP2* gene (Van Gool *et al.*, 1994). Rad26 has been suggested to enable TCR by increasing accessibility of DNA damage to repair proteins (Bucheli & Sweder, 2004).

For the lesions in DNA formed by UV or many DNA damaging agents which are not removed by NER or BER, error-free and error-prone (mutagenic) damage tolerance and translesion synthesis mechanisms exist in *S. cerevisiae*. Both these modes depend on genes within the *RAD6* epistasis group and comprise the complex post-replicative repair pathway which can be further dissected in multiple downstream subpathways (Figure 4.4).

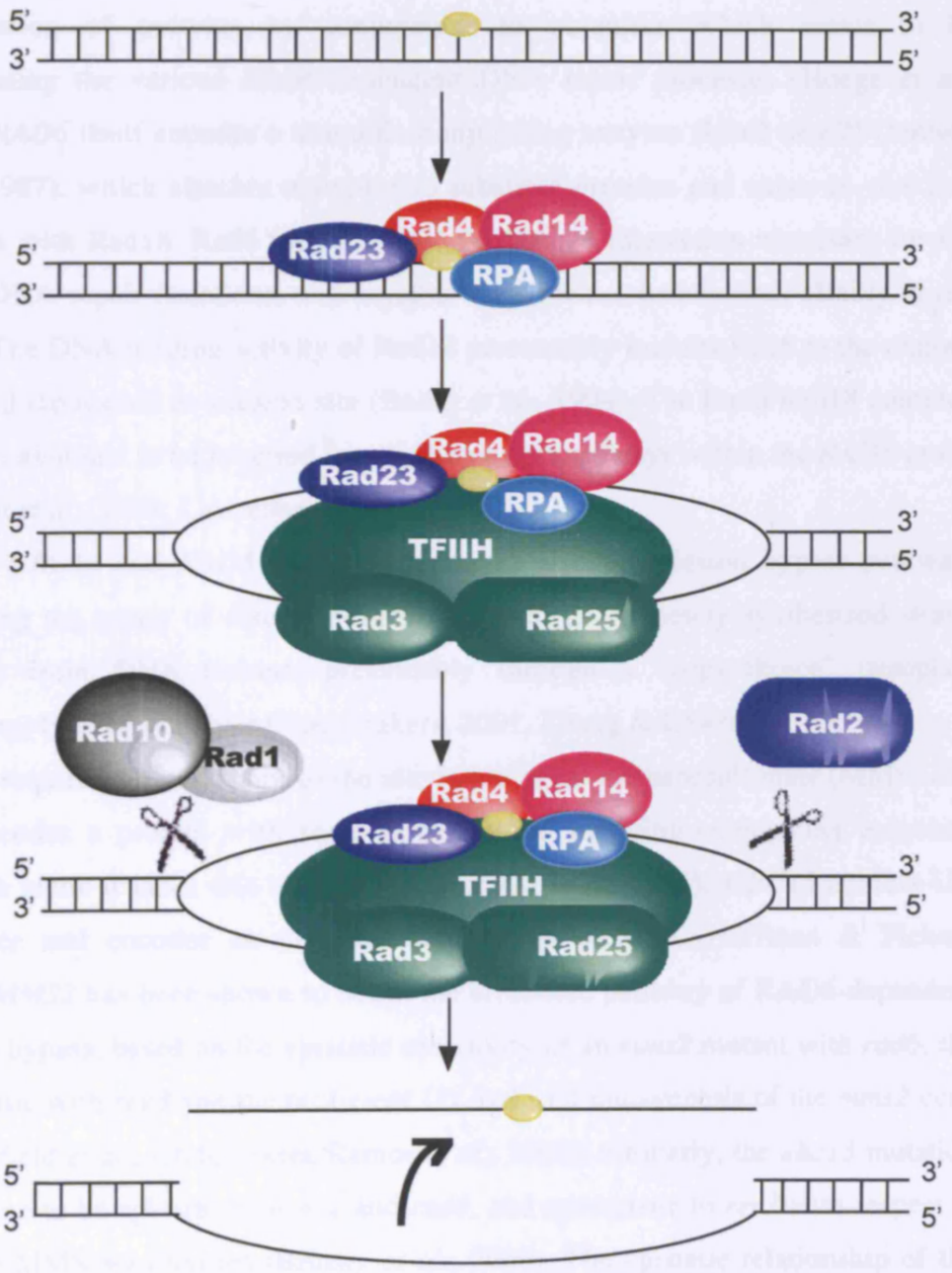

Figure 4.3 Schematic representation of the yeast NER damage recognition and incision steps.

RAD6 is the pivotal gene of the post-replicative repair pathway, required for both error-free and error-prone modes of lesion bypass. Ubiquitin is a highly conserved

76-residue protein, often found covalently joined to other proteins. It is the modification of proteins by conjugation to ubiquitin, which seems to be coordinating the various *RAD6*-dependent DNA repair processes (Hoege *et al.*, 2002). *RAD6* itself encodes a ubiquitin-conjugating enzyme (Ubc2 or E2) (Jentsch *et al.*, 1987), which attaches ubiquitin to substrate proteins and exists *in vivo* in a complex with Rad18. Rad6 interacts with Rad18, an interaction necessary for the *RAD6* DNA repair functions, and together they form a heterodimer (Bailly *et al.*, 1994). The DNA binding activity of Rad18 presumably recruits Rad6 to the regions of stalled replication at a lesion site (Bailly *et al.*, 1994). The Rad6/Rad18 complex has been assumed to be required for all known subpathways within the *RAD6* group (Prakash *et al.*, 1993; Lawrence, 1994).

MMS2, *UBC13* and *RAD5* genes comprise an error-free lesion bypass pathway, promoting the repair of discontinuities that form in the newly synthesised strand opposite from DNA lesions, presumably through a "copy-choice" (template switching) type of synthesis (Hoeijmakers, 2001, Zhang & Lawrence, 2005).

MMS2, required for resistance to the alkylating agent methanesulfonate (MMS) and UV, encodes a protein with some homology to ubiquitin-conjugating enzymes, although alone it lacks this activity (Broomfield *et al*, 1998). *UBC13* confers UV resistance and encodes an ubiquitin-conjugating enzyme (Hoffman & Pickart, 1999). *MMS2* has been shown to act in the error-free pathway of RAD6-dependent damage bypass, based on the epistatic sensitivity of an *mms2* mutant with *rad6*, the synergistic with *rev3* and the proficient UV-induced mutagenesis of the *mms2* cells (Broomfield *et al.*, 1998; Torres-Ramos *et al.*, 2002). Similarly, the *ubc13* mutation was found to be epistatic to *mms2* and *rad6*, and synergistic to *rev3* with respect to UV and MMS sensitivities (Brusky *et al.*, 2000). The epistatic relationship of the two genes for UV damage, suggests that they act in the same DNA, damage processing pathway. Additionally, the two proteins interact and form a heterodimeric complex, which promotes the assembly of polyubiquitin chains linked via the lysine 63 of ubiquitin (Hoffman & Pickart, 1999).

RAD5 is another component of the error-free system, since UV-damaged mutations still occur in a *rad5* mutant and a synergistic increase in UV sensitivity is exhibited when combined with a *rev3* mutation (Johnson *et al.*, 1992; Cejka et al., 2001). Additionally, it was found to be epistatic for UV sensitivity to *MMS2* and *UBC13* (Ulrich & Jentsch, 2000; Torres-Ramos *et al.*, 2002). The gene encodes a DNA-dependent ATPase (Johnson *et al.*, 1994) and has a ubiquitin ligase activity (Hoege *et al.*, 2002). Rad5 has been shown to transiently interact with the Mms2 / Ubc13 complex, as well as with Rad18 (Ulrich & Jentsch, 2000). It has been proposed that Rad5 recruits the Mms2 / Ubc13 complex to DNA and acts as a bridging factor to bring Ubc13 and Mms2 into contact with the Rad6 / Rad18 complex (Ulrich & Jentsch, 2000).

The Mms2 / Ubc13 protein complex was therefore placed specifically in the *RAD5*-dependent subpathway of the *RAD6* pathway and shown to be dependent on *RAD18* (Xiao *et al*, 1999; Ulrich & Jentsch, 2000).

POL30, encoding proliferating cell nuclear antigen (PCNA), a processivity factor for DNA polymerases and *POL3*, encoding polymerase δ, (Pol δ), have also been implicated in the error-free bypass of UV-damage through translesion synthesis (Torres-Ramos *et al.*, 1997). In DNA damaged yeast cells, PCNA becomes monoubiquitinated by Rad6 / Rad18, sunbsequently polyubiquitinated by Mms2 / Ubc13, through the ubiquitin ligase activity of Rad5 and is also a substrate for the small ubiquitin-related modifier, (SUMO)-conjugating enzyme (Hoege *et al.*, 2002). These modifications although affecting the same site on PCNA, direct it for alternative actions, further confirming the role of ubiquitin modifications as an important signal of the various cellular processes of PRR.

RAD30 is another member of the *RAD6* epistasis group encoding for the DNA polymerase Pol η which catalyses, in response to UV damage, error-free translesion synthesis past a thymine-thymine cyclobutane dimer (TT CDP) (Johnson *et al*, 1999). The *RAD6-RAD18-RAD30* epistasis group has been shown to be distinct to the branch comprising of *RAD6, RAD18, RAD5, UBC13* and *MMS2*, for UV sensitivity (Ulrich & Jentsch, 2000; Torres-Ramos *et al.*, 2002).

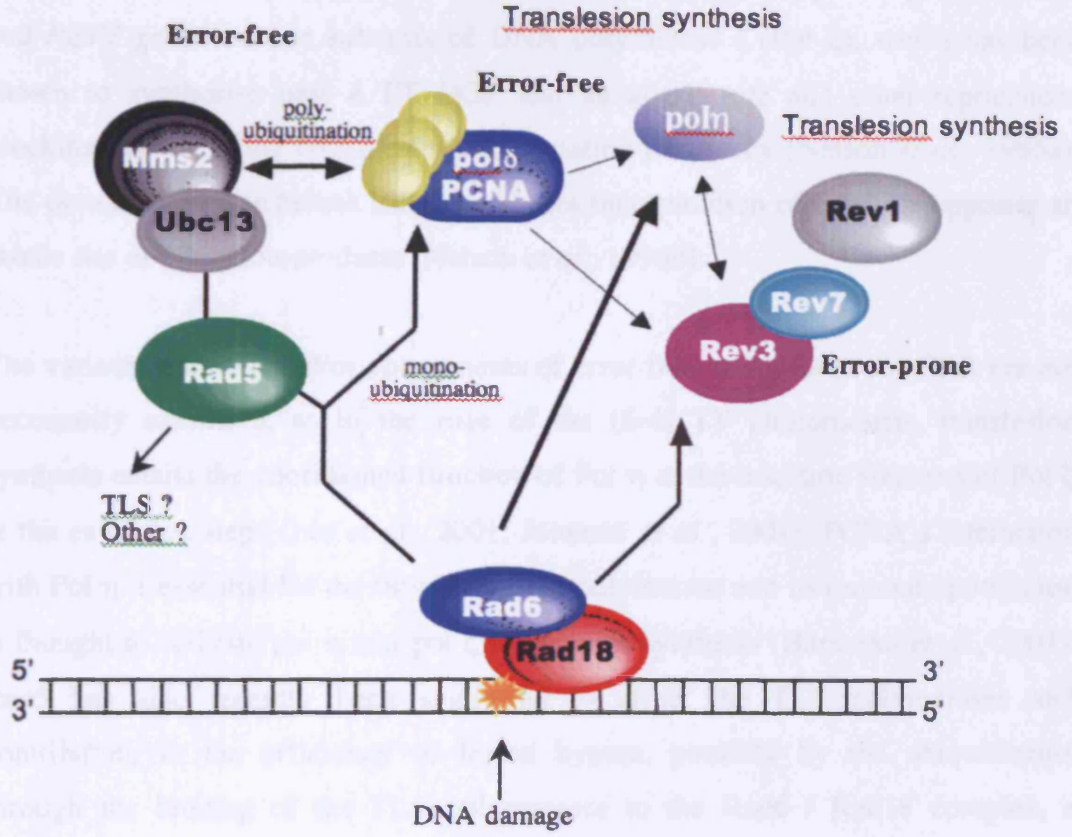

Figure 4.4 Schematic representation of the *RAD6* dependent post-replication repair subpathways. Recognition and binding to DNA damage by the Rad6/Rad18 heterodimer is required for all subsequent processes, divided in error-free and error-prone modes. The subdivision has been based on epistasis analysis of the sensitivities of the relavant mutants to UV damage and biochemical assays (see References in the text).

RAD6 and *RAD18* also mediate error-prone processes that require the proteins encoded by *REV* genes. *REV1*, *REV3*, and *REV7* genes function in mutagenic bypass as the corresponding yeast mutants, were found to decrease damage-induced

mutagenesis. Epistasis analysis indicated that the three *REV* genes function in a process independent of Pol η or Mms2 / Ubc13 mediated damage processing (Xiao *et al.*, 1999), therefore representing a distinct mutagenic subpathway. The *REV3* and *REV7* genes encode subunits of DNA polymerase ζ (Pol ζ), which has been shown to synthesise past a TT DCP and an abasic site and other replication-blocking lesions at the cost of elevated mutation frequency (Nelson *et al.*, 1996a). The deoxycitidyl transferase Rev1, promotes incorporation of cytosine opposite an abasic site or UV photoproducts (Nelson *et al.*, 1996b).

The various branches and/or components of error free and error-prone PRR are not necessarily exclusive, as in the case of the (6-4) TT photoroducts, translesion synthesis entails the cooridanted function of Pol η at the insertion step and of Pol ζ at the extension step (Guo *et al.*, 2001; Johnson *et al.*, 2001). PCNA's interaction with Pol η is essential for the function of the polymerase and its monoubiquitination is thought to activate pol η and pol ζ translesion synthesis (Haracska *et al.*, 2001). Rad5 has also recently been suggested to affect the TLS polymerases and contributing to the efficiency of lesion bypass, possibly by the ubiquitilation through the binding of the TLS polymerases to the Rad6 / Rad18 complex, a function independent of the Mms2 / Ubc13 complex (Gangavarapu *et al.*, 2006). These examples highlight the complexity of the interactions of the members of the *RAD6* epistasis group with new functions and interconnections of the member gene products, still emerging, depending on the type of DNA damage investigated.

4.1.5 Objectives of the study

Mutants of the yeast *Saccharomyces cerevisiae*, totally deficient in specific DNA repair pathways were used to identify the critical detereminants of sensitivity of the novel chiral agent TH-III-151 and the achiral one, AS-I-145. These two chemically closely related compounds were shown in chapters 2 and 3 to specifically induce adenine-N3 lesions, in a comparable, sequence specific manner. It is known that NER is important in processing the same type of lesions generated by the lead compound CC-1065, however, in the case of the novel agents, the role of the other principal excision repair pathway, BER was also investigated. Using isogenic strains disrupted for NER and BER genes, and with the inclusion of double mutants, the relative contributions of the two pathways was assessed. Large- scale sensitivity yeast screens, constructions of survival curves and epistasis analysis was performed (an outline of the experimental strategy is featured in Figure 4.5).

Based on previous findings in our lab, which implicated Rad18 in the removal of other sequence specific minor groove adducts, the sensitivity of strains deficient in genes/members of the *RAD6* epistasis group was also determined. Various members of the subpathways of the *RAD6* controlled post replication repair were considered, in an attempt to further characterise the role of this pathway.

The induction of the damage and the repair of the adducts at nucleotide resolution was examined by single-strand ligation PCR *(sslig-PCR)*, on both the transcribed and non-transcribed strands of an active gene, in repair competent and those mutant cells which had exhibited marked sensitivity. This study would provide further evidence of the adduct removal mechanisms, reveal if the excision event is transcription coupled and relate marked sensitivity to specific adduct elimination defects.

Conducting the above studies on both a chiral and an achiral compound, helped identify similarities in the repair mechanisms for the two classes of compounds and further highlighted the role of Rad18 in the repair of minor groove adducts establishing, in this case, a link between the *RAD6* pathway and NER.

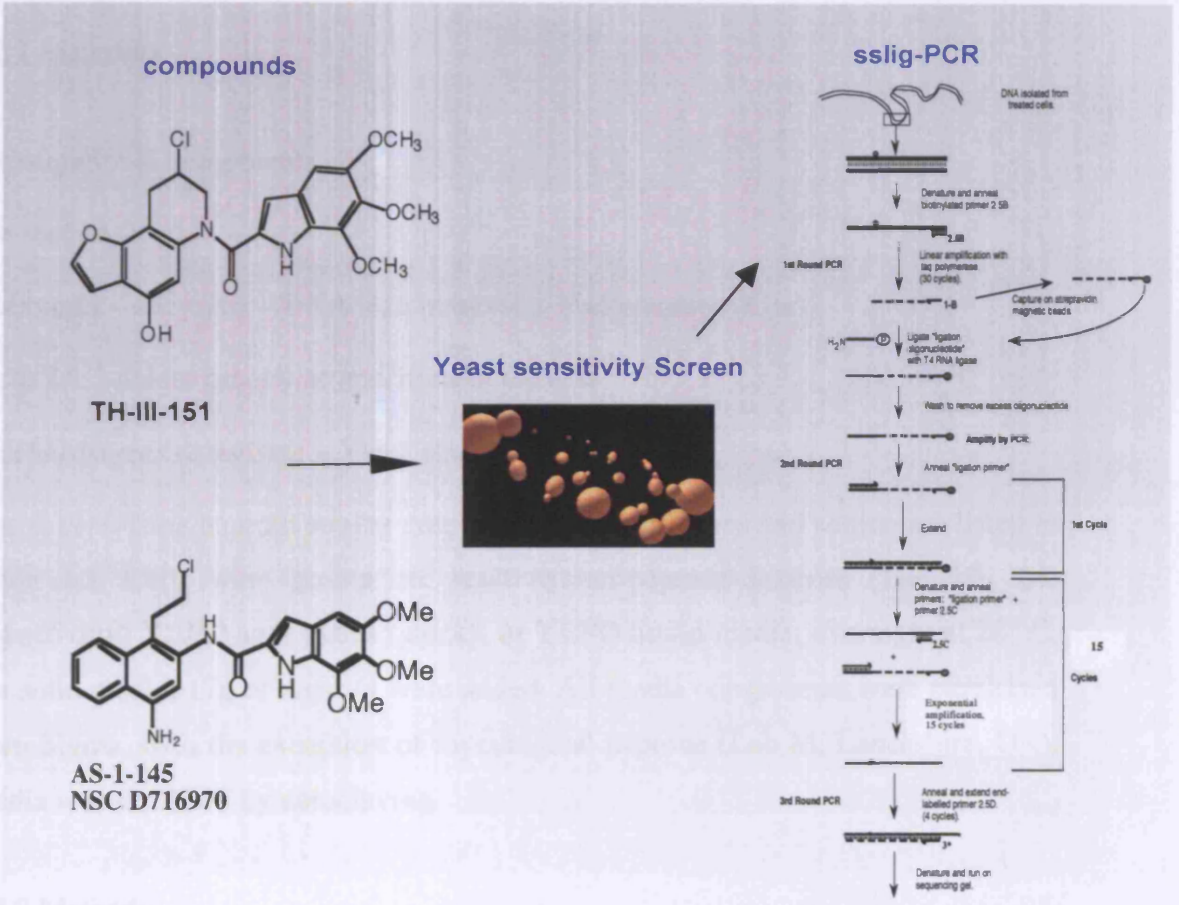

Figure 4.5 Overview of the experimental strategy followed in the yeast DNA repair studies.

4.2 Materials and Methods

4.2.1 Materials

Investigational compounds

See section 2.1.1

Chemicals – enzymes – DNA size markers – Radioisotope-Kits

As in 2.1.1 unless otherwise specified in the text.

Saccharomyces cerevisiae – Yeast strains

The *S. cerevisiae* haploid strains employed, their genotypes and source are listed in Table 4.3. Cells were grown on yeast extract-peptone-dextrose (1%, 1%, 2% respectively) YEPD agar plates (stock), or YEPD liquid media, overnight at 28° C. For solid media, 17g of Agar / l were added. All media components were purchased from Sigma, with the exception of mycological peptone (Lab M, Lancashire, UK). Media was sterilised by autoclaving.

4.2.2 Methods

4.2.2.1 Large scale sensitivity screen – Colony spotting assay

Liquid YEPD medium was inoculated with a single colony picked from a freshly streaked (YEPD) stock plate of the strain under investigation, and grown overnight at 28°C with vigorous shaking.

Cells were counted microscopically and only cultures with between 1 and 4 x 10^7 cells/ml were used. Cells were pelleted at 500 x g, 10 min, 20°C and adjusted to a final volume of 5 x 10^5 cells/ml in cold phosphate buffered saline (PBS). 1 ml aliquots were treated with increasing concentration of TH-III-151 and AS-I-145 (ranging from 0.01 μM to 10 μM), for 5 h at 28°C with vigorous shaking.

Strain	Genotype	Source	Ref.
DBY 747	*MATa his3-Δ1 leu2-3, 112 trp1-289 ura3-52*	W. Xiao	Xiao *et al.*, 1996
WXY 9394	DBY 747 with *rad4Δ::hisG-URA3- hisG*	W. Xiao	Xiao *et al.*, 1996
LP14Δ	DBY 747 with *rad14Δ::URA3*	R. Waters	-
JC 8901	DBY 747 with *mag1Δ::hisG-URA3-hisG*	L. Samson	Chen *et al.*, 1990
WXY 9345	DBY 747 with *rad4Δ::hisG-URA3- hisG mag1Δ::hisG*	W. Xiao	Xiao *et al.*, 1996
WXY 9326	DBY 747 with *rad18Δ::TRP1*	W. Xiao	Xiao *et al.*, 1996
PJM 35	DBY 747 with *rad4Δ::KanMX4 rad18Δ::TRP1*	P.J.McHugh	-
WXY 9376	DBY 747 with *rad6Δ::LEU2*	W. Xiao	Xiao *et al.*, 1996
WXY 642	DBY 747 with *mms2Δ::HIS3*	W. Xiao	Xiao *et al.*, 2000
WXY 731	DBY747 with *rad5Δ::hisG-URA3-hisG*	W. Xiao	Xiao *et al.*, 2000
WXY 732	DBY 747 with *mms2Δ::HIS3 rad5Δ::hisG-URA3-hisG*	W. Xiao	Xiao *et al.*, 2000
PJM 36	DBY 747 with *rad4Δ::KanMX4 rad5Δ::hisG-URA3-hisG*	This study	-
BY4741	*MATa his3Δ1 leu2Δ0 met15Δ0 ura3Δ0*	SGDP*	-
2085	BY4741 with *rev3Δ::KanMX4*	SGDP	-
4255	BY4741 with *rad30Δ::KanMX4*	SGDP	-
6067	BY4741 with *ung1Δ::KanMX4*	SGDP	-
393	BY4741 with *ntg1Δ::KanMX4*	SGDP	-
1734	BY4741 with *ntg2Δ::KanMX4*	SGDP	-
510	BY4741 with *ogg1Δ::KanMX4*	SGDP	-

* *Saccharomyces* Genome Deletion Project

Table 4.3 *Saccharomyces cerevisiae* strains used in this study.

After drug treatment, cells were harvested, washed twice in PBS solution and resuspended in a final volume of 1 ml of dH_2O. A series of 1:10 dilutions were performed for each strain, down to 500 cells/ml. 10 μl of the last three dilutions was

spotted onto square YEPD/agar plates with a premarked grid layout. Each line comprised a series of "spots" of one strain, containing sequentially 5000, 500, 50 cells / patch. Typically 4 or 5 strains were spotted on any one plate, and plates were spotted in triplicate. The growth phenotypes of the strains on the plates were assessed after 3 days incubation at 28°C, when plates were photographed.

4.2.2.2 Yeast survival curves

Culture conditions as above. Cells were pelleted as above and adjusted to a final density of 2 x 10^7 cells/ml this time, in cold PBS. 2 ml aliquots were then treated with TH-III-151 and AS-I-145 as above. After drug treatment, cells were washed twice in PBS solution and resuspended in a final volume of 1ml. Subsequent 1:10 serial dilutions of the stock cell suspension were performed, down to 2 x 10^3 cells/ml. 100 µl of the last dilution was plated in triplicate, onto YEPD/agar plates at a density giving rise to about 200 colonies per plate in untreated controls. The number of yeast colonies per plate was scored after 3 days incubation at 28°C. Any experiments giving rise to more than 250 colonies/plate in untreated controls were rejected. Results are expressed as percentage of the number of colonies arising from an untreated control, to enable comparison between different strains and experiments.

4.2.2.3 Single-strand ligation polymerase chain reaction (sslig-PCR).

Sslig-PCR oligonucleotides were synthesised, modified and purified by MWG, Milton Keynes, UK. All oligonucleotides were high purity salt free (HSPF) purified following synthesis and where necessary modification, and were stored at –20 °C.

For the MFA2 gene transcribed strand (TS):

2.5B 5' biotin CAT TGA CAT CAC TAG AGA CA 3'	Tm = 51 °C
2.5C 5' AGA CAC CAG CGA GCT ATC AT 3'	Tm = 58 °C
2.5D 5' AGC GAG CTA TCA TCT TCA TAC AA 3'	Tm = 61 °C

For the MFA2 gene non-transcribed strand (NTS):

2.4B 5' biotin TAT AAG AGT TTA TAG TGG TGA AG 3' Tm = 52°C

2.4C 5' AGT GGT GAA GAT AGT ACG GA 3' Tm = 54 °C

2.4D 5' GAT AGT ACG GAC TTG ATG CAC GTG 3' Tm = 61 °C

Ligation oligonucleotide:

5' p-ATC GTA GAT CAT GCA TAG TCA TA-n 3'

Ligation primer:

5' TAT GAC TAT GCA TGA TCT ACG 3'

The PCR-based technique, employed to detect induction of damage and follow the repair of the DNA adducts at the nucleotide level in cells, has been previously described for use with mammalian cells (Grimaldi *et al*, 1994; 1997). Its application on yeast cells has also been reported (Brooks *et al.*, 2000). A schematic diagram of the technique is featured in Figure 4.6.

A single colony from the appropriate yeast strain was grown overnight in 100 ml YEPD. Cells were counted, pelleted (500 g, 10 min.) and were resuspended in 60 ml PBS at a concentration of 3 x 10^7 cells/ml. 50 ml of cells were treated with 10 μM TH-III-151 for 3 h at 28°C in an orbital shaker, and 10 ml of cells were mock-treated with drug solvent. After drug treatment, cells were washed twice with PBS, 10 ml of cells were removed for the time 0 h sample and the remaining 40 ml was resuspended in YEPD medium and incubated at 28° C for 2, 4, 6 or 8 h. The mock treated samples were also incubated for 8 h. After this post treatment incubation, the cells were centrifuged at 500 g for 10 min at 20°C. The pellet was lyophilised to dryness and resuspended in 100 ml of distilled H_20. After vigorous vortexing, DNA was allowed to elute in distilled water overnight, at 4° C.

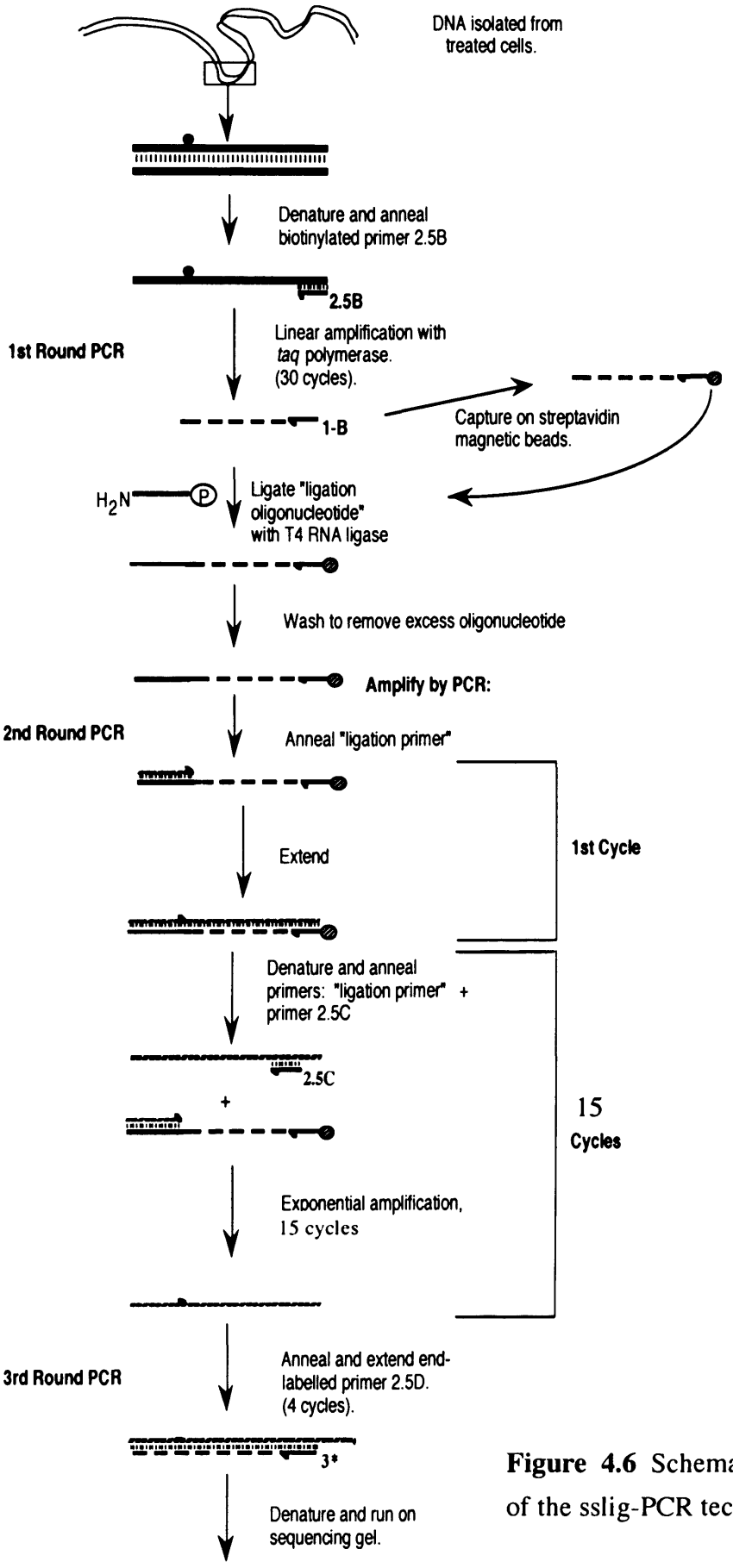

Figure 4.6 Schematic diagram of the sslig-PCR technique

Genomic DNA, from each of the time points for the repair experiments, was purified using a Nucleon Mini Kit for yeast DNA extraction (Nucleon Biosciences, UK). The genomic DNA was enzymatically cut with an appropriate endonuclease, depending on the strand under examination. 10 units of *Rsa* I (10 U / μl; New England Biolabs, Hitchin, UK) were used for analysis of the TS and the same amount of *Dde* I (10 U / μl; New England Biolabs), for analysis of the NTS. The enzymatic DNA digestions were incubated at 37°C, overnight. The DNA was finally precipitated and its concentration determined fluorimetrically.

First-Round Linear PCR

First round primer extension was carried out, in a volume of 40 μl, using 0.04 μg of the digested DNA (in 10 μl of dH_20). The single primer used in this first-round of PCR determines which region and on what strand, damage is measured (i.e. a primer complementary to the TS detects damage on the TS). Gelatin was used in the first-round linear PCR to help improve primer specificity. All the reagents for the PCR steps were stored at –20° C (except $MgCl_2$ and gelatin which were stored at 4° C), thawed if necessary and kept on ice until just prior to use, with the exception of the polymerase which was kept at –20° C at all times.

A PCR coctail mix was prepared in a 1.5-ml tube using the volumes below after multiplying by the number of samples.

4.0 μl of 10 x Thermophilic DNA polymerase buffer [as supplied with the enzyme; when diluted 1:10 it has a composition of 10 mM Tris-HCl (pH 9.0 at 25° C), 50 mM KCl and 0.1% Triton® X-100].

5.0 μl of a mixture containing 2.5 mM each dNTP

6.4 μl of $MgCl_2$ (provided with the enzyme as a stock of 25 mM) (4mM final concentration)

2.0 μl of 0.2% Gelatin

1.0 μl of biotinylated primer B (0.06 pmoles)

0.2 μl (1 U) of *Taq* DNA Polymerase (5U / μl)

11.4 μl ddH_2O

30 µl of the above PCR coctail mix was placed directly into each of the 0.5-ml tubes with the digested DNA and mixed well.

The DNA was initially denatured at 94° C for 4 min and then subjected to 30 cycles of 94° C for 1 min, Tm for 1 min, 72° C for 1 min + 1 second extension/cycle on a PT-100 thermal cycler with a hot bonnet (MJ Research, Watertown, MA, USA). The mixture was subjected to a final extension at 72° C for 5 min and then cooled to 4° C.

Capture and ligation

To capture and purify the products of biotinylated primer extension, 10 µl of 5 x washing and binding buffer (WBB; 5 mM Tris-HCl pH 7.5, 1 mM EDTA, 1 M NaCl) was added to the PCR mixture, followed by 5 µl streptavidin M-280 Dynabeads® (Dynal, Wirral, UK). The Dynabeads has been washed three times with and resuspended in 1 x WBB. The suspension was incubated for 30 min at 37° C to allow the streptavidin coated Dynabeads to bind to the biotinylated PCR products with occasional agitation for gentle mixing. The beads were sedimented in a magnetic rack and washed three times with 200 µl of 10 mM TE (pH 7.6).

After the final wash, the supernatant was carefully removed and the beads were resuspended in 10 µl ligation mixture. The ligation mix was prepared in a 1.5-ml tube using the volumes below after multiplying by the number of samples.

1.0 µl of 10 x T4 RNA ligase buffer [10 x is: 500 mM Tris-HCl (pH 8.0 at 25° C), 100 mM $MgCl_2$, 10 mM hexamine (III) cobalt chloride, 100 µg/ml bovine serum albumin, and 200 µM ATP]

1.0 µl of 20 mM ligation oligonucleotide (20 pmoles final concentration)

5.0 µl of 50% (w/v) polyethylene glycol 800 (PEG 8000)

1.0 µl (20 U) of T4 RNA ligase (20 U / ml; Promega, Southampton, UK)

2.0 µl ddH_2O

10 ml of the above mix was placed into the tubes containing the Dynabeads (using a pipette tip with the end cut off to allow the extremely viscous mixture to be pipetted) and mixed by repeating pipetting against the walls of the tubes.
The ligation reaction was incubated overnight at 22° C. The ligation oligonucleotide was supplied with a 5' phosphate, essential for ligation, and a 3' terminal amine to block its self-ligation. After ligation the beads were washed 3 times with 200 µl TE pH 7.6 and resuspended in 40 µl dH_2O for the second round PCR.

Second-Round Exponential PCR

The second round PCR mixture, in a volume of 100 µl, contained 10 pmoles of each of the primer C and the ligation primer that was complementary to the ligated oligonucleotide. The buffer composition was as for the first round PCR except that 2.5 U of *Taq* polymerase were used. The cycling conditions were: an initial denaturation at 94°C for 4 min, then 15 cycles of 94° C, 1 min, Tm, 1 min, 72° C 1 min + 1 second extension/cycle. The mixture was finally incubated at 72°C for 5 min and cooled to 4° C for 1h.

Third-Round PCR – Electrophoresis

The third round labelling reaction was carried out by adding to the 100 µl of each of the PCR-2 tubes, 10 µl of ^{32}P 5' end-labelled primer D (5 pmoles) and 1 U *Taq* polymerase in PCR reaction buffer. 5' end labelling of primer D was carried out as described in section 2.1.2.1. The mixture was subjected to 4 further cycles of 94° C, 1 min, Tm, 1 min and 72° C, 1 min, 72° C, 5 min and 4° C, 1 h. The beads were sedimented by spinning briefly in a microcentrifuge and the supernatant was carefully removed to fresh 1.5-ml tubes. The beads were rinsed with 100 µl dH_2O and the supernatant removed and added to the 1.5-ml tubes. The DNA of the collected supernatants was precipitated with ethanol and 3M NaOAc and washed twice with 70% ethanol. The lyophilised samples were finally resuspended in 5 µl formamide loading buffer. The 5 µl samples were in turn transferred to fresh tubes and the levels of radioactivity (CPM) measured with a scintillation counter. In most

cases no great deviations were recorded. This extra step was performed to ensure consistency in the levels of radioactivity in the loadings per lane.
The samples were denatured at 95° C for 3 min, cooled on ice and electrophoresed at 1500V for 3 h in a 50 cm x 21 cm x 0.4 mm, 6% polyacrylamide sequencing gel (SequaGel 6; National Diagnostics, UK). The gel was dried and autoradiographed (Kodak Hyper film, Amersham. UK). Densitometry was performed on a Bio-Rad GS-670 imaging densitometer using the Molecular Dynamics software.

4.2.2.4 DNA measurement by fluorimetry

The DNA samples were measured after extraction and enzymatic digestion for their DNA content by fluorimetry. This is one of the most accurate methods available for measuring DNA and especially very small quantities (Kowalski, 1979). The DNA concentration of each sample was determined with the Perkin-Elmer L2-SB fluorimetre using the Hoechst 33258 dye (Sigma-Aldrich, Poole, UK) and assay (Cesarone *et al.*, 1979). A standard curve was generated using 0 to 10 μg of salmon sperm DNA (Sigma-Aldrich) in 1 x SSC (15 mM sodium citrate pH 7.0, 150 mM NaCl). 2 μl of aliquots of the DNA samples were resuspended in 1 x SSC to a total volume of 2ml and 1 ml Hoechst 33258 dye (10 μg/ml). The DNA samples were fully resuspended and mixed by invertion, before measurement. After determining their DNA concentration, samples were stored at –20°C.

4.2.2.5 DNA sequencing

Di-deoxy double-stranded sequencing was carried out using the Sequenase™ 2.0 kit (Amersham Pharmacia Biotech, Little Chalfont, UK), to determine the sequence of the drug binding sites detected by sslig-PCR. The DNA fragments used for sequencing were generated by PCR using unmodified, restriction enzyme-digested DNA as a template. Typically 10-100 ng of DNA would suffice to provide high yield and high specificity. For the TS strand sequencing, the PCR fragment was

generated by the primers 2.3B (radiolabelled), which binds the NTS at positions +349 to +368 (where +1 is the start of the coding region of *MFA2*) and 2.5 C, which binds the TS at positions +943 to +924. For the NTS sequencing, the primers employed were 2.5C (radiolabelled) and 2.4C, which binds the NTS at positions +922 to +899. The fragment generated for TS is 574 bp while the one for NTS is 595 bp. Both PCR products were amplified for 35 cycles. The end products were verified by visualising on a mini agarose gel.

Sequencing was carried out according to the manufacturer's protocol using the buffers and enzymes provided in the kit. The sequencing products were resolved in parallel to the sslig-PCR products by gel electrophoresis.

4.2.2.6 PCR-based gene disruption

The following deletion primers (MWG) bearing 45 bp homology to the *RAD4* gene and 20 bp of overlap with the selective marker, were designed to generate the cassette:

RAD4 5′ DEL
5′-GGA CGA CAA GCA GAG ACA TAA CGA CAC TAT TTT TCC GCT AAA ATG CGG ATC CCC GGG TTA ATT AA-3′

RAD4 3′ DEL
5′-AAA ACA TAC TTT CCT AAT TAT TCA AAC CGT TTC AGC CTC ATT TCA GAA TTC GAG CTC GTT TAA AC-3′

The regions of homology between the primer sequences and the endogenous gene, lay at the 5′ and 3′ ends of the coding sequence (*RAD4* 5′ DEL and *RAD4* 3′ DEL respectively), to ensure complete disruption. The KanMX4 cassette template (a gift from Professor M. Longtime, Universitat Basel, Switzerland) was used to provide kanamycin selection.

Reaction mixtures were prepared in a total volume of 100 µl, comprising: 100 ng (in 10 µl) of the pFA6a KanMX4 vector; 10 µl of 1 x Thermopol buffer (NEB); 2 µl of 100 mM magnesium sulphate; 12.5 µl of 2 mM dNTPs, 250 pmol of each primer (in 2.5 µl each); 2 units of Vent Polymerase (NEB) (in 1 µl) and the rest of the volume made up with dH_20.

The PCR conditions were: 94°C for 4 min; 94°C for 1 min, 55°C 1 min, 72°C 2 min + 1 s/cycle, 30 cycles; 72°C 5 min. PCR was performed on a MJ thermocycler machine.

Six identical PCR reactions were carried out as described above. The PCR products were subsequently combined and a 1:1 volume of phenol-chloroform was added. This was centrifuged for 5 min at full speed and the aqueous (upper) layer containing the DNA, was transferred to a fresh eppendorf and subsequently mixed with 3 volumes of 95 % ethanol and $^1/_{10}$ volume of 3M sodium acetate. DNA was left to precipitate in a dry ice bath for 20 min. After spinning for 5 mins at full speed, the supenatant was carefully removed and the pellet washed twice in cold 70 % ethanol. After a final round of centrifugation and drying, the DNA pellet was resuspended in 11 µl of sterile water. 1 µl of this DNA preparation was run on an ethidium-stained, 1 % agarose gel, in 0.5 x TBE buffer,

Transformation of S. cerevisiae

A single colony from a *rad5* YEPD stock plate was inoculated in 50 ml of YEPD medium and grown overnight. After a 100-fold dilution, 10 ml of these *rad5* cells were counted with a heamacytometer, to confirm that they were in exponential phase ($2 \times 10^6 - 2 \times 10^7$ cells/ml). The cells were transformed with a single cassette using the BIO 101 Alkali-cation Yeast Transformation kit (Anachem), according to the manufacturer's instructions. Briefly, 50 ml of *rad5* cells were centrifuged at 400 x g for 5 min and the supernatant discarded. Cells were then resuspended in a total of 10 ml of TE solution (pH 7.5) and spun down further. After removal of the supernatant, the pelleted cells were resuspended in 5 ml of lithium / caesium acetate solution (100 mM) and incubated for 30 min at 30°C. The cells were subsequently

spun and resuspended in 1 ml of TE (pH 7.5), ready for transformation. A $^{1}/_{100}$ aliquot of these yeast cells (100 µl) was mixed with 10 µl of salmon sperm DNA and 10 µl of histidine solution and the 10 µl of the *RAD4-KanMX4-RAD4* cassette preparation. This suspension was mixed well and incubated at room temperature for 15 min. 1 ml of a PEG/TE/CationMixx was then added to the transformation reaction, and incubated for a further 10 min at 30°C. Reactions were heat-shocked in a water bath at 42°C for 10 min, cooled to 30°C and the cells pelleted by spinning. The pellet was resuspended in 1 ml of warm YEPD and incubated for 3 h at 28 °C to initiate expression of the selectable marker, before plating on selective media. After the incubation period, the cells were spun down, the supernatant removed and the pellet resuspended in 200 µl of YEPD.

Selection of G418-resistant cells

100 µl of the transformed cells was plated onto G418-plates (in duplicates), in order to select the cassette-bearing yeast cells. G418 (dissolved in water) had been added at a concentration of 300 mg/L in the YEPD medium (containing agar). The two G418-plates were incubated at 30°C for 48 hours. At this point, it was necessary to replica plate the G418-plates twice, in order to eliminate the background growth and obtain more prominent G418-resistant colonies. These replica plates were then incubated for a further 48-72 h at 30°C. The more prominent colonies of the transformants were then selected from the more dilute replica plate. Half of each of these colonies was then restreaked onto G418-plates, while the other half was grown in 10 ml of liquid G418-YEPD medium. Growth of the former, allowed further confirmation of the resistance to G418, while DNA preps were carried out from the cells grown in the liquid G418-YEPD.

Isolation of yeast genomic DNA

Genomic DNA was isolated from the cells that were grown in liquid G418-YEPD medium, using the Nucleon Yeast DNA Mini-prep kit (Tepnel Life Sciences, Manchester, UK). Cells were pelleted by centrifugation and resuspended in 540 µl

solution A and 60 µl solution B (supplied with the Mini-prep kit). The cell suspension was vortexed for 30 s and incubated in a 70°C heat block for 20 min. A 1:1 volume of phenol-chloroform was then added instead of the provided solution C, as this was found to result in an improved DNA yield. Samples were vortexed and spun in a microcentrifuge at full speed. The aqueous layer was transferred to a fresh eppendorf and an equal volume of isopropanol was added. Samples were mixed by inversion and spun for a further 5 min. The supernatant was carefully discarded and the pellet was washed twice with 100 µl of 70% ethanol. Pellets were dried at a 65°C heat block for 3 mins and resuspended in 100 µl of sterile water. The resuspended DNA was stored at 4 °C until use.

Confirmation of the disruption of gene disruption

Integration of the cassette at the correct locus was confirmed by PCR across the gene, using specific gene primers designed to flank the disrupted region, and template DNA derived from a single transformant colony. The primers (MWG) employed for confirmation of the *RAD4* disruption, defined as "*RAD4* 5'-CHECK" and "*RAD4* 3'- CHECK" are the following:

RAD4 5'-CHECK

5'-TGC ATG CAC AAT ATA TGC AA-3' Tm = 48 °C

RAD4 3'-CHECK

5'-GTT CTC ATT CAT TAC AAA GT-3' Tm = 49.1°C

PCR reactions to check the disrupted gene were performed in a total volume of 100 µl, containing: 10 µl (100 ng) of the genomic DNA isolated from a transformant colony. 10 µl of 10 x Thermopol buffer, 2 µl of 100 mM $MgSO_4$, 12.5 µl of 2 mM dNTPs, 2.5 µl of each "CHECK" primer (at a concentration of 10 pmol /µl), 2 units of Vent DNA polymerase (1 µl) and the rest of the volume made up with distilled water. The PCR conditions used were: 94°C 4 min; 94°C 1min, 47°C 1 min, 72°C 2

min + 1 s/cycle, 30 cycles; 72°C 5min. The PCR reactions were performed on a MJ thermocycler machine.

The size of the PCR product alone, could distinguish between disrupted genes and the wild-type. However, further verification was also obtained from restriction enzyme digests performed on the PCR products. Two restriction enzymes, *Pvu I* and *EcoR V* (NEB) were chosen that would each yield a distinct array of fragments, allowing to distinguish between the normal and disrupted genes, as visualised by agarose gel electrophoresis. Restriction digests were performed on 10 µl of PCR reaction in a total volume of 20 µl, for 1 h in a 37°C heat block and the entire reaction was subsequently run on an ethidium bromide-stained, 1% agarose gel in 0.5 x TBE buffer. Both cut and uncut control samples (containing the wild-type *RAD4* gene) were also run, along with the DNA markers, 1 kb and λ *Hind III* (NEB).

4.3 Results - TH-III-151 repair studies

The first compound selected for yeast repair studies was TH-III-151, a *seco*-CFQ agent that was shown to alkylate DNA at the N3 position of adenine, with a sequence selectivity indistinguishable to that of adozelesin (section 2.3).

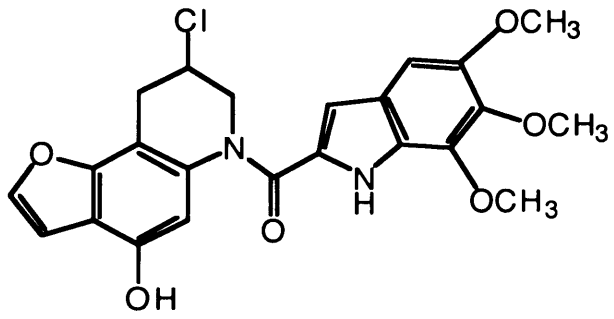

Figure 4.7 Structure of TH-III-151 (also featured in Figure 2.13).

4.3.1 NER-defective yeast cells are sensitive to TH-III-151. NER is the predominant excision repair event.

The colony-spotting assay was employed as an initial indication for the involvement of specific DNA repair and damage tolerance responses to the TH-III-151 induced A-N3 adducts. This is a qualitative screening of drug sensitivities and the involvement of the various pathways is assessed by examining the growth phenotypes of the strains defective in specific repair functions, relative to their isogenic repair proficient parental strain. Figure 4.8 shows the growth of the parent strain and key mutants belonging to the two major excision pathways, NER (*rad4*) and BER (*mag1*). The effect of simultaneous elimination of BER and NER was assessed by also including the double mutant *rad4mag1*.

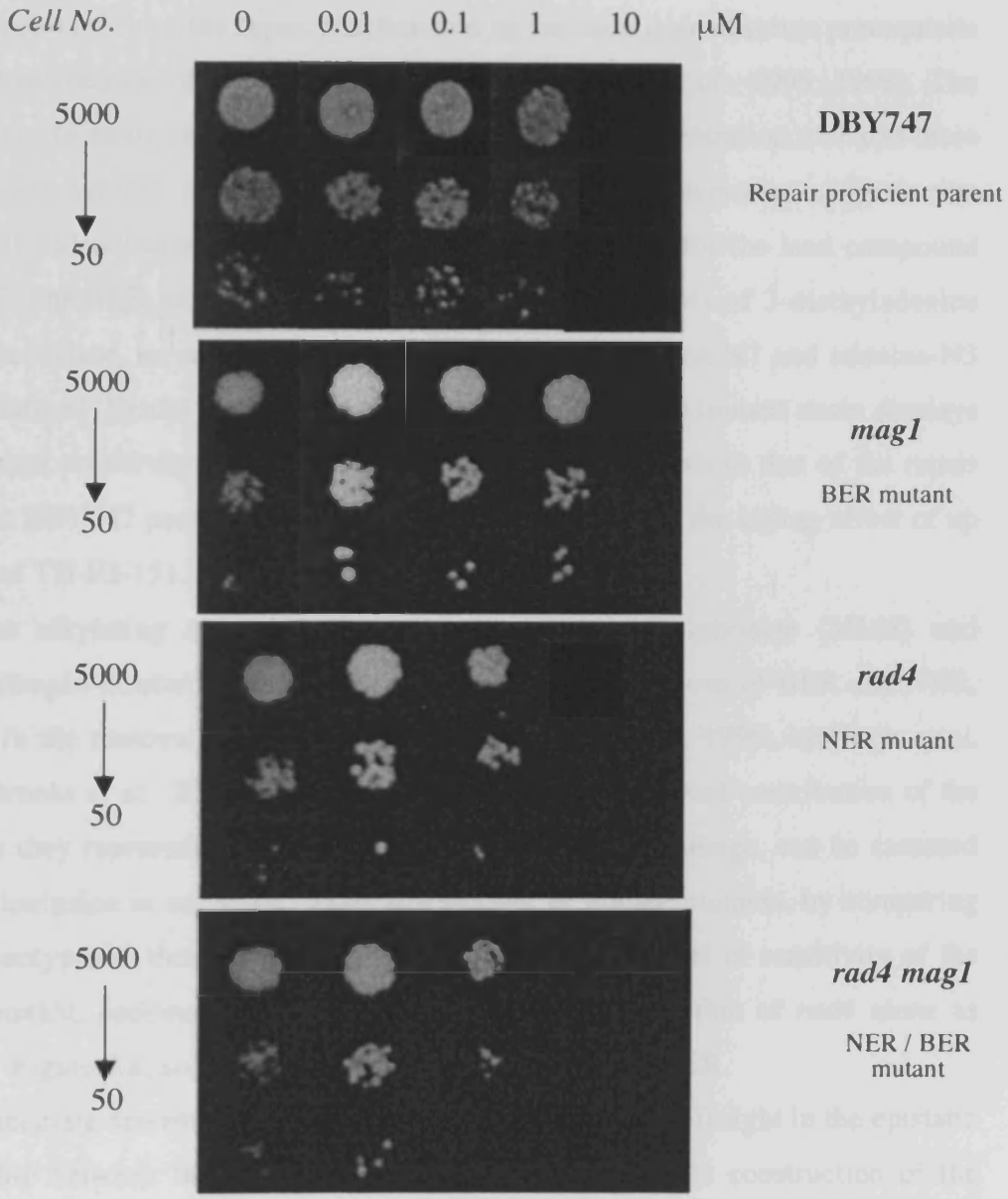

Figure 4.8 Sensitivity of the excision repair mutants *mag1* (BER) and *rad4* (NER) treated with increasing concentrations of TH-III-151. DBY474 is the repair proficient wild type.

The *rad4* cells are completely deficient in NER, as the gene has been assigned a role in an early step of the repair reaction and its function is an absolute prerequisite for the dual incision of damaged DNA by NER (Guzder *et al.*, 1995; 1998). The NER defective strain is sensitive to TH-III-151, as at a concentration of 1 μM there is no growth evident, even in the 5000 cells patch. This observation suggests that the TH-III-151 adducts are NER substrate, as was the case for the lead compound CC-1065. The BER mutant, *mag1*, is defective for the activity of 3-methyladenine DNA glycosylase, an enzyme known to repair simple guanine-N7 and adenine-N3 monalkylations (Berdal *et al.*, 1990; Bjoras *et al.*, 1995). This mutant strain displays no increased sensitivity, showing a growth pattern comparable to that of the repair proficient DBY747 parental strain and remaining resistant to the killing effect of up to 1 μM of TH-III-151.

For some alkylating agents, including methylmethane sulphonate (MMS) and simple nitrogen mustards, such as mechlorethamine, the actions of BER and NER, overlap, in the removal of the relevant adducts (Xiao *et al.*, 1996; McHugh *et al.* 1999b; Brooks *et al.*, 2000). The gene action and the functional contribution of the pathways they represent, in the process of the TH-III-151 damage, can be assessed with the inclusion in our yeast sensitivity studies, of double mutants, by comparing their phenotypes to those of each individual mutant. The level of sensitivity of the double mutant, *rad4mag1*, was found to be comparable to that of *rad4* alone as shown in Figure 4.8, suggesting a predominant role for the NER.

A more accurate determination of sensitivity, which offers an insight in the epistatic relationship between the two excision pathways, requires the construction of the corresponding survival curves of the above-mentioned strains. Figure 4.9 compares the sensitivity of the parent strain DBY747, to its isogenic *rad4* and *mag1* disruptants and the *rad4mag1* double mutant. If competition for a common lesion is occurring then a synergistic increase in damage sensitivity would be expected, when the relevant pathways are eliminated simultaneously. In this case the *rad4* strain was highly sensitive to the agent compared with the parental strain. The *mag1* cells showed no increased sensitivity over the wild type, while the double mutant

was as sensitive as the most sensitive single mutant, i.e the NER-deficient *rad4* cells. This suggests that the observed sensitivity of the double disruptant is solely dependent on the NER defect. These responses mirror the relative growth rates of the strains, as observed in the colony-spotting assay (Figure 4.8), validating its use for qualitative large-scale screening. It is therefore evident that NER is the predominant pathway in the elimination of the TH-III-151 adducts.

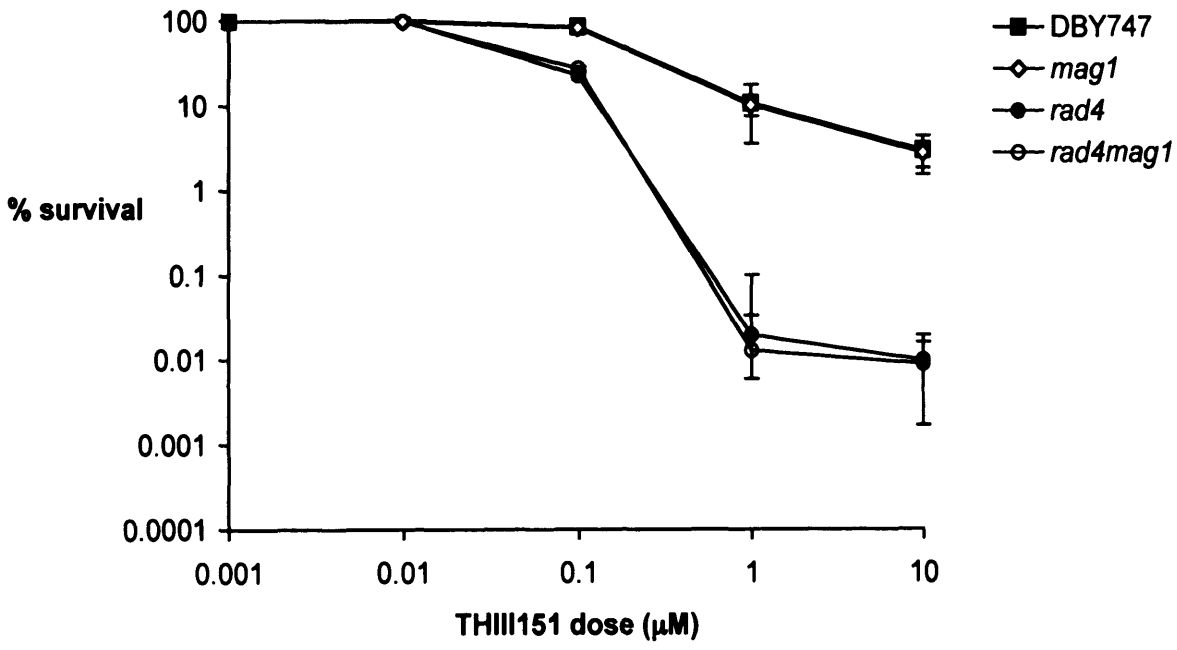

Figure 4.9 TH-III-151 sensitivity of *rad4*, *mag1*, and *rad4mag1* cells compared with their isogenic parent (DBY747). Exponentially growing cells were treated with the stated doses for 3 h at 30°C. All results shown are the mean of at least three independent experiments. The error bars represent the standard error of the mean.

The same pattern of sensitivity was observed for another BER deficient strain, *ogg1* (8-oxoguanine/formadopyrimidine glycosylase). The *OGG1* gene encodes a glycosylase endowed with an AP lyase activity (Van der Kemp *et al.*, 1996). Figure 4.10 compares the sensitivity of *ogg1*, its parent strain W303a, and the double mutant *ogg1rad14*. The *rad14* strain is another completely NER defective

disruptant, essential for the damage recognition and the subsequent incision by the Rad1-Rad10 nuclease (Prakash & Prakash, 2000; Guzder *et al.*, 2006). While the *ogg1* mutant does not show any increase in sensitivity over the wild type, elimination of both BER and NER activities confers increased sensitivity comparable to that of the *rad4mag1* double mutant. The sensitivity of the *rad14* cells to the agent is indistinguishable to that exhibited by the *rad4* mutants, further establishing the important role of NER for the cellular sensitivity to TH-III-151.

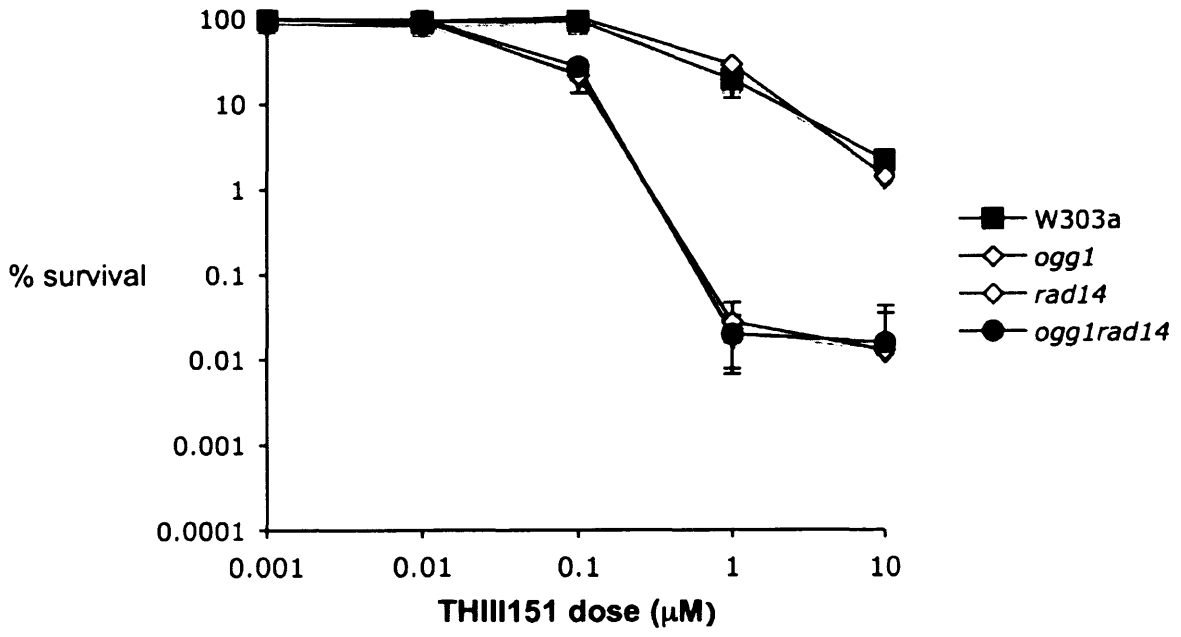

Figure 4.10 TH-III-151 sensitivity of *ogg1* with its isogenic parent W303a, *rad14* and the double mutant *ogg1rad14*.

In order to assess the potential involvement of alternative BER activities, other known BER mutants were screened for sensitivity, including the bifunctional DNA glycosylase / AP lyases *ntg1* (8-oxoguanine glycosylase/lyase), *ntg2* (related to *Escherichia coli* endonuclease III) (Alseth *et al.*, 1999) and *ung1* (uracil-DNA glycosylase) (Percival *et al.*, 1989). Figure 4.11 shows a panel of these BER

deficient strains along with their corresponding isogenic parent. The mutant strains grew at rates comparable to that of the corresponding wild type, after drug treatment with 1 μM of TH-III-151. Again it was only the *rad4* cells that exhibited sensitivity at this drug concentration, implying that NER is the predominant pathway involved in the elimination of the TH-III-151 adducts.

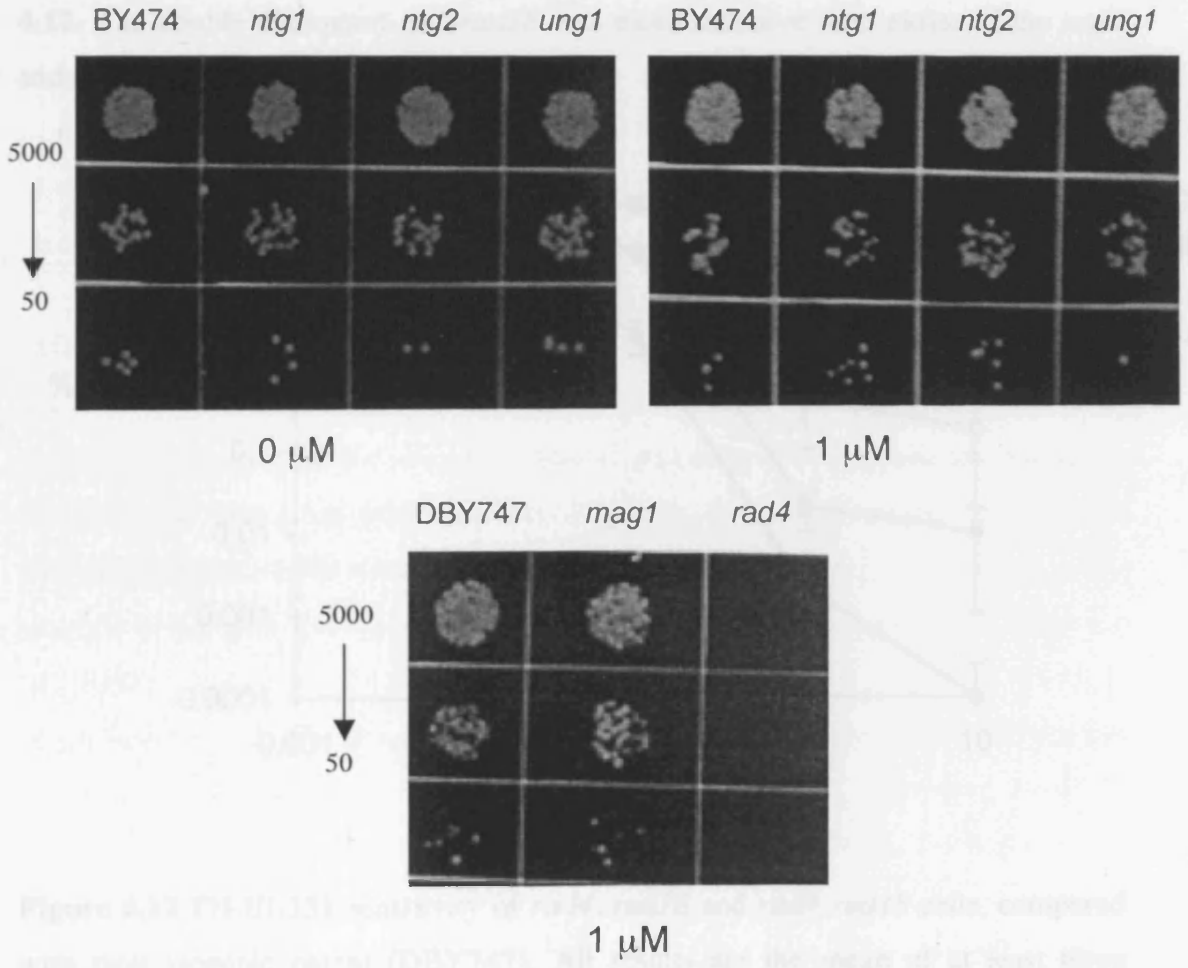

Figure 4.11 Sensitivity of the BER repair mutants *ntg1*, *ntg2* and *ung1* treated with increasing concentrations of TH-III-151, compared to their isogenic parental strain. For comparison reasons, another BER mutant *mag1* and the NER defective *rad4* strain, along with their repair proficient wild type is also included (bottom "matrix").

4.3.2 *rad18* cells are sensitive to TH-III-151

The *rad18* strain from the *RAD6* epistasis group, has been previously shown to be sensitive to the highly sequence specific minor groove adducts produced by a benzoic acid mustard tethering three pyrrole ring (Figure 4.2). A marked TH-III-151 sensitivity was also observed in a *rad18* disruptant strain as shown in Figure 4.12. The double disruptant *rad4rad18* was more sensitive than either of the *rad4* and *rad18* single mutants.

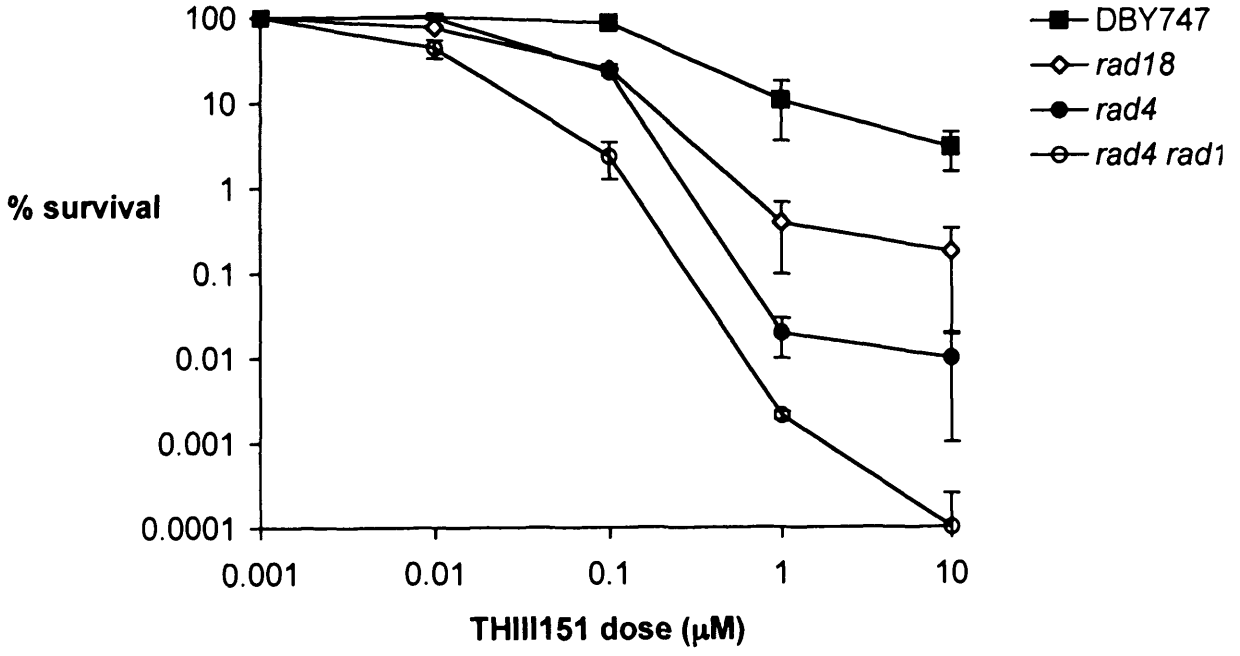

Figure 4.12 TH-III-151 sensitivity of *rad4*, *rad18* and *rad4 rad18* cells, compared with their isogenic parent (DBY747). All results are the mean of at least three independent experiments. The error bars show the standard error of the mean.

This indicates that *RAD4* and *RAD18* are not epistatic for the TH-III-151 damage response. The lack of epistasis in toxicity in survival assays is often taken to suggest that the genes act in different pathways and reactions. Inactivation of the NER

pathway might result in the lesions that would have been repaired by this pathway, to being channelled through, what seems to be a competitive pathway controlled by Rad6-Rad18, hence the synergistic interaction between the two mutations. Alternatively the TH-III-151 adducts might elicit multiple damage responses (including NER or a related excision repair process involving NER factors), which are all controlled by Rad6-Rad18. Elimination, therefore, of this additional excision-related Rad18 function, would produce an increase in sensitivity in a strain defective in both NER and *RAD18* over either single mutant.

The sensitivity of a yeast strain defective in a particular function is indicative of the involvement of a specific gene in the DNA damage response as a determinant of chemosensitivity to the agent. However, functions at molecular level are not always mirrored in the phenotypes and the responses obtained in such sensitivity assays. For example, in a *rad26* disruption mutant, preferential repair of UV-induced cyclobutane pyrimidine dimers in the transcribed strand of the active *RBP2* gene is severely impaired. Surprisingly, and in contrast to the human CS mutant, the yeast *RAD26* disruption does not confer any UV, cisplatin, or X-ray sensitivity (Van Gool *et al.*, 1994). This is particularly relevant to minor groove lesions as the sequence specific adducts induced by a nitrogen mustard-tethered distamycin analogue, while excised in the wild type strain, in a *rad18* mutant were not eliminated (Brooks *et al.*, 2000).

A molecular approach, employing a PCR-based technique was used to investigate whether the sensitivity of the *rad18* cells as exhibited in Figure 4.12, could be attributable to decreased elimination of the TH-III-151 adducts. Such possibility would extend the requirement of functional Rad18 for the excision of sequence specific adducts to yet another class of minor groove binding agents, the CC-1065 / duocarmycin family of compounds.

4.3.3 Induction and repair of TH-III-151 adducts at nucleotide resolution in cells

Single-strand ligation PCR, (slig-PCR) was employed to follow the induction and repair of TH-III-151 adducts at nucleotide resolution in intact cells of key yeast strains. The repair capacity of the highly sensitive *rad4* and *rad18* mutants (as well as the *rad6* strain) was compared to their isogenic parent DBY747. This study provides insight in the contribution of the post replication repair pathway (*rad18* and *rad6* strains) in the elimination of the TH-III-151 adducts and its requirement for the excision of minor groove sequence specific adducts.

The repair efficiencies of the various yeast strains were assessed using primers specific for both the transcribed and nontranscibed strands of the transcriptionally active *MFA2* gene. This gene produces a2 factor, a protein involved in the pheromone response pathway and has a known sequence (Mallet *et al.* 1995). *MFA2* is an a-specific gene and has an α2 operator in the control region involved in the chromatin-coupled repression of a-specific genes in α cells, through the binding of repressors (Mcm1 / α2) and nucleosome positioning in adjacent sequences (Teng *et al.*, 2000). In its active form however, in a cells, the gene exists in "open" chromatin conformation. The *MFA2* gene has been adopted as a model gene for various DNA repair investigations at nucleotide resolution, including the study of the repair of UV-induced cyclobutane pyrimidine dimers (CPDs) and the elucidation of the role of specific yeast genes in excision repair (Teng *et al.*, 1997; 1998; Teng & Waters, 2000). The same gene was also selected for the previous study of the repair of sequence specific minor groove adducts at nucleotide resolution in yeast (Brooks *et al., 2000*).

Genomic DNA extracted immediately after drug treatment and at various repair time points was digested with the *Rsa I* restriction enzyme. The first *Rsa I* site is – 337 from the start of the coding sequence of *MFA2*, which is 117 bp in length, and the second is + 416 after the end of the coding sequence. The resulting restriction fragment (869 bp) therefore contains the transcribed region of the *MFA2* gene (328

bp), the Mcm 1 binding site (part of the α2 operator) and the TATA box in the upstream control region, and downstream flanking sequences (Figure 4.13).

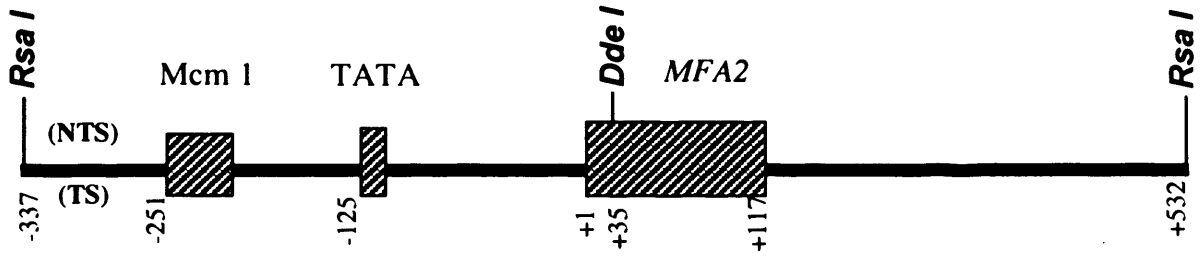

Figure 4.13 The regions of the *MFA2* gene. The *Rsa I* restriction fragment contains the Mcm1 binding site at –251 and the TATA box at –125 in the upstream control region of the *MFA2* coding region, and downstream sequences. The *Dde I* digestion was performed for analysis on the NTS. The numbers placed vertically represent the nucleotide position with respect to the *MFA2*'s coding region start point (+1).

The primers selected for the study of the transcribed strand (TS) define a region from –20 (from the start of the coding region) to the *Rsa I* site distal. Figure 4.14 depicts an autoradiograph from initial experiments examining TH-III-151 damage on the TS strand of the *Rsa I* restriction fragment of the DBY-747 wild type strain, and on isolated "naked" DNA from the same cells. This experiment was carried out to detect the level of lesions along the *MFA2* gene induced by 1 and 10 μM of TH-III-151 in order to determine the dose that gives the optimal signal under the experimental conditions employed. While bands representing TH-III-151 adducts could be detected at the lower dose of 1 μM in isolated DNA, in DNA extracted from cells treated with the agent, the higher dose of 10 μM, produced a better signal and allows detection by sslig-PCR of a wider distribution of DNA adducts formed. At this concentration, the same pattern of damage is detected between treated cells and treated naked DNA (incubation time was in both cases 3 h).

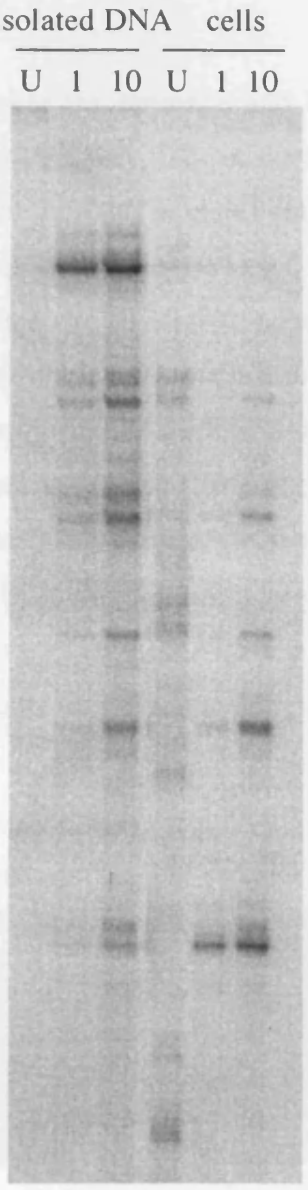

Figure 4.14 A comparison of the levels of PCR signal detected in cells and isolated DNA with different TH-III-151 concentrations. Sslig-PCR was carried out on the TS of the *MFA2* of DBY747 cells, treated with 1 and 10 μM of TH-III-151 for 3 h at 30°C. Isolated ("naked") DNA was treated with the same concentration for the same incubation time (3 h). The bands on the autoradiograph represent DNA fragments of varying lengths, which correspond to the positions of drug adducts along the sequence.

The cellular environment, despite the presence and binding of proteins does not therefore seem to significantly affect the occurrence of TH-III-151 adduct formation. The untreated control lane (U) in cells contained a ladder of background bands primarily due to non-specific polymerase stops.

In order to characterise the sites of TH-III-151 adduct formation, the sslig-PCR products were run alongside di-deoxy sequencing products. The *MFA2* fragment subjected to sequencing was amplified by PCR and defined by the sets of primers 2.3B and 2.5C for the TS and 2.5C and 2.4C for the NTS (For the primers' sequence and conditions for the generation of PCR fragments for sequencing see Methods-section 4.2.2.5). The PCR should optimally yield a single specific product of the expected size, subsequently verified with a mini agarose gel. Figure 4.15 shows the amplified PCR products for the sequencing of TS and NTS.

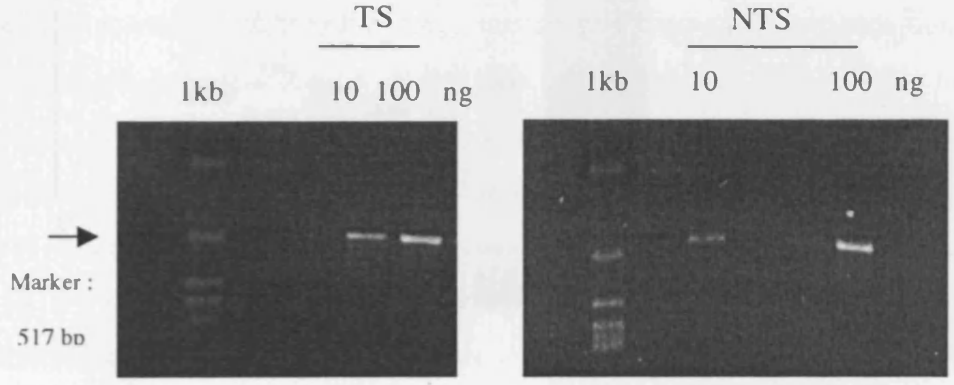

Figure 4.15 Agarose gel showing the PCR fragments used for di-deoxy sequencing. The PCR product specific for TS (left image), has a size of 574 bp, while the NTS specific fragment was 595 bps (right; since the two are not generated by identical sets of primers). A molecular mass marker (1 kb; Invitrogen) was also included as a standard. The yield differed on using different amount of the target sequence to be amplified.

In each case, one of the primers was radiolabelled and the resulting sequencing ladder, as exhibited in Figure 4.16 refers to the opposite strand of that being analysed for TH-III-151 lesions.

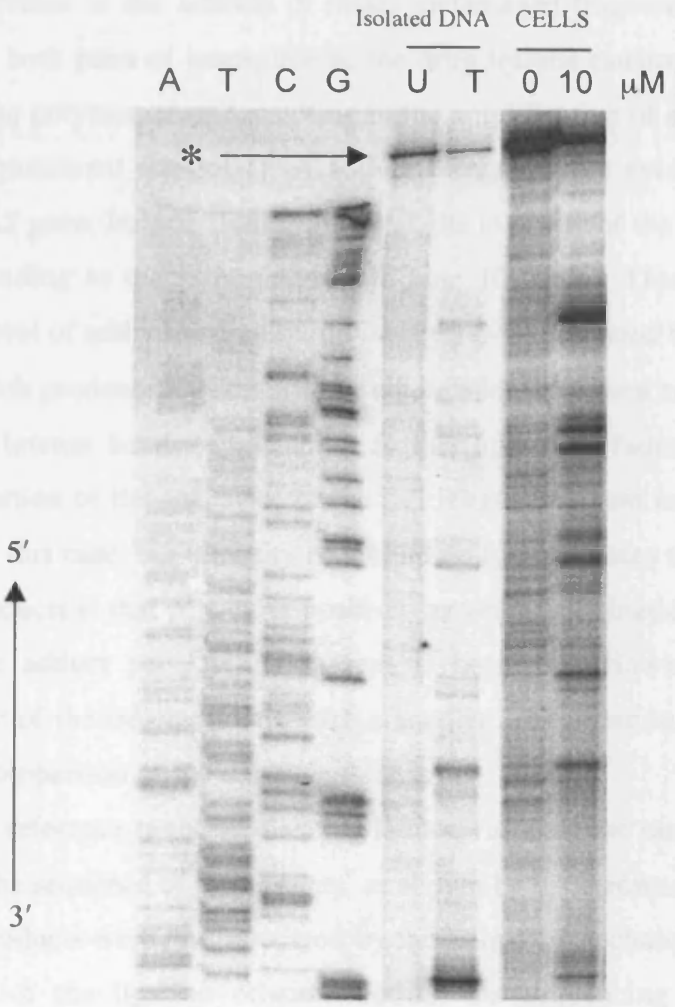

Figure 4.16 Sequencing of the TS of *MFA2* to determine sites of TH-III-151 binding. Drug treated cells and treated isolated DNA are denoted. Sequencing ladders are indicated as A, T, C, G. The full length fragments are indicated by an asterisk.

Lane U has untreated isolated genomic DNA. The single band at the top of the gel represents the intact restriction fragment. Lane T has the same DNA, treated *in vitro* with 10 μM of TH-III-151, the same drug concentration as the one used for the treatment of the yeast cells. Lane 0 has DNA extracted from DBY747 cells, mock-treated with solvent only, while lane 10 contains DNA from cells treated with TH-III-151 for three hours, and extracted immediately after drug treatment. There is a

clear decrease in the amount of intact undamaged fragments at the top of the gel between both pairs of lanes, due to the drug lesions causing downstream blockage of the *Taq* polymerase and resulting in the amplification of shorter fragments. In the several prominent sites of DNA adduct formation, are evident along the length of the *MFA2* gene. In lane T (naked DNA), the intensity of the bands is less than those corresponding to the same adducts in lane 10 (cells). This is possibly due to the higher level of adduct formation on isolated DNA, induced by the 10 μM of TH-III-151, which produced this distortion, where adducts closest to the primer correspond to more intense bands, while those further appear as fading (especially when the upper portion of the gel, close to the full length fragment is presented, as in Figure 4.16). In this case, the intensity of a band no longer relates to the relative frequency of the adducts at that particular position, as single-hit kinetics is exceeded and more than one adduct per DNA fragment is occurring. However, a darker copy or treatment of the isolated DNA with a smaller concentration of agent (Figure 4.17), allows comparison of the damage pattern.

By cross reference to the sequencing ladder, run with the samples, it was possible to deduce the sequence of the adducts, as shown by the arrows in Figures 4.17. The di-deoxy products were not processed by the sslig-PCR technique, therefore due to the addition of the ligation oligonucleotide, the sequencing products migrated 23 nucleotides further on the gel than the corresponding sslig-PCR products.

TH-III-151 reacted exclusively with adenines, showing preference for long A-tracts and AT mixed sequences, i.e the sequence specificity in the cellular environment is similar to that previously observed in plasmid DNA (chapter 2.2). In a previous study, sslig-PCR revealed a novel binding site for cisplatin in cells (Grimaldi *et al.*, 1994). In TH-III-151 treated cells however, the same set of adducts with those found in isolated, drug treated genomic DNA were detected, within the same sequence context, and with no additional lesions forming in cells (Figures 4.16 and 4.17).

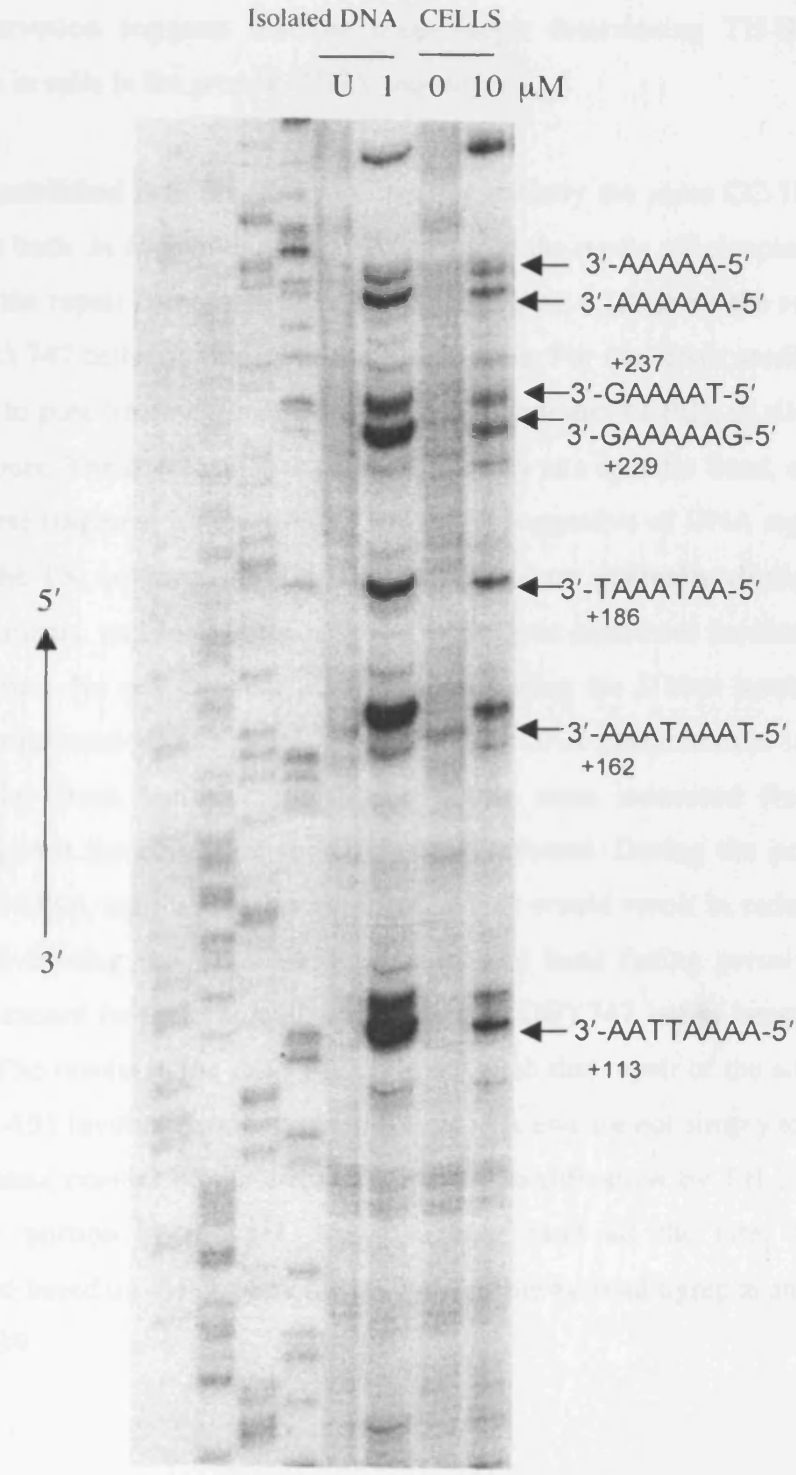

Figure 4.17 Comparison of the damage induced by 1 μM of TH-III-151 in isolated genomic DNA and that produced in cells by 10 μM of the agent. The damage pattern between the isolated DNA treated with the smaller drug concentration and that in cells, are identical. The sequencing ladders help identify the sequence and position of the adducts.

This observation suggests that the main factor determining TH-III-151 adduct formation in cells is the primary DNA sequence.

Having established that TH-III-151 targets essentially the same CC-1065-preferred sequences both *in vitro* and *in vivo* we compared the repair efficiencies of key yeast strains to the repair competent DBY747 cells. Figure 4.18 shows the repair capacity of the DBY747 cells, on the TS of the *MFA2* gene. For the repair studies, cells were subjected to post-treatment incubation in fresh medium (YEPD), to allow repair, for up to 8 hours. The decrease of the signal intensity at a specific band, corresponding to a discrete fragment for each A-N3 adduct, is suggestive of DNA repair. Repair is slow on the TS, however the TH-III-151 adducts are gradually eliminated. During the experiments, and for each time point of the post-treatment incubation, the cells were counted. No cell division was observed during the 8 hour incubation period, for any strain studied. Moreover, no increase in DNA concentration is found when the samples from various repair time points were measured fluorometrically suggesting that the cell population remained arrested. During the post-incubation periods no DNA replication should occur, which would result in reduction in band signal and diluting the TH-III-151 adducts. The band fading perceived as repair therefore cannot be the result of cell growth in DBY747 but is because of adduct removal. The results in the DBY747 cells establish that repair of the adducts formed by TH-III-151 involve elimination from the DNA and are not simply tolerated.
The sequence context of the sites of covalent modification by TH-III-151, on the resolvable portion of the gel presented here (and all the later figures), was determined based on the sequencing analysis of the autoradiographs and is shown in Figure 4.19.

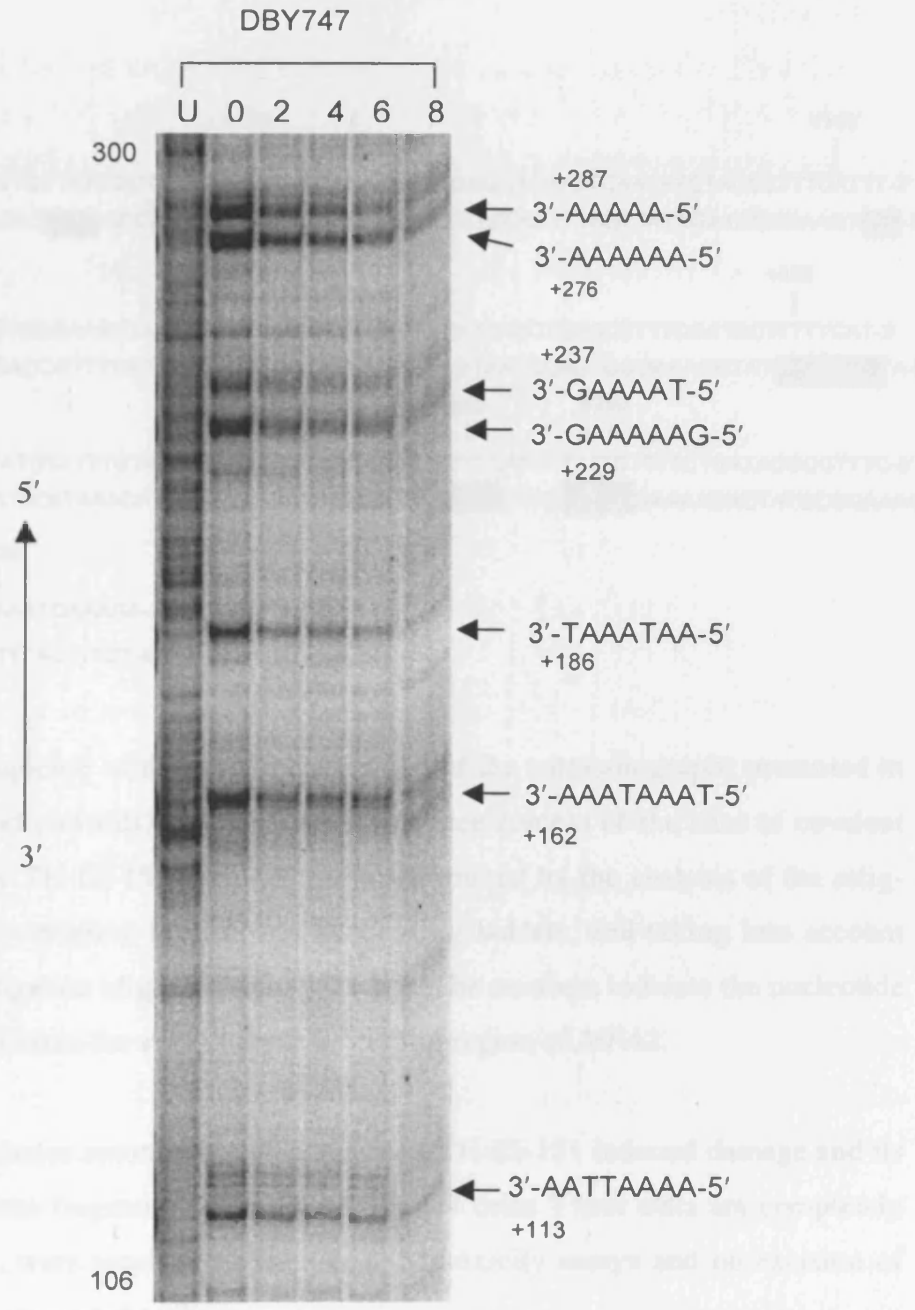

Figure 4.18 Repair of TH-III-151 adducts on the TS of *MFA2*. Exponentially growing DBY747 cells were treated with 10 μM TH-III-151 for 3 h at 30°C. Cells were harvested and DNA extracted immediately (0 h lane), or were resuspended in YEPD and allowed to repair for a further 2, 4, 6 and h prior to DNA extraction. Sslig-PCR was performed as described in the Methods section. The major adducts are indicated by arrows, along with their position relative to the start (+1) of the coding region on *MFA2*.The sequence was deduced from the analysis of the di-deoxy sequencing ladders performed previously.

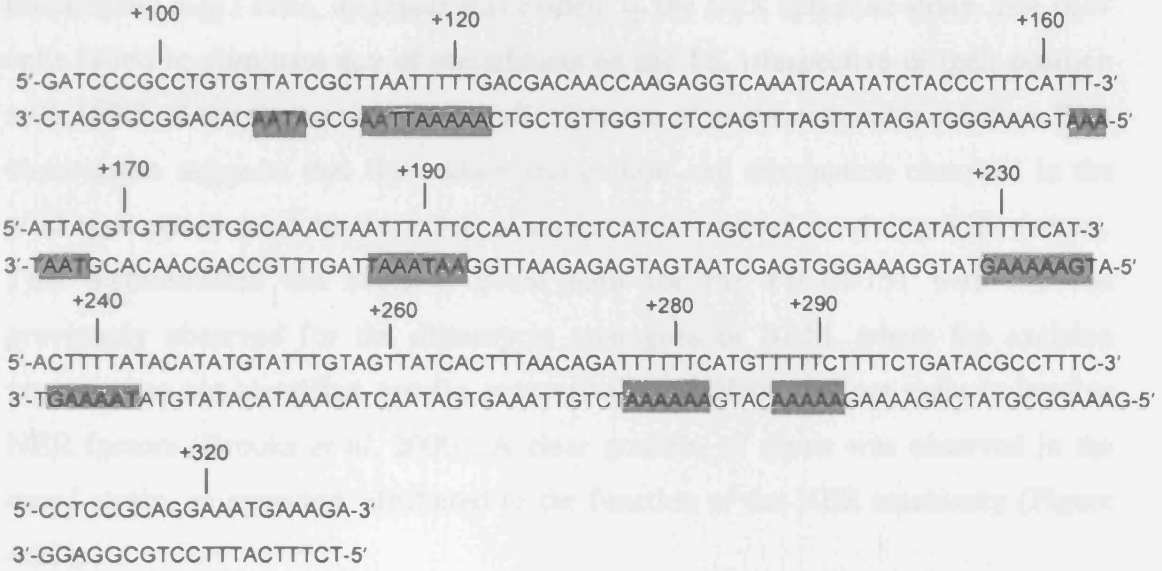

Figure 4.19 Sequence of the resolvable portion of the autoradiographs presented in Figure 4.18 (and onwards). The extended sequence context of the sites of covalent modification by TH-III-151 (shaded) were determined by the analysis of the sslig-PCR products in relation to di-deoxy sequencing ladders, and taking into account the size of the ligation oligonucleotide (23 bp). The numbers indicate the nucleotide position in relation to the start (+1) of the coding region of *MFA2*.

Figure 4.20 includes autoradiographs depicting TH-III-151 induced damage and its repair in the same fragment of the *MFA2* in *rad4* cells. These cells are completely NER-defective, were sensitive in the yeast cytotoxicity assays and no excision of the adducts was expected to occur.

Sslig-PCR on the BER-deficient *mag1* strain was also performed for comparison (Figure 4.21).

The *mag1* cells, which had not exhibited increased sensitivity to the agent in our previous experiments, would still have functional NER and should therefore be capable of removing the TH-III-151 adducts.

In sharp contrast to the repair competent DBY747 cells, as well as the NER functioning *mag1* cells, no repair was evident in the NER defective strain. The *rad4* cells failed to eliminate any of the adducts on the TS, irrespective of their position with 100% of the damage persisting after 8 hours of post-treatment incubation. This observation suggests that the adduct recognition and elimination observed in the wild type strain must be the result of an excision process involving NER factors. This differentiates the excision event seen for the TH-III-151 with the one previously observed for the distamycin analogues of BAM, where the excision process was not identified, yet the removal of the adducts did not seem to involve NER factors (Brooks *et al*, 2000). A clear gradient of repair was observed in the *mag1* strain, as expected, attributed to the function of the NER machinery (Figure 4.21).

Subsequent experiments addressed whether the high level of sensitivity of the *rad18* cells to TH-III-151 previously identified could be the result of a defect in the adduct elimination. Figure 4.22 (left) shows the repair capacity of the *rad18* strain. Repair in this strain was not simply impaired but totally defective. Strikingly the *rad18* cells were as disabled as the *rad4* cells in the elimination of the adducts on the TS. As discussed previously, the Rad18 protein physically associates with Rad6 forming a stable complex. In an attempt to clarify if the excision deficiency is the result of inactivation of the the Rad6-Rad18 complex or a phenomenon limited to Rad18 alone, *rad6* cells were also assessed for their ability to eliminate the TH-III-151 adducts. As shown in Figure 4.22 (right), *rad6* cells exhibited the same adduct repair defect. The indistinguishable defective repair profiles of both *rad6* and *rad18* cells, indicate that both proteins are required for the removal of the TH-III-151 adducts from the TS of *MFA2*.

These observations suggest that the excision of the A-N3 adducts induced by this novel CC-1065 analogue require functional Rad18.

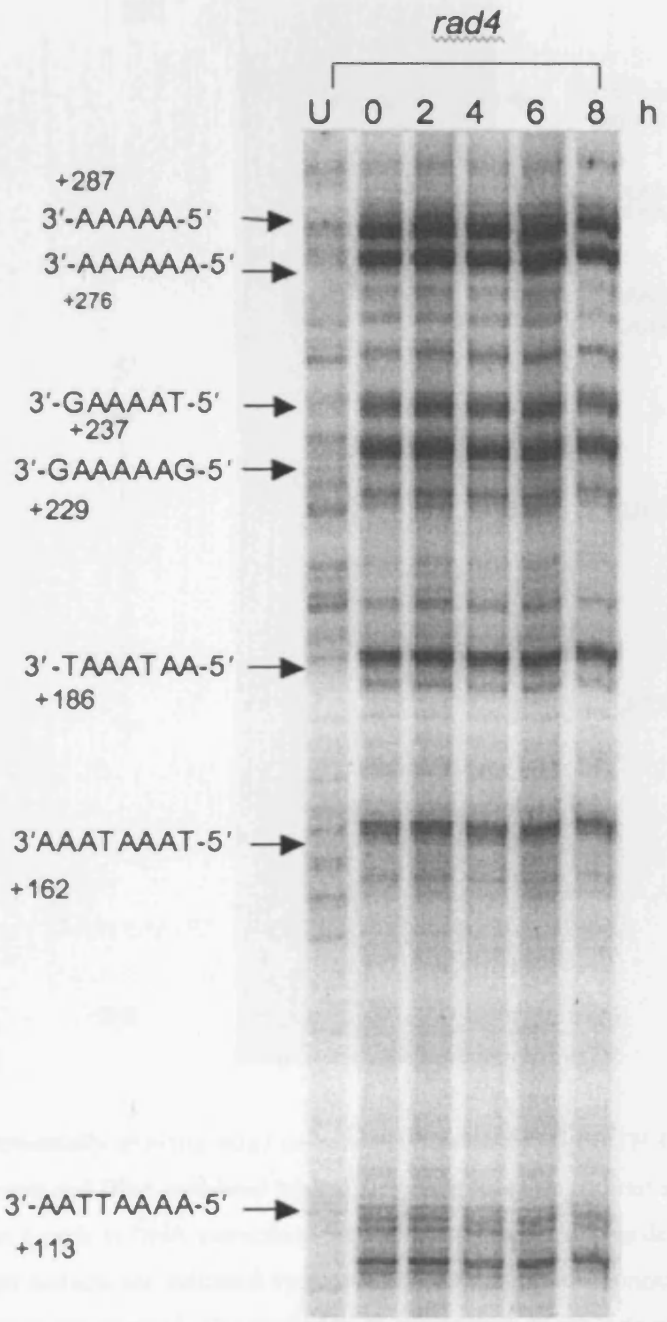

Figure 4.20 Repair of TH-III-151 adducts on the TS of *MFA2*. Exponentially growing *rad4* cells were treated with 10 μM TH-III-151 for 3 h at 30°C. Cells were harvested and DNA extracted immediately (0 h lane), or allowed to repair in YEPD for a further 2, 4, 6 and h prior to DNA extraction. Sslig-PCR was performed as described in the Methods section. The major adducts are indicated by arrow, and their sequence and nucleotide positions in relation the start of the coding region are denoted. The sequence of the portion of the gels presented here stretches from positions 106 to 300.

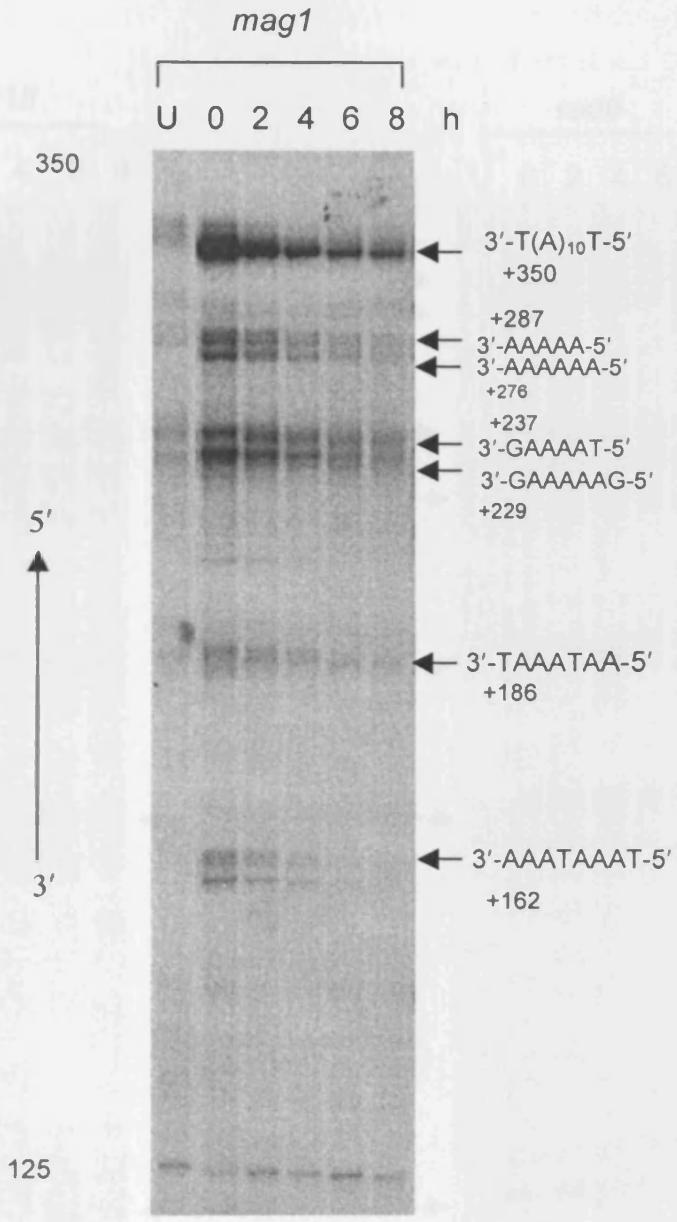

Figure 4.21 Exponentially growing *mag1* cells were treated with 10 μM TH-III-151 for 3 h at 30 °C. Cells were harvested and DNA extracted immediately (0 h lane), or allowed to repair in YEPD for a further 2, 4, 6 and h prior to DNA extraction. Sslig-PCR was performed as described in the Methods section. The major adducts are indicated by arrow, and their sequence context in relation to the start of the coding region are denoted. The sequence of the portion of the gels presented here stretches from positions 125 to 350.

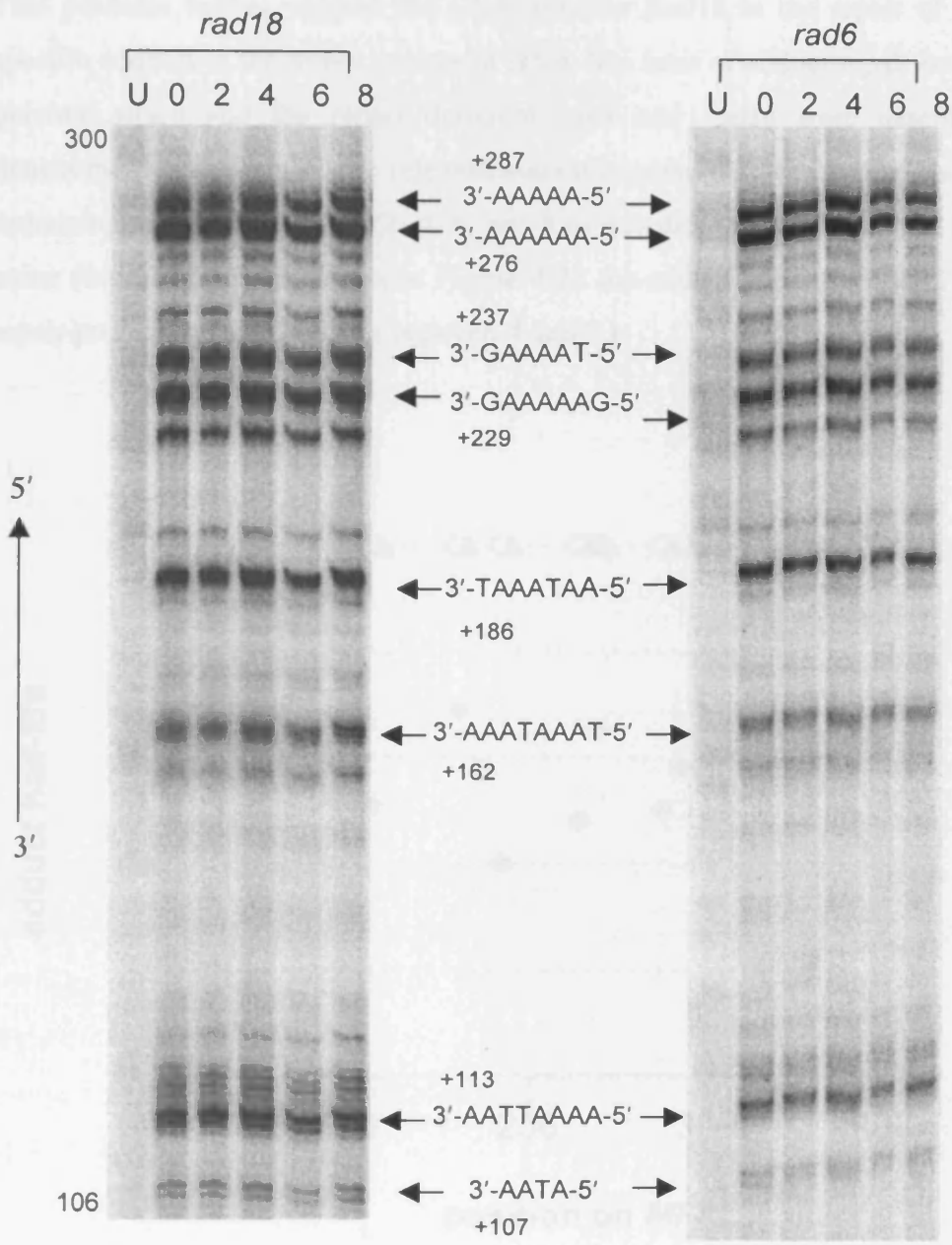

Figure 4.22 Repair of TH-III-151 adducts on the TS of *MFA2* in *rad18* and *rad6* cells treated with 10 μM TH-III-151 for 3 h at 30°C. Cells were harvested and DNA extracted immediately (0 h lane), or resuspended in YEPD and allowed to repair for a further 2, 4, 6 and h prior to DNA extraction. Sslig-PCR was performed as described in the Methods section. The sequence of the portion of the gels presented here stretches from positions 106 to 300. The locations of the major adducts is shown by the arrows. The positions of the adducts relative to the start of the coding region is also indicated.

This provides further support for a key role for Rad18 in the repair of sequence specific adducts in the minor groove of DNA The rates of adduct repair between the parental strain and the repair deficient *rad4* and *rad18* were determined by densitometric scanning of the relevant autoradiogaphs. The fraction of each adduct remaining at each time point (2, 4, 6, and 8 h) was determined relative to the initial value (0 h sample). As shown in Figure 4.23 the adduct half-life on the TS of the repair proficient DBY747 was between 4 and 7 h.

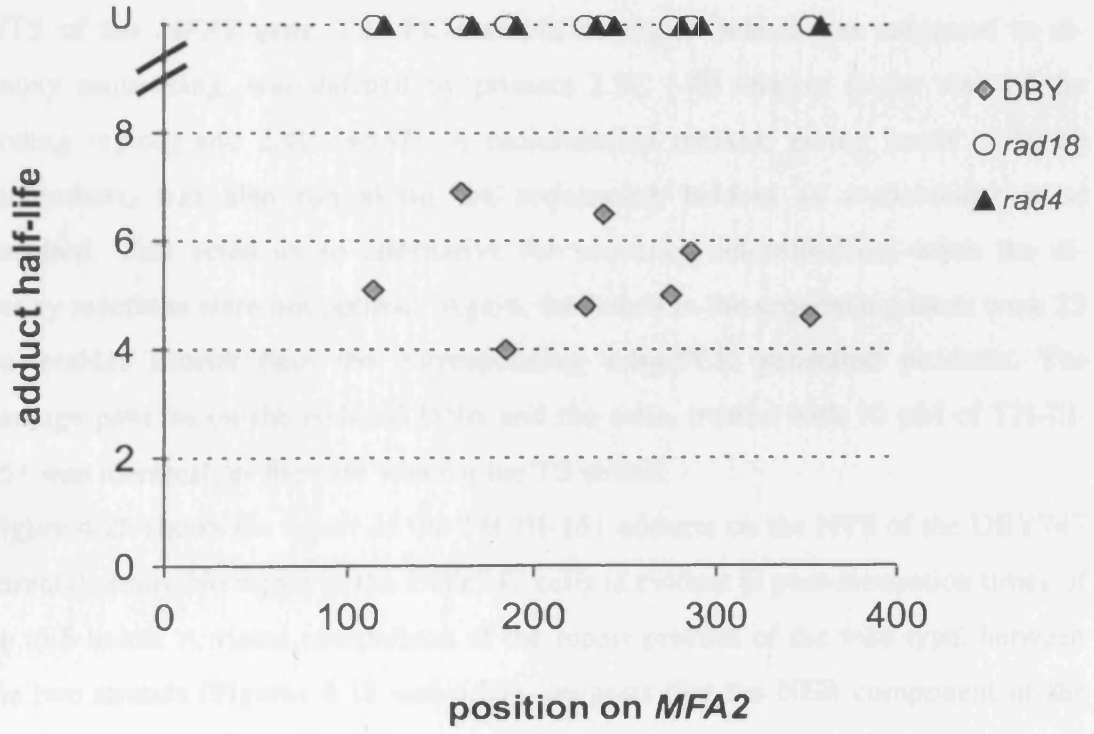

Figure 4.23 Repair rates of TH-III-151 adducts on the TS of the *MFA2* gene in the DBY747 (parental), *rad4* and *rad18* strains. The half life of each adduct is in h. Values are the mean of at least three repeats. U indicates that none of the adducts was repaired after 8 h of post-treatment incubation.

4.3.4 Repair of TH-III-151 adducts is transcription-coupled

NER is a genetically heterogeneous process and acts upon various different types of lesions (e.g. UV-induced cyclobutane pyrimidine photoproducts, cisplatin intrastrand crosslinks). Transcriptionally active regions of the genome can be subject to faster repair than silent regions and that is manifested with the TS being repaired at significantly faster rate that the NTS. This process is known as transcription-coupled repair (Hanawalt, 1989; Balajee & Bohr, 2000).

The induction and repair of the TH-III-151 adducts was also assessed using primers specific for the NTS of the *MFA2* gene. Figure 4.24 shows the sequencing of the NTS of the *MFA2* gene. The PCR amplified region which was subjected to di-deoxy sequencing, was defined by primers 2.5C (-49 relative to the start of the coding region) and 2.4C (+547). A radiolabelled marker, giving bands at 10 bp increments, was also run along the sequencing ladders as a molecular mass standard. This acted as an alternative for sequence determination, when the di-deoxy reactions were not optimal. Again, the bands in the sequencing lanes were 23 nucleotides shorter than the corresponding sslig-PCR generated products. The damage patterns on the isolated DNA and the cells, treated with 10 μM of TH-III-151 was identical, as the case was for the TS strand.

Figure 4.25 shows the repair of the TH-III-151 adducts on the NTS of the DBY747 parental strain. No repair in the DBY747 cells is evident at post-incubation times of up to 8 hours. A visual comparison of the repair profiles of the wild type, between the two strands (Figures 4.18 and 4.25), suggests that the NER component of the repair observed only on the TS may be transcription coupled, as removal of adducts preferentially occurs on this strand alone. The NTS analysis depicted in the autoradiographs of Figures 4.25 and 4.26 encompassed sequences downstream of the transcription termination site (+328), because no prominent TH-III-151 adducts were detectable further upstream and along the region examined in the repair analysis of the TS.

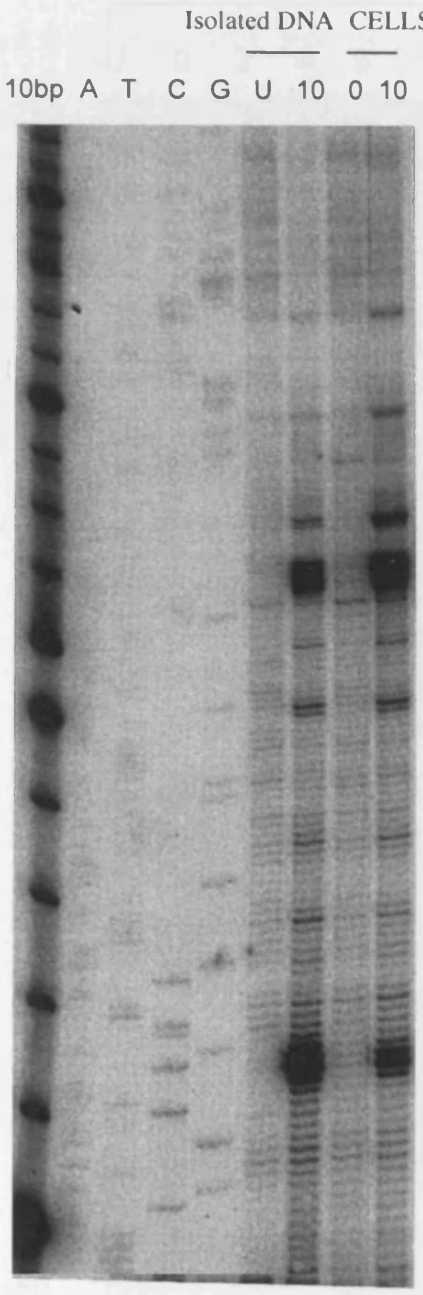

Figure 4.24 Sequencing of the NTS of *MFA2* gene, using primers 2.5C and 2.4C. Di-deoxy sequencing ladders are indicated as A, T, C, G and used to determine the sites of TH-III-151 binding. Exponentially growing DBY cells were treated with 10 μM of TH-III-151 for 3 h at t 30°C. TH-III-151 lesions were detected using the sslig-PCR technique as described in the Methods section. Lane U has untreated genomic DNA and T is for the same DNA treated with 10 μM of the agent. A molecular mass marker (increments of 10bp) was also included. The bands represent DNA fragments of varying lengths, which correspond to the positions of drug adducts along the sequence.

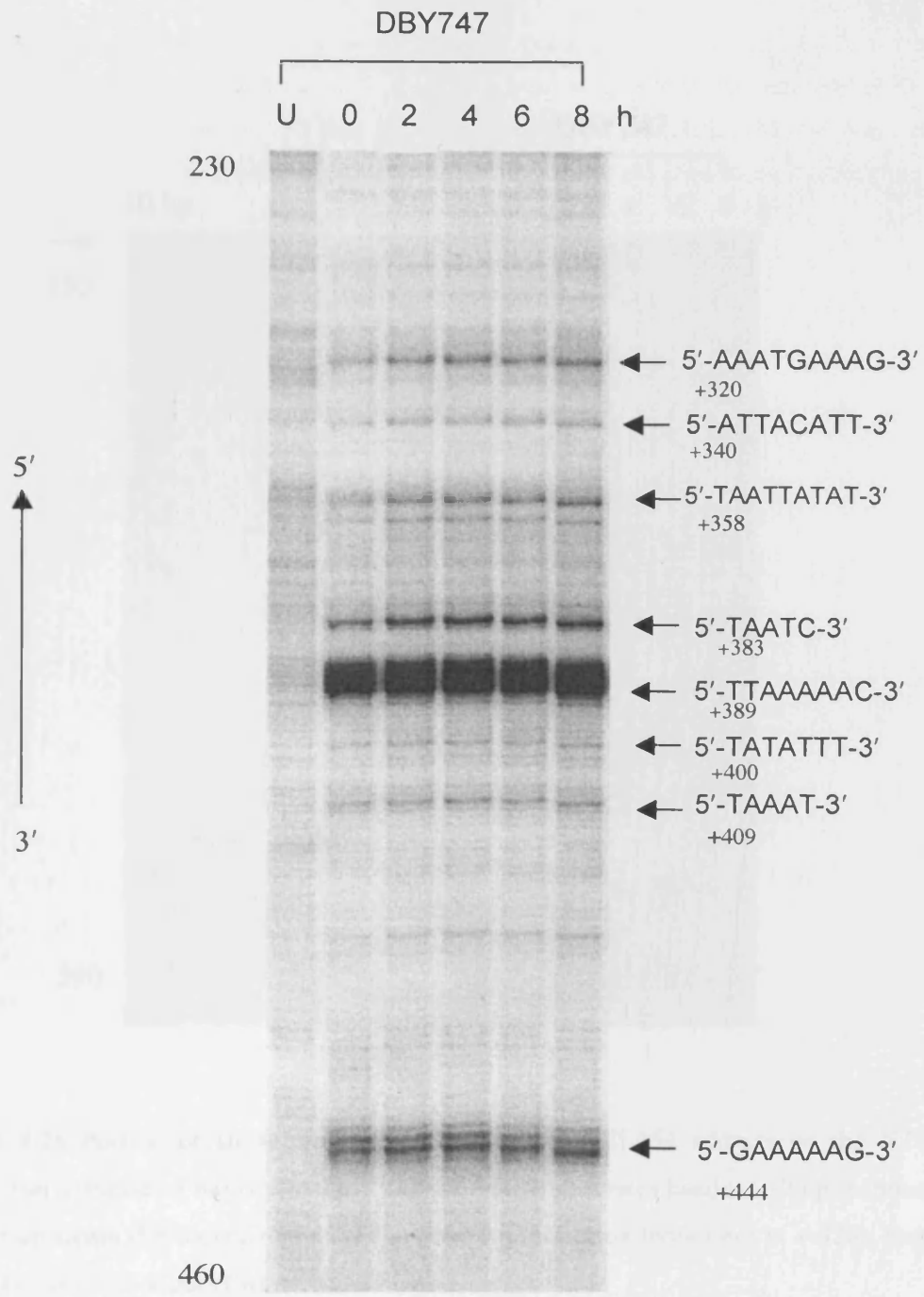

Figure 4.25 Repair of TH-III-151 adducts on the NTS of *MFA2*. Exponentially growing DBY747 cells were treated with 10 μM of TH-III-151 for 3 h at 30°C. Cells were harvested and DNA extracted immediately (0 h lane), or cells were resuspended in YEPD and allowed to repair for a further 2, 4, 6 and h prior to DNA extraction. Sslig-PCR was performed as described in the Methods section. The locations of the major adducts is shown by the arrows and their position in relation to the start of the coding region of *MFA2* is denoted. The sequence of the portion of the gels presented here stretches from positions 460 to 230.

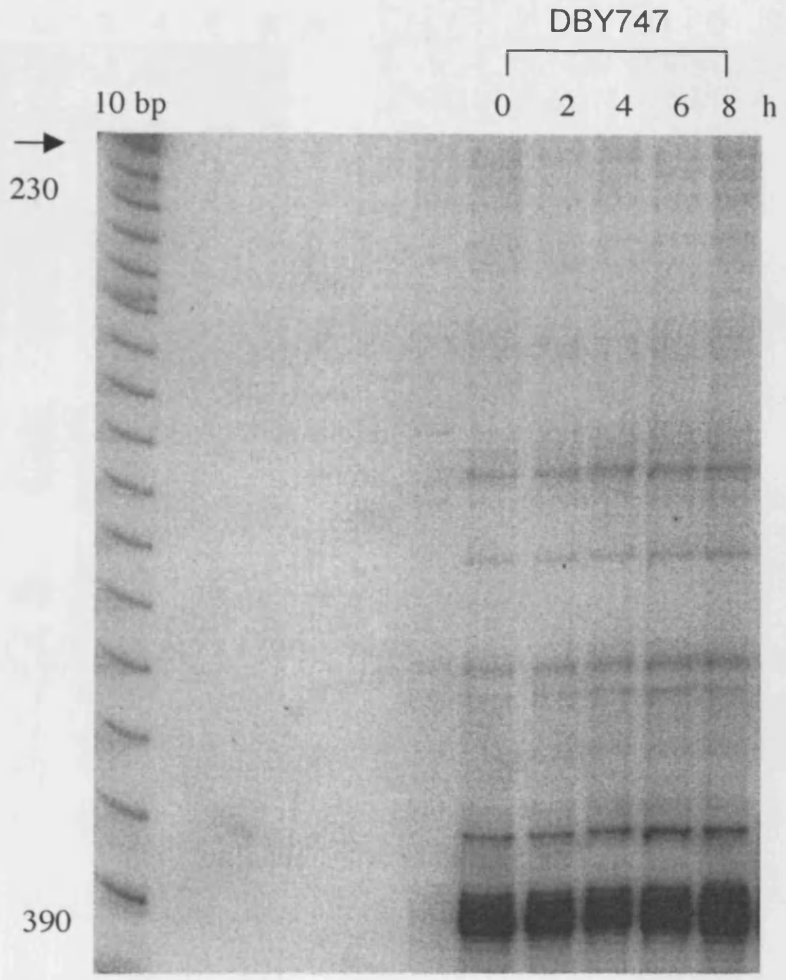

Figure 4.26 Portion of an autoradiograph showing TH-III-151 adducts on the NTS of *MFA2*, run alongside a molecular mass marker, which generates bands at 10 bp increments. Further upstream the coding region of the gene (transcription terminates at + 328), there is no visible, marked adduct formation.

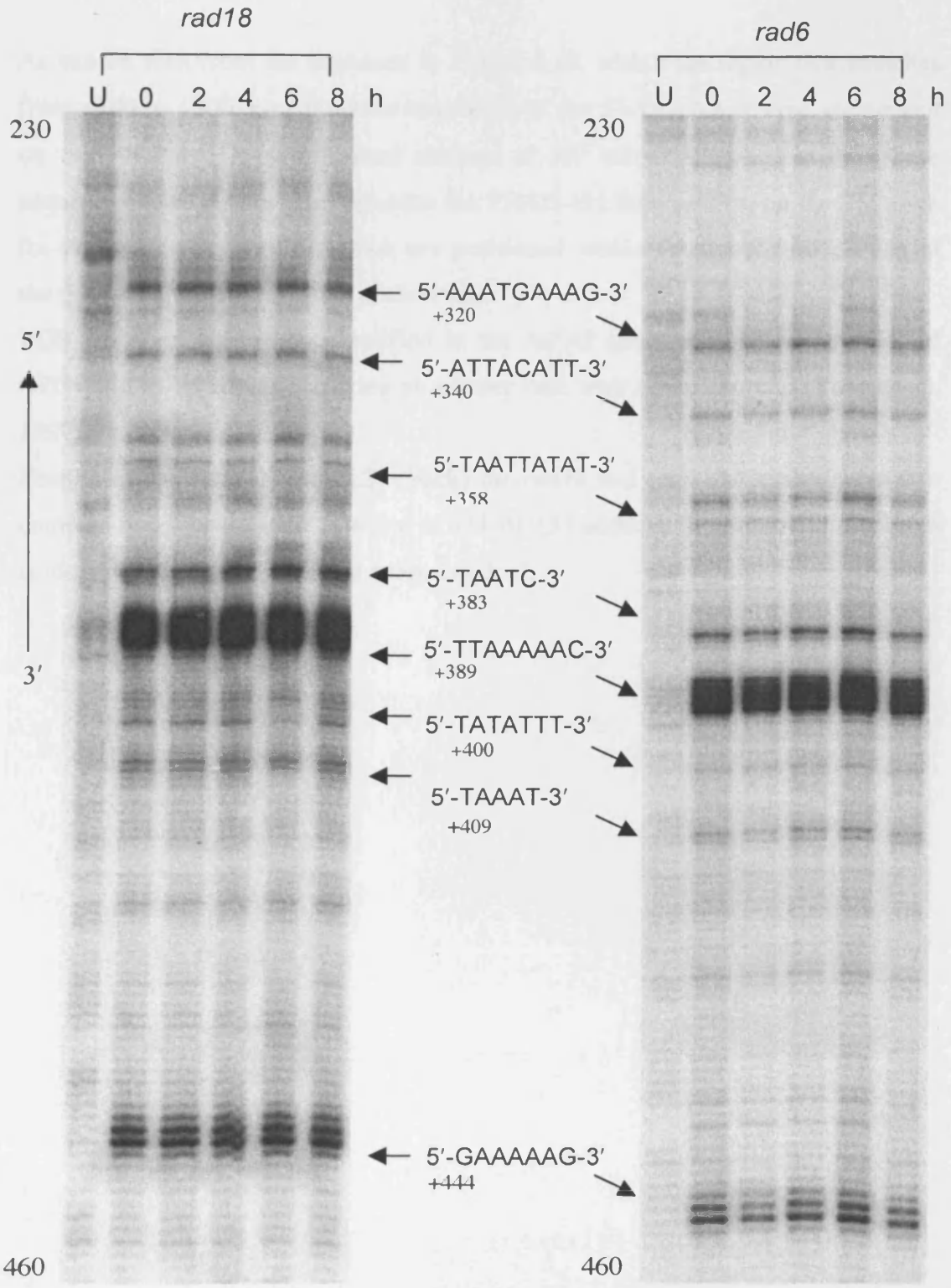

Figure 4.27 Repair of the TH-III-151 adducts on the NTS of *MFA2* of exponentially growing *rad18* and *rad6* cells. Conditions, Sslig-PCR analysis and labelling as described in legend for Figure 4.25.

As can be seen from the sequence in Figure 4.19, within the region that stretches from +100 to +300, no consensus sequences of the 5'-AAAAA-3' type are present on the NTS and only a limited number of AT mixed stretches exists. These sequences however are right opposite the TH-III-151 binding sites on the TS. Even for those adducts however which are positioned within the transcribed portion of the gene, no gradient of repair is observed.

TCR has been previously identified in the *MFA2* gene, with enhanced NER of CPDs on the TS strand occurring at a faster rate, over repair on NTS (Teng *et al.*, 1997).

Finally, as shown in Figure 4.27 (back) the *rad18* and *rad6* disruptants were also completely deficient in the removal of TH-III-151 adducts, the occurrence of which is identical among the different strains studied.

4.3.5 *RAD5* disruptants are extremely sensitive to TH-III-151

As discussed in the introduction, *RAD6* and *RAD18* are the putative members of the PRR pathway centrally controlling error-free and mutagenesis (TLS) activities. These functions have been divided in subpathways, regulated by a number of proteins (see Figure 4.4). In this way, it is possible to dissect out the contribution made to the drug response by each of the major subpathways. To this effect, key members of these subpathways were screened for TH-III-151 sensitivity. Initial studies concentrated on the *rev3* and *rad30* mutants, lacking the functions of translesion polymerases ζ and η, respectively (Johnson, *et al.*, 1999).

Figure 4.28 shows the sensitivity of these strains to TH-III-151, as exibited in the plate-based sensitivity screen.

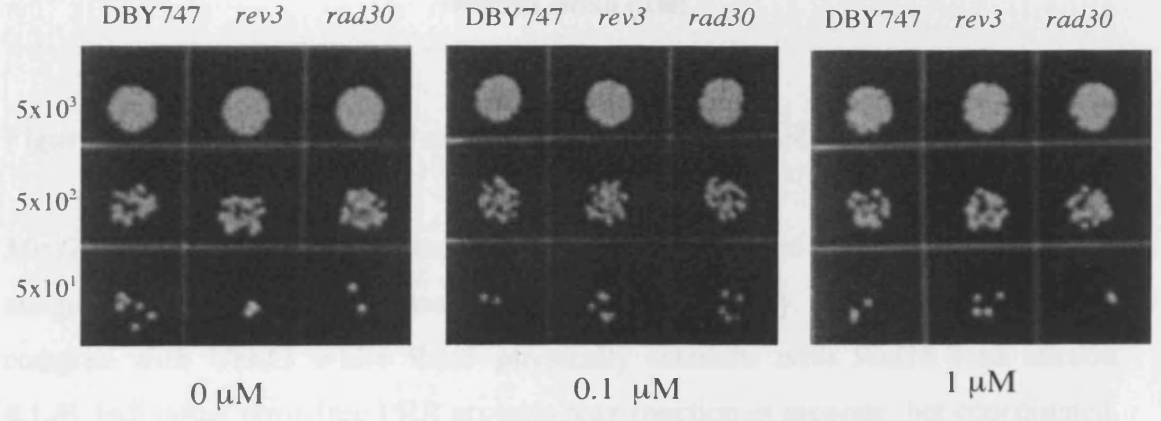

Figure 4.28 TH-III-151 sensitivity of the *rev3* and *rad30* mutant cells compared to the repair competent wild type cells.

Figure 4.29 shows the survival curve of the *rev3* strain. Disruption of *REV3* does not confer markedly increased sensitivity to the agent. These observations suggest that the PRR subpathways which contain *rev3* and *rad30* should not be involved in the processing of the TH-III-151 adducts. The NER defect therefore, reported earlier for the *rad18* and *rad6* cells, cannot be explained by the loss of the activities of either of these proteins.

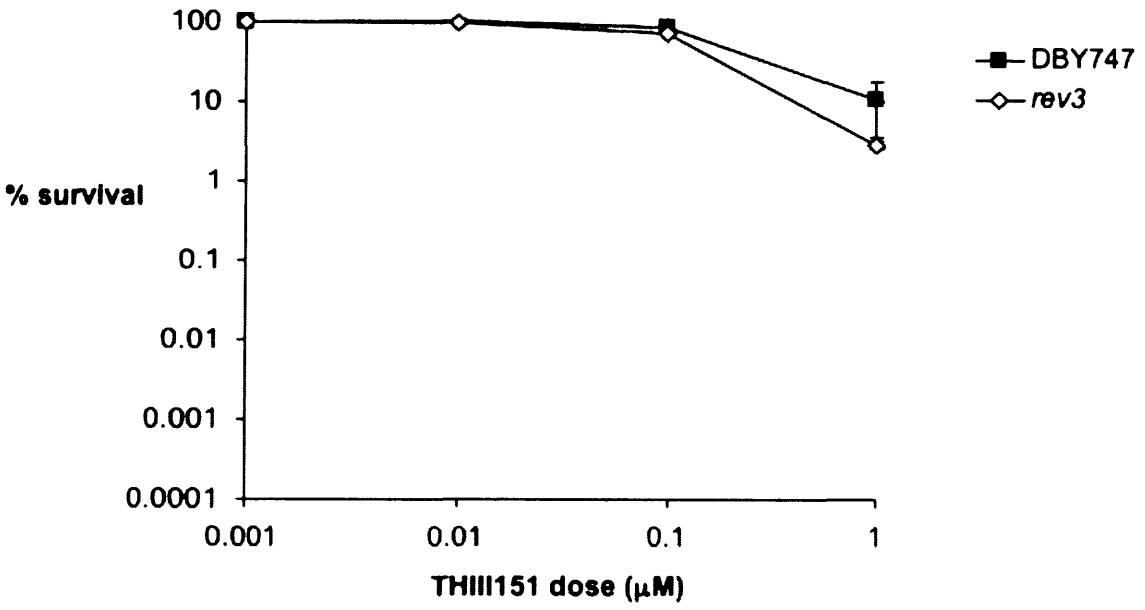

Figure 4.29 Sensitivity of *rev3* cells compared with the wild type DBY747.

Mms2 and *rad5* disruptants were also tested. Mms2 and Rad5 have both been assigned to the error-free branch of the *RAD6* pathway. Mms2 forms a stable complex with Ubc13 while Rad5 physically interacts with Rad18 (see section 4.1.4). Individual error-free PRR proteins may function in separate, but coordinated, processes, adding to the complexity of PRR. The double mutant *rad5 mms2* was therefore also included to provide an insight on the relative contribution of each protein to the TH-III-151 sensitivity. As shown in figure 4.30 the *rad5* disruptant is extremely sensitive to the agent while the *mms2* strain is moderately sensitive. It is therefore the *RAD5* defect in the double mutant which most contributes to its sensitivity, suggesting that Rad5 has the overall control of this specific Rad6-dependent subpathway for this particular response.

Having established that the error-free Rad5-controlled PRR subpathway is predominantly required for resistance to TH-III-151 toxicity, its relationship to NER was investigated.

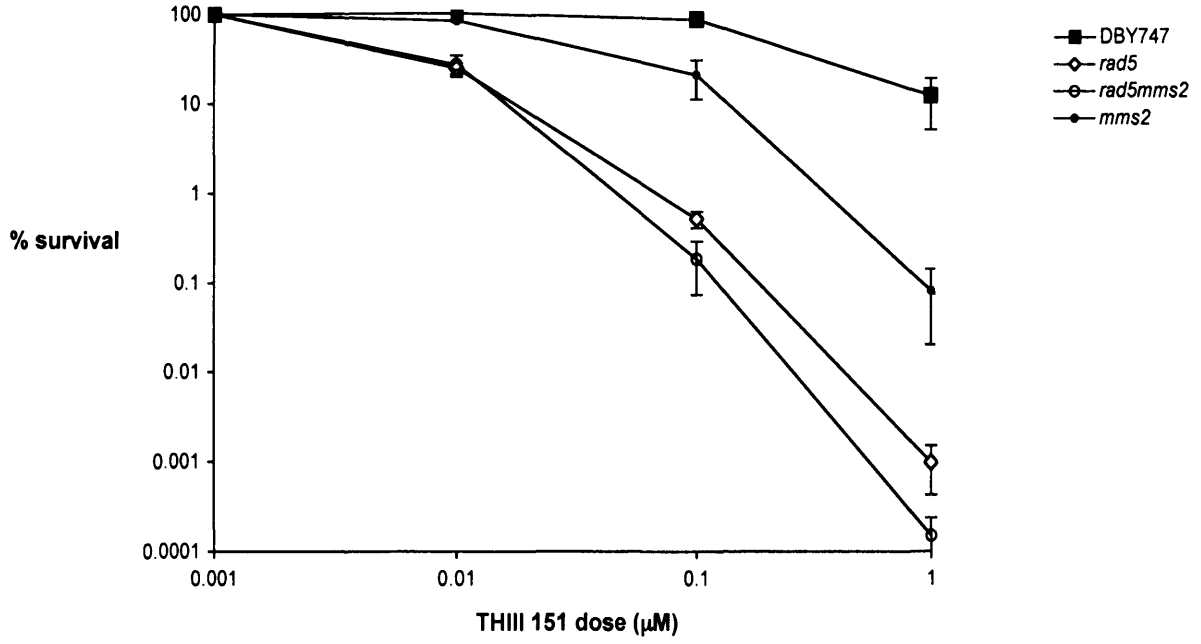

Figure 4.30 TH-III-151 sensitivity of *rad5*, *mms2*, and *rad5 mms2* cells compared with their isogenic parent DBY747.

To this effect, the *rad4 rad5* double mutant was constructed and its sensitivity compared to the individual single mutants.

In order to create the double mutant, a PCR-mediated gene disruption method was utilised (see Methods, section 4.2.2.6). This efficient technique uses gene disruption cassettes to create mutant genes in budding yeast and only requires the flanking sequences of the relevant gene. To construct the disruption cassettes, DNA sequences that flank the gene to be mutated, are cloned left and right of a marker gene using PCR. These cassettes are subsequently transformed into appropriate

yeast cells. Homologous recombination between the flanking regions on the cassette and the wild type gene in the cells, results in the disruption of the wild type gene and the simultaneous integration of the marker gene. Thus, this technique allows the disruption of the desired gene, in addition to incorporating a selection marker in a single step (Guldener *et al.*, 1996; Longtine *et al.*, 1998).

In creating the *rad4rad5* double mutant, *rad5* cells were transformed with the disruption cassette for *RAD4*. The marker used in this case was the KanMX4 expression module, which is derived from the *Escherichia coli* transposon Tn903 and the TEF promotor/terminator sequences of the fungus Ashbya gossypii (Guldener *et al.*, 1996). This marker is particularly useful, since it confers resistance to the aminoglycoside antibiotic Geneticin (G418) and therefore, provides a convenient selection for the transformed yeast cells. Additionally, since the KanMX4 marker is completely heterologous, there is no possibility of the yeast cells being resistant to G418 prior to transformation with the cassette or the marker recombining with the endogenous marker gene. The gene disruption procedure for the creation of the *rad4 rad5* is outlined in Figure 4.32. Eventually, the yeast cells that have been successfully transformed with the cassette can easily be selected based on the growth on G418 enriched plates.

Growth on G418 plates alone is not sufficient proof for the disruption of the *RAD4* gene by the *RAD4-KanMX4-Rad4* cassette, in the *rad5* cells. This only indicated that the yeast cells have been successfully transformed with the cassette, yet it is possible (around 30% possibility) for the cassette to integrate elsewhere in the genome (Guldener *et al.*, 1996).

In order to confirm that the cassette has been integrated correctly and that the *RAD4* gene has been disrupted, gel analysis of a number of enzymatic digestions on the PCR products from the *rad5* strain and its *rad4::kanMX4* disruptant was performed as a confirmation test.

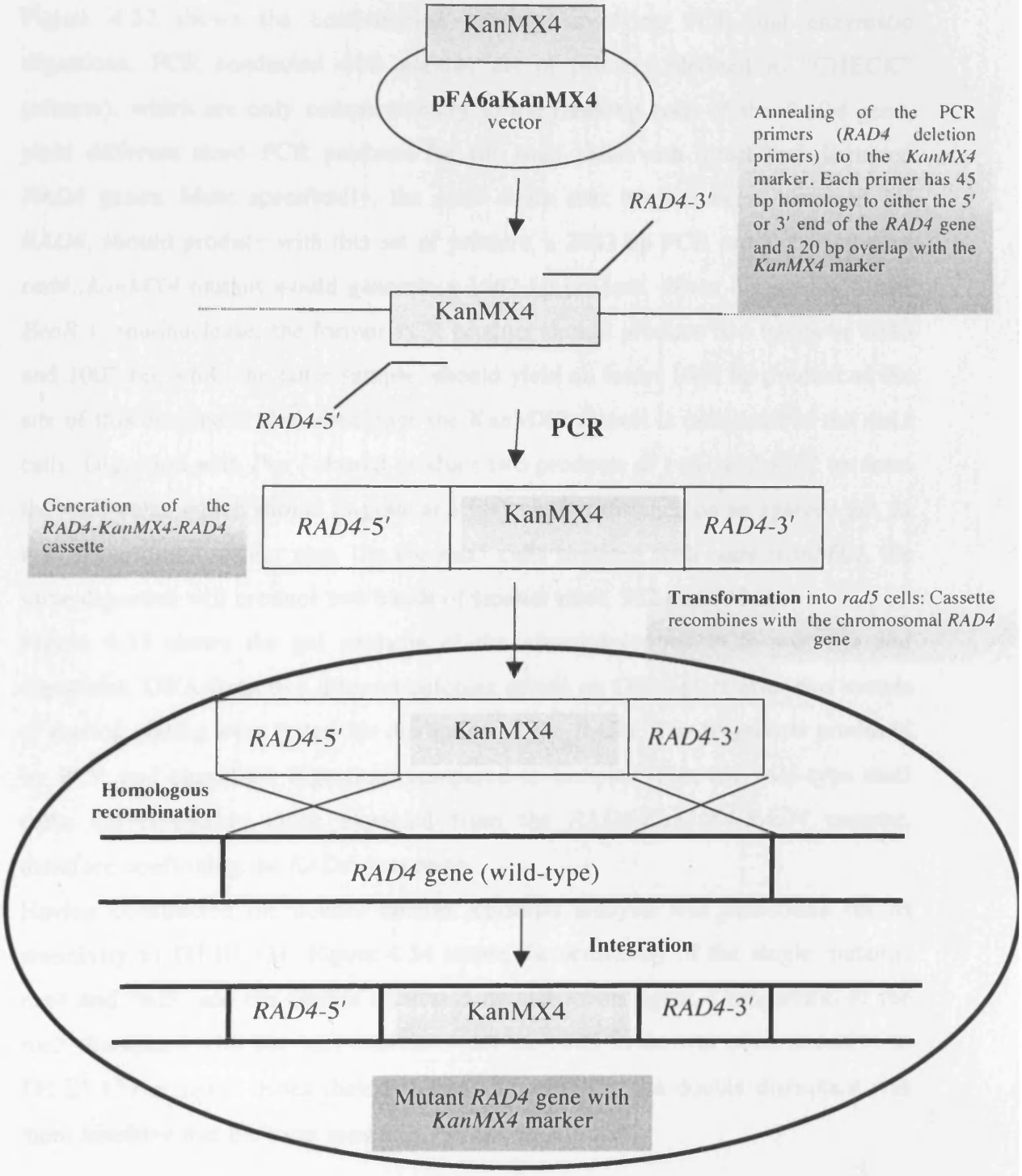

Figure 4.31 The PCR-mediated gene disruption procedure followed to create the *rad4 rad5* double mutant.

Figure 4.32 shows the confirmation strategy involving PCR and enzymatic digestions. PCR conducted with another set of primers (defined as "CHECK" primers), which are only complementary to the flanking ends of the *RAD4* gene, yield different sized PCR products for the *rad5* cells with intact and disrupted *RAD4* genes. More specifically, the *rad5* strain that has not been disrupted for *RAD4*, should produce with this set of primers, a 2443 bp PCR product, while the *rad4::kanMX4* mutant would generate a 1662 bp product. When digested with the *EcoR V* endonuclease, the former PCR product should produce two bands of 1436 and 1007 bp, while the latter sample, should yield an intact 1662 bp product as the site of this enzyme is abolished once the KanMX4 cassete is integrated in the *rad5* cells. Digestion with *Pvu I* should produce two products of 1181 and 1262 bp from the *rad5* cells, which should migrate at a very similar distance on an agarose gel, as they are of very similar size. On the *rad5* cells mutated with *rad4::kanMX4*, the same digestion will produce two bands of smaller sizes, 922 and 740 bp.

Figure 4.33 shows the gel analysis of the above-described PCR products and digestions. DNA from two diferent colonies grown on G418-plate after two rounds of replica plating were tested for disruption of the *RAD4*. The fragments produced by PCR and enzymatic digestion, compared to samples from the wild-type *rad5* cells, correspond to those expected from the *RAD4-KanMX4-RAD4* cassette, therefore confirming the *RAD4* disruption.

Having constructed the double mutant, epistasis analysis was performed for its sensitivity to TH-III-151. Figure 4.34 shows the sensitivity of the single mutants, *rad4* and *rad5*, and the double *rad4rad5* mutant to the agent. Comparison of the *rad5* disruptant with the *rad4* indicates that the *rad5* strain was more sensitive to TH-III-151 at lower doses (below 1 μM). In addition, the double disruptant was more sensitive that the most sensitive, *rad5*, single mutant.

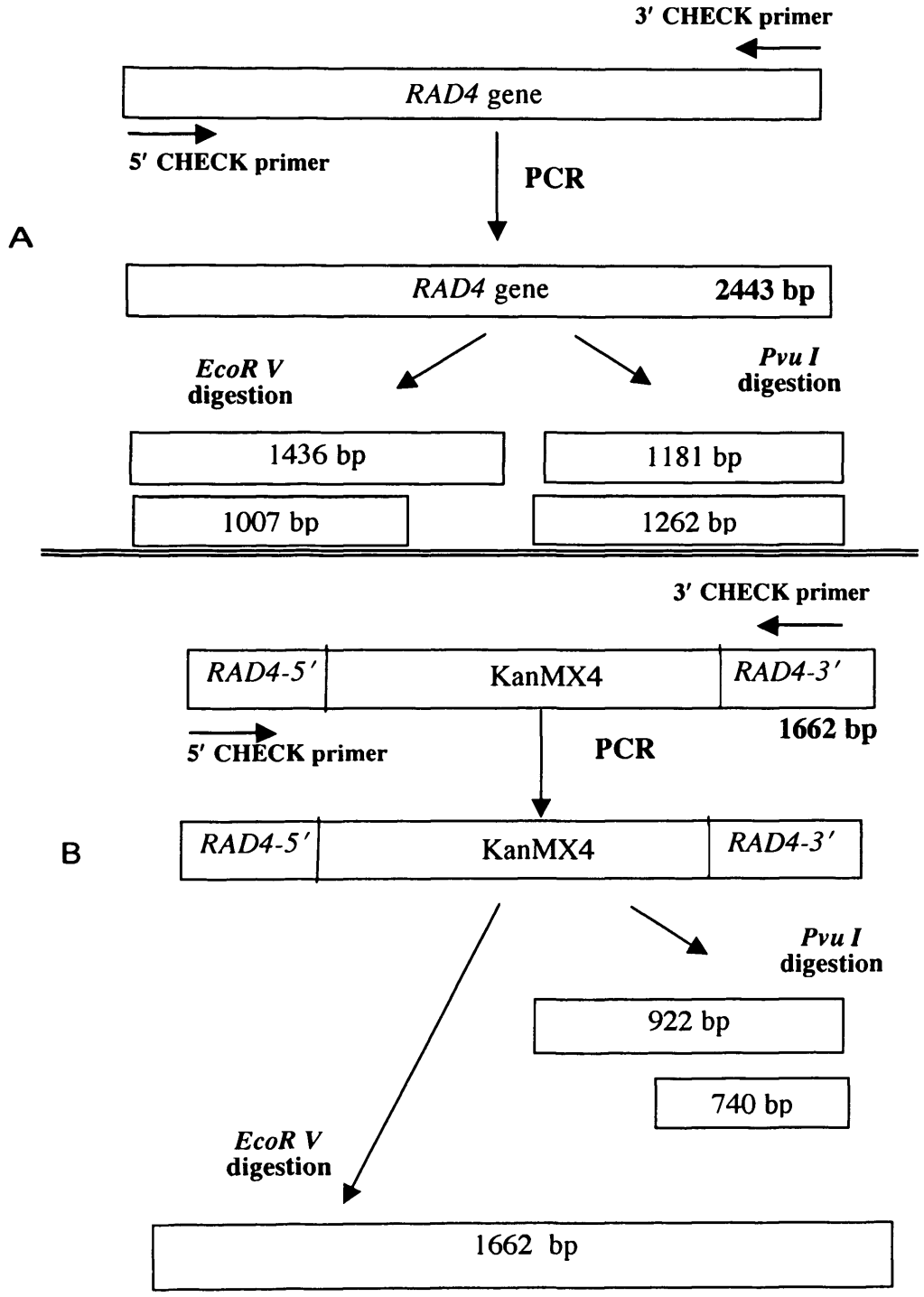

Figure 4.32 Confirmation of *RAD4* disruption using PCR and *Pvu I* and *EcoR V* digestion. PCR conducted with the CHECK primers yields different sized PCR products for the *rad5* strain with intact and disrupted *RAD4*. Digestion with the two endonucleases generates fragments of differing sizes and acts as another way of further confirming that the *RAD4* gene has indeed been disrupted in the *rad5* mutants.

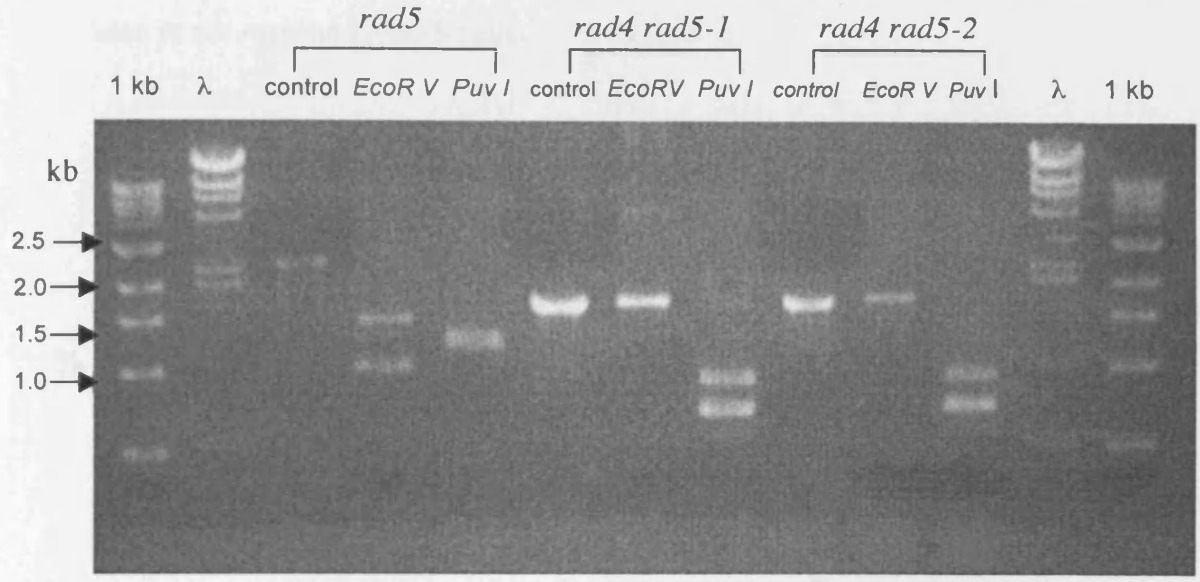

Figure 4.33 Gel analysis of undigested and *EcoR V* or *Pvu I* digested samples to confirm the creation of the *rad4 rad5* double mutant. 1 kb and λ (Lamda DNA-*Hind III* digest) are molecular weight standards. DNA samples from two different colonies grown on G418 plates (denoted as *rad4 rad5*-1 and *rad4 rad5*-2) were tested and gave identical results. As expected (and schematically drawn in Figure 4.32A and B), samples from *rad5* cells, produces a single PCR product after amplification with the CHECK primers of 2.4 kb. When this is digested with *EcoR V*, it is fragmented to give two distinct 1 kb and 1.4 kb bands (lane 4 from left). Digestion with *Puv I* gives two closely migrating bands of around 1.2 kb (lane 5 from left). Samples from G418 resistant colonies gave identical results between them. PCR amplification produced a product of 1.6 kb and In contrast to the *rad5* cells, digestion with the same endonucleases produced distinct fragments of the sizes shown in Figure 4.32B.

These cytotoxicy profiles emphasise the importance of the Rad5 defect as a determinant of the sensitivity of the NER-defective *rad4* cells to the agent.The high level of TH-III-151 sensitivity in the *rad5* strain and the exhibited complex pattern of epistasis with the *rad4* mutant, warranted direct investigation for functional evidence through the repair of the TH-III-151-induced adducts in r*ad5* cells.

Figure 4.35 shows the induction and repair of TH-III-151 adducts along the TS of the *MFA2* gene on the parental DBY747 strain (left) and the *rad5* mutant (right).

The sslig-PCR analysis revealed the same adduct elimination defect as previously seen in the *rad4* and *rad18* cells.

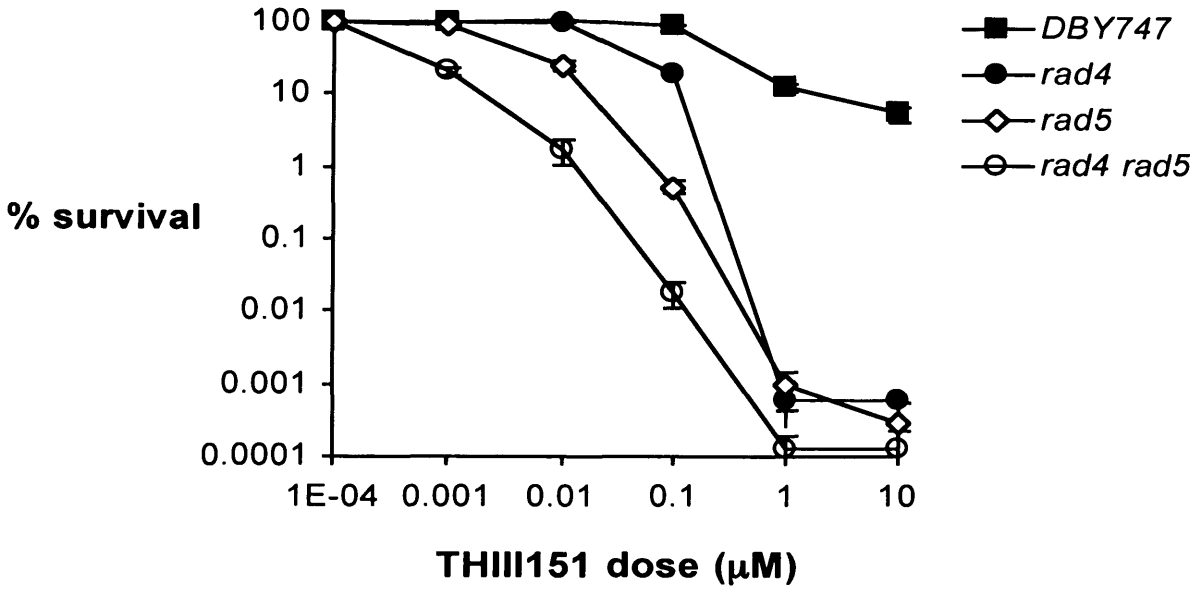

Figure 4.34 TH-III-151 sensitivity of *rad5*, *rad4* and *rad4rad5* cells compared with their isogenic parent DBY747.

The *rad5* cells failed to remove any of the adducts and 100% of the damage persisted during the 8 hour post treatment recovery period. That is in sharp contrast to the repair competent DBY747 cells. It therefore appears that it is the *RAD5* branch of the *RAD6* pathway which influences the elimination by NER of the minor groove adducts produced by this novel agent and that the interaction between these two pathways is important in controlling drug sensitivity.

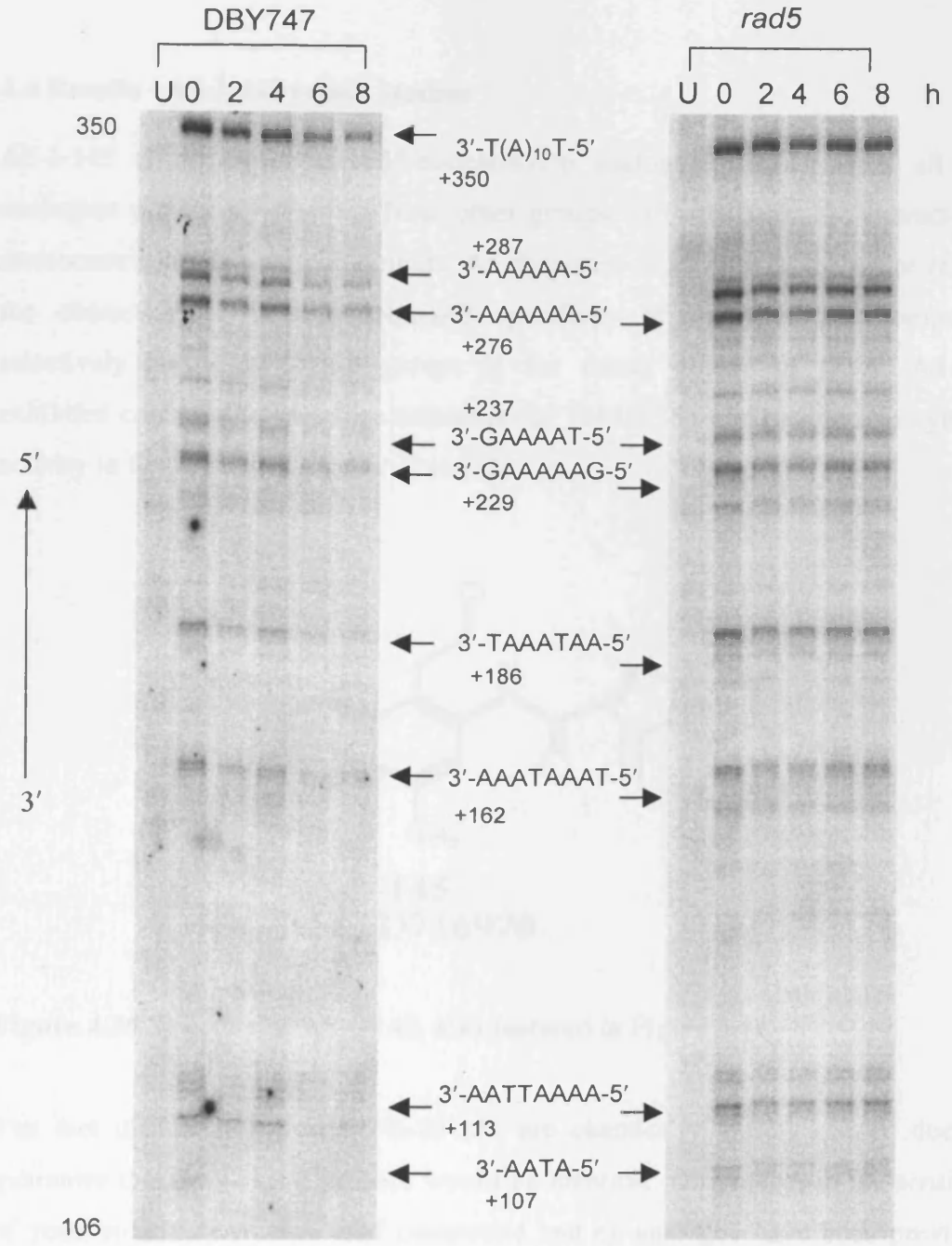

Figure 4.35 Comparison of the repair profiles of DBY747 and *rad5* cells on the TS of *MFA2*. Cells were treated with 10 μM TH-III-151 for 3 h at 30°C and harvested immediately (0 h lane), or resuspended in YEPD and allowed to repair for a further 2, 4, 6 and 8 h prior to DNA extraction. Sslig-PCR was performed as described in the Methods section. The sequence of the portion of the gels presented here stretches from positions 106 to 350. The locations of the major adducts is shown by the arrows and their position relative to the start of the coding region is also indicated.

4.4 Results - AS-I-145 repair studies

AS-I-145 is a novel CC-1065/duocarmycin analogue, distinct from all other analogues previously reported from other groups, in that it lacks the characteristic stereocentre of the lead compounds. As discussed in chapter 3, the agent retained the characteristic AT-rich sequence specificity of this class of compounds, selectively alkylating A-N3 groups in the minor groove of DNA. AS-I-145 exhibited comparable sequence selectivity to TH-III-151 and comparable cytotoxic activity in K562 cells (Chapters 2 and 3).

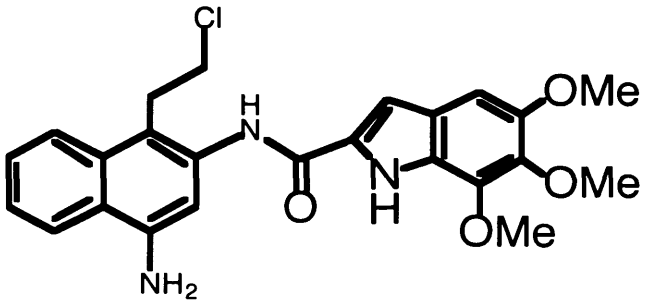

AS-1-145
NSC D716970

Figure 4.36 Structure of AS-I-145, also featured in Figure 3.11.

The fact that AS-I-145 and TH-III-151 are chemically closely related does not guarantee that their repair profiles would be identical. Differences in the sensitivity of yeast strains between a lead compound and an analogue have been previously reported as in the case of methotrexate and trimetrexate (Simon *et al.*, 2000).
Although both TH-III-151 and AS-I-145 induce the same type of damage on DNA, as demonstrated in plasmid DNA studies, the unique, novel structure of AS-I-145 and its markedly enhanced *in vivo* antitumour activity (see Chapter 6 – general discussion) made it a suitable candidate for yeast sensitivity screening.

As previously for TH-III-151, *Saccharomyces cerevisiae* strains totally defective in specific DNA repair pathways were screened for sensitivity to the agent, in an attempt to delineate the main mechanisms involved in the repair of the minor groove targeted adducts.

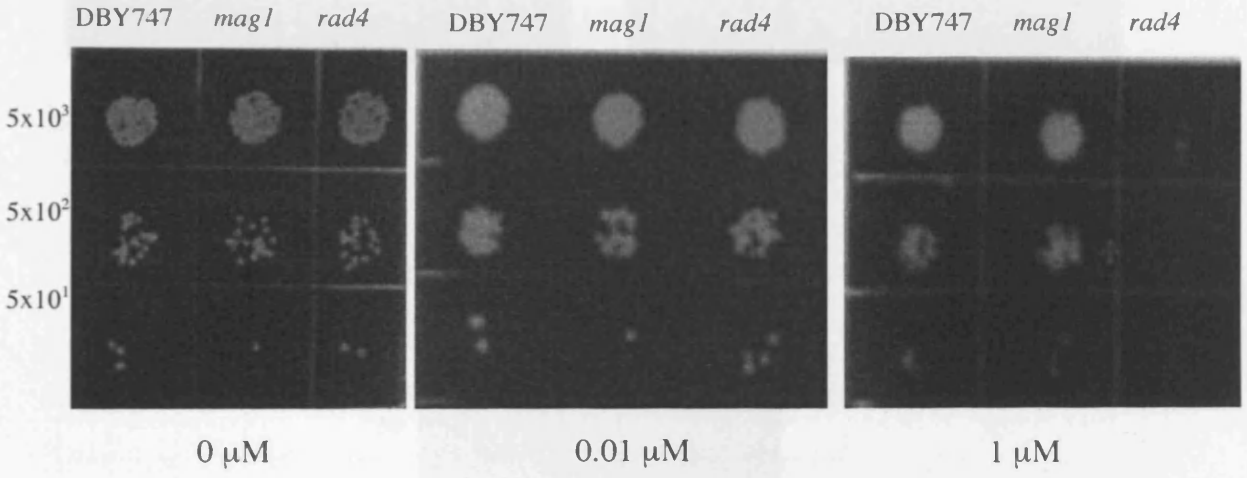

Figure 4.37 Sensitivity of the excision repair mutants *mag1* (BER), and *rad4* (NER) treated with increasing concentrations of AS-I-145. DBY747 is the repair proficient parental strain.

As was the case for TH-III-151, the NER defective strain *rad4* exhibited elevated sensitivity, since very little growth was evident at a drug concentration of 1 μM (Figure 4.37). In contrast, the insensitivity exhibited by BER mutant *mag1* suggests that the AS-I-145 adducts in yeast, are not substrate for this glycosylase.

The potential involvement of other BER functions was investigated with the screening of other glycosylases, since initiation of BER depends on the damage recognition by these enzymes (see section 4.1.4). Figure 4.38 compares the sensitivity of other known BER glycosylases to the isogenic parent. Again, no marked sensitivity was evident for any of these mutant strains, suggesting that NER is the crucial process for the elimination of the AS-I-145 adducts.

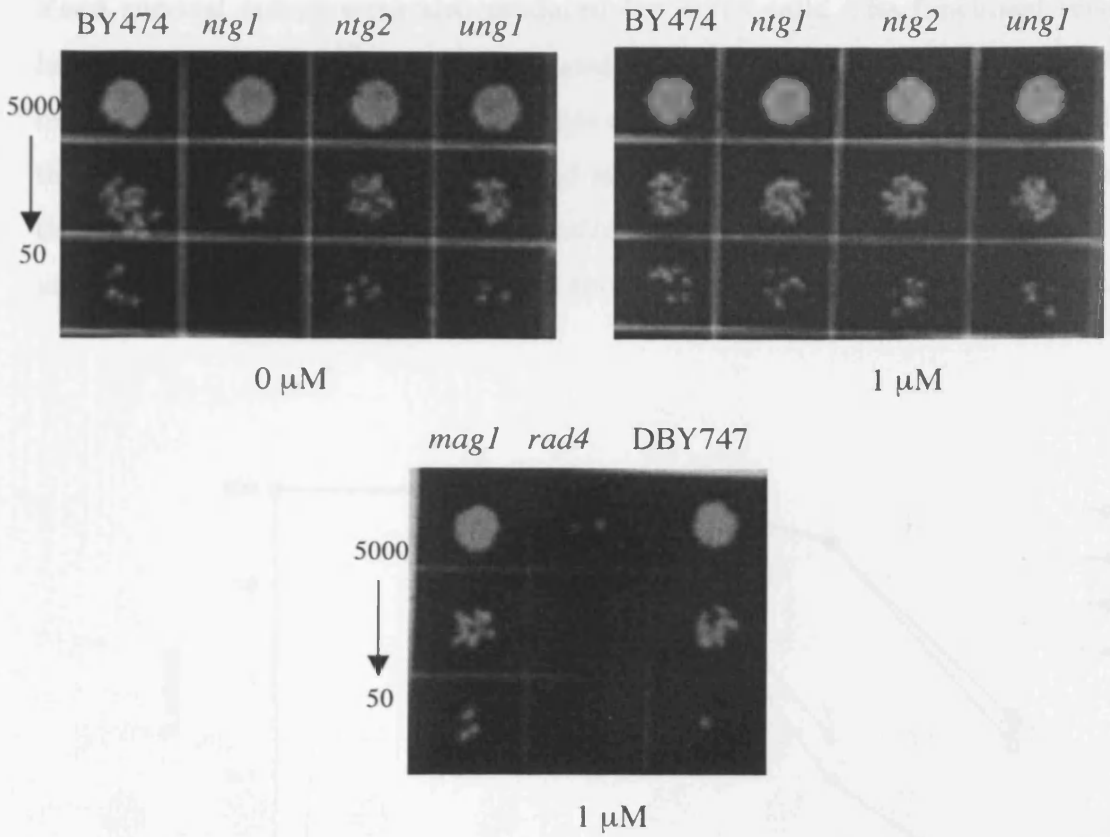

Figure 4.38 Sensitivity of the BER repair mutants *ntg1*, *ntg2* and *ung1*, all deficient in a glycosylase activity, treated with increasing concentrations of AS-I-145 compared to their isogenic parental strain. For comparison, another BER mutant *mag1* and the sensitive NER defective *rad4* strain, along with their repair proficient wild type are also included (bottom "matrix").

To further confirm the NER role as the predominant excision pathway involved in the repair of the AS-I-145 adducts, epistasis analysis was performed for the sensitivity of the *rad4* and the *mag1* cells, and the double mutant *rad4mag1*. Figure 4.39 shows the relevant survival curves. It is evident that the sensitivity possessed by the double mutant is mostly due to the NER defect as simultaneous elimination of both pathways did not markedly increase the sensitivity of the *rad4* mutant. This confirms that BER has no major contribution to the repair process and that NER is the predominant excision process.

Yeast survival curves were also produced for *rad18* cells. The functional relationship between Rad18 and NER was investigated with the inclusion of the *rad4rad18* double mutant. Figure 4.40 shows the sensitivities of the *rad4*, *rad18* and *rad4 rad18* cells. Both the *rad4* and *rad18* disruptants displayed marked sensitivity to AS-I-145. Comparison of the AS-I-145 sensitivity of the *rad4rad18* double disruptant with the single mutants indicated that *RAD4* and *RAD18* are not epistatic for the AS-I-145 damage response.

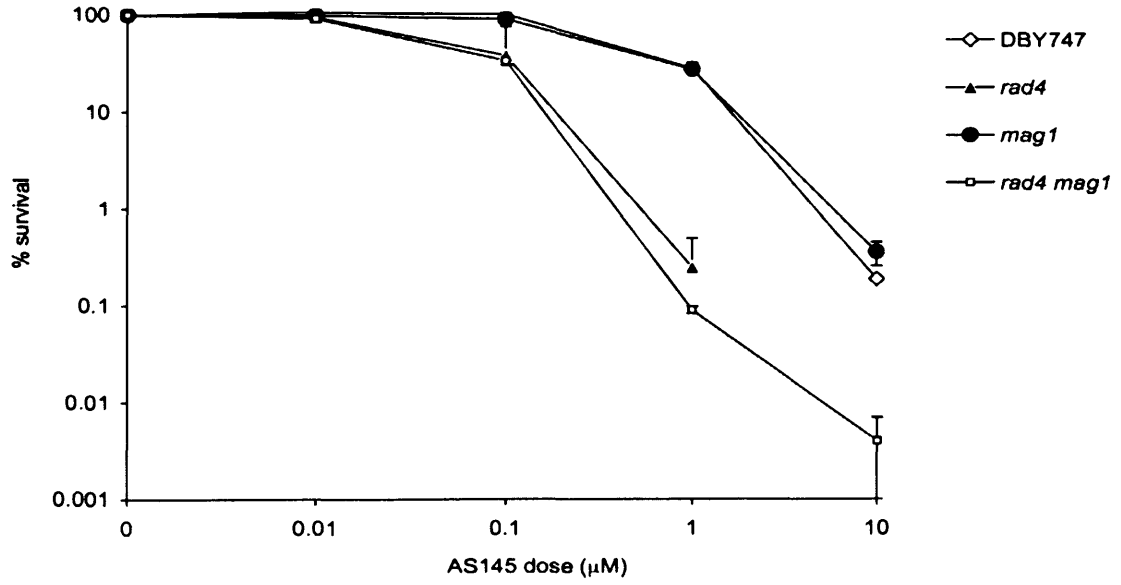

Figure 4.39 AS-I-145 sensitivity of *rad4*, *mag1*, and *rad4 mag1* cells compared with their isogenic parent (DBY747). All results shown are the mean of at least three independent experiments. The error bars represent the standard error of the mean,

The *rad4 rad18* strain was more sensitive than either the *rad4* or *rad18* single mutants, in an at least additive fashion. The TH-III-151 and AS-I-145 sensitivity profiles of the yeast strains studied, are highly similar indicating that a common response to A-N3 adducts is induced by this family of drugs.

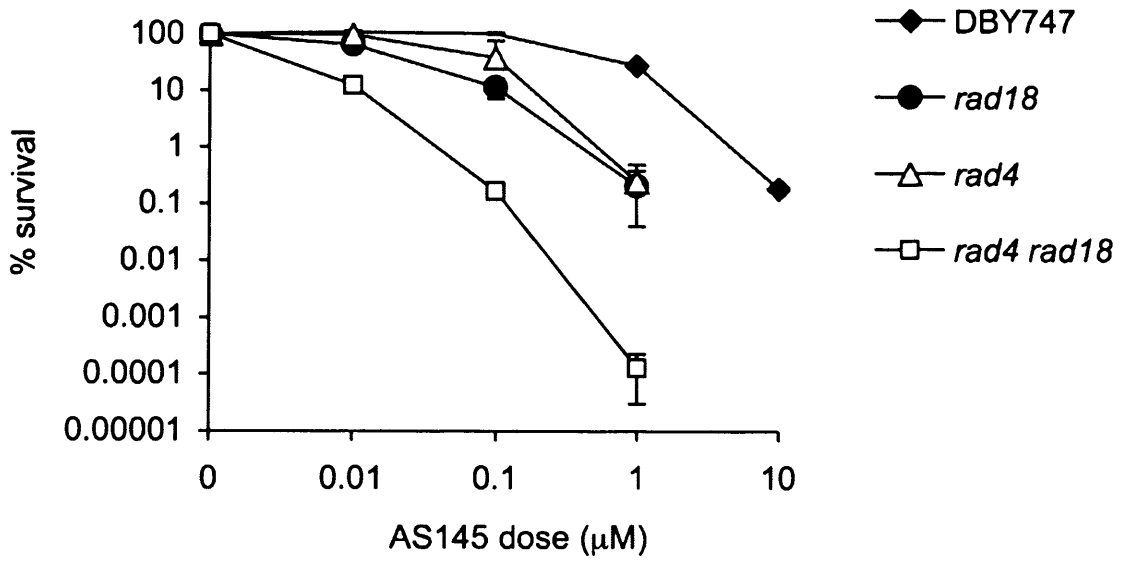

Figure 4.40 AS-I-145 sensitivity of *rad18*, *rad4*, and *rad4 rad18* cells compared with their isogenic parent (DBY747). All results shown are the mean of at least three independent experiments. The error bars represent the standard error of the mean.

The importance of the Rad18 function was previously shown to lie in the function of NER. Sslig-PCR was employed to follow the induction and repair of the AS-I-145 addducts along the the *MFA2* gene. The repair capacity of the *rad4* and the *rad18* mutants compared to their isogenic parent DBY747 was assessed using primers specific for the TS of the *MFA2*. Figure 4.41 shows the detection of the adducts by sslig-PCR, in DBY747, *rad4* and *rad18* cells. The incidence of the adducts along this region of the gene is almost identical between AS-I-145 and TH-III-151, extending our observation of their similar sequence specificity in plasmid DNA, to the cellular environment of yeast cells. It is clear that the AS-I-145 adducts are eliminated in the repair proficient parental strain, with most of the damage being repaired within 8 hours of post-treatment recovery. In contrast, no repair is observed in the *rad4* and *rad18* cells.

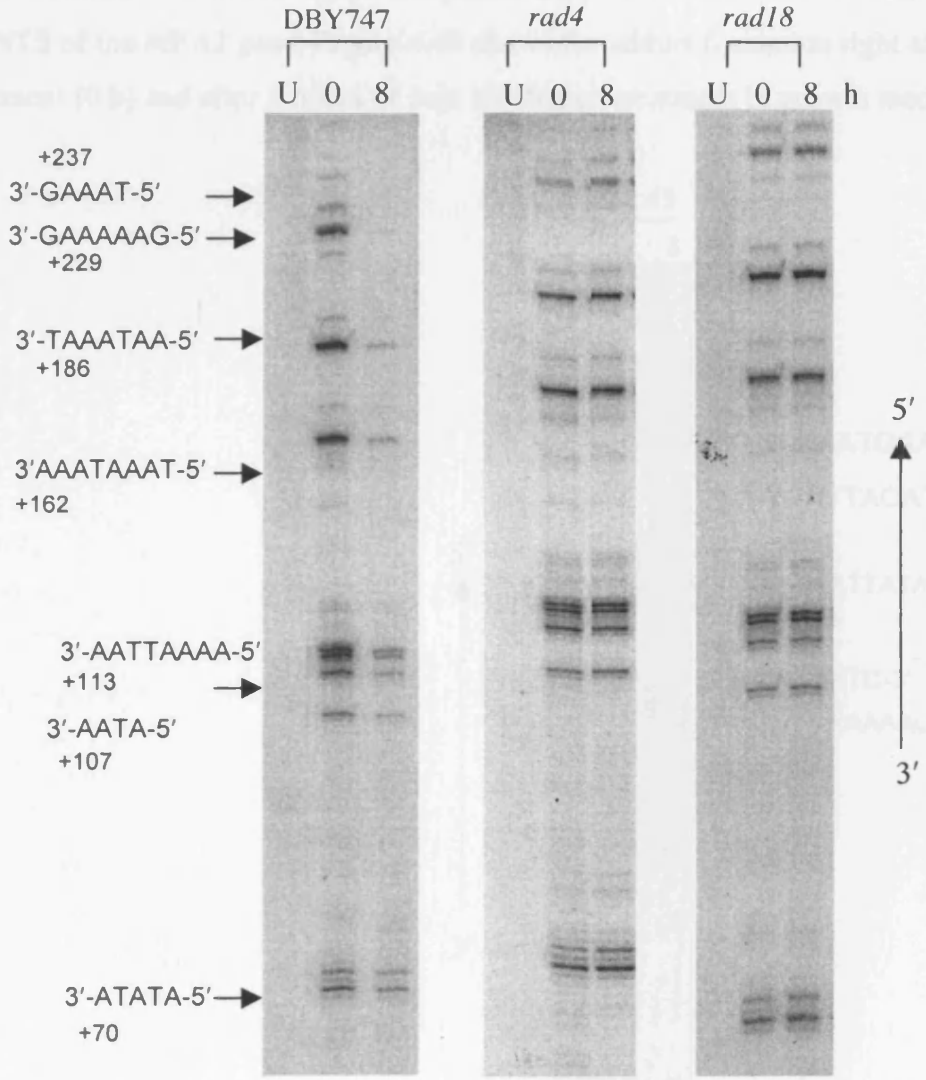

Figure 4.41 Repair of AS-I-145 adducts on the TS of *MFA2*. Exponentially growing DBY474, *rad4* and *rad18* cells were treated with 10 μM AS-I-145 for 3 h at 30 °C. Cells were harvested and DNA extracted immediately (0 h lane), or allowed to repair in YEPD for up to 8 h prior to DNA extraction. U is the untreated control. Sslig-PCR was performed as described in the Methods section. The major adducts are indicated by arrow, and their sequence and nucleotide positions in relation the start of the coding region (+1) are denoted. The sequence of the portion of the gels presented here stretches from positions +60 to +230 from the start of the gene's coding region.

Adduct elimination in the repair competent DBY747 cells, was also examined on the NTS of the *MFA2* gene. Figure 4.42 shows the adduct formation right after drug treatment (0 h) and after 8 hours of post incubation treatment in growth medium.

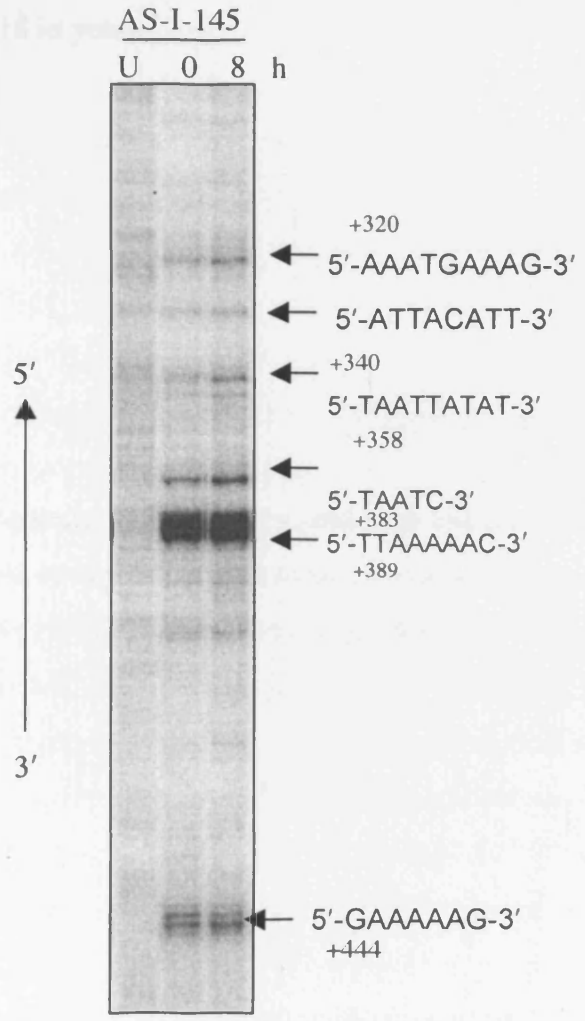

Figure 4.42 Repair of AS-I-145 adducts on the NTS of *MFA2*. Exponentially growing DBY747 cells were treated with 10 μM of AS-I-145 for 3 h at 30°C. Cells were harvested and DNA extracted immediately (0 h lane), or were resuspended in YEPD and allowed to repair for a further 2, 4, 6 and h prior to DNA extraction. Sslig-PCR was performed as described in the Methods section. The locations of the major adducts is shown by the arrows and their position in relation to the start of the coding region of *MFA2* is denoted. The sequence of the portion of the gels presented here stretches from positions 460 to 230.

No repair of any of the adducts formed along the NTS is evident. This suggests that the repair of the wild type observed in Figure 4.41 is transcription coupled.

In the case of TH-III-151 and AS-I-145, the excision event is believed to be NER, and appears to require functional Rad18 in yeast.

4.5 Discussion

The yeast repair studies of the novel chiral agent TH-III-151 and the achiral agent AS-I-145 showed that the adducts of both compounds are substrates for the NER. The NER defective *rad4* cells were sensitive to both agents (in the case of TH-III-151, the *rad14* cells also, exhibited identical levels of sensitivity as the *rad4* disruptants) and failed to eliminate the relevant adenine-N3 adducts. The observed involvement of NER is in agreement with previous repair studies on the lead compound CC-1065, which was also shown to be substrate for the NER apparatus (Gunz *et al.*, 1996; Selby & Sancar, 1988; Nazimiec *et al.*, 2001). The repair of the adducts of the two agents in the wild type, also seemed to be confined on the transcription strand of the gene tested. Such occurrence is most commonly associated with NER (Hanawalt 1989; Balajee & Bohr, 2000).

NER is proposed to be the prominent excision pathway involved in the repair of the TH-III-151 and AS-I-145 adducts. Of all the BER glycosylases tested, none was found to be more sensitive compared to the wild type, to either agent, while *mag1* mutants were proficient in eliminating the TH-III-151 lesions. These results are in agreement with previous findings suggesting that BER is not a crucial cellular response to alkylation by this class of agents. It was previously shown that the 3-methyladenine-DNA-glycosylase, the glycosylase most associated with the BER of lesions induced by alkylating agents, does not play a major role in the repair of the adenine adducts formed by CC-1065, as the introduction of the bacterial gene (*tag*) encoding this enzyme in different murine cells did not change the sensitivity of the cells to the drug (Imperatori *et al.*, 1994). Additionally, no correlation between the levels of the glycosylase and the sensitivity to CC-1065 in human cancer cell lines was found in another study (Damia *et al.*, 1996a). Finally, an adenine-N3 adduct formed by adozelesin was shown to be a substrate for the NER action of the *E.coli* endonuclease UvrABC. In sharp contrast however, the *E.coli,* 3-methyladenine glysocylase failed to excise the adozelesin lesions (Jin *et al.*, 2001).

This is the second time an interconnection of the *RAD6* pathway and NER is proposed for the repair of highly sequence specific minor groove adducts. For both agents in this study, the excision of their adducts by NER appeared to require functional Rad18. *RAD18* is a pivotal gene controlling through its interaction with *RAD6* a variety of subpathways and processes, which could be utilised following inactivation of NER, as in the case of a *rad4* mutant. Interestingly, the lack of Rad18, not only increased the sensitivity of the cells to the two compounds, but impaired the NER of their adducts. Additionally, in the case of TH-III-151, further enhancement in sensitivity and again a clear NER defect was also observed in a *rad5* strain, indicating that *RAD5* could also be involved in the proposed interplay of the Rad6-Rad18 complex with NER. An early indication that Rad5 might affect lesion excision came from a study of the kinetics of repair of UVC-induced cyclobutane dimers and 6-5 photoproducts in a large collection of yeast mutants (McCready, 1994). Both a *rad18* and a *rad5* mutant exhibited reduced capacity in eliminating both classes of adducts.

MMS2, which has been assigned to the same subpathway as *RAD5* (see section 4.1.4) was initially shown to be epistatic to *rad4* for UV response (Broomfield *et al.*, 1998). However, later epistasis analysis found a synergistic enhancement in UV sensitivity in a combination of a *rad4* and an *mms2* mutation (Torres-Ramos *et al.*, 2002). *RAD5* has been shown to be epistatic to *MMS* for UV response (Ulrich & Jentsch, 2000; Torres-Ramos *et al.*, 2002). Although the *mms2* strain is not as UV sensitive as the *rad5* strain, yet it displays a much more severe repair defect (Torres-Ramos *et al.*, 2002). The discrepancy between the sensitivities of *rad5* and *mms2* led the authors to hypothesize that Rad5 could have an additional role to that in post replication repair, and possibly promote the repair of UV lesions by participating in other processes. Additionally, such inconsistency between levels of sensitivity and repair efficiencies, also previously found for *RAD26* (Van Gool *et al.*, 1994), further supports the idea of seeking functional evidence for the role of a repair gene product, as in this thesis, though the study of the repair rates on a gene.

The findings in chapter 4 suggest that such an additional role of Rad5 could be in the NER of, in this case, the TH-III-151 minor groove lesions. Rad5 could possibly help preferentially target, through its interaction with Rad6 and Rad18, NER repair factors to the poorly "displayed" lesions of TH-III-151 in the minor groove. CC-1065 adducts have been shown to be poorly recognised by human NER factors *in vitro* (Gunz *et al.*, 1996). This is attributed to the low level of helical distortion induced by CC-1065 and the thermodynamic stabilisation of the double helix (Reynolds *et al.*, 1986). Recognition of minor groove adducts and recruitment of repair factors required for their elimination has been previously assigned to Rad18 (Brooks *et al.*, 2000). This could also be the case for both the TH-III-151 and AS-I-145 adducts. This function of Rad18 may be influenced by Rad5, (as it derives from the TH-III-151 studies), acting in the error-free subpathway, downstream of the Rad6-Rad18 complex.

CHAPTER 5

CYTOTOXICITY OF AS-I-145 IN NER DEFECTIVE CHINESE HAMSTER OVARY CELL LINES

5.1 Introduction - Aim

Chinese hamster ovary (CHO) cell lines provide a useful model mammalian system for identifying the pattern of sensitivity and understanding the mechanisms of cytotoxicity of a number of chemotherapeutic agents. Mutant cell lines with defined deficiencies in DNA repair pathways can be utilised to investigate the mechanisms involved in the repair of the adducts of a number of compounds, such as alkylating agents to which DNA repair-deficient cells often show altered sensitivity. Such studies in CHO cells have been conducted for both the minor groove binding drugs discussed in the introduction and currently in clinical trials, ET-743 (Damia *et al.*, 2001a; Takebayashi *et al.*, 2001b) and SJG-136 (Clingen *et al.*, 2005). The sensitivity of CHO cells to CC-1065, the lead compound of the analogues investigated in this thesis, has also been reported (Damia *et al.*, 1996b).

To complement the studies in yeast and further corroborate the critical role of NER in the repair of the adducts induced by the novel achiral analogue, AS-I-145, a panel of CHO cell lines (Table 5.1) with specific defects in different components of the NER apparatus was employed in cytotoxicity studies.

The aim is to investigate the relative role of various NER functional defects in the sensitivity of mammalian cells to the agent AS-I-145.

5.2 Materials and Methods

5.2.1 Materials

Cell lines and culture conditions

The cells used in this study are listed in Table 5.1. The AA8, UV23, UV42, UV61, and UV96 cell lines were obtained from Dr. M. Stefanini (Istituto di Genetica Biochimica ed Evoluzionistica, Pavia, Italy), and UV135 was purchased from the American Type Culture Collection (ATCC number CRL-1867). All cell lines were grown in T80 cm^2 tissue culture flasks (Gibco Life Technologies, UK), as a monoloayer, in F12-Ham-HEPES medium (Sigma, Poole, U.K.), supplemented with 2 mM glutamine (Sigma) and 10% foetal calf serum (FCS) (Autogenbioclear, Witshire, UK). The latter had been heat-inactivated by a 30 minutes treatment at 65°C. Cells were grown at 37°C in a 5% CO_2 humidified incubator and harvested using trypsin-EDTA 1x solution (Autogenbioclear, Witshire, UK).

Investigational compounds

AS-I-145 was kindly provided by Professor Moses Lee, Furman University, Greenville, South Carolina, USA. The drug was dissolved in DMA (Sigma) at a 10 mM stock concentration and stored at -20°C until immediately prior to use.

Materials

- 0.4% (wt/vol) SRB in 1% acetic acid.
- 10 mM Tris Base
- 10% Trichloroacetic acid (TCA)
- 1% Acetic acid
- 96-well flat-bottomed tissue culture plates (VWR International).

- Sulphorhodamine B (Sigma)

5.2.2 Methods

Sulphorhodamine B Growth Inhibition Assay

Growth inhibition was assessed using the Sulphorhodamine B (SRB) assay (Skehan *et al.*, 1990). This assay was developed as an alternative to tetrazolium assays for use in the NCI *in vitro* primary drug screen. A series of protein and biomass stains were investigated and the SRB reagent gave the best combination of stain intensity, signal-to-noise ratio, and linearity with cell number. SRB is a bright pink anionic dye that in dilute acetic acid binds electrostatically to the basic amino acids of (TCA)-fixed cells. The SRB assay also has the distinct advantage of a stable endpoint (i.e., not time-critical, in contrast to the tetrazolium assays (Boyd, 2004).

Stock cultures were trypsinised and 3 x 10^3 cells were seeded into each well of 96-well, flat-bottomed microtiter plates, in a volume of 100 µl and left to adhere overnight at 37°C. The desired concentrations of AS-I-145 were prepared in culture medium (without FCS) immediately before use. Medium in wells was removed and 100 µl of drug-medium mixture was added. Six replicates were used for each drug concentration. One solvent control lane was included in each experiment. Plates were incubated for 1 hour at 37°C. At the end of the drug treatment, the media was replaced with 200 µl of fresh complete growth medium, and the plates were further incubated for three days in a humidified incubator at 37°C with 5% CO_2. The medium in the wells was removed and 100 µl of ice-cold 10% (wt/vol) TCA was added per well, to fix the cells. The plates were then incubated at 4°C for 20 minutes and were subsequently washed four times with tap water. Cells were stained with 100 µl of 0.4% (wt/vol) SRB in 1% acetic acid, per well, to allow visualisation of cellular proteins, for 20 minutes at room temperature. Unbound dye was removed by washing five times with 1% acetic acid, and plates were left to air-

dry overnight at room temperature. The next day, the dye was solubilised by the addition of 100 µl of 10 mM Tris base into each well. Plates were left at room temperature for 20 minutes, and the optical density (OD) at 540 nm was determined using a Tecan microplate reader (Flow laboratories). Growth inhibition was expressed as the fraction of control A_{540} (surviving fraction) and calculated from the following equation: Fraction of control A_{540} = OD of drug-treated wells / OD of untreated control. The mean surviving fraction for each drug concentration with standard deviations was calculated. Dose response curves were plotted and the IC_{50} values, i.e. the drug concentration required to produce 50% of the OD of the untreated control, were determined from the respective curves. When comparing parental and mutant cell lines, the relative sensitivity was determined by the following equation:

Relative sensitivity = IC_{50} value in parent cell line / IC_{50} value in the mutant cell line.

5.3 Results and discussion

The mutant cell lines UV47 and UV96 are defective in XPF and ERCC1, respectively. These two proteins form a tight heterodimeric complex with a structure-specific endonuclease activity and are responsible for the 5' incision, 16-25 nucleotides from the damage site, during NER (Bessho *et al.* 1997; De Laat *et al.*, 1998). Similar to its yeast counterpart (Rad 1 and Rad10 proteins) XPF/ERCC1 is multifunctional, also participating in homology-dependent recombination reactions, including DNA single strand annealing (SSA) and gene targeting (Adair *et al.*, 2000; Motycka *et al.*, 2004) and in the repair of DNA interstrand crosslinks, where it is needed to release one arm of the cross-link or to remove them by recombination (De Silva *et al.*, 2002; Clingen *et al.*, 2005).

UV23 and UV42 cell lines bear mutations in the *XPB* and *XPD* gene products. The two helicases have opposite polarities (3'→5' and 5'→3', respectively) and induce localised unwinding of double-stranded DNA at the damaged regions. The two

helicases are subunits of the basal transcription factor TFIIH, which is implicated in both trancription initiation and NER (Hwang *et al*, 1996; Schaeffer *et al.*, 1994). UV135 cells are defective in XPG, a structure-specific endonuclease responsible for the initial incision step, which occurs approximately 2-9 nucleotides to the 3′ side of the damage during NER of DNA (O'Donovan *et al.*, 1994). Besides its catalytic endonuclease activity, the physical presence of XPG is also required for subsequent 5′ incision by ERCC1/XPF (Wakasugi *et al.*, 1997).

Finally the DNA repair defect in the UV61 cells is homologous to that of Cockayne's syndrome complementation group B (CSB) cells. These cells, unlike all the previous ones which have total NER deficiency, have proficient global-genome, GG-NER but deficient transcription-coupled, TC-NER (Orren *et al.*, 1996).

Figure 5.1 features a schematic representation of the human GG-NER, also showing the function of the gene products that are defective in the mutant CHO cell lines under investigation (Table 5.1). All these NER factors participate in the common steps of GC-NER and TC-NER, with the exception of CSB, which converges with CSA at the damaged sites on the transcribed strand, where RNA polymerase II becomes stalled.

Mutant cell line	**Parent cell line**	**Defective gene**
UV23	AA8	*XPB*
UV42	AA8	*XPD*
UV47	AA8	*XPF*
UV61	AA8	*CSB*
UV96	AA8	*ERCC1*
UV135	AA8	*XPG*

Table 5.1 The NER-deficient Chinese hamster cell lines used in this study.

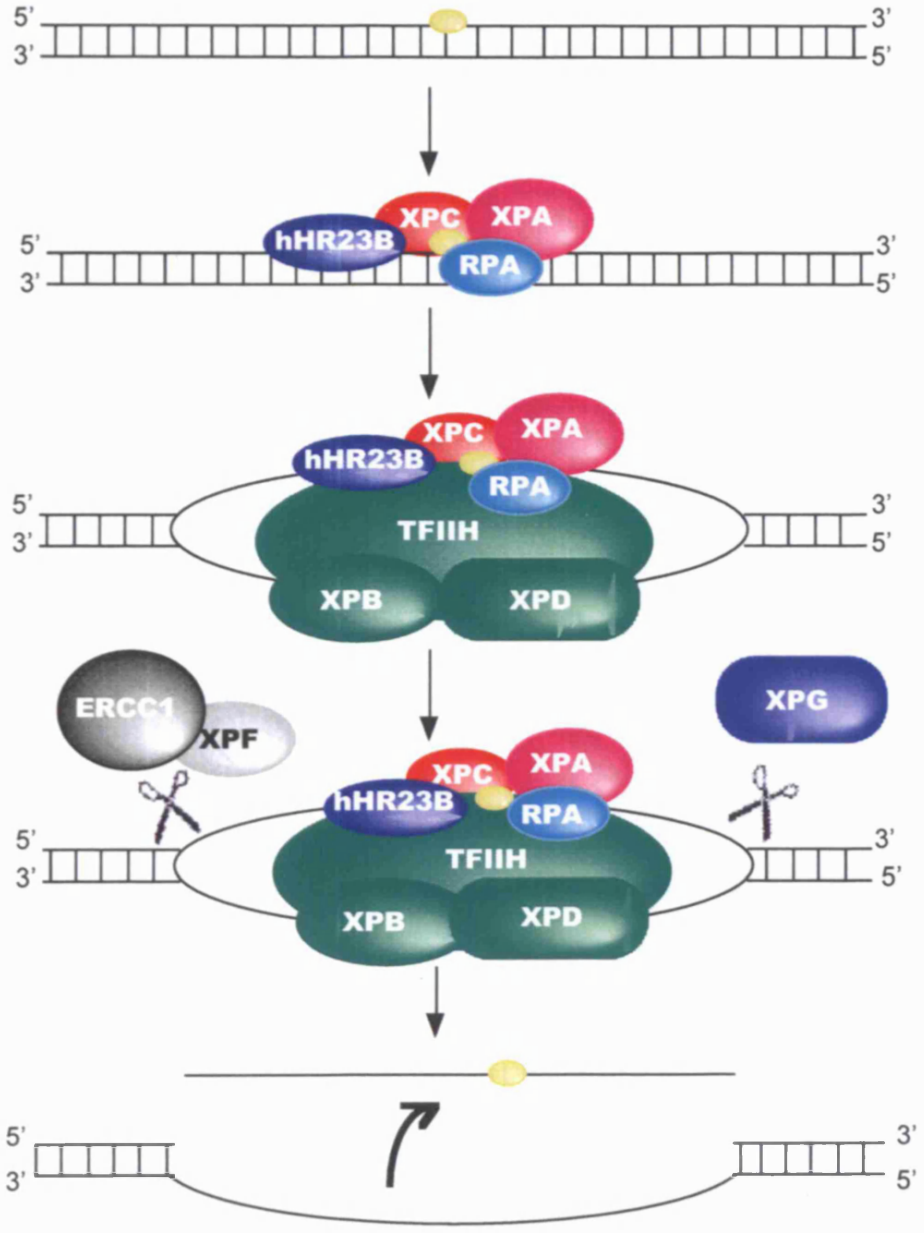

Figure 5.1 Schematic representation of the "recognition", "formation of the open structure", "dual incision and excision of the damage-containing, single-stranded oligonucleotide", steps of GG-NER in human cells. Repair is completed with DNA resynthesis (gap-filling) and ligation in the presence of DNA replication factors.

The sensitivity of the CHO cells to AS-I-145 was assessed using the SRB growth inhibition assay after a 1-hour exposure to increasing concentrations of the agent. The data presented in Figure 5.2 show the sensitivity of the wild type (AA8) and the NER defective repair mutants to AS-I-145.

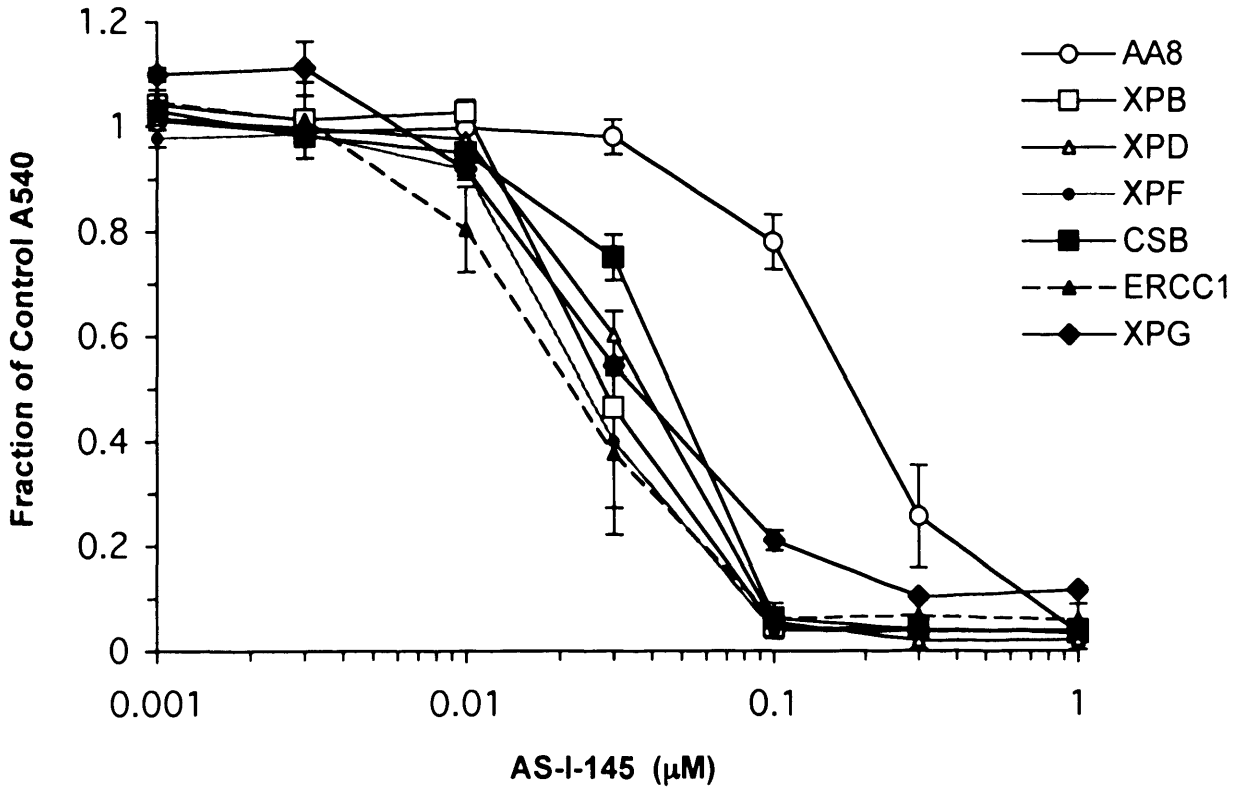

Figure 5.2 AS-I-145 sensitivity in parental AA8 cells and NER mutants XPB (UV23), XPD (UV42), XPF (UV47), CSB (UV61), ERCC1 (UV96) and XPG (UV135). Growth inhibition was determined using the SRB assay and the fraction of control A_{540} calculated as described in the Methods. All the results are the mean of at least two independent experiments and error bars show the standard error of the mean.

After treatment with the agent, all the NER deficient mutant cell lines were shown to be more sensitive to AS-I-145 than the repair proficient, parental AA8 cell line. Table 5.2 shows a comparison of the AS-I-145 IC_{50} values (concentration of drug to give an A_{540} reading of treated cells 50% of the reading of the control-untreated cells) obtained in the AA8 and the mutant cell lines. Among those, UV47 and UV96, defective in XPF and ERCC1 were the most sensitive to the cytotoxic effects of AS-I-145, with IC_{50} values 7.3- and 7.9- times lower, respectively, when compared to their isogenic parent cell line.

Cell line	Gene Defect	AS-I-145 IC_{50} (μM)	Sensitivity Ratio
AA8		0.19	
UV23	*XPB*	0.0285 ± 0.0007	6.6
UV42	*XPD*	0.036 ± 0.0056	5.3
UV47	*XPF*	0.026 ± 0.007	7.3
UV61	*CSB*	0.047 ± 0.0028	4.0
UV96	*ERCC1*	0.024 ± 0.0113	7.9
UV135	*XPG*	0.0346 ± 0.0032	5.5

Table 5.2 IC_{50} values of AS-I-145 in the CHO parental (AA8) and repair deficient mutant cell lines, as obtained by interpolation of the dose-response curves in the different cell lines. Each value is the mean ± S.D of at least two independent experiments. Numbers in the ratio column represent the fold increase in sensitivity of the mutant cell lines compared to the parental cell line AA8.

Cellular sensitivity to AS-I-145 seems to be comparably dependent to all the other components of the core NER pathway considered in this study as compromise of these NER functions confers a similar degree of chemosensitivity. This is expressed with an increase in the relative rate of sensitivities of all other repair mutant cell

lines ranging from 4 to 6.6-fold. This similar degree of sensitivities indicates an equally important role of these NER proteins in the response to the adenine-N3 lesions induced by the compound.

These results are in agreement with a previous study on the sensitivity of CHO mutants to various anticancer agents. In that case, the UV23, UV42, UV47, and UV96 cells displayed increased sensitivity (2-fold) to the minor groove alkylating agents tallimustine and CC-1065, in a colony formation assay (Damia *et al.*, 1996b).

Additionally, the implication of TC-NER in the cellular response to the AS-I-145 adducts, as suggested by the observations on the removal of the AS-I-145 adducts in the yeast studies was confirmed in this mammalian system, with a TC-NER deficiency contributing to the agent's cytotoxicity. More specifically, a 4-fold enhanced activity of AS-I-145 was observed in the UV61 cell line, defective in CSB, the Cockayne's syndrome-related factor involved in the transcriptional coupling of NER. Relevant to this result, higher efficiency of CC-1065 adduct removal and significantly faster repair in the transcribed strand than in the nontranscribed strand of the dihydrofolate reductase (*DHFR*) gene was previously observed in CHO cells. This preferential repair was attributed to transcription-coupled repair of active genes (Tang *et al.*, 1994).

The cytotoxicity profiles of the mutant cell lines emphasised the importance of the defects in NER as a determinant of chemosensitivity to the AS-I-145 adducts in mammalian cells.

CHAPTER 6

GENERAL DISCUSSION

The therapeutic area of oncology is characterised by a pressing need for new drugs, as it remains one of the most challenging medical fields for the discovery of efficient therapies. With an average of only one in nine experimental compounds making it through development and acquiring approval by the US / European regulatory authorities and an overall clinical success rate of 11%, as featured in a study of the various therapeutic areas, oncology has a successful rate of 5%, only one quarter of that of cardiovascular disease (20%) (Kola & Landis, 2004). It is indicative that the failure rate of investigational oncology compounds in phase II clinical trials is 70%, in phase III, 59% and even at the registration stage, 30% of experimental anticancer agents undergo attrition (Kola & Landis 2004). Amidst the poor results, the urgent need for new treatments is reflected in the fact that there are currently more than 550 phase I trials open to cancer patients in the United States at any given time, and this number is steadily increasing (Roberts *et al.*, 2004). According to a 2003 survey, there were 395 agents for the treatment of cancer in clinical trials, more than any other therapeutic class of medicine (Chabner & Roberts Jr, 2005; Reference therein). On the other hand, the overall objective response rate for 213 single-agent, phase I trials, involving 6474 cancer patients with solid tumours and spanning a 12-year period (1991-2002) was determined to be 3.8%, with the odds of a patient responding decreasing in the later years of the study period (1999-2002) (Roberts *et al.*, 2004).

In recent years there has been a focus shift in cancer drug discovery towards the development of targeted agents for cancer therapeutics, selectively exploiting dominant molecular aberrations between cancer and normal cells. Such efforts culminated in the discovery of imatinib mesylate (STI571, Gleevec; Novartis), an inhibitor of the tyrosine kinase BCR-ABL. The drug is currently used as a first-line therapy for chronic myeloid leukemia (CML), surpassing previous therapies,

including alkylating agents (Capdeville *et al.*, 2002). However, most tumours are characterized by multiple molecular alterations and conventional cytotoxic agents are in many instances the only therapeutic option still available.

Alkylating agents still remain at the core of several single-agent or combination chemotherapeutic regimens, despite being the oldest class of drugs introduced in the clinic for the treatment of cancer since the 1950s. Chlorambucil for example remains the preferred first-line therapy for chronic lymphocytic leukemia (CLL) (Andritsos & Khoury, 2002) and oxaliplatin for colorectal cancer (Saunders & Iveson, 2006), while alone or in combination, cisplatin is part of the standard chemotherapy for testicular germ-cell tumours (today more than 80% of men with metastatic TGCTs can be cured with cisplatin-based combination chemotherapy) (Einhorn, L.H. 2002), melphalan for multiple myeloma (MM) (Jagannath, S. 2005), cyclophosphamide for breast cancer (Kirshner *et al.*, 2004) to name but a few. Apart from the established compounds, novel alkylating agents currently emerge from the pipeline providing previously unavailable therapeutic interventions. One such recent example, the naturally derived ET-743 (Yondelis; section 1.3.3) was granted orphan drug status by the FDA for the treatment of soft tissue sarcoma in April 2005. It is the first active agent for this type of tumour in the last 25 years (Jimeno *et al.*, 2004). This drug highlights not only the potential the alkylating agents still hold, but also the continuing role that natural products have in the cancer drug discovery.

Natural products have been the source of many human therapeutics. Of the 877 small-molecule "New Chemical Entities" (NCE), introduced between 1981-2002, approximately half, (49%), were natural products, semi-synthetic analogues or synthetic compounds based on natural product pharmacophores (Newman *et al.*, 2003). More specifically, in the area of cancer and between the same time frame, 62% of the introduced small molecule, new chemical entities that are nonsynthetic, were of natural origin (Newman *et al.*, 2003).

Natural products can also serve as leads for the design of novel, synthetic, biologically active structures with potentially improved properties. A series of novel

chiral and achiral analogues of the natural products CC-1065 and the duocarmycins were presented in this thesis (Chapters 2 and 3). The alkylation properties of all analogues were determined on plasmid DNA. Sites of covalent modification were revealed using the *Taq* polymerase stop assay and purine-N3 alkylation in the minor groove was probed using the thermally-induced cleavage assay. The cytotoxicity of the agents was also determined in most cases, using the MTT assay. The objective of the alkylation studies was to determine whether the structural modifications of the analogues would have any effect on their alkylation efficiencies / sequence selectivity compared to those reported for the natural lead compounds. A recent paper highlighted the validity of such studies on naked-DNA and their importance as a valuable tool and a good approximation to the agents' properties in cells (Trzupek *et al.*, 2006). More specifically, the DNA alkylation properties of both enantiomers of DUMSA and Yatakemycin were determined on protein-free DNA and on the same sequence bound in nucleosome core particle (NCP), modeling the state of DNA in eukaryotic cells. The relative efficiencies of the agents to alkylate DNA and their sequence selectivity were shown to remain unaltered in both instances. The observed alkylation sites were the same, no unexpected sites were detected and alkylation proceeded even at the most accessible challenging sites on NCPs, unaffected by the conformational perturbations and in an identical manner to free-DNA. The NCPs packaging is a close approximation of nuclear DNA and these findings highlighted that for this class of compounds, observations on their sequence-selective alkylation deriving from studies on free-DNA could actually correlate well with their intracellular behaviour and binding *in vivo* (Trzupek *et al.*, 2006). The same has recently been demonstrated for another minor-groove agent, SJG-136. Sslig-PCR experiments showed that the agent would bind the same sites with the same degree of sequence selectivity in naked DNA and in cells (Martin *et al.*, 2005). The same assay was also previously employed to study lesion formation by alkylating agents, such as nitrogen mustards. The pattern of adduct formation by uracil and quinacrine mustards was identical in isolated DNA, in cells and to that observed earlier, in plasmid DNA (Grimaldi *et al.*, 1994; Ponti *et al.*, 1991).

The novel chiral agents presented in Chapter 2, featured either established pharmacophores like the *seco*-CI alkylating moiety coupled to varying, extended DNA binding subunits (sections 2.2 and 2.4) or incorporation of the novel pharmacophores *seco*-iso-CFI and *seco*-CFQ (section 2.3). All the analogues studied readily alkylated the high affinity CC-1065 alkylation site 5'-AAAAA-3', with variations observed for the alkylation of secondary AT sites.

The *seco*-iso-CFI indoline agent TH-III-149 and the *seco*-CFQ quinoline, TH-III-151 were assessed in the National Cancer Institute's large scale *in vitro* cell screen (Boyd, 2004). The current model of this screen uses approximately 60 human tumour cell lines representing haematologic malignancies, melanoma and cancers of the lung, colon, breast, brain, kidney, and prostate. The method uses continuous drug incubation for 48 hours and the viability of the cells is evaluated by staining cells with the protein-binding dye, sulforhodamine (SRB). The screen data are visualised with the characteristic "fingerprint" chart. The mean graph representation for the LC_{50} values, of all the cell lines responses (concentration for killing 50% of the cells) to TH-III-149 and TH-III-151 can be seen in Appendix-I (Professor M. Lee – personal communication). The two agents exhibited differential toxicity and were most active primarily against cells derived from solid tumours such as melanoma, renal and certain CNS and colon cell lines. None of the leukemic cell lines included in the screen exhibited increased sensitivity to either of the agents.

Both compounds then advanced to preliminary *in vivo* assessment of their potential anticancer activity based on the hollow fibre assay (Hollingshead *et al.*, 2004). TH-III-149 received an IP (referring to hollow fibres implanted intraperitoneally) score of 14 and an SC (hollow fibres implanted subcutaneously) score of 4, resulting to a total score of 18. TH-III-151 received an IP score of 16 and an SC score of 4, acquiring a total score of 20. Both agents were found to be capable of producing cell kill (Professor M. Lee – personal communication). The criteria for further *in vivo* evaluation of an experimental agent subjected to the hollow fibre assay are a minimum combined IP + SC score of 20, a SC score 8 or a net cell kill of one or more cell lines. Finally the cytotoxicity of TH-III-159 and TH-III-151 to murine

bone marrow cells was assessed using a commercially available colony-forming assay (StemCell technologies, Inc., Vancouver, Canada). While TH-III-149 was found to be toxic (no colonies), TH-III-151 displayed significantly less toxicity (45 ± 10 colonies, compared to 60 ± 3 colonies for untreated control) (Professor M. Lee – personal communication).

The favourable activity against tumour cell lines, the "active" status based on the hollow fibre assessment and the low toxicity to murine bone marrow cells render, primarily TH-III-151, a worthy candidate for further drug development studies. These results underline the potential of structurally modifying the alkylation subunit of the lead compounds. The introduction therefore of the furan ring with a new orientation in the case of TH-III-149 and the unique *seco*-CFQ warhead of TH-III-151 which was an "unexpected" product, derived from the rearrangement of the intermediate permitted by the reaction kinetics during synthesis, generated active compounds with anti-cancer activity. These novel alkylating functionalities may serve as valid alternatives to the established CBI pharmacophore.

In the quest for improved antitumour agents a series of novel achiral analogues was also assessed for their alkylation properties and cytotoxicity (Chapter 3). The introduction of an achiral pharmacophore was a strategy that was not extensively pursued in the past. Chirality has now emerged as a central issue in drug design and development. A clear trend for the development of enatiomerically-pure compounds over racemates, which dominated previous decades, was gradually established due to a better appreciation of stereoselective pharmacology and the differential relative contributions of each enantiomer to the overall drug action. Single-enantiomer drugs now comprise ~75% of the new drugs that are introduced to the market, rising from ~25% ten years ago (Agranat *et al.*, 2002). This trend however does not preclude the development of achiral agents. The advantages of the design of achiral compounds over racemates was discussed in the introduction. Of the new molecular entitites approved in the U.S between 1998-2001, 52% were achiral, 30% single enantiomers with several chiral centres, 7% single enantiomers with one chiral centre, 7% racemates and 4% multiple diastereomers. The corresponding

distribution for the NCEs approved in the UK, between 1996-2000 is: 36% achiral, 48% single enantiomers and 16% racemates (Agranat *et al.*, 2002 and references therein).

Embarking on the design of achiral agents it was initially imperative to determine whether the chiral centre present in all CC-1065 / duocarmycin analogues reported in the literature and in this thesis, was absolutely required for DNA interaction and cytotoxicity. The "first generation" of achiral analogues, incorporating the achiral *seco*-hydroxy-CI and *seco*-amino-CI alkylation subunits (section 3.2) were shown to be able to efficiently perform the characteristic adenine-N3 alkylation of the lead compounds.

The achiral *seco*-hydroxy-CI-TMI compound SC-III-147 (Figure 3.5) was submitted for testing in the NCI 60 cell line screen. The agent exhibited activity in the micromolar range while the screening profile manifested differential cytotoxicity. Again none of the leukaemia cell lines included in the assay were found to be more sensitive than the average sensitivity of the full 60-cell panel (Appendix-II). In sharp contrast, all the melanoma cells exhibited increased sensitivity to SC-III-147. The agent was selected for preliminary *in vivo* testing with the hollow fibre assay. The composite IP and SC score was 22, however no cell kill was observed. Based on the combined score being > 20 and its unique achiral structure, the compound advanced for further *in vivo* testing using human tumour xenografts. The tumour model tested was the human UACC-257 melanoma. SC-III-147 treatments were initiated on day 16 after implantation, at the maximum tolerated dose of 134 mg/kg/dose and administered IP. Therapeutic results from the experiments are presented in terms of increases in lifespan reflected by the median survival times of treated (T) versus control (C) groups of mice (%T/C) and any long term survivors (> 60 days). The T/C value at day 51 was 40, which according to the NCI's evaluation criteria, renders SC-III-147 an "active" compound (Alley *et al.*, 2004). At the dose administered to the animals, no significant weight loss was observed, indicating that the compound was relatively non-toxic (Professor M. Lee, personal communication).

Compounds incorporating the achiral *seco*-hydroxy-CBI and *seco*-amino-CBI alkylating moieties were also able to efficiently alkylate in the cluster of the five adenines and did so with enhanced efficiency compared to their achiral-CI counterparts (section 3.3). The achiral *seco*-amino-CBI-TMI compound, AS-I-145 (Figure 3.11) was also submitted for *in vitro* cytotoxicity testing at the NCI 60-cell screen. The agent exhibited activity in the sub-micromolar range and similarly to the sensitivity profiles obtained for the previous compounds tested, AS-I-145 was not particularly active against leukemic cells but showed differential activity against certain cell lines from solid tumours including melanoma, lung, colon, renal, breast and CNS (Appendix-III).

AS-I-145 was subsequently accepted for *in vivo* anticancer activity assessment by the NCI standard hollow fibre assay. It received an IP score of 46 and an SC score of 8, resulting to a total score of 54 (out of a possible 96). These results render AS-I-145 one of the most active compounds (top 5%) tested in this assay to date. This is particularly important as of the compounds tested up until 2004, only 16.3% had a total score of 20 or greater (Hollingshead *et al.*, 2004). Such level of activity guaranteed further *in vivo* evaluation of the agent. Tumour xenograft studies involved a model of the advanced stage human SC-OVCAR-3 ovarian cancer and were carried by the NCI. Drug treatments of 11.20 mg/kg, IP were able to inhibit the growth of the tumour cells, providing a % T/C value of 24% on day 33. The mean time for doubling of the tumour weight was 25.3 days, compared to 13 days for the control untreated animals. According to the NCI evaluation criteria, this result deems AS-I-145 as an active compound. Importantly, the treated animals did not experience any toxicity or weight loss, indicating that the agent is well tolerated. This compound is significantly less toxic than its chiral counterparts including the clinically investigated adozelesin, which was found to be toxic at a dose of 1 mg/kg. Further *in vivo* studies on the B16-F0 murine melanoma cells, and the MDA-MB-435, human breast cancer xenograft, were conducted by Taiho Pharmaceutical Co., Ltd, Japan. AS-I-145 exhibited significant activity when administered IP (15 mg/kg) without toxicity and was also active when administered orally. Finally, the

toxicity of AS-I-145 against hematopoietic progenitor cells was assessed. Bone marrow cells were taken from the fermus of healthy mice that had not been previously treated with the agent. The cells were then treated with equal concentrations (0.0084 μM, the IC_{50} value of the racemic *seco*-hydroxy-CBI-TMI against L1210 cells, for a 3-days continuous exposure) of AS-I-145 and *seco*-hydroxy-CBI-TMI. No colonies were observed for the chiral agent. However, AS-I-145 was less toxic, allowing formation of colonies (25 versus 0, respectively; untreated control gave 60 colonies) (Professor M. Lee – personal communication).

The results of the studies on the achiral agents revealed that the chiral centre of CC-1065 and the duocarmycins is not absolutely required for DNA sequence specific interaction and anticancer activity. The achiral *seco*-amino / hydroxy-CBI and CI alkylating moieties constitute therefore feasible substitutes to the established chiral pharmacophores and offer a template for alternative drug design of novel analogues.

TH-III-151 incorporating the novel *seco*-CFQ warhead and AS-I-145, one of the most active compounds ever tested in the NCI *in vitro* screen and representing the novel class of achiral analogues, were chosen for DNA repair studies.

In the yeast *Saccharomyces cerevisiae*, nucleotide excision repair is the predominant pathway for the repair of the adenine-N3 adducts of both TH-III-151 and AS-I-145, which seem to share common mechanisms of cytotoxicity despite their different stereochemistry (Chapter 4). This excision repair was in both instances transcription coupled and appeared to depend upon functional Rad18. The role of Rad18 as a potential sensor of damage by this class of compounds and its function as a prerequisite for the elimination of the relevant adducts by NER, render Rad18 a key determinant of chemosensitivity to these agents. Studies in mammalian cells, also revealed a role of NER in the repair of AS-I-145 induced damage, judged by the increased sensitivity of a panel of NER deficient CHO cell lines compared to the repair proficient wild type (Chapter 5).

A reported potential determinant of chemosensitivity to the CC-1065/duocarmycins class of compounds is the cellular protein, named duocarmycin-DNA adduct

recognising protein (DARP) (Asai *et al.*, 1999). This protein of an estimated molecular weight ~ 60 kDa was present in nuclear extracts from human cervical carcinoma HeLa S3 cells. DARP was detected through gel mobility shift assays, shown to bind with increased affinity to DUMSA modified DNA and was subsequently partially purified. Apart from DUMSA, DARP was also shown to be capable of recognising the DNA adduct of the structurally related CC-1065 and that of anthramycin, another potent minor groove binder, but did not recognised damage induced by major groove binding drugs such cisplatin (Asai *et al.*, 1999). The selective interaction of DARP with DNA adducts generated only by certain minor groove agents was attributed to the protein's ability to recognise the altered structure of DNA upon modification by these drugs, and particularly the induced bend toward the minor groove, a characteristic shared by these specific agents. Despite the lack of further molecular and functional characterisation, it was initially suggested that DARP could be one of the components involved in the nucleotide excision repair pathway, as CC-1065 adducts are known NER substrates (Asai *et al.*, 1999).

Human Rad18 gene encodes for a protein of an expected size of 56 kDa. Use of the commercially available RAD18 antibody in a western blot, detects a band of ~ 60 kDa (Abcam plc, Cambridge, UK).

DARP also appeared to be different from another protein of ~100 kDa, previously identified to recognise DNA damage induced specifically by AT-specific, minor groove binding agents such as distamycin, Hoechst 33258 and CC-1065 (Colela *et al.*, 1996). Since DARP's specificity was restricted only to a certain chemotype of minor groove drugs, it presented a potential factor that might selectively modulate the antitumour activity of the CC-1065/duocarmycin class of compounds in tumour cells. The protein was eventually further purified and sequenced by the same group (Taguchi *et al.*, 2004). DARP was once again detected by its ability to bind to DUMSA-DNA adduct in gel shift assays. Three partial amino acid sequences were obtained which were found to completely match parts of the predicted human heterogenous nuclear ribonucleoprotein L (hnRNP L), thus rendering hnRNP L a

candidate for DARP's described activity. There are approximately 20 major members of the hnRNP family and participate in a variety of processes involving RNA, including transcription, splicing, processing, translation etc. High expression of some of these proteins has been reported in several human malignancies like lung and breast cancer. Differential intracellular localisation of hnRNP L was demonstrated among human lung cancer cell lines. Transfectants of hnRNP L possessed increased sensitivity to the growth inhibitory effect of KW-2189, a duocarmycin derivative. hnRNP L therefore enhances cell sensitivity to a member of the CC-1065/duocarmycin class of compounds while no difference in sensitivity was observed to cisplatin and mitomycin C (Taguchi *et al.*, 2004). Similarly DARP had not been able to recognise the DNA adducts of those two major groove agents in the initial study (Asai *et al.* 1999). These observations suggest that DARP could be hnRNP L. Critically however, the use of anti-hnRNP L antibody failed to produce a supershift of the retardation complex of DUMSA modified DNA in a gel mobility shift assay.

TH-III-151 and AS-I-145 coulbe be used to damage the oligonucleotide used by Asai *et al.* This modified template can be subsequently used for gel mobility shift assays to detect a possible hRad18 binding manifested as a retarded band corresponding to the hRad18/DNA complex. The use of the commercially available hRad18 antibody would result in a band of even lower mobility ("supershift") at the expense of the original retarded band. That would indicate binding of the complex by the antibody and would unambiguously confirm the binding of hRad18 to the damaged DNA probe. This method could help further establish the notion of hRad18 as a damage recognition factor of minor groove agents and assign hRad18 as another possible candidate for the DARP activity.

The identification of the key pathways involved in the repair of DNA damage induced by chemotherapeutic agents is important for understanding the ability of cancer cells to recognize damage and initiate DNA repair and in some cases explaining mechanisms of therapeutic resistance. At the same time, these pathways

constitute potential sites for intervention, which could enhance the efficacy of DNA damaging agents. The resistance phenotype for example, of a series of cisplatin-resistant, human ovarian cancer cell lines was shown to be due to overexpression of NER associated proteins, in particular ERCC1, resulting in increased DNA adduct removal (Ferry *et al.*, 2000). NER, the main pathway responsible for the removal of cisplatin damage and ERCC1 in particular, the NER component correlated with resistance, were subsequently "targeted" in an attempt to sensitise the resistant ovarian cell lines to the cytotoxic effects of cisplatin. Disturbing the NER in those cells by perturbing levels of ERCC1 resulted in enhanced cisplatin cytotoxicity up to 8.1-fold, in the cell lines under investigation (Selvakumaran *et al.*, 2003). Another way of modulating DNA repair is through pharmacological intervention. A small molecule inhibitor of vascular endothelial growth factor, SU5416 was shown to downregulate DNA repair activity by reducing the expression of ERCC1 and enhancing cisplatin cytotoxicity up to 5.5-fold, in resistant human ovarian cancer cells (Zhong *et al.*, 2003).

The repair studies of TH-III-151 and AS-I-145 revealed that Rad18 has a special role in the function of the NER of the minor groove adducts induced by the two agents. In light of the above examples where DNA repair inhibition is used as a means for modulating chemosensitivity, this Rad18 function described in this thesis could be further exploited as an alternative way of impairing NER. Instead of directly targeting an NER component, as described above for ERCC1 and cisplatin sensitivity, NER could be modulated by targeting Rad18, for agents like TH-III-151 and AS-I-145. Our observations for the moment are restricted in yeast. The role of mammalian *RAD18* and its possible involvement in the mammalian NER of the adducts of this class of minor groove agents should be also investigated. Imbalances in the levels of hRad18 exist in many tumours and could lead to changes in drug sensitivity. *hRAD18*, the human homologue of the yeast *RAD18* maps on chromosome 3p24-25, where deletions are often found in lung, breast, ovary and testis cancers (Tateishi *et al.*, 2000). As with their yeast counterparts, hRad18 has been shown to physically associate *in vivo* with hHR6A/hHR6B (*hHR6A* and

hHR6B being the human homologues of the yeast *RAD6* gene (Tateishi *et al.*, 2000). Human breast cancer cells engineered to overexpress *hHR6B* were shown to be resistant to the cytotoxic effects of cisplatin. In contrast, cells depleted of this protein exhibited increased sensitivity (Lyakhovich & Shekhar, 2004). Cells could be sensitized *in vitro* by the employment of *RAD18* antisense RNA to downregulate the levels of hRad18. It would be interesting to assess the extent of the NER of minor groove adducts, in hHR6B or hRad18 depleted cells. Would an NER defect be observed in such cells as it was in yeast for TH-III-151, AS-I-145 and BAM-Py_3 induced, sequence specific lesions? (Brooks *et al.*, 2000; this thesis). Deficiency of the human cells to excise the adenine-N3 adducts when *hRAD18* is silenced would confirm the involvement of hRad18 in the NER of these adducts. It is important to also investigate any correlation in the levels of Rad18 expression in various tumour types with the sensitivity to the above-mentioned agents and the extent and efficiency of NER. If such a correlation is established, it could be used as a predictive tool for susceptibility of specific tumours to drug toxicity. It is conceivable that altered levels of hRad18 or hRad6, either occurring constitutively in certain cancers, as mentioned above, or resulting through modulatation (e.g. by the identification and use of a small molecule inhibitor) could cause cancer cells to be impacted more, by such DNA damaging agents, through crippling their NER capacity. This would be most important in cases of resistance emerging due to enhanced activity of NER, where the toxic effects of agents are neutralized.

hRad18's possible requirement in mammalian NER and particularly its implication in the early, recognition steps of NER and subsequent recruitment of NER proteins could be, as mentioned above, an attractive target for pharmacological intervention. Block or disruption of the of hRad18-DNA interaction through interference with hRad18's ability to bind DNA, will ultimately interfere with DNA repair and help manipulate cellular sensitivity to TH-III-151 and AS-I-145. In a similar attempt, a high-throughput screen for the identification of inhibitors of replication protein A, RPA's binding to DNA was described by Andrews & Turchi in 2004. From 2000 pure and synthetic products provided by the structural diversity set of the NCI, their

fluorescence-based screen identified 79 compounds as potential inhibitors. Of those, 9 were further validated with gel mobility shift assays and an *in vitro* NER incision assay employing site-directed cisplatin adducts and were shown to efficiently inhibit RPA's binding to DNA (Andrews & Turchi, 2004).

In chapter 4, it was shown that *rad6* cells were as disabled as *rad18* in the elimination of the TH-III-151 damage, suggesting that it is the inactivation of the Rad18-Rad6 complex that impairs the NER of these adducts and is not a phenomenon only limited to Rad18. The interaction of the two proteins presents another potential site for intervention that could ultimately impair NER, once established that hRad18 / hRad6 are required for the NER removal of TH-III-151 / AS-I-145 adducts in mammalian cells. In an analogous manner, it has been previously shown that reduction between the binding of ERCC1 to XPA in cell extracts, induced by the agent UCN-01, caused reduction of the amount of the NER incision and therefore suppression of the NER of cisplatin-induced lesions (Jiang & Yang, 1999). Such interventions however have to be vigorously tested for safety and efficacy validation, ensuring that the desired therapeutic phenotype does not occur with other off-target activities. Rad6 for example in yeast is a pleiotropic protein involved in many cellular functions, unlike Rad18, which plays no known additional role in cellular metabolism (Bailly *et al.*, 1994). Deletion of *hRAD6 (hHR6A* and *hHR6B)* showed that the gene is "necessary but not central" to normal human breast cell profileration and growth. Cells lacking hRad6 failed to plate down and proliferate effectively while cells expressing low amounts of hRad6 retained ability of those functions (Lyakovich & Shekhar, 2004). Such implications must be addressed when considering the feasibily of developing dual therapies consisting of agents, which would interfere with relevant repair pathways and potentiate the efficacy of specific DNA damaging drugs.

The natural anti-tumour compound illudin S and its semisynthetic derivative irofulven (MGI-114, 6-hydroxymethylacylfulvene, HMAF; NSC 683863) both belong in the family of illudins. Although the exact mechanism of action of the two

agents has not been elucidated, their capacity to bind covalently to DNA and proteins, characterise them as alkylating agents (Herzig *et al.*, 1999). Radioactive irofulven in particular, was shown to bind to intracellular DNA in a non-reversible manner while the lack of bifunctional lesions led to the further characterisation of irofulven as a monofunctional alkylating agent (Woynarowski *et al.*, 1997). The two agents have been shown to induce DNA damage processed by NER in human fibroblasts. CS-A and CS-B cells with a selective defect in TC-NER were also sensitive to the drugs, at levels similar to the XP mutants, suggesting that illudin / irofulven cell survival depends on TC-NER. Additionally no increased sensitivity to a BER mutant CHO cell line was observed suggesting that BER does not play a crucial role in the processing of the adducts. Finally, RAD18-deficient chicken lympoma cells were hypersensitive to illudin S while absence of polymerase η (RAD30A) in XP-variant fibroblasts did not affect illudin toxicity (Jaspers *et al.*, 2002). NER as a crucial factor in the cellular sensitivity to irofulven was further confirmed in a later study, where human NER-deficient cells showed increased sensitivity to the cytotoxic effects of the drug e.g. 30-fold in the case of XPA cells, 20-fold in XPB and XPD and > 10 in CS cells, compared to NER-proficient cells (Koeppel *et al.*, 2004). The susceptibility to NER deficiency, the involvement of TC-NER and the sensitisation in RAD18 mutants comprise a repair pattern reminiscent of the findings in yeast for TH-III-151 and AS-I-145, as described in chapter 4.

Irofulven exhibits activity *in vitro* towards a panel of human carcinoma cell lines. The cytotoxic effect of irofulven was most pronounced toward non-small cell lung and ovarian carcinomas while also showing potent activity toward malignant glioma cells. In contrast, limited activity was observed against leukemia cell lines. These findings correlated well with the results obtained for the same cell lines at the NCI 60 cell line screen (Poindessous *et al.*, 2003). Irofulven has been investigated in several clinical trials including phase I (Bomgaars *et al.*, 2006) and phase II (Seiden *et al.*, 2006) for pediatric solid tumours and ovarian cancer, respectively. Currently, irofulven remains in various phase II clinical trials against a wide variety of solid

tumors and has demonstrated activity in ovarian, prostate, gastrointestinal, and non-small cell lung cancer (Paci *et al.*, 2006; references therein). Again the preferential activity of irofulven against solid tumours over leukemias is reminiscent of the sensitivity patterns obtained for TH-III-151 and AS-I-145 in the NCI *in vitro* screen (Appendix-I, III).

The reported involvement of the same mechanisms for the repair of the respective adducts and the similar tissue specific sensitivities suggests that irofulven and TH-III-151/AS-I-145 could elicit similar cellular responses. The full characterization of the DNA interaction of irofulven is however required to extrapolate further conclusions. The observation in one of the early studies, of (partial) inhibition of *Taq* Polymerase extension on a DNA template isolated from irofulven-treated cells (Woynarowski *et al.*, 1997), along with the reported interaction of irofulven with calf-thymus DNA (Herzig *et al.*, 1999) suggests that the *Taq* Polymerase stop assay could initially be a useful technique to gain more insight in the sequence specificity of the interaction of the agent with DNA. Finally, the COMPARE program based on the sensitivity profiles to the agents of the cells at the NCI 60-line screen could be also used to determine the correlation coefficient between the two classes of agents. Such comparison could provide more insight to a possible common mechanism of action.

The National Cancer Institute estimates that approximately 10.1 million Americans with a history of cancer were alive in January 2002. Some of these individuals were cancer-free, while other still had evidence of cancer and may have been undergoing treatment. The 5-year survival rate for all cancers diagnosed between 1995 and 2001 is 65%, up from 50% in 1974-1976. This improvement is largely due to advances in detection and new and/or improved treatments. While these have helped some developed nations lower incidence and improve survival rate for certain cancers, for most parts of the world cancer is a growing problem. Cancer killed 6.7 million people around the world in 2002 and this figure is expected to rise to 10.3 million in 2020 (World cancer report – World Health Organisation).

Despite increased cure rates for certain cancer types and survival improvements, routine cure or long term management of cancer as a chronic disease remain elusive with treatment options for cancer patients still being marginal for most cancer types. The need for the development of new therapeutic compounds with improved antitumour activity and decreased clinical toxicity remains persistent and demanding. In the current, postgenomic era, there has been a transition in drug development from cytotoxic drugs to targeted therapies. However, the same principles that have hampered the "cytotoxic era" like variations of response due to tumour heterogeneity, tumour relapse and eventual development of therapy resistance seem to also pertain the targeted strategies. Combination therapies are therefore one alternative for a more efficient tumour eradication. Studies have demonstrated synergy between targeted molecules and traditional chemotherapy. Gleevec for example synergistically sensitizes CLL cells to chlorambucil, from 2 to 20 fold (Aloyz *et al.*, 2005). A synergistic interaction between Gleevec and cisplatin has also been demonstrated *in vitro* in adenoic cystic carcinoma and squamous cell carcinoma of the head and neck (HNSCC) (Bruce *et al.*, 2005). Concurrent administration of Gleevec and chemotherapy has finally been shown to have a greater antileukemic effect in patients with acute lymphoblastic leukemia (ALL) (Wassman *et al.*, 2006).

The potent toxicities of existing DNA-reactive agents can result in an immediate reduction in tumour burden and this can be a prerequisite for optimal results of newer sophisticated targeted therapies. Such a setting of minimal residual disease achieved with standard chemotherapy has been suggested to be the best strategy for the use of telomerase inhibitors. In that way, it is believed that rare cancer stem cells, a possible source of chemoresistance, which also happen to be telomerase-positive, are best targeted by use of combination regimens (Shay & Wright, 2006). Conventional cytotoxics, like the alkylating agents will therefore still hold a place in the cancer therapeutic regimens for the years to come.

As part of a long lasting programme of rational drug design, this thesis presented a series of novel chiral and achiral analogues of the natural products CC-1065 and the duocarmycins. A new platform for the development of active analogues is provided and could be exploited in various synthetic schemes in the future. Compounds like ET-743 and irofulven have been associated with what could be a "resurgence for alkylating therapy in cancer" (Dent & Grant, 2004). The achiral design can therefore become a new paradigm and a new focus in further exploiting nature's lead compounds CC-1065/duocarmycins and maintaining their relevance in today's drug development. The identification on the other hand of key cellular determinants that are implicated in the DNA damage response can explain susceptibility to drug toxicity and provide leads for the modulation of the drug response.

APPENDIX

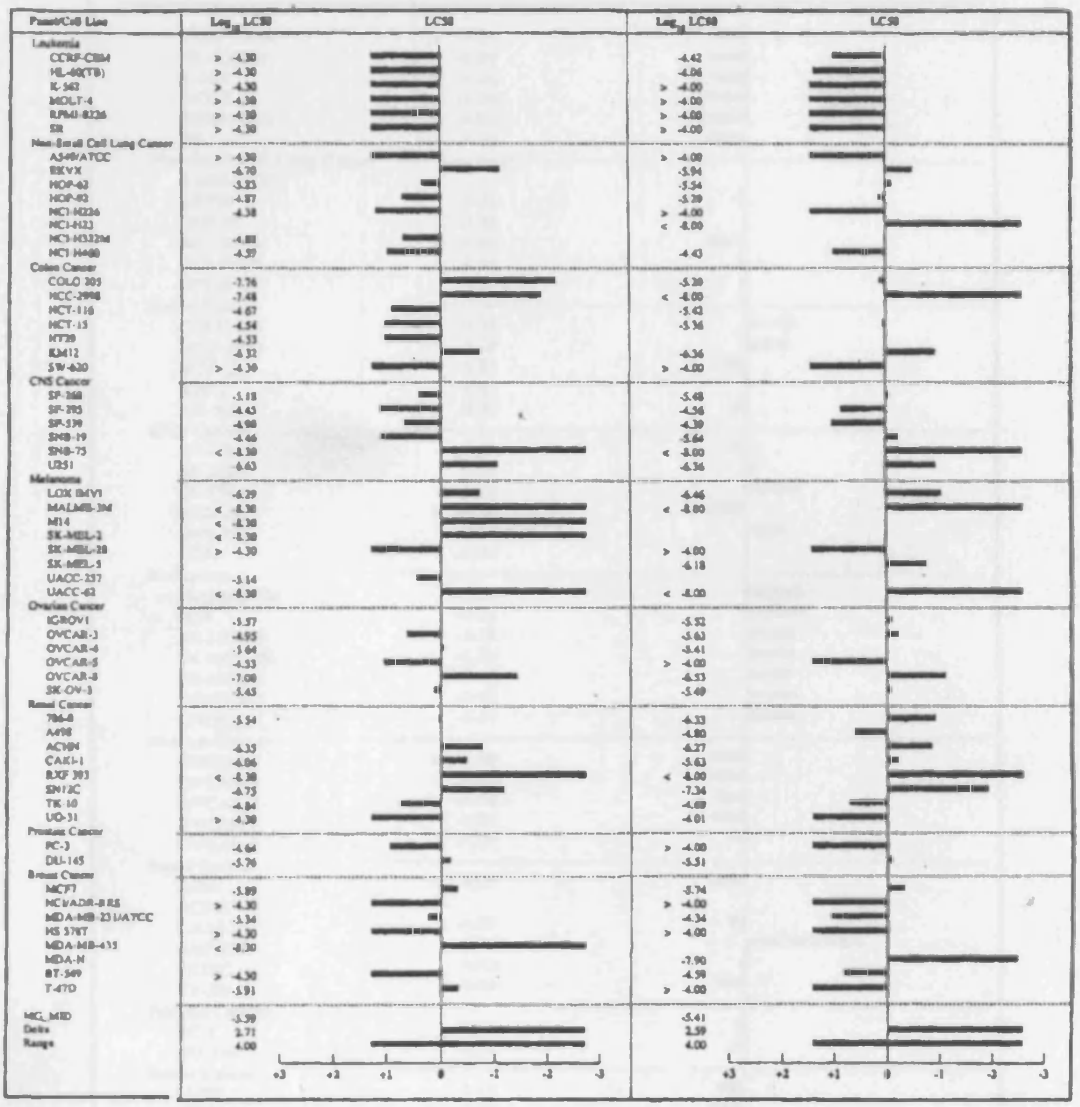

I. NCI mean graph (log LC_{50} values) of the 60 human tumour cell line anticancer drug screen for compounds TH-III-149 (left) and TH-III-151 (right). The testing of an agent in the 60-cell line screen generates a corresponding set of 60 dose response curves. The screening data are then respresented as a "mean graph" in which a mean of the logarithms of the concentrations of the agent under investigation, that produces a particular level of response (in this case LC_{50}, 50% cytotoxicity) for all the cell lines in the screen, forms an anchor point for this graphic representation. The individual response of each cell line to the agent is then depicted by horizontal bars, that extend from the average sensitivity (represented by the central vertical line), either to the right or to the left of the mean, depending on whether the response of the cell line is either more or less sensitive than the average response. The length of each bar is proportional to the relative sensitivity compared with the mean determination.

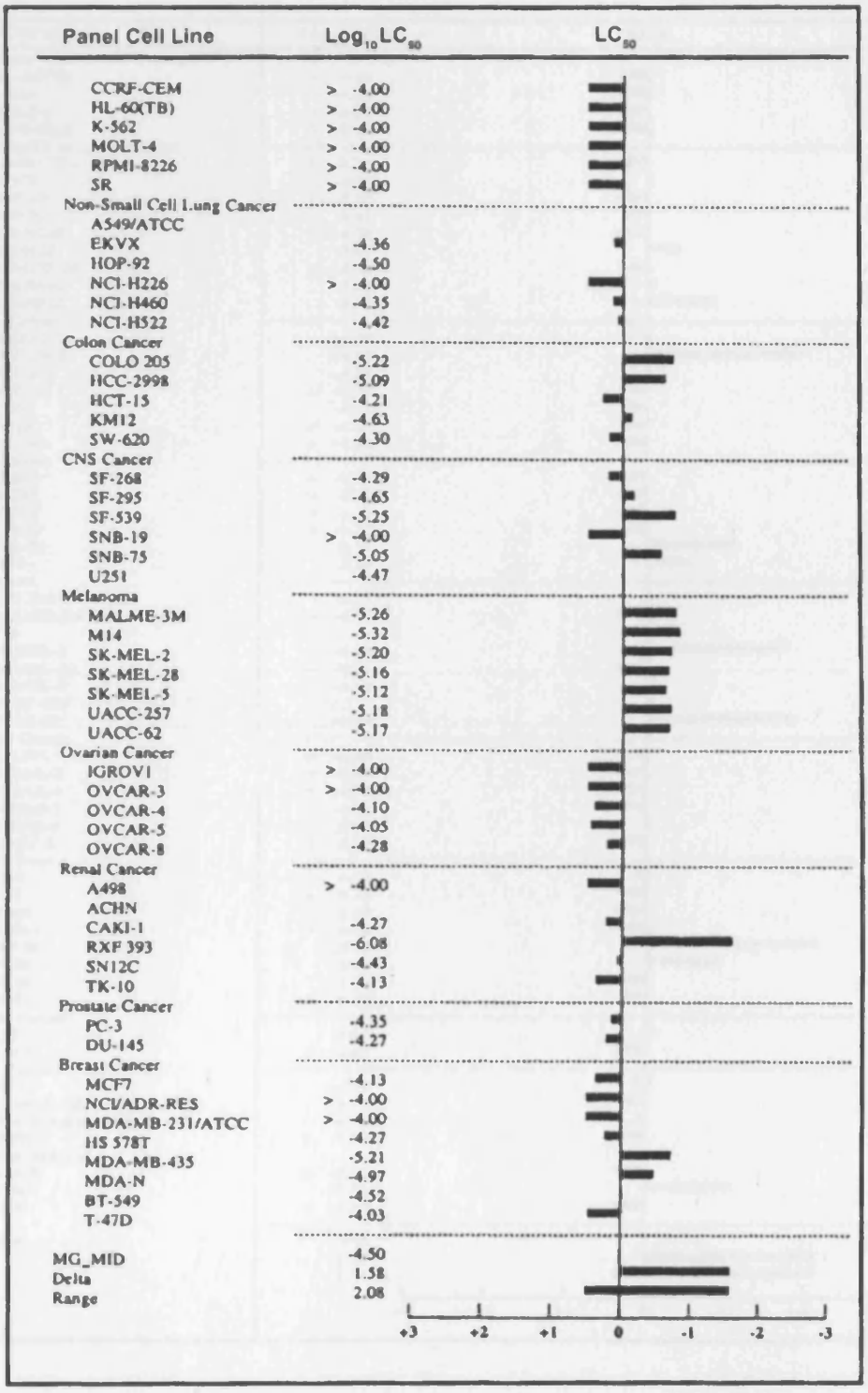

II. NCI mean graph (log LC_{50} values) of the 60 human tumour cell line anticancer drug screen for compound SC-III-147.

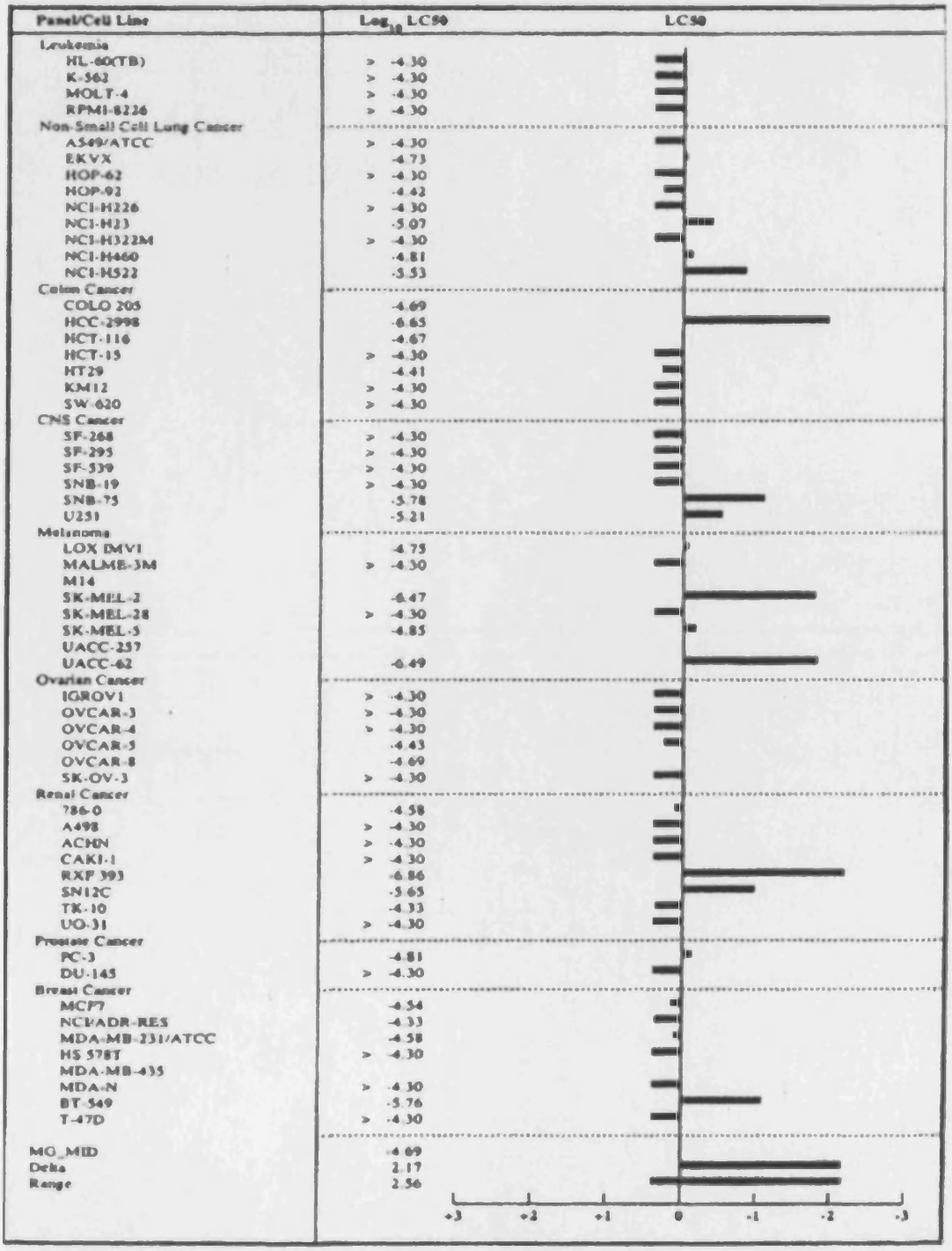

III. NCI mean graph (log LC_{50} values) of the 60 human tumour cell line anticancer drug screen for compound AS-I-145.

REFERENCES

Adair, G.M., Roling, R.L., Moore-Fever, D., Zabelshansky, M., Wilson, J.H. & Nairn, R.S. **2000** Role of the ERCC1 in removal of long non-homologous tails during targeted homologous recombination. *EMBO J.* **19**, 5552-5561.

Adams, E.G., Badiner, G.J. & Bhuyan, B.K. **1988** Effects of U-71,184 and several other CC-1065 analogues on cell survival and cell cycle of Chinese Hamster Ovary Cells. *Cancer Res.* **48**, 109-116.

Afonina, I., Zivarts, M., Kutyavin, I., Lukhtanov, E., Gamper, H. & Meyer, R.B. **1997** Efficient priming of PCR with short oligonucleotides conjugated to a minor groove binder. *Nucleic Acids Res.* **25** (13), 2657-2660.

Agranat, I., Caner, H. & Caldwell, J. **2002** Putting chirality to work: The strategy of chiral switches. *Nature Rev. Drug Discov.* **1**, 753-768.

Alberts, S.R., Erlichman, C., Reid, J.M., Sloan, J.A., Ames, M.M., Richardson, R.L. & Goldberg, R.M. **1998** Phase I study of the duocarmycin semisynthetic derivative KW-2189 given daily for five days every six weeks. *Clin. Cancer. Res.* **4** (9), 2111-2117.

Alley, M.C., Hollingshead, M.G., Dykes, D.J. & Waud, W.R. Human tumor xenograft models in NCI drug development. Pp 125-152 in: *Anticancer Drug Development Guide: Preclinical Screening, Clinical Trials, and Approval.* Teicher, B.A., Andrews, P.A.(eds), 2nd edition, 2004, Humana Press Inc. Totowa, N.J.

Alley, M.C., Hollingshead, M.G., Pacula-Cox, C.M. et al., **2004** SJG-136 (NSC 694501), A novel rationally designed DNA minor groove interstrand cross-linking

agent with potent and broad spectrum antitumour activity. Part 2: Efficacy evaluations. *Cancer Res.* **64**, 6700-6706.

Aloyz, R., Grzywacz, K., Xu, Z.Y., Loignon, M., Alaoui-Jamali, M.A., Panasci, L. **2005** Imatinib sensitizes CLL lymphocytes to chlorambucil. *Leukemia* **19** (6), 1103-1105.

Alseth, I., Eide, L., Pirovano, M., Rognes, T., Seeberg, E. & Bjoras, M. **1999** The *Saccharomyces cerevisiae* homologues of endonuclease III from *Escherichia coli*, Ntg1 and Ntg2 are both required for efficient repair of spontaneous and induced oxidative DNA damage in yeast. *Mol. Cell. Biol.* **19** (5), 3779-3787.

Ambroise, Y. & Boger, D.L. **2002** The DNA phosphate backbone is not involved in catalysis of the duocarmycin and CC-1065-DNA alkylation reaction. *Bioorg. Med. Chem. Lett.* **12**, 303-306.

Andrews, B.J. & Turchi, J.J. **2004** Development of a hight-throughput screen for inhibitors of replication protein A and its role in nucleotide excision repair. *Mol. Cancer. Ther.* **3** (4), 385-391.

Andritsos, L. & Khoury, H. **2002** Chronic lymphocytic leukemia. *Curr. Treat. Options Oncol.* **3**, 225-231.

Aristoff, P.A, Johnson, P.D, Sun, D. & Hurley, L.H. **1993** Synthesis and biochemical evaluation of the CBI-PDE-I-dimer, a benzannelated analog of (+)-CC-1065 that also produces delayed toxicity in mice. *J.Med. Chem.* **36** (14), 1956-1963.

Asai, A., Yano, K., Mizukami, T. & Nakamo, H. **1999** Characterisation of a Duocarmycin-DNA adduct recognising protein in cancer cells. *Cancer Res.* **59**, 5417-5420.

Atwell, G.J., Tercel, M., Bboyd, M., Wilson, W.R. & Denny, W.A. **1998** Synthesis and cytotoxicity of 5-amino-1-(chloromethyl)-3-[95,6,7-trimethoxyindol-2-yl)carbonyl]-1,2-dihydro-3H-benz[e]indole (Amino-*seco*-CBI-TMI) and related 5-alkylamino analogues: New DNA minor groove alkylating agents. *J. Org. Chem.* **63**, 9414-9420.

Atwell, G.J., Wilson, W.R. & Denny, W.A **1997** Synthesis and cytotoxicity of amino analogues of the potent DNA alkylating agent *seco*-CBI-TMI *Bioorg. Med. Chem. Lett.* **7** (12), 1493-1496.

Awada, A., Punt, C.J.A., Piccart, M.J., Tellingn, O.V., Manen, L.V., Kerger, J., Groot, Y., Wanders, J., Verweij, J. & Wagener, D.J.Th. **1999** Phase I study of Carzelesin (U-80,244) given (4-weekly) by intravenous bolus schedule. *Br. J. Cancer* **79**, 1454-1461.

Bailly, V, Lamb, J., Sung, P., Prakash, S. & Prakash, L. **1994** Specific complex formation between yeast RAD6 and RAD18 proteins: a potential mechanism for targeting RAD6 ubiquitin-conjugating activity to DNA damage sites. *Genes Dev.* **8** (7), 811-820.

Baird, R. & Winstein, S. **1963** Neighboring Carbon and Hydrogen. Dienones from Ar-3' participation. Isolation and behavior of Spiro(2,5)octa-1,4-diene-3-one. *J. Am. Chem. Soc.* **85**, 576-578.

Balajee, A.S. & V.A. Bohr. **2000**. Genomic heterogeneity of nucleotide excision repair. *Gene* **250**, 15-30.

Bando, T., Narita, A., Saito, I. & Sugiyama, H. **2002** Molecular design of pyrrole-imidazole hairpin polyamides for effective DNA alkylation. *Chem. Eur. J.* **8** (20), 4781-4790.

Bando, T., Narita, A., Saito, I. & Sugiyama, H. **2003** Highly Efficient sequence-specific DNA interstrand cross-linking by pyrrole/imidazole CPI conjugates. *J. Am. Chem. Soc.* **125**, 3471-3485.

Bando, T., Narita, A., Sasaki, S. & Sugiyama, H. **2005** Specific adenine alkylation by pyrrole-imidazole CBI conjugates. *J. Am. Chem. Soc.* **127** (40), 13890-13895.

Baraldi, P.G., Balboni, G., Cacciari, B., Guitto, A., Manfredini, S., Romagnoli, R., Spalluto, G., Howard, P.H., Thurston, D.E., Bianchi, N., Rutigliano, C., Mischiati, C. & Gambari, R. **1999** Synthesis, antiproliferative activity and DNA-binding properties of hybrid molecules containing pyrrolo [2,1-c][1,4]benzodiazepine (PBD) and minor groove binding. *J. Med. Chem.* **42**, 5131-5141.

Baraldi, P.G., Balboni, G., Pavani, M.G., Spalluto, G., Tabrizi, M.A., Clercq, E.D., Balzarini, J., Bando, T., Sugiyama, H. & Romagnoli, R. **2001** Design, synthesis, DNA binding, and biological evaluation of water-soluble hybrid molecules containing two pyrazole analogues of the alkylating cyclopropylpyrroloindole (CPI) subunit of the antitumour agent CC-1065 and polypyrrole minor groove binders. *J. Med. Chem.* **44**, 2536-2543.

Baraldi, P.G., Bovero, A., Fruttarolo, F., Pretti, D., Tabrizi, M.A., Pavani, M.G. & Romagnoli, R. **2004** DNA minor groove binders as potential antitumour and antimicrobial agents. *Med. Res. Rev.* **24** (4), 475-528.

Baraldi, P.G., Cacciari, B., Pineda de las Infantas, M.J., Romagnoli, R., Spalluto, G, Cozzi, P. & Mongelli, N. **1997** Synthesis, chemical solvolytic stability and preliminary biological evaluation of (+/-)-N-Boc-CpzI: a pyrazole analog of the left-hand segment of the antitumour agent CC-1065. *Anticancer Drug Des.* **12** (1), 67-74.

Baraldi, P.G., Romagnoli, R., Entrena Guadix, A., Pineda de las Infantas, M.J., Gallo, M.A., Espinosa, A., Martinez, A., Bingham, J.P. & Hartley, J.A. **2002** Design, synthesis and biological activity of hybrid compounds between uramustine and DNA minor groove binder distamycin A. *J. Med. Chem.* **45** (17), 3630-3638.

Barberis, A., Gunde, T., Berset, C., Audetat, S. & Luthi, U. **2005** Yeast as a screening tool. *Drug Discovery Today : Technologies* **2** (2) 187-192.

Bardwell, A.J., Bardwell, L. Tomkinson, A.E. & Friedberg, E.C **1994** Specific cleavage of model recombination and repair intermediates by the yeast Rad1-Rad10 DNA endonuclease. *Science* **265** (5181), 2082-2085.

Barret, J.M., Cadou, M. & Hill, B.T. **2002** Inhibition of nucleotide excision repair and sensitisation of cells to DNA cross-linking anticancer drugs by F11782, a novel fluorinated epipodophylloid. *Biochem. Pharmacol.* **63** (2), 251-258.

Bedalov, A., Gatbonton, T., Irvine, W.P., Gottschling, D.E. & Simon, J.A. **2001** Identification of a small molecule inhibitor of Sir2p. *Proc. Natl Acad. Sci. USA* **98**(26), 15113-15118.

Belitsky, J.M., Leslie, S.J., Arora, P.S., Beerman, T.A. & Dervan, P.B. **2002** Cellular uptake of N-methylpyrrole/N-methylimidazole polyamide–dye conjugates. *Bioorg. Med. Chem.* **10**, 3313-3318.

Berdal, K.G., Bjoras, M., Bjelland, S. & Seeberg, E. **1990** Cloning and expression in *Escherichia coli* of a gene for an alkylbase DNA glycosylase from *Saccharomyces cerevisiae*; a homologue to the bacterial alkA gene. *EMBO J.* **9** (13), 4563-4568.

Bessho, T., Sancar, A., Thompson, L.H. & Thelen, M.P. **1997** Reconstitution of human excision nuclease with recombinant XPF-ERCC1 complex. *J. Biol. Chem.* **272**, 3833-3837.

Best, T. P., Edelson, B.S., Nickols, N.G. & Dervan, P.B. **2003** Nuclear localisation of pyrrole-imidazole polyamide-fluorescein conjugates in cell culture. *Proc. Natl. Acad. Sci. USA* **100** (21), 12063-12068.

Bhuyan, B.K., Crampton, S.L. & Adams, E.G. **1983** Cell Cycle Effects of CC-1065. *Cancer Res.* **43**, 4227-4232.

Bhuyan, B.K., Newell, K.A., Crampton, S.L., & Von Hoff., D.D. **1982** CC-1065 (NSC 298223), a most potent antitumour agent: Kinetics of inhibition of growth, DNA synthesis, and cell survival. *Cancer Res.* **42**, 3532-3537.

Bianchi, N., Spalluto, G., Cacciari, B., Romagnoli, R., Feriotto, G., Mischiati, C., Rutigliano, C., Borsetti, E., Baraldi, P.G. & Gambari, R. **1999** Selective binding to human genomic sequences of two synthetic analogues structurally related to U-71184 and adozelesin. *Drug Dev. Res.* **46**, 96-106.

Bjoras, M., Klungland, A., Johansen, R.F. & Seeberg, E. **1995** Purification and properties of the alkylation repair DNA glycosylase encoded the *MAG* gene from *Saccharomyces cerevisiae*. *Biochemistry* **34** (14), 4577-4582.

Boger, D.L. **1994** Design, synthesis, and evaluation of DNA minor groove binding agents: the duocarmycins. *Pure & Appl. Chem.* **66** (4), 837-844.

Boger, D.L., Bollinger, B., Hertzog, D.L., Johnson, D.S., Cai, H., Mesini, P., Garbaccio, R.M., Jin, Q. & Kitos, P. **1997a** Reversed and sandwiched analogs of duocarmycin SA: Establishment of the origin of the sequence-selective alkylation

of DNA and new insights into the source of catalysis. *J. Am. Chem. Soc.* **119** (21), 4987-4998.

Boger, D.L. & Boyce, C.W. **2000** Selective metal cation activation of a DNA alkylation agent: Synthesis and evaluation of methyl 1,2,9,9a-tetrahydrocyclopropa[c]pyrido[3,2-e]indol-4-one-7-carboxylate (CpyI). *J. Org. Chem.* **65**, 4088-4100.

Boger, D.L., Boyce, C.W., Garbaccio, R.M. & Goldberg, J.A. **1997b** CC-1065 and the Duocarmycins: Synthetic Studies. *Chem Rev.* **97**, 787-828.

Boger, D.L. & Coleman, R.S. **1988** Total synthesis of (±)-N^2-(Phenylsulfonyl)-CPI, (±)-CC-1065, (+)-CC-1065, ent-(-)-CC-1065, and the precise functional agents (±)-CPI-$CDPI_2$, (+)-$CDPI_2$ and (-)-$CDPI_2$. *J. Am. Chem. Soc.* **110**, 4796-4807.

Boger, D.L., Coleman, R.S. & Invergo, B.J. **1987** Studies on the total synthesis of CC-1065: Preparation of a synthetic, simplified 3-carbamoyl-1,2-dihydro-3H-pyrrolo[3,2-e]indole dimer/ trimer/ tetramer (CDPI dimer/ trimer/ tetramer) and development of methodology for PDE-I dimer methyl ester formation. *J. Org. Chem.* **52**, 1521-1530.

Boger, D.L., Coleman, R.S., Invergo, B.J., Sakya, S.M., Ishizaki, T., Munk, S.A., Zarrinmayeh, H., Kitos, P.A. & Thompson, S.C. **1990a** Synthesis and evaluation of aborted and extended CC-1065 functional analogues: (+)- and (-)- CPI-$PDE\text{-}I_1$, (+)- and (-)-CPI-$CDPI_1$, and (±)-, (+)-, and (-)- CPI-$CDPI_3$. Preparation of key partial structures and definition of an additional functional role of the CC-1065 central and right-hand subunits. *J. Am. Chem. Soc.* **112**, 4623-4632.

Boger, D.L. & Garbaccio, R.M. **1997** Catalysis of the CC-1065 and duocarmycin DNA alkylation reaction: DNA binding induced conformational change in the agent results in activation. *Bioorg. Med. Chem.* **5** (2), 263-276.

Boger, D.L. & Garbaccio, R.M. **1999a** Shape-Dependent catalysis: Insights into the source of catalysis for the CC-1065 and duocarmycin DNA alkylation reaction. *Acc. Chem. Res.* ***32***, 1043-1052.

Boger, D.L. & Garbaccio, R.M. **1999b** Are the duocarmycin and CC-1065 DNA alkylation reactions acid-catalysed? Solvolysis pH-rate profiles suggest they are not. *J. Org. Chem.* **64**, 5666-5669.

Boger, D.L. & Garbaccio, R.M. **1999c** A novel class of CC-1065 and duocarmycins analogues subject to mitomycin-related reductive activation. *J. Org. Chem.* **64**, 8350-8362.

Boger, D.L., Garbaccio, R.M. & Jin. Q. **1997c** Synthesis and evaluation of CC-1065 and duocarmycin analogues incorporating the Iso-CI and Iso-CBI alkylation subunits: Impact of relocation of the C-4 carbonyl. *J. Org. Chem.* **62**, 8875-8891.

Boger, D.L. & Han, N. **1997** CC-1065/duocarmycin and bleomycin A2 hybrid agents: lack of enhancement of DNA alkylation by attachment to noncomplementary DNA binding subunits. *Bioorg. Med. Chem.* **5** (2), 233-243.

Boger, D.L., Han, N., Tarby, C.M., Boyce, C.W., Cai, H., Jin, Q. & Kitos, P.A. **1996b** Synthesis, chemical properties, and preliminary evaluation of substituted CBI analogs of CC-1065 and the duocarmycins incorporating the 7-cyano-1,2,9,9a-tetrahydrocyclopropa[c]benz[e]indol-4-one alkylation subunit: Hammett quantitation of the magnitude of electronic effects in functional reactivity. *J. Org. Chem.* **61**, 4894-4912.

Boger, D.L., Hertzog, D.L., Bollinger, B., Johnson, D.S., Cai, H, Goldberg, J. & Turnbull, P. **1997d** Duocarmycin SA shortened, simplified, and extended agents: A systematic examination of the role of the DNA binding subunit. *J. Am. Chem. Soc.* **119**, 4977-4986.

Boger, D.L., Hughes, T.V. & Hedrick, M.P. **2001** Synthesis, chemical properties, and biological evaluation of CC-1065 and duocarmycin analogues incorporating the 5'-methoxycarbonyl-1,2,9,9a-tetrahydrocyclopropa[c]benz[e]indol-4-one alkylation subunit. *J. Org. Chem.* **66**, 2207-2216.

Boger, D.L., Invergo, B.J., Coleman, R.S., Zarrinmayeh, H., Kitos, P.A., Collins-Thompson, S., Leong, T. & McLaughlin, L.W. **1990d** A demonstration of the intrinsic importance of stabilising hydrophobic binding and non-covalent van der waals contacts dominant in the non-covalent CC-1065/B-DNA binding. *Chem. Biol. Interact.* **73**, 29-52.

Boger, D.L. & Ishizaki, T. **1990** Resolution of a CBI precursor and incorporation into the synthesis of (+)-CBI, (+)-CBI-$CDPI_1$, (+)-CBI-$CDPI_2$: enhanced functional analogs of (+)-CC-1065. A critical appraisal of a proposed relationship between electrophile reactivity, DNA binding properties, and cytotoxic potency. *Tetrahedron Lett.* **31** (6), 793-796.

Boger, D.L., Ishizaki, T., Sakya, S.M. & Munk, S.A. **1991** Synthesis and preliminary evaluation of (+)-CBI-$indole_2$: an enhanced functional analog of (+)-CC-1065. *Biiorg. Med, Chem. Lett.* **1** (2), 115-120.

Boger, D.L., Ishizaki, T., Wysocki, Jr, R.J. & Munk, S.A. **1989** Total synthesis and evaluation of (±)-N-(tert-Butyloxycarbonyl)-CBI, (±)-CBI-$CDPI_1$, and (±)-CBI-$CDPI_2$: CC-1065 functional agents incorporating the equivalent 1,2,9,9a-

tetrahydrocycloprop[1,2-c]benz[1,2-e]indol-4-one (CBI) left-hand subunit. *J. Am. Chem. Soc.* **11**, 6461-6463.

Boger, D.L., Ishizaki, T. & Zarrinmayeh, H. **1990c** Synthesis and preliminary evaluation of agents incorporating the pharmacophore of the duocarmycin/pyrindamycin alkylation subunit: identification of the CC-1065/Duocarmycin common pharmacophore. *J. Org. Chem.* **55**, 4499-4502

Boger, D.L., Ishizaki. T., Zarrinmayeh, H., Munk, S.A., Kitos, P.A. & Suntornwat, O. **1990b** Duocarmycin–Pyrindamycin DNA alkylation properties and identification, synthesis, and evaluation of agents incorporating the pharmacophore of the duocarmycin-pyrindamycin alkylation subunit. Identification of the CC-1065-duocarmycin common pharmacophore. *J. Am. Chem. Soc.* **112**, 8961-8971.

Boger, D.L. & Jenkins T.J. **1996** Synthesis, X-ray Structure, and Properties of Fluorocyclopropane Analogs of the Duocarmycins Incorporating the 9,9-Difluoro-1,2,9,9a-tetrahydrocycloprop*a*[*c*]benzo[*e*]indol-4-one (F_2CBI) Alkylation Subunit. *J. Am. Chem. Soc.* **118**, 8860-8870.

Boger, D.L & Johnson, D.S. **1995** Second definitive test of proposed models for the origin of the CC-1065 and duocarmycin DNA alkylation selectivity. *J. Am. Chem. Soc.* **117**, 1443-1444.

Boger, D.L. & Johnson, D.S. **1996** CC-1065 and the Duocarmycins: Understanding their biological function through mechanistic studies. *Angew. Chem. Int. Ed. Engl.* **35**, 1438-1474.

Boger, D.L., Johnson, D.S., Palanki, M.S.S., Kitos, P.A., Chang, J. & Dowell, P. **1993** Evaluation of functional Analogs of CC-1065 and the Duocarmycins incorporating the cross-linking 9a-chloromethyl-1,2,9,9a-

tetrahydrocyclopropa[*c*]benz[*e*]indol-4-one (C_2BI) alkylation subunit. *Bioorg. Med. Chem.* **1** (1), 27-38.

Boger, D.L., Johnson, D.S. & Yun, W. **1994b** (+)- and *ent*-(-)-Duocarmycin SA and (+)- and *ent*-(-)-N-BOC-DSA DNA alkylation properties. Alkylation site models that accommodate the offset AT-rich adenine N3 alkylation selectivity of the enatiomeric agents. *J. Am. Chem. Soc.* **116**, 1635-1656.

Boger, D.L., Johnson, D.S., Yun, W & Tarby, C.M **1994a** Molecular basis for sequence selective DNA alkylation by (+)- and ent-(-)-CC-1065 and related agents: alkylation site models that accommodate the offset AT-rich adenine N3 alkylation selectivity. *Bioorg. Med. Chem.* **2** (2), 115-135.

Boger, D.L. & McKie, J.A. **1995** An efficient synthesis of 1,2,9,9a-Tetrahydrocyclopropa[c]benz[e]indol-4-one (CBI): An enhanced and simplified analog of CC-1065 and duocarmycin alkylation subunits. *J. Org. Chem.* **60**, 1271-1275.

Boger, D.L., McKie, J.A., Cai, H.C., Cacciari, B. & Baraldi, P.G. **1996a** Synthesis and properties of substituted CBI analogs of CC-1065 and the duocarmycins incorporating the 7-methoxy-1,2,9,9a-tetrahydrocyclopropa[c]benz[e]indol-4-one (MCBI) alkylation subunit: Magnitude of electronic effects on the functional reactivity. *J. Org. Chem.* **61**, 1710-1729.

Boger, D.L. & Messini, P. **1995** DNA alkylation properties of CC-1065 and duocarmycin analogs incorporating the 2,3,10,10a-tetrahydrocyclopropa[d]benzo[f]quinol-5-one alkylation subunit: Identification of subtle structural features that contribute to the regioselectivity of the adenine N3 alkylation reaction. *J. Am. Chem. Soc.* **117**, 11647-11655.

Boger, D.L. & Munk, S.A. **1992** DNA alkylation properties of enhanced analogs of CC-1065 incorporating the 1,2,9,9a-tetrahydrocyclopropa[1,2-c]benz[1,2-e]indol-4-one (CBI) alkylation subunit. *J. Am. Chem. Soc.* **114** (14), 5487-5496.

Boger, D.L., Munk, S.A. & Ishizaki, T. **1991c** (+)-CC-1065 DNA alkylation: Observation of an unexpected relationship between cyclopropane electrophile reactivity and the intensity of DNA alkylation. *J. Am. Chem. Soc.* **113**, 2779-2780.

Boger, D.L., Munk, S.A. & Zarrinmayeh, H. **1991b** (+)-CC-1065 DNA alkylation: Key studies demonstrating a noncovalent binding selectivity contribution to the alkylation selectivity. *J. Am. Chem. Soc.* **113**, 3980-3983.

Boger, D.L. & Palanki, M.S.S. **1992** Functional Analogs of CC-1065 and the Duocarmycins incorporating the 9a-(Chloromethyl)- 1,2,9,9a-tetrahydrocyclopropa[c]benz[elindol-4-one (C_2BI) Alkylation Subunit: Synthesis and Preliminary DNA Alkylation Studies. *J. Am. Chem. Soc.* **114**, 9318-9327.

Boger, D.L. & Sakya, S.M. **1992** CC-1065 partial structures: Enhancement of noncovalent affinity for DNA minor groove binding through introduction of stabilising electrostatic interactions. *J. Org. Chem.* **57**, 1277-1284.

Boger, D.L., Santillan, Jr., A., Searcey, M. & Jin, Q. **1998** Critical role of the linking amide in CC-1065 and the duocarmycins: Implications on the source of DNA alkylation catalysis. *J. Am. Chem. Soc.* **120**, 11554-11537.

Boger, D.L., Searcey, M., Tse, W.C. & Jin, Q. **2000b** Bifunctional alkylating agents derived from duocarmycin SA: Potent antitumour activity with altered sequence specificity. *Bioorg. Med. Chem. Lett.* **10**, 495-498.

Boger, D.L., Stauffer, F. & Hedrick, M.P. **2001b** Substituent effects within the DNA binding subunit of CBI analogues of the duocarmycins and CC-1065. *Bioorg. Med. Chem. Lett.* **11**, 2021-2024.

Boger, D.L. & Turnbull, P. **1997** Synthesis and evaluation of CC-1065 and duocarmycin analogs incorporating the 1,2,3,4,11,11a-hexahydrocyclopropa[c]naphtha[2,1-b]azepin-6-one (CNA) alkylation subunit: Structural features that govern reactivity and reaction regioselectivity. *J. Org. Chem.* **62**, 5849-5863.

Boger, D.L. & Turnbull, P. **1998** Synthesis and evaluation of a carbocyclic analogue of the CC-1065 and duocarmycin alkylation subunits: Role of the vinylogous amide and implications on DNA alkylation catalysis. *J. Org. Chem.* **63**, 8004-8011.

Boger, D.L., Wolkenberg, S.E. & Boyce, C.W. **2000a** A new method of *in situ* activation for a novel class of DNA alkylating agents: Tunable metal cation complexation and activation. *J. Am. Chem. Soc.* **122**, 6325-6326.

Boger, D.L. & Wysocki, Jr. R.J. **1989** Total synthesis of (±)-N-(Phenylsulfonyl)- and (±)-N-(tert-Butyloxycarbonyl)-CI, (±)-CI-CDPI$_1$, and (±)-CI-CDPI$_2$: CC-1065 functional analogues incorporating the parent 1,2,7,7a-Tetrahydrocycloprop[1,2-c]indol-4-one (CI) left-hand subunit. *J. Org. Chem.* **54**, 1238-1240.

Boger, D.L. & Yun, W. **1993** Reversibility of the duocarmycin A and SA DNA alkylation reaction. *J. Am. Chem. Soc.* **115**, 9872-9873.

Boger, D.L. & Yun, W. **1994** Role of the CC-1065 and duocarmycin N2 substituent: Validation of a direct relationship between solvolysis, chemical stability and *in vitro* biological potency. *J. Am. Chem. Soc.* **116**, 5523-5524.

Boger, D.L. & Yun, W. **1994b** CBI-TMI: Synthesis and Evaluation of a key analog of the duocarmycins. Validation of a direct relationship between chemical solvolytic stability and cytotoxic potency and confirmation of the structural features responsible for the distinguishing behaviour of enantiomeric pairs of agents. *J. Am. Chem. Soc.* **116**, 7996-8006.

Boger, D.L., Yun, W., Cai, H. & Han, N. **1995c** CBI-CDPBO$_1$ and CBI-CDPBI$_1$: CC-1065 analogs containing deep seated modifications in the DNA binding subunit. *Bioorg. Med. Chem.* **3** (6), 761-775.

Boger, D.L., Yun, W. & Han, N. **1995b** 1,2,9,9a-Tetrahydrocyclopropa[c]benz[e]indol-4-one (CBI) analogs of CC-1065 and the duocarmycins: Synthesis and evaluation. *Bioorg. Med. Chem.* **3** (11), 1429-1453.

Boger, D.L., Yun, W., Han, N. & Johnson, D.S. **1995a** CC-1065 CBI analogues: An example of enhancement of DNA alkylation efficiency through interaction of stabilising electrostatic interactions. *Bioorg. Med. Chem.* **3** (6), 611-621.

Boger, D.L., Yun, W. & Teergarden, B.R. **1992** An improved synthesis of 1,2,9,9a-Tetrahydrocyclopropa[c]benz[e]indol-4-one (CBI): A simplified analogue of the CC-1065 alkylation subunit. *J. Org. Chem.* **57**, 2873-2876.

Boger, D.L., Zarrinmayeh, H., Munk, S.A., Kitos, P.A. & Suntornwat, O. **1991a** Demonstration of a pronounced effect of noncovalent binding selectivity on the (+)-CC-1065 DNA alkylation and identification of the pharmacophore of the alkylation subunit. *Proc. Natl. Acad. Sci. USA* **88**, 1431-1435.

Bomgaars L.R., Megason, G.C., Pullen, J., Langevin, A.M., Dale Weitman, S., Hershon, L., Kuhn, J.G., Bernstein, M. & Blaney, S.M. **2006** Phase I trial of

irofulven (MGI 114) in pediatric patients with solid tumours. *Pediatr. Blood Cancer* **47** (2), 163-168.

Bose, D.S., Thompson, A.S., Ching, J.S., Hartley, J.A., Berardini, M.D., Jenkins, T.C., Neidle, S., Hurley, L.H and Thurston, D.E. **1992a** Rational design of a highly efficient irreversible DNA interstrand cross-linking agent based on pyrrolobenzodiazepine ring-system. *J. Am. Chem. Soc.* **114**, 4939-4941.

Bose, D.S., Thompson, A.S., Smellie, M., Berardini, M.D., Hartley, J.A. *et al.* **1992b** Effect of linker length on DNA-binding affinity, cross-linking efficiency and cytotoxicity of C8-linked pyrrolobenzodiazepine dimers. *Chem. Commun.* 1518-1520.

Boyd, M.R. The NCI Human Tumour Cell Line (60-cell line) screen. Concept, Implementation, and Applications. Pp 41-61 in: *Anticancer Drug Development Guide: Preclinical Screening Clinical Trials, and Approval.* Teicher, B.A. & Andrews, P.A.(eds), 2nd edition, **2004**, Humana Press Inc. Totowa, N.J.

Braña, M.F., Cacho, M., Gradillas, A., de Pascual-Teresa, B. & Ramos. A. **2001** Intercalators as anticancer drugs. *Curr. Pharm. Des.* **7**, 1745-1780.

Broggini, M., Coley, H.L., Pesenti, E., Wyatt, M.D., Hartley, J.A. & D'Incalci, M. **1995** DNA sequence-specific adenine alkylation by the novel antitumour drug Tallimustine (FCE 24517), a benzoyl nitrogen mustard derivative of distamycin. *Nucleic Acids Res.* **23** (1), 81-87.

Brooks, N., McHugh, P.J., Lee, M. & Hartley, J.A. **2000** Alteration in the choice of DNA repair pathway with increasing sequence selective DNA alkylation in the minor groove. *Chem. Biol.*, **7**, 659-668.

Broomfield, S. Chow, B.L. & Xiao, W. **1998** *MMS2*, encoding a ubiquity-conjugating-enzyme-like protein, is a member of the yeast error-free replication repair pathway. *Proc. Natl. Acad. Sci. USA* **95**, 5678-5683.

Bruce, I.A., Slevin, N.J., Homer, J.J., McGown, A.T., Ward, T.H. **2005** Synergistic effects of imatinib (ST1 571) in combination with chemotherapeutic drugs in head and neck cancer. *Anticancer Drugs* **16** (7), 719-726.

Brusky, J., Zhu, Y. & Xiao, W. **2000** *UBC13*, a DNA-damage-inducible gene is a member of the error-free postreplication repair pathway in *Saccharomyces cerevisiae*. *Curr. Genet.* **37**, 168-174.

Bryson, T.A & Roth, G.A. **1988** *Tetrahedron Lett.* **29**, 2197

Bucheli, M. & Sweder, K. **2004** In UV-irradiated *Saccharomyces cerevisiae*, overexpression of Swi2/Snf2 family member Rad26 increases transcription-coupled repair and repair of the non-transcribed strand. *Mol. Biol.* **52** (6), 1653-1663.

Capdeville, R., Buchdunger, E., Zimmermann, J. & Matter, A **2002** Glivec (STI571, imatinib), a rationally developed, targeted anticancer drug. *Nature Rev. Drug Discov.* **1**, 493-502.

Carbonero-Garcia, R., Supko, J.G., Manola, J., Seiden, M.V., Harmon, D., Ryan, D.P., Quigley, M.T., Merriam, P., Canniff, J., Goss, G., Matulonis, U., Maki, R.G., Lopez, T.A., Puchalski, T.A., Sancho, M.A., Gomez, J., Guzman, C., Jimeno, J. & Demetri, G.D. **2004** Phase II and pharmacokinetic study of ecteinascidin 743 in patients with progressive sarcomas of soft tissues refractory to chemotherapy. *J Clin Oncol.* **22** (8), 1480-90.

Carmichael, J., DeGraff, W.G., Gazdar, A.F., Minna, J.D. & Mitchell, J.B **1987** Evaluation of a tetrazolium-based semiautomated colorimetric assay: Assessment of chemosensitivity testing. *Cancer Res.* **47**, 936-942.

Carter, C.A., Waud, W.R., Li, L.H., DeKoning, T.F., McGovern, J.P., Plowman, J. **1996** Preclinical antitumour activity of bizelesin in mice. *Clin. Cancer Res.* **2** (7), 1143-1149.

Castedo, L., Delamano, J., Enjo, J., Fernadez, J., Gravalos, D.G., Leis, R., Lopez, C., Marcos, C.F., Rios, A. & Tojo, G. **2001** Derivatives of methyl 5-methyl-4-oxo-1,2,4,5,8,8a-hexahydrocyclopropa[c]-pyrrolo[3,2-e]indole-7-carboxylate: A case of inverse electronic effects on the reactivity of CC-1065 derivatives. *J. Am. Chem. Soc.* **123**, 5102-5103.

Cejka, P., Vondrejs., V. & Storchova, Z. **2001** Dissection of the functions of the *Saccharomyces cerevisiae RAD6* postreplicative repair group in Mutagenesis and UV sensitivity. *Genetics* **159**, 953-963.

Cesarone, C.F., Bolognesi, C. & Santi, L. **1979** Improved microfluorometric DNA determination in biological material using 33259 Hoechst. *Anal. Biochem.* **100**, 188-197.

Chabner, B.A. & Roberts Jr., T.G. **2005** Chemotherapy and the war on cancer. *Nature Rev. Cancer* **5**, 65-72.

Chang, A.Y. & Dervan, P.B. **2000** Strand selective cleavage of DNA by diastereomers of hairpin polyamide-seco-CBI conjugates. *J. Am. Chem. Soc.* **122**, 4856-4864.

Chen J, Derfler, B & Samson, L. **1990** *Saccharomyces cerevisiae* 3-methyladenine DNA glycosylase has homology to the AlkA glycosylase of *E. coli* and is induced in response to DNA alkylation damage. *EMBO J.* **9**, 4569-4575.

Chiang, S.Y., Welch, J., Rauscher III, F.J. & Beerman, T.A. **1994** Effects of minor groove binding drugs on the interaction of TATA box binding protein and TFIIA with DNA. *Biochemistry* **33**, 7033-7040.

Chidester, C.G., Krueger, S.A., Mizsak. D.J., Duchamp. D.J. & Martin. D.G. **1981** The structure of CC-1065, a potent antitumour agent, and its binding to DNA. *J. Am. Chem. Soc.* **103**, 7629-7635.

Churchill, M.E., Hayes, J.J. & Tullius, T.D. **1990** Detection of drug binding to DNA by hydroxyl radical footprinting. Relationship of distamycin binding sites to DNA structure and positioned nucleosomes on 5S RNA genes of Xenopus. *Biochemsitry* **29** (25), 6043-6050.

Cobuzzi Jr., R.J., Burhans, W.C. & Beerman, T.A. **1996** Inhibition of initiation of simian virus 40 DNA replication in infected BSC-1 cells by the DNA alkylating drug adozelesin. *J. Biol. Chem.* **271** (33), 19852-19859.

Colella, G., Bonfanti, M., D'Incalci, M. & Broggini, M. **1996** Characterisation of a protein recognising minor groove binders–damaged DNA. *Nucleic Acids Res.* **24** (21), 4227-4233.

Coull, J.J., He, G.C., Melander, C., Rucker, V.C., Dervan, P.B., & Margolis, D.M. **2002** Targeted derepression of the human immunodeficiency virus type 1 long terminal repeat by pyrrole-imidazole polyamides. *J. Virol.* **76**, 12349-12354.

Clingen, P.H., De Silva, I.U., McHugh, P.J., Ghadessy, F.J., Tilby, M.J., Thurston, D.E. & Hartley, J.A. **2005** The XPF-ERCC1 endonuclease and homologous recombination contribute to the repair of minor groove DNA interstrand crosslinks in mammalian cells produced by the pyrrolo[2,1-c][1.4]benzodiazepine dimer SJG-136. *Nucleic Acids Res.* **33** (10), 3283-3291.

Cunningham, R.P. **1997** DNA glycosylases. *Mutat. Res.* **383** (3), 189-196.

D'Incalci, M., Colombo, T., Ubezio, P., Nicoletti, I., Giavazzi, R., Erba, E., Ferrarese, L., Meco, D., Riccardi, R., Sessa, C., Cavallini, E., Jimeno, J. & Faircloth, G.T. **2003** The combination of yondelis and cisplatin is synergistic against human tumour xenografts. *Eur. J. Cancer* **39**, 1920-1926.

Damia, G., Imperatori, L., Citti, L., Mariani, L. & D'Incalci, M. **1996a** 3-methyladenine-DNA-glycosylase and O^6-alkylguanine-DNA-alkyltransferase activities and sensitivity to alkylating agents in human cancer cell lines. *Br. J. Cancer* **73**, 861-865.

Damia, G., Imperatori, L., Stefanini, M. & D'Incalci M. **1996b** Sensitivity of CHO mutant cell lines with specific defects in nucleotide excision repair to different anti-cancer agents. *Int. J. Cancer* **66**, 779-783.

Damia, G., Silvestri, S., Carassa, L., Filiberti, L., Faircloth, G.T., Liberi, G., Foiani, M. & D'Incalci, M. **2001** Unique pattern of ET-743 activity in different cellular systems with defined deficiencies in DNA-repair pathways. *Int. J. Cancer* **92**, 583-588.

Damia, G., Silvestri, S., Filiberti, L., Broggini, M. & D'Incalci, M. **1999** Importance of DNA repair mechanisms for the sensitivity of tumour cells to ET-

743. Proceeding of the 1999 AACR-NCI-EORTC International Conference on Molecular Targets and Cancer Therapeutics, p. 3872.

De Laat, W.L., Appeldoorn, E., Jaspers, N.G.J. & Hoeijmaker, J.H.J. **1998** DNA structural elements required for ERCC1-XPF endonuclease activity. *J. Biol. Chem.* 273, 7835-7842.

De Silva, I, U., McHugh, P.J., Clingen, P.H. & Hartley, J.A. **2002** Defects in interstrand cross-link uncoupling do not account for the extreme sensitivity of ERCC1 and XPF cells to cisplatin. *Nucleic Acids Res.* **30** (17), 3848-3856.

Dempcy, R.O., Kutyavin, I.V., Mills, A.G., Lukhtanov, E.A. & Meyer, R.B. **1999** Linkers designed to intercalate the double helix greatly facilitate DNA alkylation by triplex-forming oligonucleotides carrying a cyclopropapyrroloindole reactive moiety. *Nucleic Acids Res.* **27** (14), 2931-2937.

Dent, P. & Grant, S. **2004** Irofulven: a resurgence for alkylating therapy in cancer ? *Cancer Biol. Ther.* **3** (11), 1143-1144.

Dervan, P.B. & Edelson, B.S. **2003** Recognition of the DNA minor groove by pyrrole-imidazole polyamides. *Curr. Opin. Struct. Biol.* **13**, 284-299.

Dickinson, L.A., Gulizia, R.J., Traugerm J.W., Baird, E.E., Mosier, D.E., Gottesfeld, J.M. & Dervan, P.B. **1998** Inhibition of RNA polymerase II transcription in human cells by synthetic DNA-binding ligands. *Proc. Natl. Acad. Sci. USA* **95**, 12890-12895.

Dickinson, L.A., Trauger, J.W., Baird, E.E., Ghazai, P., Dervan, P.B. & Gottesfeld, J.M. **1999** Anti-repression of RNA polymerase II transcription by pyrrole-imidazole polyamides. B*iochemistry* **38**, 10801-10807.

Ding, Z.M., Harsley, R.M. & Hurley, L.H. **1993** (+)-CC-1065 as a structural probe of Mu transposase-induced bending of DNA: overcoming limitation of hydroxyl-radical footprinting. *Nucleic Acid Res.* **21** (18), 4281-4287.

Doetsch, P.W. & Cunningham, R.P. **1990** The enzymology of apurinic/ apyrimidinic endonucleases. *Mutat. Res.* **236**, 173-201.

Einhorn, L.H. **2002** Curing metastatic testicular cancer. *Proc. Natl. Acad. Sci. U.S.A* **99** (7), 4592-4595.

Erba, E., Bergamaschi, D., Bassano, L., Damia, G., Ronzoni, S., Faircloth, G.T. & D'Incalci, M. **2001** Ecteinascidin-743 (ET-743), a natural marine compound, with a unique mechanism of action. *Eur. J. Cancer* **37**, 97-105.

Ferry, K.V., Hamilton, T.C. & Johnson, S.W. **2000** Increased nucleotide excision repair in cisplatin-resistant ovarian cancer cells. *Biochem. Pharmacol.* **60**, 1305-1313.

Fleming, G.F., Ratain, M.J., O'Brien, S.M. *et al.* **1994** Phase I study of adozelesin administered by 24-hour continuous intravenous infusion. *J. Natl. Cancer Inst.* **86** (5), 368-372.

Foster, B.J., Lorusso, P.M., Poplin, E., Zalupski, M., Valdivieso, M., Wozniak, A., Flaherty, L., Kasunic, D.A., Earhart, R.H. & Baker, L.H. **1996** Phase I trial of Adozelesin using the treatment schedule of daily x 5 every 3 weeks. *Invest. New Drugs* **13** (4), 321-326.

Foury, F. **1997** Human genetic diseases: a cross-talk between man and yeast. *Gene* **195**, 1-10.

Fox, K.R. & Waring, M.J. **1984** DNA structural variations produced by actinomycin and distamycin as revealed by DNase I footprinting. *Nucleic Acids Res.* **12** (24), 9271-9285.

Fregeau, N.L., Wang, Y., Pon, R.T., Wylie, W.A. & Lown, J.W. **1995** Characterisation of a CPI-Lexitropsin Conjugate-Oligonucleotide covalent complex by ^{1}H NMR and restrained molecular dynamics simulation. *J. Am. Chem. Soc.* **117**, 8917-8925.

Friedberg, E.C, Walker, G.C. & Siede, W. (eds). **1995** *DNA Repair and Mutagenesis*, ASM Press, Washington D.C.

Friedman, D., Hu, Z., Kolb, A., Gorfajn, B. & Scotto, K.W. **2002** Ecteinascidin-743 inhibits activated but not constitutive transcription. *Cancer Res.* **62**, 3377-3381.

Fujimoto, K., Iida, H., Kawakami, M., Bando, T., Tao, Z-F. & Sugiyama, H. **2002** Sequence-specific protection of plasmid DNA from restriction endonuclease hydrolysis by pyrrole-imidazole-cyclopropapyrroloindole conjugates. *Nucleic Acids Res.* **30** (17), 3748-3753.

Fujiwara, T., Tao, Z.H., Ozeki, Y., Saito, I., Wang, A.H-J., Lee, M. & Sugiyama, H. **1999** Modulation of sequence specificity of duocarmycin-dependent DNA alkylation by pyrrole-imidazole triamides. *J. Am. Chem. Soc.* **121**, 7706-7707.

Gajate, C., An, F. & Mollinedo, F. **2002** Differential cytostatic and apoptotic effects of Ecteinascidin-743 in cancer cells. Transcription-dependent cell cycle arrest and transcription-independent JNK and mitochondrial mediated apoptosis. *J. Biol. Chem.* **277** (44), 41580-41589.

Gangavarapu, V., Haracska, L., Unk, I., Johnson, R.E., Prakash, S. & Prakash, L. **2006** Mms2-Ubc13 dependent and independent roles of Rad5 ubiquitin ligase in postreplication repair and translesion DNA synthesis in *Saccharomyces cerevisiae*. *Mol. Cell. Biol.* 26 (10), 7783-7790.

Gilman, A & Philips, F.S. **1946** The biological actions and therapeutic applications of β-chloroethyl amines and sulfides. *Science* **103** (2675), 409-415.

Goffeau, A., Barrell, B.G., Bussey, H., Davis, R.W., Dujon, B., Feldmann, H., Galibert, F., Hoheisel, J.D., Jacq, C., Johnston, M. *et al.* **1996** Life with 6000 genes. *Science* **274** (546), 563–567.

Gottesfeld, J.M., Neely, L., Trauger, J.W., Baird, E.E. & Dervan, P.B. **1997** Regulation of gene expression by small molecules. *Nature* **387**, 202-205.

Gregson, S.J., Howard, P.W., Hartley, J.A., Brooks, N.A., Adams, L.J., Jenkins, T.C., Kelland, L.R. & Thurston, D.E. **2001** Design, synthesis, and evaluation of a novel pyrrolobenzodiazepine DNA-interactive agent with highly efficient cross-linking ability and potent cytotoxicity. *J. Med. Chem.* **44** (5), 737-748.

Grimaldi, K.A., McAdam, S.R., Souhami, R.L. & Hartley, J.A. **1994** DNA damage by anti-cancer agents resolved at the nucleotide level of a single copy gene: evidence for a novel binding site for cisplatin in cells. *Nucleic Acids Res.* **22** (12), 2311-2317.

Grimaldi, K.A., McGurk, C.J., McHugh, P.J. & Hartley, J.A. **2002** PCR-based methods for detecting DNA damage and its repair at the sub-gene and single nucleotide levels in cells. *Molecular Biotechnology*, **20**, 181-196.

Guldener, U., Heck, S., Fielder, T., Beinhauer, J. & Hegemann, J.H. **1996** A new efficient gene disruption cassette for repeated use in budding yeast. *Nucl. Acids Res.* **24**, 2519-2524.

Gunz, D., Hess, M.T. & Naegeli, H. **1996** Recognition of DNA adducts by human nucleotide excision repair. *J. Biol. Chem.* **271** (41), 25089-25098.

Guo, D.G., Wu, X., Rajpal, D.K., Taylor, J.S. & Wang, Z. **2001** Translesion synthesis by yeast DNA polymerase ζ from templates containing lesions of ultraviolet radiation and acetylaminofluorene. *Nucleic Acids Res.* **29** (13), 2875-2883.

Guzder, S.N., Habraken, Y., Sung, P., Prakash, L. & Prakash, S. **1995** Reconstitution of Yeast nucleotide excision repair with purified Rad proteins, replication protein A, and Transcription Factor TFIIH. *J. Biol. Chem.* **270** (22), 12973-12973.

Guzder, S.N., Sommers, C.H., Prakash, L. & Prakash, S. **2006** Complex formation with damage recognition protein Rad14 is essential for *Saccharomyces cerevisiae* Rad1-Rad10 nuclease to perform its function in nucleotide excision repair *in vivo*. *Mol. Cell. Biol.* **26** (3), 1135-1141.

Guzder, S.N., Sung, P. Prakash, L & Prakash, S. **1993** Yeast DNA-repair gene *RAD14* encodes a zinc metalloprotein with affinity for ultraviolet-damaged DNA. *Proc Natl. Acad. Sci. USA* **90** (12), 5433-5437.

Guzder, S.N., Sung, P., Prakash, L. & Prakash, S. **1997** Yeast Rad7-Rad16 complex, specific for the nucleotide excision repair of the nontranscribed DNA strand, is an ATP-dependent DNA damage sensor. *J. Biol. Chem.* **272** (35), 21665-21668.

Guzder, S.N., Sung, P., Prakash, L. & Prakash, S. **1998** Affinity of yeast nucleotide excision repair factor 2, consisting of the Rad4 and Rad23 proteins, for ultraviolet damaged DNA. *J. Biol. Chem.* **273** (47), 31541-31546.

Habraken, Y., Sung, P., Prakash, L. & Prakash, S. **1993** Yeast excision repair gene *RAD2* encodes a single-stranded DNA endonuclease. *Nature* **366**, (6453), 365-368.

Halas, A., Baranowska, H., Policinska, Z. & Jachymczyk, W.J. **1997** Involvement of the *REV3* gene in the methylated base-excision repair system. Co-operation of two DNA polymerases, δ and Rev3p, in the repair of MMS-induced lesions in the DNA of *Saccharomyces cerevisiae*. *Curr. Genet.* **31**, 292-301.

Han, F.X. & Hurley, L.H. **1996** A model for the T-Antigen-Induced structural alteration of the SV40 replication origin based upon experiments with specific probes for bent, straight, and unwound DNA. *Biochemistry* **35**, 7993-8001.

Hanawalt, P.C. **1989** Preferential repair of damage in actively transcribed DNA sequences *in vivo*. *Genome*, **31**(2), 605-611.

Hanka L.J, Dietz, A., Gerpheide, S.A, Kuentzel, S.L. & Martin, D.G. **1978** CC-1065 (NSC-298223), A new antitumour antibiotic. Production, *in-vitro* biological activity, microbiological assays, and taxonomy of the producing microorganism. *J. Antibiot.* **31**, 1211-1217.

Haracska, L., Kondratick, C.M., Unk, I., Prakash, L. & Prakash, S. **2001** Interaction with PCNA is essential for yeast DNA polymerase η function. *Mol. Cell.* **8**, 407-415.

Hartley, J.A. Alkylating agents Pp 639-654 in: *Oxford textbook of Oncology.* Souhami, R.L., Tannock, I., Hohenberger, P. & Horiot, J.C. (eds), 2nd edition, **2002**, Oxford university press.

Hartley, J.A., Berardini, M.D. & Souhami, R.L. **1991** An agarose gel method for the determination of DNA interstrand crosslinking applicable to the measurement of the rate of total and "second-arm" crosslink reaction. *Anal. Biochem.* **193**, 131-134.

Hartley, J.A., Spanswick, V.J., Brooks, N., *et al.* **2004** SJG-136 (NSC 694501), a novel rationally designed DNA minor groove interstrand cross-linking agent with potent and broad spectrum antitumour activity. Part I: cellular pharmacology, *In vitro* and initial *In vivo* antitumour activity. *Cancer Res.* **64**, 6693-6699.

Herman, D.M., Baird, E.E. & Dervan, P.B. **1999b** Tandem hairpin motif for recognition in the minor groove of DNA by pyrrole-imidazole polyamides. *Chem. Eur. J.* **5**, 975-983.

Herman, D.M., Turner, J.M., Baird, E.E. & Dervan, P.B. **1999a** Cycle polyamide motif for recognition of the minor groove of DNA. *J. Am. Chem. Soc.* **121**, 1121-1129.

Herzig, M.C., Arnett, B., MacDonald, J.R. & Woynarowski, J.M. **1999** Drug uptake and cellular targets of hydroxymethylacylfulvene (HMAF). *Biochem. Pharmacol.* **58** (2), 217-225.

Herzig, M.C., Rodriguez, K.A., Trevino, A.V., Dziegielewski, J., Arnett, B., Hurley, L.H. & Woyanarowski, J.M. **2002** The genome factor in region-specific DNA damage: The DNA-reactive drug U-78779 prefers mixed A/T-G/C sequences at the nucleotide level but is region-specific for long pure AT islands at the genomic level. *Biochemistry* **41**, 1545-1555.

Hoege, C., Pfander, G.L., Moldovan, G. Pyrovolakis, G. & Jentsch, S. **2002** RAD6-dependent DNA repair is linked to modification of PCNA by ubiquitin and SUMO. *Nature* **419**, 135-141.

Hoeijmakers, J.H. Genome maintenance mechanisms for preventing cancer. **2001** *Nature* **411**, 366-374.

Hoffman, R.M. & Pickart, C.M. **1999** Noncanonical *MMS2*-encoded ubiquitin-conugating enzyme functions in assembly of novel polyubiqiotin chains for DNA repair. *Cell* **96**, 645-653.

Hollingshead, M.G., Alley, M.C., Kaur, G., Pacula-Cox, C.M. & Stinson, S.F. NCI specialised procedures in preclinical drug evaluations. Pp 153-156 in: *Anticancer Drug Development Guide: Preclinical Screening Clinical Trials, and Approval.* Teicher, B.A. & Andrews, P.A.(eds), 2nd edition, **2004**, Humana Press Inc. Totowa, N.J.

Hughes, T.R. **2002** Yeast and drug discovery *Funct. Integr. Genomics* **2**, 199-211.

Hurley, L.H. **2002** DNA and its associated processes as targets for cancer therapy. *Nat. Rev. Cancer* **2**, 188-200.

Hurley, L.H., Lee, C.S., McGovern, J.P., Warpehoski, M.A., Mitchell, M.A., Kelly, R.C. & Aristoff, P.A. **1988b** Molecular basis for sequence-specific DNA alkylation by CC-1065. *Biochemistry* **27**, 3886-3892.

Hurley, L.H., Needham-VanDevanter, D.R. & Lee, C.S **1987** Demonstration of the asymmetric effect of CC-1065 on local DNA structure using a site-directed adduct in a 117-base-pair fragment from M13mp1. *Proc. Natl. Acad. Sci. USA* **84**, 6412-6416.

Hurley, L.H., Reynolds, V.L., Swenson, D.H., Petzold, G.L. & Scahill, T.A. **1984** Reaction of the antitumour antibiotic CC-1065 with DNA: Structure of a DNA adduct with DNA sequence specificity. *Science* **226**, 843-844.

Hurley, L.H., Reck, T., Thurston, D.E., *et al.* **1988a** Pyrrolo[1,4]benzodiazepine antitumour antibiotics: relationship of DNA alkylation and sequence specificity to the biological activity of natural synthetic compounds. *Chem. Res. Toxicol.* **5**, 258-268.

Hurley, L.H. & Sun, D. **1994a** (+)-CC-1065 as a probe for intrinsic and protein-induced bending of DNA. *J. Mol. Recognit.* **7**, 123-132.

Hurley, L.H. & Sun, D. **1994b** Binding of Sp1 to the 21-bp repeat region of SV40 DNA: effect of intrinsic and drug-induced DNA bending between GC boxes. *Gene* **149** (1), 165-172.

Hurley, L.H., Warpehoski, M.A., Lee, C.S., McGovern, J.P., Scahill, T.A., Kelly, R.C., Mitchell, M.A., Wicnienski, N.A., Gebhard, I., Johnson, P.D. & Bradford, V.S. **1990** Sequence specificity of DNA alkylation by the unnatural enantiomer of CC-1065 and its synthetic analogues. *J. Am. Chem. Soc.* **112**, 4633-4649.

Hwang, J.R., Moncollin, V., Vermeulen, W., Seroz, T., Van Vuuren, H., Hoeijmakers, J.H.J. & Egly, J.M. **1996** A 3′→5′ XPB helicase defect in Repair/Transcription factor TFIIH of Xeroderma Pigmentosum group B affects both DNA repair and transcription. *J. Biol. Chem.* **271** (27), 15898-15904.

Igarashi, Y., Futamata, K., Fujita, T., Sekine, A., Senda, H., Naoki, H. & Furumai, T. **2003** Yatakemycin, a novel antifungal antibiotic produced by Streptomyces sp. TP-A0356. *J. Antibiot. (Tokyo).* **56** (2), 107-13.

Imperatori, L., Damia, G., Taverna, P., Garattini, E., Gitti, L., Boldrini, L. & D'Incalci, M. **1994** 3T3 NIH murine fibroblasts and B78 murine melanoma cells expressing the *Escherichia coli* N3-methyladenine-DNA-glycosylase I do not become resistant to alkylating agents. *Carcinogenesis* **15** (3), 533-537.

Jagannath, S. **2005** Treatment of myeloma in patients not eligible for transplantation *Curr. Treat. Options Oncol.* **6**, 241-253.

Jaspers, N.G.J., Raams, A., Kelner, M.J., Ng, J.M.Y., Yamashita, Y.M., Takeda, S., McMorris, T.C. & Hoeijmakers, J.H.J. **2002** Anti-tumour compounds illudin S and Irofulven induce DNA lesions ignored by global repair and exclusively processed by transciption- and replication-coupled repair pathways. *DNA repair* **1**, 1027-1038.

Jentsch, S., McGrathand, J.P. & Varshavsky, A. **1987** The yeast DNA repair gene *RAD6* encodes a ubiquiting-conjugating enzyme. *Nature* **329**, 131-134.

Ji, J., Wang, H.K., Bastow, K.F., Zhu, X.K., Cho, S.J., Cheng, Y.C. & Lee, K.H. **1997** Design, synthesis and biological evaluation of novel etoposide analogs bearing pyrrolecarboxamido group as DNA *topoisomerase II* inhibitors. *Bioorg. Med. Chem. Lett.* **7**, 607-612.

Jia, G., Iida, H. & Lown, J.W. **1999** Synthesis of an unsymmetrical bis-lexitropsin-1,2,9,9a-tetrahydrocyclopropa[c]benzo[e]indol-4-one (CBI) conjugate. *Chem. Commun.* 119-120.

Jia, G & Lown, J.W. **2000** Design, synthesis and cytotoxicity evaluation of 1-chloromethyl-5-hydroxy-1,2-dihydro-3*H*-benz[*e*]indole (*seco*-CBI) dimers. *Bioorg. Med. Chem.* **8** (7), 1607-1617.

Jiang, H. & Yang, L.Y. **1999** Cell cycle checkpoint abrogator UCN-01 inhibits DNA repair: association with attenuation of the interaction of XPA and ERCC1 nucleotide excision repair proteins. *Cancer Res.* **59**, 4529-4534.

Jimeno, J., Lopez-Martin, J.A., Ruiz-Casado, A., Izquierdo, M.A., Scheuer, P.J. & Rinehart, K. **2004** Progress in the clinical development of new marine-derived anticancer compounds. *Anti-Cancer Drugs* **15** (4), 321-328.

Jin, S.G., Choi, J.H., Ahn, B., O'Connor, T.R., Mar, W. & Lee, C.S. **2001** Excision repair of adozelesin-N3 adenine adduct by 3-methyladenine-DNA glycosylase and UvrABC nuclease. *Mol. Cells.* **11** (1), 41-47.

Jin, S., Gorfajn, B., Faircloth, G. & Scotto, K.W. **2000** Ecteinascidin 743, a transcription-targeted chemotherapeutic that inhibits MDR1 activation. *Proc. Natl. Acad. Sci. USA* **97**, 6775-6779.

Johnson, R.E., Haracska, L., Prakash, S. & Prakash, L. **2001** Role of DNA polymerase η in the bypass of a (6-4) TT photoproduct. *Mol. Cell. Biol.* **21**, 3558-3563.

Johnson, R.E., Henderson, S.T., Petes, T.D., Prakash, S., Bankmann, M & Prakash, L. **1992** *Saccharomyces cerevisiae* RAD5-encoded DNA repair protein contains DNA helicase and zinc-binding sequence motifs and affects the stability of simple repetitive sequences in the genome. *Mol. Cell. Biol.* **12**, 3807-3818.

Johnson, R.E., Prakash, S. & Prakash, L. **1999** Efficient bypass of a thymine-thymine dimmer by yeast polymerase, pol η. *Science* **283**, 1001-1004.

Johnson, R.E., Prakash, S. & Prakash, L. **1994** Yeast DNA repair protein RAD5 that promotes instability of simple repetitive sequences is a DNA-dependent ATPase. *J. Biol. Chem.* **269**, 28259-28262.

Jolivet, J., Cowan, K.H., Curt, G.A., Clendeninn, N.J. & Chabner, B.A. **1983** The pharmacology and clinical use of methotrexate. *N. Eng. J. Med.* **309**, 1094-1104.

Kamal, A., Reddy, P.S.M.M., Reddy, D.R., Laxman, E. & Murthy, Y.L.N. **2004** Synthesis of fluorinated analogues of SJG-136 and their DNA-binding potential. *Bioorg. Med. Chem. Lett.* **14**, 5699-5702.

Kelly, R.C., Gebhard, I., Wicnienski, N., Aristoff, P.A., Johnson, P.D. & Martin, D.G. **1987** Coupling of cyclopropapyrroloindole (CPI) derivatives. The preparation of CC-1065, ent-CC-1065, and analogues. *J. Am. Chem. Soc.* **109**, 6837-6838.

Kielkopf, C.L., Bremer, R.E., White, S., Szewczyk, J.W., Turner, J.M., Baird, E.E., Dervan, P.B. & Rees, D.C. **2000** Structural effects of DNA sequence on TA recognition by hydroxypyrrole/pyrrole pairs in the minor groove. *J. Mol. Biol.* **295**, 557-567.

Kim, D.Y., Shih, D.S., Cho, D.Y. & Swenson, D.H. **1995** Helix-stabilizing compounds CC-1065 and U-71,184 bind to RNA-DNA and DNA-DNA duplexes containing modified internucleotide linkages and stabilize duplexes against thermal melting. *Antisense Res. De.* **5** (1), 49-57.

Kirshner, J., Hatch, M., Hennessy, D.D., Fridman, M. & Tannous, R.E. **2004** Anemia in Stage II and III breast cancer patients treated with adjuvant doxorubicin and cyclophosphamide chemotherapy. *The Oncologist* **9** (1), 25-32.

Kissinger, K., Krowicki, K., Dabrowiak, J.C. & Lown, J.W. **1987** Molecular recognition between oligopeptides and nucleic acids: monocationic lexitropsins that display enhanced GC sequence dependent DNA binding. *Biochemistry* **26**, 5590-5595.

Koberle, B., Masters, J.R.W., Hartley, J.A. & Wood, R.D. **1999** Defective repair of cisplatin-induced DNA damage caused by reduced XPA protein in testicular germ cell tumours. *Curr. Biol.* **9** (5), 273-276.

Koeppel, F., Poindessous, V., Lazar, V., Raymond, E., Sarasin, A. & Larsen, A.K. **2004** Irofulven cytotoxicity depends on transcription-coupled nucleotide excision repair and is correlated with XPG expression in solid tumour cells. *Clin. Cancer Res.* **10**, 5604-5613.

Kola, I. & Landis, J. **2004** Can the pharmaceutical industry reduce attrition rates? *Nature Rev. Drug Discov.* **3**, 711-715.

Kopka, M.L., Yoon, C., Goodshell, D., Pjura, P. & Dickerson, R.E. **1985** The molecular origin of DNA-drug specificity in netropsin and distamycin. *Proc. Natl. Acad. Sci. USA* **82**, 1376-1380.

Kowalski, D. **1979** A procedure for the quantitation of relaxed closed circular DNA in the presence of superhelical DNA: an improved fluorometric assay for nicking-closing enzyme. *Anal. Biochem.* **93**, 346-354.

Krowicki, K. & Lown, J.W. **1987** Synthesis of novel imidazole-containing DNA minor groove binding oligopeptides related to the antiviral antibiotic netropsin. *J. Org. Chem.* **52** (16), 3493-3501.

Krueger, W.C., Hatzenbuhler, N.T., Prairie, M.D. & Shea, M.H. **1991** DNA sequence recognition by the antitumour antibiotic CC-1065 and analogs of CC-1065. *Chem-Biol. Interactions* **79**, 265-286.

Kumar, R. & Lown, W.J. **2003** Synthesis and cytotoxicity evaluation of novel C7-C7, C7-N3 and N3-N3 dimers of 1-chloromethyl-5-hydroxy-1,2-dihydro-3H-benzo[e]indole (seco-CBI) with pyrrole and imidazole polyamide conjugates. *Org. Biomol. Chem.* **1**, 2630-2647.

Kumar, R., Rai, D., Marcus, S.L., Ko, S.C.C. & Lown, J.W. **2004** Synthesis and cellular uptake of fluorescently labelled 1-chloromethyl-5-hydroxy-1,2-dihydro-3H-Benz[e]indole (*seco*-CBI)-pyrrole polyamide conjugates. *Letters in Organic Chemistry* **1**, 154-158.

Kumar, S., Reed, M.W., Gamper, Jr. H.B., Gorn, V.V., Lukhtanov, E.A., Foti, M., West, J., Meyer, Jr. R.B., & Schweitzer, B.I. **1998** Solution structure of a highly stable DNA duplex conjugated to a minor groove binder. *Nucleic Acids Res.* **26** (3) 831-838.

Kurtz, S, Luo, G., Hahnenberger, K.M., Brooks, C., Gecha, O., Ingalls, K., Numata, K. & Krystal, M. **1995** Growth impairment resulting from expression of influenza virus M2 protein in *Saccharomyces cerevisiae*: identification of a novel inhibitor of influenza virus. *Antimicrob. Agents Chemother.* **39** (10) 2204-2209.

Lawrence, C. **1994** The *RAD6* DNA repair pathway in Saccharomyces cerevisiae: what does it do, and how does it do it? *Bioessays* **16**, 253-258.

Lee, C.S. & Gibson, N.W. **1993** Nucleotide Preferences for DNA interstrand cross-linking induced by the cyclopropylpyrroloindole analogue U-77,779. *Biochemistry* **32**, 2592-2600.

Lee, C.S., Pfeifer, G.P. & Gibson, N.W. **1994** Mapping of DNA alkylation sites induced by adozelesin and bizelesin in human cells by ligation-mediated polymerase chain reaction. *Biochemistry* **33**, 6024-6030.

Lee, C.S., Sun, D., Kizu, R. & Hurley, L.H. **1991** Determination of the structural features of (+)-CC-1065 that are responsible for bending and winding of DNA. *Chem. Res. Toxicol.* **4**, 203-213.

Lee, M., Hartley, J.A., Pon, R.T., Krowicki, K. & Lown, J.W. **1988** Sequence specific molecular recognition by a monocationic lexitropsin of the decadeoxynucleotide d-[(CATGGCCATG]2 : structural and dynamic aspects deduced from high field 1H-NMR studies. *Nucleic Acids Res.* **16** (2), 665-684.

Lee, M., Pon, R.T., Krowicki, K. & Lown, J.W. **1988b** Stuctural and dynamic aspects of the sequence specific binding of netropsin and its bis-imidazole analogue on the decadeoxyribonucleotide d-[CGCAATTGCG]$_2$. *J. Biomol. Struct. Dyn.* 5 (4), 939-949.

Li, L.H., DeKoning, T.F., Kelly, R.C., Krueger, W.C. *et al.* **1992** Cytotoxicity and antitumour activity of carzelesin, a prodrug cyclopropylpyrroloindole analogue. *Cancer Res.* **52** (18), 4904-4913.

Li, M.C., Hertz, R. & Bergenstal, D.M. **1958** Therapy of choriocarcinoma and related trophoblastic tumours with folic acid and purine antagonists. *N. Eng. J. Med.* **259**, 66-74.

Li, L.H., Swenson, D.H., Schpok, S.L.F., Kuentzel, B.D., Dayton, B.D. & Krueger, W.C. **1982** CC-1065 (NSC 298223), a novel antitumour agent that interacts strongly with double-stranded DNA. *Cancer Res.* **42**, 999-1004.

Lin, C.H., Beale, J.M., & Hurley, L.H. **1991** Structure of the (+)-CC-1065-DNA adduct: Critical role of ordered water molecules and implications for involvement of phosphate catalysis in the covalent reaction. *Biochemistry* **30**, 3597-3602.

Lin, C.H., Hill, G.G., & Hurley, L.H. **1992** Characterisation of a 12-mer duplex d(GGCGGAGTTAGG)·d(CCTAACTCCGCC) containing a highly reactive (+)-CC-1065 sequence by ^{1}H and ^{31}P NMR, hydroxyl-radical footprinting, and NOESY restrained molecular dynamics calculations. *Chem. Res. Toxicol.* **5**, 167-182.

Lin, C.H. & Hurley, L.H. **1990** Determination of the major tautomeric form of the covalently modified adenine in the (+)-CC-1065-DNA adduct by ^{1}H and ^{15}N NMR studies. *Biochemistry* **29**, 9503-9507.

Liu, X.D., Liu, P.C.C., Santoro, N. & Thiele, D.J. **1997** Conservation of a stress response: human heat shock transcription factors functionally substitute for yeast HSF. *EMBO J.* **16** (21), 6466-6477.

Longtine, M.S., McKenzie, A., Demarini, D.J., Shah, N.G., Wach, A., Brachat, A., Philippsen, P. & Pringle, J.R. **1998** Additional modules for versatile and economical PCR-based gene deletion and modification in *Saccharomyces cerevisiae*. *Yeast* **14**, 953-961.

Lown J.W. **1988** Lexitropsins: rational design of DNA sequence reading agents as novel anti-cancer agents and potential cellular probes. *Anticancer Drug Des.* **3** (1), 25-40.

Lown, J.W., Krowicki, K. & Bhat, U.G. **1986** Molecular recognition between oligopeptides and nucleic acids: Novel imidazole-containing oligopeptides related to netropsin that exhibit altered DNA sequence specificity. *Biochemistry* **25**, 7408-7416.

Lukhtanov, E.A., Mills, A.G., Kutyavin, I.V., Gorn, V.V., Reed, M.W. & Meyer, R.B. **1997** Minor groove DNA alkylation directed by major groove triplex forming oligodeoxyribonucleotides. *Nucleic Acids Research* **25** (24), 5077-5084.

Lukhtanov, E.A., Podyminogin, M.A., Kutyavin, I.V., Meyer Jr., R.B. & Gamper, H.B. **1996** Rapid and efficient hybridisation-triggered crosslinking within a DNA duplex by an oligodeoxyribonucleotide bearing a conjugated cyclopropyrroloindole. *Nucleic Acids Res.* **24** (4), 683-687.

Lyakhovich, A. & Shekhar, M. **2004** *RAD6B* overexpression confers chemoresistance: *RAD6* expression during cell cycle and its redistribution to chromatin during DNA damage-induced response. *Oncogene* 1-10.

Maine, I.P., Sun, D., Hurley, L.H. & Kodadek, T. **1992** The antitumour agent CC-1065 inhibits helicase-catalysed unwinding of duplex DNA. *Biochemistry* **31**, 3968-3975.

Mallet, L., Bussereau, F. & Jacquet, M. **1995** A 43.5 kb segment of yeast chromosome XIV, which contains MFA2, MEP2, CAP/SRV2, NAM9, FKB1/FRP1/RBP1, MOM22 and CPT1, predicts an adenosine deaminase gene and 14 new open reading frames. *Yeast* **11**, 1195-1209.

Mapp, A.K., Ansari, A.Z., Ptashne, M. & Dervan, P.B. **2000** Activation of gene expression by small molecule transcription factors. *Proc. Natl. Acad. Sci. USA* **97**, 3930-3935.

Marques, M.A., Doss, R.M., Foister, S. & Dervan, P.B. **2004** Expanding the repertoire of heterocycle ring pairs for programmable minor groove DNA recognition. *J. Am. Chem. Soc.* **126**, 10339-10349.

Martin, D.G, Biles C., Gerpheide, S.A., Hanka, L.J., Krueger, W.C., McGovern, J.P., Mizsak, S.A., Neil, G.L., Stewart, J.C. & Visser, J. **1981** CC-1065 (NSC-298223), a potent new antitumour agent-improved production and isolation, characterisation and antitumour activity. *J. Antiobiot.* **34**, 1119-1125.

Martin, C., Ellis, T, McGurk, C.J., Jenkins, T.C., Hartley, J.A., Waring, M.J. & Thurston, D.E. **2005** Sequence-selective interaction of the minor-groove interstrand cross-linking agent SJG-136 with naked and cellular DNA: Footprinting and Enzyme inhibition studies. *Biochemistry* **44** (11), 4135-4147.

Martin, D.G., Kelly, R.C., Watt, W., Wicnienski, N., Mizsak, S.A., Nielsen, J.W. & Prairie, M.D. **1988** Absolute configuration of CC-1065 by X-ray crystallography on a devitalised chiral fragment (CPI) from the natural antibiotic. *J.Org. Chem.* **53**, 4610-4613.

Masters, J.R.W. & Köberle, B. **2003** Curing metastatic cancer: Lessons from testicular germ-cell tumours. *Nature Rev. Cancer* **3**, 517-520.

McCready, S. **1994** Repair of 6-4 photoproducts and cyclobutane pyrimidine dimers in rad mutants of *Saccharomyces cerevisiae*. *Mutat. Res.* **315** (3), 261-273.

McGovern, J.P, Clarke, G.L., Pratt, E.A. & Dekoning, T.F. **1984** Preliminary toxicity studies with the DNA binding antibiotic CC-1065, a potent antitumour antibiotic. *J. Antibiot.* **37**, 63-70.

McHugh, M.M., Kuo, S.R., Walsh O'Beirne, M.H., Liu, J.S., Melendy, T. & Beerman, T.A. **1999a** Bizelesin, a bifunctional cyclopropylpyrroloindole alkylating agent, inhibits simian virus 40 replication in *trans* by induction of an inhibitor. *Biochemistry* **38**, 11508-11515.

McHugh, M.M., Woynarowski, J. M., Mitchell, M.A., Gawron, L.S., Weiland, K.L. & Beerman, T.A. **1994** CC-1065 bonding to intracellular and purified SV40 DNA: Site specificity and functional effects. *Biochemistry* **33**, 9158-9168.

McHugh, P.J., Gill. R.D., Waters, R. & Hartley, J.A. **1999b** Excision repair of nitrogen mustard-DNA adducts in *Saccharomyces cerevisiae. Nucleic Acids Res.* **27** (16), 3259-3266.

McHugh, P.J., Sones, W.R. & Hartley, J.A. **2000** Repair of intermediate structures produced at DNA interstrand cross-links in *Saccharomyces cerevisiae. Mol. Cell. Biol.* **20** (10), 3425-3433.

McHugh, P.J., Spanswick, V. & Hartley, J.A. **2001** Repair of DNA interstrand crosslinks: molecular mechanisms and clinical relevance. *Lancet Oncol.* **2** (8), 483-490.

Memisoglu, A. & Samson, L. **2000** Base excision repair in yeast and mammals. *Mutat. Res.* **451**, 39-51.

Middendorp, O., Ortler, C., Neumann, U., Paganetti, P., Luthi, U. & Barberis, A. **2004** Yeast growth selection system for the identification of cell-active inhibitors of beta-secretase. *Biochim. Biophys. Acta* **1674** (1) 29-39.

Milbank, J.B., Tercel, M., Atwell, G.J., Wilson, W.R., Hogg, A. & Denny, W.A. **1999** Synthesis of 1-substituted 3-(Chloromethyl)-6-aminoindoline (6-amino-*seco*-CI) DNA minor groove alkylating agents and structure-activity relationships for their cytotoxicity. *J. Med. Chem.* **42**, 649-658.

Minuzzo, M., Marchini, S., Broggini, M., Faircloth, G., D'Incalci, M. & Mantovani, R. **2000** Interference of transcriptional activation by the antineoplastic drug ecteinascidin-743. *Proc. Natl. Acad. Sci. USA* **97**, 6780-6784.

Mitchell, M.A., Johnson, P.D., Williams, M.G. & Aristoff, P.A **1989** Interstrand DNA crosslinking with dimers of the spirocyclopropyl alkylating moiety of CC-1065. *J. Am. Chem. Soc.* **111**, 6428-6429.

Mitchell, M.A., Kelly, R.C., Wicniensky, N.A., Hatzenbuhler, N.T., Williams, M.G., Petzold, G.L., Slightom, J.L. & Siemieniak, D.R. **1991** Synthesis and DNA cross-linking by a rigid CPI dimer. *J. Am. Chem. Soc.* **113**, 8994-8995.

Mohamadi, F., Spees, M.M., Staten, G.S., Marder, P., Kipka, J.K. & Johnson, D.A. **1994** Total synthesis and biological properties of novel antineoplastic (chloromethyl) furanoindoles: An asymmetric hydroboration mediated synthesis of the alkylation subunits. *J. Med. Chem.* **37**, 232-239.

Moore, B.M., Seaman, F.C. & Hurley, L.H. **1997** NMR-based model of an ecteinascidin 743-DNA adduct. *J. Am. Chem. Soc.* **119**, 5475-5476.

Moorthamer, M., Panchal, M., Greenhalf, W & Chaudhuri, B. **1998** The p16(INK4A) protein and flavopiridol restore yeast cell growth inhibited by Cdk4. *Biochem. Biophys. Res. Commun.* **250**(3), 791-797.

Mossman, T. **1986** Rapid colorimetric assay for cell growth and survival; application to proliferation and cytotoxicity assays. *J. Immunol. Methods* **89**, 271-277.

Motycka, T.A., Bessho, T., Post, S.M., Sung, P. & Tomkinson, A.E. **2004** Physical and Functional Interaction between the XPF/ERCC1 Endonuclease and hRad52. *J. Biol. Chem.* **279** (14), 13634-13639.

Moy, B.C., Prairie, M.D., Krueger, W.C. & Bhuyan, B.K. **1989** Interaction of CC-1065 and its analogues with mouse DNA and chromatin. *Cancer Res.* **49**, 1983-1988.

Mrksich, M. & Dervan, P.B. **1994** Design of a covalent peptide heterodimer for sequence specific recognition in the minor groove of double helical DNA. *J. Am. Chem. Soc.* **116**, 3663-3664.

Mrksich, M. & Dervan, P.B. **1993a** Antiparallel side-by-side heterodimer for sequence specific recognition in the minor groove of DNA by a distamycin / 1-Methylimidazole-2-carboxamide-netropsin pair. *J. Am. Chem. Soc.* **115**, 2572-2576.

Mrksich, M. & Dervan, P.B. **1993b** Enhanced sequence specific recognition in the minor groove of DNA by covalent peptide dimers: bis(pyridine-2-carboxaminodonetropsin) $(CH_2)_{3-6}$. *J. Am. Chem. Soc.* **115**, 9892-9899.

MrKsich, M., Parks, M.E. & Dervan, P.B Hairpin Peptide Motif. **1994** A New Class of Oligopeptides for Sequence-Specific Recognition in the Minor Groove of Double-Helical DNA. *J. Am. Chem. Soc.* **116**, 7983-7988.

Murty, M.S.R.C. & Sugiyama, H. 2004 Biology of N-methylpyrrole-N-methylimidazole hairpin polyamide. *Biol. Pharm. Bull.* **27** (4), 468-474.

Naegeli, H., Bardwell, L. & Friedberg, E.C. **1993** Inhibition of Rad3 DNA helicase activity by DNA adducts and abasic sites: Implications for the role of a DNA Helicase in Damage-Specific incision of DNA. *Biochemistry* **32**, 613-621.

Nazimiec, M., Lee, C.S., Tang, Y.L., Ye, X., Case, R. & Tang, M.S. **2001** Sequence-dependent interactions of the two forms of UvrC with DNA helix-stabilising CC-1065-N3-Adenine adducts. *Biochemistry* **40**, 11073-11081.

Needham-VanDevanter, D.R. & Hurley, L.H. **1986** Construction and characterisation of a site-directed CC-1065-N3-Adenine adduct within a 117 base pair DNA restriction fragment. *Biochemistry* **25**, 8430-8436.

Needham-VanDevanter, D.R., Hurley, L.H., Reynolds, V.L., Theriault, N.Y., Krueger, W.C. & Wierenga, W. **1984** Characterisation of an adduct between CC-1065 and a defined oligodeoxynucleotide duplex. *Nucleic Acids Res.* **12** (15), 6159-6168.

Neil, G.L., Clarke, G.L. & McGovern, J.P. **1981** Antitumour activity and acute toxicity of CC-1065 (NSC-298223) in the mouse. *Proc. Am. Assoc. Cancer Res.* **22** : 244.

Nelson, J.R., Lawrence, C.W. & Hinkle, D.C. **1996a** Thymine-thymine dimmer bypass by yeast DNA polymerase x. *Science* **272**, 1646-1649.

Nelson, J.R., Lawrence, C.W. & Hinkle, D.C. **1996b** Deoxycytidyl transferase activity of yeast REV1 protein *Nature* **383**, 729-731.

Newman, D.J., Gragg, G.M. & Snader, K.M. **2003** Natural products as a source of new drugs over the period 1981-2002. *J. Nat. Prod.* **66** (7), 1022-1037.

O'Donovan, A., Davies, A.A., Moggs, J.G., West, S.C. and Wood, R.D. **1994** XPG endonuclease makes the 3′ incision in human DNA nucleotide excision repair. *Nature* **371** (6496), 432-435.

Olenyuk, B.Z., Zhang, G.J., Klco, J.M., Nickols, N.G., Kaelin, W.G. & Dervan, P.B. **2004** Inhibition of vascular endothelial growth factor with a sequence-specific hypoxia response element antagonist. *Proc. Natl. Acad. Sci. USA* **101** (48), 16768-16773.

Orren, D.K., Dianov, G.L. & Bohr, V.A. **1996** The human CSB (ERCC6) gene corrects the transcription-coupled repair defect in the CHO cell mutant UV61. *Nucleic Acids Res.* **24** (17), 3317-3322.

Oyoshi, T., Kawakami, W., Narita, A., Bando, T. & Sugiyama, H. **2003** Inhibition of transcription at a coding sequence by alkylating polyamide. *J. Am. Chem. Soc.* **125**, 4752-4754.

Paci, A., Rezai, K., Deroussent, A., De Valeriola, D., Re, M., Weill, S., Cvitkovic, E., Kahatt, C., Shan, A., Waters, S., Weems, G., Vassal, G. & Lokiec, F. **2006** Pharmacokinetics, metabolism, and routes of excretion of intravenous irofulven in patients with advanced solid tumours. *Drug Metab. Dispos.* **34** (11), 1918-1926.

Parrish, J.P., Kastrinsky, D.B., Hwang, I. & Boger, D.L. **2003a** Synthesis and evaluation of duocarmycin and CC-1065 analogues incorporating the 1,2,9,9a-tetrahydrocyclopropa[c]benz[e]-3-azaindol-4-one (CBA) alkylation subunit. *J. Org. Chem.* **68** (23), 8984-8990.

Parrish, J.P., Kastrinsky, D.B., Wolkenberg, S.E., Igarashi, Y. & Boger, D.L. **2003c** DNA alkylation properties of Yatakemycin. *J. Am .Chem. Soc.* **125**, 10971-10976.

Parrish, J.P., Hughes, T.V., Hwang, I. & Boger, D.L. **2003b** Establishing the parabolic relationship between reactivity and activity fro derivatives and analogues of the duocarmycin and CC-1065 alkylation subunits. *J. Am. Chem. Soc.* **126**, 80-81.

Passadore, M., Bianchi, N., Feriotto, G., Mischiati, C., Rutigliano, C. & Gambari, R. **1997** *In vitro* and *In vivo* binding of CC-1065 analogue to human gene sequences: a polymerase-chain reaction study. *Eur. J. Pharmacol.* **319**, 317-325.

Patel, V.F., Andis, S.L., Enkema, J.K., Johnson, D.A., Kennedy, J.H., Mohamadi, F., Schultz, R.M., Soose, D.J. & Spees, M.M. **1997** Total Synthesis of *seco* (+)- and *ent*-(-)-Oxaduocarmycin SA: Construction of the (Chloromethyl)indoline Alkylating Subunit by a Novel Intramolecular Aryl Radical Cyclization onto a Vinyl Chloride. *J. Org. Chem.* **62** (25), 8868-8874.

Pati, H., Howard, T., Townes, H., Lingerfelt, B., McNulty, L. & Lee, M. **2004** Unexpected synthesis of *seco*-cyclopropyltetrahydroquinolines from a radical 5-exo-trig cyclization reaction: Analogs of CC-1065 and the Duocarmycins. *Molecules* **9**, 125-133.

Patterson, H.G. & Simpson, R.T **1994** Nucleosomal location of STE6 TATA box and Mat alpha 2p-mediated repression. *Mol. Cell. Biol.* **14**, 4002-4010.

Pavlidis, N., Aamdal, S., Awada, A., Calvert, H., Fumoleau, P., Sorio, R., Punt, C., Verwij, J., Van Oosterom, A., Morant, R., Wanders, J. & Hanauske, A.R. **2000** Carzelesin phase II study in advanced breast, ovarian, colorectal, gastric, head and neck cancer, non-Hodgkin's lymphoma and malignant melanoma: a study of the EORTC early clinical studies group (ECSG). *Cancer Chemother. Pharmacol.* **46**, 167-171.

Paz, M.M., Das, A. & Tomasz, M. **1999** Mitomycin C linked to DNA minor groove binding agents: Synthesis, reductive activation, DNA binding and cross-linking properties and in vitro antitumour activity. *Bioorg. Med. Chem.* **7**, 2713-2726.

Pelton, J.G. & Wemmer, D.E. **1989** Structural characterisation of a 2:1 distamycin A.d(CGCAAATTGGC) complex by two-dimensional NMR. *Proc. Natl. Acad. Sci. USA.* **86** (15), 5723-5727.

Percival, K.J., Klein, M.B. & Burgers, P.M. **1989** Molecular cloning and primary structure of the uracil-DNA-glycosylase gene from *Saccharomyces cerevisiae. J. Biol. Chem.* **264** (5), 2593-2598.

Perkins, E., Sun, D., Nguyen, A., Tulac, S., Francesco, M., Tavana, H., Nguyen, H., Tugendreich, S., Barthmaier, P., Couto, J., Yeh, E., Thode, S., Jarnagin, K. Jain, A., Morgans, D. & Melese, T. **2001** Novel inhibitors of poly(ADP-ribose) polymerase/PARP1 and PARP2 identified using a cell-based screen in yeast. *Cancer Res.* **61**(10), 4175-4183.

Prakash, S. & Prakash, L. **2000** Nucleotide excision repair in yeast. *Mut. Res.* **451**, 13-24.

Prakash, S., Sung, P. & Prakash, L. **1993** DNA repair genes and proteins of *Saccharomyces cerevisiae. Annu. Rev. Genet.* **27**, 33-70.

Pratt, W.B., Ruddon, R.W., Ensminger, W.D. & Maybaum, J. (eds). **1994** Antimetabolites. Pp 69-107 in : *The Anticancer Drugs*, Oxford Univeristy Press, NY.

Pilot, H.C., Reid, J.M., Sloan, J.A., Ames, M.M., Adjei, A.A., Rubin, J., Bagniewski, P.G., Atherton, P., Rayson, D., Goldberg, R.M. & Erlichman, C. **2002** A Phase I study of Bizelesin (NSC 615291) in patients with advanced solid tumours. *Clin. Cancer Res.* **8**, 712-717.

Poindessous, V., Koeppel, F., Raymond, E., Comisso, M., Waters, S.J. & Larsen, A. K. **2003** Marked activity of irofulven (MGI 114) toward human carcinoma cells: comparison with cisplatin and ecteinascidin (ET-743). *Clin. Cancer Res.* **9**, 2817-2828.

Pommier, Y., Kohlagen, G., Bailly, C., Waring, M., Mazumder, A. & Kohn, K.W. **1996** DNA sequence- and structure-selective Alkylation of guanine N2 in the DNA minor groove by Ecteinascidin 743, a Potent antitumour compound from the Caribbean Tunicate *Ecteinascidia turbinara. Biochemistry* **35**, 13303-13309.

Ponti, M., Forrow, S.M., Souhami, R.L., D'Incalci, M. & Hartley, J.A. **1991** Measurement of the sequence specificity of covalent DNA modification by antineoplastic agents using *Taq* DNA polymerase. *Nucleic Acids Res.* **19** (11), 2929-2933.

Portugal, J. & Waring, M.J. **1987** Hydroxyl radical footprinting of the sequence-selective binding of netropsin and distamycin to DNA. *FEBS Lett.* **225**, 195-200.

Roberts Jr., T.G., Goulart, B.H., Squitieri, L., Stallings, S.C., Halpern, E.F., Chabner, B.A., Gazelle, G. S., Finkelstein, S.N. & Clark, J.W. **2004** Trends in the risks and benefits to patients with cancer participating in phase I clinical trials. *JAMA* **292**, 2130-2140.

Reddy, B.S.P., Sondhi, S.M. & Lown, J.W. **1999** Synthetic DNA minor groove-binding drugs. *Pharmacol. Ther.* **84**, 1-111.

Reddy, P. M., Toporowski, J.W., Kahane, A.L. & Bruice, T.C. **2005** Recognition of a 10 base pair sequence of DNA and stereochemical control of the binding affinity of chiral hairpin polyamide-Hoechst 33258 conjugates. *Bioorg. Med. Chem. Lett.* **15**, 5531-5536.

Rennenberg, D. & Dervan, P.B. **2003** Imidazopyridinie/Pyrrole and Hydroxybenzimidazole/Pyrrole pairs for DNA minor groove recognition. *J. Am. Chem. Soc.* **125**, 5705-5716.

Reynolds, V.L., Molineaux, I.J., Kaplan, D.J., Swenson, D.H. & Hurley, L.H. **1985** Reaction of the antitumour antibiotic CC-1065 with DNA. Location of the site of thermally induced strand breakage and analysis of DNA sequence specificity. *Biochemistry* **24**, 6228-6237.

Rinehart, K.L., Gravalos, L.G., Faircloth, G. & Jimeno, J. **1995** ET-743: preclinical antitumour development of a marine derived natural product. *Proc. Am. Ass. Cancer Res.* **36**, 2322.

Rosenberg, B., Van Camp, L., & Krigas, T. **1965** Inhibition of cell division in Escherichia coli by electrolysis products from a platinum electrode. *Nature* **205**, 698-699.

Ruddon, R.W. & Johnson, J.M. **1968** The effects of nitrogen mustard on DNA template activity in purified DNA and RNA polymerase systems. *Mol. Pharmacol.* 4, 258

Sancar, A. & Sancar, G.B. **1988** DNA Repair enzymes *Annu. Rev. Biochem.* **57**, 29-67.

Saunders, M. & Iveson, T. **2006** Management of advanced colorectal cancer: state of the art. *Br. J. Cancer* **95** (2), 131-138.

Scahill, T.A., Jensen, R.M., Swenson, D.H., Hatzenbuhler, N.T., Petzold, G., Wierenga, W. & Brahme, N.D. **1990** An NMR study of the covalent and noncovalent interactions of CC-1065 and DNA. *Biochemistry* **29**, 2852-2860.

Schaeffer, L., Moncollin, V., Roy, R., Staub, A., Mezzina, M., Sarasin, A., Weeda, G., Hoeijmakers, J.H. & Egly, J.M. **1994** The ERCC2/DNA repair protein is associated with the class II BTF2/TFIIH transcription factor. *EMBO J.* **13** (10), 2388-2392.

Schnell, J.R., Ketchem, R.R., Boger, D.L. & Chazin, W.J. **1999** Binding-induced activation of DNA alkylation by duocarmycin SA: Insights from the structure of an indole derivative-DNA adduct. *J. Am. Chem. Soc.* **121**, 5645-5652.

Schwartz, G.H., Patnaik, A., Hammond, L.A., Rizzo, J., Berg, K., Von Hoff, D.D. & Rowinsky, E.K. **2003** A phase I study of bizelesin, a highly potent and selective DNA-interactive agent, in patients with advanced solid malignancies. *Ann. Oncol.* **14** (5), 775-782.

Seaman, F.C. & Hurley, H. **1998** Molecular basis for the DNA sequence selectivity of ecteinascidin 736 and 743: evidence for the dominant role of direct readout via hydrogen bonding. *J. Am. Chem. Soc.* **120**, 13028-13041.

Seiden, M.V., Gordon, A.N., Bodurka, D.C., Matulonis, U.A., Penson, R.T., Reed, E., Alberts, D.S., Weems, G., Cullen, M. & McGuire, W.P. 3rd. **2006** A phase II study of irofulven in women with recurrent and heavily pretreated ovarian cancer. *Gynecol. Oncol.* **101** (1), 55-61.

Selby, C.P. & Sancar, A. **1998** ABC excinuclease incises both 5' and 3' to the CC-1065-DNA-adduct and its incision is stimulated by DNA helicase II and DNA polymerase I. *Biochemistry* **27**, 7184-7188.

Selvakumaran, M., Pisarcik, D.A., Bao, R., Yeung, A.T. & Hamilton, T.C. **2003** Enhanced cisplatin cytotoxicity by disturbing the nucleotide excision repair pathway in ovarian cancer cell lines. *Cancer Res.* **63**, 1311-1316.

Shamdas, G.J., Alberts, D.S., Modiano, M., Wiggins, C., Power, J., Kasunic, D.A., Elfing, G.L. & Earhart, R.H. **1994** Phase I study of adozelesin (U-73,975) in patients with solid tumours. *Anticancer Drugs* **5** (1), 10-14.

Shay, J.W. & Wright, W.E. **2006** Telomerase therapeutics for cancer: challenges and new directions. *Nature Rev. Drug Discov.* **5** (7), 577-584.

Shinohara, K-I., Narita, A., Oyoshi, T., Bando, T., Teraoka, H. & Sugiyama, H. **2004** Sequence-Specific gene silencing in mammalian cells by alkylating pyrrole-imidazole polyamides. *J. Am. Chem. Soc.* **126**, 5113-5118.

Shishido, K., Haruna, S., Yamamura, C., Litsuka, H., Nemoto, H., Shinohara, Y. & Shibuya, M. **1997** Synthesis and evaluation of the hybrid molecules possessing DNA-cleaving activity. *Bioorg. Med. Chem. Lett.* **7** (20), 2617-2622.

Simon, J.A. & Bedalov, A. **2004** Yeast as a model system for anticancer drug discovery. *Nat. Rev. Cancer* **4**, 1-8.

Simon, J.A., Szankasi, P., Nguyen, D.K., Ludlow, C., Dunstan, H.M., Roberts, C.J., Jensen, E.L., Hartwell, L.H. & Friend, S. H. **2000** Differential toxicities of anticancer agents among DNA repair and checkpoint mutants of *Saccharomyces cerevisiae*. *Cancer Res.* **60**, 328-333.

Skehan, P., Storeng, R., Scudiero, D., Monks, A., McMahon, J., Vistica, D., Warren, J.T., Bokesch, H., Kenney, S. & Boyd, M.R. **1990** New colorimetric cytotoxicity assay for anticancer-drug screening. *J. Natl. Cancer Inst.* **82** (13), 1107-1112.

Small, E.J., Figlin, R., Petrylak, D., Vaughn, D.J. *et al.* **2000** A phase II pilot study of KW-2189 in patients with advanced renal cell carcinoma. *Investigational New Drugs* **18**, 193-197.

Smith, J.A., Bifulco, G., Case, D.A., Boger, D.L., Gomez-Paloma, L. & Chazon, W.J. **2000** The structural basis for *in situ* activation of DNA alkylation by duocarmycin SA. *J. Mol. Biol.* **300**, 1195-1204.

Spanswick, V.J., Craddock, C., Sekhar, M., Mahendra, P., Shankaranarayana, P., Hughes, R.G., Hockhauser, D. & Hartley, J.A. **2002** Repair of interstrand crosslinks as a mechanism of clinical resistance to melphalan in multiple myeloma. *Blood* **100** (1), 224-229.

Stewart, B.W. & Kleihues, P. (eds) *World Cancer Report* **2003** International Agency for Research on Cancer Scientific Publications.

Sugiyama, H., Fujiwara, T., Ura, A., Tashiro, T., Yamamoto, K., Kawanishi, S. & Saito, I. **1994** Chemistry of the thermal degradation of abasic sites in DNA. Mechanistic investigation on thermal DNA strand cleavage of alkylated DNA. *Chem. Res. Toxicol.* **7**, 673-683.

Sugiyama, H., Lian, C., Isomura, M., Saito, I. & Wang, A.H-J. **1996** Distamycin A modulates the sequence specificity of DNA alkylation by duocarmycin A. *Proc. Natl. Acad. Sci. USA* **93**, 14405-14410.

Sugiyama, H., Ohmori, K., Chan, K.L., Hosoda, M., Asai, A., Saito, H. & Saito, I. **1993** A novel guanine N3 alkylation by antitumour antibiotic duocarmycin A. *Tetrahedron Lett.* **34** (13), 2179-2182.

Sun, D. & Hurley, L.H. **1992a** Effects of the (+)-CC-1065-(N3-adenine) DNA adduct on *in vitro* DNA synthesis mediated by *Escherichia coli* DNA polymerase. *Biochemistry* **31**, 2822-2829.

Sun, D. & Hurley, L.H **1992b** Structure-activity relationships of (+)-CC-1065 analogues in the inhibition of helicase-catalysed unwinding of duplex DNA. *J. Med. Chem.* **35**, 1773-1782.

Sun, D. & Hurley, L.H **1992c** Inhibition of T4 DNA ligase activity (+)-CC-1065: demonstration of the importance of the stiffening and winding effects of (+)-CC-1065 on DNA. *Anti-Cancer Drug Design* **7**, 15-36.

Sun, D. & Hurley, L.H. **1994** Cooperative Bending of the 21-base-pair repeats of the SV40 viral early promoter by human Sp1. *Biochemistry* **33**, 9578-9587.

Sun, D., Lin, C.H. & Hurley, L.H **1993** A-tract and (+)-CC-1065-induced bending of DNA. Comparison of structural features using non-denaturing gel analysis, hydroxyl-radical footprinting, and High-field NMR. *Biochemistry* **32**, 4487-4495.

Sung, P., Guzder, S.N., Prakash, L. & Prakash, S. **1996** Reconstitution of TFIIH and requirement of the DNA helicase subunits, Rad3 and Rad25, in the incision step of nucleotide excision repair. *J. Biol. Chem.* **271** (18), 10821-10826.

Sung, P., Prakash, L. & Prakash, S. **1987** RAD3 protein of *Saccharomyces Cerevisiae* is a DNA helicase. *Proc. Natl. Acad. Sci. USA* **84**, 8951-8955.

Svetomir, M., Vera, S., Allen, V. *et al.* 2002 Phase II trial of KW-2189 in patients with advanved malignant melanoma. *American J. Clin. Oncol.* **25** (3), 308-312.

Swalley, S.E., Baird, E.E., Dervan, P.B. **1998** Effects of γ-turn and β-tail amino acids on sequence specific recognition of DNA by hairpin polyamides. *J. Am. Chem. Soc.* **121**, 1113-1120.

Swenson, D.H., Li, L.H., Hurley, L.H., Rokem, J.S., Petzold, G.L., Dayton, B.D., Wallace, T.L., Lin, A.H. & Krueger, W.C. **1982** Mechanism of interaction of CC-1065 (NSC 298223) with DNA. *Cancer Res.* **42**, 2821-2828.

Taguchi, F., Kusaba, H., Asai, A., Iwamoto, Y., Yano, K., Nakano, H., Mizukami, T., Saijo, N., Kato, H. & Nishio, K. **2004** hnRNP L enhances sensitivity of the cells to KW-2189. *Int. J. Cancer* **108**, 679-685.

Takahasi, R., Bando, T. & Sugiyama, H. **2003** Specific alkylation of human telomere repeats by hairpin pyrrole-imidazole polyamide. *Bioorg. Med. Chem.* **11**, 2503-2509.

Takebayashi, Y., Goldwasser, F., Urasaki, Y., Kohlhagen, G. & Pommier, Y. **2001a** Ecteinascidin 743 induces protein-linked DNA breaks in human colon carcinoma HCT116 cells and is cytotoxic independently of *topoisomerase I* expression. *Clin. Cancer Res.* **7**, 185-191.

Takebayashi, Y., Pourquier, P., Yoshida, A., Kohlhagen, G. & Pommier, Y. **1999** Poisoning of human DNA *topoisomerase I* by ecteinascidin 743, an anticancer drug that selectively alkylates DNA in the minor groove. *Proc. Natl. Acad. Sci.* **96**, 7196-7201.

Takebayashi, Y., Pourquier, P., Zimonjic, D.B., Nakayama, K., Emert, S., Ueda, T., Urasaki, A., Kanzaki, S., Akiyama, S., Popescu, N., Kraemer, K.H. & Pommier, Y. **2001b** Antiproliferative activity of ecteinascidin 743 is dependent upon transcription-coupled nucleotide-excision repair. *Nature Med.* **7**, 961-966.

Tang, M.S., Qian, M. & Pao, A. **1994** Formation and repair of antitumour antibiotic CC-1065-induced DNA adducts in the adenine phosphoribosyltransferase and amplified dihydrofolate reductase genes of Chinese hamster ovary cells. *Biochemistry* **33**, 2726-2732.

Tao, Z.F., Fujiwara, T., Saito, I. & Sugiyama, H. **1999a** Sequence-specific DNA alkylation by hybrid molecules between segment A of duocarmycin A and pyrrole / imidazole diamide. *Angew. Chem. Int. Ed.* **38** (5), 650-653.

Tao, Z.F., Fujiwara, T., Saito, I. & Sugiyama, H. **1999b** Rational design of sequence- specific DNA alkylating agents based on duocarmycin A and pyrrole-imidazole hairpin polyamides. *J. Am. Chem. Soc.* **121**, 4961-4967.

Tao, Z.F., Saito, I. & Sugiyama, H. **2000** Highly cooperative DNA dialkylation by the homodimer of imidazole-pyrrole diamide-CPI conjugate with vinyl linker. *J. Am. Chem. Soc.* **122**, 1602-1608.

Tateishi, S., Sakuraba, Y., Masuyama, S., Inoue, H. & Yamaizumi, M. **2000** Dysfunction of human Rad18 results in defective postreplication repair and hypersensitivity to multiple mutagens. *Proc. Natl. Acad. Sci. U.S.A* **97** (14), 7929-7932.

Teichmann, M., Dieci, G., Huet, J., Rüth, J., Sentenac, A. & Seifart, K.H. **1997** Functional interchangeability of TFIIIB components from yeast and human cells in vitro *EMBO J.* **16** (15), 4708–4716.

Teng, Y, Longhese, M., McDonough, G. & Waters, R. **1998** Mutants with changes in different domains of yeast replication protein A exhibit differences in repairing the control region, the transcribed strand and the non-transcribed strand of the *Sacchraomyces cerevisiae MFA2* gene. *J. Mol. Biol.* **280**, 355-363.

Teng, Y., Shisheng, L., Waters, R. & Reed, S. H. **1997** Excision Repair at the level of the nucleotide in the *Saccharomyces cerevisiae MFA2* gene: Mapping of where enhanced repair in the transcribed strand begins and ends and identification of only a partial Rad16 requisite for repairing upstream control sequences. *J. Mol. Biol.* **267**, 324-337.

Teng, Y. & Waters, R. **2000** Excision repair at the level of the nucleotide in the upstream control region, the coding sequence and in the region where transcription terminates of the *Saccharomyces cerevisiae MFA2* gene and the role of *RAD26*. *Nucleic Acids Res.* **28** (5), 1114-1119.

Tercel, M., Denny, W.A. & Wilson, W.R. **1996** Nitrogen and sulfur analogues of the *seco*-CI alkylating agent: synthesis and cytotoxicity. *Bioorg. Med. Chem. Lett.* **6**, 2735-2740.

Tercel, M. Stribbling, S.M., Sheppard, H., Siim, B.G., Wu, K., Pullen, S.M., Botting, K.J., Wilson, W.R. & Denny, W.A. **2003** Unsymmetrical DNA cross-linking agents: Combination of the CBI and PBD pharmacophores. *J. Med. Chem.* **46**, 2132-2151.

Tietze, L.F., Herzig, T., Fecher, A., Haunert, F. & Schuberth, I. **2001b** Highly selective glycosylated prodrugs of cytostatic CC-1065 analogues for antibody-directed enzyme tumour therapy. *ChemBioChem* **2**, 758-765.

Tietze, L.F., Lieb, M., Herzig, T., Haunert, F. & Schuberth, I. **2001a** A strategy for tumour-selective chemotherapy by enzymatic liberation of *seco*-duocarmcyin SA-derivatives from nontoxic prodrugs. *Bioorg. Medic. Chem.* **9**, 1929-1939.

Torres-Ramos, C. A., Prakash, S. & Prakash, L **1997** Requirement of yeast DNA polymerase δ in post-replication repair of UV-damaged DNA. *J. Biol. Chem.* **272** (41), 25445-25448.

Torres-Ramos, C. A., Prakash, S. & Prakash, L. **2002** Requirement of RAD5 and MMS2 for postreplication repair of UV-damaged DNA in *Saccharomyces cerevisiae*. *Mol. Cel. Biol.* **22** (7), 2419-2426.

Trauger, J.W., Baird, E.E. & Dervan, P.B. **1996** Recognition of DNA by designed ligands at subnanomolar concentrations. *Nature* **387**, 202-205.

Trzupek, J.D., Gottesfeld, J.M. & Boger, D.L. **2006** Alkylation of duplex DNA in nucleosome core particles by duocarmycin SA and yatakemycin. *Nat. Chem. Biol.* **2**(2), 79-82.

Turner, P.R. & Denny, W.A. **2000** The genome as a drug target: Sequence specific minor groove binding ligands. *Current Drug Targets* **1**, 1-14.

Turner, J.M., Swalley, S.E., Baird, E.E. & Dervan, P.B. **1998** Aliphatic/aromatic amino acid pairings for polyamide recognition in the minor groove of DNA. *J. Am. Chem. Soc.* **120**, 6219-6226.

Ulrich, H.D. & Jentsch, S. **2000** Two RING finger proteins mediate cooperation between ubiquitin-conjjugating enzymes in DNA repair. *EMBO J.* **19** (13), 3388-3397.

Van der Kemp, P.A., Thomas, D., Barbey, R., de Oliveira, R. & Boiteux, S. **1996** Cloning and expression in *Escherichia coli* of the *OGG1* gene of *Saccharomyces cerevisiae*, which codes for DNA glycosylase that excises 7,8-dihydro-8-

oxoguanine and 2,6-diamino-5-hydroxy-5-N-methylformamidopyrimidine. *Proc. Natl. Acad. Sci. USA* **93** (11), 5197-5202.

Van Dyke, M.W., Hertzberg, R.P. & Dervan, P.B. **1982** Map of distamycin, netropsin and actinomycin binding sites on heterogenous DNA:DNA cleavage-inhibition patterns with methidiumpropyl-EDTA.Fe(II). *Proc. Natl. Acad. Sci. USA* **79** (18), 5470-5474.

Van Glabbeke, M., Verweij, J., Judson, I. & Nielsen, O.S. **2002** Progression-free rate as the principal end-point for phase II trials in soft- tissue sarcomas. *Eur. J. Cancer* **38**, 543-549.

Van Gool, A.J., Verhage, R., Swagemakers, S.M., Van de Putte, P., Brouwer, J., Troelstra, C., Bootsma, D., Hoeijmakers, J.H. **1994** *RAD26*, the functional *S. cerevisiae* homolog of the cockayne syndrome B gene ERCC6. *EMBO J.* **13** (22), 5361-5369.

Van Kesteren, C., Vooght, M.M.M., Lopez-Lazaro, L., Mathot, R.A.A., Schellens, J.H.M., Jimeno, J.M. & Beijnen, J.H. **2003** Yondelis® (trabectedin, ET-743): the develolpment of an anticancer agent of marine origin. *Anti-Cancer drugs* **14**, 487-502.

Volpe, D.A. Tomaszewski, J.E., Parchment, R., Garg, A., Flora, K.P., Murphy, M.J. & Grieshaber, C.K. **1996** Myelotoxic effects of the bifunctional alkylating agent bizelesin on human, canine and murine myeloid progenitor cells. *Cancer Chemother Pharmacol.* **39**, 143-149.

Wakasugi, M., Reardon, J.T. & Sancar, A. **1997** The non-catalytic function of XPG protein during dual incision in human nucleotide excision repair. *J. Biol. Chem.* **272** (25), 16030-16034.

Wang Y., Gupta, R., Huang, L., Luo, W. & Lown, J.W. **1996** Design, synthesis, cytotoxic properties and preliminary DNA sequencing evaluation of CPI-N-methylpyrrole hybrids. Enhancing effect of a trans double bond linker and role of the terminal amide functionality on cytotoxic potency. *Anti-Cancer Drug Design* **11**, 15-34.

Wang, Y., Yuan, H., Ye, W., Wright, S.C., Wang, H. & Larrick, J.W. **2000** Synthesis and preliminary biological evaluations of CC-1065 analogues: Effects of different linkers and terminal amides on biological activity. *J. Med. Chem.* **43**, 1541-1549.

Wang, Y., Yuan, H., Ye, W., Wright, S.C., Wang, H. & Larrick, J.W. **2001** Synthesis and preliminary cytotoxicity study of a cephalosporin-CC-1065 analogue prodrug. *BMC Chemical Biology* **1** (4). This article is available from http://www.biomedcentral.com/1472-6769/1/4.

Wang, Y., Yuan, H., Wright, S.C., Wang, H. & Larrick, J.W. **2002** Synthesis and cytotoxicity of a biotinylated CC-1065 analogue . BMC Chemical Biology 2 (1). This article is available from http://www.biomedcentral.com/1472-6769/2/1

Ward, B., Rechfuss, R., Goodisman, J. & Dabrowiak, J.C. **1988** Determination of netropsin-DNA binding constants from footrprinting data. *Biochemistry* **27** (4), 1198-1205.

Warpehoski, M.A., Harper, D.E., Mitchell, M.A. & Monroe, T.J. **1992** Reversibility of the covalent reaction of CC-1065 and analogues with DNA. *Biochemistry* **31**, 2502-2508.

Warpehoski, M.A. & Hurley, L.H. **1988** Sequence selectivity of DNA covalent modification. *Chem. Res. Toxicol.* **1**, 315-333.

Warpehoski, M.A., Kelly, G.R.C., Krueger, W.C., Li, L.H., McGovern, J.P., Prairie, M.D., Wicnienski, N. & Wierenga, W. **1988** Stereoelectronic factors influencing the biological activity and DNA interaction of synthetic antitumour agents modelled on CC-1065. *J. Med. Chem.* **31**, 590-603.

Wartell, R.M., Larson, J.E. & Wells, R.D. **1974** Netropsin. A specific probe for A-T regions of duplex deoxyribonucleic acid. *J. Biol. Chem.* **249**, 6719-6731.

Wassmann, B, Pfeifer, H., Goekburget, N., Beelen, D.W. *et al.* **2006** Alternating versus concurrent schedules of imatinib and chemotherapy as front line therapy for Philadelphia positive acute lymphoblastic leukemia (Ph^+ ALL). *Blood* **108** (5), 1469-1477.

Weber, C.A., Salazar, E.P., Stewart, S.A. & Thomson, L.A. **1990** *ERCC2*: cDNA cloning and molecular characterisation of a nucleotide excision repair gene with high homology to yeast *RAD3*. *EMBO J.* **9**, 1343-1347.

Weiland, K.L. & Dooley, T.P. **1991** *In vitro* and *in vivo* bonding by the CC-1065 analogue U-73975. *Biochemistry* **30**, 7559-7565.

White, R.H., Parsons, P.G., Prakash, A.S. & Young, D.J. **1995** The *in vitro* cytotoxicity and DNA alkylating ability of the simplest functional analogues of the *seco* CC-1065 alkylating subunit. *Bioorg. Medic. Chem. Lett.* **5** (16), 1869-1874.

White, S., Szewczyk, J.W., Turner, J.M., Baird, E.E., Dervan, P.B. **1998** Recognition of the four Watson-Crick base pairs in the DNA minor groove by synthetic ligands. *Nature* **391**, 468-471.

Woynarowski, J. M. **2002** Targeting critical regions in genomic DNA with AT-specific anticancer drugs. *Biochim. Biophys. Acta* **1587**, 300-308.

Woynarowski, J.M. & Beerman, T.A. **1997** Effects of Bizelesin (U-77,779), a bifunctional alkylating minor groove binder, on replication of genomic and simian virus 40 DNA in BSC-1 cells. *Biochim. Biophys. Acta* **1353** (1), 50-60.

Woynarowski, J.M., Napier, C., Koester, S.K., Chen, S.F., Troyer, D., Chapman, W., & MacDonald, J.R. **1997** Effects on DNA integrity and apoptosis induction by a novel antitumour sesquiterpene drug, 6-hydroxymethylacylfulvene (HMAF, MGI 114). *Biochem. Pharmacol.* **54** (11), 1181-1193.

Woynarowski, J.M., Napier, C., Trevino, A.V. & Arnett, B. **2000** Region-specific DNA damage by AT-specific DNA-reactive drugs is predicted by drug-binding specificity. *Biochemistry* **39** (32), 9917-9927.

Wrasidlo, W., Johnson, D.S. & Boger, D.L. **1994** Induction of endonucleolytic DNA fragmentation and apoptosis by the duocarmycins. *Bioorg. Medic. Chem. Lett.* **4** (4), 631-636.

Wyatt, M.D., Garbiras, B.J., Haskell, M.K., Lee, M., Souhami, R.L. & Hartley, J.A. **1994** Structure-activity relationship of a series of nitrogen mustard- and pyrrole-containing minor groove-binding agents related to distamycin. *Anti-cancer Drug Des.* **9**, 511-525.

Wyatt, M.D., Lee, M., Garbiras, B.J., Souhami, R.L. & Hartley, J.A **1995** Sequence specificity of alkylation for a series of nitrogen mustard-containing analogues of distamycin of increasing binding site size: evidence for increased cytotoxicity with enhanced sequence specificity. *Biochemistry* **34**, 13034-13041.

Xiao, W., Chow, B.L.. Broomfield, S. & Hanna, M. **2000.** The *Saccharomyces cerevisiae RAD6* group is composed of an error-prone and two error-free postreplication repair groups. *Genetics* **155**, 1633-1641.

Xiao, W., Chlow, B.L., Fontanie, T., Ma, L., Bacchetti, S., Hryciw, T. & Broomfield, S. **1999** Genetic interactions between error-prone and error-free postreplication repair pathways in *Saccharomyces Cerevisiae. Mutat. Res.* **435**, 1-11.

Xiao, W., Chow, B.L. & Rathgeber, L. **1996** The repair of DNA methylation damage in *Saccharomyces cerevisiae. Curr. Genet.* **30**, 461-468.

Xie, Y., Miller, G.G., Cubitt, S.A., Soderlind, K.J., Allalunis-Turner, M.J., & Lown, J.W. **1997** Enediyne-lexitropsin DNA-targeted anticancer agents. Physicochemical and cytotoxic properties in human neoplastic cells *in vitro*, and intracellular distribution. *Anti-Cancer Drug Design* **12**, 169-179.

Yamamoto, K., Sugiyama, H. & Kawanishi, S. **1993** Concerted DNA recognition and novel site-specific alkylation by duocarmycin A with distamycin A. *Biochemistry* **32**, 1059-1066.

Zakrzewska, K., Randrianarivelo, M. & Pullman, B. **1987** Theoritical study of the sequence specificity in the covalent binding of the antitumour drug CC-1065 to DNA. *Nucleic Acids Res.* **15** (14), 5775-5785.

Zewail-Foote, M. & Hurley, L.H. **1999** Ecteinascidin 743: a minor groove alkylator that bends DNA toward the major groove. *J. Med. Chem.* **42**, 2493-2497.

Zewail-Foote, M. & Hurley, L.H. **2001** Differential rates of reversibility of Ecteinascidin 743-DNA covalent adducts from different sequences lead to migration to favored binding sites. *J. Am. Chem. Soc.* **123**, 6485-6495.

Zewail-Foote, M., Ven-Shun, L., Kohn, H., Bearss, D., Guzman, M. & Hurley, L.H. **2001** The inefficiency of incisions of ecteinascidin 743-DNA adducts by the UvrABC nuclease and the unique structural feature of the DNA adducts can be used to explain the repair-dependent toxicities of this antitumor agent. *Chem. Biol.* **8**, 1033-1049.

Zhang, H. & Lawrence, C.W. **2005** The error-free component of *RAD6/RAD18* DNA damage tolerance pathway of budding yeast employs sister-strand recombination. *Proc. Nat. Acad. Sci. USA* **102**, 15954-15959.

Zhong, X., Li, Q.Q. & Reed, E. **2003** SU5416 sensitizes ovarian cancer cells to cisplatin through inhibition of nucleotide excision repair. *Cell. Mol. Life Sci.* **60**, 794-802.

Zhou, Q., Duan, W., Simmons, D., Shayo, Y., Raymond, M.A., Dorr, R.T. & Hurley, L.H. **2001** Design and synthesis of a novel DNA-DNA intrestrand Adenine-Guanine Cross-linking Agent. *J. Am. Chem. Soc.* **123**, 4865-4866.

Zimmer, C., Marck, C., Schneider, C., Guschlbauer, W. **1979** Influence of nucleotide sequence on dA.dT-specific binding of Netropsin to double stranded DNA. *Nucleic Acids Res.* **6** (8), 2831-2837.

Zsido, T.J., Woynarowski, J.M., Baker, R.M., Gawson, L.S. & Beerman, T.A. **1991** Induction of heat-labile sites in DNA of mammalian cells by the antitumour alkylating drug CC-1065. *Biochemistry* **30**, 3733-3738.

PUBLICATIONS RESULTING FROM THIS THESIS

Howard, T.T., Lingerfelt, B.M., Purnell, B.L., Scott, A.E., Price, C.A., Townes, H.M., McNulty, L., Handl, H.L., Summerville, K., Hudson, S.J., Bowen, J.P., Kiakos, K., Hartley, J.A. & Lee, M. **2002** Novel furano analogues of duocarmycin C1 and C2: design, synthesis, and biological evaluation of *seco*-iso-cyclopropylfurano[2,3-e]indoline (*seco*-iso-CFI) and *seco*-cyclopropyltetrahydrofurano[2,3-f]quinoline (seco-CFQ) analogues. *Bioorg. Med. Chem.* **10** (9), 2941-2952.

Toth, J.L., Price, C.A., Madsen, E.C., Handl, H.L., Hudson, S.J., Hubbard, R.B. 3rd, Bowen, J.P., Kiakos, K., Hartley, J.A. & Lee, M. **2002** Sequence selective recognition of DNA by hairpin conjugates of a racemic *seco*-cyclopropaneindoline-2-benzofurancarboxamide and polyamides. *Bioorg. Med. Chem. Lett.* **12** (16), 2245-2248.

Kiakos, K., Howard, T.T., Lee, M., Hartley, J.A., McHugh, P.J. **2002** *Saccharomyces cerevisiae RAD5* influences the excision repair of DNA minor groove adducts. *J. Biol. Chem.* **277** (46), 44576-44581.

Toth, J., Henry, J., Taherbhai, Z., Staples, A., Summerville, K., Handl, H., Hudson, S., Kiakos, K., Hartley, J. & Lee, M. **2003** Cytotoxicity and sequence specificity of C- and N- terminus conjugates of N-methylpyrrole polyamides with *seco*-cyclopropaneindoline. *Med. Chem. Res.* 12:2, 87-93.

Kupchinsky, S., Centioni, S., Howard, T., Trzupek, J., Roller, S., Carnahan, V., Townes, H., Purnell, B., Price, C., Handl, H., Summerville, K., Johnson, K., Toth, J., Hudson, S., Kiakos, K., Hartley, J.A. & Lee M. **2004** A novel class of achiral *seco*-analogs of CC-1065 and the duocarmycins: design, synthesis, DNA binding, and anticancer properties. *Bioorg. Med. Chem.* **12** (23), 6221-36.

Price, C.A., Lingerfelt, B.M., Handl, H.L., Kiakos, K., Hartley, J.A. & Lee, M. **2005** Sequence specific recognition of DNA by tailor-made hairpin conjugates of achiral *seco*-cyclopropaneindoline-2-benzofurancarboxamide and pyrrole-imidazole polyamides. *Bioorg. Med. Chem. Lett.* 15 (12), 3151-3156.

Sato, A., McNulty, L., Cox, K., Kim, S., Scott, A., Daniell, K., Summerville, K., Price, C., Hudson, S., Kiakos, K., Hartley, J.A., Asao, T. & Lee, M. **2005** A novel class of *in vivo* active anticancer agents: achiral *seco*-amino- and *seco*-hydroxycyclopropylbenz[e]indolone (*seco*-CBI) analogues of the duocarmycins and CC-1065. *J. Med. Chem.* **48** (11), 3903-3918.

Toth, J.L., Trzupek, J.D., Flores, L.V., Kiakos, K., Hartley, J.A., Pennington, W.T. & Lee, M. **2005** A novel achiral *seco*-amino-cyclopropylindoline (CI) analog of CC-1065 and the duocarmycins: design, synthesis and biological studies. *Med Chem.* **1** (1), 13-19.